

ERDA Symposium Series

QL  
739  
L879  
1973

An abstract graphic on a dark, textured background. It features a dense cluster of small, light-colored dots arranged in a roughly triangular shape, with a few scattered dots extending from the main group. The dots vary slightly in brightness, giving a sense of depth or movement.

# MAMMALIAN CELLS: Probes and Problems



# MAMMALIAN CELLS: Probes and Problems

Proceedings of the First Los Alamos  
Life Sciences Symposium  
held at Los Alamos, New Mexico  
October 17-19, 1973

Sponsored by  
Los Alamos Scientific Laboratory  
U. S. Atomic Energy Commission  
and  
National Cancer Institute

## Editors

C. R. Richmond  
D. F. Petersen  
P. F. Mullaney  
E. C. Anderson  
Los Alamos Scientific Laboratory

1975

Published by

Technical Information Center, Office of Public Affairs  
U. S. Energy Research and Development Administration

QL  
739  
L672  
1973

Available as CONF-731007 for \$7.60 (foreign, \$10.10) from

National Technical Information Service  
U. S. Department of Commerce  
Springfield, Virginia 22161

International Standard Book Number 0-87079-017-4  
Library of Congress Catalog Card Number 75-600009  
ERDA Distribution Category UC-48

Printed in the United States of America  
USERDA Technical Information Center, Oak Ridge, Tennessee  
March 1975; latest printing, June 1975



## PREFACE

The symposium entitled "Mammalian Cells: Probes and Problems" was the first Los Alamos Life Sciences Symposium. We wanted very much to begin the series with a symposium subject that was both timely and relevant in the scientific sense and one to which I believe the biomedical research personnel at Los Alamos Scientific Laboratory have made significant contributions.

The symposium, jointly sponsored by the Los Alamos Scientific Laboratory, the Division of Biomedical and Environmental Research, U. S. Atomic Energy Commission, and the National Cancer Institute, was held on October 17–19, 1973, at Los Alamos, New Mexico. Our plan was to arrange a setting for researchers to meet and exchange information on how techniques such as image analysis and flow systems for cell analysis and sorting currently are being used to solve both practical and basic biomedical research problems. Going a step further, we asked certain speakers to look into the future to see what might appear to be interesting avenues of research and applications. This is a difficult task at best since it must cover a fixed vantage point in time. However, the task is necessary, for, although it is important that we remember the past so as not to repeat it, we must continually look to the future and remember that today is tomorrow's yesterday. I think the contributors to the summary sessions did an excellent job of looking into the future and deserve special thanks.

I was gratified to see the intensive interaction among engineers, physicists, biologists (and their hybrid cousins, the biophysicists), and physicians. The efficient exploitation of such rapidly evolving techniques as flow microfluorometry systems for cell analysis and sorting, scanning cytophotometry, and cytographic analysis requires just such an interdisciplinary approach to solving biomedical problems.

## PREFACE

These powerful techniques now allow us to measure cell volume, number, and area, to probe the interior of the cell, and to interrogate the important cell surface upon which important biological and chemical events occur and through which all things must pass to enter the cell. It is important that we actively pursue the development and application of these powerful tools to study, for example, subcellular entities, but it is perhaps even more important to exchange information in this rapidly developing area where the potential breakthroughs offer not only significant progress in biomedical research but also notable benefits to those who support such efforts—that is, society in general. In summary, this interaction is what the symposium was all about.

As symposium coordinator and on behalf of the editors, I should like to thank the sponsors, the authors, and all the others who helped to make our First Los Alamos Life Sciences Symposium a success. I also want to thank Elizabeth M. Sullivan for gently but firmly extracting manuscripts from the speakers, for assembling manuscripts for these proceedings, and for attending to seemingly endless detail. Special acknowledgment must go to the Office of Public Affairs, U. S. Energy Research and Development Administration, for publication of this volume, both to Robert F. Pigeon, Science Services Branch, for administration and to members of the Editorial Branch, Technical Information Center, for preparing the proceedings, particularly to Joan Roberts, who worked during as well as after the symposium to transform several days of technical meetings into these symposium proceedings. Last, but certainly not least, I want to thank the many people at the Los Alamos Scientific Laboratory who, each in his own way, helped to guarantee the success of the symposium.

C. R. Richmond\*  
*Symposium Coordinator*

---

\*Presently Associate Director for Biomedical and Environmental Sciences at Holifield National Laboratory, Oak Ridge, Tennessee.

# CONTENTS

## IMAGE-ANALYSIS TECHNIQUES

Image-Analysis Techniques: Opening Remarks . . . . .	1
<i>George L. Wied</i>	
Scanning Cytophotometry: Principles and Practice . . . . .	3
<i>Brian H. Mayall</i>	
Extraction and Evaluation of Information from Digitized Cell Images . . . . .	15
<i>Peter H. Bartels and George L. Wied</i>	
Slit-Scanning Cell-Analysis Methods . . . . .	29
<i>Leon L. Wheelless, Jr.</i>	
Analysis of DNA Synthesis Changes in Cells Infected with SV40 Virus . . . . .	38
<i>John M. Lehman</i>	
Computer-Assisted Analysis of Irradiated Lymphocytes . . . . .	44
<i>Robert E. Anderson, George B. Olson, John L. Howarth, and Peter H. Bartels</i>	
Image-Analysis Techniques: Session Summary . . . . .	55
<i>Mortimer L. Mendelsohn</i>	

## FLOW-SYSTEMS CELL ANALYSIS AND SORTING

Flow-Systems Cell Analysis and Sorting: Opening Remarks . . . . .	59
<i>M. A. Van Dilla</i>	
Multiparameter Cell Sorting and Analysis . . . . .	61
<i>John A. Steinkamp</i>	

## CONTENTS

DNA Content in Normal, Transformed, and Revertant Mouse Cell Lines . . . . .	76
<i>Arthur Vogel, Brad Ozanne, and Robert Pollack</i>	
Factors Affecting the Choice of Cellular Specimens for Automated Examinations . . . . .	89
<i>M. R. Melamed</i>	
Cell Preparation and Staining for Flow Systems . . . . .	94
<i>Harry A. Crissman</i>	
Fluorescence-Activated Cell Sorting and Its Applications . . . . .	107
<i>Michael H. Julius, Richard G. Sweet, C. Garrison Fathman, and Leonard A. Herzenberg</i>	
Flow-Systems Cell Analysis and Sorting: Closing Remarks . . . . .	122
<i>M. A. Van Dilla</i>	

## CELL-CYCLE ANALYSIS

Cell-Cycle Analysis: Opening Remarks . . . . .	125
<i>Donald F. Petersen</i>	
Biochemical Events in the S Phase of Replicating Animal Cells . . . . .	128
<i>Gerald C. Mueller</i>	
Cycle-Dependent Enzyme Induction . . . . .	145
<i>Gordon M. Tomkins</i>	
Sequential Biochemical Events in the Mammalian Cell Cycle . . . . .	152
<i>Robert A. Tobey, Lawrence R. Gurley, C. E. Hildebrand, Paul M. Kraemer, Robert L. Ratliff, and Ronald A. Walters</i>	
Cycle-Dependent Therapeutic Agents . . . . .	168
<i>Vincent H. Bono, Jr., and Robert L. Dion</i>	
Cell-Cycle Analysis: Session Summary . . . . .	179
<i>Donald F. Petersen</i>	

## THE CELL NUCLEUS

The Cell Nucleus: Opening Remarks . . . . .	181
<i>J. Herbert Taylor</i>	

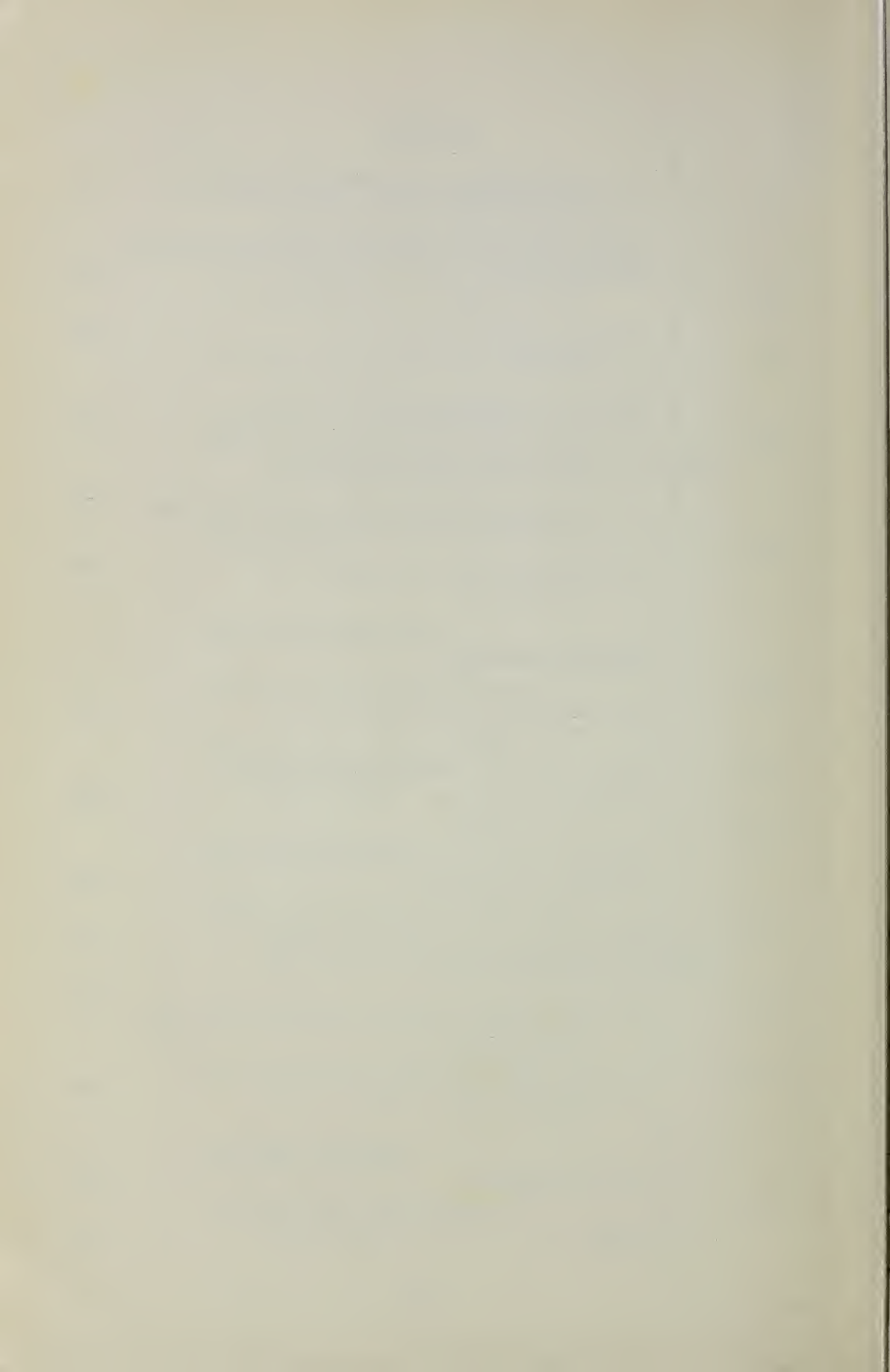
## CONTENTS

The Cell Cycle and DNA Synthesis in Mammalian Cells . . .	184
<i>Joel A. Huberman</i>	
Genetic Conservatism in Phylogeny with Special References to Chromosomes . . . . .	200
<i>Frances E. Arrighi</i>	
On Chromosome Organization . . . . .	208
<i>T. C. Hsu</i>	
Chromosome G-Banding and DNA Constancy in Aneuploid Cell Populations . . . . .	212
<i>Larry L. Deaven, Phyllis C. Sanders, Julie L. Grilly, Paul M. Kraemer, and Donald F. Petersen</i>	
Genetic Markers Associated with Hamster Chromosomes . .	228
<i>E. H. Y. Chu, N. C. Sun, and C. C. Chang</i>	
The Cell Nucleus: Session Summary . . . . .	239
<i>J. Herbert Taylor</i>	

## THE CELL SURFACE

The Cell Surface: Opening Remarks . . . . .	242
<i>Paul M. Kraemer</i>	
Current Views on the Molecular Organization of Biological Membranes . . . . .	246
<i>Garth L. Nicolson</i>	
On Signals Generated by the Binding of Multivalent Antigens to Lymphocytes . . . . .	254
<i>George I. Bell</i>	
Heterogeneity of Antibody-Binding Affinity . . . . .	277
<i>Gregory W. Siskind</i>	
Cell Adhesion . . . . .	284
<i>Carl G. Hellerqvist, Warren L. Rottmann, Bernt T. Walther, and Saul Roseman</i>	
The Cell Surface: Session Summary . . . . .	296
<i>Paul M. Kraemer</i>	
List of Participants . . . . .	299
Index . . . . .	303





## SESSION I

### IMAGE-ANALYSIS TECHNIQUES: OPENING REMARKS

George L. Wied, *Session Chairman*

Departments of Obstetrics and Gynecology and of Pathology, University of Chicago,  
Chicago, Illinois

---

I have been given the privilege of making a few introductory remarks and, since this session is concerned with automation of cytology, I will discuss some of the clinical goals of quantitative cytology. Diagnostic cytology has been proven to be the most effective means for early detection of many malignant diseases and has, within the past 25 years, found worldwide acceptance. The recognition of the value of the method in disease management and the anticipated demand are such that substantial research efforts are being made toward automation of routine diagnostic cytology despite the fact that even now one can hardly call clinical cytology a quantitative science. Approaches taken by the exact sciences in the past have been far too simplistic to do justice to the complexities of actual clinical cell samples.

Several in this audience today participated in or attended the First International Tutorial on Quantitative Cytochemistry, sponsored by the International Academy of Cytology and held at the Center for Continuing Education at the University of Chicago in 1965, and took part in our subsequent tutorials on the subject. The Chicago meeting had a purpose very similar to the one for this meeting here at Los Alamos: to bring together and explain in simple terms the most advanced methods that basic exact science can bring to bear on improvement of cytological diagnosis. The emphasis in 1965 was on measurements of total amounts of DNA in cells. The mathematics were relatively simple: one-way analysis of variance and correction for distributional errors in photometric measurements that by current standards must be considered generally crude. The program of this meeting reflects the changes in the field of cytology in the past years. The emphasis today is on information extraction from cells and on the immunological capabilities of cells. We have seen cytology emerge as an objective and quantitative science. There is a great challenge in

applying the principles and methodology from such seemingly unrelated fields as communication theory, computer science, and control theory to clinical cytology, where complex mathematical models, multivariate statistics, and analytical procedures are applied practically. An exciting and surprising aspect is the active involvement of researchers from so many different and widely varying disciplines. What is also new is that mathematics is used not only to ascertain and to secure facts already detected by biological experimentation but also to discover new relationships that can be established as consistent and significant even before the biological meaning is known.

At a time when the potential of exact methodology becomes applicable to clinical cytology, it may be appropriate for someone deeply involved in the practice of diagnostic cytology to comment on the envisioned goals. With our increased capabilities to extract information from cells and cell samples, we will be able to set up objective standards for diagnostic decisions. These standards will be defined by sets of expected values of multivariate confidence regions and estimates of the involved covariances. We will collect reliable data as to what cellular composition samples, taken at a given time, are expected to have in patients belonging in well-defined groups with comparable clinical histories. We will have precise estimates for the properties of cells of different diagnostic significance. We will be able to assess precisely the effects of different antineoplastic agents and to develop even more refined pharmacokinetic models to monitor drug response in patients. We will be able to follow on the cellular level the effects of therapeutic radiation, to screen pharmaceuticals, and to determine the environmental hazards of commercially used chemicals as well as low-level radiation. It can be expected that we will be able to determine standards of irreversibility on certain cellular alterations (for instance, when a severely dysplastic cellular abnormality cannot be expected to regress any longer to benign epithelial conditions). However, most important is the greatly increased capability to measure small differences between single cells and sets of cells to discover trends and to discriminate. We now have the potential to set up a finely structured cytotaxonomy. The field of leukocyte classification serves as an example. The basic types of leukocytes have already been incremented by the two subcategories of thymus-derived T cells and bone marrow-derived B cells within small lymphocytes with their different immune capabilities. There already is evidence that at least the T cells contain two consistently present subgroups of as yet unconfirmed biological significance. We may reasonably expect this development to continue in the future. It does not take much imagination to perceive eventual clinical methods that would assess the differential count of such subcategories of immunologically engaged cells and very possibly use such methods to evaluate the immunological surveillance competence of a patient. This would be a very definite achievement toward prognostic medical care and may be far ahead of early detection of disease processes already in progress.

# SCANNING CYTOPHOTOMETRY: PRINCIPLES AND PRACTICE

BRIAN H. MAYALL

Biomedical Division, Lawrence Livermore Laboratory, Livermore, California

---

## ABSTRACT

Cytophotometry allows quantitation of individual cells and cell components. Absorption cytophotometry is compared with conventional spectrophotometry, the theory of scanning instruments is developed, and sources of error are identified. Illustrative applications include cytochemical studies of bull sperm differentiation and of hemoglobin synthesis in the developing chick embryo. The DNA-based measurement of human chromosomes is an application in which scanning cytophotometry is combined with computer image analysis to provide previously unobtainable information. The power of this approach is shown by the analysis of chromosomes from leukemic cells of a patient with chronic myelogenous leukemia; the measurements confirmed the suspected 9q+/22q- translocation and revealed an unsuspected 9+/20- translocation.

Cytophotometry uses optical probes to measure and analyze individual cells. Such probes include measurement of light absorption, fluorescence emission, phase retardation, polarizing activity, light scattering, and other optical properties of cells. Applications of cytophotometry range from simple counting and sizing of cells through quantitation of cellular components to analysis of the spatial distribution and the molecular organization of specific macromolecules within the cell. Many of the broader applications of cytophotometry are discussed by other contributors to this symposium. The prime concern of this presentation is the use of absorption measurements as applied to the quantitation of DNA and other macromolecules in individual cells and in chromosomes.

In absorption cytophotometry a major problem arises in that DNA and most other cellular constituents show little absorption in the visible part of the spectrum. Caspersson, in his pioneering studies,<sup>1</sup> avoided this problem by measuring DNA with ultraviolet light, but this approach has never been used



widely because of the associated expense and technical problems. The alternative is first to stain the cellular component of interest with either an absorption or a fluorescent dye and then to make measurements in the visible part of the spectrum. Ideally the staining reaction will be both specific and stoichiometric for the component of interest so that the stain content is directly proportional to substrate and the quantitation of dye quantitates the amount of substrate in the cell. In practice this ideal is rarely met, because the cytochemistry is modified by steric hindrance and competitive inhibition from other cellular components. Fortunately cytophotometric experiments usually are concerned with relative effects rather than with absolute measurements and so can tolerate some uncertainty in stoichiometry of staining, provided that the experimental design includes proper controls and that staining is specific and proportional.

Cytophotometry requires special instrumentation. Two classes of instrumental approach have been developed—flow systems and imaging systems. In flow systems, cells in suspension are measured at rates of a thousand or more cells per second; in imaging systems, cells are attached to an optical surface, such as a microscope slide, and are measured at a rate of about one cell per minute. The higher speed of the flow system is balanced by the accessibility of morphology in the imaging systems. In flow systems it is difficult to relate the measurements to other characteristics of the individual cells. By contrast, in imaging systems the cells are immobilized on a surface and so can be located, mapped, examined, and identified by conventional morphologic criteria. This allows the characterization of individual cells by morphology and by cytochemical procedures, including autoradiographic and other noncytophotometric techniques. The differences between the two classes of instrumentation are narrowing; there now are flow systems that capture some morphologic information and imaging systems that measure at rates approaching those of flow systems.

This presentation is concerned with imaging systems, more specifically with absorption cytophotometry and scanning cytophotometers. The theory of absorption cytophotometry and scanning is developed, sources of error and design criteria are considered, and usefulness of the approach is illustrated by the application of DNA cytophotometry to work currently in progress at the Lawrence Livermore Laboratory.

## ABSORPTION CYTOPHOTOMETRY

Absorption cytophotometry is a modification of conventional photometry. The left side of Fig. 1 illustrates a familiar situation—a solution of chromophore being measured spectrophotometrically in a cuvette. The measured intensity of light passing through the system is  $I$ , and the measured intensity when there is no chromophore in the cuvette is  $I_0$ . The transmission ( $T$ ) through the system is the ratio of these two measurements, and the absorption or optical



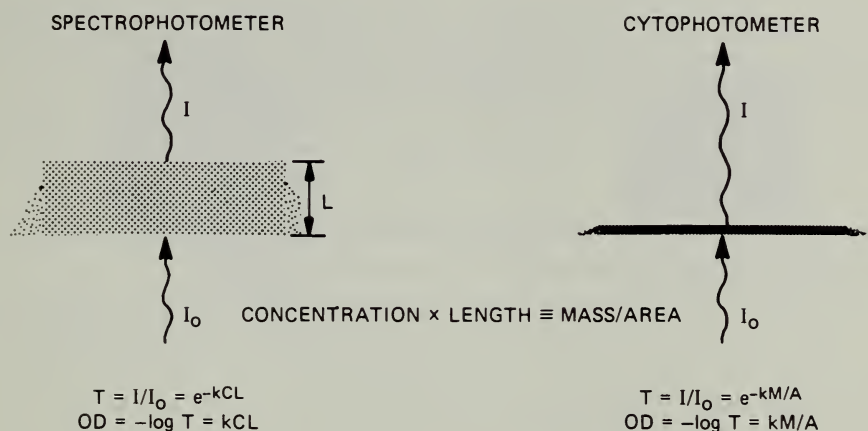


Fig. 1 Comparison of absorption spectrophotometry in a cuvette and absorption cytophotometry on a slide. Absorption law requires (1) monochromatic collimated illumination; (2) no glare, no flare, no scattering; and (3) homogeneous distribution of chromophore.

$I$	Measured intensity of light passing through the system
$I_0$	Measured intensity with no chromophore in the cuvette
$T$	Transmission through the system
$OD$	Optical density
$k$	Specific absorption of the chromophore at the measuring wavelength
$C$	Concentration of chromophore
$L$	Path length of the cuvette
$M/A$	Mass of chromophore per unit area

density (OD) is the negative logarithm of the transmission. Thus

$$OD = -\log T = -\log (I/I_0) \quad (1)$$

The optical density is directly proportional to the concentration of chromophore in the cuvette, provided that the following four conditions are met:

1. The illumination is monochromatic and collimated perpendicularly to the cuvette.
2. There is no glare, no flare, and no scattering in the system.
3. The chromophore is homogeneously distributed throughout the cuvette.
4. The specific absorption of the chromophore is not changed by the molecular environment (i.e., no hyperchromic, hypochromic, or metachromatic effects).

Failure to satisfy any of the preceding conditions leads to measuring errors. But when the conditions are all satisfied, the concentration of chromophore (C) can be calculated directly from the measured optical density as

$$OD = kCL \quad (2)$$

where  $k$  is the specific absorption of the chromophore at the measuring wavelength and  $L$  is the path length of the cuvette.

The right side of Fig. 1 illustrates the situation in absorption cytophotometry. The total amount of absorbing material is the same in this example as in the one on the left, but here it has precipitated out of solution and formed a uniform thin layer. The mass of chromophore in a given area of this layer is the same as the mass of chromophore contained in the cuvette in a volume subtended by the same cross-sectional area. Simple algebra shows that the mass of chromophore per unit area ( $M/A$ ) is directly proportional to the optical density measured in the cytophotometer, provided only that the chromophore is uniformly distributed within the measuring area and that the other three conditions of the absorption laws are satisfied. Thus

$$OD = kM/A \quad (3)$$

Since the chromophore in the cell is not homogeneously distributed on the microscope slide, one of the requirements for valid photometry is not satisfied. This can result in distributional error, potentially the most serious of the systematic errors associated with cytophotometry.<sup>2-6</sup> Distributional error occurs because a measurement through any photometric field averages the transmissions through all of the fractional elements of the field. Taking the negative logarithm of this average transmission will lead to the systematic underestimation of the amount of chromophore present whenever there is heterogeneity in the field. Distributional error is a simple consequence of the algebraic relationship that the logarithm of the mean of different values is not the same as the mean of the logarithms of the values, i.e.,

$$\log (\overline{A + B}) < \overline{(\log A + \log B)} \quad (A, B > 1; A \neq B) \quad (4)$$

Distributional error is always negative, and its magnitude increases both with the mean optical density and with the heterogeneity of the chromophore distribution.

Scanning is the most versatile of the several cytophotometric approaches that have been developed to minimize the effect of distributional error. In scanning cytophotometers, the field containing the cell is divided into a large number of regularly spaced picture elements. Optical density is measured for each element. Figure 2, which illustrates the basic process of scanning, shows a

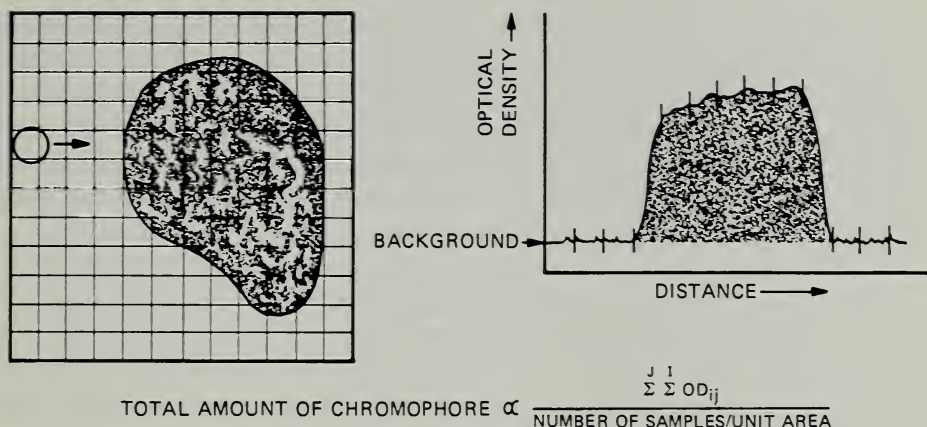


Fig. 2 Principle of scanning cytophotometry. When the absorption laws are obeyed, the total amount of chromophore in the field is proportional to the sum of the optical density values for all the picture elements of the field.

measuring field containing a cell surrounded by clear background. The field is scanned in a regular fashion by a measuring spot whose size is matched to the resolution of the optical system and which is small enough to make distributional error inconsequential.<sup>5,6</sup> Typically, the spot scans continuously across the field in a rectilinear raster. The right-hand portion of Fig. 2 shows the signal trace from a single scan line. The vertical bars superimposed on this continuous trace correspond to the points at which measurements are taken.

The algebra of scanning cytophotometry is straightforward.<sup>6</sup> The total amount of chromophore present in the measuring field is directly proportional to the integrated optical density for all the picture elements. This sum can be corrected for sampling density by dividing by the number of elements sampled per unit area. Thus changes in magnification or sampling rate are factored out, and measurements made on different instruments or under different conditions can be compared.

The reliability of measurements made with scanning systems depends on linearity and resolution in both the spatial and photometric senses.<sup>4-7</sup> Spatial linearity is a readily understood function of the scanning system and the optics and implies freedom from such effects as pin-cushion or barrel distortion. Spatial resolution depends on the sampling density and on the optical resolution of the system, including accurate focus. Photometric linearity implies not only linearity in the detection system and associated electronics but also measurements made under conditions permitting valid application of the absorption laws. Photometric resolution is concerned with the signal-to-noise ratio of the system and thus is a function of such factors as brightness of illumination and sampling speed.



A common problem in cytophotometry is associated with establishing the base line of zero optical density. Since measurements are made relative to this clear-area base line, the system should be calibrated so that background-scan elements containing no chromophore have zero optical density. Four different approaches have been used for the base-line problem. The simplest approach is to make a scan with the base line at some arbitrary but unknown positive value and thus to add a background constant to every measurement of optical density. The cell then is removed, and a neighboring clear area is scanned. The sum of the clear-area measurements estimates the background constant and is subtracted from the original sum to give the integrated optical density. In the second approach either the first element of a scan or the first element of each line of a scan is sampled; these values are assumed to give good estimates of what the background will be for the rest of the scan, and these values are used to zero the system. The third approach is used in the IMANCO Quantimet system which detects the whitest elements of the field. The system first is zeroed against these values; then it adjusts automatically to maintain the calibration. In the fourth approach image-processing techniques are used to sample clear areas in the vicinity of the objects being measured; the clear-area values are used to set a local background for each object. This approach is particularly useful when the background shows local structure, as is frequently the case with metaphase chromosome preparations.

## APPLICATIONS

Imaging systems are uniquely suited to the cytophotometric applications that require morphological identification, multiple analysis, or spatial partitioning.

Gledhill's studies of cytochemical changes in differentiating bull spermatozoa illustrate an application in which morphological identification of the individual cells is crucial.<sup>8</sup> The cells can be assigned to different successive stages of differentiation on the basis of morphological criteria alone. Thus cells of each stage can be identified in different preparations, and various cytochemical properties can be correlated with the stage of differentiation. Gledhill's studies included measurements of DNA content by ultraviolet absorption and Feulgen stain content, basic protein content (bromphenol blue reaction), protein-bound arginine (Sakaguchi reaction), and available DNA phosphate (with the intercalating dyes methyl green and acridine orange). In addition, he used the hyperchromicity of ultraviolet absorption and metachromatic shift in acridine orange fluorescence to investigate the thermal stability of the deoxyribonucleoprotein complex as a function of differentiation.<sup>9</sup> These studies demonstrated that during sperm differentiation substantial changes occur in the nucleoprotein complex without any detectable loss of DNA.

With imaging systems it is possible to measure multiple cytochemical properties of the same cell. Campbell, studying primitive erythrocytes in the developing chicken embryo, was able to correlate hemoglobin synthesis and hemoglobin content with phase in the cell cycle.<sup>10</sup> Five-day-old embryos were treated with tritiated thymidine immediately prior to bleeding. Blood smears were mapped and primitive cells identified. The hemoglobin content of the mapped cells was measured on a scanning cytophotometer using the natural absorption of hemoglobin at the 415-nm Soret band. Hemoglobin then was removed from the cells with hydrochloric acid, the cells were stained for DNA with the Feulgen reaction, and the cells were remeasured. Finally, the preparation was exposed to autoradiography to establish which cells were in DNA synthesis at the time of harvesting. The results of autoradiography were correlated with the DNA Feulgen measurements to establish the cell-cycle phase for each cell, and this in turn was correlated with hemoglobin content. The work showed that hemoglobin is synthesized at an almost constant rate throughout the cell cycle and suggested that in the primitive chicken erythrocyte hemoglobin synthesis and cell cycle are independent processes.

Scanning cytophotometry can be combined with image analysis to give quantitative topological analysis or image partitioning. Examples include partitioning of cells into cytoplasm and nucleus,<sup>11-13</sup> partitioning of metaphase cells into individual chromosomes,<sup>14-16</sup> and partitioning of giant polytene chromosomes into individual bands.<sup>17</sup> This combined approach to cytophotometry is exemplified by the chromosome-analysis program at Livermore, in which DNA-based measurements are used to characterize morphologically identified human metaphase chromosomes.<sup>18,19</sup>

Conventional metaphase spreads are made from blood cultures, stained with quinacrine hydrochloride, and examined under the fluorescent microscope. Cells suitable for analysis are selected and photographed, and their fluorescent banding patterns are used to identify all the chromosomes in the selected metaphase cells. The preparations then are destained, treated with ribonuclease, restained specifically and stoichiometrically for DNA with galloycyanin-chrome alum at pH 1.64, and mounted in oil of matching refractive index.<sup>19</sup>

The scanning of the metaphase cells is done with the CYDAC system,<sup>7</sup> a flying-spot scanning cytophotometer in which the light source is the continuously moving spot of a cathode-ray-tube (CRT) raster located in the image plane of the microscope. Light passes in the reverse direction through the microscope, which demagnifies the spot and the raster. The demagnified image of the spot scans across the specimen and is modulated by it. The modulated light is collected by the substage condenser and detected by the data photomultiplier. An optically equivalent reference channel continuously monitors the intensity of the spot on the CRT. The electronic signals from the two channels are converted to their logarithms and are differenced in an analog photometer circuit whose gain can be adjusted to match the contrast of the



specimen. The output from this circuit is sampled at 6 kHz and is digitized to 255 levels to give values directly proportional to the optical density under the spot at the time the sample was taken. The eight-bit digital values are passed to a minicomputer that stores them on magnetic tape for subsequent image processing and data reduction.

The CYDAC system acts as a passive transducer in that spatial and optical-density information is captured without transformation, and it is nonautomatic in that the operator must select and position the cell. A novel focus-assist device is used to ensure optimum focus for every scan.<sup>20,21</sup> The scanning and recording specifications of the CYDAC system are given in Table 1.

**TABLE 1**  
**CHARACTERISTICS OF THE CYDAC**  
**CRT SCANNER**

Specified optical conditions	
Magnification, $\times$	800
Objective (100 $\times$ Plan Apo) numerical aperture	1.30
Condenser numerical aperture	0.80
Wavelength, nm	500 $\pm$ 50
Resolution (50% modulation transfer), lines/mm	1150
Sampling interval and line separation, $\mu\text{m}$	0.25
Scan size (180 $\times$ 180), $\mu\text{m}$	45 $\times$ 45
Sampling rate, kHz	6
Digitization (variable scale), number of levels	255
Signal-to-noise ratio (per picture element)	$\sim 100 : 1$

A scan of a metaphase spread includes many chromosomes. Extensive and relatively complex processing of the digital image is required to isolate the individual chromosomes and to extract their integrated optical densities and centromeric indices.<sup>19,22,23</sup> In addition, the investigator interacts with the analysis to identify objects, to resolve ambiguities, and to correct processing errors or inadequacies.<sup>24</sup>

Processing is complicated by the inherently fuzzy nature of chromosomes and by the closeness of their width to the resolution limit of the light microscope. The grayness of each chromosome extends for a considerable distance out from the chromosome boundary (as defined by the inflection of the chromosome edge profile); thus, to include all the grayness, the analysis develops shells extending 1  $\mu\text{m}$  beyond the chromosome boundary.<sup>23</sup> All picture elements extending to the outermost shell are assigned to the chromosome and are included in the estimate of its optical density. When two chromosomes are so close together that their shells overlap, the points are assigned to the nearest chromosome. The background value is defined individually for each chro-

mosome on the basis of the average value of all the samples that lie in the vicinity of the chromosome but outside any chromosome shells.

The centromeric index is determined by a two-stage analysis. The first stage finds the major axis of the chromosome and provisionally assigns a centromere location based on the minimum distance between the opposite sides of the chromosome. The second stage uses this information to generate a rectangular slit parallel to the orientation of the provisional assignment. The slit is passed along the major axis of the chromosome, and optical-density values are summed for each position of the slit to generate a profile of distribution of optical density along the chromosome axis. This profile passes through a minimum at the centromere, whose location is defined to a fraction of a micrometer using a quadratic fit.<sup>19</sup> The total optical density of the chromosome then is partitioned between the two sides of the centromere line, and the centromeric index is expressed as the ratio of the optical density of the large arm to the optical density of the whole chromosome.

A typical experiment involves about 10 cells from a single individual and yields measurements on nearly 500 chromosomes. For each cell the chromosomal density measurements are normalized by expressing them on a corrected scale in which the sum of the measurements for the 44 autosomal chromosomes is 100 units. This procedure removes the effect of cell-to-cell changes in staining efficiency, which can vary by 5%. The normalized measurements are then subjected to a multilevel statistical analysis. First they are examined in isolation to detect any outlying values, e.g., values resulting from chromosome misclassification or from processing errors. Then the chromosomal pairs are analyzed with a recently developed test to detect and to get an unbiased estimate of any differences between their paternal and maternal homologs.<sup>25</sup> Significant homolog differences are uncommon but are detected occasionally. In the absence of any significant homolog difference, the measurements for each chromosome pair are pooled across all the cells to give estimates of the mean and the variance for the chromosomes of the individual.

The chromosomal means for five adults are illustrated in Fig. 3. Numbers 221 through 231 refer to white males, and number 232 refers to a black female. Each solid symbol indicates a chromosomal mean that differs significantly from the means of the other four persons. In general, the five means for any chromosome cluster closely and are well separated from the means of other chromosomes; the major regions of confusion are among the D group chromosomes (D13, D14, and D15) and among the G group chromosomes (G21, G22, and Y).

We are interested in making DNA-based chromosomal measurements in abnormal conditions. For instance, chronic myelogenous leukemia is known to be associated with a major deletion of chromosome G22, and Rowley<sup>26</sup> has suggested that this material probably was translocated to chromosome C9. Recently we measured the DNA stain content of chromosomes from a patient with chronic myelogenous leukemia.<sup>27</sup> The affected chromosome G22 showed a

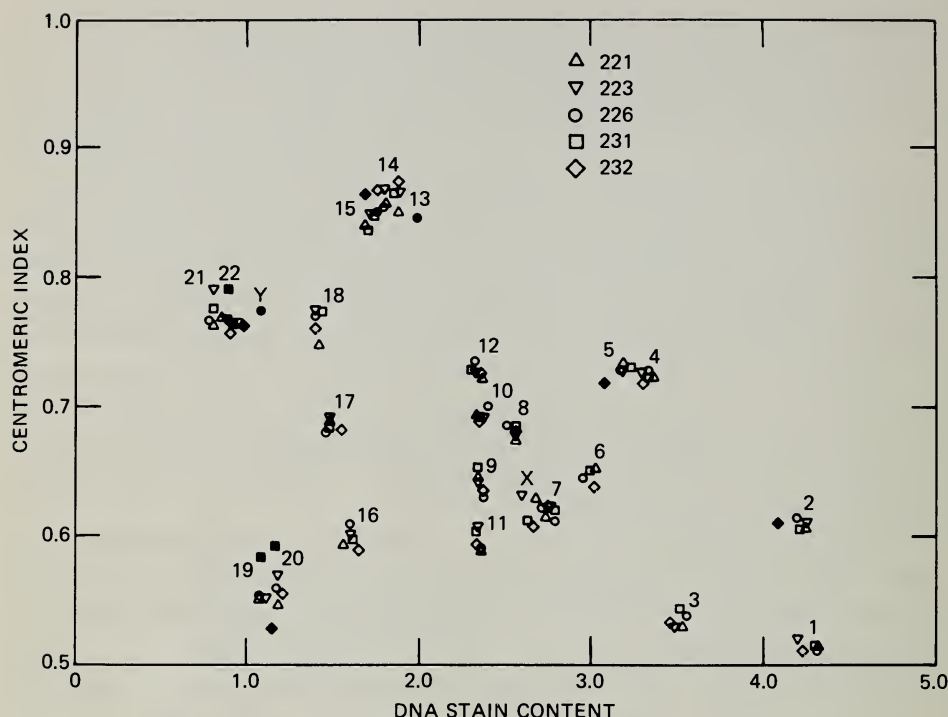


Fig. 3 Mean chromosome data for five adults. Abscissa: normalized optical density expressed as a percent of autosomal total. Ordinate: centromeric index, the ratio of large-arm optical density to total optical density. The symbols indicate measurement means for each of the 22 autosome pairs and the sex chromosomes for each of the five persons. Means that differ significantly ( $P > 0.01$ ) from those of the other adults are indicated by solid symbols.

DNA loss of 0.42 unit, and the affected chromosome C9 showed an increase of the same amount. Furthermore, the measurements also revealed an unsuspected DNA loss of 0.12 unit from one chromosome F20 and the presumptive translocation of this material to the other chromosome C9. Other cases of chronic myelogenous leukemia must be studied to establish the generality of these initial findings; nevertheless, it is clear from this one case that DNA measurements of chromosomes support and complement conventional cytogenetic analysis.

These few examples indicate the power of scanning cytophotometry in applications of biological and clinical significance, and they show how this approach can detect and quantitate subtle effects at the cellular and subcellular levels. The principles of scanning cytophotometry now are well established, practice is a reality, and future applications are limited only by time, funds, and the creative ingenuity of scientists.



## ACKNOWLEDGMENT

This work was performed under the auspices of the U. S. Atomic Energy Commission and was supported in part by U. S. Public Health Service Grant 7R01 GM20291.

## REFERENCES

1. T. Caspersson, *Cell Growth and Cell Function*, Norton, New York, 1950.
2. L. Ornstein, The Distributional Error in Microspectrophotometry, *Lab. Invest.*, **1**: 250-262 (1952).
3. K. Patau, Absorption Microphotometry of Irregular-shaped Objects, *Chromosoma*, **5**: 341-362 (1952).
4. M. L. Mendelsohn, Absorption Cytophotometry: Comparative Methodology for Heterogeneous Objects, and the Two-Wavelength Method, in *Introduction to Quantitative Cytochemistry*, G. L. Wied (Ed.), pp. 201-214, Academic Press, Inc., New York, 1966.
5. B. H. Mayall and M. L. Mendelsohn, Errors in Absorption Cytophotometry: Some Theoretical and Practical Considerations, in *Introduction to Quantitative Cytochemistry*, **2**, G. L. Wied and G. F. Bahr (Eds.), pp. 171-197, Academic Press, Inc., New York, 1970.
6. B. H. Mayall, and M. L. Mendelsohn, Deoxyribonucleic Acid Cytophotometry of Stained Human Leukocytes. II. The Mechanical Scanner of CYDAC, the Theory of Scanning Photometry and the Magnitude of Residual Errors, *J. Histochem. Cytochem.*, **18**: 383-407 (1970).
7. M. L. Mendelsohn, B. H. Mayall, J. M. S. Prewitt, R. C. Bostrom, and W. G. Holcomb, Digital Transformation and Computer Analysis of Microscopic Images, in *Advances in Optical and Electron Microscopy*, Vol. 2, V. Cosslett and R. Barer (Eds.), pp. 77-150, Academic Press, Inc., New York, 1968.
8. B. L. Gledhill, M. P. Gledhill, R. Rigler, Jr., and N. R. Ringertz, Changes in Deoxyribonucleoprotein During Spermiogenesis in the Bull, *Exp. Cell Res.*, **41**: 652-665 (1966).
9. N. R. Ringertz, B. L. Gledhill, and Z. Darzynkiewicz, Changes in Deoxyribonucleoprotein During Spermiogenesis in the Bull: Sensitivity of DNA to Heat Denaturation, *Exp. Cell Res.*, **62**: 204-218 (1970).
10. G. LeM. Campbell, H. Weintraub, B. H. Mayall, and H. Holtzer, Primitive Erythropoieses in Early Chick Embryogenesis. II. Correlation Between Hemoglobin Synthesis and Mitotic History, *J. Cell Biol.*, **50**: 669-681 (1971).
11. J. M. S. Prewitt and M. L. Mendelsohn, The Analysis of Cell Images, *Ann. N. Y. Acad. Sci.*, **128**: 1035-1053 (1966).
12. G. L. Wied, G. F. Bahr, and P. H. Bartels, Automatic Analysis of Cell Images by TICAS, in *Automated Cell Identification and Cell Sorting*, G. L. Wied and G. F. Bahr (Eds.), pp. 195-360, Academic Press, Inc., New York, 1970.
13. J. W. Bacus and E. E. Gose, Leukocyte Pattern Recognition, *IEEE (Inst. Elec. Electron. Eng.), Trans. Systems, Man, and Cybernetics*, **2**: 513-526 (1972).
14. R. S. Ledley and F. H. Ruddle, Automatic Analysis of Chromosome Karyograms, in *Mathematics and Computer Science in Biology and Medicine*, pp. 189-209, Medical Research Council, London, 1965.
15. P. W. Neurath, A. Falek, B. L. Bablouzian, T. H. Warms, and R. C. Serbagi, Human Chromosome Analysis by Computer—An Optical Pattern Recognition Problem, *Ann. N. Y. Acad. Sci.*, **128**: 1013-1028 (1966).

16. J. Hilditch and D. Rutovitz, Chromosome Recognition, *Ann. N. Y. Acad. Sci.*, **157**: 339-364 (1969).
17. G. T. Rudkin, Replication in Polytene Chromosomes, in *Results and Problems in Cell Differentiation*, Vol. 4, W. Beerman (Ed.), pp. 59-85, Springer-Verlag New York Inc., 1972.
18. M. L. Mendelsohn, B. H. Mayall, E. Bogart, D. H. Moore II, and B. H. Perry, DNA Content and DNA-Based Centromeric Index of the 24 Human Chromosomes, *Science*, **179**: 1126-1129 (1973).
19. M. L. Mendelsohn and B. H. Mayall, Chromosome Identification by Image Analysis and Quantitative Cytochemistry, in *Human Chromosome Methodology*, J. Yunis (Ed.), pp. 311-346, Academic Press, Inc., New York, 1974.
20. M. L. Mendelsohn and B. H. Mayall, Computer-Oriented Analysis of Human Chromosomes. III. Focus, *Comput. Biol. Med.*, **2**: 137-150 (1972).
21. M. A. Kujoory, B. H. Mayall, and M. L. Mendelsohn, Focus-Assist Device for a Flying-Spot Microscope, *IEEE (Inst. Elec. Electron. Eng.) Trans. Bio-Med. Eng.*, **20**: 126-132 (1973).
22. M. L. Mendelsohn, B. H. Mayall, and J. M. S. Prewitt, Approaches to the Automation of Chromosome Analysis, in *Image Processing in Biological Science*, Diane M. Ramsey (Ed.), pp. 119-136, University of California Press, Berkeley, Calif., 1969.
23. M. L. Mendelsohn, B. H. Mayall, and B. H. Perry, Generalized Grayness Profiles as Applied to Edge Detection and the Organization of Chromosome Images, in *Advances in Medical Physics*, J. S. Laughlin and E. W. Webster (Eds.), pp. 327-341, The Second International Conference on Medical Physics, Inc., Boston, Mass., 1971.
24. B. H. Mayall, A Survey of Digital Image-Processing Activities at Lawrence Livermore Laboratory. Part II. Biomedical Applications, *Computer*, **7**(5): 81-87 (1974).
25. D. H. Moore II, Do Homologous Chromosomes Differ? Two Statistical Tests, *Cytogenet. Cell Genet.*, **12**: 305-314 (1973).
26. J. D. Rowley, A New Chromosomal Abnormality in Chronic Myelogenous Leukemia Identified by Quinacrine Fluorescence and Giemsa Staining, *Nature*, **243**: 290-293 (1973).
27. B. H. Mayall, A. V. Carrano, and J. D. Rowley, DNA Cytophotometry of Chromosomes in a Case of Chronic Myelogenous Leukemia, *Clin. Chem.*, **20**: 1080-1088 (1974).



# EXTRACTION AND EVALUATION OF INFORMATION FROM DIGITIZED CELL IMAGES

PETER H. BARTELS\* and GEORGE L. WIED†

\*Department of Microbiology and Medical Technology and the Optical Sciences Center  
University of Arizona, Tucson, Arizona, and †Departments of Obstetrics and Gynecology  
and Pathology, University of Chicago, Chicago, Illinois

---

## ABSTRACT

Digitized cell images contain highly specific information in the mutual dependencies of the recorded optical density values. Small changes or differences in the chromatin distribution patterns can be extracted, and substantiated, by computer programs. Essential processing steps are feature extraction and feature selection, dimensionality reduction, and supervised and unsupervised learning programs. This paper describes some of the methods and program sections of the TICAS program system.

The functional combination of rapid-scanning microphotometers and computers in on-line operation has made it possible to acquire substantial numbers of digitized cell images.<sup>1</sup> The recorded optical density (OD) values express the distribution patterns of the chromatin in the nucleus. The granule size distribution, spatial arrangement, and staining density indicate the functional state of the cell; they can be rapidly evaluated by computer. It is possible to extract "computable" information from cell images, information that may not have a visually perceivable counterpart in the image.<sup>2</sup> The array of OD values can be considered as a stochastic process extending in two dimensions and, as such, can be determined by a set of parameters.<sup>3,4</sup> Visual evaluation would never yield a value for one of the coefficients of an eigenvector of the covariance matrix of a set of mutually dependent OD values in the image;<sup>5</sup> neither would visual assessment be capable of determining the probabilities with which certain OD values or value sequences are followed by other values or value sequences.<sup>6</sup> Computable image information of this type has opened new approaches to quantitative cytology. This paper describes the extraction and methods of evaluation of such computable image information in cytologic research.

The classical cytometric measures of cell size, nuclear size, nucleus-to-cytoplasm ratio, and total amount of dye bound can be readily computed. Essential here are the performance criteria of automatic nucleus-finding routines, to separate nucleus from cytoplasm.<sup>7,8</sup>

The histogram of OD values renders much useful information. Cells from malignant material<sup>9</sup> and cells undergoing transformation<sup>10</sup> frequently exhibit histograms extending into the higher OD ranges<sup>9</sup> (see Fig. 1). Lymphocytes

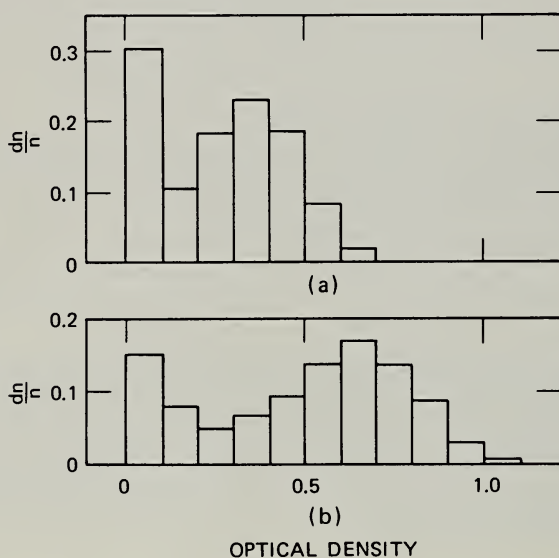


**Fig. 1** Histograms of OD values for cells from a tissue culture of (a) human embryonic lung and (b) human epidermoid carcinoma. Measurements were taken at 260 nm. Note the extended histogram in the malignant cell material.

responding to immunologic challenge,<sup>11</sup> to chemotherapeutic agents,<sup>12</sup> or to ionizing radiation (Anderson et al., this volume) have exhibited marked shifts toward lower OD values, indicating that dense and coarse granules disappear and that the nuclear chromatin stains more homogeneously and lighter on the average.

Reducing data to histogram form is a rough procedure, however. The recorded OD values are considered as independent events. For each, merely the count of the relative frequency of occurrence in the correct histogram interval is incremented. No mutual dependencies between adjacently measured values are considered at all. The mutual dependencies of pairs of adjacent OD values are used in a data-reduction scheme that computes the transition probability for an OD value in any given interval to be followed, along the scan line, by a value in the same or any other OD interval. Such a Markov process with order of dependence of two results in a transition-probability matrix as shown in Table 1.

TABLE 1  
TRANSITION-PROBABILITY MATRIX

Ranges	0.01 to 0.20	0.21 to 0.40	0.41 to 0.60	0.61 to 0.80	0.81 to 1.00	1.01 to 1.20	1.21 to 1.40	1.41 to 1.60	Null
0.01 to 0.20	0.76	0.06	0.05	0.01					0.10
0.21 to 0.40	0.16	0.69	0.12						
0.41 to 0.60		0.17	0.59	0.21					
0.61 to 0.80			0.27	0.51	0.17	0.02			
0.81 to 1.00				0.40	0.36	0.19	0.02		
1.01 to 1.20				0.03	0.33	0.37	0.25		
1.21 to 1.40					0.05	0.29	0.56	0.08	
1.41 to 1.60							0.36	0.63	
Null	0.35		0.01	0.05					0.57

Its elements can be arranged in a suitably ordered sequence and often form highly informative profiles such as those in Fig. 2. Only the main diagonal elements and the elements one position above the main diagonal elements were selected.

Mutual dependencies extending farther can be computed by having the computer program find the center of the nucleus and positioning a frame around it. Then within the frame the correlations can be computed for all values immediately adjoining each other or removed from each other by one, two, or more measuring spots. Such a correlation matrix is shown in Fig. 3. The first column reflects the existing order of dependence, as determined by granule sizes and spatial arrangement. The diagonals indicate the stationarity of the process, i.e., whether a given dependence between adjacent values is constant over the entire nuclear area included in the frame. Figures 4 and 5 show examples where consistent differences in the order of dependence were found between normal and malignant cell material.

Consistently positioned line-scan segments of predetermined length can be considered as samples from a multivariate distribution.<sup>13</sup> For cell sets of different origin, both mean vectors and covariance matrices can be estimated. Unknown cell images can then be classified on the basis of a greater likelihood. This is shown in Fig. 6 for cells from adenocarcinoma of the endometrium and hyperplastic cells. The error rate decreases continuously as the scan segment increases in length.

In all these procedures mutual value dependencies were considered only in the direction of the scan line. They exist, in fact, in two dimensions, and models taking such two-dimensional dependencies into account have been developed.<sup>3,4</sup> So that the data reduction is computationally feasible, a limited order of dependence is assumed. Figure 7 shows how a given column vector in a two-dimensional array of OD values could be predicted if only the two



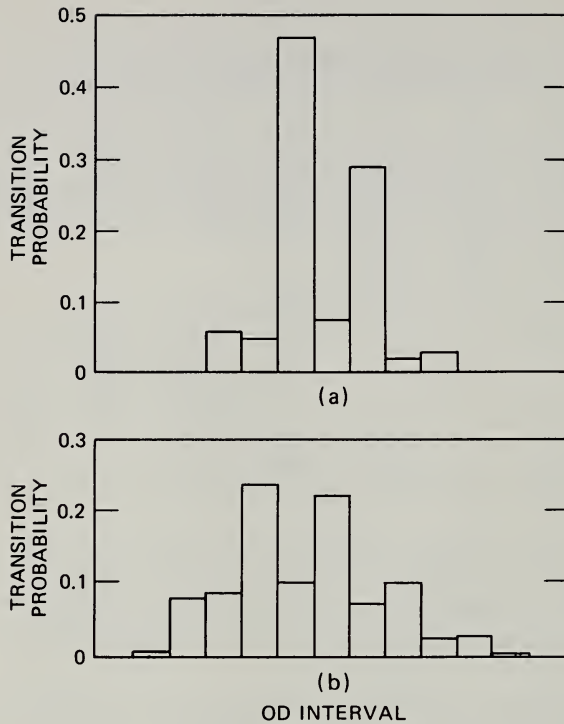


Fig. 2 Transition probabilities between OD values along the scan line in digitized images of (a) parabasal ectocervical cells and (b) cells from nonkeratinizing dysplasia. Each OD interval was chosen 0.20 OD units wide. On the ordinate the transition probabilities are plotted between two consecutive scan-line values; on the abscissa the OD transitions are plotted in the following order: interval 1 to interval 1; interval 1 to interval 2; interval 2 to interval 2; interval 2 to interval 3; interval 3 to interval 3; interval 3 to interval 4; etc.

immediately preceding column vectors were known. This order of dependence implies that, for any given element in such a column vector, only points within a restricted distance contribute to the prediction. It is thus possible to model the two-dimensional dependencies existing in a large array with only a small number of regression coefficients and only a small number of eigenvalues of the multivariate random process. The eigenvectors are known and given by the assumed model.

Schemes of this type have been tested and found most useful in cell-image synthesis. They appear not to be sufficiently robust for real-world cell-image recognition when even moderate inhomogeneity in the nuclear texture exists between different cells of the same classification since, as regression schemes, they are sensitive to outliers in the training sets.<sup>14</sup>

The image properties described so far are all general and should for any specific discrimination problem be augmented by problem-specific features.

ORDER OF DEPENDENCE	2	0.881						
	3	0.657	0.905					
	4	0.427	0.681	0.911				
	5	0.176	0.474	0.761	0.923			
	6	0.028	0.268	0.587	0.831	0.943		
	7	0.139	0.390	0.679	0.871	0.952	0.979	
	8	0.502	0.746	0.838	0.800	0.775	0.679	0.797
	9	0.662	0.796	0.725	0.592	0.481	0.379	0.502
								0.883

STATIONARITY

Fig. 3 Correlation matrix.

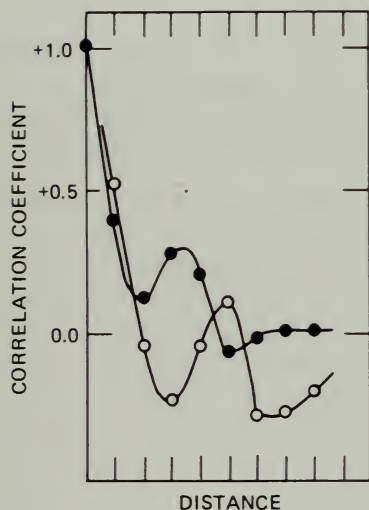


Fig. 4 Correlogram for a string of OD values centered in the nuclei of images from small lymphocytes from the nodes of patients with benign lymphadenitis (○) and from patients with malignant lymphoma (●).

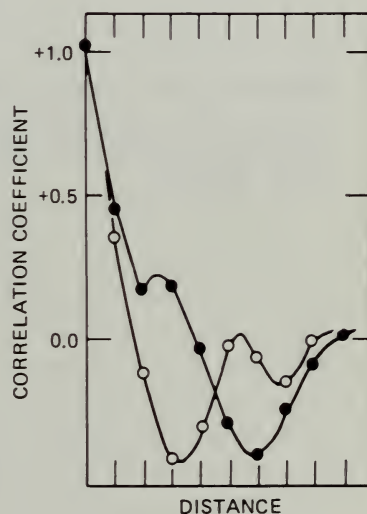


Fig. 5 Correlogram for a string of OD values centered in the nuclei of images for cells from normal endometrium (○) and from adenocarcinoma of the endometrium (●).

Procedures for the evaluation of information from cell images fall into three groups:

1. Applications in completely automated or computer-assisted cytodiagnosis. The extracted information is submitted to *supervised learning algorithms* to derive a classification rule.<sup>15,16</sup>

2. Applications in *multivariate trend analysis*. The primary image information is used to follow gradual changes in the properties of a set of cells.



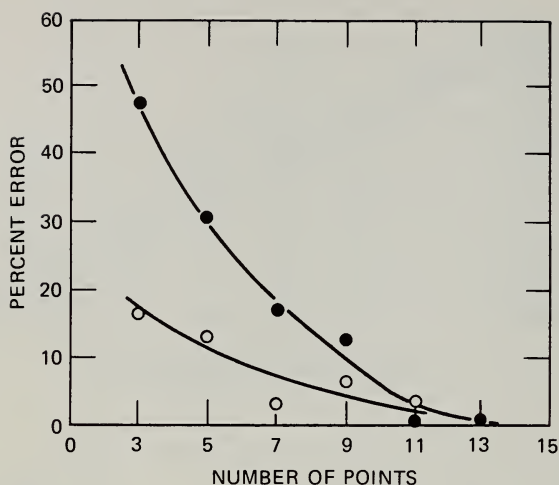


Fig. 6 Error rates in the classification of cell images for cells from adenocarcinoma of the endometrium ( $\circ$ ) and for hyperplastic cells ( $\bullet$ ). A string of values centered through the nucleus is recorded, considered as a sample from a multivariate distribution, and then classified on the basis of greater likelihood.

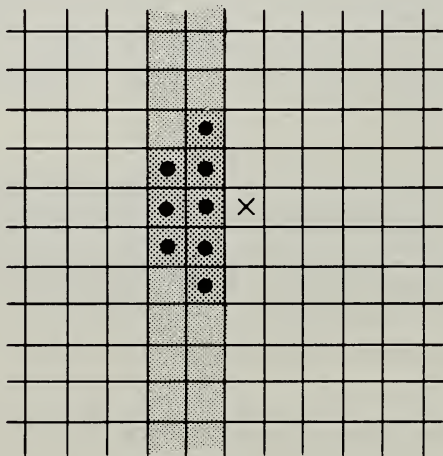


Fig. 7 Scheme for order of two-dimensional dependence. The column vector marked by X is predicted by the values found in the two preceding column vectors (shaded area). The value in the location marked X depends under the given scheme only upon the values found in the dotted locations of the two preceding column vectors.

Secondary information is then derived, e.g., parameters such as time constants of a trend. It is often of interest to select features or a linear combination of features which best reflects the observed trend. Such trend descriptors should retain most of the information while reducing the dimensionality significantly.

3. In both of the previously described applications, the question of homogeneity of the examined set of cells arises. In lymphocytes, cells that seem morphologically equivalent have been shown to possess different immunobiologic capabilities. It has been possible to recognize these existing subsets on the basis of computable image information. On the other hand, in some applications image scanning can be used to detect subsets with consistently differing chromatin distribution patterns. Such analyses involve *unsupervised learning algorithms*,<sup>17</sup> or programs aimed at the automatic detection of subsets of cells.

The principle of a supervised learning program in brief is as follows: External information—such as that supplied by an expert cytopathologist—is used to establish truth values for the classification of each of the cell images from different sets. Cell images of the same classification are then combined into “training sets.” A common set of features is extracted from each image, and it is finally represented by a feature vector having as many components as there are extracted features. The program then searches for components of the feature vectors that have clearly differing distributions for the two training sets of cells to be discriminated. These features are selected and combined into a linear combination. Weights, based on differences of feature means, and their variances in both training sets are assigned. Finally, a classification rule is derived. A classification success criterion is computed for both sets and is used as a merit function to optimize the weights. The final classification rule then is tested for consistency on feature vectors of known truth value that had not been included in the training sets. The supervised learning program is summarized in Fig. 8. Figure 9 shows an example for a linear discriminant separating nuclei of superficial cervical cells from nuclei of carcinoma in situ cells. On a CDC 6400, the supervised learning program takes approximately 40 sec to extract all features from two sets of 125 cells each and an additional 15 sec to derive a classification rule.

As in any statistical classifier, the same features are extracted initially for any set of cells to be discriminated. A sharp reduction of the dimensionality and an improved discrimination for any given discrimination problem can be attained when the feature specifications are made self-adaptive to the discrimination problem at hand.

From a given feature set, one may have an algorithm select the minimum required number of features and then adaptively change their specifications according to an objective function so that optimum classification success is attained. Assume that the relative frequencies of occurrence of OD values in the interval from 0.40 to 0.49 give good discrimination. The algorithm then adapts the feature specifications by, for example, extending the interval width to 0.33

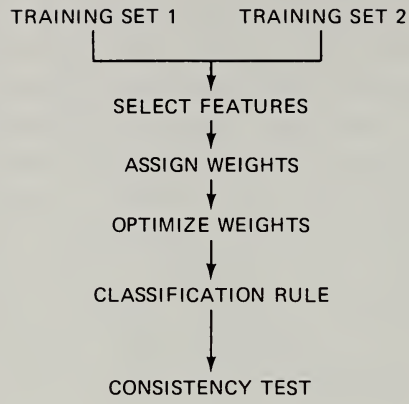


**Fig. 8** Supervised learning.

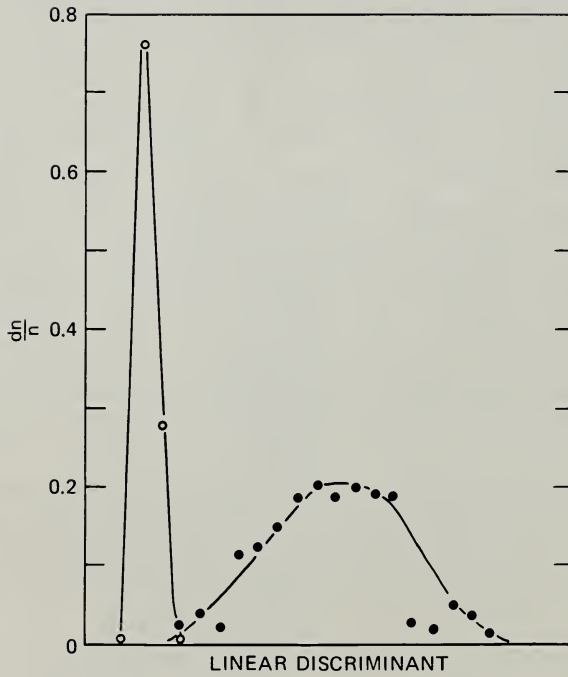


**Fig. 9** Discrimination derived by the supervised learning program for nuclei of superficial squamous cells ( $\circ$ ) and nuclei from carcinoma in situ ( $\bullet$ ).

and 0.65 or by moving interval boundaries in from 0.49 to 0.46, to optimize the objective function. This is shown in Fig. 10.

In unsupervised learning a single set of feature vectors is submitted to an algorithm. The program then proceeds to partition the data set into subsets whose members are more "similar" to each other than to vectors assigned to another subset. Similarity here is measured by some distance metric. In this, it is absolutely essential to test for multivariate statistical significance of a particular partitioning and to have a validity test in the program. Finding a statistically valid partitioning suggests the presence of cells with consistently different chromatin distribution patterns. It is up to biologic experimentation to explore the biologic significance of the subsets.

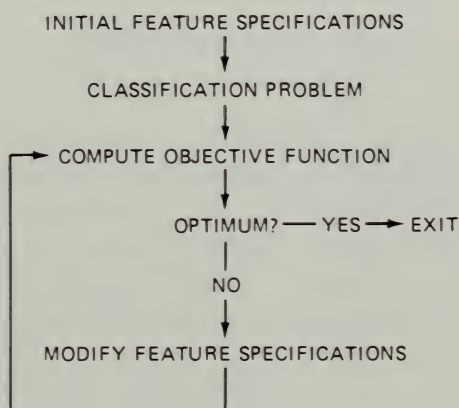


Fig. 10 Adaptive change of feature specifications to meet a particular discrimination problem.

Unsupervised learning techniques often require substantial core in the computer, and feature selection is a problem. In the TICAS program system, this is approached as shown in Fig. 11. The unsupervised learning algorithm is started off with a small enough set of features to be computationally feasible. The features are arbitrarily selected but usually are based on past experience. If a validity test<sup>18</sup> for the resulting partitioning is passed, the subsets are entered as training sets into the supervised learning program, the full feature set being used. This program establishes which features separate the subsets best. They may now be adaptively optimized in their specifications. After a suitable feature set is thus selected and adapted, it is used to process further data for the unsupervised learning process on the same data set.

Cells responding to experimental conditions, such as treatment with chemotherapeutica, ionizing radiation, or immunologic agents, often show continuous changes in a number of image properties. The representation of such



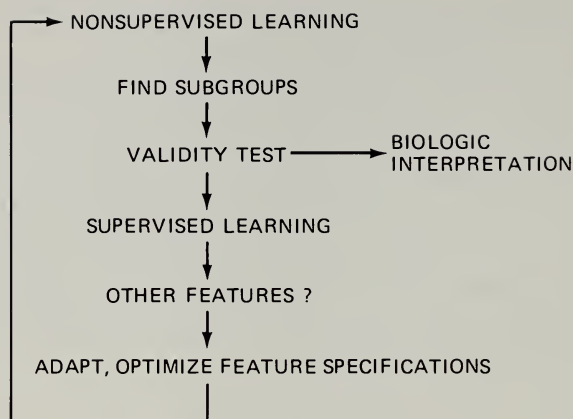


Fig. 11 Nonsupervised learning.

changes by a trend indicator, as a function of the causative process, and in a space of low dimensionality will be described next. The information of interest is carried in two sets of variables. First, there are the observed image properties. They are given as a set of feature vectors. One may now simply compute the mean feature vector for the observed cell sample and its trend as a function of the trend variable, such as time, dosis, etc. The mean feature vector may show a continuous change in all or in some of its components.

For a set of feature vectors, however, more than just the mean value is known. For each component the variance is known and so is the covariance of each component with each other component. The entire multivariate process thus is defined by a  $k$ -dimensional mean vector and a  $k \times k$ -variance-covariance matrix. Trends in the mean vector may be, but are not necessarily, accompanied by changes in the mutual dependencies of the components. If the covariance matrix is considered a multivariate probability density distribution in  $k$ -space, a change in the mutual component dependencies corresponds to a deformation of the covariance matrix.

It is difficult, though, to follow small changes in a covariance matrix of high dimensionality, and, in fact, this is not even necessary. For histograms of OD values, one can show that the first three eigenvalues carry as a rule approximately 95% of the information. The intrinsic dimensionality of such data thus is 3 rather than 18 (for an OD range from 0.00 to 1.80 and 0.10-unit intervals).<sup>5</sup> A highly efficient trend indicator can be derived if one plots only the coefficients of the eigenvector associated with the largest eigenvalue. For each eigenvector the coefficients form a discrete distribution, but for the purposes here the coefficient values will be connected by an envelope. When the coefficients are plotted as a function of the treatment, a surface results. It shows very clearly which pair of coefficients exhibits the greatest divergence. Using these variables and computing their correlation coefficient as a function of the

trend variable yields a most efficient reduction of the dimensionality of the representation.

This is best demonstrated by examples. Mouse thoracic-duct lymphocytes were exposed to increasing doses of ionizing radiation. The histogram showed a marked shift, and a pronounced change in the covariance matrix occurred. Figure 12 shows the coefficients of the first eigenvector for these data. One can see that the third and sixth coefficients have the greatest divergence. Their correlation is plotted as a function of time after treatment in Fig. 13.

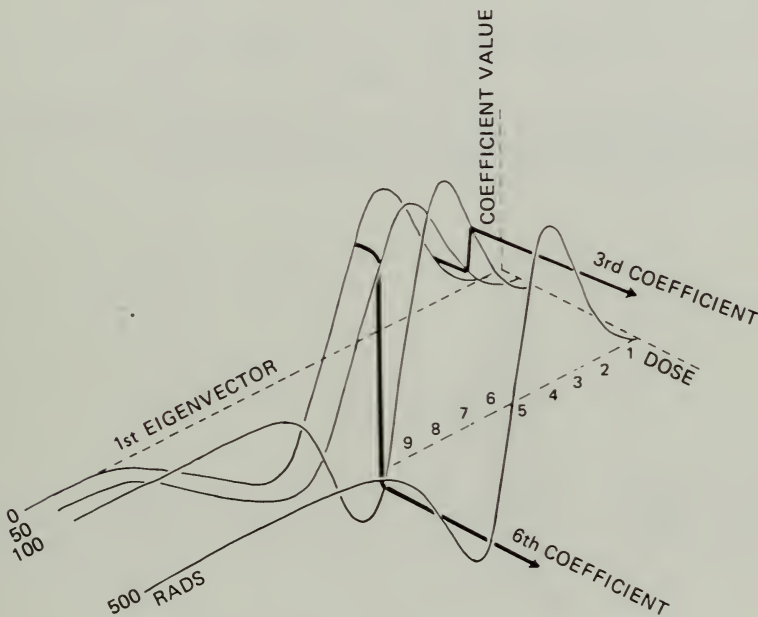


Fig. 12 Scheme for efficient dimensionality reduction to derive a trend indicator for the response of mouse thoracic-duct lymphocytes to X rays.

Trends, however, do not have to be associated with some experimental treatment. In cervical cytology several cell types of ectocervical cells are distinguished and are considered as discrete entities. It is interesting to observe the coefficients of the first eigenvector of the OD histograms of these cells<sup>19</sup> as shown in Fig. 14. The distributions appear to represent a continuous family of curves. If one defines a descriptive statistic—such as the point on the abscissa where the envelope passes through the coefficient value zero, for example, or through  $-1.5$ —one can map the cell types from an equidistantly arranged nominal scale onto an ordinal scale of progression toward abnormalities (see Fig. 15). The impression of continuity of change toward malignant cell types is

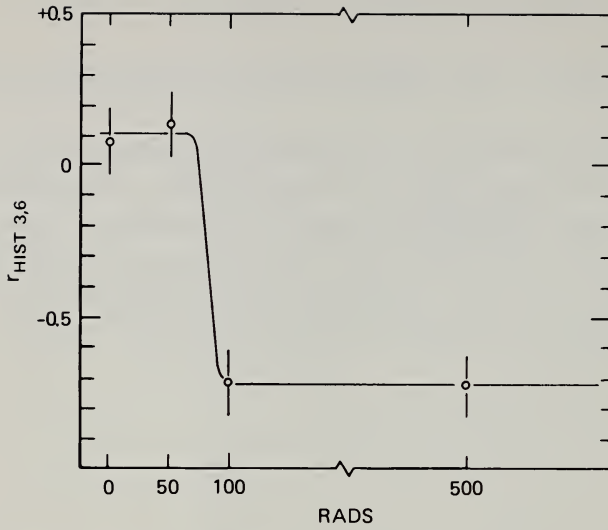


Fig. 13 Trend indicator for the response of mouse thoracic-duct lymphocytes to X rays (Fig. 12), with  $r$  denoting the correlation coefficient.

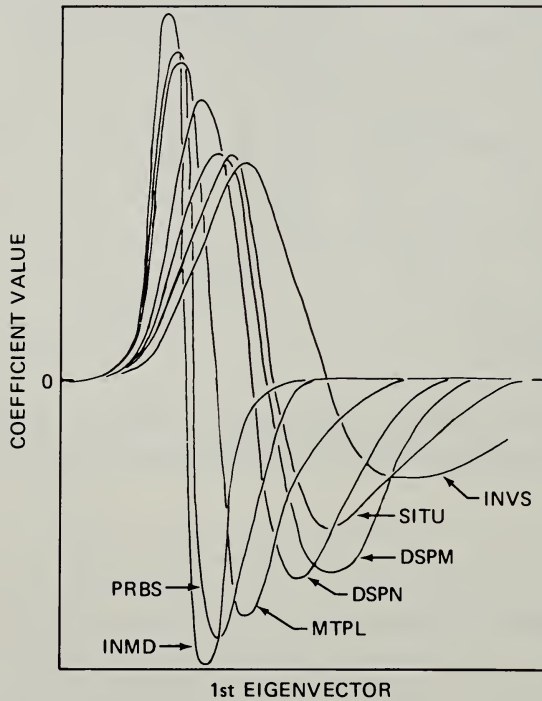


Fig. 14 Nuclei of ectocervical cells exhibiting continuous changes in the covariance structure of their histogram data. The coefficients of the first eigenvector of the covariance matrix of the OD histograms here were connected by an envelope. Intermediate, INMD; parabasal, PRBS; metaplastic, MTPL; slight dysplasia, DSPN; severe dysplasia, DSPM; carcinoma in situ, SITU; and invasive carcinoma, INVS.

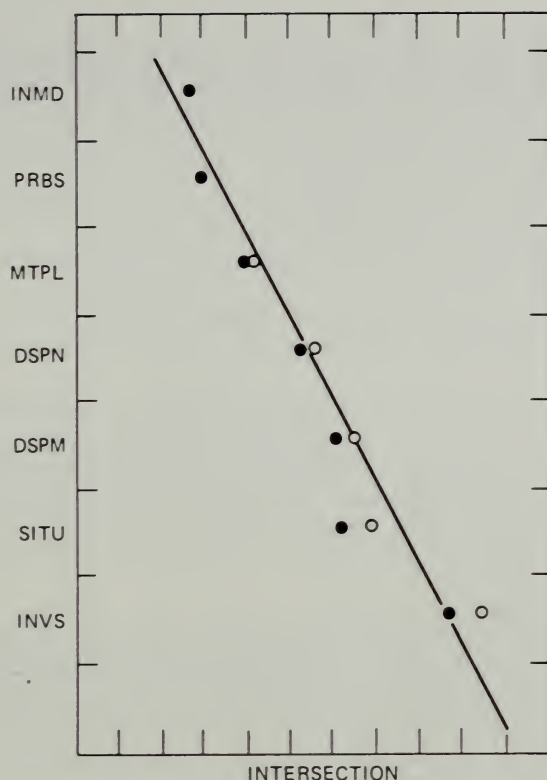


Fig. 15 Horizontal lines placed into Fig. 14 render a useful descriptive statistic to map the nominal scale of cell types onto an ordinal scale of development toward cellular atypia. ●, coefficient value zero; ○, coefficient value  $-1.5$ .

inescapable. It raises fundamental questions of cytologic diagnostic procedure such as the following: Are there, in fact, discretely different cell types in existence, or are these cell types an artifact introduced by the human need for categorization? And, if there is a continuous trend in one direction, is there any possibility of reversibility?

The extraction of computable image information and its evaluation by self-adaptive and self-learning computer programs appear to hold considerable promise. Objective and quantitative descriptions of cell images often showing no visually discernible differences can be obtained. Small differences in the patterns of chromatin distribution can be measured, followed, and statistically substantiated. Unsupervised learning techniques show the existence of subsets of cells with small but significantly different chromatin distribution patterns; these techniques represent one example in which artificial intelligence can be employed to support further cytologic research.<sup>20</sup>



## REFERENCES

1. G. L. Wied, P. H. Bartels, G. F. Bahr, and D. G. Oldfield, Taxonomic Intra-Cellular Analytic System (TICAS) for Cell Identification, *Acta Cytol.*, **12**: 180-204 (1968).
2. P. H. Bartels, G. F. Bahr, M. Bibbo, and G. L. Wied, Objective Cell Image Analysis, *J. Histochem. Cytochem.*, **20**: 239 (1972).
3. P. K. Bhattacharya, Order of Dependence in a Stationary Normally Distributed Two-Way Series, *Ann. Math. Statist.*, **43**: 1792-1807 (1972).
4. P. H. Bartels, P. K. Bhattacharya, J. C. Bellamy, G. F. Bahr, and G. L. Wied, Computer Generated, Synthetic Cell Images, *Acta Cytol.*, **18**: 155-164 (1974).
5. P. H. Bartels, G. F. Bahr, W. S. Jeter, G. B. Olson, J. Taylor, and G. L. Wied, Evaluation of Correlational Information in Digitized Cell Images, *J. Histochem. Cytochem.*, **22**: 69-79 (1974).
6. P. H. Bartels, G. F. Bahr, and G. L. Wied, Cell Recognition from Line Scan Transition Probability Profiles, *Acta Cytol.*, **13**: 210-217 (1969).
7. J. M. S. Prewitt, Parametric and Nonparametric Recognition by Computer: An Application to Leukocyte Processing, *Advan. Computers*, **12**: 285-414 (1972).
8. G. L. Wied, G. F. Bahr, P. H. Bartels, M. Bibbo, D. L. Richards, and J. Taylor, Jr., Computerized Nucleus-Finding Routines for Automated Cell Analyses: A Comparative Study, *Acta Cytol.*, in press.
9. M. Bibbo, P. H. Bartels, G. F. Bahr, J. Taylor, Jr., and G. L. Wied, Computer Recognition of Cell Nuclei from the Uterine Cervix, *Acta Cytol.*, **17**: 340-350 (1973).
10. P. H. Bartels, G. F. Bahr, F. Griep, H. Rappaport, and G. L. Wied, Computer Analysis on Lymphocytes in Transformation. A Methodologic Study, *Acta Cytol.*, **13**: 557-568 (1969).
11. T. E. Kiehn, Computer Analysis of Transforming Lymphocytes, Ph.D. Thesis, University of Arizona, Department of Microbiology, 1972.
12. P. H. Bartels, W. S. Jeter, and J. R. Cole, Computer Analysis of In Vivo Response to 5FUdR in Guinea Pig Lymphocytes, in preparation.
13. P. H. Bartels, T. L. Jarkowski, J. C. Bellamy, G. F. Bahr, and G. L. Wied, Cell Recognition by Multivariate Gray Value Analysis in Digitized Images, *Acta Cytol.*, **15**: 284-288 (1971).
14. P. H. Bartels, P. K. Bhattacharya, J. Bellamy, G. F. Bahr, and G. L. Wied, Cell Recognition from the Statistical Dependence of Gray Values in Digitized Cell Images, *Acta Cytol.*, **18**: 165-169 (1974).
15. P. H. Bartels, G. F. Bahr, J. C. Bellamy, M. Bibbo, D. L. Richards, and G. L. Wied, A Self-Learning Computer Program for Cell Recognition, *Acta Cytol.*, **14**: 486-494 (1970).
16. P. H. Bartels and J. Bellamy, Self-Optimizing, Self-Learning System in Pictorial Pattern Recognition, *Appl. Opt.*, **9**(11): 2453-2458 (1970).
17. P. H. Bartels, W. S. Jeter, G. B. Olson, and G. L. Wied, Computer Analysis of Lymphocytes: Unsupervised Learning Algorithms, *Acta Cytol.*, in press.
18. M. G. Kendall, Cluster Analysis, in *International Conference on Frontiers of Pattern Recognition*, Honolulu, Jan. 18-20, 1971, S. Watanabe (Ed.), pp. 291-307, Academic Press, Inc., New York, 1972.
19. P. H. Bartels, M. Bibbo, G. F. Bahr, and G. L. Wied, Cervical Cytology. Descriptive Statistics for Nuclei of Normal and Atypical Cell Types, *Acta Cytol.*, **17**: 449-453 (1973).
20. P. H. Bartels, G. B. Olson, R. E. Anderson, and G. L. Wied, Computer Discrimination of Mouse T and B Lymphocytes, *Acta Cytol.*, in press.

# SLIT-SCANNING CELL-ANALYSIS METHODS

LEON L. WHEELLESS, JR.

Departments of Pathology and Electrical Engineering,  
The University of Rochester, Rochester, New York

---

## ABSTRACT

The basic principles of the slit-scan cell-analysis technique for single cells are described. The slit-scan contour is obtained by recording the secondary fluorescence of a cell through a slit aperture at discrete intervals as the aperture is passed over the cell. This method permits cell measurements that yield information on such parameters of pathological values as cell diameter, nuclear diameter, nuclear- to cell-diameter ratio, and nuclear and cytoplasmic fluorescence at one or more wavelengths. The usefulness of the slit-scan technique is illustrated in the prescreening of acridine orange-stained material from the human female genital tract.

In many cell-analysis systems, particularly in prescreening, one is faced with the conflicting requirements of obtaining sufficient information on each cell to make some type of decision on that cell while maintaining a throughput rate of several hundred cells per second. A slit-scan technique offers a compromise solution to this problem of resolution and throughput by providing a more complete set of cellular parameters than is available with a zero-resolution optical system without producing the large data matrix associated with high-resolution scanning systems. This paper is confined to slit scanning in cytofluorometry with the understanding that slit scanning may be equally useful when applied to light-absorption or light-scatter measurements.

Slit scanning in cytofluorometry involves sequentially recording the secondary fluorescence of an elongated portion of a cell (generally traversing the width of the cell) at discrete time intervals as that cell moves relative to the slit-producing aperture. In a static-cell instrument, this can be accomplished, as shown in Fig. 1, by recording the secondary fluorescence through a slit aperture at discrete time intervals as the aperture is passed over the cell.<sup>1</sup> This would

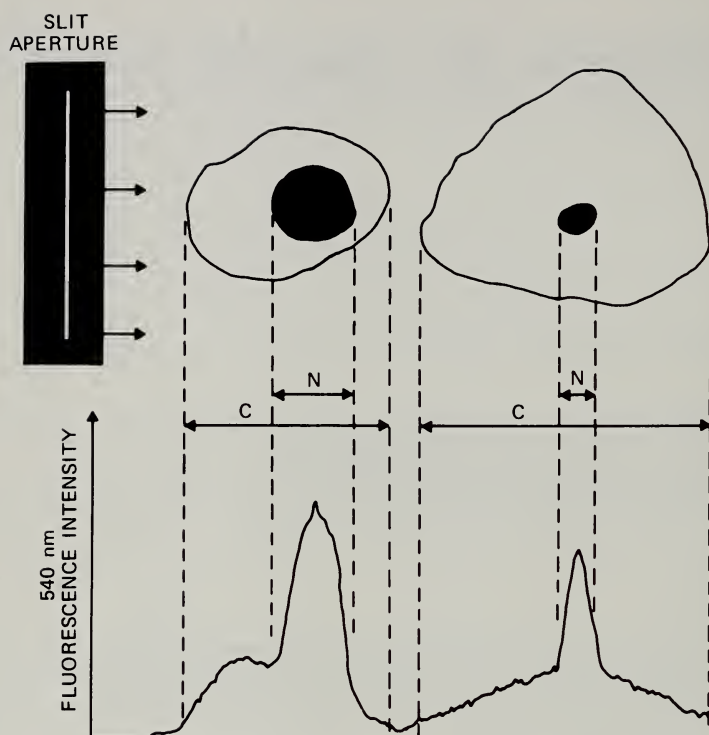


Fig. 1 Slit-scan technique and resulting fluorescence contours, with the correlation shown between the fluorescence contours and cell diameter (C) and nuclear diameter (N).

correspond in a flow system to a recording of secondary fluorescence from a cell as it flows through a thin "wall" of excitation illumination. In either case the slit aperture, or wall of excitation illumination, ideally would be much smaller than the features of the cell of interest. A slit width of  $5\ \mu\text{m}$  was used for our studies.

This type of low-resolution slit scan provides, as illustrated by the graphic fluorescence contour at the bottom of Fig. 1, a plot of the averaged fluorescence along the cell. From these contours the following features (cellular parameters) are available: cell diameter, nuclear diameter, nuclear- to cell-diameter ratio, nuclear fluorescence at one or more wavelengths, and cytoplasmic fluorescence at one or more wavelengths.

In addition, because the slit-scan technique is basically a low-resolution scanning system, it provides information related to the position of the nucleus in a cell as well as information on cell overlap. Partially overlapping cells present a unique slit-scan contour which allows their recognition and measurement. Therefore, using a slit-scan technique, one has a fairly complete set of cellular parameters available while still being consistent with the throughput constraints imposed by a flow system. Each contour need only be generated by a maximum of 20 to 30 measurements taken on a cell.



An example of one application of this technique is our work in developing a prescreening system for cytopathology. Our goal has been to develop a prescreening system based on the recognition of normal cellular material and known noncellular artifacts. Any specimen containing one or more cells which the instrument does not recognize as being normal would be returned to the cytopathologist for processing by conventional techniques. Such an instrument must be sensitive to the entire spectrum of cellular abnormalities that exist in the vagina, uterine cervix, or endometrium. In addition, it must also identify the inadequate sample.

Our approach, based upon the slit-scan technique, has been to establish and perfect a data base using a static-cell instrument. Cellular material was collected by cervical scrape, placed upon a Nuclepore filter, and stained with acridine orange. Cell measurements were recorded on a computerized slit-scan cytofluorometer. This instrument records the fluorescent slit-scan contour of a cell at 540 nm and analyzes it to determine the cellular and nuclear boundaries and nuclear fluorescence. The cell and nuclear boundaries are displayed as vertical lines on the computer scope together with the raw slit-scan data. The operator types on the teletype a two-letter code identifying the specific normal or abnormal cell type. This code word, along with the raw slit-scan data, is then recorded on magnetic tape.

Figure 2 depicts the raw slit-scan data, cell and nuclear boundaries, and calculated parameters for a normal intermediate squamous cell. In contrast, Fig. 3 illustrates the same data from a nonkeratinizing dysplastic cell. The dysplastic cell shows an increase in both nuclear- to cell-diameter ratio (NCR) and nuclear fluorescence (FN3) as compared with the normal intermediate cell.

Following the measurement of cells on one slide, a graphical output is generated plotting the recorded parameters of nuclear fluorescence and nuclear- to cell-diameter ratio for each measured cell. Results on material from a patient with a small-cell carcinoma in situ with coexisting dysplasia are presented in Fig. 4. Intermediate squamous cells exhibit the same nuclear fluorescence as stripped intermediate-cell nuclei but differ in nuclear- to cell-diameter ratio. However, the metaplastic and nonkeratinizing dysplastic cells and the cells derived from small-cell carcinoma in situ are clearly separated from the normal cell population because of an increase in nuclear fluorescence.<sup>2</sup>

The use of nuclear fluorescence avoids the problems of nonspecific cytoplasmic fluorescence associated with the measurement of total cell fluorescence and provides much better separation of normal and abnormal cell populations.

The other feature, nuclear- to cell-diameter ratio, allows the separation of superficial and intermediate squamous cells from other normal cell populations, such as endocervical cells, stripped nuclei, and white blood cells. This allows samples containing less than a preset number of superficial and intermediate squamous cells to be tagged for reexamination to determine the adequacy of the sample.



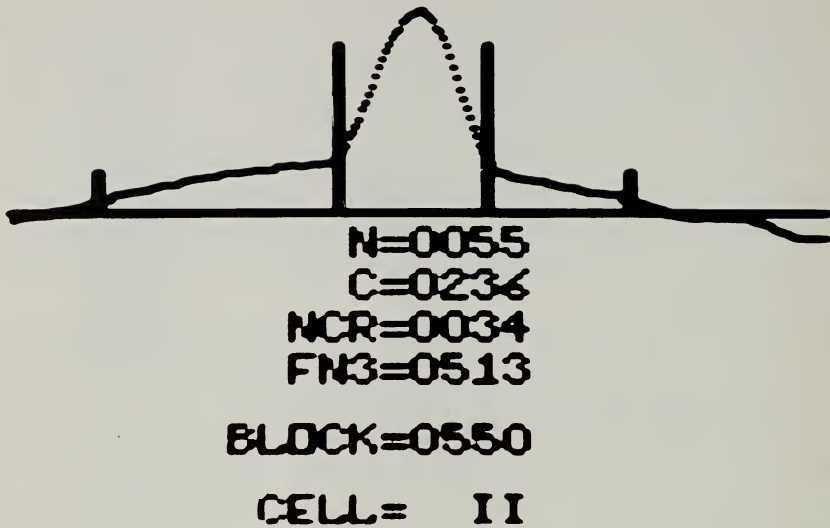


Fig. 2 Oscilloscope display of slit-scan contour of normal intermediate squamous cell with computer-determined cell and nuclear boundaries and calculated parameters.

N Nuclear diameter

NCR Nuclear- to cell-diameter ratio

C Cell diameter

FN3 Nuclear fluorescence

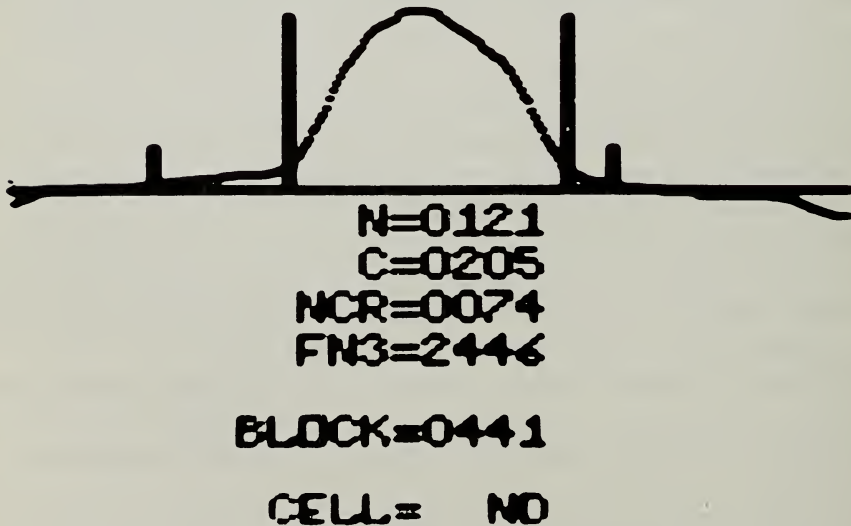


Fig. 3 Oscilloscope display of slit-scan contour of nonkeratinizing dysplastic cell with computer-determined cell and nuclear boundaries and calculated parameters.

N Nuclear diameter

NCR Nuclear- to cell-diameter ratio

C Cell diameter

FN3 Nuclear fluorescence

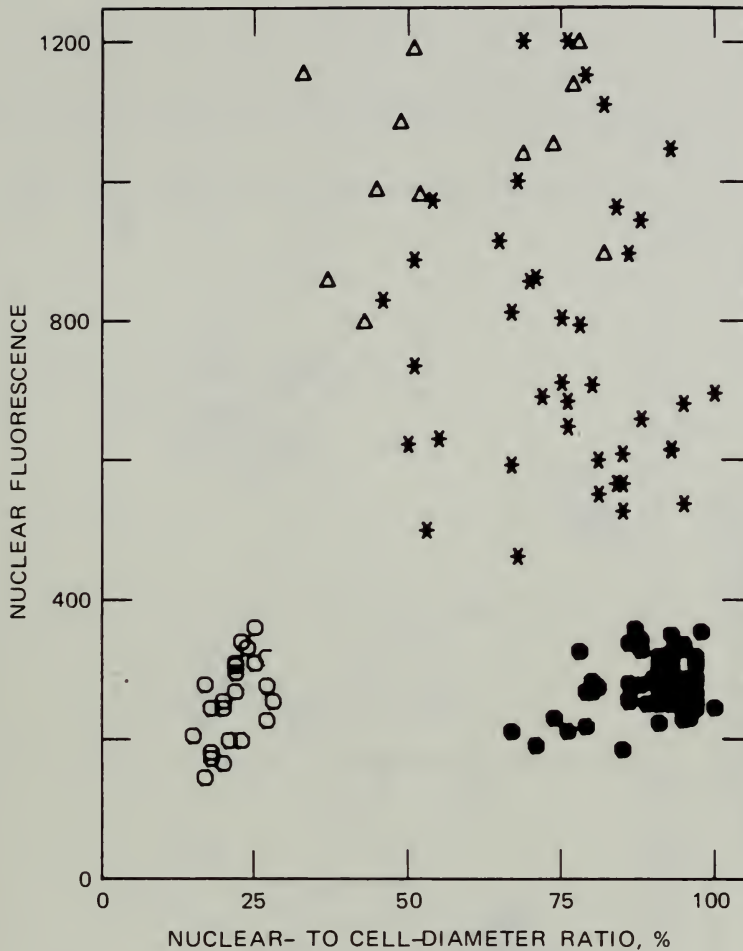


Fig. 4 Nuclear fluorescence vs. nuclear- to cell-diameter ratio in percent for intermediate squamous cells (○), stripped intermediate-cell nuclei (●), non-keratinizing dysplastic cells (△), and cells derived from a small-cell carcinoma in situ (\*).

Figure 5 exhibits data from a patient with dysplasia. Here again, nuclear fluorescence is sufficient to separate the pattern classes of normal and abnormal cells.

Figures 6 and 7 illustrate the sensitivity of the technique to other cellular abnormalities. In each case the specimen was split, with half being stained by the conventional slide technique. The other half was stained in suspension with a 0.01% acridine orange solution. The static-cell cytofluorometer was used to record measurements on cells stained by both techniques to demonstrate the equivalence of the two staining techniques with respect to the measured parameters.<sup>3</sup> This suspension-staining technique was developed for use in a slit-scan flow system now under fabrication.

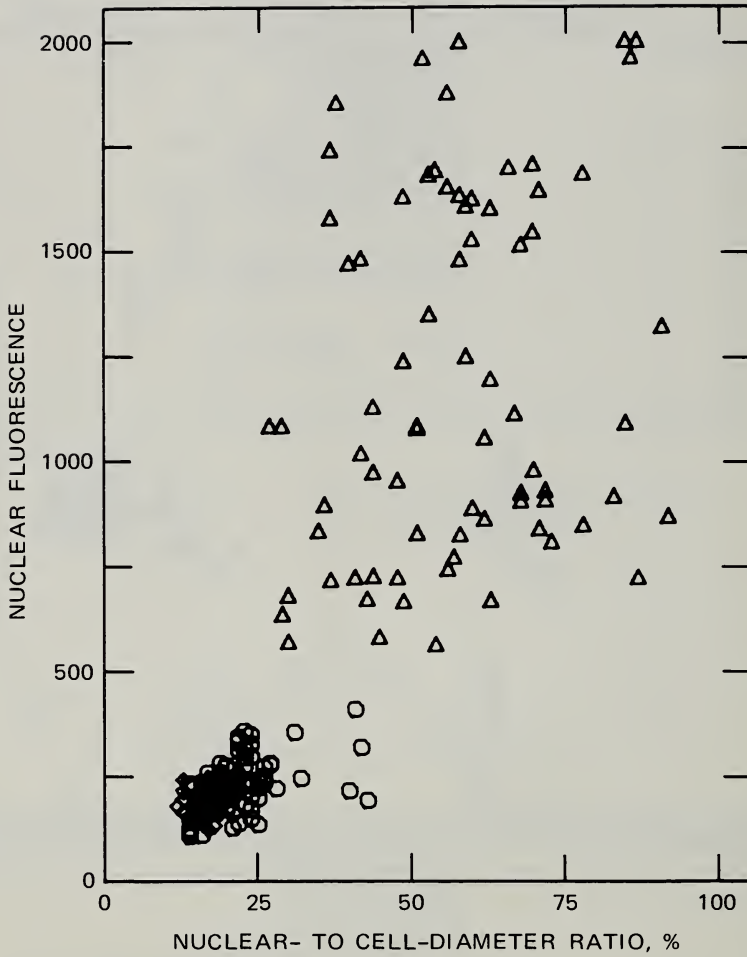


Fig. 5 Nuclear fluorescence vs. nuclear- to cell-diameter ratio in percent for superficial squamous cells (◇), intermediate squamous cells (○), and non-keratinizing dysplastic cells (△).

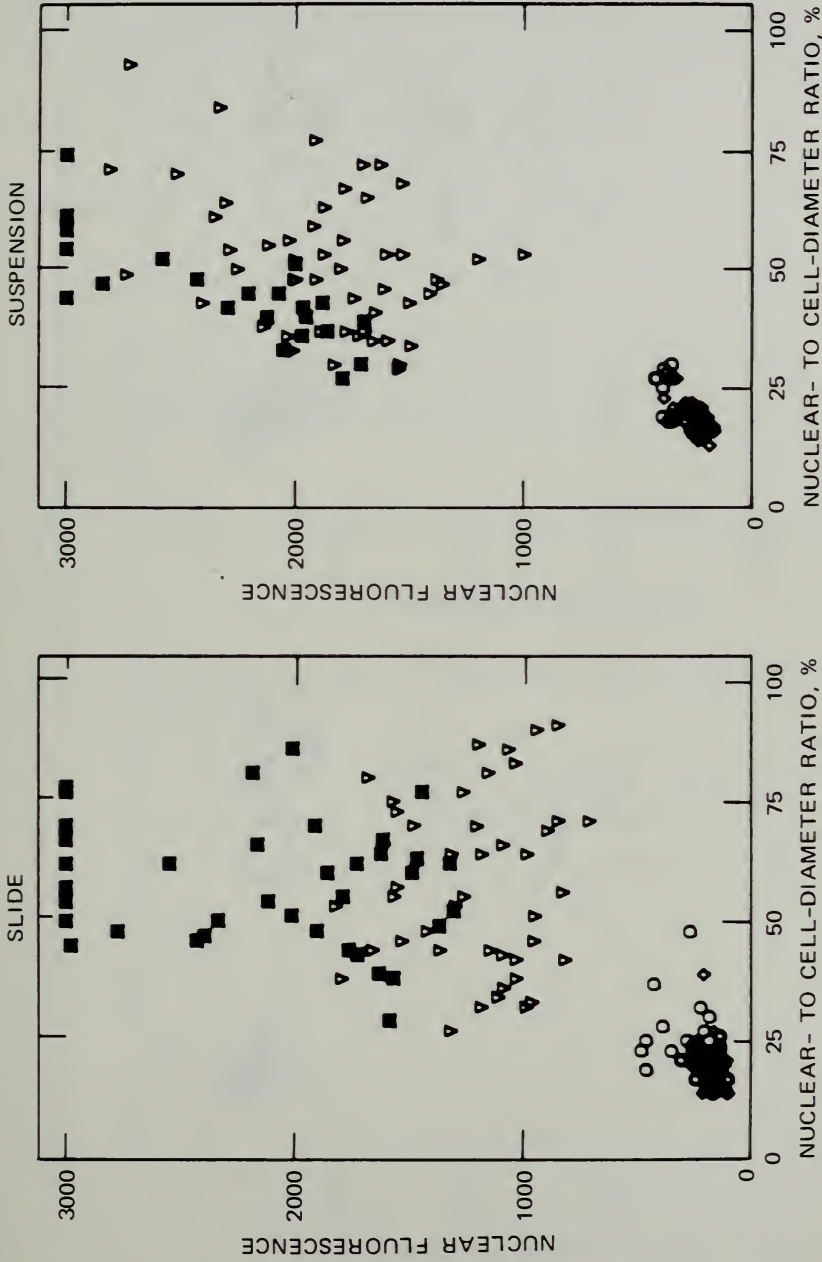


Fig. 6 Nuclear fluorescence vs. nuclear- to cell-diameter ratio in percent for superficial ( $\circ$ ) and intermediate ( $\triangle$ ) squamous cells, dysplastic cells ( $\nabla$ ), and cells derived from a keratinizing squamous-cell carcinoma ( $\blacksquare$ ). Half the specimen was stained on a slide; the other half, stained in suspension.



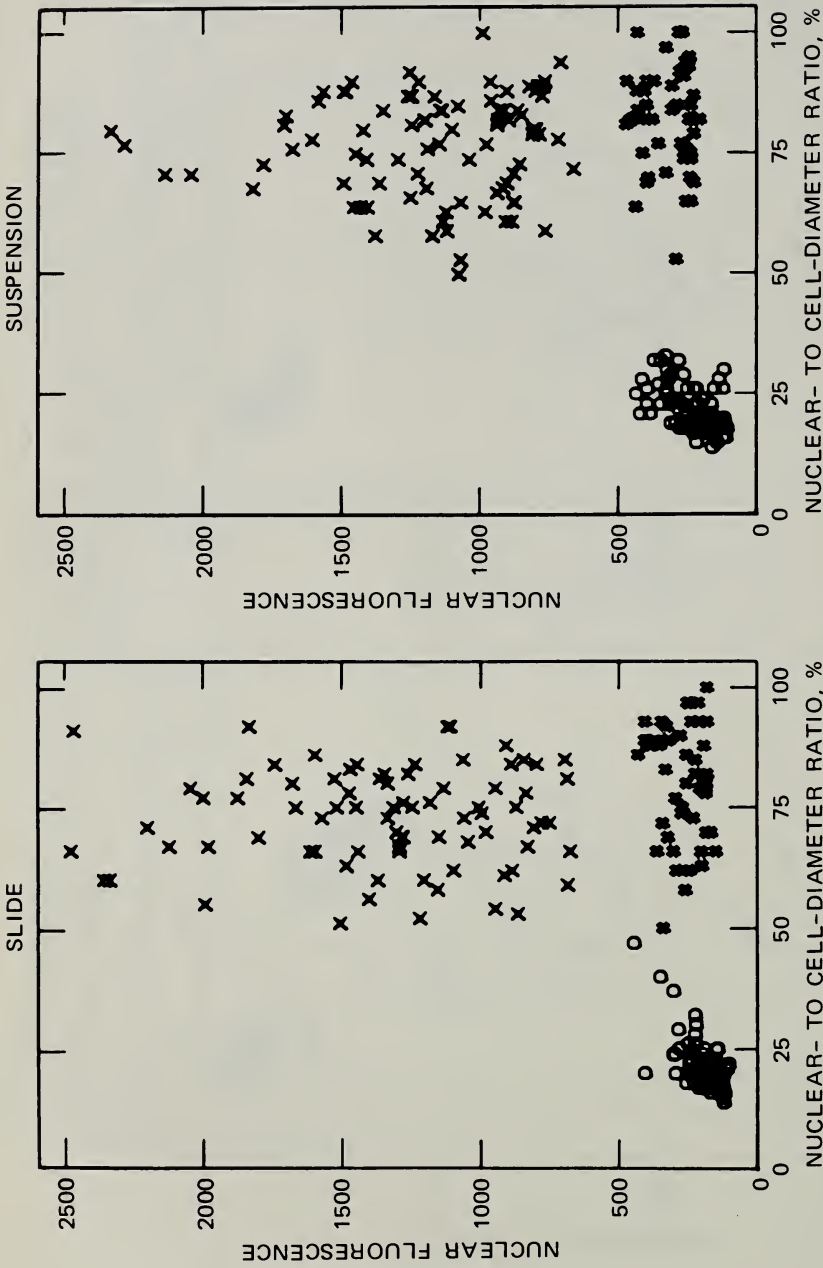


Fig. 7 Nuclear fluorescence vs. nuclear- to cell-diameter ratio in percent for intermediate squamous cells (○), lymphocytes (#), and cells derived from a metastatic endometrial stromal sarcoma (X). Half the specimen was stained on a slide; the other half, in suspension.

The slit-scan technique has shown itself to be extremely useful in the additional parameters it provides. The combination of nuclear fluorescence and nuclear- to cell-diameter ratio represents a unique and powerful set of measurable cell parameters which have already been documented as forming a viable data base for prescreening cells from the human female genital tract.

Current efforts are directed toward expanding the data base to other body systems and the fabrication of a slit-scan flow system.

## REFERENCES

1. L. L. Wheeless and S. F. Patten, Slit-Scan Cytofluorometry, *Acta Cytol.*, **17**: 333-339 (1973).
2. L. L. Wheeless and S. F. Patten, Slit-Scan Cytofluorometry: Basis for an Automated Cytopathology Prescreening System, *Acta Cytol.*, **17**: 391-394 (1973).
3. L. L. Wheeless, S. F. Patten, and M. A. Onderdonk, Quantitative Comparison of Slide and Suspension Technique for Acridine Orange Staining of Human Cells, *Acta Cytol.*, **18**: 8-12 (1974).

# ANALYSIS OF DNA SYNTHESIS CHANGES IN CELLS INFECTED WITH SV40 VIRUS

JOHN M. LEHMAN

Department of Pathology, University of Colorado Medical School, Denver, Colorado

---

## ABSTRACT

Simian virus 40 (SV40) recruits cells into unscheduled rounds of DNA synthesis. Cytophotometric determinations of nuclear DNA content show that a significant percentage (10 to 20%) of polyploid cells are induced within 24 hr postinfection. The polyploid cells arise by stimulation of cells into two or more simultaneous S periods without an intervening mitosis. The majority (80%) of these cells are tetraploid, and no specific chromosome changes were seen. Hypotetraploid and hypertetraploid cells (30 to 50%) were enriched in the transformed cell population, a fact suggesting that these cells are capable of cell division. Polyploidization with subsequent chromosome imbalance may be a necessary step in the malignant transformation of cells by SV40 virus. Further experiments are outlined to define the role of polyploid cells in transformation by SV40 virus.

The small DNA tumor viruses (SV40 and polyoma) have the ability to induce unscheduled rounds of cellular DNA synthesis.<sup>1</sup> This viral event is unique to this group of viruses since most other viral agents cause a depression or shutoff of host DNA, RNA, and protein synthesis. Thus a possible relationship may exist between the viral induction of cellular DNA synthesis by these viruses and the oncogenic potential of the viruses.

The phenomenon of viral-induced cellular DNA synthesis was first described in cells infected with polyoma virus (PY) both in the presence and in the absence of viral replication. A number of laboratories have reported that PY could induce into the S phase of the cell cycle cells that were arrested in the cell cycle because of contact inhibition,<sup>2</sup> temperature,<sup>3</sup> X ray,<sup>2</sup> 5-fluorouracil,<sup>4</sup> and state of cellular differentiation.<sup>5</sup> Myoblasts that fuse in tissue culture into multinucleated, striated myotubes are unable to undergo cellular DNA synthesis or cell division just prior to cell fusion.<sup>6</sup> If a small number of myoblasts are infected with PY virus prior to cell fusion, a few PY T-antigen-positive nuclei are

incorporated into the myotube. Within a few hours cell nuclei that were negative for the intranuclear SV40 T antigen undergo cellular DNA synthesis and eventually enter mitosis. Thus the infected nuclei are able by intranuclear transfer of a preposed viral-specific product to induce cells into DNA synthesis and mitosis.<sup>5</sup> The nature of this substance or its interaction with the nuclear DNA is not known; however, recent results suggest that the viral product is also able to induce mitochondrial DNA to replicate.<sup>7</sup> The newly replicated cellular DNA is normal.<sup>8</sup> Concomitant with this DNA replication is a stimulation of the synthesis of histones and other chromosomal proteins.<sup>9</sup>

Other DNA tumor viruses, adenoviruses,<sup>10</sup> and Epstein-Barr virus<sup>11</sup> have also been shown to stimulate an unscheduled round of cellular DNA synthesis in both permissive and nonpermissive cells.

We have demonstrated with CYDAC (cytophotometric data conversion) and FMF (flow microfluorometry) a population of tetraploid-polyploid cells produced following infection of a Chinese hamster (ChH) cell strain with SV40 virus. This paper will outline the results and further studies to define the relationship of this population of cells to transformation by SV40 virus.

The studies discussed in this paper used secondary-passage Chinese hamster embryo cells and a contact-inhibited strain of Chinese hamster cells. In earlier studies<sup>12</sup> secondary ChH cells were shown to be (1) highly susceptible to SV40 infection since approximately 90 to 100% of the cells produced the SV40-specific intranuclear T antigen within 48 hr postinfection, (2) nonpermissive to complete virus replication (blocked before viral DNA synthesis), and (3) transformed at a frequency of 0.1 to 5%. The other cell system used in the studies described was a ChH cell strain with the previously listed properties in addition to being contact inhibited.<sup>13</sup> Both cell systems were diploid, and this made possible an analysis of the early chromosomal changes that resulted from SV40 infection.<sup>12,13</sup>

It was determined by autoradiography that within 16 to 20 hr after infection with SV40 virus a large percentage (80 to 90%) of the infected population was recruited into cellular DNA synthesis. Pulse-labeling (1 hr) experiments showed an increase in the number of infected cells undergoing DNA synthesis in the time period, 18 to 24 hr postinfection.<sup>12</sup> This result could be explained by an increase in recruitment of cells into S or by a lengthening of the S period.

A cytophotometric analysis<sup>14</sup> of the infected population was made with CYDAC to resolve which of the two preceding hypotheses was correct. By optical-density measurements, this system allowed a determination of the DNA content of a single nucleus which had been stained by a modified Feulgen procedure. At early times postinfection (16, 20, 24, and 34 hr), 200 nuclei of control and infected cultures were measured for their DNA content. The infected culture at 16 hr began to show a twofold increase in the tetraploid-polyploid cell population. The control population at all times analyzed exhibited a 2.0 to 2.5% polyploid population. By 24 and 34 hr there was an eightfold and a ninefold increase, respectively, of polyploid cells in the infected populations.



Of interest was the fact that in the infected population (24 and 34 hr) a proportion of the cells that had cycled from  $G_1$  and S into  $G_2$  remained in  $G_2$ , apparently not undergoing mitosis. These  $G_2$  cells may be the  $G_1$  cells of the tetraploid population. Analysis of the CYDAC data showed that a larger portion of the infected population cycled through S and  $G_2$ , and this suggested an increased recruitment of infected cells into S.

In four separate experiments the chromosome number mode, the presence or absence of abnormal metaphase chromosomes, and the percentage of polyploid mitoses were analyzed.<sup>15</sup> All four experiments showed a significant increase in the polyploid metaphases (10%). Therefore the polyploid interphase cells studied by cytophotometric analysis were capable of undergoing mitosis. Although the majority of the polyploid cells were tetraploid, occasionally higher ploidy (16X, 32X, 64X) values were observed (5 to 6%). Approximately 20 to 30% of these polyploid metaphases were abnormal, with breaks, abnormal chromosomes, and loss and addition of chromosomes. The remaining polyploid metaphases were normal. The specific chromosomal changes were observed in either the diploid or the polyploid population. Of interest is the fact that no endoreduplicated metaphases were found.

What relationship did these polyploid cells play in the transformation of cells by SV40 virus? This question we attempted to answer by analyzing the chromosome mode of the transformed cell population. With the secondary ChH cell strain, we detected transformants within 3 to 4 weeks and made a cytogenetic analysis of the transformed cells to determine their chromosome characteristics. In three clones of transformed cells, a significant portion of the mitoses were hypotetraploid or hypertetraploid (30 to 50%).<sup>12,15</sup> Thus a proportion of the polyploid cells seen early after infection were capable of replication and were enriched in the transformed population. The contact-inhibited ChH cell strain allowed an analysis of the early cells that break through contact inhibition after SV40 infection. This cell strain would reach a density of  $1.1 \times 10^6$  cells per 60-mm petri dish; then the cells would not enter DNA synthesis.<sup>13</sup> Following infection with SV40, a burst of mitotic activity would occur within 24 to 48 hr. This population was analyzed with and without Colcemid block. Fifty percent of the metaphases were tetraploid-polyploid, and 5% of all mitoses were multipolar (tri- or tetra-). We also used time-lapse cinemicrography showing the occurrence of multipolar mitoses shortly after infection.<sup>12</sup> This information establishes the fact that the SV40 virus induces unscheduled rounds of cellular DNA synthesis in Chinese hamster cells and that a population of polyploid cells results from this stimulated DNA synthesis. While a direct relationship has not been defined for the involvement of the polyploid cells in the transformation by SV40 virus, the data suggest that polyploidization may be a step in the neoplastic transformation.

Primary Syrian hamster tumors induced by SV40 virus exhibit a new tetraploid chromosome mode.<sup>16</sup> Polyoma tumors, on the other hand, have a pseudodiploid-aneuploid chromosome mode.<sup>17</sup> Therefore the chromosome

mode of the SV40 primary tumors suggests that polyploidy may be a step in the transformation *in vivo*.

We next looked at the possible mechanism for the origin of these polyploid cells. The cytophotometric (CYDAC) and chromosome analyses showed the presence of the polyploid cells within 24 hr postinfection (22 hr generation time for the ChH cells). There are four possible explanations for the origin of these cells: (1) replication of tetraploid cells already present in the cell population (3%); (2) fusion of cells; (3) DNA synthesis following an incomplete karyokinesis; and (4) two or more simultaneous S periods without a mitosis.<sup>1,2</sup> For hypothesis 1 to be operational, the tetraploid population (2%) would have to undergo at least three generations with a much shorter generation time to produce 16% polyploid cells at 24 hr. The SV40 virus has not been described as a fusion virus, and experiments suggested that in Chinese hamster cells fusion was not occurring. Therefore both hypotheses 1 and 2 were untenable. In early work with PY virus, Dulbecco and Vogt<sup>1,8</sup> suggested on the basis of anaphase and metaphase analysis that a mechanism of transformation might be incomplete karyokinesis. To decide whether hypothesis 3 or hypothesis 4 was correct, we took time-lapse cinemicrographs of infected cultures. Of the 670 mitoses that were photographed, all underwent complete karyokinesis and cytokinesis. The life histories of eight cells determined to be polyploid by CYDAC were followed in the film. None of the eight cells underwent a faulty karyokinesis.<sup>1,2</sup> Further evidence to support the fourth hypothesis was obtained by the use of 5-bromodeoxyuridine as a DNA density marker. In the presence of Colcemid which prevented mitosis, a fraction of the infected population underwent two periods of DNA synthesis which was detected by the presence of heavy-heavy DNA.<sup>1,9</sup> This heavy-heavy DNA was replicated 24 to 48 hr postinfection and was cellular DNA as determined by DNA-DNA hybridization. Autoradiography experiments showed that a fraction of the infected cells replicate their DNA in two complete cycles. The evidence presented suggests that after infection with SV40 virus a portion of the Chinese hamster cell population undergoes two cycles of DNA synthesis without an intervening mitosis.

The observation of increased polyploidy after infection with SV40 virus has been described for mouse embryo fibroblasts<sup>1,5</sup> and mouse macrophages.<sup>2,0</sup> Earlier work with the human diploid fibroblasts<sup>2,1</sup> also detected an increased tetraploidy and general heteroploidy at about the time of morphological transformation following infection with SV40 virus.

To further define the mechanism of origin and relationship of polyploid cells to transformation by SV40, we are utilizing FMF to analyze quantitatively<sup>2,2,2,3</sup> the generation of these cells. Once isolated, this population will be studied in relation to its transformation efficiency and tumorigenicity. Preliminary results<sup>2,3,2,4</sup> suggest that FMF may be used to isolate the population. We also plan to study such parameters as relationship of cell-cycle period to transformation and changes in cell cycle after infection with SV40 virus.

Boveri<sup>25</sup> postulated that malignancy might result from chromosome imbalance following multipolar mitoses. He suggested that the chromosome imbalance may lead to a population of cells that, after successive generations, have a propensity to replicate, not obeying normal growth restraints. Of importance for transformation by SV40 virus may be polyploidization followed by chromosome imbalance and the integration of the SV40 viral genome<sup>26</sup> into cellular DNA. Evidence that chromosome balance may regulate the expression of malignancy has been described for chemically and virally transformed revertants.<sup>27</sup> This cell-virus system offers a model to study mechanisms of carcinogenesis and cell regulations.

## ACKNOWLEDGMENTS

This work was supported in part by Public Health Service Training Grants T01-CA-05163 and T01-CA-05164 from the National Cancer Institute and Grant DT-14-0 from the American Cancer Society.

## REFERENCES

1. E. Winocour, Some Aspects of the Interaction Between Polyoma Virus and Cell DNA, in *Advances in Virus Research*, pp. 153-200, Academic Press, Inc., New York, 1969.
2. D. Gershon, L. Sachs, and E. Winocour, The Induction of Cellular DNA Synthesis by Simian Virus 40 in Contact-Inhibited and in X-Irradiated Cells, *Proc. Nat. Acad. Sci. U.S.A.*, **56**: 918-925 (1966).
3. L. Ossovski and L. Sachs, Temperature Sensitivity of Polyoma Virus, Induction of Cellular DNA Synthesis, and Multiplication of Transformed Cells at High Temperature, *Proc. Nat. Acad. Sci. U.S.A.*, **58**: 1938-1943 (1967).
4. T. Ben-Porat, A. S. Kaplan, and R. W. Tennant, Effect of 5-Fluorouracil on the Multiplication of a Virulent Virus (Pseudorabies) or an Oncogenic Virus (Polyoma), *Virology*, **32**: 445-456 (1967).
5. M. Fogel and V. Defendi, Infection of Muscle Cultures from Various Species with Oncogenic DNA Viruses (SV40 and Polyoma), *Proc. Nat. Acad. Sci. U.S.A.*, **58**: 967-973 (1967).
6. K. Okazaki and H. Holtzer, Myogenesis: Fusion, Myosin Synthesis, and the Mitotic Cycle, *Proc. Nat. Acad. Sci. U.S.A.*, **56**: 1484-1489 (1966).
7. A. Levine, Induction of Mitochondrial DNA Synthesis in Monkey Cells Infected by SV40 and (or) Treated with Calf Serum, *Proc. Nat. Acad. Sci. U.S.A.*, **68**: 717-720 (1971).
8. T. Ben-Porat, C. Coto, and A. S. Kaplan, Unstable DNA Synthesized by Polyoma Virus-Infected Cells, *Virology*, **30**: 74-81 (1966).
9. E. Winocour and E. Robbins, Histone Synthesis in Polyoma and SV40 Infected Cells, *Virology*, **40**: 307-315 (1970).
10. J. E. Zimmerman, K. Raska, and W. A. Strohl, The Response of BHK21 Cells to Infection with Type 12 Adenovirus, *Virology*, **42**: 1147-1150 (1970).
11. P. Gerber and B. H. Hoyer, Induction of Cellular DNA Synthesis in Human Leucocytes by Epstein-Barr Virus, *Nature (London)*, **231**: 46-47 (1971).
12. J. M. Lehman and V. Defendi, Changes in Deoxyribonucleic Acid Synthesis Regulation in Chinese Hamster Cells Infected with Simian Virus 40, *J. Virol.*, **6**: 738-749 (1970).



13. J. M. Lehman, Biological Characteristics and Viral Transformation of a Contact-Inhibited Chinese Hamster Cell Strain, in preparation.
14. B. H. Mayall and M. L. Mendelsohn, Deoxyribonucleic Acid Cytophotometry of Stained Human Leukocytes. II. The Mechanical Scanner of CYDAC, the Theory of Scanning Photometry, and the Magnitude of Residual Errors, *J. Histochem. Cytochem.*, **18**: 383-407 (1970).
15. J. M. Lehman, Early Chromosome Changes in Diploid Chinese Hamster Cells After Injection with Simian Virus 40, *Int. J. Cancer*, **13**: 164-172 (1974).
16. J. M. Lehman and P. Bloustein, Chromosome Analysis and Agglutination by Concanavalin A of Primary Simian Virus 40 Induced Tumor, *Int. J. Cancer*, in press.
17. V. Defendi and J. M. Lehman, Biological Characteristics of Primary Tumors Induced by Polyoma Virus in Hamsters, *Int. J. Cancer*, **1**: 525-540 (1966).
18. M. Vogt and R. Dulbecco, Steps in the Neoplastic Transformation of Hamster Embryo Cells by Polyoma Virus, *Proc. Nat. Acad. Sci. U.S.A.*, **49**: 171-179 (1963).
19. K. Hirai, J. M. Lehman, and V. Defendi, Reinitiation Within One Cell Cycle of the Deoxyribonucleic Acid Synthesis Induced by Simian Virus 40, *J. Virol.*, **8**: 828-835 (1971).
20. J. M. Lehman, J. Mauel, and V. Defendi, Regulation of DNA Synthesis in Macrophages Infected with Simian Virus 40, *Exp. Cell Res.*, **67**: 230-233 (1971).
21. P. S. Moorhead and E. Saksela, The Sequence of Chromosome Aberrations During SV40 Transformation of a Human Diploid Cell Strain, *Hereditas*, **52**: 271-284 (1965).
22. M. A. Van Dilla, T. Trujillo, P. F. Mullaney, and J. R. Coulter, Cell Microfluorometry: A Method for Rapid Fluorescence Measurement, *Science*, **163**: 1213-1214 (1969).
23. P. F. Mullaney, J. A. Steinkamp, H. A. Crissman, L. S. Cram, and D. M. Holm, Laser Flow Microphotometrics for Rapid Analysis and Sorting of Individual Mammalian Cells, in *Laser Applications in Medicine and Biology*, M. L. Wolbarsht (Ed.), Plenum Publishing Corporation, 1973.
24. P. K. Horan, J. H. Jett, A. Romero, and J. M. Lehman, Flow Microfluorometry Analysis of DNA Content in Chinese Hamster Cells Following Infection with Simian Virus 40, *Int. J. Cancer*, in press.
25. T. Boveri, *The Origin of Malignant Tumors*, translated by M. Boveri, Baillière, Tindall, and Cox, London, 1929.
26. K. Hirai, J. M. Lehman, and V. Defendi, Integration of Simian Virus 40 Deoxyribonucleic Acid into the Deoxyribonucleic Acid of Primary Chinese Hamster Cells, *J. Virol.*, **8**: 708-715 (1971).
27. A. Rabinowitz and L. Sachs, Control of the Reversion Properties in Transformed Cells, *Nature (London)*, **225**: 136-139 (1970).



# COMPUTER-ASSISTED ANALYSIS OF IRRADIATED LYMPHOCYTES

ROBERT E. ANDERSON,\* GEORGE B. OLSON,† JOHN L. HOWARTH,‡ and  
PETER H. BARTELS†§

\*Department of Pathology, School of Medicine, University of New Mexico,  
Albuquerque, New Mexico; †Department of Microbiology and Medical Technology,  
University of Arizona, Tucson, Arizona; ‡Departments of Physics and Radiology,  
University of New Mexico, Albuquerque, New Mexico; §Optical Sciences Center,  
University of Arizona, Tucson, Arizona

---

## ABSTRACT

Computer-assisted morphometric analysis of murine thoracic-duct lymphocytes reveals two subpopulations of small lymphocytes. Similar analysis of uniform populations of lymphocytes confirms that these are T (thymus-derived lymphocytes) and B (bone-marrow-derived lymphocytes) cells.

The nuclei of T cells are significantly larger than those of B cells, and their Feulgen-positive material is more evenly distributed with fewer densely staining aggregates.

Radiation-induced morphologic alterations are evident at relatively small doses with respect to both T and B cells. The latter appear to demonstrate a progressive enlargement of the nucleus associated with a more even dispersion of the nuclear chromatin and formation of intranuclear vacuoles. The T cells initially also show a more even dispersion of Feulgen-positive material as a function of dose, but at 2000 rads they appear to exhibit marked chromatin clumping. This alteration is associated with a decrease in nuclear size, and vacuoles are not evident.

The exquisite radiosensitivity of the small lymphocyte is well known.<sup>1-9</sup> However, most of the attendant experiments were completed before the definition of immunologically distinct subpopulations of lymphocytes. Some of the differences between T (thymus-derived) and B (bone-marrow-derived) lymphocytes are summarized in Table 1.

Recently, a series of experiments suggested that T and B cells are not equally radiosensitive.<sup>10,11</sup> These experiments employed a variety of functional parameters, and the data support the concept that B cells are more radiosensitive

TABLE 1  
CHARACTERISTICS OF THYMIC-DERIVED VS.  
BONE-MARROW-DERIVED LYMPHOCYTES

Characteristics	Bone-marrow-derived lymphocytes	Thymic-derived lymphocytes
Origin	Bone-marrow stem cell	Bone-marrow stem cell
Ontogenic control of differentiation	Bursa fabricious (avian); bursa equivalent (mammalian)	Thymus
Life span	6 to 8 weeks	4 to 6 months
Recirculating pool	Minority (15 to 25% in mouse)	Majority (80 to 85% in mouse)
Major tissue localization		
Lymph nodes	Follicles and medulla	Deep cortical; perifollicular
Spleen	Follicles and peripheral of white pulp	Periarteriolar sheath
Peyer's patches	Follicles	Interfollicular
Functions		
Cell-mediated immunity	±	4+
Induction of humoral immunity	4+	4+
Antibody synthesis	4+	0
Specific receptors	F <sub>c</sub> fragment; complement	θ alloantigen (mouse)
Ultrastructure	Numerous surface microvilli	Questionably larger than B cell; few surface microvilli
"Mitogenic" response	Lynopolysaccharide	Phytohemagglutinin, concanavalin-A, lentil
Memory	No	Yes

than T cells. The purpose of the experiments reported here was to explore the morphologic correlates of these functional differences.

## METHODS AND RESULTS

Cells for analysis were obtained from the thoracic ducts of congenitally athymic "nude" (nu/nu) and CBA mice of both sexes according to the cannulation technique of Boak and Woodruff.<sup>12</sup> The relative numbers of T and B cells were ascertained by an anti-θ cytotoxicity test (T cells) and an immunofluorescence assay using labeled anti-Ig (B cells).<sup>13</sup> Cells suspended in

minimal essential medium (MEM) were irradiated at room temperature at a concentration of  $3$  to  $6 \times 10^6$  cells/ml with a standard X-ray machine. Irradiated cell suspensions were immediately applied to slides, fixed, and stained for DNA with a Feulgen reaction.<sup>14</sup> Evaluation of the digitized images of Feulgen-stained lymphocytes was accomplished as outlined by Bartels (Bartels and Wied, this volume).

Figure 1 depicts the distribution of optical-density (OD) values from Feulgen-stained thoracic-duct lymphocytes (TDL) in CBA mice (CBA). The resultant histograms indicate the relative frequencies of occurrence of OD values grouped as indicated. As shown in this figure, the majority of values are concentrated in the range 0 to 1.0 OD units. This observation is supported by visual inspection of histogram data for individual lymphocytes where the majority (73%) possess histograms with values that do not extend beyond 1.00 OD. However, a minor subpopulation (27%) contains very densely staining Feulgen-positive aggregates with values up to 1.50 units. The minor subpopulation is designated Mode I and the major subpopulation is referred to as Mode II. Evaluation of an aliquot of this population of TDL with anti- $\theta$  and fluorescein-conjugated anti-Ig indicates that 87% are positive for the  $\theta$  antigen (and therefore represent T cells) and 13% are positive for Ig determinants (B cells). This observation supports the concept that T and B cells can be differentiated by computer-assisted morphometric analysis.

For a further investigation of this hypothesis, the distribution of OD values from uniform populations of Feulgen-stained T and B cells was analyzed and compared with Modes I and II. Pure B cells were obtained by cannulation of the thoracic duct of congenitally athymic "nude" mice. A uniform population of T cells was obtained by passage of CBA TDL through a nylon fiber column.<sup>15</sup> As shown in Fig. 2, an analysis of a uniform B-cell population indicates histograms which extend to values of 1.5 OD and which are almost identical to Mode I. On the other hand, a uniform population of T cells shows histograms concentrated at lower OD values without the dense Feulgen-positive aggregates evident with respect to B cells. Again, the histogram data for Mode II and the T-cell subpopulation are virtually superimposable.

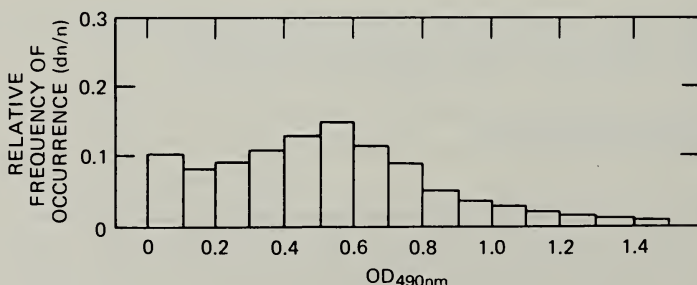


Fig. 1 Distribution of optical-density (OD) values for thoracic-duct lymphocytes from CBA mice.

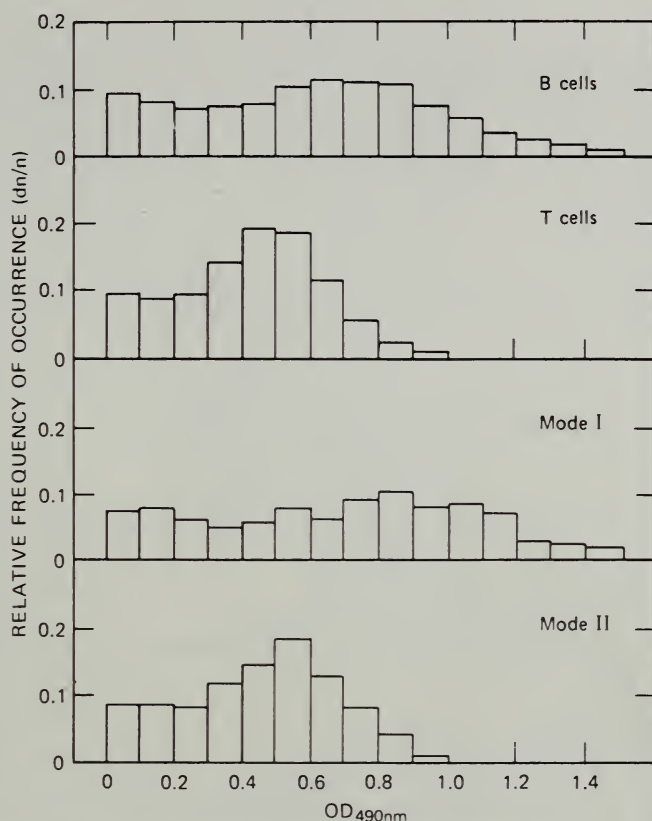


Fig. 2 Distribution of optical-density (OD) values for Mode I, Mode II, T cells, and B cells.

The preceding comparisons are summarized in Table 2, in which T and B cells are compared with respect to the relative nuclear area and total OD. As seen in Table 2, T cells have a somewhat larger nuclear area than B cells and slightly more total Feulgen-positive material.

Figure 3 shows the distribution of OD values as a function of radiation dose for CBA TDL. An initial shift toward lower OD values is evident, followed by a marked spreading of OD values at 2000 rads. Comparable results have been obtained from a similar experiment.

In this connection it is important to recall that thoracic-duct lymph contains two primary subpopulations of lymphocytes. Therefore the dose-response data of Fig. 3 may reflect dissimilarities between T and B cells with respect to relative radiosensitivity and/or dissimilar morphologic alterations caused by radiation. A series of experiments, summarized in Figs. 4 to 9, were set up to investigate these possibilities.

Figures 4 and 5 show the change in relative nuclear area for TDL upon exposure to 500 rads. The major subpopulation (T cells) shows relatively little



TABLE 2

MEANS AND CONFIDENCE LIMITS OF RELATIVE NUCLEAR AREA AND TOTAL OPTICAL DENSITY IN MOUSE T AND B LYMPHOCYTES

Cell type	Relative nuclear area	Total optical density
T cell	$97.8 \pm 1.5^*$	$4178 \pm 43^*$
B cell	$65.0 \pm 1.5$	$3980 \pm 43$

\*95% confidence limits, based on mean-square estimates from analysis of variance table.

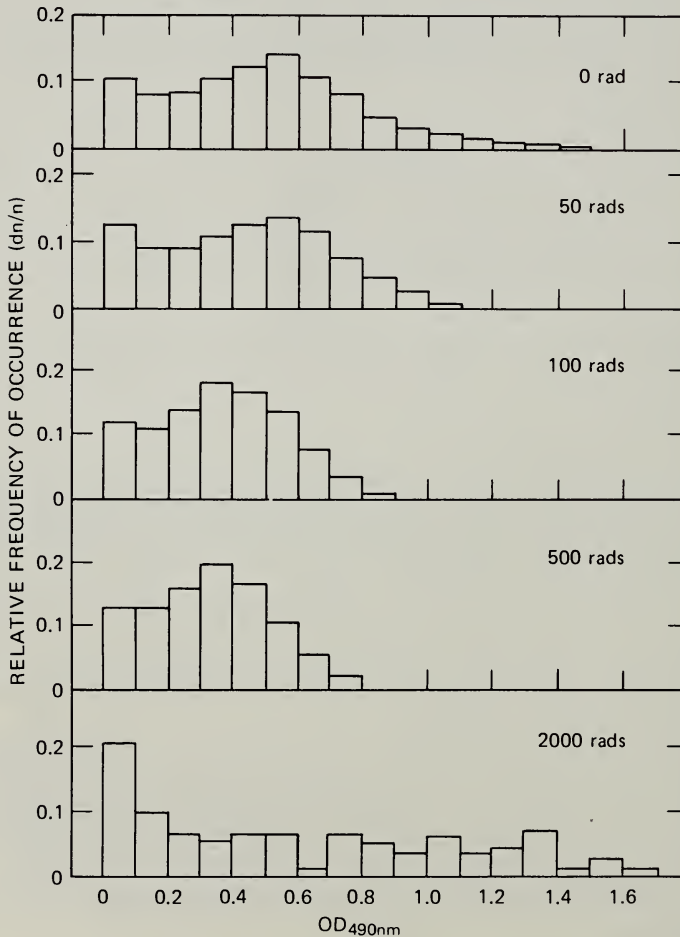


Fig. 3 Distribution of optical-density (OD) values as a function of dose for thoracic-duct lymphocytes from CBA mice.

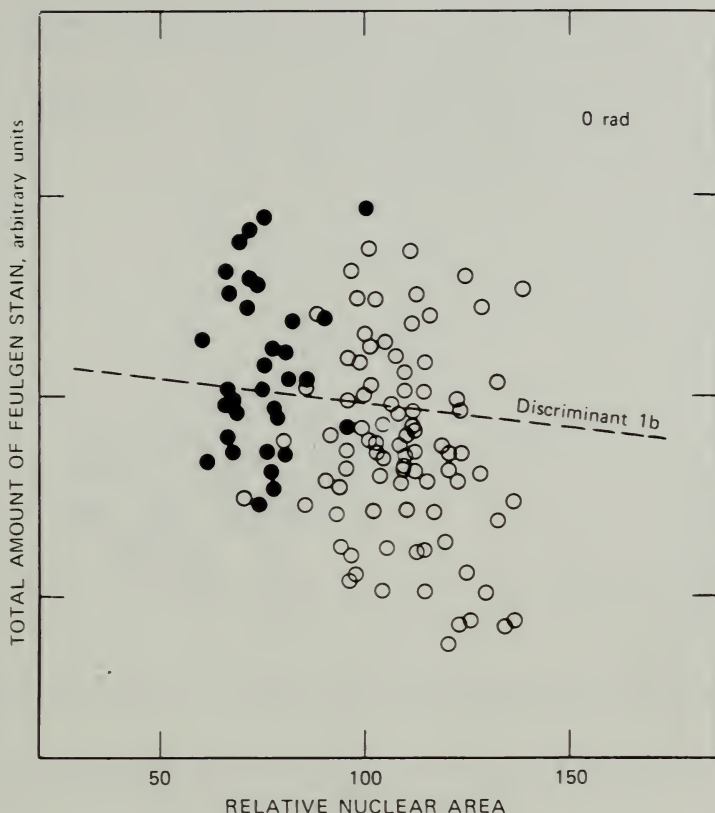


Fig. 4 Distribution of total optical density as a function of relative nuclear area for T cells (○) and B cells (●) from nonirradiated CBA mice.

change. However, the minor subpopulation (B cells) shows a rather striking increase in relative area at this dose.

A similar phenomenon is apparent when two of the histogram intervals (HIST 4 and HIST 5), which show a consistent and pronounced change as a function of dose, are plotted vs. one another. Again, in Figs. 6 and 7 relatively little change follows 500 rads for the T-cell subpopulation, but a distinct shift is evident with respect to the minor (B-cell) subpopulation.

For a further analysis of the morphologic changes occasioned by ionizing radiation, uniform populations of T and B cells were exposed to a variety of doses. Figure 8 shows the distribution of OD values as a function of dose for CBA TDL passaged through the nylon fiber column. Note the shift toward lower OD values at doses up to 100 rads. However, at 2000 rads there is a marked spreading of the OD values.

Figure 9 shows similar data for a uniform B-cell subpopulation obtained by cannulation of congenitally athymic "nude" mice. Note the shift of histograms toward lower values as a function of dose. In addition, Wright-Giemsa-stained

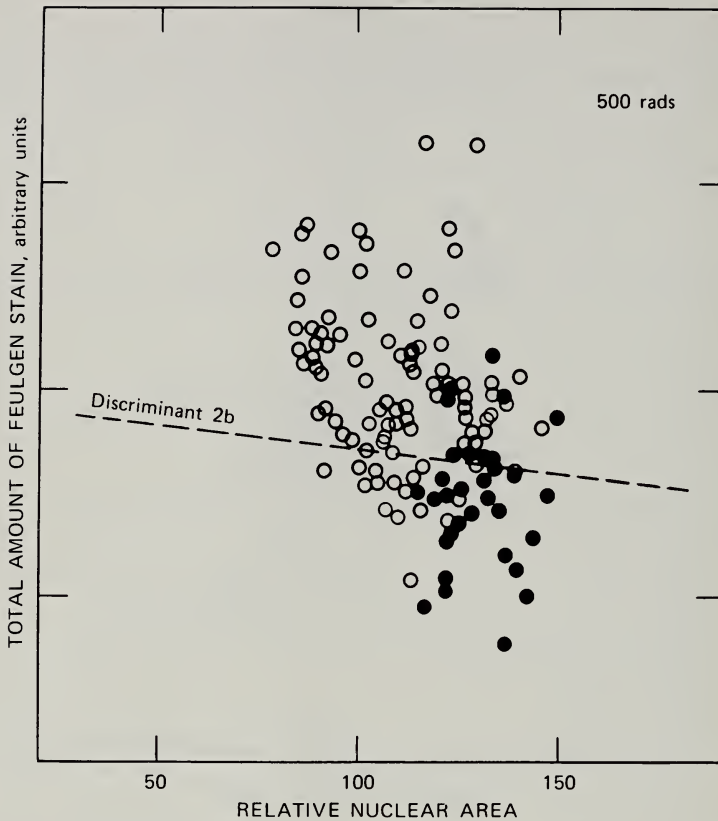


Fig. 5 Distribution of total optical density as a function of relative nuclear area for T cells (○) and B cells (●) from CBA mice after a 500-rad exposure.

smears from aliquots showed marked vacuolization of the nuclei at each of the dose levels. Similar vacuoles were not evident among the irradiated T cells at any of the doses.

## DISCUSSION

Despite morphologic homogeneity, at least at the light-microscope level, two subpopulations of small lymphocytes can be distinguished by computer-assisted morphometric analysis. The nuclei of T cells are significantly larger than those of B cells, and their Feulgen-positive material is more evenly distributed throughout the nucleus with fewer densely staining aggregates than are noted with B cells.

Considerable evidence now exists to support the presence of subpopulations of T and B cells. Suppressor T cells represent perhaps the best defined example in this regard.<sup>1,6</sup> To date, the majority of the data have been derived from functional studies, but recent studies of lymphocyte populations from several

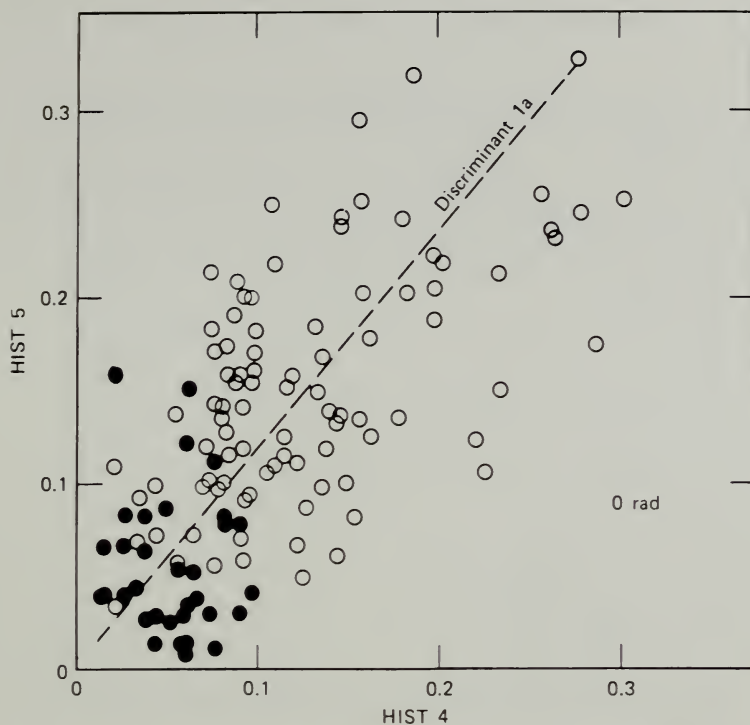


Fig. 6 Distribution of HIST 4 vs. HIST 5 for T cells ( $\circ$ ) and B cells ( $\bullet$ ) from nonirradiated CBA mice.

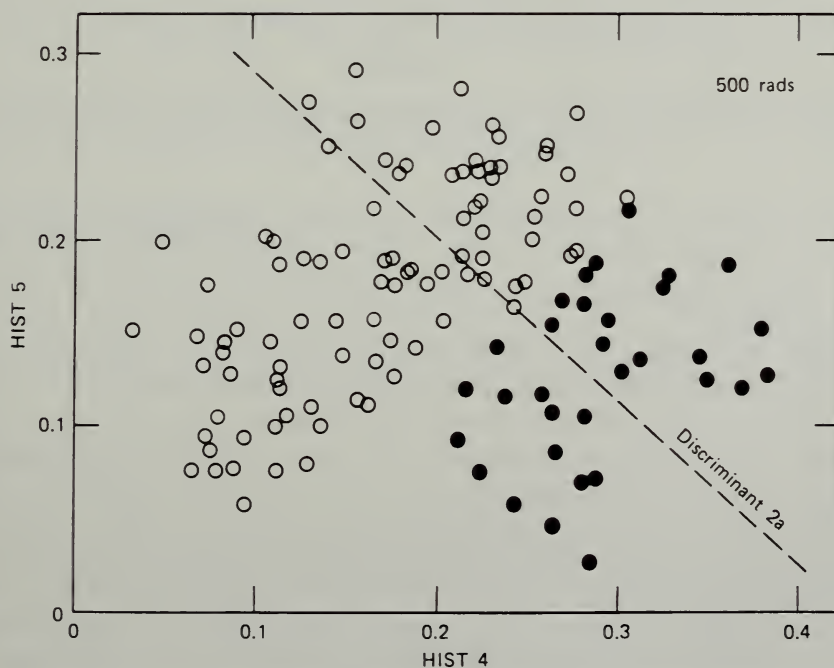


Fig. 7 Distribution of HIST 4 vs. HIST 5 for T cells ( $\circ$ ) and B cells ( $\bullet$ ) from CBA mice after a 500-rad exposure.



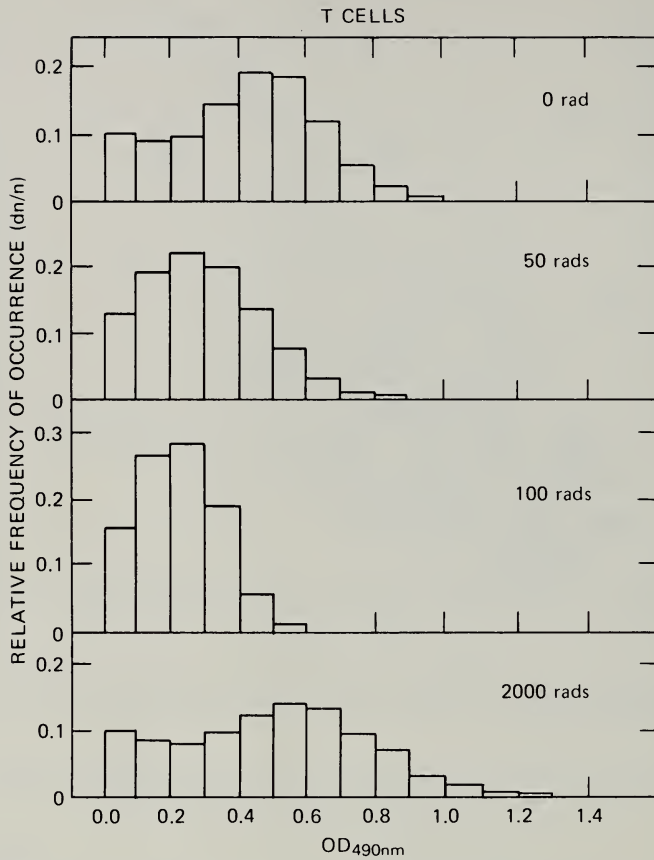


Fig. 8 Distribution of optical-density (OD) values as a function of dose for T cells.

sources evaluated by scanning electron microscopy also appear to support the presence of subpopulations of T cells.<sup>17</sup> We are currently reexamining our data from "pure" populations of T and B cells for the presence of putative subpopulations.

Given the morphologic differences between T and B cells summarized previously, it is not surprising that the two subpopulations also differ in their radiosensitivity. However, the observation that radiation-induced injury of T and B cells is manifested by dissimilar morphologic responses is unexpected. Irradiated B cells develop enlarged nuclei with a more even dispersion of the nuclear chromatin. Eventually vacuoles appear which are readily evident on Wright-Giemsa-stained smears examined in standard fashion. Vacuoles are not evident among irradiated T cells, at least up to 2000 rads. Rather, T cells exposed to small to moderate doses exhibit slight dispersion of their Feulgen-positive nuclear material with little change in nuclear size. At large dosages, T cells developed marked clumping of their Feulgen-positive material with a decrease in nuclear size. An understanding of these differences may permit

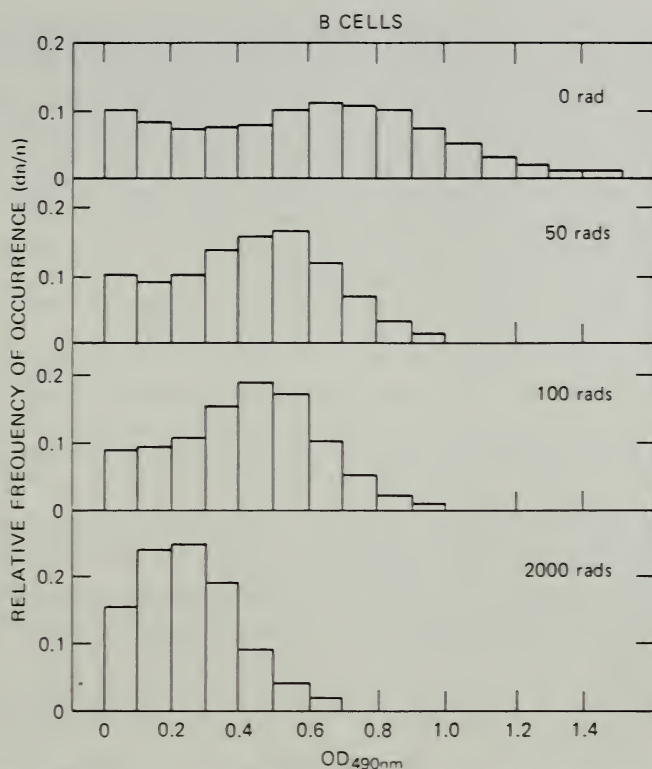


Fig. 9 Distribution of optical-density (OD) values as a function of dose for B cells.

definition of the physical-chemical basis of the marked radiosensitivity of small lymphocytes, particularly with respect to interphase death.

## ACKNOWLEDGMENTS

This research was supported in part by U. S. Public Health Service Grant CA13805, by the Albuquerque Veterans Administration Research Funds, and by a National Institutes of Health Institutional Grant to the University of Arizona.

## REFERENCES

1. S. Stefani and R. Schrek, Cytotoxic Effect of 2 and 5 Roentgens on Human Lymphocytes Irradiated in vitro, *Radiat. Res.*, **22**: 126-129 (1964).
2. R. Schrek, Qualitative and Quantitative Reactions of Lymphocytes to X-Rays, *Ann. N.Y. Acad. Sci.*, **95**: 839-848 (1961).
3. G. Brecher, K. M. Endicott, H. Gump, and H. P. Brawner, Effects of X-Ray on Lymphoid and Hemopoietic Tissues of Albino Mice, *Blood*, **3**: 1259-1274 (1948).
4. R. Schrek, Cytologic Changes in Thymic Glands Exposed in vivo to X-Rays, *Amer. J. Path.*, **24**: 1055-1066 (1948).

5. P. F. Harris, Changes in Thymus and Lymph Node Activity, and Alterations in Bone Marrow Lymphocyte Levels During Recovery of the Guinea-Pig from Whole Body Gamma Irradiation, *Brit. J. Exp. Pathol.*, **39**: 557-573 (1958).
6. E. P. Frenkel, Y. Sugino, R. C. Bishop, and R. L. Potter, Effect of X-Radiation on DNA Metabolism in Various Tissues of the Rat. VI. Correlative Morphologic and Biochemical Changes During the Regeneration of the Thymus, *Radiat. Res.*, **19**: 701-716 (1963).
7. R. Schrek, Dark-Field Observations on Lymphocytes Exposed to X-Rays and Other Injurious Agents, *Proc. Soc. Exp. Biol. Med.*, **64**: 381-384 (1947).
8. R. Schrek, Primary and Secondary Vacuoles in Thymic Cells Exposed in vitro to X-Rays, *J. Cell Comp. Physiol.*, **30**: 203-224 (1947).
9. H. Akaiwa and M. Takeshima, The Reaction of Lymphoid Tissue to Roentgen Radiation, *Amer. J. Roentgenol. Radium Ther.*, **24**: 42-46 (1930).
10. R. E. Anderson, J. Sprent, J. F. A. P. Miller, Radiosensitivity of T and B Lymphocytes. I. Effect of Irradiation on Cell Migration, *Eur. J. Immunol.*, **4**: 199-203 (1974).
11. J. Sprent, R. E. Anderson, J. F. A. P. Miller, Radiosensitivity of T and B Lymphocytes. II. Effect of Irradiation on Response of T Cells to Alloantigens, *Eur. J. Immunol.*, **4**: 204-210 (1974).
12. J. L. Boak and M. F. A. Woodruff, A Modified Technique for Collecting Mouse Thoracic Duct Lymph, *Nature (London)*, **205**: 396-397 (1965).
13. M. C. Raff, M. Sternberg, and R. B. Taylor, Immunoglobulin Determinants on the Surface of Mouse Lymphoid Cells, *Nature (London)*, **225**: 553-554 (1970).
14. R. E. Stowell, Feulgen Reaction for Thymonucleic Acid, *Stain Technol.*, **20**: 45-58 (1945).
15. M. C. Raff, T and B Lymphocytes and Immune Responses, *Nature (London)*, **242**(5392): 19-23 (1973).
16. R. R. Rich and C. W. Pierce, Biological Expressions of Lymphocyte Activation. II. Generation of a Population of Thymus-Derived Suppressor Lymphocytes, *J. Exp. Med.*, **137**: 649-659 (1973).
17. A. Polliack, N. Lampen, B. D. Clarkson, E. DeHarven, Z. Bentwich, F. P. Siegal, and H. G. Kunkel, Identification of Human B and T Lymphocytes by Scanning Electron Microscopy, *J. Exp. Med.*, **138**: 607-624 (1973).

# IMAGE-ANALYSIS TECHNIQUES: SESSION SUMMARY

MORTIMER L. MENDELSON, *Session Chairman*

Biomedical Division, Lawrence Livermore Laboratory, Livermore, California

---

In this session we have been given a brief, broad, and interesting sampling of image analysis as applied to cellular problems. We have seen the multidisciplinary nature of a field that includes applied and theoretical optics, computer science, cytochemistry, cell biology, and much hard engineering. We have been gently introduced to some aspects of machine perception, to the partitioning of scenes, the delineation of objects of interest, and the extraction of relevant parameters. We have discussed the complexities and power of decision making in multidimensional, abstract space. We have been exposed to applications areas in basic biology and in the clinic, and we have had a glimpse of the parallel effort to engineer total systems that have the robustness and versatility to survive effectively in the routine laboratory away from the protective environment that surrounds their one-of-a-kind predecessors.

Biological image analysis is a complex, expensive field that is just reaching the point of giving a return to its investors. With the typical bias of the overcommitted, those of us in the field are fascinated by its open-ended potential. We are convinced that machines have a major perceptive role in biology as well as in many other human pursuits. I would like to share some of our optimism with you by reviewing briefly the kinds of applications we envisage in biology and medicine.

## ROUTINE TASKS

The easiest roles for man to accept for a perceptive machine are enumeration and similar tedious, uninspiring, mundane, simple-minded tasks. The human technician knows how to do these jobs, but the technician is expensive, restless, and distractable; more often than not his counting is unreliable or statistically inadequate. A good example is the routine differential blood count, a procedure



done by the millions each year across the United States. Now machines, some commercially available and some about to become available, can identify and count the major types of white blood cells, can carry the differential count to numbers that for the first time are statistically meaningful, and can do this economically in the context of a clinical hematology laboratory. Some of these machines are image analyzers, and some are flow analyzers. They are prototypes for a general class of machines that will soon be counting biological particles, bacteria, colonies, and cells under a wide variety of circumstances.

## QUANTITATIVE TASKS

We seldom measure anything without some form of mechanical assistance, but we may find it difficult to accept the fact that perceptive machines can make optical measurements more effectively and quantitatively than can the human. Machines can now measure platelet volume, the distribution of red-cell diameters, or the motility of sperm with speed and consistency far exceeding human capacity. Perhaps more importantly the machines can do quantitative photometry, a capability the human eye does not have. Thus, with appropriate staining reactions or with natural chromophores, the photometrically perceptive machine can measure the amount of hemoglobin in a red cell, the DNA in a chromosome, or the cytochromes in a mitochondria. There are many examples of such applications, including a variety of measurements of the blood film, size and shape measurements of sperm, bacterial measurements, mitochondrial sizing, radiographic and electron-microscopic measurements, grain counting, chromosome and chromosomal-band measurements, cell-cycle analysis, and many more.

## COMPLEX TASKS

Man has difficulty with some perceptive problems because of the amount of data involved or the transformation required. Two related examples are neuron tracking and three-dimensional reconstruction. We easily identify neurons in single sections, and we may even be able to reconstruct and mentally visualize the image of a particular neuron as it traverses several sections. But our capacity to do this is severely limited and is unequal to the neuroanatomist's need for the delineation of detailed neuronal connections. Computer systems can work interactively with the anatomist by storing his decisions and later displaying the results in a coherently integrated format. The machines can even do the entire job on their own by carrying out the necessary recognition to track neurons and using memory and intelligence to assemble the results at the end. Similarly, for many problems in neuroanatomy and other fields, it is desirable to expand a series of two-dimensional views into a three-dimensional whole and to

be able to rotate the three-dimensional image to any orientation. Such techniques are now being used for macromolecules, subcellular architecture, tissue anatomy, and even radiographs of entire organs.

## SOPHISTICATED TASKS

Finally, there is a large area which for want of a better term I am going to call "sophisticated tasks". These are the tasks of the large comprehensive systems and include those intriguing and humbling examples where the artificial intelligence of perceptive machines can see things we cannot see or have not yet learned to see for ourselves. The distinction of T and B cells is a case of such perception, and I would not be surprised if a similar approach soon teaches us to identify cells in S and G<sub>2</sub> on the basis of their anatomical features. I use the word "teach" advisedly because man should be able to learn some of this perception from the machine. Sometimes the recognition task becomes trivial once we learn to make the proper association. The Barr body, for example, was seen for a century before the correlation was made between it and the sex of the cell. This relationship was discovered by a man, but, when machines have good optical information and are routinely using multiparametric analysis and the kind of decision capability Peter Bartels talked of, we should soon have many examples of such discoveries being made by machine.

Comprehensive systems are the foundation for the creativity and productiveness of machine perception, but such systems require large commitments of human and material resources, and their optimal development and deployment can be a very difficult problem. Consider, for example, the machines for chromosomal karyotype analysis under development in over a dozen laboratories around the world. In the early 1960s when this effort began, the goal of the karyotyping machines was to classify human chromosomes into the 10 subgroups that were then identifiable by man on the basis of chromosomal size and shape. By 1970 the technology had developed to a point where two groups in the United States were offering machine-done karyotype analysis on a commercial basis. But then Caspersson discovered banding in human chromosomes and suddenly cytogeneticists everywhere could identify all the chromosomes and readily classify them into 24 groups. Overnight the machines that in aggregate took millions of dollars to develop became obsolete, in part because the cytogeneticist's specifications changed and in part because his need for machine assistance changed. As good as our machines may be, they are far from having the flexibility of the human observer. The very characteristics that make a complex mechanical system stable enough to survive in the field also prevent it from rapidly adapting to new biological and technical developments.

Yes, our machines are cumbersome, inflexible, expensive, obtuse, and sometimes cantankerous, but they are also increasingly perceptive and should be

playing an expanding role in biology and medicine. The immediate tasks are in exfoliative cytology, hematology, cytogenetics, biological dosimetry, and radiographic and cellular diagnosis. Probes are now available for specific enzymes, molecular orientation and mobility, cell-surface markers, antigens, physiological indicators such as redox potential, many biochemical constituents, and even for subcellular elemental analysis across the entire Periodic Table. These probes, coupled to an increasingly intelligent artificial intelligence, give an enormous promise of things to come. The effective application of this armamentarium requires the insight and cooperation of the potential user community, and I would hope that if and when you are faced with some monstrous, mysterious, maybe even ego-shattering machine you will do your best to work with it and treat it as fairly as you can.

## SESSION II

### FLOW-SYSTEMS CELL ANALYSIS AND SORTING: OPENING REMARKS

M. A. VAN DILLA, *Session Chairman*

Biomedical Division, Lawrence Livermore Laboratory, Livermore, California

---

I would like to begin this session with a little historical background on the development and biological applications of cell analysis and sorting by high-speed flow-systems methods. Cell analysis is part of the broader field of particulate analysis, to which engineers interested in mine dusts and industrial aerosols made important contributions in the 1940s and 1950s. F. T. Gucker developed a flow-systems approach to measuring the size of particles in mine dust which is very similar to the one we are using today. He injected the aerosol into a moving air sheath that entrained a small stream of dust particles flowing one at a time through a light beam. He then looked at the light scattered by each dust particle with a photomultiplier tube and obtained a scatter distribution. Lagerquist in Sweden was the first to count erythrocytes by photoelectric methods. Crosland-Taylor in England used a liquid-sheath flow system with entrainment and photoelectric detection in an improved electronic erythrocyte counter. Hodgkinson in England published a theoretical treatment of light scattering by particles. Then a new technique appeared which was very simple and powerful. Electrical-resistance counting, invented by Wallace Coulter and known as "Coulter counting," came along in the mid-1950s. Because it was simple and convenient, it became the method of choice for a large number of applications. Coulter's original development was carried further by a number of workers in this country and abroad, including Kubitchek at Argonne National Laboratory, Gregg et al. at Western Reserve University, Van Dilla et al. at the Los Alamos Scientific Laboratory, and Grover et al. in Israel. The usefulness and wide applicability of Coulter counting and volume spectrometry led to a reexamination of optical methods, including not only scattering but also absorption and fluorescence of stained and unstained cells. This led to the development of flow microfluorometry in essentially parallel and independent efforts by Van Dilla and a group at Los Alamos Scientific Laboratory, by



Kamentsky et al. at IBM Watson Laboratory (now at Biophysics Systems Inc.) and Memorial Hospital for Cancer and Allied Diseases, New York City, by Sandritter and a group in Freiburg, Germany, and by Göhde and Dittrich and a group in Münster, Germany. These efforts emphasized fluorescent staining; at the same time light scattering and absorption were being examined in much more detail by Mullaney and Brunsting at the Los Alamos Scientific Laboratory, Wyatt at Science Spectrum, Kamentsky et al., and Technicon (concerned with the automation problem associated with white-blood-cell differential determination). These various approaches to cell sensing led to the development of cell-sorting systems. Electronic-cell sorting using the Coulter principle was invented by Fulwyler at the Los Alamos Scientific Laboratory. Sorting triggered by fluorescence sensing was then developed by Hulett et al. at Stanford and extended to multiparameter sorting by Fulwyler and Steinkamp at Los Alamos Scientific Laboratory.

Biological applications are the real motivation for all these developments, and these applications have proliferated in such fields as life-cycle analysis of cell populations, studies of leukocytes and leukemia, mechanism of the immune response, studies of transformation and tumor cells, effects of radiation and drugs on cell-cycle traverse, cell-surface studies, and attempts to automate screening of exfoliative cytology material for cancer cells. The session will give us illustrations of current technological developments and biological applications.

# MULTIPARAMETER CELL SORTING AND ANALYSIS

JOHN A. STEINKAMP

Biophysics and Instrumentation Group, Los Alamos Scientific Laboratory,  
Los Alamos, New Mexico

---

## ABSTRACT

Improved multisensor cell-sorting instrumentation for quantitative analysis and sorting of cells has been developed. Cells stained with fluorescent dyes enter a flow chamber where sensors for cell volume, fluorescence, and light scatter simultaneously measure multiple cellular properties. Cells then emerge in a liquid jet that is broken into uniform liquid droplets. Sensor signals are electronically processed in one of several ways and are displayed as pulse-amplitude frequency-distribution histograms with a multichannel pulse-height analyzer. Processed signals activate cell sorting according to preselected parameters by electrically charging droplets containing cells and electrostatically deflecting them into collection vessels. Examples are given of multiparameter cell analysis and sorting in experiments using cultured mammalian cells, a model mouse-tumor-cell system, and animal leukocytes.

The development of high-speed flow-system cell-sorting methods based on physical and biochemical measurements of single cells has provided a new dimension to biological investigation by making it possible to isolate from a heterogeneous mixture the cells with particular properties.<sup>1-3</sup> Such systems have been used to differentiate and sort human leukocytes on the basis of volume measurement,<sup>4</sup> to isolate antigen-binding cells which are precursors to antibody-producing cells by the use of immunofluorescence,<sup>5</sup> and to analyze and separate cells on the basis of ultraviolet absorption and visible light scatter.<sup>2</sup> Improved instrumentation for separating cells by simultaneous measurement of cell volume, total or two-color fluorescence, and light scatter has recently been developed<sup>6</sup> and has been used to analyze and separate acridine orange-stained human leukocytes on the basis of red fluorescence of cytoplasmic granulation.<sup>7</sup> By the incorporation of several existing analytical techniques, this system permits multiple measurements to be performed on the same cell. Coupled with

cell sorting, multiparameter-analysis methods provide unusual versatility in experimental cell research by measuring and processing several cell characteristics simultaneously and separating cells according to selected combinations of parameters. Cell sorting permits the correlation of machine-measured cell properties with cell morphology and cell enrichment (i.e., concentration of cell subclasses).

This paper describes the cell analysis and sorting techniques made possible with new multisensor instrumentation.<sup>6</sup> Validation of the method is discussed, with examples of multiparameter analysis and cell sorting on the basis of single parameters, ratios, and two-parameter combinations of cell volume, cell surface area, and fluorescence. Examples of multiparameter analysis include (1) CHO cells reacted with fluorescein isothiocyanate-conjugated concanavalin-A and (2) HeLa cells doubly stained for protein and DNA contents. Other examples include (1) normal and tumor (MCA-1) mouse spleen cells sorted on the basis of DNA content, (2) dog leukocytes sorted into lymphocyte, neutrophil, and eosinophil subpopulations on the basis of cytoplasmic granulation, and (3) HeLa cells sorted on the basis of DNA-cell volume relationships.

## INSTRUMENTATION

A comprehensive description of the instrumentation has been given elsewhere.<sup>6</sup> Cells stained with fluorescent dyes that label specific biochemical components are suspended in normal saline and introduced into the flow chamber (Fig. 1) at approximately 500 cells/sec. Cells first pass centrally through a 75- $\mu$ m-diameter cell-volume-sensing orifice (Coulter principle) and then across a fluid-filled viewing region intersecting an argon laser beam (488-nm wavelength), causing fluorescence and light scatter. Cell-volume pulses also can be raised to the two-thirds power to produce signals proportional to cell surface area.<sup>8</sup> Both fluorescence and light scatter are electrooptically measured, the fluorescence sensor being a dual-photomultiplier-tube array that measures total (above 520-nm wavelength) or two-color fluorescence of selectable color-separation regions. Light scatter also can be measured by optically focusing the forward-scattered light onto a photodiode. After optical measurement the liquid stream carrying suspended cells emerges into air as a jet and is broken into uniform droplets (45,000 droplets/sec). Thus cells are isolated into droplets, with approximately 1% of the droplets containing a cell.

Parametric signals from the cell-sensor amplifiers are processed on a cell-by-cell basis as single parameters, ratios (analog pulse divider), and gated single parameters with a multiparameter signal processing unit<sup>6</sup> developed at Los Alamos Scientific Laboratory (LASL). A multichannel pulse-height analyzer accumulates and displays processed signals as pulse-amplitude frequency-distribution histograms. Gated-single-parameter analysis permits the examination of particular subclasses of cells within selectable ranges on different cellular

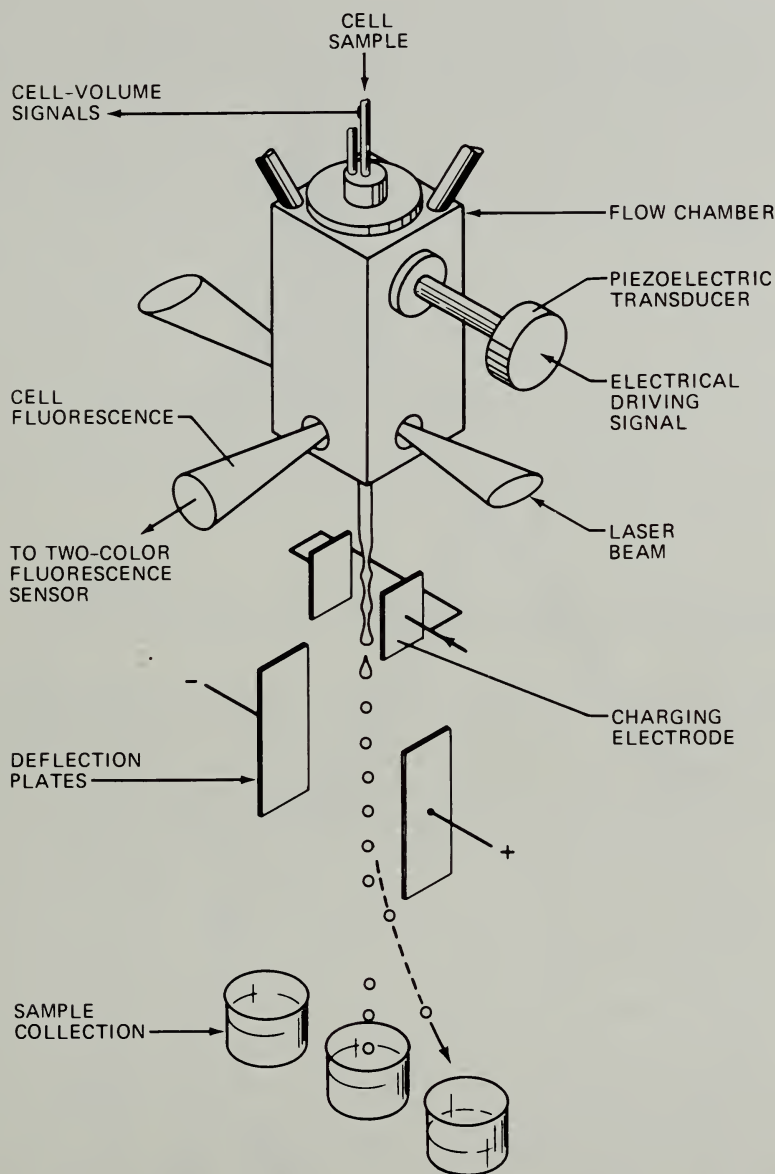


Fig. 1 Multiparameter cell separator illustrating the flow chamber; laser illumination; droplet generation, charging, and deflection scheme; and sample collection.

property values. For example, the volume distribution for  $G_1$  cells can be obtained by analyzing only the processed volume signals from cells determined by fluorescence measurement as yielding  $G_1$  DNA content. That is, only if the DNA-content signal falls within the  $G_1$  DNA-content range (as determined by adjustable signal-amplitude gates) will the associated volume signal be accumu-



lated and displayed. Gated-single-parameter techniques also permit distributions to be obtained from weakly fluorescing signals (e.g., fluorescent antibody) by requiring electronic coincidence with cell-volume, surface-area, or light-scatter signals. In this manner fluorescence signals from debris are eliminated. Complete two-parameter analysis also is available by selecting two processed signals as inputs to a dual-parameter pulse-height analyzer and displaying subsequent three-dimensional pulse-height distributions and two-dimensional contour views.

Processed signals activate cell sorting if the amplitudes fall within preselected ranges of single-channel pulse-height analyzers. An electronic time delay is activated which subsequently triggers a positive or a negative droplet-charging pulse and thus causes a group of droplets containing a cell to be charged and deflected by a static electric field into a collection vessel. The cells not satisfying the sorting criteria pass undeflected into a separate collection vessel. The sorted suspension is introduced into a cytocentrifuge and deposited on microscope slides for counterstaining and microscopic examination.

## EXAMPLES OF MULTIPARAMETER ANALYSIS AND SORTING

Figure 2 shows cell surface fluorescence and surface-area measurements being combined as a surface density function (ratio) to study lectin binding per unit of cell surface area. Gated-single-parameter analysis methods are also used to eliminate signals created by fluorescing debris. Chinese hamster cells (line CHO) reacted with fluorescein isothiocyanate-conjugated concanavalin-A (con A-F)<sup>9</sup> are used to demonstrate these techniques. Figure 2a shows the single-parameter cell volume and cell surface-area distributions for randomly grown CHO cells. Dispersion of the distribution for cell surface area is less than that of the cell-volume plot. This is due to the surface area being proportional to cell diameter squared, whereas cell volume is proportional to cell diameter cubed. Figure 2b shows the distributions for both the single-parameter and gated-single-parameter cell surface fluorescence. Small fluorescent debris is responsible for the high number of background counts to the left side of the ungated fluorescence distribution. These background counts are virtually eliminated by requiring coincidence of cell fluorescence signals with cell surface-area signals by gated-single-parameter methods. This is accomplished by displaying only those fluorescence signals having cell area signals between channels 23 and 40 of Fig. 2a, as illustrated by the shaded region. The resulting distribution of the gated cell surface fluorescence is essentially free from background interference but contains dispersions due to cell-size variability. The correlation of lectin-binding sites to cell surface by ratio analysis is shown in Fig. 2c. The distribution of the gated cell surface fluorescence-to-surface area ratio provides a new method for studying the surface density of lectin-binding sites per unit of cell surface area.<sup>8</sup>

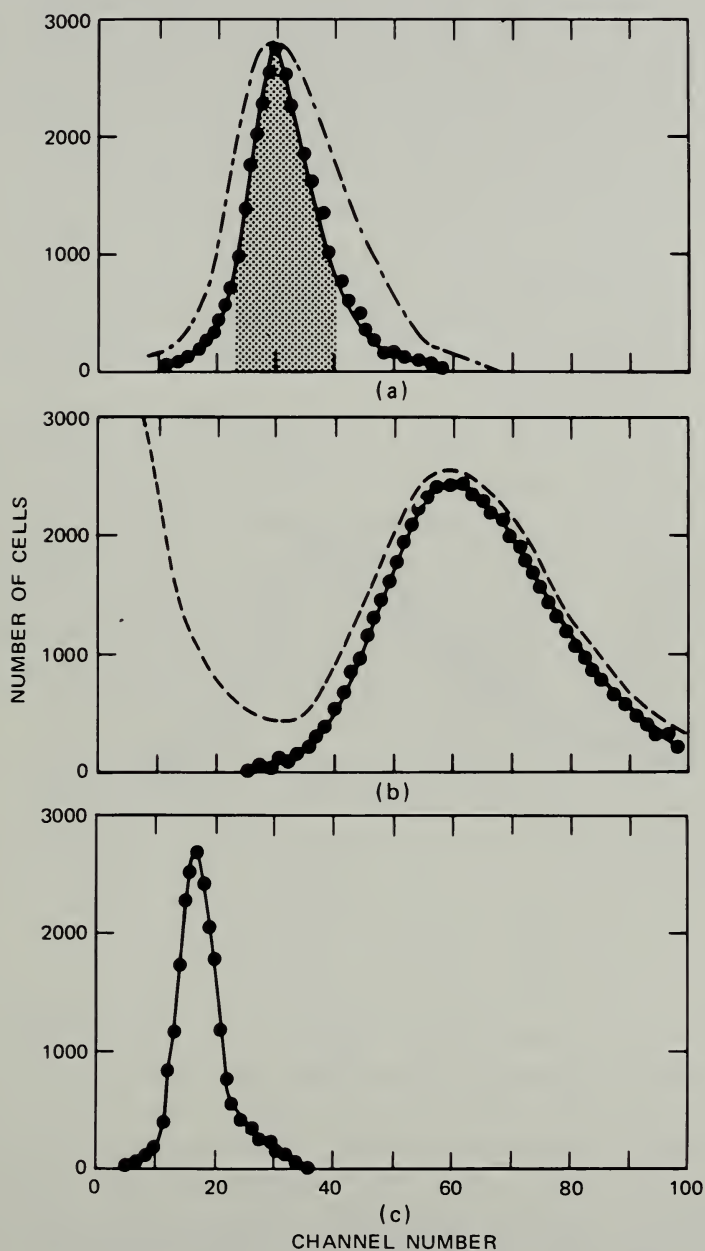


Fig. 2 Frequency-distribution histograms of CHO cells reacted with con A-F. Distributions are shown for (a) cell volume (---) and cell surface area (●); (b) ungated (---) and gated (●) cell surface fluorescence; and (c) gated cell surface fluorescence-to-surface area ratio.

Figure 3 shows single-parameter DNA- and protein-content distributions of HeLa cells doubly stained with propidium iodide (DNA) and fluorescein isothiocyanate (protein),<sup>10</sup> illustrating two-color fluorescence analysis. The distributions for the cell volume and the protein-to-cell volume ratio are also shown. The DNA-content distribution (Fig. 3a) shows two peaks: the first peak represents  $G_1$  cells, and the second peak,  $G_2 + M$  cells having twice the DNA content. Cells synthesizing DNA (S phase) lie in the region between the peaks. The coefficient of variation for  $G_1$ -phase cells is about 4.5%. The protein and cell-volume distributions (Fig. 3b) are broad, unimodal, and typical of a cell population in exponential growth. The distribution of the protein-to-cell volume ratio shown in Fig. 3c is unimodal (the coefficient of variation is near 6%) and shows the high degree of correlation between protein content and cell volume as measured on a cell-by-cell basis.

Complete two-parameter analysis of DNA-protein content relationships is demonstrated in Fig. 4, which shows a three-dimensional frequency-distribution histogram (isometric view) and a two-dimensional contour view that is a base-plane sectional view of the isometric display. The contour view shows the correlation of DNA and protein around the cell cycle, with additional fine structure capable of being observed with this type of analysis. Two-parameter analysis also provides a method to quantitate the number of cells within a given range of two cellular properties and permits cell-cycle-dependent events to be studied. This method has recently been used to demonstrate these relationships on other cultured mammalian cell lines.<sup>10</sup>

Figure 5 shows the DNA-content distributions for normal mouse spleen and methylcholanthrene-induced mouse tumor (MCA-1) cells<sup>11</sup> prepared and stained with acriflavine by the fluorescent-Feulgen procedure.<sup>12</sup> The mouse-spleen-cell DNA distribution (Fig. 5a) provides an indication for normal 2C diploid DNA content. The DNA distribution of MCA-1 tumor cells (Fig. 5b) shows three peaks: the first peak represents cells with a normal 2C diploid DNA content, and the second and third peaks represent cells with 4C and 8C DNA contents, respectively. The tumor-cell population was sorted on the basis of DNA content into two groups, designated by sort regions 1 and 2 (Fig. 5b). Figure 5c is a photomicrograph of dispersed and counterstained tumor cells prior to sorting. Cells with normal DNA content from sort region 1 are leukocytes (Fig. 5d), whereas cells with an elevated or abnormal DNA content from sort region 2 are tumorigenic cells (Fig. 5e), the two subpopulations being morphologically distinct. The second and third peaks of Fig. 5b are  $G_1$  and  $G_2 + M$  phase tumor cells, with S phase cells between the peaks. These results have been verified for MCA-1 tumor cells cultured *in vivo* and *in vitro*.<sup>11</sup>

The red- and green-fluorescence pulse-amplitude distributions of normal dog (beagle) leukocytes vitally stained with acridine orange<sup>13</sup> are shown in Fig. 6. The green-fluorescence distribution (Fig. 6a) is unimodal, illustrating uniform nuclear staining, whereas the red-fluorescence distribution (Fig. 6b) shows three distinct peaks, characterizing dog leukocytes primarily into three subpopulations

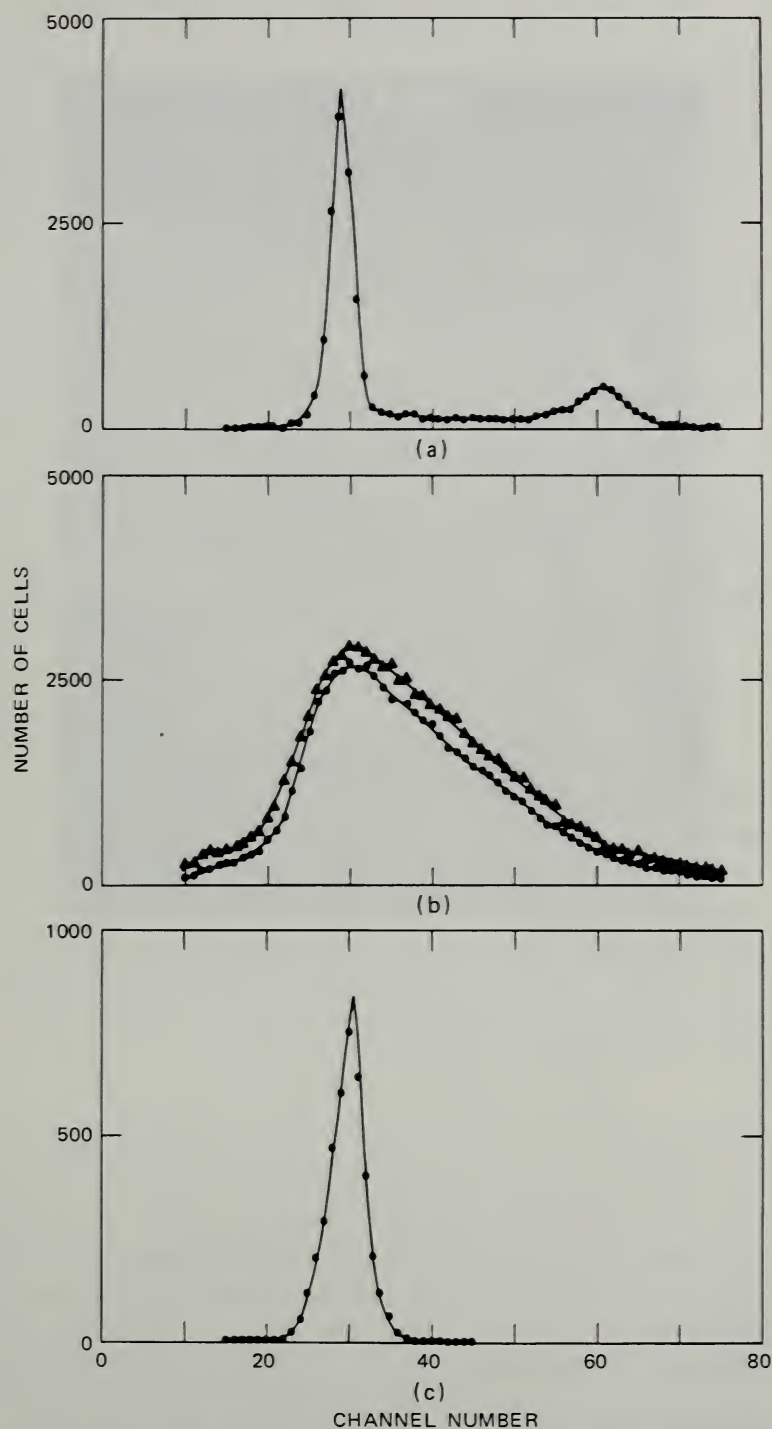


Fig. 3 Frequency-distribution histograms of HeLa cells doubly stained with propidium iodide (DNA) and fluorescein isothiocyanate (protein). Distributions are shown for (a) DNA content (red fluorescence); (b) protein (▲) and cell volume (○); and (c) protein-to-cell volume ratio.



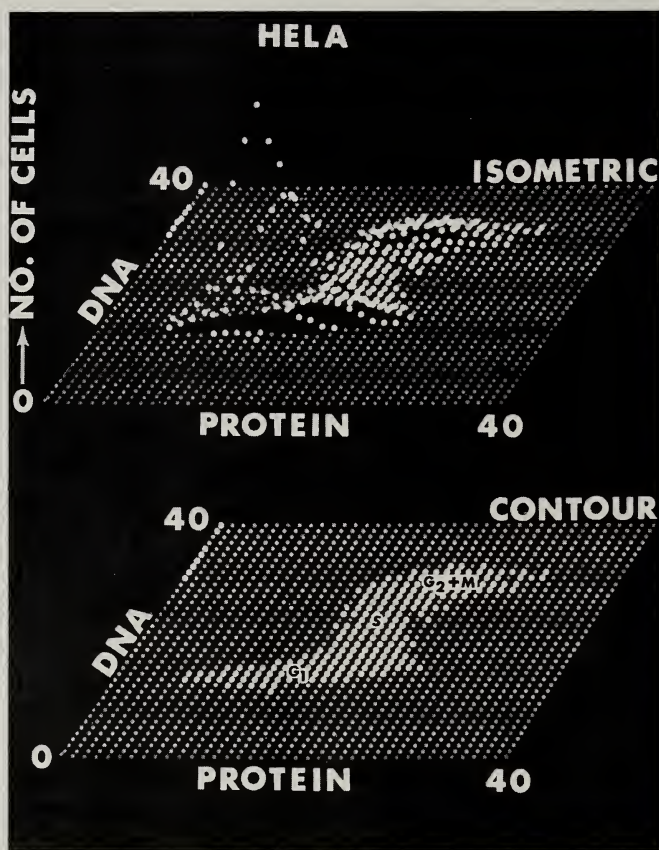


Fig. 4 Two-parameter DNA-protein frequency-distribution histogram (isometric view) and contour view of HeLa cells stained with fluorescein isothiocyanate (protein) and propidium iodide (DNA). The contour view was recorded near the zero-cell-number level.

on the basis of cytoplasmic granules that exhibit red fluorescence. Leukocytes having red-fluorescence signal amplitudes corresponding to sort regions 1, 2, and 3 (Fig. 6b) were separated, counterstained, and identified by microscopic examination as principally consisting of lymphocytes, neutrophils, and eosinophils, respectively. Figures 6d to 6g are photomicrographs of the blood smear and sorted leukocyte fractions. Eosinophils are characterized by coarse cytoplasmic granules compared to finer (dustlike) granulation in lymphocytes and neutrophils as exemplified in the red-fluorescence distribution. Dog leukocytes were also characterized on the basis of measurements of green-to-red-fluorescence ratio (Fig. 6c). Leukocytes having ratio signal amplitudes corresponding to sort regions 4, 5, and 6 were separated and identified as eosinophils, neutrophils, and lymphocytes, respectively.

Cell analysis and sorting on the basis of two parameters are demonstrated by using acriflavine-Feulgen-stained HeLa cells.<sup>12</sup> Single-parameter DNA-content

and cell-volume distributions were first recorded (Fig. 7a), as was the DNA-cell volume two-parameter plot (Fig. 7c). The DNA-content and cell-volume distributions are similar to those in Fig. 3. Figure 7c shows a three-dimensional DNA-cell volume distribution (isometric view) and a two-dimensional contour view. The contour display illustrates the correlation of DNA content and cell volume around the cell cycle.

By use of gated-single-parameter analysis methods, the individual  $G_1$  and  $G_2 + M$  cell-volume distributions were next recorded (Fig. 7b) by analyzing the volume of cells having  $G_1$  and  $G_2 + M$  DNA content, respectively (channels 25 to 33 and 58 to 70 of the DNA distribution). Equal numbers of cells were then sorted into two groups, designated by sort regions 1 and 2 (Fig. 7b). This resulted in the collection of small-volume  $G_1$  and large-volume  $G_2 + M$  cells. The two subpopulations were mixed together and rerun through the cell sorter, and the DNA-cell volume two-parameter distribution was recorded (Fig. 7d). The two-parameter DNA-cell volume distribution of the combined sorted populations vividly illustrates this method of cell sorting and provides additional capability to measure quantitatively and to characterize cell properties on the basis of two or more parameters.

## CONCLUSIONS

We have presented several examples of analysis and sorting of mammalian cells on the basis of single- and two-parameter combinations of cell volume, cell surface area, and total or two-color fluorescence. Multiparameter signal processing, coupled with cell sorting, provides a versatile and extremely useful method for cell biology research, with the range of applications expanding as new methods of obtaining information on cells become available. In principle, other cell-sensing and analysis methods may give meaningful information on physical and biochemical cellular characteristics since both instrumental development and biological applications are in initial stages of growth.

## ACKNOWLEDGMENTS

I thank H. A. Crissman and P. M. Kraemer for cell preparation and staining; P. K. Horan for growing of MCA-1 tumor cells and subsequent staining; A. Romero for cell counterstaining; Julia Grilly for photomicrography of sorted cells; and L. M. Holland for obtaining animal blood samples. The MCA-1 tumor was obtained from the Laboratory of Pathology, National Cancer Institute of the National Institutes of Health, Bethesda, Md.

This work was performed at the Los Alamos Scientific Laboratory, Los Alamos, N. Mex., under the joint sponsorship of the U. S. Atomic Energy Commission and the National Cancer Institute.

(Text continues on page 75.)

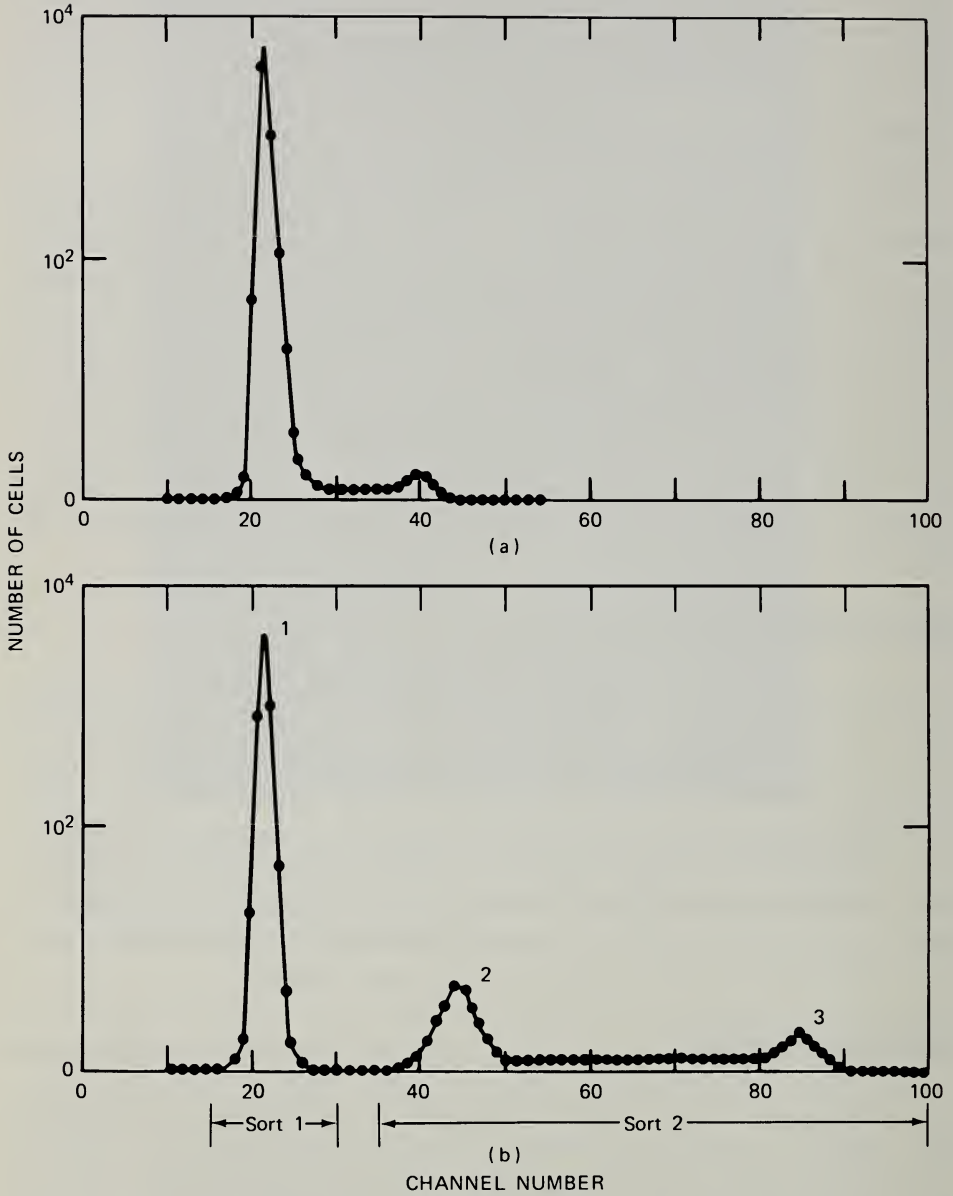


Fig. 5 Frequency-distribution histograms of acriflavine-Fuelgen-stained mouse (C3H/HeJ) spleen and MCA-1 tumor cells. DNA-content distributions are shown for (a) normal spleen cells and (b) MCA-1 tumor cells. Both DNA content distributions (a) and (b) were measured at the same fluorescence channel-amplifier gain setting.

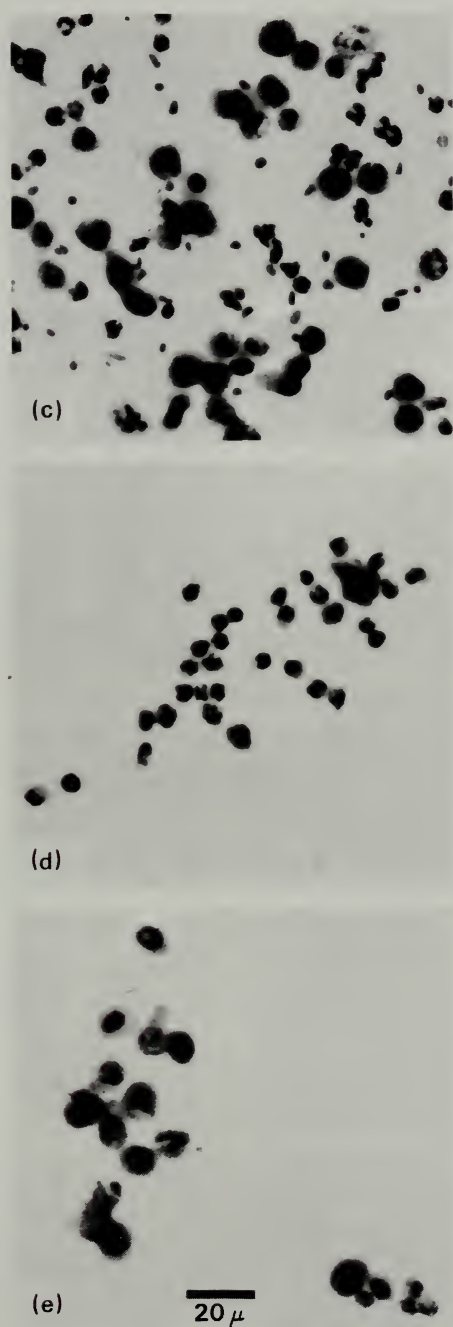


Fig. 5 (Continued). Photomicrographs for (c) dispersed tumor cells prior to sorting; (d) sorted mouse leukocytes of sort region 1; and (e) sorted tumorigenic cells of sort region 2.



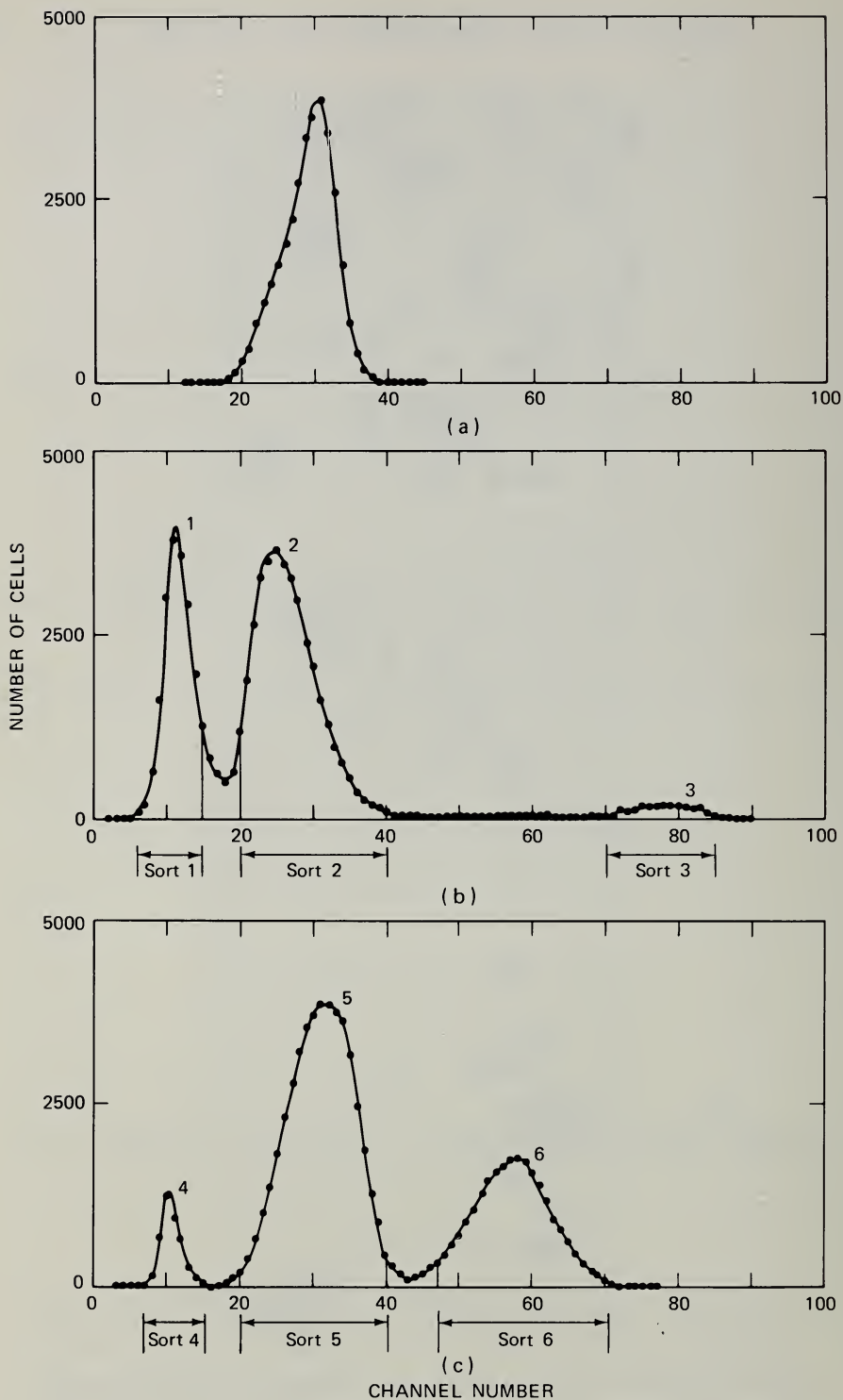


Fig. 6 Frequency-distribution histograms of acridine orange-stained normal dog (beagle) leukocytes: (a) green-fluorescence distribution; (b) red-fluorescence distribution; and (c) green- to red-fluorescence ratio distribution.

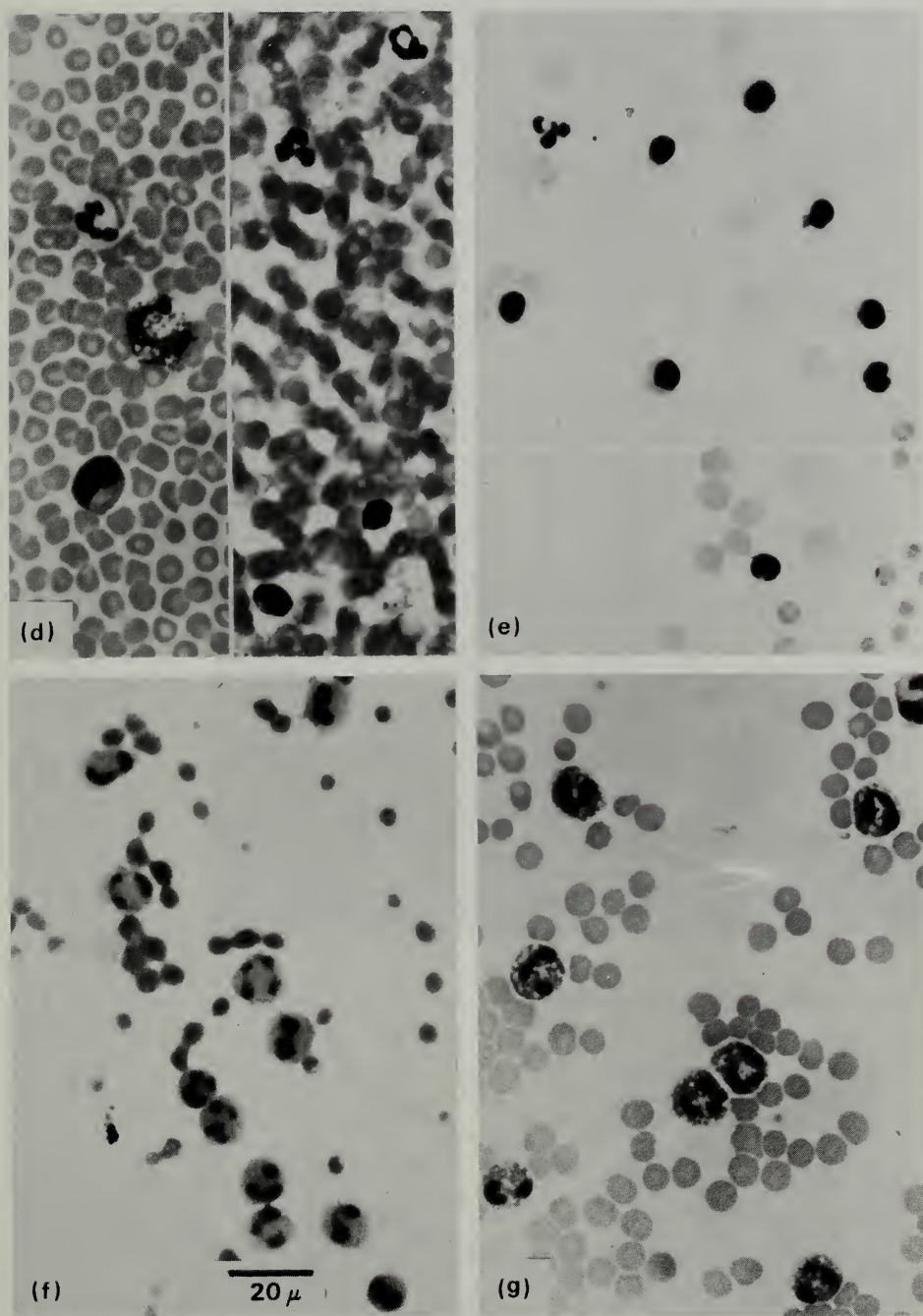


Fig. 6 (Continued). Photomicrographs for (d) blood smear prior to sorting; (e) sorted lymphocytes; (f) sorted neutrophils; and (g) sorted eosinophils. Erythrocytes in the photomicrographs were separated along with selected leukocytes.

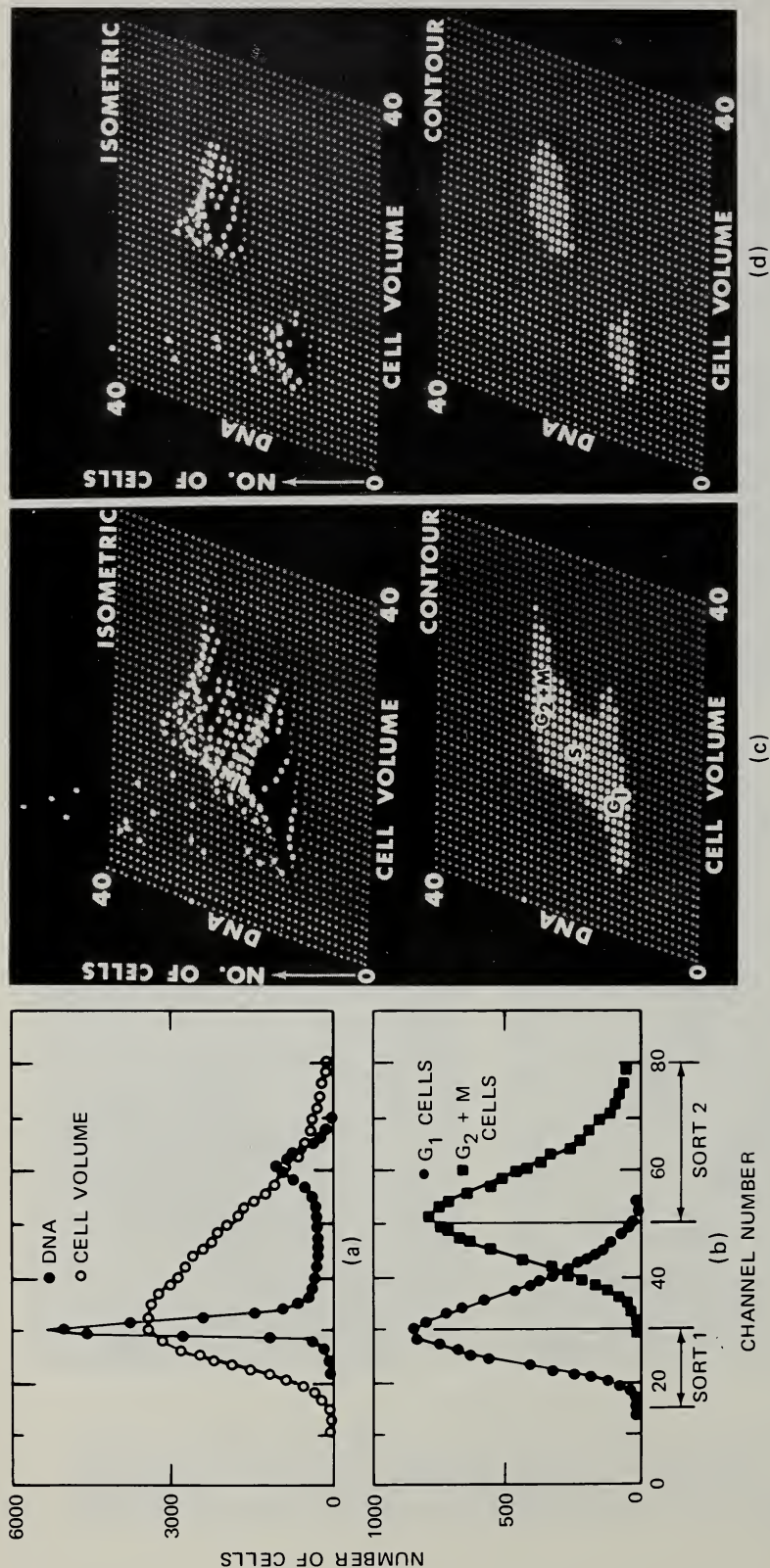


Fig. 7 Frequency-distribution histograms of acriflavine-Feulgen-stained HeLa cells: (a) DNA-content ( $\bullet$ ) and cell-volume ( $\circ$ ) distributions; and (b) cell-volume distributions of  $G_1$  ( $\bullet$ ) and  $G_2 + M$  ( $\blacksquare$ ) cells obtained by gated-single-parameter analysis. Two-parameter DNA-cell volume plots illustrate (c) three-dimensional isometric and two-dimensional contour views of cells prior to sorting and (d) cells reanalyzed after sorting. The contour views were recorded near the zero-cell-number level.



## REFERENCES

1. M. J. Fulwyler, Electronic Separation of Biological Cells by Volume, *Science*, **150**: 910-911 (1965).
2. L. A. Kametsky and M. R. Melamed, Spectrophotometric Cell Sorter, *Science*, **156**: 1364-1365 (1967).
3. H. R. Hulett, W. A. Bonner, J. Barrett, and L. A. Herzenberg, Cell Sorting: Automated Separation of Mammalian Cells as a Function of Intracellular Fluorescence, *Science*, **166**: 747-749 (1969).
4. M. A. Van Dilla, M. J. Fulwyler, and I. U. Boone, Volume Distribution and Separation of Normal Human Leucocytes, *Proc. Soc. Exp. Biol. Med.*, **125**: 367-370 (1967).
5. M. H. Julius, T. Masuda, and L. A. Herzenberg, Demonstration That Antigen-Binding Cells Are Precursors of Antibody-Producing Cells After Purification with a Fluorescence-Activated Cell Sorter, *Proc. Nat. Acad. Sci. U.S.A.*, **69**: 1934-1938 (1972).
6. J. A. Steinkamp, M. J. Fulwyler, J. R. Coulter, R. D. Hiebert, J. L. Horney, and P. F. Mullaney, A New Multiparameter Separator for Microscopic Particles and Biological Cells, *Rev. Sci. Instr.*, **44**: 1301-1310 (1973).
7. J. A. Steinkamp, A. Romero, and M. A. Van Dilla, Multiparameter Cell Sorting: Identification of Human Leukocytes by Acridine Orange Fluorescence, *Acta Cytol.*, **17**: 113-117 (1973).
8. J. A. Steinkamp and P. M. Kraemer, Flow Microfluorometric Studies of Lectin Binding to Mammalian Cells. II. Estimation of the Surface Density of Receptor Sites by Multiparameter Analysis, *J. Cell Physiol.*, **84**: 197-204 (1974).
9. P. M. Kraemer, R. A. Tobey, and M. A. Van Dilla, Flow Microfluorometric Studies of Lectin Binding to Mammalian Cells. I. General Features, *J. Cell. Physiol.*, **81**: 305-314 (1973).
10. H. A. Crissman and J. A. Steinkamp, Rapid Simultaneous Measurement of DNA, Protein, and Cell Volume in Single Cells from Large Mammalian Cell Populations, *J. Cell Biol.*, **59**: 766-771 (1973).
11. P. K. Horan, A. Romero, J. A. Steinkamp, and D. F. Petersen, Detection of Heteroploid Tumor Cells, *J. Nat. Cancer Inst.*, **52**: 843-848 (1974).
12. R. A. Tobey, H. A. Crissman, and P. M. Kraemer, A Method for Comparing Effects of Different Synchronizing Protocols on Mammalian Cell Cycle Traverse. The Traverse Perturbation Index, *J. Cell Biol.*, **54**: 638-645 (1972).
13. L. R. Adams and L. A. Kametsky, Machine Characterization of Human Leukocytes by Acridine Orange Fluorescence, *Acta Cytol.*, **15**: 289-291 (1971).



# DNA CONTENT IN NORMAL, TRANSFORMED, AND REVERTANT MOUSE CELL LINES

ARTHUR VOGEL, BRAD OZANNE, and ROBERT POLLACK  
Cold Spring Harbor Laboratory, Cold Spring Harbor, New York

---

## ABSTRACT

Revertants of SV40-transformed 3T3 cells have been examined for the chromosome number and the amount of DNA per cell. All classes of revertants have more DNA and chromosomes per cell than 3T3 or SV40-transformed 3T3 cells.

The conversion of a normal cell to a malignant cell is often accompanied by alterations in the chromosome number.<sup>1</sup> Many tumors, either spontaneously arising<sup>2</sup> or induced by carcinogens,<sup>3-5</sup> display karyotypic abnormalities. The acquisition of the ability to grow in vitro is also associated with increases in the chromosome number, and many established cell lines will form tumors when injected into suitable hosts.<sup>6-8</sup> However, the chromosome change is not sufficient for tumorigenesis, because nontumorigenic, aneuploid established cell lines exist.<sup>9,10</sup> The mouse fibroblast line 3T3, an example of such an established cell line, has been used as the prototype "normal" cell line in studies of viral oncogenesis.

The growth of normal 3T3 cells is regulated by many environmental factors. They are unable to grow in low concentrations of serum (1%) and require high concentrations of serum for growth.<sup>11,12</sup> They grow to low saturation density in 10% calf serum and must be anchored to a solid substrate to grow.<sup>9,10,13</sup> Transformation by SV40 abolishes some or all of these forms of growth regulation.<sup>12-15</sup> Fully transformed SV3T3 (i.e., 3T3 transformed by SV40 virus) cells grow well in 1% calf serum, grow to high saturation density in 10% calf serum, and form colonies when single cells are suspended in a methyl-cellulose medium.

The SV40 transformation also leads to alterations in other cellular properties. Transformed cells have a SV40-specific intranuclear antigen.<sup>16</sup> Cyclic

AMP concentrations in growing cultures of transformed cells are lower than in similarly growing 3T3 cells.<sup>17,18</sup> Transformants are also more susceptible to agglutination by such plant lectins as concanavalin-A (con-A).<sup>19</sup>

The use of different selection procedures can result in the isolation of variant sublines from populations of SV3T3 cells that have reverted to a 3T3-like state.<sup>20-26</sup> Revertants are isolated by plating transformed cells in conditions that support the growth of transformants only and then adding a drug to kill dividing cells. The revertant cells are unable to divide and therefore survive the selection procedure. Various classes of revertants have been isolated (Tables 1 and 2): Density revertants are selected to have a low saturation density in excess serum concentrations. They are isolated by plating transformed cells at high density in 10% calf serum and adding FUDR, BUdR, or colchicine to kill the cells capable of dividing in dense culture<sup>20,22,25-26</sup> (Table 1). Serum revertants are selected to be unable to grow in 1% calf serum or in 10% agamma-depleted calf serum<sup>26</sup> (Table 1). Sublines resistant to con-A are isolated by exposing transformed cells to high concentrations of con-A.<sup>21,23-24</sup> Some of these survivors have altered growth properties. Revertants isolated in different ways have unique growth properties. In particular, selection for reversion in one growth property does not necessarily result in reversion in all growth properties (Table 3).

Chromosome studies have been performed on transformed and revertant cell lines to further investigate the relationship between alterations in growth control and karyotypic changes. A common finding among revertants is an increase in chromosome number compared to the transformed parents.<sup>22,27-29</sup> The revertants contain more chromosomes than the subtetraploid number found in

TABLE 1  
ISOLATION OF REVERTANTS OF SV40-TRANSFORMED 3T3 CELLS\*

Type of revertant	Growth conditions		Selective agent
	Cell density	Serum concentration	
Density	Dense	10%	FUDR
Density	Dense	10%	BUdR and ultraviolet light
Density	Dense	10%	Colchicine
Serum	Sparse	1%	BUdR and ultraviolet light
Serum	Sparse	10% agamma depleted	BUdR and ultraviolet light
Con-A resistant	Subconfluent	10%	Con-A

\*Transformed cells were plated in the conditions described and treated with various agents toxic to growing cells.

TABLE 2  
GROWTH PROPERTIES OF REVERTANT CELL LINES\*

Line	Anchorage Growth in Methocel†	Density Saturation density in 10% calf serum, 10 <sup>4</sup> (cells/cm <sup>2</sup> )	Serum	
			Doubling time, hr	
			1%	10%
3T3	0.001	5	85	21
SV101	20	>45 (peels)	30	16
Density revertants				
FlSV101	0.01	9	36	25
BuSV2	0.02	13	50	22
ColSV4	0.07	14	>100	24
Serum revertants				
LsSV2	0.04	12	>120	22
AγSV5	11	10	>120	21
Con-A revertant				
CA <sup>r</sup> 32	0.005	10	36	22

\*Cells were inoculated at  $0.1$  to  $0.2 \times 10^4$  cells/cm<sup>2</sup> in 1 or 10% calf serum, and the number of cells per plate was determined daily by trypsinization and counting on a Coulter counter. The medium was changed every 3 days in all growth determinations.

†For Methocel growth,  $10^5$ ,  $10^4$ ,  $10^3$ , and  $10^2$  cells were plated in 4 ml of Methocel medium and incubated for 21 days with 4 ml of fresh Methocel medium added every week.<sup>2,5</sup> Only colonies larger than 0.2 mm in diameter were scored.

3T3 cells or SV40-transformed 3T3 cells. Using the Los Alamos flow microfluorometer, we have found that the revertants also contain more DNA than the transformed parent.<sup>2,5</sup>

## GROWTH PROPERTIES OF REVERTANTS

Lines of SV40-transformed 3T3 cells differ from 3T3 cells in many of their growth properties (Fig. 1 and Table 2). Revertants of SV3T3 cells have lost some or all of these transformed growth properties, and these sublines show varying combinations of normal and transformed phenotypes (Fig. 1 and Tables 2 and 3).

Density revertants isolated with FUDR (FlSV101) or BUdR (BuSV2) grow to low saturation density in 10% calf serum and cannot form colonies in Methocel. However, they grow in 1% calf serum with a doubling time similar to SV3T3 cells (Fig. 1 and Table 2). Thus these variant sublines have reverted in only two of the three transformed growth properties. The con-A revertant CA<sup>r</sup>32 is also reverted in its density and anchorage properties but not in its

TABLE 3  
GROWTH PROPERTIES OF REVERTANT CELL LINES  
ISOLATED FROM SV40-TRANSFORMED 3T3 CELLS

Line	Saturation density*	Serum requirement†	Anchorage requirement‡
3T3	Normal	Normal	Normal
SV101	Transformed	Transformed	Transformed
Density revertants selected with			
FUDR	Normal	Transformed	Normal
BUDR	Normal	Transformed	Normal
Colchicine	Normal	Normal	Normal
Con-A revertant CA <sup>r</sup> 32	Normal	Transformed	Normal
Serum revertants selected in			
1% calf serum	Normal	Normal	Normal
A $\gamma$ -depleted calf serum	Normal	Normal	Transformed

\*Normal cells have saturation densities less than  $15 \times 10^4$  cells/cm<sup>2</sup> in 10% calf serum.

†Assayed by growth in 1% calf serum. Normal cells have doubling times greater than 80 hr; transformed cells double in 35 hr or less.

‡Assayed by ability to form a colony in Methocel. Normal cells do not form colonies in Methocel but transformed cells do.

serum requirement for growth (Table 2). Density revertants isolated with colchicine have reverted in all three growth properties since they also grow poorly in 1% calf serum (Fig. 1 and Table 2).

Two classes of serum revertants exist with respect to these growth parameters. The revertant line selected not to grow in 1% calf serum (LsSV2) has reverted in the other two growth parameters as well. Serum revertant A $\gamma$ SV5, selected for its inability to grow in 10% agamma-depleted calf serum,<sup>30</sup> grows to low saturation density in excess serum but can form colonies in Methocel (Table 2). This line represents a unique class of cells which displays only a transformed anchorage property. Table 3 summarizes the growth properties of the revertants.

## CHROMOSOMES AND DNA CONTENT PER CELL

Diploid mouse-embryo fibroblasts (MEF) contain 40 chromosomes per metaphase. Line 3T3, a continuous cell line derived from mouse-embryo fibroblasts, is subtetraploid and contains a mean chromosome number of



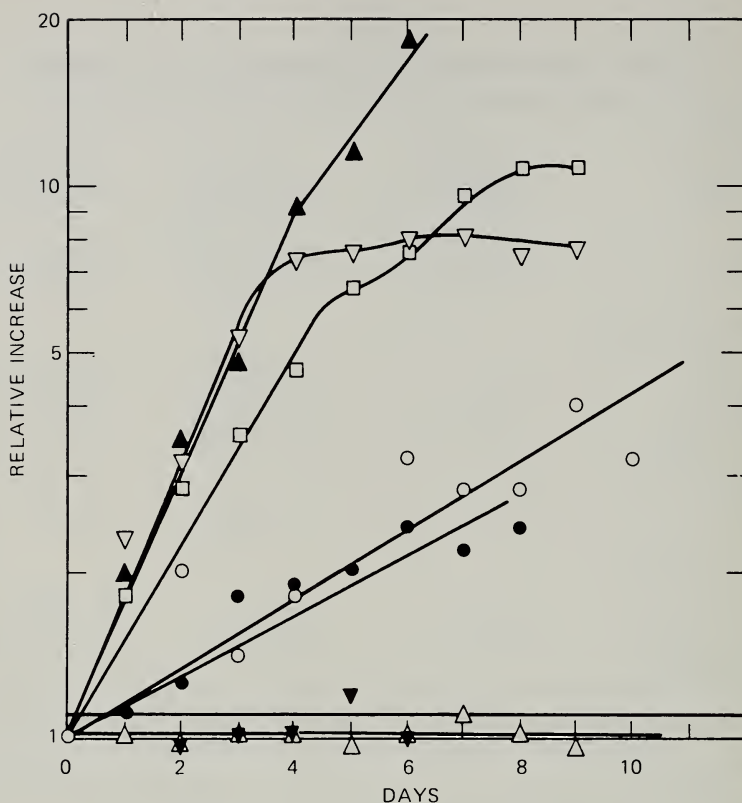


Fig. 1 Revertant growth in 1% calf serum. Growth determinations were done as described in Table 2. ○, 3T3; ▲, SV101; ▽, FLSV101; □, BuSV3; ●, ColSV2; Δ, LsSV2; ▼, AγSV5.

approximately 70 chromosomes per metaphase (Fig. 2 and Table 4). The SV40-transformed 3T3 cells contain the same number of chromosomes per cell as the 3T3 cells. All revertants show an increase in chromosome number per cell (Fig. 2 and Table 4). Such increases can be marked, as in BuSV3 or FLSV101 where the mean value has increased to 95 to 110 chromosomes per metaphase, or they can be slight, as in the colchicine or con-A revertants, where the mean value has increased to 75 to 85 chromosomes per metaphase.

The chromosome increase is accompanied by an increase in DNA content per cell (Table 4). The 3T3 and SV3T3 cells contain approximately three haploid amounts of DNA (Table 4). The DNA measurements were made on individual cells using the Los Alamos flow microfluorometer and cells stained specifically for DNA (acriflavine-Feulgen procedure). The histograms of DNA per cell are shown<sup>31</sup> in Fig. 3. The G<sub>1</sub> peaks are relatively narrow, even for FLSV101, which has more than three times the amount of DNA of a diploid mouse-embryo fibroblast. With a few exceptions the increase in DNA content appears to be directly correlated with the increase in chromosomes (Fig. 4). The line with the

TABLE 4  
MEAN CHROMOSOME NUMBER AND DNA CONTENT  
IN REVERTANT CELL LINES\*

Line	Number of metaphases counted	Mean number of chromosomes	Standard deviation	DNA per cell†
MEF		40		2
3T3	15	68.4	14.5	3
SV101	25	69.6	6.9	3
SV3T3(B)	18	75.9	12.0	3.5
A $\gamma$ 61	31	64.0	20.9	3.0
A $\gamma$ 256	25	58.4	11.8	3.3
Density revertants				
BuSV2	30	98.6	22.9	6.0
BuSV3	28	96.5	20.3	6.0
FISV101	29	111.0	23.2	7
ColSV1	30	83.0	12.5	5
ColSV3	32	78.4	9.4	3.5
Con-A revertants				
CA <sup>r</sup> 30	25	78.8	12.9	5.8
CA <sup>r</sup> 32	28	78.8	16.8	5.8
CA <sup>r</sup> 41	23	84.0	16.7	4.4
Serum revertants				
LsSV1	30	95.7	22.3	4.2
LsSV2	30	94.0	18.3	3.5
A $\gamma$ SV4	30	100.3	12.9	4.7
A $\gamma$ SV5	30	92.6	18.1	4.4

\*Chromosome analysis was done as described in Ref. 27.

†The DNA content per cell was measured on the Los Alamos flow microfluorometer as described in Ref. 25.

most chromosomes per cell, FISV101, also contains the most DNA per cell. Con-A revertants and ColSV1, however, contain five haploid amounts of DNA without manifesting a large increase in chromosome number (Table 4).

This increase in DNA content per cell is specific for the revertant phenotype and is not the result of cells simply surviving the selection procedure. The DNA per cell does not increase in lines surviving BUdR treatment, which still maintain all transformed properties (A $\gamma$ 12d2, A $\gamma$ 61, and A $\gamma$ 256) (Fig. 2 and Table 4). Furthermore, rerevertants of FISV, selected for their ability to form colonies on 3T3 monolayers, have also reverted in their chromosome number to a value similar to the transformed parent line (Fig. 5).

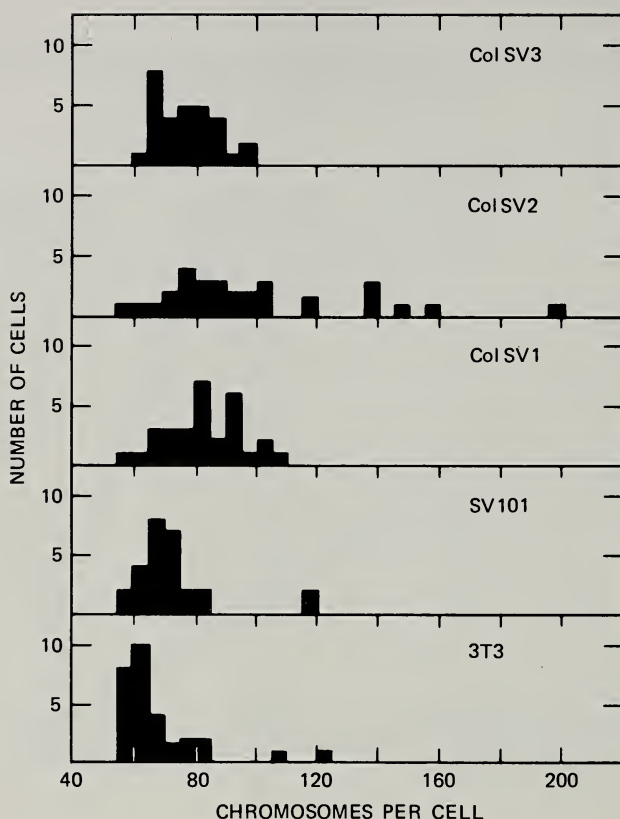


Fig. 2 Chromosomes per cell in various mouse cell lines. Chromosomes were analyzed as described in Ref. 27.

## DISCUSSION

Each revertant has been selected for alteration in a specific growth property, and the selected alteration may or may not be accompanied by reversion in other growth parameters. However, in our hands the reversion process always leads to an increase in DNA, independent of the particular phenotype of the revertant.

These variant sublines are selected for reversion to a more "normal" state of growth control. It is surprising that, in every case, this reversion to a "normal" type of growth control is accompanied by what may be thought of as an "abnormal" increase in the amount of DNA per cell, which in some cases can be very marked (FLSV101). It should be emphasized that a variant line with less DNA per cell than the transformed parent was never found by us, although such variants of polyoma-transformed BHK cells have been reported by others.<sup>28</sup>

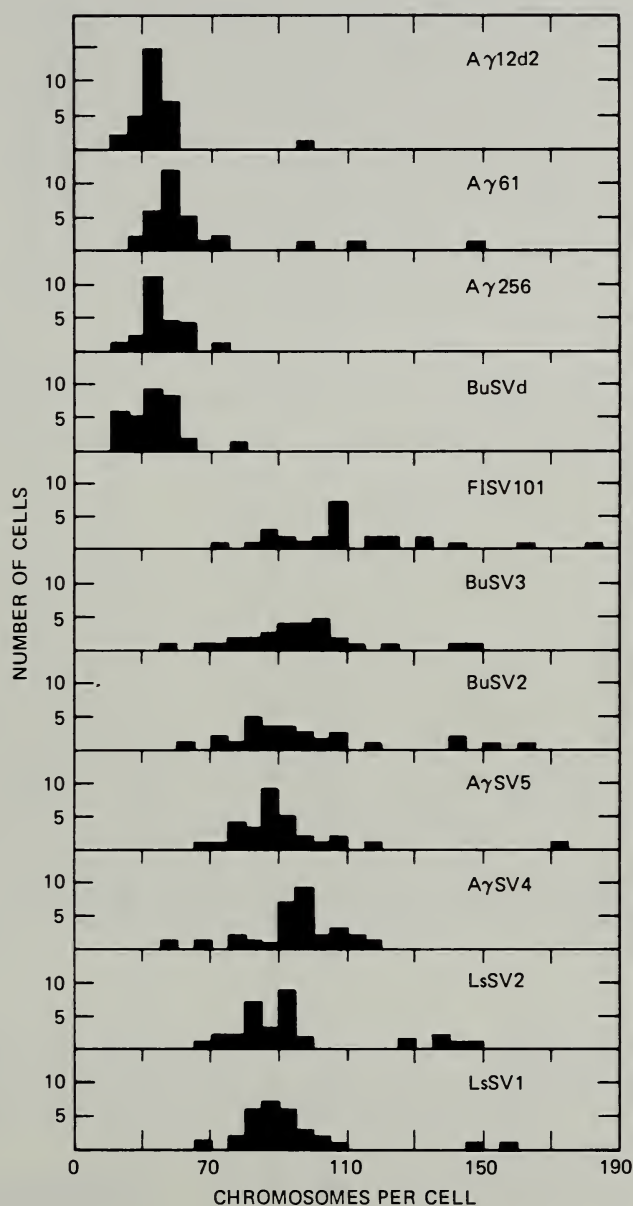


Fig. 2 (Continued).

We as yet do not understand the relationship of the increase in DNA to the reversion process. This phenomenon has been reported in many laboratories.<sup>21-22,25-29</sup> The revertants that we have isolated to date still contain the SV40 genome since they are SV40 T antigen positive and contain SV40 DNA and RNA.<sup>20,25,29,32</sup> It has been difficult to rescue SV40 from the revertants by fusion with permissive monkey cells, but the virus that has been rescued is wild type with respect to its ability to transform 3T3 cells.<sup>24-25</sup> Thus the



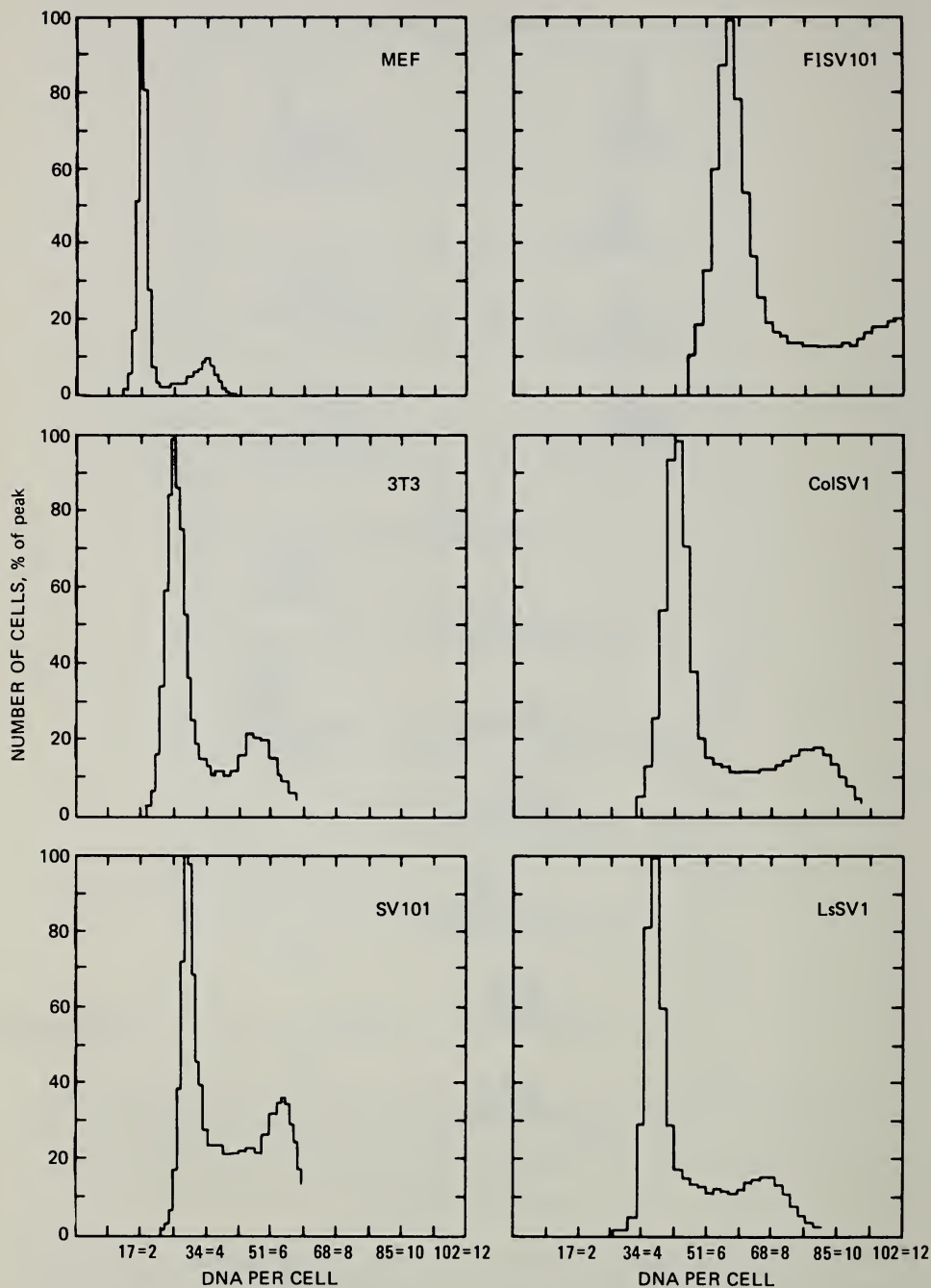


Fig. 3 Histograms of DNA content per cell in normal, transformed, and revertant mouse cell lines. The DNA content is measured in haploid equivalents of cell DNA, relative to mouse-embryo fibroblasts. (From A. Vogel, J.Oey, and R. Pollack, Two Classes of Revertants Isolated from SV40-Transformed Mouse Cells, in Control of Proliferation of Animal Cells, Cold Spring Harbor Laboratory, Cold Spring Harbor, New York, 1974.)

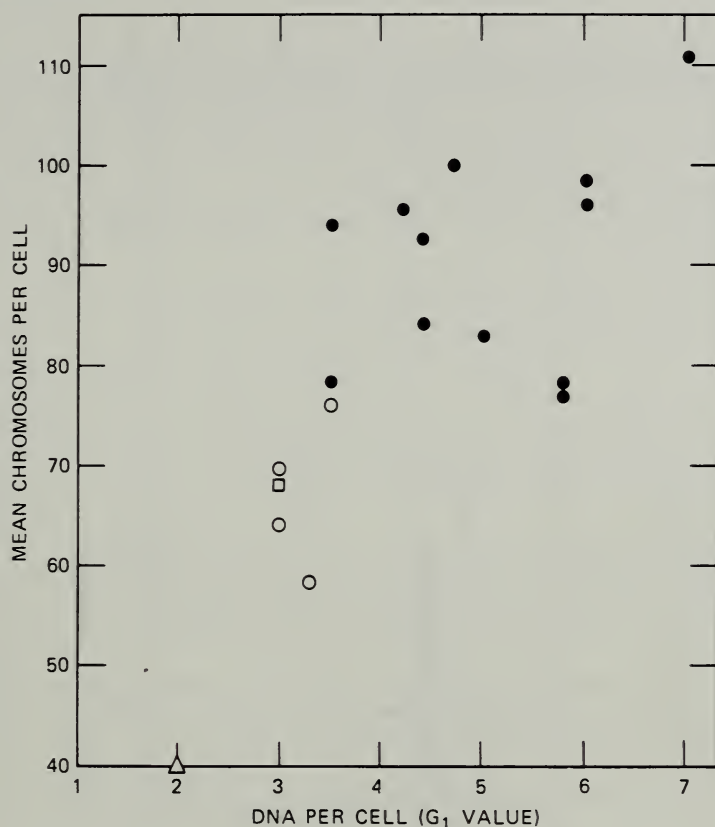


Fig. 4 Chromosomes per cell vs. DNA content per cell. The DNA content is expressed in haploid equivalents of DNA.  $\Delta$ , MEF;  $\square$ , 3T3;  $\circ$ , transformant;  $\bullet$ , revertant.

revertants may represent classes of cells which have managed to overcome the effects of the SV40 still present in these cells. If this is the case, then the increase in DNA may be involved in this cellular alteration.

## ACKNOWLEDGMENTS

We wish to thank Don Petersen of the Los Alamos Scientific Laboratory for allowing us to use the flow microfluorometer and Scott Cramm and Harry Crissman, also of the Los Alamos staff, for their invaluable assistance in running the experiments.

This work was supported by National Institutes of Health grant 1-PO1-CA13106-01 from the National Cancer Institute. Arthur Vogel is supported by National Institutes of Health training grant 5-TO5-GM01668 from the National Institute of General Medical Science.

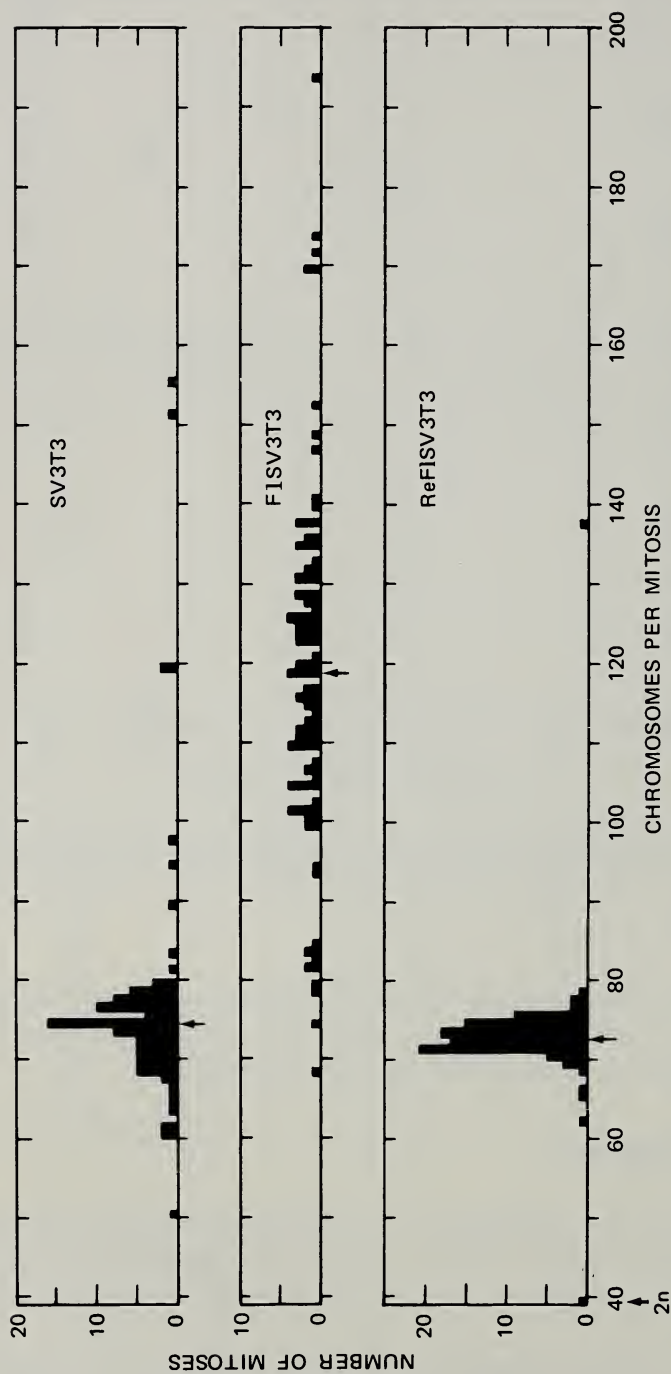


Fig. 5 Chromosomes per cell in SV3T3, F1SV3T3, and a revertant of F1SV3T3.

## REFERENCES

1. P. C. Koller, The Role of Chromosomes in Cancer Biology, in *Recent Results in Cancer Research*, p. 38, Springer-Verlag, New York, 1972.
2. T. S. Hauschka, The Chromosomes in Ontogeny and Oncogeny, *Cancer Res.*, **21**: 957-974 (1961).
3. C. E. Ford, J. L. Hamerton, and R. H. Mole, Chromosomal Changes in the Primary and Transplanted Reticular Neoplasms of the Mouse, *J. Cell. Comp. Physiol.*, **52**: 235-270 (1958).
4. K. E. Hellström, Chromosomal Studies in Primary Methylcholanthrene Induced Sarcomas in the Mouse, *J. Nat. Cancer Inst.*, **23**: 1019-1034 (1959).
5. K. Moriwaki, H. T. Imai, and T. H. Yoshida, Polyploidization and Protein Synthesis in Mammalian Cells, *Jap. J. Genet.*, **44**(Suppl. 1): 71-83 (1969).
6. W. R. Earle and A. Nettleship, Production of Malignancy In Vitro. V. Results of Injections of Cultures into Mice, *J. Nat. Cancer Inst.*, **4**: 213-227 (1943).
7. G. O. Gey, Cytological and Cultural Observations on Transplantable Rat Sarcomata Produced by Inoculation of Altered Normal Cells Maintained in Continuous Culture, *Cancer Res.*, **1**: 737 (1941).
8. A. Levan and J. J. Bieseke, Role of Chromosomes in Cancerogenesis as Studied in Serial Tissue Culture of Mammalian Cells, *Ann. N. Y. Acad. Sci.*, **71**: 1022-1027 (1958).
9. G. Todaro and H. Green, Quantitative Studies on the Growth of Mouse Embryo Cells in Culture and Their Development into Established Lines, *J. Cell. Biol.*, **17**: 299-313 (1963).
10. S. Aaronson and G. Todaro, Basis for the Acquisition of Malignant Potential by Mouse Cells Cultivated In Vitro, *Science*, **162**: 1024-1026 (1968).
11. R. Holley and J. Kiernan, "Contact Inhibition" of Cell Division in 3T3 Cells, *Proc. Nat. Acad. Sci.*, **60**: 300-304 (1968).
12. R. Dulbecco, Topoinhibition and Serum Requirement of Transformed and Untransformed Cells, *Nature*, **227**: 802-806 (1970).
13. P. H. Black, Transformation of Mouse Cell Line 3T3 by SV40: Dose Response Relationship and Correlation with SV40 Tumor Antigen Production, *Virology*, **28**: 760-763 (1966).
14. R. Risser and R. Pollack, A Non-Selective Analysis of SV40 Transformation of Mouse 3T3 Cells, *Virology*, **59**: 477-489 (1974).
15. G. Todaro, H. Green, and B. Goldberg, Transformation of Properties of an Established Cell Line by SV40 and Polyoma Virus, *Proc. Nat. Acad. Sci.*, **51**: 66-73 (1964).
16. P. Black, W. Rowe, H. Turner, and R. Huebner, A Specific Complement-Fixing Antigen Present in SV40 Tumor and Transformed Cells, *Proc. Nat. Acad. Sci.*, **50**: 1148-1156 (1963).
17. J. Otten, G. Johnson, and I. Pastan, Cyclic AMP Levels in Fibroblasts: Relationship to Growth Rate and Contact Inhibition of Growth, *Biochem. Biophys. Res. Commun.*, **44**: 1192-1198 (1971).
18. J. Sheppard, Difference in the cAMP Levels in Normal and Transformed Cells, *Nature (London) New Biol.*, **236**: 14-16 (1972).
19. M. Inbar and L. Sachs, Interaction of the Carbohydrate-Binding Protein Concanavalin A with Normal and Transformed Cells, *Proc. Nat. Acad. Sci.*, **63**: 1418-1425 (1969).
20. R. Pollack, H. Green, and G. Todaro, Growth Control in Cultured Cells: Selection of Sublines with Increased Sensitivity to Contact Inhibition and Decreased Tumor-Producing Ability, *Proc. Nat. Acad. Sci.*, **60**: 126-133 (1968).
21. B. Ozanne and J. Sambrook, Isolation of Lines of Cells Resistant to Agglutination by Concanavalin A from 3T3 Cells Transformed by SV40, *Lepetit Colloq. Biol. Med.*, **2**: 248-253 (1971).



22. L. Culp, W. Grimes, and P. Black, Contact-Inhibited Revertant Cell Lines. I. Biologic, Virologic and Chemical Properties, *J. Cell Biol.*, **50**: 682-690 (1971).
23. L. Culp and P. Black, Contact-Inhibited Revertant Cell Lines Isolated from Simian Virus 40-Transformed Cells. III. Concanavalin A Selected Revertant Cells, *J. Virol.*, **9**: 611-620 (1972).
24. B. Ozanne, Variants of Simian Virus 40-Transformed 3T3 Cells That Are Resistant to Concanavalin A, *J. Virol.*, **12**: 79-89 (1973).
25. A. Vogel, R. Risser, and R. Pollack, Isolation and Characterization of Revertant Cell Lines. III. Isolation of Density Revertants of SV40-Transformed 3T3 Cells Using Colchicine, *J. Cell. Physiol.*, **82**: 181-188 (1973).
26. A. Vogel and R. Pollack, Isolation and Characterization of Revertant Cell Lines. IV. Direct Isolation of Serum-Revertant Sublines of SV40-Transformed 3T3 Mouse Cells, *J. Cell. Physiol.*, **82**: 189-198 (1973).
27. R. Pollack, S. Wolman, and A. Vogel, Reversion of Virus Transformed Cell Lines: Hyperploidy Accompanies Retention of Viral Genes, *Nature*, **228**: 938, 967-970 (1970).
28. S. Hitotsumachi, Z. Rabinowitz, and L. Sachs, Chromosomal Control of Reversion in Transformed Cells, *Nature*, **231**: 511-514 (1971).
29. B. Ozanne, P. Sharp, and J. Sambrook, Transcription of Simian Virus 40. II. Hybridization of RNA Extracted from Different Lines of Transformed Cells to the Separated Strands of Simian Virus 40 DNA, *J. Virol.*, **12**: 90-98 (1973).
30. H. Smith, C. Scher, and G. Todaro, Induction of Cell Division in Medium Lacking Serum Growth Factor by SV40, *Virology*, **44**: 359-370 (1971).
31. A. Vogel, J. Oey, and R. Pollack, Two Classes of Revertants Isolated from SV40-Transformed Mouse Cells, in Control of Proliferation of Animal Cells, Cold Spring Harbor Laboratory, Cold Spring Harbor, New York, 1974.
32. B. Ozanne, A. Vogel, P. Sharp, W. Keller, and J. Sambrook, Transcription of SV40 DNA Sequences in Different Transformed Cell Lines, *Lepetit Colloq. Biol. Med.*, **4**: 176-182 (1974).

# FACTORS AFFECTING THE CHOICE OF CELLULAR SPECIMENS FOR AUTOMATED EXAMINATIONS

M. R. MELAMED

Memorial Hospital for Cancer and Allied Diseases, New York, New York

---

## ABSTRACT

The clinical laboratory requires automation in many areas as diverse as record keeping, specimen preparation, and specimen analysis. In the case of cellular specimens, the design of analytic instruments will be greatly affected both by the type of specimen and by the purpose of the test. Factors that affect the choice of cellular specimens for automated examination are discussed, with comments on the general philosophy of cytology automation.

There are three very different aspects of automation in the laboratory. I would like to mention them briefly, for perspective, though only one of the three concerns us here.

One is record keeping. It may well be that the most urgent, if unglamorous, need in many cytology laboratories is an efficient, automated, probably computerized record-keeping system. Certainly somewhere between a quarter and a half of the cost and space in the laboratory is concerned with records, reports, billing, and quality control with patient follow-up.

A second aspect of cytology automation is in specimen handling, i.e., in specimen collection, selective concentration of certain cell populations, preparation of slides, staining, coverslipping, and labeling or otherwise identifying specimens. Although there is some work in this area and useful machines will probably come from it, I do not think this amounts to more than an improvement in techniques, and it will not substantially alter our way of life.

The third area of cytology automation is what concerns us primarily. I would define it as automated, instrumented cell measurement, cell analysis, and interpretation. I hesitate to use the word "diagnosis" here because I think that means interpretation of cytologic findings within the context of other medical findings and what I am speaking of in cytology automation is perhaps better defined as artificial intelligence.

What do we who are directors of clinical medical laboratories want, need, most from a system that will automatically measure, analyze, and interpret the cellular contents of cytologic specimens? For what *kind* of specimen and what *kind* of test would we like to apply such a system? The tests that we would most like to automate can be described by the following:

First, they are high-volume tests; i.e., in most hospital and outpatient clinical laboratories, these are the tests that are carried out in large numbers and every day. Many are performed routinely on all patients and are frequently repeated.

Second, they are tests which can be done by relatively unskilled personnel and which require little or no judgment and no basic medical training, or even any understanding of the test and its meaning. The laboratory people who perform these tests have the highest rate of absenteeism, the greatest job turnover, and the least reliability. It would be nice to have the option of automation.

The third feature can be summarized simply and inclusively as tests that are unpleasant to perform—not only those which are physically unpleasant or distasteful but also those which are repetitious or tedious and therefore are avoided, when possible, by many of the good laboratory technicians.

Fourth would be tests with limited expected variation of specimen and a limited choice of possible different results or with results that can be expressed numerically. It would not be feasible, for example, to automate the examination of biopsies that may cover multiple sites and an almost infinite range of possible interpretations.

A fifth feature favoring automation for a particular test would be the requirement or the desirability of precise and reproducible results. This probably will be achieved more readily by instrumentation than is possible manually. There is a decided statistical advantage in the use of instrumentation for counting or measuring large numbers of cells.

Finally, I would recommend automation, obviously, for tests that cannot be performed manually or are not performed well. I can predict that we will see new tests devised to exploit new instruments as time goes by, and some of these will be tests that cannot be performed manually. Recently I saw a publication by Dr. Wied and his colleagues describing morphological differences between leukemic and normal lymphocytes that were identifiable by TICAS but not by visual examination. Later Dr. Kamensky and I will describe changes in the vital staining of blood leukocytes during infection which are recognized instrumentally but cannot be perceived manually.

I would like to come back to this final point later because I think it is one that is philosophically of great importance to us.

Conversely, of course, we would not want to automate a test that can be performed rapidly and more easily manually. Again, the interpretation of biopsies would be a good example of the type of test that is not suitable for automation.



So much for the features that describe the kind of tests we would like to automate. Specifically, we can list some of the tests as follows:

At the top of the list, I would put what are commonly called the routine blood counts, and clearly others agree with me if we judge by the effort devoted to the development of instrumentation for this specific purpose in recent years. With or without a differential white cell count, the routine blood count probably is the most frequently requested and performed clinical cytologic examination; thus it meets the first requirement for high-volume usage. Further, for all but a very few special-category patients, the blood counts require very little judgment and relatively little training to perform. They are repetitive and tedious, results can be expressed numerically, and it would certainly be desirable to have precise and reproducible results so far as possible. In addition to total counts of red and white blood cells, we are moving quickly toward some type of clinical instrument that will automate the differential white blood cell count, reticulocyte and platelet counts, and perhaps some new descriptors of blood cells based on function as well as morphology.

My second choice for a clinical laboratory cellular specimen to be examined by automated instrumentation may not be so easily accepted by everyone here. I would choose the routine urinalysis. It is a test that is called for with almost the same frequency as the routine blood count. It is the most neglected and probably the most poorly performed test in the clinical laboratory. While some judgment, skill, and knowledge are needed to properly interpret the cellular sediment, these seem to be dispensed with in actual practice. The urinalysis is not exactly a glamour test; it is not terribly pleasant to do, and I do not think the technicians would miss it if they had to give it up. In fact, morale might be improved. Certainly accuracy would be improved. Results lend themselves to numerical reporting, and, if quantitative reproducible counts of the various cells and other formed elements in the urinary sediment could be obtained, they would be very useful in following diseases of the kidney, as Dr. Addis showed in tediously performed manual counts on some of his patients many years ago.

Cytologic examinations for cancer detection I would put third on my list of potential applications for cytology automation. A large and growing number of uterine cervical cytology specimens are examined each year, and there are more and more cytologic examinations of sputum for lung cancer and of urine for bladder cancer. Even though the total number of these tests does not approach that of hematologic examinations or urinalysis, cytologic examinations for cancer are done in sufficiently large numbers by most good laboratories to profit by automation. More important, in smaller laboratories with relatively few abnormal specimens, it is difficult to maintain a high level of diagnostic skill. For such laboratories cytology automation would be performing a task that is not well performed manually.

The goals for automation of cytologic cancer-detection specimens are somewhat different from those for hematologic examinations or routine



urinalysis. In this application we are not looking for precise counting or classification of all cell types present. Possibly we are not even interested in the presence or absence of certain types of cells. In the most general terms, we would like to know: Is this specimen normal for this patient? Is it abnormal? Does it show cancer or a precancerous lesion? We are interested only in the presence or absence of certain kinds of abnormal cells, and, within broad limits, the number of abnormal cells is immaterial. As an initial goal, if we can simply identify all the specimens that are entirely normal, we should be able to reduce the amount of work performed manually by 50 to 75%.

At the same time we would reduce both the boredom that results from examining too many normal specimens and, we would hope, the errors that come from lagging attention.

Alternatively, it would be desirable to develop a system that would select, mark, or concentrate abnormal cells or cell groups to facilitate subsequent manual review and evaluation. Such cells may vary tremendously in number. In a recent study of the urinary cytology from 50 patients with bladder cancer, Miss Nancy Morse, from our laboratory, found that a single slide of the four usually prepared from the cellular sediment of 25 ml of urine could contain fewer than a thousand cells or as many as 800,000. In this mixture of leukocytes, red blood cells, and epithelial cells, the transitional epithelial cells arising from bladder mucosa varied from as few as 35 cells in one patient to 165,000 in another. There was no relationship between overall cellularity and the number of transitional bladder cells present. The number of cancer cells varied from about 50 to nearly 700 per 1000 total transitional bladder cells. If these sometimes very few cancer cells could be concentrated or identified by instrumentation or if all abnormal bladder epithelial cells were so marked, even without specification of the abnormality, it would be of considerable practical help and an important first step toward a fully automated system.

Fourth on my list of priorities for clinical laboratory tests of cellular specimens that should be automated would be the typing and cross matching of blood in the blood bank. This is another test that accounts for a substantial part of the total laboratory work load. It is repetitive and really requires little judgment to perform or interpret, though an error could be disastrous, of course. Results are simply expressed, with a minimum number of possible choices. The greatest danger of error lies in mislabeling or mishandling specimens, a danger that should be less with properly designed instrumentation than with manual examinations. Furthermore, the processes involved in mixing precise amounts of test specimens and reagents under controlled conditions of time and temperature can be done very well by machines, and the end product, which is cell clumping, is a rather gross feature to recognize instrumentally, compared with the features we look for to distinguish cancer and benign epithelial cells or different kinds of leukocytes.

I will only mention other possible applications of cytology automation that come to mind. They include chromosome karyotyping, which is in a state of

flux today due to the introduction of the banding techniques for defining individual chromosomes; identification and counting of bacteria; tissue typing by mixed lymphocyte culture; immunofluorescent classification of blood lymphocytes and, possibly soon, epithelial or other cells; and the identification of rare circulating cells in peripheral blood, including megakaryocytes, immature leukocytes, nucleated red blood cells, and possibly circulating cancer cells. Perhaps even some noncellular particulates such as chylomicrons will be identified in peripheral blood and prove of clinical significance in the diagnosis of atherosclerosis.

In any system of cytologic examination, whether it be manual or instrumental, a key factor is the proper selection of cellular characteristics or attributes that can be used to distinguish two or more different cell types. Until now, we have talked primarily about morphology, and instrumentation has been morphology-minded by design. The reason for this, obviously, is that the light microscope and morphology have been essentially our only tools to classify cells. I think that is changing. Recent advances in cell physiology, particularly in immunology, are suggesting new specific ways of distinguishing functionally different categories of cells. Unexpected, real differences between cells that appear morphologically identical by light microscopy are going to be brought out with the instrumentation that is being designed and used by the people here today. We will be finding new cell attributes, some rational and others empirical but all potentially useful for classification and subclassification in an automated cytologic system. What could be more logical than to use these new instruments to find new ways for distinguishing cells? As time goes by, the number of useful cell attributes we will find surely will increase—it cannot decrease—and our ability to discriminate new categories of cells will increase correspondingly.

And this brings up a final, very interesting philosophical question. Our goal to date has been to find ways for automatically classifying cells in the same way that they have been classified since we first began to look at them with the light microscope. We have merely been searching for a new, faster, more reliable automated way to duplicate a manual task. Do we really want to continue down that path? Do we assume that the light microscope is the best way to classify cells because it was the first and, for a long time, the only way? What would we have done had we not had the microscope but instead were studying cells with some of the black boxes developed by people in this room, comparing results with clinical observations just as the nineteenth century microscopists studied cell morphology in relation to clinical disease. I am not proposing that we throw away the microscope, but I do think we ought to leapfrog it on occasion. It is possible, in fact probable, that new instrumentation and newly specified cell attributes will give us a cell-classification system much more informative for many purposes than the classification now in use.

# CELL PREPARATION AND STAINING FOR FLOW SYSTEMS

HARRY A. CRISSMAN

Biophysics and Instrumentation Group, Los Alamos Scientific Laboratory, Los Alamos,  
New Mexico

---

## ABSTRACT

Techniques are presented for dispersal and staining of cells in liquid suspension for subsequent analysis in flow systems. Cell dispersal involving the use of proteolytic enzymes such as trypsin is achieved with minimal cell loss and yields cell suspensions containing large populations of single cells free of excessive cellular debris or cell clumps. Classical staining methods have been adapted to accommodate cells in suspension and to provide for the specific fluorochroming of cellular DNA or protein or both as well as fluoresceinated antibody or lectin tagging of cells.

The successful application of flow systems for rapid, individual cell analysis is critically dependent upon preparative techniques that maintain the cells in a monodispersed state during fixation, staining, and measurement. In instances where fluorescent-staining techniques are used, the quality and specificity of cellular staining must also be evaluated to ascertain the reliability of analytical results. Automated analytical systems permit rapid and precise measurement of individual cells; however, such systems cannot be relied upon to distinguish fluorescent cellular debris or cell clumps from properly stained single cells. Therefore, sample preparation involving both the disaggregation of cellular tissue into single-cell entities and cell staining plays an extremely important role in flow-system methodology. Experience has shown that failure to obtain reliable and reproducible data has more often been caused by poorly prepared samples than by faulty instrumentation. The fact remains that a flow system operating at peak performance can produce no better data than the input cell sample can provide.

During the past few years, considerable effort has been invested in devising adequate cell-dispersal protocols and quantitative, reproducible cell-staining



methods that provide quality single-cell suspensions for subsequent flow-instrument analysis. Although most of the material analyzed in the past has consisted of cells from tissue culture, more recently attention has been directed toward techniques useful for dispersing and staining exfoliative cervical material, as well as human and animal tumors.

## METHODS FOR CELL DISPERSAL

The preparation of monodispersed cell suspensions is a difficult but not necessarily insurmountable task. A number of methods are available for disaggregation or dispersal of cells, most of which involve various enzymatic procedures. For instance, a routine preparative method at Los Alamos Scientific Laboratory (LASL) uses trypsin, ethylenediaminetetraacetic acid (EDTA), and DNase for dispersing cells from suspension or monolayer cultures.<sup>1</sup> Modifications of the technique can be used for disaggregating solid tissue, including tumors. Other laboratories have used such enzyme combinations as hyaluronidase and collagenase<sup>2</sup> or hyaluronidase alone<sup>3</sup> to remove cellular aggregating factors. Collagenase has also been effective in dispersing cells in cervical samples.<sup>4</sup> These samples contain large populations of degenerating cells that are susceptible to lysis when treated with trypsin. There are many enzymes that may be better suited for a particular cell type than those just described; however, the adaptation of any specific enzymatic protocol requires preliminary studies to determine the enzyme concentration and time period of incubation which produce optimal cell dispersal and minimal cell loss. In instances where proteolytic enzymes may remove a biochemical component of interest such as a cell-surface moiety, the use of EDTA-saline may be quite satisfactory.<sup>5</sup> Obviously no single preparative technique will be adequate for every cell sample, but whichever technique is chosen it must satisfy the criteria that demand minimizing clumping, cell doublets, cellular debris, and cell loss. Microscopic examination of the cell sample is a stringent requirement for assuring that these criteria are satisfied.

## FIXATION OF CELLS IN SUSPENSION

There is a real need for the development of fixation protocols that minimize cell clumping and cell loss. Existing methods, generally designed for cell preparation on slides, often require certain modifications to be of value for flow-system analysis. New fixative procedures should always be tested and evaluated in cell-suspension systems in conjunction with specific staining methods, since the two protocols are most often interdependent.

### Requirements of Cellular Fixatives

The ideal fixative is one that prevents cellular autolysis and bacterial growth and preserves all the biochemical and cellular components but neither interferes



with the specificity of subsequent staining reactions nor induces gross changes in cell morphology. Many fixatives presently in use fulfill only a few of these criteria. For instance, Formalin is regarded as an all-purpose fixative for nucleic acids, proteins, and lipids; however, many carbohydrates, including glycogen and some mucopolysaccharides, are not preserved and thus are leached from the cell. Alternatively, methyl and ethyl alcohol are excellent fixatives for glycogen, but they solubilize cellular lipids. Obviously every fixative has certain advantages as well as disadvantages.

At LASL, 10% Formalin (saline GF; Formalin in a balanced salt solution with glucose)<sup>1</sup> is used routinely for fixing cells in liquid suspension for subsequent staining by the Feulgen procedure. However, formaldehyde is a strong cross-linking agent and interferes with the intensity of staining when intercalating fluorescent dyes such as ethidium bromide<sup>6</sup> or propidium iodide<sup>7</sup> are used to fluorochrome DNA. In this instance, cold 70% ethanol proves to be the better fixative. For immunofluorescent studies of viral antigens, acetone seems to be the fixative often favored.<sup>8</sup> Acetic-alcohol (glacial acetic acid-ethanol, 1:3) causes excessive cell loss when applied to cells in liquid suspension. Cells in suspension appear to be more susceptible to strong acid fixatives than cells adhering to slides. Since a number of histochemical references<sup>9,10</sup> prescribe the best fixatives for a given biochemical moiety in cells, the subject will not be elaborated upon here. However, a word of caution should be given concerning overfixation or prolonged fixation of cells, especially in Formalin. It has been observed that cells fixed in this medium for 2 weeks or more, depending on cell type, tend to exhibit considerable nonspecific cytoplasmic staining following the Feulgen reaction. As judged from the coefficient of variation of cellular DNA distributions, best results are obtained when cells are fixed no longer than one week in Formalin. If cells must be stored longer, it is advised that they be transferred to 70% ethanol. Fixation should always take place at refrigerated temperatures.

## CELL STAINING IN LIQUID SUSPENSION

In contrast to conventional methods for staining cells on slides, flow systems require that the cell samples be stained in liquid suspension. This requires the centrifugation of cells after each step of the staining protocol. After each centrifugation, cells are dispersed by mildly vortexing the sample tube to avoid cell clumping.

### DNA-Specific Staining Methods

Trujillo and Van Dilla<sup>11</sup> have previously described a method for auramine O-Feulgen staining of cells in suspension. This procedure has recently been modified by substituting the dye acriflavine<sup>12,13</sup> for auramine O and incorporating the cell disaggregation and fixation techniques mentioned

previously.<sup>14</sup> These modifications serve to reduce cell aggregation and to facilitate dispersal of cells after centrifugation. Cells stained with acriflavine-Schiff are about 10 times brighter than those stained with auramine O; thus the coefficient of variation is improved by a factor of 2. Hydrolysis of cells in hydrochloric acid (HCl) prior to acriflavine-Schiff staining can be accomplished with the least cell loss by using 4*N* HCl for 20 min at room temperature. Deitch, Wagner, and Richart<sup>15</sup> and Fand<sup>16</sup> have also noted that hydrolysis of cells at room temperature in elevated HCl normalities is preferable over the use of normal HCl at 60°C. Investigations at LASL support the findings of these authors and show that cells hydrolyzed for periods varying from 12 to 60 min show little difference in fluorescence intensity after staining. In some instances the dye flavophosphine N has been used successfully in place of acriflavine.<sup>12</sup> Figure 1 shows cells that have been stained by the Feulgen procedure and demonstrates the specificity of the reaction for DNA.

Two fluorescent dyes, ethidium bromide (EB)<sup>6</sup> and propidium iodide (PI)<sup>7</sup>, which have been demonstrated to be intercalating agents of double-stranded nucleic acids, can also be used for staining DNA as alternatives to the Feulgen procedure. Dittrich and Göhde<sup>17</sup> have described a method using EB staining for DNA after digestion of cellular RNA with RNase. Similar results have been obtained at LASL with PI, an analog of EB.<sup>18</sup> The cellular DNA distributions obtained from Feulgen-stained or PI-stained cells (Fig. 2) are strikingly similar even though the modes of staining are not necessarily the same. Staining procedures using EB or PI do not involve acid hydrolysis; thus cell loss is less than with the Feulgen procedure.

Preliminary studies indicate that another intercalating dye, mithramycin, might be used to stain DNA. Since mithramycin appears to be highly specific for DNA, RNase treatment of cells before staining is not necessary. Staining and analysis can be accomplished in about 20 min. Details concerning the protocol are discussed elsewhere.<sup>19</sup>

### Protein-Specific Dyes

The use of a number of protein-specific dyes, including ANSA,\* dansyl chloride, brilliant sulfaflavine, fluorescein isothiocyanate (FITC), rhodamine B isothiocyanate, and Fluoram (fluorescamine), has been investigated. Of these, the recently synthesized dye Fluoram<sup>20</sup> appears to stain the most rapidly. The compound is nonfluorescent until bound to primary amino groups, and the unreacted portion of the compound is decomposed in several seconds in aqueous solution. Dye-protein interaction time is less than 1 sec. Although the dye is excited suboptimally by the lines available in our present laser system, the rapidity, versatility, and sensitivity of staining with the dye make it worthy of

\*ANSA, 8-anilino-1-naphthalenesulfonic acid.

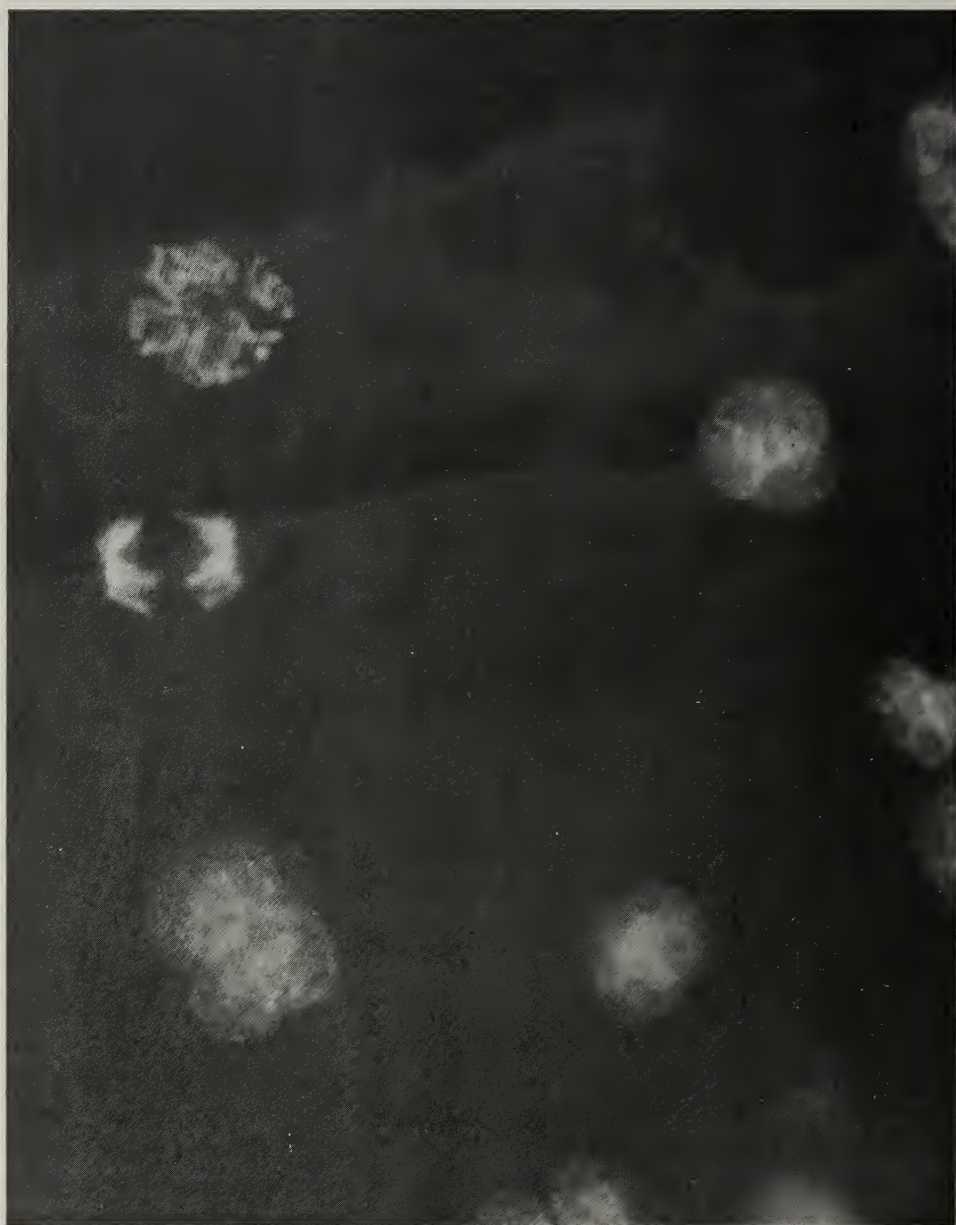


Fig. 1 Chinese hamster cells (line CHO) stained by the Feulgen procedure. Note particularly the specificity of staining with respect to the mitotic figures.



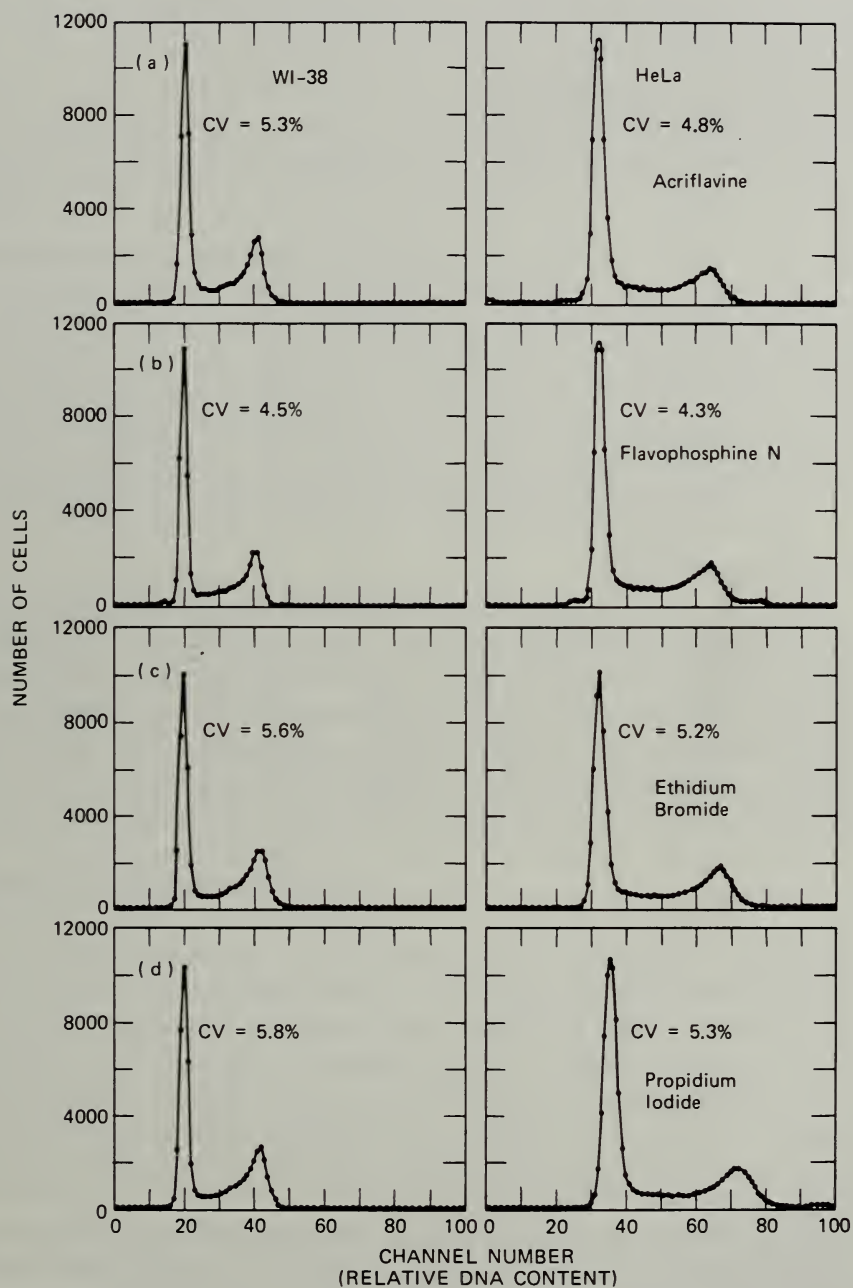


Fig. 2 Analytical results obtained for WI-38 and HeLa cells stained with either (a) acriflavine, (b) flavophosphine N, (c) ethidium bromide, or (d) propidium iodide. Results of staining for each cell type compare favorably. Coefficient of variation (CV): standard deviation  $\times$  100 divided by the mean.



further study. It may prove useful as a protein stain for use with dyes such as PI in two-color analysis.

### DNA- and Protein-Specific Staining

Cells can be double stained for both DNA and protein by using two fluorescent dyes with similar absorption but differing emission spectra. Dittrich et al.<sup>21</sup> have used EB and FITC for staining cellular DNA and protein, respectively. Ethidium bromide and propidium iodide fluoresce orange-red, and FITC fluoresces a greenish yellow. However, better spectral separation is obtained by using the PI-FITC combination, since PI has an emission maximum near 590 nm as compared with 580 nm for EB and 530 nm for FITC when bound to cells. Analytical data presented earlier (Steinkamp, this volume) have already demonstrated and validated the application of two-color analysis of PI-FITC-stained cells. Figure 3 shows DNA and protein distributions of CHO, HeLa, and L-929 cells. The staining protocol is described in detail elsewhere.<sup>18</sup>

### Acridine Orange Staining

Use of the metachromatic dye acridine orange (AO) as a quantitative vital stain for DNA and RNA in cells has been proposed by a number of investigators.<sup>22,23</sup> However, Kasten<sup>24</sup> has warned against such premature assumptions without proper controls for assuring DNA and RNA specificity of staining. Attempts to use AO supravivally at concentrations of  $10^{-6}$  g/ml or less, at which cells exhibit only green fluorescence, have failed to yield DNA distributions similar to those obtained for cells stained by Feulgen procedures or by intercalating dyes mentioned previously. Cellular AO distributions are more often strikingly similar to cell-volume distributions. In Fig. 4 are AO green fluorescence and cell-volume frequency distributions for HeLa cells. This figure demonstrates a good but not necessarily direct correlation between green fluorescence of acridine orange and cell volume. Microscopic examination of AO-stained cells reveals pale green fluorescence over the entire cell and the absence of nuclear specificity. Mullaney and West<sup>25</sup> have stained CHO cells with AO at concentrations as low as  $10^{-8}$  M and analyzed light scattering and green fluorescence from cells to obtain a higher signal-to-noise ratio and have had similar results. Small-angle light scattering that was relative to particle size also showed a fluorescence-to-cell size correlation.

It appears that, at least for the present, AO cannot be relied upon to serve as a quantitative stain for DNA or RNA in cells even though the stain seems to react in a quantitative manner with nucleic acids in solution.<sup>26,27</sup> However, the use of AO as a vital stain does appear to have application in studies involving differential analysis of human leukocytes. Adams and Kametsky<sup>28</sup> demonstrated that various human leukocyte types in whole blood could be resolved into three distinct populations on the basis of red fluorescence after staining in AO ( $10^{-6}$  g/ml). Red blood cells do not seem to take up the dye

significantly at this concentration. More recently Steinkamp, Romero, and Van Dilla<sup>29</sup> confirmed these findings and, in fact, electronically sorted cells from each of the three populations. Microscopic examination of the sorted cells showed that the segregated cell types were lymphocytes, monocytes, and granulocytes, respectively, in order of increasing red fluorescence as predicted by others.<sup>28</sup> Data from these experiments were presented earlier (Steinkamp, this volume).

### Cell-Surface Binding of Fluorescein-Conjugated Lectins

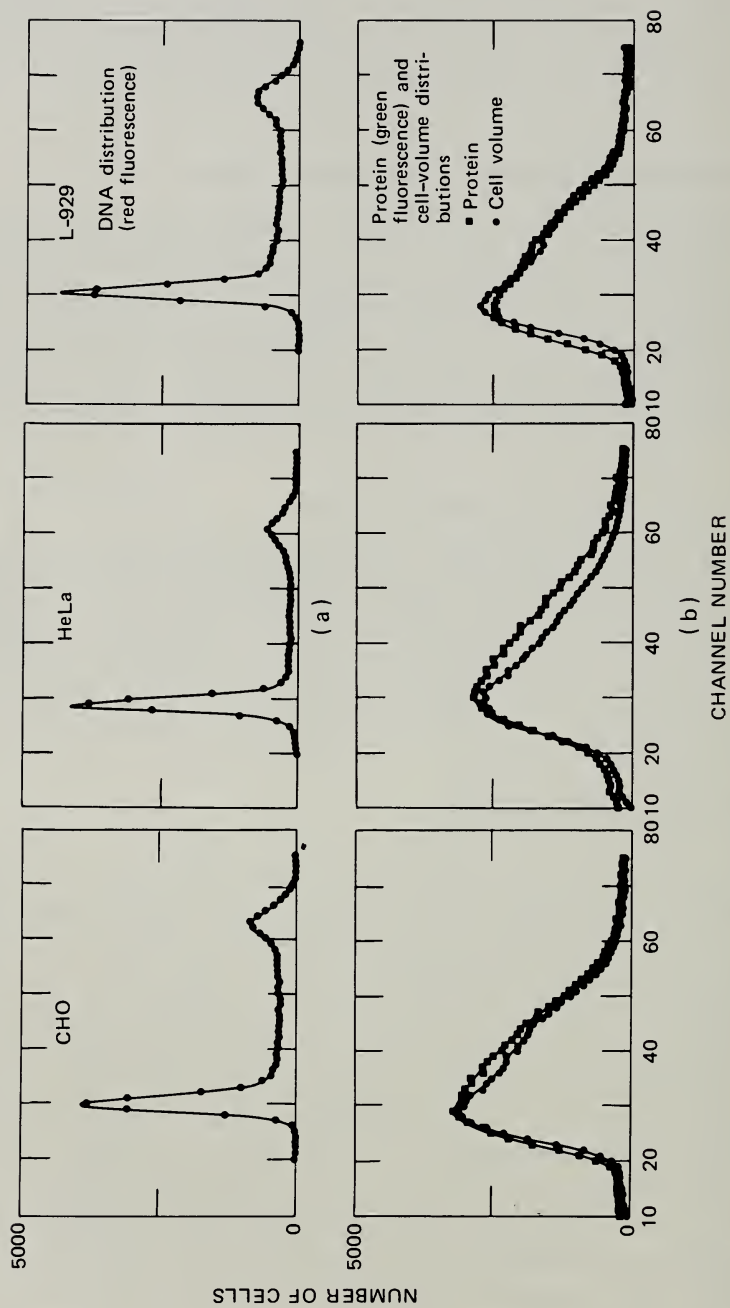
Quantitative studies of concanavalin-A binding to the cell surface have recently been made by tagging cells with the fluoresceinated conjugate of this lectin (con A-F).<sup>30</sup> It appears that conjugation does not significantly interfere with the biological activity of con A. In these experiments EDTA-saline was used for cell dispersal since trypsin has a pronounced effect on cell-surface binding sites. More-recent studies involving multiparameter analysis of con A-F per unit surface area have been discussed earlier (Steinkamp, this volume).

### Tagging Cells with Fluorescein-Labeled Antibody

Studies at LASL by Cram et al.<sup>31</sup> have demonstrated that cells in suspension can be labeled with fluorescein-conjugated antibody and subsequently analyzed in flow systems. Julius, Masuda, and Herzenberg<sup>32</sup> have made somewhat similar observations. These techniques provide a means of estimating the amount of antigen or antibody per cell. Possible future applications of these and similar techniques will be extremely useful in the diagnosis of animal or human diseases.

## SUMMARY AND CONCLUSIONS

At the present time the application of flow systems for cell analysis is limited mainly by the cell-preparation aspects of the methodology. Although automated analytical capabilities are now available for making a large number of biological studies, such investigations must await new or modified cell-preparation methods that will permit the initiation of these studies. Techniques for improved cell dispersal and rapid cell staining are urgently needed to expand the usefulness of flow systems for various cytological investigations. In addition to the biochemical cellular components presently being studied, fluorescent-staining protocols should be devised for staining cellular RNA, histones, and lipids since these moieties also appear to play an important role in cell metabolism. In other studies various fluorogenic substrates could be used for quantitating specific enzyme systems in cells provided optimal conditions for incubating cells in suspension are ascertained. The applications of flow systems certainly seem theoretically almost endless; however, new cytological studies will require the same diligent efforts that have produced the techniques used routinely today.



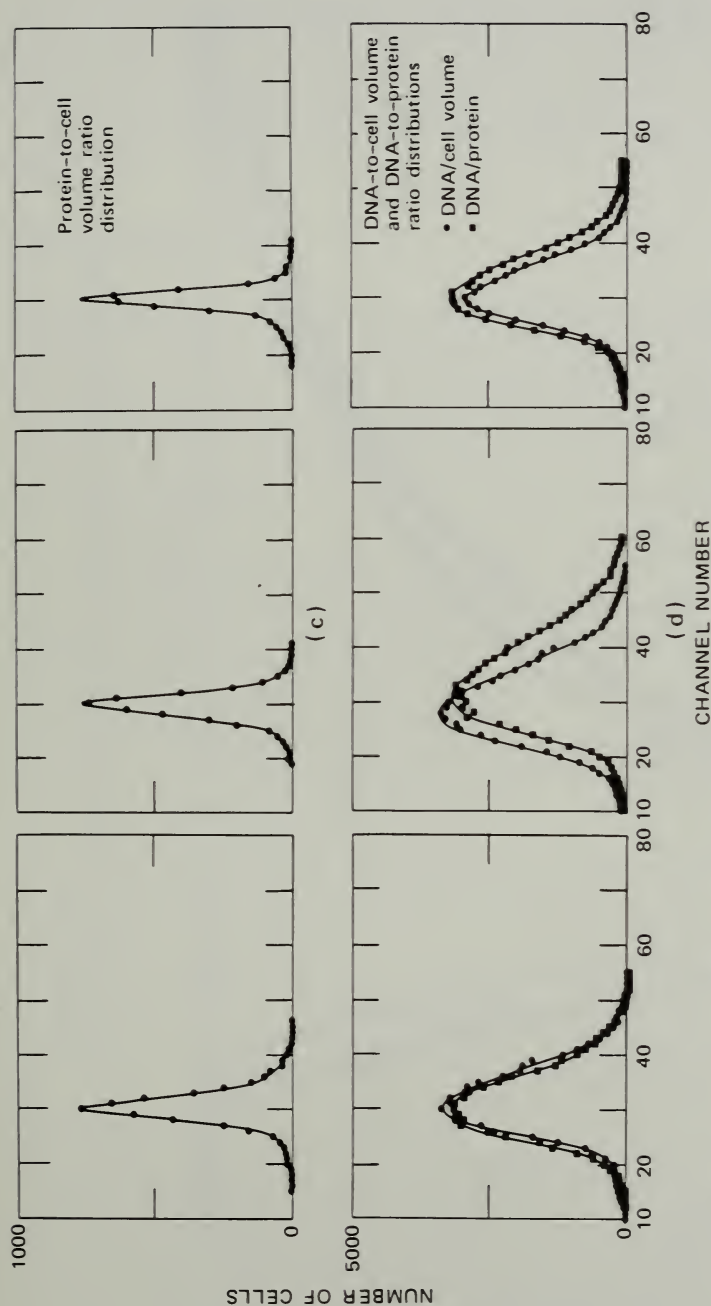


Fig. 3 DNA, protein, and cell-volume distributions for CHO, HeLa, and L-929 cells. Protein-to-cell volume ratios (c) were obtained by using both the green fluorescence and cell-volume signals from each cell to produce electronically a ratio with an analog divider system. The coefficients of variation (standard deviation  $\times 100$  divided by the mean) of the ratio distributions are 6.8%, 6.5%, and 5.3%, respectively, for CHO, HeLa, and L-929 cells. DNA-to-protein ratios were obtained similarly by analysis of both red and green fluorescence signals for each cell. The abscissa scale (channel number) has a depressed zero but otherwise is proportional to either DNA content, protein content, or cell volume. The constants of proportionality are different for the various cell types.



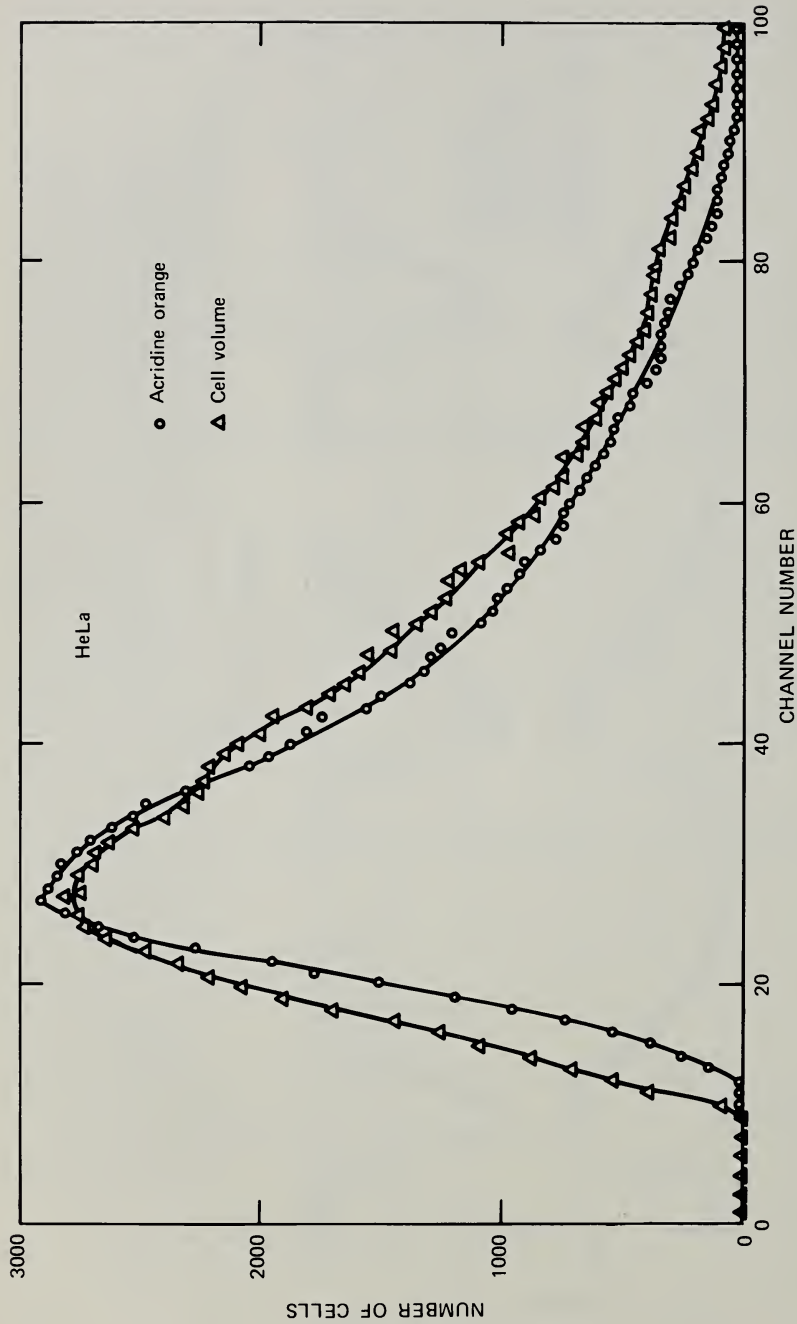


Fig. 4 Green fluorescence and cell-volume distributions of acridine orange-stained HeLa cells.

## ACKNOWLEDGMENTS

The author wishes to thank J. A. Steinkamp, L. S. Cram, T. T. Trujillo, P. K. Horan, J. H. Jett, P. N. Dean, E. C. Anderson, P. M. Kraemer, P. F. Mullaney, R. A. Tobey, D. F. Petersen, P. C. Sanders, J. Grilly, A. Romero, and J. C. Forslund for their generous contributions to this study.

This work was performed under the auspices of the U. S. Atomic Energy Commission.

## REFERENCES

1. P. M. Kraemer, L. L. Deaven, H. A. Crissman, and M. A. Van Dilla, DNA Constancy Despite Variability in Chromosome Number, in *Advances in Cell and Molecular Biology*, Vol. 2, pp. 47-108, E. J. DuPraw (Ed.), Academic Press, Inc., New York, 1972.
2. M. Müller, M. Schreiber, J. Kartenbeck, and G. Schreiber, Preparations of Single-Cell Suspensions from Normal Liver, Regenerating Liver and Morris Hepatomas 9121 and 5123tc, *Cancer Res.*, **32**: 2568-2576 (1972).
3. B. Pessac and V. Defendi, Cell Aggregation: Role of Acid Mucopolysaccharides, *Science*, **175**: 898-900 (1972).
4. A. Romero and P. K. Horan, Disaggregation of Gynecological Specimens for Flow-System Analysis, submitted to *Acta Cytol.*, 1974.
5. A. L. Kisch, R. O. Kelley, H. Crissman, and L. Paxton, DMSO Induced Reversion of Several Features of Polyoma Transformed BHK-21 Cells: Alterations in Growth and Morphology, *J. Cell Biol.*, **57**: 38-53 (1973).
6. J. B. LePecq and C. Paoletti, A Fluorescent Complex Between Ethidium Bromide and Nucleic Acids, *J. Mol. Biol.*, **27**: 87-106 (1967).
7. B. Hudson, W. B. Upholt, J. Devinny, and J. Vinograd, The Use of an Ethidium Bromide Analogue in the Dye-Buoyant Density Procedure for the Isolation of Closed Circular DNA: The Variation of the Superhelix Density of Mitochondrial DNA, *Proc. Nat. Acad. Sci. U.S.A.*, **62**: 813-820 (1969).
8. L. S. Cram and A. Brunsting, Fluorescence and Light Scattering Measurements on Hog Cholera-Infected PK-15 Cells, *Exp. Cell Res.*, **78**: 209-213 (1973).
9. A. G. Pearse, *Histochemistry: Theoretical and Applied*, 3rd ed., Vol. 1, Little, Brown and Company, Boston, 1968.
10. D. Hopwood, Fixatives and Fixation: A Review, *Histochem. J.*, **1**: 323-360 (1969).
11. T. T. Trujillo and M. A. Van Dilla, Adaptation of the Fluorescent Feulgen Reaction to Cells in Suspension for Flow Microfluorometry, *Acta Cytol.*, **16**: 26-30 (1972).
12. F. H. Kasten, Schiff-Type Reagents in Cytochemistry, *Histochemie*, **1**: 466-509 (1959).
13. C. Culling and P. Vassar, Desoxyribose Nucleic Acid. A Fluorescent Histochemical Technique, *Arch. Pathol.*, **71**: 88-92 (1961).
14. R. A. Tobey, H. A. Crissman, and P. M. Kraemer, A Method for Comparing Effects of Different Synchronizing Protocols on Mammalian Cell Cycle Traverse, *J. Cell Biol.*, **54**: 638-645 (1972).
15. A. D. Deitch, D. Wagner, and R. M. Richart, Conditions Influencing the Intensity of the Feulgen Reaction, *J. Histochem. Cytochem.*, **16**: 371-379 (1968).
16. S. Fand, Environmental Conditions for Optimal Feulgen Hydrolysis, in *Introduction to Quantitative Cytochemistry*, Vol. II, pp. 209-221, G. L. Wied and G. F. Bahr (Eds.), Academic Press, Inc., New York, 1970.
17. W. Dittrich and W. Göhde, Impulse Fluorometry with Single Cells in Suspension, *Z. Naturforsch.*, **24B**: 360 (1969).

18. H. A. Crissman and J. A. Steinkamp, Rapid, Simultaneous Measurement of DNA, Protein and Cell Volume in Single Cells from Large Mammalian Cell Populations, *J. Cell Biol.*, **59**: 766-771 (1973).
19. H. A. Crissman and R. A. Tobey, Cell-Cycle Analysis in 20 Minutes, *Science*, **184**: 1297-1298 (1974).
20. S. Undenfriend, S. Stein, P. Böhlen, W. Dairman, W. Leimgruber, and M. Weigle, Fluorescamine: A Reagent for Assay of Amino Acids, Peptides, Proteins and Primary Amines in the Picomole Range, *Science*, **178**: 871-872 (1973).
21. W. Dittrich, W. Göhde, E. Severin, and G. Reiffenstuhl, The Nucleus-Cytoplasm Relation in Impulse Cytophotometry of Cervical and Vaginal Smears, Lecture, Fourth International Congress on Cytology, London (1971).
22. R. Rigler, Acridine Orange in Nucleic Acid Analysis, *Ann. N. Y. Acad. Sci.*, **157**: 211-224 (1969).
23. S. S. West, Fluorescence Microspectrophotometry of Supravivally Stained Cells, in *Physical Techniques in Biological Research*, Vol. III, Part C, pp. 253-269, A. W. Pollister (Ed.), Academic Press, Inc., New York, 1969.
24. F. H. Kasten, Cytochemical Studies with Acridine Orange and the Influence of Dye Contaminants in the Staining of Nucleic Acids, in *International Review of Cytology*, Vol. 21, pp. 141-202, G. H. Bourne and J. F. Canielli (Eds.), Academic Press, Inc., New York, 1967.
25. P. F. Mullaney and W. T. West, A Dual-Parameter Flow Microfluorometer for Rapid Cell Analysis, *J. Phys. E (London)*, **6**: 1006-1008 (1973).
26. R. Rigler, Microfluorometric Characterization of Intracellular Nucleic Acids and Nucleoproteins by Acridine Orange, *Acta Physiol. Scand.*, **67**(Suppl. 267): 5-122 (1966).
27. S. Ichimura, M. Zama, and H. Fujita, Quantitative Determination of Single Stranded Sections in DNA Using the Fluorescent Probe Acridine Orange, *Biochim. Biophys. Acta*, **240**: 485-495 (1971).
28. L. R. Adams and L. A. Kametsky, Machine Characterization of Human Leukocytes by Acridine Orange Fluorescence, *Acta Cytol.*, **15**: 289-291 (1971).
29. J. A. Steinkamp, A. Romero, and M. A. Van Dilla, Multiparameter Cell Sorting: Identification of Human Leukocytes by Acridine Orange Fluorescence, *Acta Cytol.*, **17**: 113-117 (1973).
30. P. M. Kraemer, R. A. Tobey, and M. A. Van Dilla, Flow Microfluorometric Studies of Lectin Binding to Mammalian Cells. I. General Features, *J. Cell. Physiol.*, **81**: 305-314 (1973).
31. L. S. Cram, J. C. Forslund, P. K. Horan, and J. A. Steinkamp, Application of Flow Microfluorometry (FMF) and Cell Sorting Techniques to the Control of Animal Diseases, in *Automation in Microbiology and Immunology*, proceedings of the Symposium on Rapid Methods and Automation in Microbiology, June 3-8, 1973, Stockholm, Sweden, John Wiley & Sons, Inc., New York, in press.
32. M. H. Julius, T. Masuda, and L. A. Herzenberg, Demonstration that Antigen-Binding Cells Are Precursors of Antibody-Producing Cells After Purification with a Fluorescence-Activated Cell Sorter, *Proc. Nat. Acad. Sci. U.S.A.*, **69**: 1934-1938 (1972).

# FLUORESCENCE-ACTIVATED CELL SORTING AND ITS APPLICATIONS

MICHAEL H. JULIUS, RICHARD G. SWEET, C. GARRISON FATHMAN,\*  
and LEONARD A. HERZENBERG

Department of Genetics, Stanford University School of Medicine,  
Stanford, California

---

## ABSTRACT

The Fluorescence Activated Cell Separator (FACS) separates cells according to fluorescence, light-scattering characteristics, or selected combinations of these two parameters. The instrument can process up to 5000 cells/sec and separate two nearly pure fractions with independently specified ranges of fluorescence and light-scattering cross sections for each fraction. The FACS can differentiate between viable and dead cells on the basis of light scattering. Appropriate threshold setting permits "gating out" of the dead-cell population so that cell populations can be separated or analyzed on the basis of viable-cell content. Using the FACS in combination with fluorescein-conjugated antigens to visualize antigen-binding cells by fluorescence, we have obtained viable and functional populations of antigen-binding cells enriched up to 400-fold from spleens of primed and unprimed mice. We have directly demonstrated that antigen-binding cells in both primed and unprimed mouse spleen contain the precursors of antibody-forming cells. Moreover, the antigen-binding precursor cells are functionally specific, and the avidity of the antibody formed is directly correlated with the avidity of the antigen receptors on the antigen-binding precursor cells.

## DESCRIPTION OF THE INSTRUMENT

The Fluorescence Activated Cell Separator (FACS) separates cells according to fluorescence, light-scattering characteristics, or selected combinations of the two parameters. Figure 1 is a simplified block diagram of the system. Cells in liquid suspension are forced under pressure through a micronozzle into the center of a stream of cell-free fluid and then out an effluent nozzle 50  $\mu\text{m}$  in diameter. This design creates a coaxial flow that keeps the cells near the axis of the effluent jet.

---

\*Present address: Immunology Branch, National Cancer Institute, National Institutes of Health, Bethesda, Md.



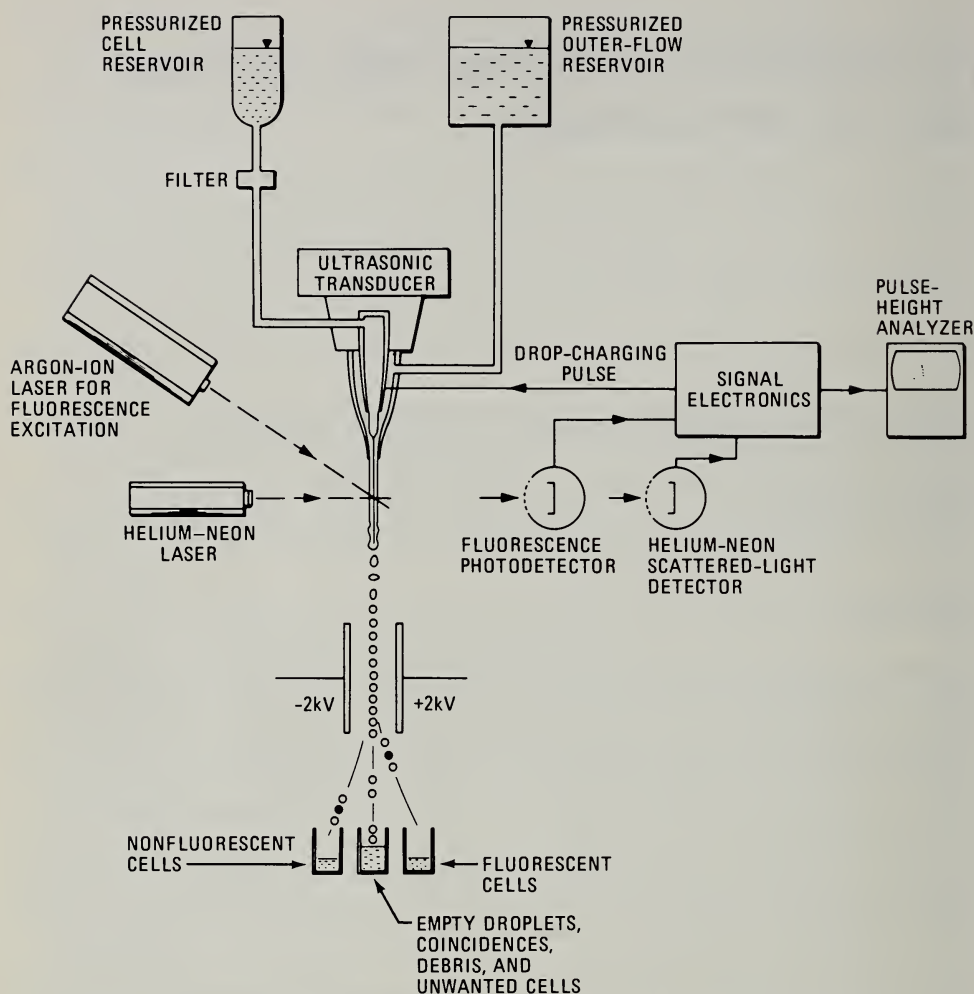


Fig. 1 Simplified block diagram of the Fluorescence Activated Cell Separator (FACS).

The nozzle assembly is vibrated axially at 40 kHz, breaking the jet into 40,000 uniform droplets per second. Immediately below the nozzle, before droplet formation occurs, the jet is illuminated by two lasers. Low-angle scattered light from one, a helium-neon unit operating at 632.8 nm, falls on a red-sensitive photodetector and produces a signal related to cell volume. The second laser, an argon-ion unit operating at one of a number of lines between 454 and 514 nm, excites fluorescence in cells tagged with appropriate fluorescent material. Some of the fluorescent light falls on a second photodetector and provides a signal proportional to the number of fluorescent residues on the cell. Signals produced in the scatter and/or fluorescent channels are processed, delayed, and combined as required to produce electrical pulses, which are used to charge the liquid stream at the time the droplet containing the desired cell is forming. Droplets

broken off while the stream is charged retain their charge. Further downstream, the droplets pass through an electric field between two charged plates. Charged droplets are deflected appropriately, while uncharged droplets continue on their original course. The charging pulse lasts for three droplet periods, centered on the time the cell is expected to enter a droplet, to ensure that the droplet containing a desired cell is charged and thus deflected. The charging pulses are synchronized with the ultrasonic droplet generator so as to ensure that all drops formed during the charging period are equally charged. Further details of basic instrument operation can be found in the article by Bonner et al.<sup>1</sup> A more recent instrument, presently being tested, uses illumination by a single argon-ion laser for both scatter and fluorescence.

Analog signal pulses produced by the scatter and fluorescent-light detectors are converted to digital logic signals by circuits that respond only to signals within selected amplitude limits. These digital signals are combined logically to define two cell fractions, each fraction corresponding to scatter and fluorescence signal ranges that can be independently specified. Droplets containing cells in one fraction (D1) are deflected in one direction, and droplets containing cells in the other fraction (D2) are deflected in the opposite direction. Logic circuits prohibit deflection of droplets containing detected cells or particles not meeting the D1 or D2 criteria and cells too closely spaced to separate properly.

## INSTRUMENT PERFORMANCE

The instrument can detect fluorescence of single cells with more than 3000 bound molecules of fluorescein per cell. Cells or particles having a uniform fluorescence much greater than the detectable minimum produce a single amplitude distribution having a coefficient of variation of about 9%. This uncertainty in amplitude measurement, contributed by the instrument, defines its fluorescence amplitude resolving capability. The instrumental spread for scattered light signals from uniform spherical particles also corresponds to a coefficient of variation of about 9%, but signals from nonspherical cells may vary more than this because of differences in orientation as they cross the laser beam.

Final fraction purities of greater than 95% are typically obtained in a one-pass separation at processing rates up to 5000 cells/sec. At this processing rate, up to about 30% of the desired cells are too closely spaced for proper separation and are discarded in the nondeflected droplet fraction by the coincidence-detection circuits. For separation of cells comprising a relatively small fraction—less than about 3%—of the input sample, it is often faster to make a preliminary separation at a very high processing rate, e.g., 20,000 cells/sec or more. Since nearly every wanted cell is accompanied by one or more unwanted “passengers,” the circuitry for discarding closely spaced cells must be disabled. The highly enriched separated fraction is then sorted again to achieve the desired final purity.

## ANALYTICAL APPLICATIONS OF THE FACS

The FACS has been used for analysis and cell separation. It has the useful capabilities of allowing analysis of murine lymphoid cells by two independent parameters—fluorescence and scatter. With appropriate fluorescein-conjugated antisera, it is possible to specifically label certain subpopulations for analysis or separation. This section describes two of the analytical applications of the FACS which were studied in this laboratory

### Detection of Dead Cells by Light Scattering

One application of the FACS which was recognized during early analytical studies is the detection and analysis of viable cells. Treatment of cell populations with the fluorogenic compound fluorescein diacetate (FDA) renders only viable cells fluorescent,<sup>2</sup> and the dead cells do not become fluorescent. Therefore, in a population treated with FDA, analysis of the scatter signals from fluorescent cells only (i.e., fluorescence-gated scatter, or FGS) generates the scatter profile of viable cells in that population. Figure 2 shows the scatter profile (S) of

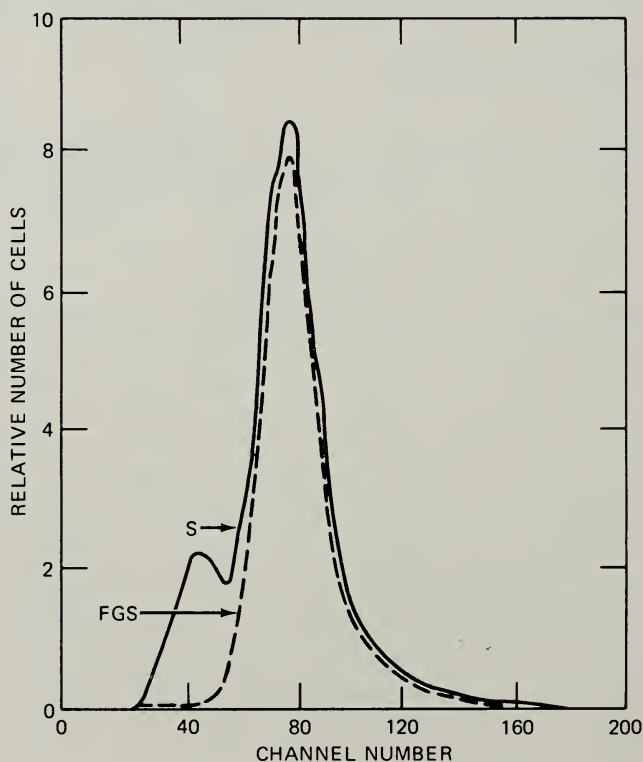


Fig. 2 Scatter profile (S) of murine thymocytes compared with FGS profile of FDA-stained thymocytes.

murine thymocytes. Superimposed on this distribution is the FGS profile of FDA-fluorescent thymocytes. The nonfluorescent dead cells constitute a subpopulation that can be clearly differentiated on the basis of scatter alone. Appropriate threshold settings enable us to "gate out" the dead cells so that any subsequent separation or analysis of the population can be based on viable-cell content. This characteristic dead-cell scatter profile is obtained from cells of all lymphoid organs studied thus far.

### Detection of Functionally Distinct Cells by Immunofluorescent Staining and FGS

Murine lymphoid cells can be divided into two major subpopulations that contain cells with different functional characteristics and ontogeny. One subpopulation contains bone-marrow-derived B cells, which differentiate into antibody-forming cells.<sup>3</sup> The other major subpopulation contains cells that have undergone differentiation within the thymus and are required for the differentiation of B cells into antibody-forming cells in response to most antigens. These are called T cells.<sup>3</sup> The B cells bear easily detectable surface immunoglobulin,<sup>4</sup> whereas T cells bear the alloantigenic marker Thy-1 ( $\theta$ ).<sup>4</sup> With fluorescein-conjugated antibodies, it is possible to differentially label these cell types in single-cell suspensions of lymphoid organs. Once labeled, the cells can be analyzed by the FACS. Figure 3 shows the scatter profile (S) of splenic

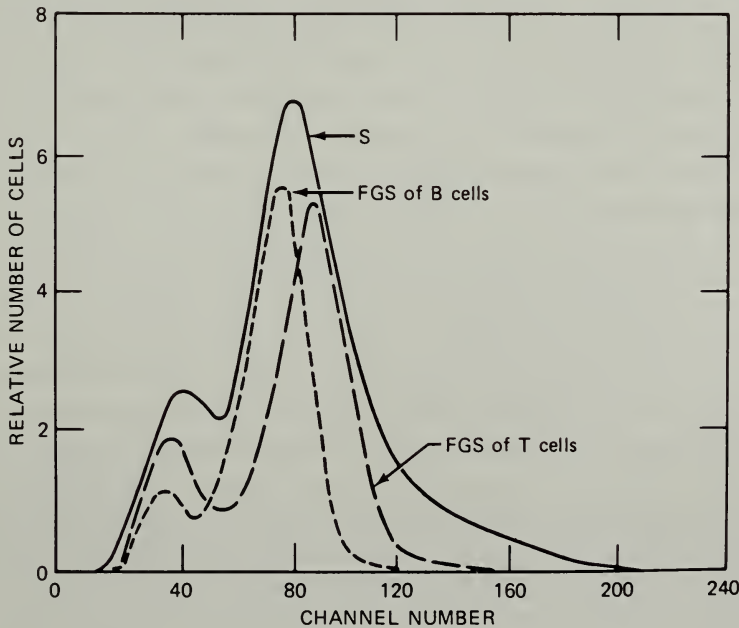


Fig. 3 Scatter profile (S) of splenic lymphocytes compared with FGS profiles of B and T cells.



lymphocytes with superimposed FGS profiles of T and B cells, detected by the appropriate fluorescent antisera.

It is apparent that T cells are larger than B cells. This is in agreement with the data of Howard, Hunt, and Gowans,<sup>5</sup> who used unit gravity sedimentation analysis of lymphocyte populations and assayed for the presence of T and B cells in the populations of cells sedimenting at various rates. They found that the more rapidly sedimenting (larger) cells were substantially enriched for T cells, whereas the majority of the more slowly sedimenting (smaller) cells were B cells. We also found that T and B cells present in lymph nodes exhibit the same scatter distribution as those in the spleen.

In addition to permitting us to routinely separate and analyze the viable cells in heterogeneous cell populations, the FACS provides a powerful tool in the analysis of functionally distinct cell subpopulations involved in the immune process.

## **ISOLATION AND FUNCTIONAL CHARACTERIZATION OF ANTIBODY-FORMING CELL PRECURSORS IN MICE**

The development of the FACS has enabled us to isolate functionally active populations of cells involved in the immune response. For the first time we have the opportunity to directly address two problems of long standing in cellular immunology.

First, are specific antigen-binding cells the precursors of antibody-forming cells? Other investigations have shown that depletion of specific antigen-binding cells from a lymphocyte population results in the inability of that population to respond to the specific antigen.<sup>6,7</sup> These studies, however, provide only indirect evidence for the precursor role of antigen-binding cells. We have isolated almost pure populations of antigen-binding cells from primed and unprimed mouse spleen and tested their ability to respond to antigen after being transferred into irradiated recipients. We have already established that a population of cells binding Keyhole Limpet Hemocyanin (KLH), isolated by the FACS from spleens of mice immunized with KLH, contains the precursors of anti-KLH antibody-forming cells necessary to give an adoptive secondary response.<sup>8</sup> Similarly, as the data presented here demonstrate, cells binding dinitrophenyl (DNP), isolated from unprimed mouse spleen, contain precursors of anti-DNP antibody-forming cells required for an adoptive primary response. Thus the precursors of antibody-forming cells in both primary and secondary adoptive responses are contained in the population of specific antigen-binding cells.

Second, since we can isolate precursors of specific antibody-forming cells, we can directly determine the relationship between the avidity of the antibody formed and the avidity of the antigen receptors on the isolated antigen-binding precursors. In adoptive-primary-transfer experiments, the avidity of anti-DNP antibody-forming cells in recipients of high-avidity DNP-binding cells was

100-fold higher than the avidity of the antibody-forming cells in recipients of unfractionated spleen. The data clearly demonstrate that high-avidity antigen-binding precursor cells give rise to high-avidity antibody-forming cells.

### **Demonstration That Antigen-Binding Cells Are Precursors of Antibody-Forming Cells**

#### *Adoptive Secondary Response to KLH: Functional Specificity of KLH-Binding Cells*

Having already established the precursor activity of KLH-binding cells derived from KLH-primed spleen,<sup>8</sup> we tested the functional specificity of these cells using the following experimental design. The KLH-binding cells were isolated (the FACS and fluorescein-conjugated KLH being used to visualize KLH-binding cells) from spleens doubly primed to KLH and Human Gamma Globulins (HGG), and the resulting population, depleted of KLH-binding cells, was tested (in separate groups of mice) for its ability to respond to KLH and HGG in an adoptive transfer. If the KLH-binding cells include only specific precursors for anti-KLH antibody-forming cells, then transfer of the depleted population should give a diminished anti-KLH response but an equivalent anti-HGG response in comparison to the responses of unfractionated spleen.

As the data in Table 1 show, transfer of unseparated KLH and HGG doubly primed spleen cells (containing 1% KLH-binding cells) into irradiated recipients gave an anti-KLH hemagglutination titer ( $\log_2$ ) of 8.4 and an anti-HGG titer ( $\log_2$ ) of 8.6 when challenged with KLH or HGG, respectively. No detectable anti-HGG titer resulted when KLH was used as the challenging antigen, and, conversely, no measurable anti-KLH titer resulted when HGG was used as the challenging antigen. When the population depleted (undeflected) of KLH-binding cells (containing <0.1% KLH-binding cells) was transferred and challenged with KLH, the resulting anti-KLH titer of 4.0 was more than tenfold lower than the titer elicited by transfer of unseparated spleen; however, when the undeflected population was challenged with HGG, the resulting anti-HGG titer of 9.6 was comparable to that given by unseparated spleen. Transfer of the population enriched for KLH-binding cells (70%) alone gave very little if any response to either KLH or HGG, but admixture with undeflected cells (Table 1) or a known source of cooperating cells<sup>8</sup> (which themselves do not respond) to the KLH-binding cells completely restored the anti-KLH response to the level of the unseparated spleen.

The depleted population from which the KLH-binding cells were isolated was unable to give an adoptive response to KLH, although it was as efficient as unseparated spleen cells in transferring a secondary response to an unrelated antigen, HGG. Thus the precursors of antibody-forming cells in a secondary response are detected only among antigen-binding cells, and these cells reflect the specificity of their commitment.

TABLE 1

FUNCTIONAL SPECIFICITY OF KLH-BINDING CELLS  
(Fluorescent Cells: Unseparated, 1%; Deflected, 70%; Undeflected, <0.1)

Number of cells transferred ( $\times 10^6$ )*				Log <sub>2</sub> anti-KLH titer†	Log <sub>2</sub> anti-HGG titer†
Unsep.	Defl.	Undefl.	Antigen		
3			KLH	8.4 $\pm$ 0.8	<1
		3	KLH	4.0 $\pm$ 0.5	<1
	0.05		KLH	1.4 $\pm$ 0.4	<1
	0.05	3	KLH	8.2 $\pm$ 0.4	<1
3			HGG	<1	8.6 $\pm$ 0.2
		3	HGG	<1	9.6 $\pm$ 0.5
	0.05		HGG	<1	<1
	0.05	3	HGG	<1	9.4 $\pm$ 0.6

\*Spleen cells from KLH and HGG doubly primed mice were transferred into irradiated (600 R) congenic hosts along with  $3 \times 10^6$  congenic bone-marrow cells and either 100  $\mu$ g KLH or 400 mg heat-aggregated HGG.

†Log<sub>2</sub> titers (0.01M dithioerythritol resistant)  $\pm$  standard error at day 15 after transfer. Four animals per group.

### *Adoptive Primary Response to DNP*

Adoptive primary responses are inefficient with respect to the number of cells required to transfer a response compared to the number for adoptive secondary responses. This relative inefficiency is due to the limiting number of cooperators available in unprimed spleen populations. To study the adoptive primary response to DNP, we are using the DNP-KLH hapten-carrier system since carrier primed cooperators greatly increase the efficiency of the response. Since we are interested in finding out whether isolated DNP-binding cells contain the precursors for anti-DNP antibody-forming cells, populations of carrier primed cooperators (required for the differentiation and maturation of DNP-precursor cells) must be depleted of DNP-precursor cells that would be confused with the activity of the isolated DNP-binding cells. To remove precursors from the cooperator population, we used the nylon wool depletion method developed originally for this purpose in this laboratory.<sup>9</sup>

As shown in Table 2, KLH-primed spleen, containing 44% immunoglobulin-bearing (B) cells and 46% thymus-derived (T) cells as assayed by immunofluorescence, after being transferred into irradiated recipients resulted in  $21 \times 10^3$  antibody-forming cells (plaque-forming cells, or PFC) per spleen (measured in the Cunningham plaquing assay)<sup>10</sup> and an anti-KLH hemagglutination titer of 1100. Incubation of KLH-primed spleen with nylon wool resulted in a tenfold depletion of immunoglobulin-bearing cells (4%) and a complementary twofold enrichment of T cells (89%). The T-cell-enriched

population was depleted of both the ability to transfer a primary response to DNP, giving rise to  $2 \times 10^3$  PFC per spleen, and the ability to transfer a secondary response to KLH, resulting in an anti-KLH titer of 17. Thus the nylon wool efficiently removes DNP-precursor cells as well as KLH-memory B cells. However, the T-cell-enriched population contained the same cooperator activity per T cell as did the intact (unfiltered) KLH-primed spleen. Transfer of KLH-primed T cells with unprimed spleen, providing a source of DNP-precursor cells, resulted in  $49 \times 10^3$  PFC per spleen (Table 2). The anti-DNP response was twice that obtained with unfiltered KLH-primed spleen since T cells are limiting and the number of T cells transferred was double the number present in unfiltered primed spleen.

### *Isolation and the Adoptive Response of DNP-Binding Cells*

The DNP-binding cells present in unprimed spleen populations were visualized by staining spleen cell suspensions with fluorescein-conjugated DNP mouse immunoglobulin ( $^F$ DNP-MIg). As shown in Table 3, the proportion of detectable DNP-binding cells depends on the concentration of  $^F$ DNP-MIg used in the staining procedure. If unprimed spleen is stained with  $^F$ DNP-MIg at 55  $\mu$ g/ml, 0.77% of the population binds detectable quantities. However, if a

TABLE 2

#### REMOVAL OF B PRECURSOR AND MEMORY CELLS BY NYLON WOOL

Cells transferred*	Percent† stained		Direct anti-DNP PFC per spleen‡ ( $\times 10^2$ )	Anti-KLH titer§
	Ig	T		
KLH-primed spleen¶	44%	46%	210	1100
KLH-primed T cells** (nylon wool column effluent)	4%	89%	20	17
Unprimed spleen	Not done		16	20
KLH-primed T cells plus unprimed spleen	Not done		490	140

\*Irradiated (600 R) animals received  $5 \times 10^6$  of each cell type and 100  $\mu$ g alum-precipitated DNP-KLH on day 0. Animals were boosted with 10  $\mu$ g DNP-KLH (aqueous) on day 5 and were bled and sacrificed on day 12.

†Indirect stain with either rabbit anti-MIg or anti-T and  $R_{goat}$  anti-RIg (rhodamine-conjugated goat anti-rabbit Ig).

‡Arithmetic mean.

§Geometric mean.

¶Primed with 100  $\mu$ g KLH (aqueous) 3 months before sacrifice.

\*\*KLH-primed spleen depleted of Ig-bearing cells by passage through nylon wool column.



TABLE 3  
INHIBITION OF DNP-BINDING CELLS

Staining concentration of $^F$ DNP-MIg, $\mu\text{g/ml}$	Molarity of DNP on $^F$ DNP-MIg	Molarity of $\epsilon$ -DNP-lysine in staining mixture	Percent labeled cells	Percent inhibition
55	$8.7 \times 10^{-6}$		0.77*	
		$8.7 \times 10^{-5}$	0.63	18
		$8.7 \times 10^{-4}$	0.64	18
18	$2.9 \times 10^{-6}$		0.22†	
		$2.9 \times 10^{-5}$	0.12	45
		$2.9 \times 10^{-4}$	0.05	77
6	$9.7 \times 10^{-2}$		0.04‡	
		$9.7 \times 10^{-6}$	0.02	55
		$9.7 \times 10^{-5}$	0.009	78

\*3000 lymphocytes counted.

†10,000 lymphocytes counted.

‡30,000 lymphocytes counted.

concentration of 6  $\mu\text{g/ml}$  is used in the staining procedure, only 0.04% of the spleen cells bind detectable quantities of  $^F$ DNP-MIg. Moreover, if we try to inhibit the binding of  $^F$ DNP-MIg by staining in the presence of excess quantities of  $\epsilon$ -DNP-lysine, which will compete with the  $^F$ DNP-MIg for available binding sites on the cell surface, only the DNP-binding cells visualized by using low concentrations of  $^F$ DNP-MIg are easily inhibitable (Table 3). Presumably only high-avidity binding cells are labeled at low antigen concentration and are readily inhibitable with excess antigen, whereas higher concentrations of antigen are required to visualize lower avidity binding cells which are less readily inhibited by excess antigen.

Table 4 illustrates the adoptive primary response of isolated DNP-binding cells. In this experiment a high concentration of  $^F$ DNP-MIg (150  $\mu\text{g/ml}$ ) was used to visualize the DNP-binding cells in unprimed spleen. In the unseparated spleen population, 1.5% of the cells bound detectable antigen and were isolated by the FACS. The purified (deflected) population contained 90% DNP-binding cells, while the depleted (undeflected) population contained 0.2% DNP-binding cells. In the transfer of unseparated spleen cells, KLH-primed (T) cooperators, the deflected population, or the undeflected population alone, low but detectable anti-DNP PFC responses were obtained. When  $5 \times 10^6$  unseparated cells were combined with  $7.5 \times 10^6$  cooperators and transferred, the resulting response was  $28 \times 10^3$  anti-DNP PFC per spleen. Transfer of only  $5 \times 10^4$  purified DNP-binding cells with  $7.5 \times 10^6$  cooperators gave a comparable response,  $23 \times 10^3$  anti-DNP PFC per spleen. Thus, by enriching for

DNP-binding cells in the deflected fraction, we have also enriched 100-fold for DNP-precursor activity.

Transfer of  $5 \times 10^6$  undeflected cells with  $7.5 \times 10^6$  cooperators resulted, as expected, in a diminished response,  $8 \times 10^3$  anti-DNP PFC per spleen, compared with unseparated spleen. Whether these PFC are qualitatively different from those derived on transfer of unseparated spleen is discussed further in the following section.

TABLE 4

## ADOPTIVE RESPONSE OF DNP-BINDING CELLS

(Fluorescent Cells: Unseparated, 1.5%; Deflected, 90%; Undeflected, 0.2%)

Number of cells transferred* ( $\times 10^6$ )				Direct anti-DNP PFC per spleen† ( $\times 10^3$ )	
Unsep.	KLH-primed T	Defl.	Undefl.		
5	7.5	0.05	5	4	(3 to 6)
				4	(2 to 7)
				0.2	(0.1 to 3)
	7.5	0.05	5	0.6	(0.5 to 0.7)
5	7.5	0.05	5	28	(25 to 32)
	7.5			23	(19 to 26)
	7.5			8	(8 to 9)

\*Cells were transferred into irradiated (600 R) congenic hosts intravenously. Animals received 100  $\mu$ g alum-precipitated DNP-KLH on day 0 and 10  $\mu$ g aqueous DNP-KLH on day 5 and were sacrificed on day 12.

†Geometric mean and standard error. Four animals per group.

### Relationship Between Avidity of DNP-Binding Precursor Cells and Avidity of Resulting Anti-DNP PFC

Analogous to the inhibition of DNP-binding cells with  $\epsilon$ -DNP-lysine, the avidity of PFC was determined by varying concentrations of  $\epsilon$ -DNP-lysine incorporated in the plaquing medium. High-avidity PFC will be inhibited by low concentrations of  $\epsilon$ -DNP-lysine, but inhibition of lower avidity PFC will require higher concentrations of  $\epsilon$ -DNP-lysine. Figure 4 shows the inhibition profiles of the adoptive primary response to DNP discussed in Table 4.

The inhibition curves for the unseparated whole spleen and for the purified DNP-binding cells are virtually identical and represent a heterogeneous population of PFC with respect to avidities. However, the depleted population (non-DNP-binding cells) which gave a reduced number of anti-DNP PFC (Table 4) exhibits a striking difference when the avidities of the PFC are compared with the other populations. The avidities of the PFC derived from the depleted population are at least 1000-fold lower than the avidities derived from

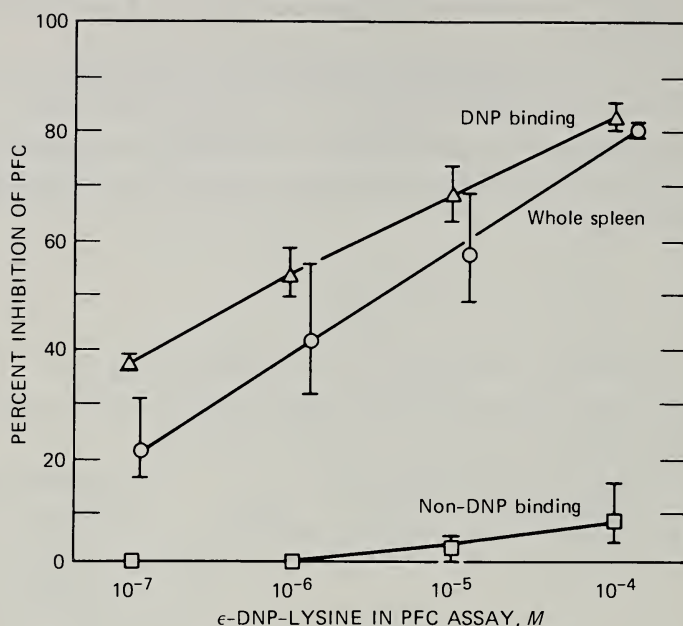


Fig. 4 Inhibition of anti-DNP PFC with  $\epsilon$ -DNP-lysine.

either the unseparated or the DNP-binding populations. Thus a concentration of  $^F$ DNP-MIg as high as 150  $\mu$ g/ml used to visualize DNP-binding cells is not sufficient to label all the DNP precursors since there appear to be DNP-precursor cells of sufficiently low binding avidity to be undetectable and therefore not separated.

These data led us to expect that, as we select higher avidity precursors, by decreasing the concentration of  $^F$ DNP-MIg used in staining, the avidity of the PFC derived from these precursors will increase. As a test of this prediction, DNP-binding cells visualized by using  $^F$ DNP-MIg at 10  $\mu$ g/ml were separated by the FACS. The results of the adoptive primary DNP transfer using these putatively high-avidity precursor cells are shown in Table 5.

Of the unseparated population, 0.2% bound detectable  $^F$ DNP-MIg. The deflected population contained 80% DNP-binding cells, and the undeflected fraction contained 0.01% binding cells. Transfer of  $5 \times 10^6$  unseparated cells with  $7.5 \times 10^6$  carrier primed cooperators again gave a much higher anti-DNP PFC response ( $77 \times 10^3$  PFC per spleen) than did  $5 \times 10^6$  unseparated cells transferred alone ( $21 \times 10^3$  PFC per spleen). Again transfer of primed cooperators, deflected population, or undeflected population alone gave low but detectable responses. The transfer of  $5 \times 10^4$  purified DNP-binding cells combined with  $7.5 \times 10^6$  carrier primed cooperators resulted in a significant response ( $27 \times 10^3$  PFC per spleen), indicating substantial enrichment of DNP-precursor activity concomitant with enrichment of DNP-binding cells.

Transfer of  $5 \times 10^6$  undeflected cells with  $7.5 \times 10^6$  primed cooperators resulted in  $22 \times 10^3$  PFC per spleen. The depleted response derived from the undeflected fraction was somewhat lower than what we would have predicted on the basis of the small fraction of DNP-binding cells removed.

Figure 5 represents the avidity profiles of the anti-DNP PFC responses derived from the different populations described in Table 5. The undeflected fraction shows the identical inhibition profile as the unseparated population. One might predict that if we had removed the high-avidity precursors from the undeflected fraction the resulting PFC should show a complementary depletion of high-avidity PFC. However, because the high-avidity PFC represent only a small proportion of the total response, we were unable to detect the depletion.

TABLE 5

ADOPTIVE RESPONSE OF HIGH-AVIDITY DNP-BINDING CELLS  
(Fluorescent Cells: Unseparated, 0.2%; Deflected, 80%; Undeflected, 0.01%)

Number of cells transferred* ( $\times 10^6$ )				Direct anti-DNP PFC per spleen† ( $\times 10^3$ )
Unsep.	KLH-primed T	Defl.	Undefl.	
5				21 (17 to 27)
	7.5			4 (3 to 5)
		0.05		0.4 (0.3 to 0.5)
			5	2 (1 to 3)
5	7.5			77 (64 to 94)
	7.5	0.05		27 (17 to 43)
	7.5		5	22 (18 to 26)

\*Cells were transferred into irradiated (600 R) congenic hosts intravenously. Animals received 100  $\mu$ g alum-precipitated DNP-KLH on day 0 and 10  $\mu$ g aqueous DNP-KLH on day 5 and were sacrificed on day 12.

†Geometric mean and standard error. Four animals per group.

The inhibition profile of the anti-DNP PFC response derived from the purified DNP-binding cells is significantly different from the profiles of the other two populations. Purified DNP-binding cells gave rise to anti-DNP PFC that were 100-fold more avid than the PFC derived from either the unseparated or the undeflected populations. Thus high-avidity DNP-binding cells detected with low concentrations of  $^F$ DNP-MIg contain DNP precursors for high-avidity anti-DNP PFC.

Using the FACS, we have clearly demonstrated that antigen-binding cells in both primed and unprimed mouse spleen contain the precursors of antibody-forming cells. Moreover, the antigen-binding precursor cells are functionally specific, and the avidity of the antibody formed is directly correlated with the avidity of the antigen receptors on the antigen-binding precursors.



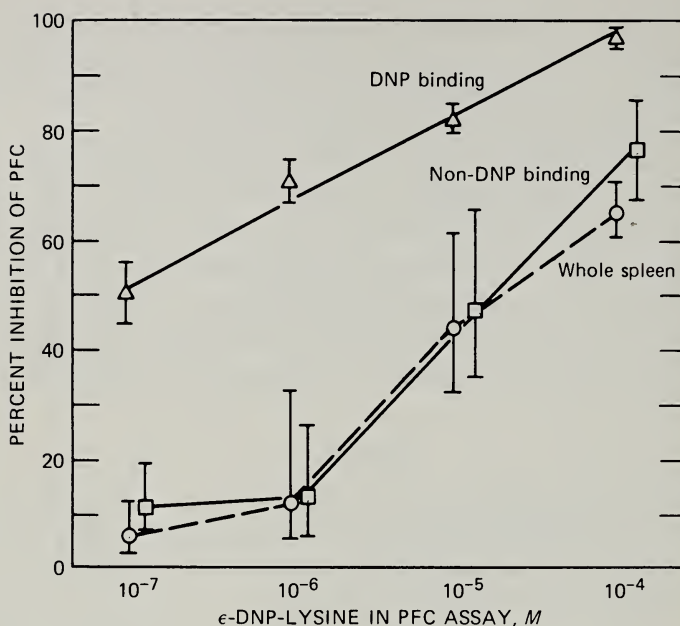


Fig. 5 Inhibition of anti-DNP PFC with  $\epsilon$ -DNP-lysine.

## ACKNOWLEDGMENTS

The work described in this paper was supported by National Institutes of Health grants AM-01-006 and GM 17367.

## REFERENCES

1. W. A. Bonner, H. R. Hulett, R. G. Sweet, and L. A. Herzenberg, Fluorescence Activated Cell Sorting, *Rev. Sci. Instrum.*, **43**: 404-409 (1972).
2. B. Rotman and B. W. Papermaster, Membrane Properties of Living Mammalian Cells as Studied by Enzymatic Hydrolysis of Fluorogenic Esters, *Proc. Nat. Acad. Sci. U.S.A.*, **55**: 134-141 (1966).
3. J. F. A. P. Miller and G. F. Mitchell, Thymus and Antigen Reactive Cells, *Transplant. Rev.*, **1**: 3-42 (1969).
4. M. C. Raff, Two Distinct Populations of Peripheral Lymphocytes in Mice Distinguishable by Immunofluorescence, *Immunology*, **19**: 637-650 (1970).
5. J. C. Howard, S. V. Hunt, and J. L. Gowans, Identification of Marrow-Derived and Thymus-Derived Small Lymphocytes in the Lymphoid Tissue and the Thoracic Duct Lymph of Normal Rats, *J. Exp. Med.*, **135**: 200-219 (1972).
6. G. L. Ada and P. Byrt, Specific Inactivation of Antigen-Reactive Cells with  $^{125}\text{I}$ -Labelled Antigen, *Nature*, **222**: 1291-1292 (1969).
7. H. Wigzell and O. Makela, Separation of Normal and Immune Lymphoid Cells by Antigen-Coated Columns, *J. Exp. Med.*, **132**: 110-126 (1970).

8. M. H. Julius, T. Masuda, and L. A. Herzenberg, Demonstration That Antigen-Binding Cells Are Precursors of Antibody Producing Cells After Purification with a Fluorescence-Activated Cell Sorter, *Proc. Nat. Acad. Sci. U.S.A.*, **69**: 1934-1938 (1972).
9. M. H. Julius, E. Simpson, and L. A. Herzenberg, A Rapid Method for the Isolation of Functional Thymus-Derived Murine Lymphocytes, *Eur. J. Immunol.*, **3**: 645 (1973).
10. A. J. Cunningham and A. Szenberg, Further Improvements in the Plaque Technique for Detecting Single Antibody-Forming Cells, *Immunology*, **14**: 599-600 (1968).

# FLOW-SYSTEMS CELL ANALYSIS AND SORTING: CLOSING REMARKS

M. A. VAN DILLA, *Session Chairman*

Biomedical Division, Lawrence Livermore Laboratory, Livermore, California

---

I will not attempt to summarize the talks, which covered both engineering techniques and applications to various biomedical problems. Instead, I will comment on what might emerge from future developments in this whole area and what approaches, experiments, and ideas might be fruitful.

1. Cell preparation, dispersal, and cytochemistry are crucial aspects that need strengthening. Present Feulgen methods need improvement, and Feulgen chemistry needs to be understood better. For example, at the Lawrence Livermore Laboratory, Joe Gray and Pat Lindl have found that, if bisulfite is omitted from the staining solution in the Feulgen procedure using acriflavine, staining quality and specificity are affected hardly at all. Since the  $\text{SO}_2$  is thought to be a key reactant in the formation of the fluorescent final product, this is surprising; we do not understand what is going on here. We need other DNA fluorescent stains that are more specific and more widely applicable than the present ones. We need fluorescent stains for a variety of other cellular components, e.g., total nucleic acid, RNA, proteins, membrane properties, hemoglobin, and antigens. Also very important is the need for vital stains specific for DNA and other cellular components which will enable live, viable populations to be sorted. One method holding much potential for broad usage is enzyme assay in cells using fluorogenic substrates that produce fluorescent products after enzymatic modification.

2. In addition to fluorescence stains, a wide variety of absorption stains are known to the microscopist. How can they be utilized in flow systems? Some cellular components have absorption peaks, e.g., 260 nm for nucleic acids and 420 nm for hemoglobin. It will be necessary to correct for distributional error by adapting the techniques developed in conventional cytophotometry.

3. Cell clumps complicate data analysis. For example, in a population of proliferating cultured cells, two  $G_1$  cells stuck together are confused with one

G<sub>2</sub> cell. Or in cervical cytology material two normal cells stuck together can be confused with an abnormal aneuploid cell. Since cell-dispersal techniques probably will never become perfect, there is need for an instrumental method for clump detection, possibly by pulse-shape analysis.

4. The light-scattering pattern of a cell contains considerable information available for measurement. The problem is to decipher the message. Several questions need answers. Can light scattering yield information on the cell interior? Can it recognize mitotic cells? Can it determine cell orientation and shape? Can it tell clumps from single cells? Can the techniques of Fourier optics help us to understand the light-scattering pattern?

5. Another question is the limit of sensitivity. Can bacteria, viruses, and subcellular components such as mitochondria or chromosomes be measured in flow systems? The chromosomes are of especial interest because of the recent developments in fluorescent banding and staining techniques which suggest possibilities for high-speed analysis and sorting.

6. Commercial instruments need maximum reliability, ease of operation, stability of optical lineup, and improved data-collection and processing facilities. We need a larger variety of commercial instrumentation, especially in the sorter area. We urgently need fluorescence and size standards that will enable us to use instruments more easily in a quantitative and reproducible way.

Biomedical applications for this technology seem limited only by problems of cell preparation and the imagination of the experimenter. In life-cycle analysis of cultured cell populations, study of synchronized and other non-steady-state populations by flow systems can yield more information than is currently obtained. Cell kinetics of normal, solid tissues needs investigation. Applications in tumor-cell kinetics could be of clinical importance in radiology. Aging of cultured cell populations is an area to which cell sorting could contribute. In the area of mutagenesis, sorting of mutant cells labeled by appropriate cytochemical agents could be very useful. Studies of cell transformation and cancer have begun, but the field is open for much more work. Studies of cell hybrids and heterokaryons should be fruitful. Studies have been made of the effects of a wide variety of such agents as radiation, drugs, hormones, chemotherapeutic agents, medium composition, etc., on cell growth, but this is a big field with much left to be done. The same can be said for studies of the mechanism of the immune response, where there are opportunities for multiparameter analysis using double immunofluorescent labeling and scattering signals. Cell-surface-fluorescent probes have also been utilized successfully, but again this area has a much larger potential than has been tapped so far. Clinical applications to a wide variety of cell-analysis problems can make solid contributions to improved health care. Tests of cell function rather than identification of cell morphology become possible; for the first time the relationship between the two can be studied and used. New ways of looking for leukocyte subsets may reveal new hematological information, and new ways of looking for cancer cells in exfoliative cytologic material may make possible the automation of cancer



screening. It seems clear that both the technology and the biomedical applications of flow systems have a very promising future and that improvement in cytochemical and cell-preparative methods is necessary for that future to be realized.

### **ACKNOWLEDGMENT**

This work was performed under the auspices of the U. S. Atomic Energy Commission.

## SESSION III

### CELL-CYCLE ANALYSIS: OPENING REMARKS

DONALD F. PETERSEN, *Session Chairman*

Cellular and Molecular Radiobiology Group, Los Alamos Scientific Laboratory,  
Los Alamos, New Mexico

---

This session deals primarily with phenomena of the cycling cell, but to be complete we will also consider the cell that does not cycle. By way of introduction, a few words about the rationale for the organization of this program are probably in order. The conference has been structured and the attendees of this meeting were invited with considerable malice aforethought. We wanted to gather together the experts in the field of this new instrumentation and then, reflecting our prejudices, to gather together experts in those fields of cellular biology which we felt could be most appropriately exploited by the use of these new and convenient measuring systems. Our biological prejudice is that the cell cycle, the cell nucleus, and the cell surface are probably the areas that are ripe for exploitation with currently existing methodology. Twenty years ago, Howard and Pelc first saw the peculiar distribution of phosphorus-32 in root tips and correctly interpreted their results to yield the formalism of a cell cycle, albeit lacking in detail. I am not sure they appreciated at the time how much anguish they were going to cause an entire generation of cell biologists in terms of the tedium of conventional methods for cell-cycle analysis. The use of radioactive labels, particularly thymidine, and the tedious business of counting labeled cells day after day have necessarily forced the cell-biology community to consider that the cell-cycle parameters of a particular cell line are indeed stable features of that cell line. Many of the estimates describing the temporal subdivision of the cell cycle were made 10 to 12 years ago, and I know we are as guilty as anyone here today of being very, very sure of the duration of *our* cell cycle.

If we consider, in a broader sense, what constitutes the cell cycle, it is clearly in biochemical terms an ordered sequence of events. If all events proceed as programmed, the cell indeed traverses  $G_1$ , S, and  $G_2$ , divides, and repeats the entire process time after time. Even though the life-cycle analysis business is now

20 years old, no one has much notion about how many events are really involved. No one knows whether all events in the cycle are crucial. No one knows the total number of putative events or how many, in fact, are important. One interesting notion that has been dealt with speculatively for some time but for which evidence does not exist is whether this sequence can be altered in any way. For example, can certain events occur ahead of or behind other events? Is the whole process locked in a single linear sequence, or are there parallel paths? These are largely unanswered questions today. Are there features in the cell cycle that, under general conditions of culture, remain unexpressed? Can these features be induced? What are the differences between noncycling and cycling cells, and, finally, what can we find out about the effects of pharmacologic agents on cycling cells and what can we find out about cycling cells by using pharmacologic agents?

It is clear from data given previously that life-cycle analysis is no longer a tour de force. It can be accomplished with trivial ease, and it can be done many times, if necessary, during the course of a single experiment. In other words, every data point can be properly controlled by a complete description of cell-cycle distribution. All that is required is sufficient material to perform the analyses.

In closing, I would like to mention very briefly some results that we have recently obtained at the Los Alamos Scientific Laboratory. The work has been a collaborative effort of Harry Crissman, Jim Jett, Phil Dean, Marv Van Dilla, and me. The problem stems from our original attempts to find out whether the microfluorometric measurements for which you have seen data were, in fact, a proper reflection of the cell cycle. Consequently the experiments involved the tedious conventional life-cycle analysis in parallel with the newer microfluorometric measurements. It is now quite clear that the two methods agree within a very few percent. If aliquots from the same culture are pulse-labeled with  $^3\text{H}$ -thymidine (1  $\mu\text{Ci/ml}$ ) and prepared for autoradiographic estimation of the fraction of cells in the S period and, in addition, are analyzed by the fluorescent-Feulgen staining procedure, the answer is virtually identical. However, the fluorescent-Feulgen procedure has the distinct advantage of providing a direct measurement of each cycle phase rather than necessitating estimates of  $G_2$  by the accumulation function and  $G_1$  by difference. This observation led to the experiment I will describe.

We wanted to know first whether monolayer and suspension-culture cells of the same line had different cycle parameters. From a parent culture we prepared two experimental cultures: one grown in monolayer and the other grown in suspension. We then removed samples at frequent intervals, approximately hourly, and looked at the life-cycle distribution across the dynamic range of exponential growth from about 50,000 to about 500,000 cells/ml. We found, much to our dismay, that at the low cell densities generally used in work on anchorage-dependent systems, indeed, the S phase of the Chinese hamster (CHO) cell was long—much longer than we usually see—because most of our work in

biochemically related areas requires large cell samples. We crowd them up as far as we can, for economic reasons, within the constraints of exponential growth. By the time cultures reach densities of 300,000 to 400,000 cells/ml, the S period of the CHO line has shrunk from 8 to 4 hr with a concomitant increase in duration of  $G_1$  from 4 to 8 hr. The phenomenon occurs in both suspension culture and monolayers to about the same extent, and we conclude that it reflects density rather than anchorage or suspension. Across the dynamic exponential growth range, the growth rate on which we have always relied as a very accurate estimate of the stability of the culture in reality is telling us nothing about cycle distribution. The expansion of  $G_1$  and the contraction of S are hiding inside an extremely stable growth rate. Therefore the take-home message of these remarks is that traditional cell-cycle-phase values are clearly not fixed parameters and that much technical disagreement from laboratory to laboratory concerning the response of cultures to various agents can probably be explained by these observations. A case in point would be the disagreements related to cycle-dependent radiosensitivity—still not clearly resolved after 15 years.



# BIOCHEMICAL EVENTS IN THE S PHASE OF REPLICATING ANIMAL CELLS

GERALD C. MUELLER

McArdle Laboratory for Cancer Research, The University of Wisconsin,  
Madison, Wisconsin

---

## ABSTRACT

The control of animal cell replication is discussed in terms of the biochemical events that make up the cell cycle. It is proposed that cells in the  $G_1$  or  $G_0$  state are restrained by membrane-mediated reactions which regulate the availability of some inducing principle that is necessary for switching on replication genes. Through perturbation of the stabilized membrane state, which may be characteristic for each cell type in  $G_1$ , this inducing principle is made available or active. Its action, in turn, causes a concerted expression of the genes leading to the synthesis of specific proteins that carry out DNA replication. The DNA replication process has been analyzed in subcellular systems and has been found to be an ordered, but discontinuous, process involving the action of a number of enzymes and protein factors which have been partially fractionated and used in reconstitution experiments. The progress of DNA replication regulates the synthesis of histones, provides the framework for the assembly of both basic and acidic proteins into newly replicated chromatin, and triggers the expression of genes necessary for the  $G_2$  and mitotic events of the cell cycle.

The structure and function of organized tissues are the products of a delicate balance between cell replication and differentiation. Each cell, living in an environment contributed by its neighbors, senses the specific mitogenic stimuli that prompt it to engage in nuclear replication. The important achievement in this triggering event is the induced expression of the genes for the synthesis and assembly of the DNA replication machinery (i.e., DNA replicase). It appears that, once DNA replication has been initiated, the actual progression guides and paces the synthesis and assembly of nuclear proteins in the formation of the daughter chromosomes and in addition sets the stage for the subsequent cell-cycle events leading to cytokinesis.<sup>1,2</sup> Inherent in nuclear replication is also the setting of the cell phenotype. By some mechanism, as yet undefined, the

newly replicated chromatin is processed during the S phase into expressible or repressed forms, with the resultant recapitulation of cell phenotype or differentiation along new lines. Since the cell phenotype in turn defines the character and intensity of the mitogenic stimuli that are required to trigger nuclear replication, one comes full circle to be confronted with the conclusion that an understanding of growth regulation in both normal and malignant states depends on obtaining molecular insights into the nuclear replication processes. In this paper biochemical approaches to the dissection of S-phase reactions are described along with emerging concepts on the nature of the genetic controls that operate in this interval of the cell cycle.

Our studies have been carried out largely in synchronized cultures of HeLa cells. As previously described,<sup>1</sup> logarithmically growing eucaryotic cells can best be visualized as traversing such a cell cycle as is depicted in Fig. 1. Studies with inhibitors of RNA and protein synthesis have revealed that this cycle is the product of sequential genetic expressions in which the main event is the move to duplicate the chromosomes. The majority of cells carry out the S-phase-associated reactions in 6 to 9 hr and are guided by the ordered synthesis of nuclear DNA. After chromosome condensation in the G<sub>2</sub> interval, the cells undergo cytokinesis and give rise to daughter cells. Cells in the G<sub>1</sub> interval display the phenotypic capabilities that identify them as a particular cell type (i.e., liver, kidney, mammary, or other). In contrast to the rest of the cell cycle, the G<sub>1</sub> interval varies greatly from cell to cell and probably reflects the delicate operation of growth control mechanisms that are so fundamental to the maintenance of organized tissues. In this interval a cell exhibits the ability to stabilize against the activation of genes coding for replication machinery. Evidence is accumulating that the overriding of these controls depends on one or more combinatorial events occurring in the cell membranes. The nature of these controls has been difficult to establish in the absence of significant markers for the G<sub>1</sub> interval. Accordingly we have sought to gain perspective on the problem by first defining the S-phase reactions that are the targets of these controls. The status of our progress concerning the reactions involved in the synthesis of histones, acidic proteins, and DNA of the chromosomes will be described.

## CONTROL OF HISTONE SYNTHESIS

Nuclei of eucaryotic cells in general contain a mass of histones equivalent to that of DNA. These proteins, which are easily extracted with dilute acids, are readily resolved by electrophoresis in polyacrylamide gels into four major fractions plus a number of minor components. With synchronized cell populations, it has been demonstrated<sup>3</sup> that the accumulation of histones during the S period is tightly coupled to the progression of DNA synthesis (Fig. 2). Initiation of DNA synthesis is attended by induction of histone synthesis, which is easily followed by isotopic labeling of the accumulated products. Interruption

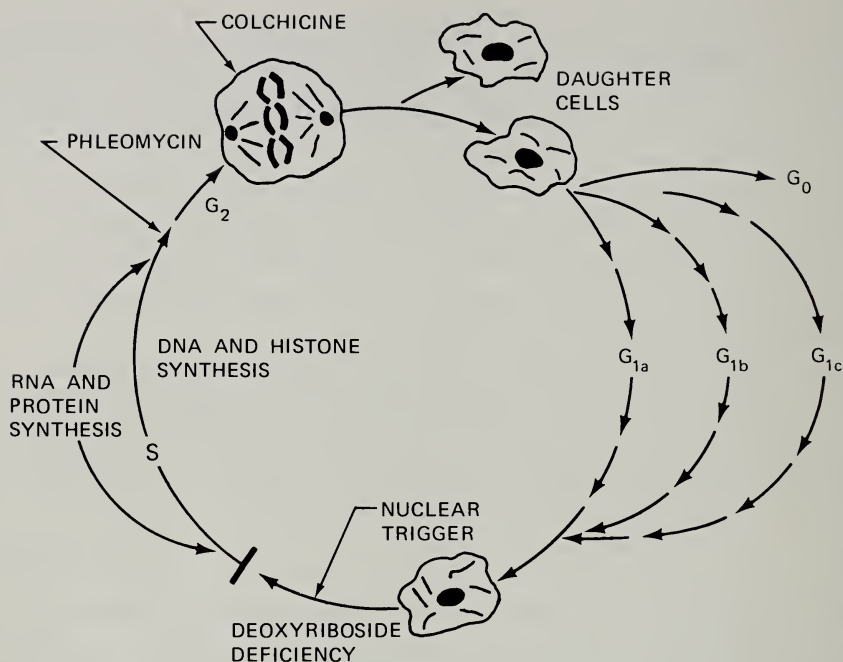


Fig. 1 Diagram of a cell cycle. The replication of animal cells is a highly ordered sequence of molecular events requiring the expression of specific genetic information at certain steps in the cycle. S phase, an interval lasting 6 to 7 hr in many cells, is concerned with synthesis of a complete complement of DNA and histones; progression through this interval requires the timely synthesis of RNA as well as DNA and proteins. The  $G_2$  interval, i.e., mitosis and cell division, requires approximately 2 to 3 hr and is concerned with the formation of newly synthesized chromatin into chromosome pairs and the distribution of the condensed chromosomes into the daughter cells. Progression into the  $G_2$  interval requires the completion of DNA synthesis and the antecedent synthesis of RNA and protein. In HeLa cells phleomycin blocks the cell cycle near the end of the DNA synthesis period. Colchicine and other agents active against the microtubules block the progression of cells through metaphase. Cells with different replication times vary mainly in the duration of the  $G_1$  interval and are depicted in the diagram as  $G_{1a}$ ,  $G_{1b}$ ,  $G_{1c}$ , and  $G_0$ . During this interval the cell expresses the phenotypic character of its particular differentiated state. Depending on intracellular and extracellular factors, cells progress through  $G_1$  and become triggered for nuclear replication; at this point they have achieved the ability to initiate DNA replication and to express the genes for histone synthesis. [From G. C. Mueller, *Biochemical Events in the Animal Cell Cycle*, *Fed. Proc.*, 28: 1781 (1969).]

of DNA synthesis midway through the S period is followed by a quick cessation of histone synthesis. Experiments with cell lysates have shown<sup>4,5</sup> that the synthesis of histones occurs on cytoplasmic polysomes that have been informed for this process (Fig. 3). When cells are exposed to <sup>3</sup>H-uridine during active DNA replication (Fig. 4), the RNA isolated from histone-synthesizing polysomes

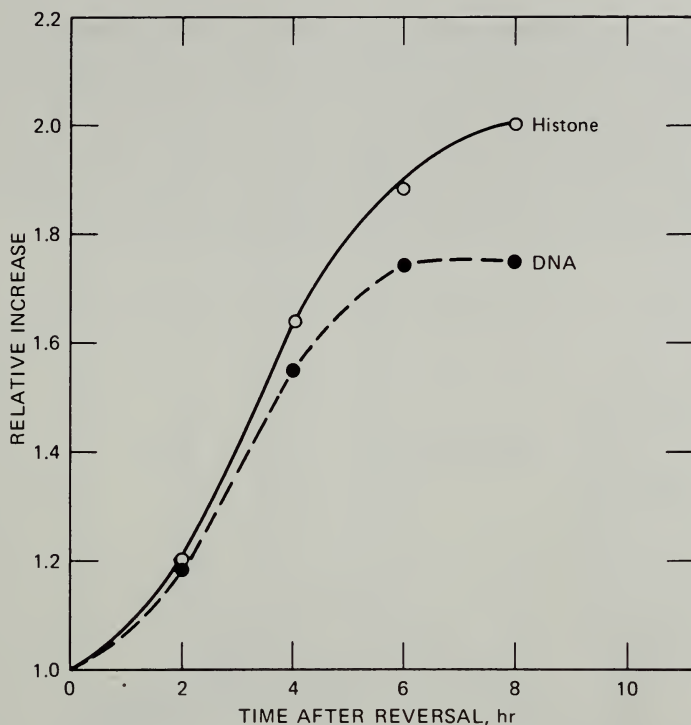


Fig. 2 Relationship of histone and DNA synthesis. Cells synchronized by an amethopterin-induced thymidineless state were reversed after 16 hr by the addition of thymidine and allowed to go through a single S phase. The relative accumulations of DNA and histones are plotted with respect to the time of reversal. [From G. C. Mueller, *Biochemical Events in the Animal Cell Cycle*, *Fed. Proc.*, 28: 1785 (1969).]

reveals at least three electrophoretically separable RNA species (6 to 8S) which on isolation are capable of informing a new polysome system for the synthesis of histones.<sup>6-8</sup> Interruption of DNA synthesis is attended by the rapid disappearance of this messenger RNA on the polysomes; on resumption of DNA synthesis, this messenger once again is synthesized and makes its appearance in the polysomes.<sup>4,9-12</sup> After compiling these observations into a diagram describing the nature of the coupling of histone synthesis to DNA replication (Fig. 5), we conclude that the initiation of DNA synthesis activates certain cistrons for transcription into histone messengers; these transcripts migrate from the nucleus to inform cytoplasmic polysomes for the synthesis of histones.<sup>10</sup> Newly synthesized histones rapidly transfer back to the nucleus where they enter into association with the newly replicated DNA. Experiments with inhibitors of protein synthesis suggest that the incoming histones, on association with the protein-deficient DNA of replicating nuclei, tend to shut down further histone-messenger production, possibly by direct association with these templates. Only through the continued synthesis of DNA are such sites kept active.



In this scheme the movement of some proteins (possibly histones alone) within the chromatin structure to protein-deficient regions of DNA during the process of DNA replication is proposed as the means of opening the histone cistrons for messenger production. This process, in turn, is paced by the cytoplasmic production of histones which, on entering the nucleus, tend to saturate such sites. In this concept histones can be viewed as possible repressors for the function of the genes that code for histone-messenger production.

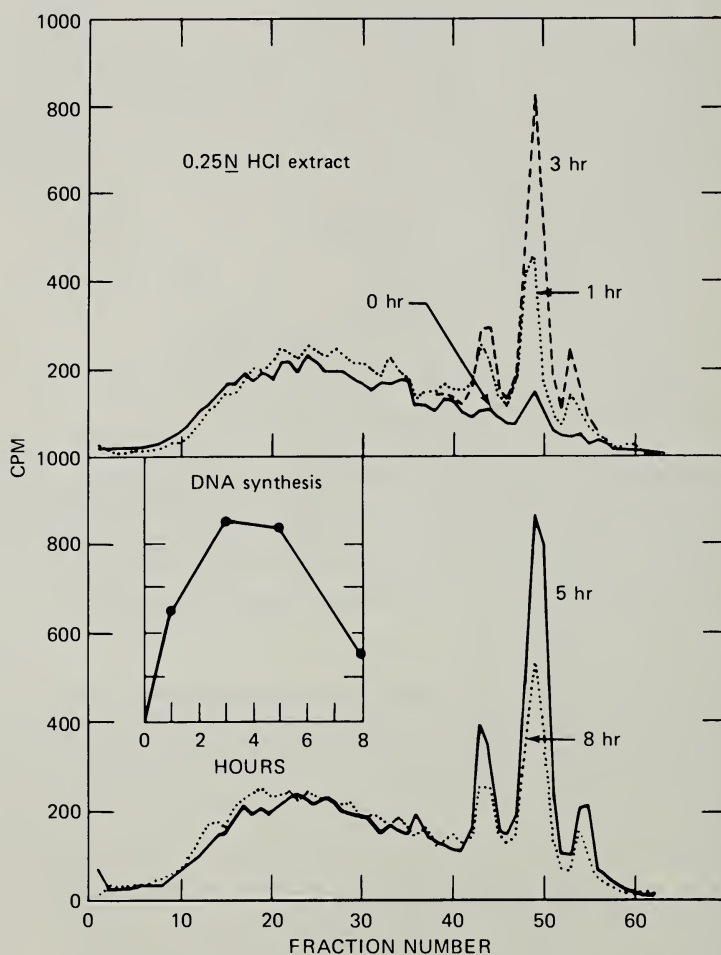


Fig. 3 Acid-soluble proteins synthesized *in vitro* on microsomes prepared at different times in S phase. HeLa cells were synchronized with amethopterin for 16 hr, and microsomes were prepared before and at different times after DNA synthesis was initiated with thymidine. Acid-soluble proteins were labeled *in vitro* with  $^3\text{H}$ -leucine and  $^3\text{H}$ -lysine 1 hr, 3 hr, 5 hr, and 8 hr after initiation of DNA synthesis. Electrophoresis was performed at pH 4.3. Thymidine was incorporated into DNA in 30-min pulses at different times after initiation of DNA synthesis (see inset). (Figure is replotted from data in Ref. 4.)

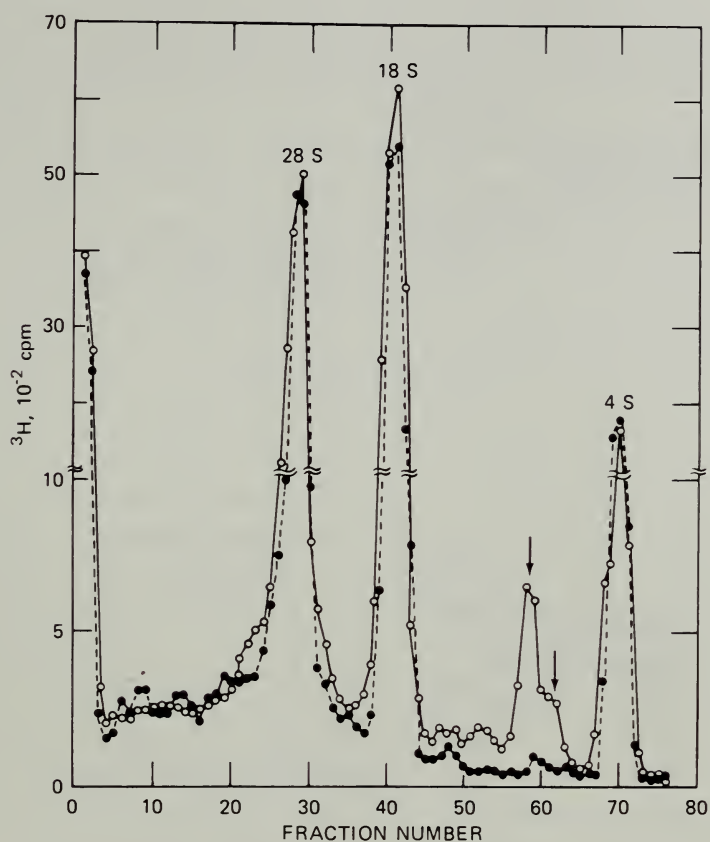


Fig. 4 Comparison of the labeled microosomal RNA isolated from HeLa cells in S phase and RNA from cells in which DNA synthesis was blocked with hydroxyurea. ○,  $125 \times 10^6$  cells synchronized with amethopterin and labeled with 600  $\mu\text{Ci}$  of 5- $^3\text{H}$ -uridine (specific activity, 25.1 Ci/mmol) for 100 min after initiation of DNA synthesis with the addition of thymidine. ●,  $5 \times 10^{-3} M$  hydroxyurea added during the last 45 min of the labeling period to block DNA synthesis during this interval. The RNA species were resolved electrophoretically in 2.0% acrylamide gels containing 0.5% agarose. [From D. Gallwitz and G. C. Mueller, RNA from HeLa Cell Microsomes with Properties of Histone Messenger, *FEBS (Fed. Eur. Biochem. Soc.) Lett.*, 6: 84 (1970).]

## SYNTHESIS OF ACIDIC NUCLEAR PROTEINS DURING THE CELL CYCLE

In contrast to the remarkable constancy of the histone-DNA ratio among eucaryotic cells, both the amount and the character of the acidic nuclear proteins vary dramatically with the functional state of a given cell;<sup>1,13</sup> they also vary with changes in cell phenotype.<sup>14</sup> The electrophoretic resolution of the acidic proteins in SDS-polyacrylamide gels reveals a minimum of 50 to 60

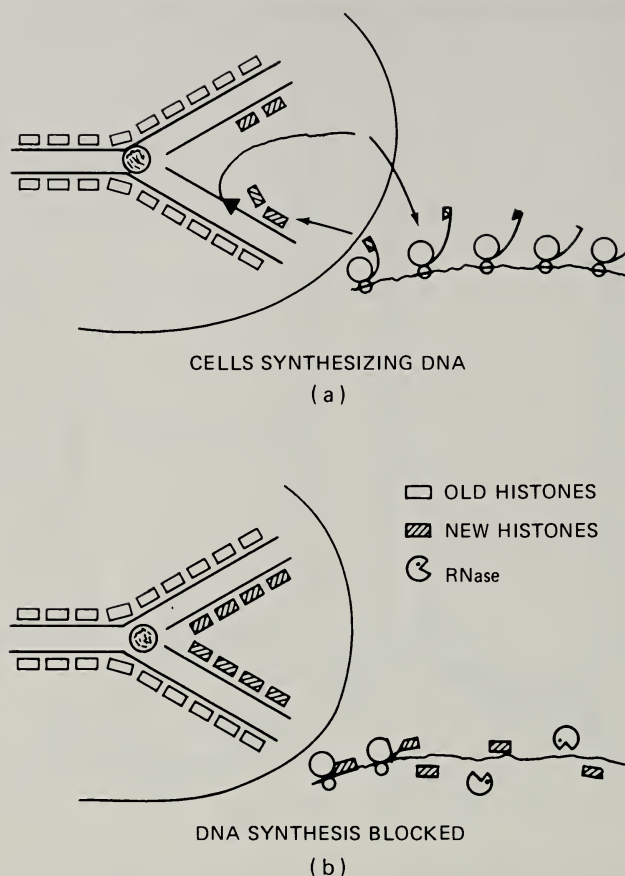


Fig. 5 Model for the control of histone synthesis by DNA replication. (a) It is proposed that the process of DNA replication opens or activates the templates for transcription of the different species of histone messenger RNA. The histones are synthesized on cytoplasmic polysomes that quickly migrate to the nucleus to be associated with newly replicated or other histone-deficient DNA regions. DNA replication in a normal S period paces this process. (b) Blocking DNA synthesis is followed by a transitory accumulation of newly synthesized histones in the cytoplasm which transfer to the nucleus, saturate the DNA, and contribute to a repression of the gene for histone-messenger production. [From W. B. Butler and G. C. Mueller, Control of Histone Synthesis in HeLa Cells, *Biochim. Biophys. Acta*, 294: 495 (1973).]

characteristic bands of proteins. In contrast to the situation with histones, the synthesis of acidic nuclear proteins is not directly coupled to the replication of DNA; instead, there is a constant turnover of these proteins in the nucleus throughout all intervals of the cell cycle.<sup>1,13</sup> Labeling experiments reveal that the synthesis and turnover of particular acidic protein species may be influenced by culture conditions, hormone treatments, and the state of differentiation of the cell.<sup>15</sup> As DNA accumulates during the S period, however, there is a

simultaneous accumulation of acidic nuclear proteins similar to the situation with histones. It appears that newly replicated DNA provides a framework for sequestering or assembling these proteins during the formation of the daughter chromosomes.

Studies of the labeling of acidic proteins indicate that the turnover of these components reflects functional events at the various chromosomal sites. This view is supported by experiments in which the genetic capability of the DNA has been modified by the substitution of bromodeoxyuridine (BUdR) for the normal thymidine in this structure.<sup>16</sup> Cells with BUdR in the DNA synthesized in the first half of the S phase exhibit a turnover pattern of their acidic proteins in the subsequent G<sub>1</sub> interval different from that of comparable cells containing BUdR in the DNA replicated during the last half of the S phase (Fig. 6). Since the cells containing BUdR in early replicating DNA are genetically blocked from engaging in nuclear replication and the cells with BUdR in late replicating DNA continue to replicate,<sup>17</sup> it is tempting to conclude that the altered labeling patterns of the acidic proteins are a manifestation of their altered phenotypes.

Although our understanding of the role and function of acidic proteins in cell biology is very limited at this time, it is nevertheless clear that the overall accumulation of these components during the S phase follows, like histones, in the wake of DNA replication; their turnover, however, continues throughout the cycle. It is likely that the selective synthesis of specific components or the establishment of unique associations of certain acidic proteins with particular segments of DNA at certain times in the cycle may play a role in the subsequent definition of cell phenotype. Optimal pursuit of problems in this attractive area of study awaits the isolation of specific nuclear proteins and the development of improved techniques for studying their association with specific DNA segments and interaction with adjacent proteins in chromatin.

## REPLICATION OF NUCLEAR DNA

Synchronized cultures of HeLa cells provide a unique opportunity for studying the enzymatic mechanisms involved in the replication of chromosomal DNA. Treatment of HeLa cultures with amethopterin to inhibit the endogenous synthesis of thymidine for 16 hr collects the cells at the entry into the S period.<sup>1</sup> The addition of exogenous thymidine to such cultures stimulates the synchronous initiation of DNA synthesis in a majority of the cells, and this process, once initiated, continues in an ordered manner to replicate the complete HeLa genome. Cells from such cultures constitute an excellent starting material for the preparation of DNA replicating systems of different levels of complexity. For example, the simple hypotonic shocking of the cells renders cells permeable to nucleotide triphosphates and greatly simplifies the study of metabolic events leading to the establishment of the replication sites. In practice this is achieved by suspending the HeLa cells in a hypotonic solution [TEMB = 0.01M *tris*-HCl,



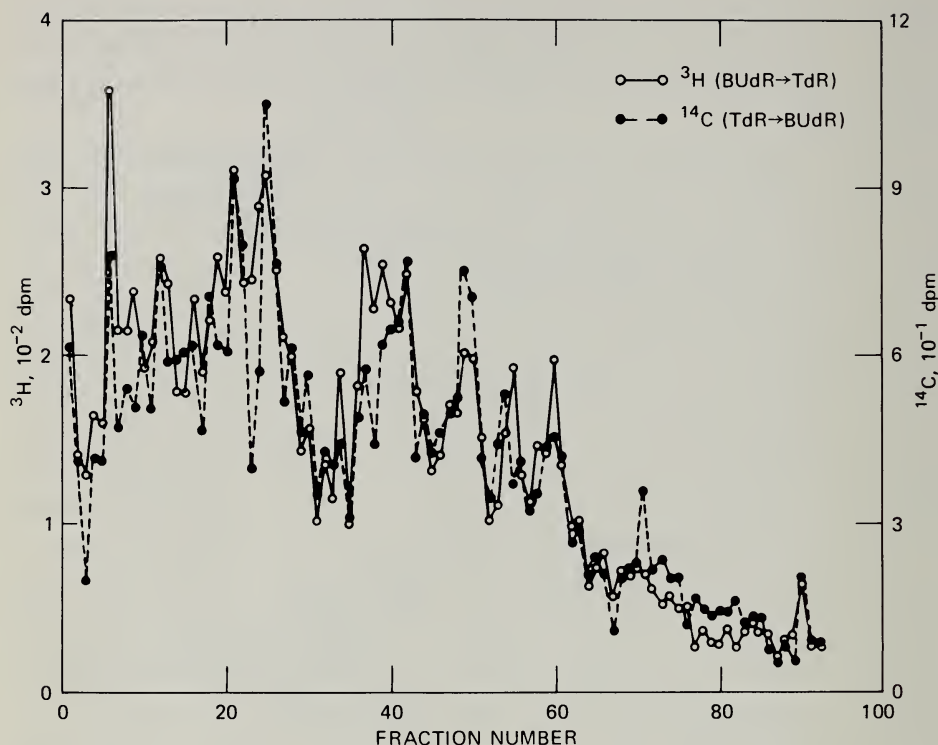


Fig. 6 Effect of incorporating 5-bromodeoxyuridine (BUdR) into cellular DNA on the synthesis of acidic nuclear proteins. Amethopterin-synchronized cultures of HeLa were caused to synthesize the DNA made in either the first 3 hr (BUdR  $\rightarrow$  TdR) or the last 3 hr (TdR  $\rightarrow$  BUdR) of the S period from exogenous BUdR; the remaining DNA of the S periods was synthesized from exogenous thymidine (TdR). In the ensuing  $G_1$  interval (16 hr after reversal of the thymidineless state), the cells were labeled for 30 min with  $^3\text{H}$ - or  $^{14}\text{C}$ -leucine. The nuclei were isolated, extracted with 0.25  $N$  HCl to remove the histones, and mixed samples of the acid-insoluble residues were solubilized and electrophoresed in SDS-polyacrylamide gels.

4mM  $\text{MgCl}_2$ , 1mM EDTA (pH 7.8), and 6mM 2-mercaptoethanol] and allowing them to stand in an ice bath for 30 min followed by sedimentation and two additional washes in the hypotonic solution. S-phase cells treated in this manner synthesize DNA for periods as long as 2 hr when the cells are supplied with the four deoxyriboside triphosphates and adenosine triphosphate (ATP). An amount of DNA equivalent to 5% of the HeLa cell genome can be replicated in this interval. The synthesis continues from sites that were actively replicating in the cells of origin. The process is semiconservative, and the omission of a single nucleotide abolishes the DNA replication process.<sup>18</sup>

With this type of preparation, the level of DNA replicase has been assayed throughout the S period of synchronized HeLa cultures. Under conditions of

complete thymidine restriction, the amethopterin-treated cells show little or no increase in the level of replicase activity<sup>19</sup> during the 16 hr of the synchronization interval (Fig. 7). Reversal of the thymidineless state by the addition of exogenous thymidine is attended by a synchronous initiation of DNA synthesis in a majority of the cells and a rapid rise in the level of DNA replicase activity, as measured by the incorporation of exogenous nucleotides into the DNA of permeable cells. The level of replicase activity correlates closely with the rate of DNA synthesis throughout the S period in the intact living cells. On completion of DNA synthesis in the S phase, the replicase activity falls to a level that can be accounted for by the partial asynchrony of the population. The rapid rise in

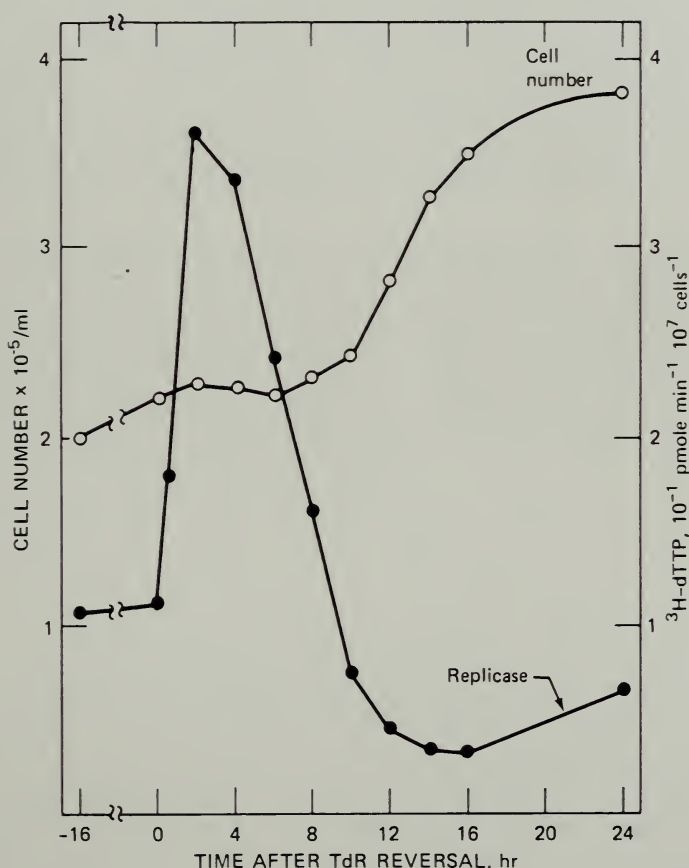


Fig. 7 Variation of DNA replicase activity during replication of HeLa cells. Logarithmically growing suspensions of HeLa cells were synchronized by treatment with amethopterin for 16 hr. At 0 hr thymidine (TdR) was added to reverse the thymidineless state and to initiate a synchronous wave of DNA synthesis. DNA replicase activity was assayed with cells that were made permeable to nucleotides (see text). Cell number was followed by direct counting with a Coulter counter.<sup>18</sup>

replicase activity after addition of thymidine to the cultures is prevented by levels of actinomycin D which block 95% of the RNA synthesis in the cultures. A delay of 1 hr in the addition of actinomycin D after a sizable fraction of the DNA replicase activity had already been accrued severely restricted further increase in replicase activity and led to a rapid and premature decline in the level of this activity. MPB, or 2-mercapto-1-( $\beta$ -4-pyridethyl)benzimidazole, a reversible inhibitor of RNA synthesis, yields analogous results; reversal of this inhibitor by medium change and resumption of RNA synthesis is attended by a rapid rise in replicase activity.

The rapid increase in replicase activity associated with the initiation of DNA synthesis after thymidine is added to amethopterin-synchronized cultures appears also to require the synthesis of some new protein. Levels of puromycin or cycloheximide which prohibit protein synthesis in the living cells also prevent the rise in replicase activity. Cells treated with cycloheximide for an interval and then returned to control media, to allow protein synthesis to resume, exhibit a rapid rise in replicase activity. Blocking protein synthesis in cells after replicase activity has been elevated causes a precipitous drop in replicase activity. Again, resumption of protein synthesis is attended by a recovery of the lost replicase activity.<sup>19</sup>

In addition to a requirement for the synthesis of new RNA and protein in the establishment of replicase activity in synchronized cultures of HeLa, this entire response appears also to depend on the actual replication of some DNA; reversal of the thymidineless state when DNA synthesis is further blocked by hydroxyurea is not accompanied by the expected increases in replicase activity. However, the amount of DNA synthesis required to establish the replicase activity is quite small. Cultures reversed with an amount of thymidine that provides for the replication of only 3% of the DNA of the HeLa nucleus acquire a major fraction of the attainable replicase activity. Once established, this replicase activity is remarkably stable even though the progression of DNA replication is interrupted by the exhaustion of thymidine. The inhibition of DNA synthesis by cytosine arabinoside in thymidine-reversed cultures prohibited the rise in replicase activity when this agent was added at the time of reversal of the amethopterin-induced thymidineless state. However, the addition of cytosine arabinoside to block further DNA synthesis (after the high levels of replicase activity have been established) maintains this activity for many hours and prevents the drop in activity that is associated with a normal progression of the S phase.<sup>19</sup>

In summary, the establishment of DNA replicase activity at specific chromosomal sites in synchronized HeLa cultures appears to require the synthesis of RNA, protein, and some DNA. The data suggest that cells synchronized at the point of entry into S phase, though already actively synthesizing the RNA and protein needed for establishment of active replicase sites in the chromatin, require the actual synthesis of some DNA for the capture and assembly of the necessary components. The studies with inhibitors of RNA

and protein synthesis also indicate that the required protein is turning over continuously in the S-phase nuclei and is in relatively short supply throughout the DNA replication interval. All studies to date are in accord with the concept that the limiting protein is essential to the stabilization of replicase sites.<sup>19</sup>

Some leads to the identity of the factors involved in DNA replication of chromosomal DNA have been obtained through a study of the DNA replication process in cell lysates. As described previously, S-phase cells<sup>20,21</sup> lysed in hypotonic media continue to synthesize DNA at sites that are biologically active in the living cells when the lysates are supplemented with the four deoxyriboside triphosphates, ATP,  $MgCl_2$ , and the proper ionic environment. Fractionation of the lysates demonstrates that the nuclei from S-phase cells depend on factors present in the soluble cytoplasmic fraction (CF) of the cell (Fig. 8). Attempts to fractionate the soluble cytoplasmic protein fraction for replicase-supporting activity have been frustrated by the instability of this activity. Gel-filtration experiments, however, have revealed that the activity falls into several fractions, some of which are completely separable from the DNA polymerase contained in the cell extracts.<sup>1</sup> Chromatography of the soluble proteins on columns of diethylaminoethyl cellulose, phosphocellulose, and hydroxyapatite provides further evidence that the activity of the cytoplasmic fraction in supporting the nuclear replication of DNA is not accounted for by the DNA polymerase activity of the preparations. The possibility remains, however, that the polymerase of the cytoplasmic fraction has to be modified by some other principle present in the soluble protein fraction in order to play a role in supporting DNA replication in nuclei. Since the activity of the cytoplasmic fraction is rapidly lost on exposure to organic solvents or hydrophobic surfaces, it is possible that a lipoidal component or lipoprotein complex is involved.

Although the activity of the cytoplasmic fraction from synchronized cultures of HeLa cells increases somewhat with the onset of each S phase, there is nevertheless considerable activity at all points in the cell cycle. This observation, coupled with the inability of cytoplasmic fractions to initiate DNA synthesis in  $G_1$  nuclei, agrees with the concept that the cytoplasmic factors support the performance of active replicase sites but do not themselves initiate DNA synthesis or carry out the  $G_1 \rightarrow S$  transition.<sup>21</sup> Analysis of the DNA synthesized,<sup>22</sup> however, reveals that the ligation of newly synthesized DNA fragments is strikingly limited in the absence of the cytoplasmic factors (Fig. 9). Thus it appears that the soluble cytoplasmic protein fraction provides at least some essential ligase for the DNA replication mechanism. Current experiments are concerned with isolating this ligase from the cytoplasmic fraction and studying its role in the DNA replication process as this occurs in the eucaryotic chromosome.

Studies of DNA replication in lysates of cells undergoing the transition from the  $G_1$  state to S phase reveal that the limiting event in this transition is the establishment of active replicating sites in the nuclei, which in turn function cooperatively with cytoplasmic factors present throughout the cell cycle of



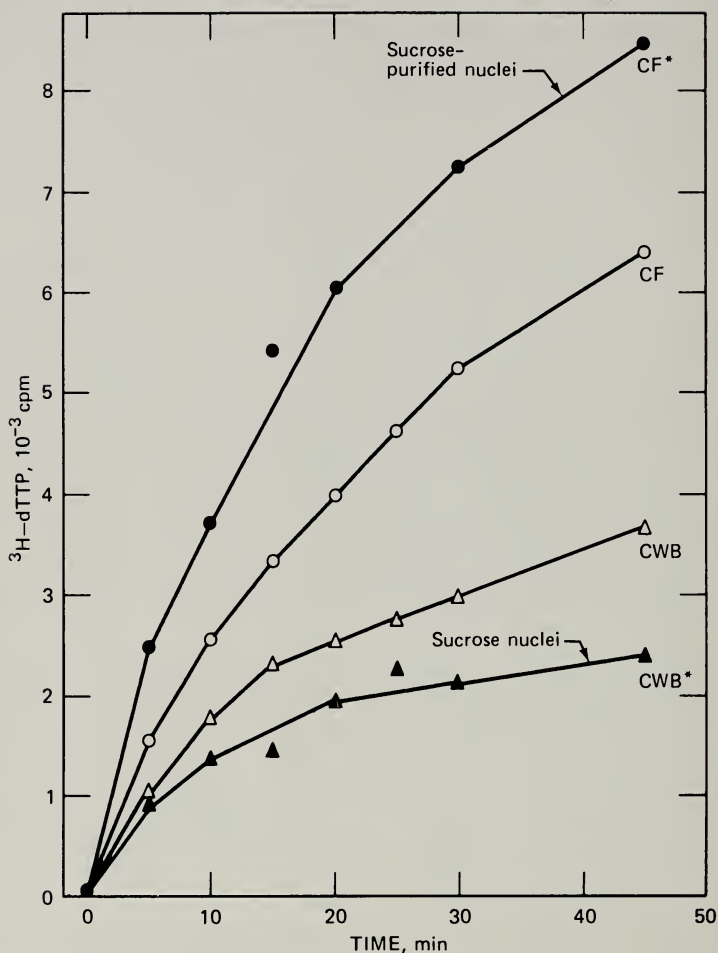


Fig. 8 Effect of cytoplasmic factors on the DNA replicating activity of isolated nuclei. Nuclei and the soluble cytoplasmic proteins were prepared according to the system of Hershey, Stieber, and Mueller<sup>2,1</sup> from synchronized HeLa cells in mid S phase (2 hr after reversal of the thymidineless state). A fraction of the nuclei was further purified by sedimentation through 0.88M sucrose. Both types of nuclei were assayed for DNA replicase activity<sup>2,1</sup> in the presence and absence of the soluble cytoplasmic proteins (CF). Cell-wash buffer solution (CWB) was used as the control solution in the absence of CF. The asterisk (\*) indicates adjustment to same number of nuclei. Data are expressed as counts per minute of <sup>3</sup>H-thymidine triphosphate incorporated into DNA per 10<sup>7</sup> nuclei during the indicated intervals.

logarithmically growing HeLa cells. In an attempt to identify the operating units of such replication sites, extensive efforts have been made to disperse the molecular components of the replicating sites, to fractionate them biochemically, and to reconstitute the activity again from identifiable fractions. After much investigation it was found that simple extraction of the nuclei with 0.27M

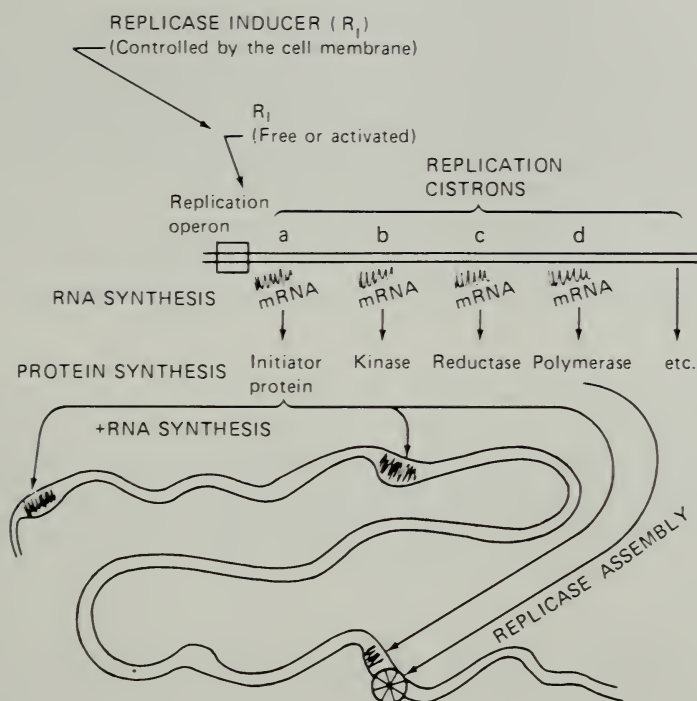


Fig. 9 Scheme for induction of DNA replication. It is proposed that the cell membrane regulates the concentration or activity of a replication inducer (or repressor), which in turn activates (or inactivates) a replication operon controlling the transcription of cistrons for messenger RNA (mRNA), leading to the production of proteins involved in DNA replication. Certain of the proteins are concerned with production of nucleotide precursors for DNA replication, and others are directly operative as components of active replicase sites.

NaCl in the TEMB buffer reduces the level of replicase activity to approximately 5% of that of the starting nuclear preparation.<sup>19</sup> This treatment leaves the overall nuclear structure intact. Activity of the nuclear residues is stimulated five- to six-fold by the addition of the cytoplasmic factors; the maximal activity, however, is limited to 25 to 30% of that of the starting cell lysate. In contrast, the addition of the nuclear extracts to such systems after reduction of the NaCl concentration permits the replicase activity to increase to a level approximating that of the starting nuclei. The reconstituted system was completely dependent on the presence of all four deoxyriboside triphosphates, ATP, and the proper ionic balance.

The active principle in the salt extracts appears to be carried by material that becomes insoluble in solutions of low ionic strength containing  $Mg^{2+}$ . Chromatographic resolution of the components in these precipitates on phosphocellulose columns reveals the presence of a DNA polymerase and of two protein fractions

that appear to synergize with this DNA polymerase to reconstitute nuclear replicase activity in salted extracted nuclear residues. This DNA polymerase activity has properties different from those found in the cytoplasm. Current experiments concern the further characterization of this polymerase activity and the helping factors; these entities appear to be distinct from known polymerases and ligase. It can be stated in passing that the salt extracts of nuclei from puromycin-treated S-phase cells exhibited the same activity as did the controls; however, the nuclear residue after salt extraction appears to contain the replicase component whose activity depends on the continued synthesis of proteins.<sup>19</sup>

## SUMMARY

The results of these studies are in accord with the concept that cells entering S phase activate an operon controlling genes that lead to the synthesis of a whole group of proteins involved in DNA replication (Fig. 9). Data from many sources indicate that production of an inducer for the replication operon, or destruction of a repressor, is regulated by the state of the cell membrane. Changes in the membrane caused by incoming mitogens, hormones, or special nutrients appear to contribute to the probability that some combinatorial event will take place which effects a switch-on of the replication operon. When deoxyribonucleotides become available, some of the replication components are assembled into active DNA replicase complexes at multiple sites throughout the chromatin. Although little is known concerning the localization of the initiation sites, the action of an initiator protein, possibly an endonuclease, on specific DNA sequences along the chromatin is suspected of opening the way for the assembly of the replicase components. DNA synthesis then proceeds bidirectionally<sup>23,24</sup> and discontinuously from such sites.<sup>22,25,26</sup> The small and intermediate-size fragments are subsequently ligated together (Fig. 10). An involvement of RNA synthesis in the initiation and maturation of these segments is inferred from preliminary studies,<sup>27,28</sup> but the actual role of this synthesis requires further study. From metabolic and reconstitution experiments, replication sites clearly contain at least two components essential for replicase activity: (1) a salt-extractable protein available in S-phase nuclei and absent in G<sub>1</sub> nuclei and (2) a nuclear residue factor whose presence or activity depends on the continued synthesis of RNA and protein throughout the S phase.<sup>19</sup> Chromatographic analysis of the salt-extracted fraction reveals the presence of a modified DNA polymerase that is distinct from the polymerase residing in the cytoplasm. Two additional factors are separated which appear to work synergistically with the modified polymerase and the nuclear residue factor.<sup>19</sup> For optimal activity, however, the reconstituted nuclear system also requires the presence of the soluble fraction of the cytoplasm. This fraction again contains at least three principles: a DNA polymerase and two factors that separate on phosphocellulose. One of the factors may be ligase.

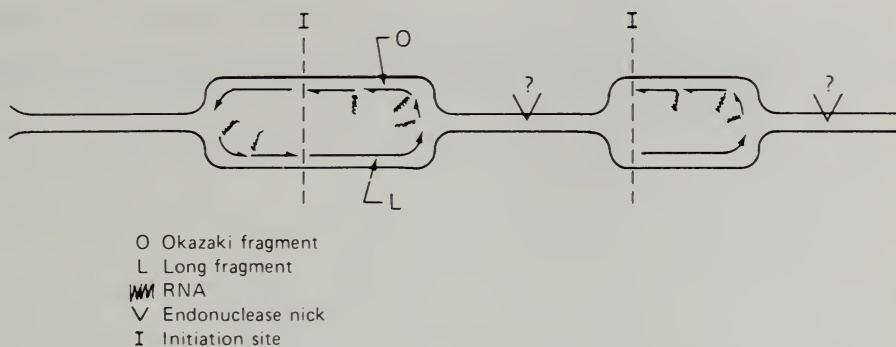


Fig. 10 A diagram of DNA replication. The process of DNA replication is presented as initiating at multiple sites throughout the genome, perhaps in the vicinity of endonuclease-mediated single-strand nicks. DNA replication is bidirectional and discontinuous, involving the synthesis of short segments of DNA starting from a primary or adapter RNA. The process is considered to involve the action of a series of enzymes referred to as DNA replicase.

Once the DNA-synthesizing machinery has been assembled, the actual progression of DNA replication appears to guide the synthesis and accumulation of histones as well as the accumulation of the acidic nuclear proteins that are synthesized throughout the cell cycle.<sup>1,2</sup> Further studies on the integration of DNA replication and the assembly of nuclear proteins along the maturing, newly replicated DNA are urgently needed since such processes may be involved in the recapitulation or differentiation of the cell phenotype.

## REFERENCES

1. G. C. Mueller, Biochemical Events in the Animal Cell Cycle, *Fed. Proc.*, **28**: 1780-1789 (1969).
2. G. C. Mueller, *The Cell Cycle and Cancer*, pp. 269-307, Marcel Dekker, Inc., New York, 1971.
3. J. Spalding, K. Kajiwara, and G. C. Mueller, The Metabolism of Basic Proteins in HeLa Cell Nuclei, *Proc. Nat. Acad. Sci. U.S.A.*, **56**: 1535-1542 (1966).
4. D. Gallwitz and G. C. Mueller, Histone Synthesis In Vitro on HeLa Cell Microsomes, *J. Biol. Chem.*, **244**: 5947-5952 (1969).
5. E. Robbins and T. W. Borun, The Cytoplasmic Synthesis of Histones in HeLa Cells and Its Temporal Relationship to DNA Replication, *Proc. Nat. Acad. Sci. U.S.A.*, **57**: 409-416 (1967).
6. D. Gallwitz and G. C. Mueller, RNA from HeLa Cell Microsomes with Properties of Histone Messenger, *FEBS (Fed. Eur. Biochem. Soc.) Lett.*, **6**: 83-85 (1970).
7. T. W. Borun, M. D. Scharff, and E. Robbins, Rapidly Labeled, Polyribosome-Associated RNA Having the Properties of Histone Messenger, *Proc. Nat. Acad. Sci. U.S.A.*, **58**: 1977-1983 (1968).
8. M. Breindl and D. Gallwitz, Identification of Histone Messenger RNA from HeLa Cells, *Eur. J. Biochem.*, **32**: 381-391 (1973).



9. D. Gallwitz and G. C. Mueller, Histone Synthesis In Vitro by Cytoplasmic Microsomes from HeLa Cells, *Science*, **163**: 1351-1353 (1969).
10. W. B. Butler and G. C. Mueller, Control of Histone Synthesis in HeLa Cells, *Biochim. Biophys. Acta*, **294**: 481-496 (1973).
11. M. Jacobs-Lorena, C. Baglioni and T. W. Borun, Translation of Messenger RNA for Histones from HeLa Cells by a Cell-Free Extract from Mouse Ascites Tumor, *Proc. Nat. Acad. Sci. U.S.A.*, **69**: 2095-2099 (1972).
12. M. Adesnik and J. E. Darnell, Biogenesis and Characterization of Histone Messenger RNA in HeLa Cells, *J. Mol. Biol.*, **67**: 397-406 (1972).
13. G. S. Stein and T. W. Borun, The Synthesis of Acidic Chromosomal Proteins During the Cell Cycle of HeLa S-3 Cells, *J. Cell Biol.*, **52**: 292-307 (1972).
14. F. Chytil and T. C. Spelsberg, Tissue Differences in Antigenic Properties of Non-Histone Protein-DNA Complexes, *Nature (London) New Biol.*, **233**: 215-218 (1971).
15. G. Rovera and R. Baserga, Effect of Nutritional Changes on Chromatin Template Activity and Non-Histone Chromosomal Protein Synthesis in WI-38 and 3T6 Cells, *Exp. Cell Res.*, **78**: 118-126 (1973).
16. K. Kajiwara and G. C. Mueller, McArdle Laboratory for Cancer Research, The University of Wisconsin, unpublished results.
17. K. Kajiwara and G. C. Mueller, Molecular Events in the Reproduction of Animal Cells. III. Fractional Synthesis of Deoxyribonucleic Acid with 5-Bromodeoxyuridine and Its Effect on Cloning Efficiency, *Biochim. Biophys. Acta*, **91**: 486-493 (1964).
18. S. Seki, M. LeMahieu, and G. C. Mueller, McArdle Laboratory for Cancer Research, The University of Wisconsin, in preparation.
19. S. Seki and G. C. Mueller, McArdle Laboratory for Cancer Research, The University of Wisconsin, in preparation.
20. D. L. Friedman and G. C. Mueller, A Nuclear System for DNA Replication from Synchronized HeLa Cells, *Biochim. Biophys. Acta*, **161**: 455-468 (1968).
21. H. V. Hershey, J. F. Stieber, and G. C. Mueller, DNA Synthesis in Isolated HeLa Nuclei: A System for Continuation of Replication In Vivo, *Eur. J. Biochem.*, **34**: 383-394 (1973).
22. W. R. Kidwell and G. C. Mueller, The Synthesis and Assembly of DNA Subunits in Isolated HeLa Cell Nuclei, *Biochem. Biophys. Res. Commun.*, **36**: 756-763 (1969).
23. J. A. Huberman and A. Tsai, Direction of DNA Replication in Mammalian Cells, *J. Mol. Biol.*, **75**: 5-12 (1973).
24. H. Weintraub, Bi-directional Initiation of DNA Synthesis in Developing Chick Erythroblasts, *Nature (London) New Biol.*, **236**: 195-197 (1972).
25. R. Okazaki, T. Okazaki, K. Sakabe, K. Sugimoto, and A. Sugino, Mechanism of DNA Chain Growth. I. Possible Discontinuity and Unusual Secondary Structure of Newly Synthesized Chains, *Proc. Nat. Acad. Sci. U.S.A.*, **59**: 598-605 (1968).
26. K. Sugimoto, T. Okazaki, and R. Okazaki, Mechanism of DNA Chain Growth. II. Accumulation of Newly Synthesized Short Chains in *E. coli* Infected with Ligase-Defective T4 Phages, *Proc. Nat. Acad. Sci. U.S.A.*, **60**: 1356-1362 (1968).
27. S. Sato, S. Ariake, M. Saito, and T. Sugimura, Properties of Nascent DNA of Ehrlich Ascites Tumor Cells Obtained by Nitrocellulose Column Chromatography, *Biochem. Biophys. Res. Commun.*, **49**: 270-277 (1972).
28. S. Sato, S. Ariake, M. Saito, and T. Sugimura, RNA Bound to Nascent DNA in Ehrlich Ascites Tumor Cells, *Biochem. Biophys. Res. Commun.*, **49**: 827-834 (1972).

# CYCLE-DEPENDENT ENZYME INDUCTION

GORDON M. TOMKINS

Department of Biochemistry and Biophysics, University of California, San Francisco, California

---

## ABSTRACT

Hormones interact with cells either by complexing with specific surface receptors and exerting regulatory effects without physical connection through the agency of conformational changes in membrane and consequent changes in the concentration of intracellular mediators or by diffusing through membrane, complexing with intracellular receptors, and subsequently binding to DNA. The induction of tyrosine aminotransferase (TAT), which is representative of the second mechanism, has been useful in developing a model for gene expression. The allosteric protein receptor for the steroid inducer exists in equilibrium between two forms, active and inactive. The inducer presumably binds to the active form. The complex interacts with a structural gene that codes for the enzyme or a regulatory gene that codes for a labile product capable of destabilizing the enzyme messenger RNA. Control of TAT occurs only during part of  $G_1$  and the S period. Both the structural and regulatory genes are blocked during the remainder of the cycle; this confers stability on residual messenger. Turnover of the enzyme remains constant throughout the cell cycle.

Dr. Mueller's presentation (this volume) focused on the two cellular structures, membranes and chromosomes, most intimately concerned with enzyme induction. I shall discuss some aspects of how hormones, which interact with these structures, can be used as convenient stimuli to study control of gene expression.

There are specific membrane receptors for the large number of hormones that interact with the outside of the cell. The receptor-hormone interaction triggers the cellular response, usually in a rather complicated way since there is no direct physical connection between the hormone and the machinery under its control. As a result of the effector-receptor interaction, conformational changes in the membrane lead to alterations in the concentrations of intracellular mediators, such as the cyclic nucleotides. These substances produce a number of effects, including changes in the production of specific proteins and in the rates

of cell proliferation. Receptor—hormone interactions might, therefore, serve as models for the action of other specific effectors, e.g., antigens and embryonic inducers.

Members of another class of hormones act inside rather than outside the cell. This group contains the steroids and probably thyroxine. These effectors must penetrate the cell membrane to combine with their specific intracellular receptors, and the hormone—receptor complexes thus formed interact directly with the chromatin.

Clearly, therefore, before we can understand the details of either enzyme induction or hormone action, we must know more about the structures of membranes and chromosomes. Conversely, specific hormone—receptor interactions might serve as useful probes for these structures.

The glucocorticosteroid induction of tyrosine aminotransferase (TAT) in cultured rat hepatoma cells (HTC) has been studied extensively.<sup>1</sup> When glucocorticoids are added to the culture medium, there is a rapid increase in the level of TAT activity and in the rate of TAT synthesis<sup>2</sup> and a parallel increase in the accumulation of polysomes making the enzyme.<sup>3</sup> Induction can be terminated rapidly either by removing the hormone or by adding an anti-inducing steroid.<sup>4</sup> This is illustrated by the experiment shown in Fig. 1, where the inducer is cortisol. Progesterone, an anti-inducer, stops TAT induction, and its enzymic activity falls because of the rapid turnover of both enzyme<sup>5</sup> and active messenger RNA<sup>3</sup> (mRNA) molecules.

Several years ago we investigated the inducibility of tyrosine aminotransferase during the HTC cell cycle.<sup>6,7</sup> The results showed that the enzyme is not inducible during G<sub>2</sub>, M, or the first 3 hr of G<sub>1</sub>. Similar experiments have been reported for another hepatoma line as well.<sup>8</sup>

Interestingly, TAT deinduction can take place only during the inducible portions of the cycle.<sup>6-8</sup> Figure 2 summarizes these observations.

The early steps in the action of glucocorticoids (and probably the other steroid hormones as well) are shown in Fig. 3. The steroid penetrates the plasma membrane<sup>9</sup> (probably by diffusion) and associates with allosteric protein receptor molecules.<sup>10</sup> These molecules are thought to equilibrate between inactive and active forms. We assume that inducing steroids have preferential affinity for the active configuration, which, following a temperature-dependent activation step,<sup>11</sup> enters the nucleus<sup>12</sup> and associates with the DNA.<sup>13</sup> Steroid receptors are therefore nonhistone chromosomal proteins with known functions (but unknown mechanisms of action).

Glucocorticoid receptors are found in a wide variety of cultured cells and of animal tissues.<sup>14</sup> Regulation by the glucocorticoids, although almost universal, apparently is not essential for the life of an individual cell since cell variants that do not contain glucocorticoid binding activity remain viable.<sup>15,16</sup> The receptors can be partially purified by affinity chromatography<sup>17</sup> or more conventional techniques.<sup>18</sup>

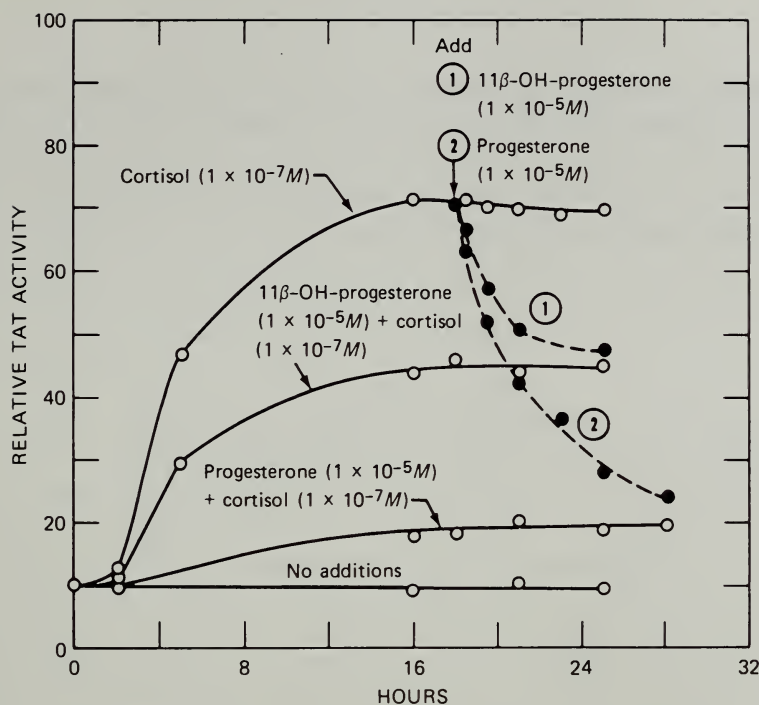


Fig. 1 Effect of steroids on TAT induction. The ordinate represents TAT specific activity, and the abscissa, hours after the start of the experiment. [From H. H. Samuels and G. M. Tomkins, *Journal of Molecular Biology*, 52: 64 (1971).]

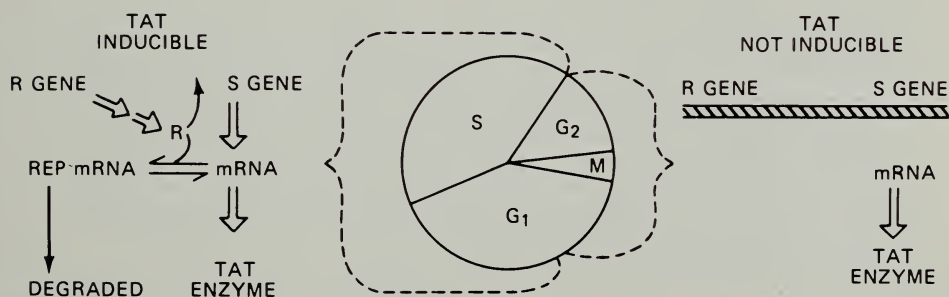


Fig. 2 Regulation of the biosynthesis of TAT during the cell-generation cycle. The S phase of the cycle is the DNA synthetic period, and  $G_1$  and  $G_2$  are, respectively, the postmitotic and premitotic phases separating S phase from mitosis (M). The TAT regulatory and structural genes are R gene and S gene, respectively. The labile posttranscriptional repressor of TAT synthesis is R; mRNA is the messenger RNA of TAT; and rep mRNA is repressed TAT mRNA through which mRNA is degraded. The cross-hatched bar on the right-hand side of the figure (under R gene and S gene) symbolizes the absence of transcription of the R and S genes during the noninducible periods. [From D. W. Martin and G. M. Tomkins, *Proceedings of the National Academy of Sciences USA*, 65: 1064 (1970).]



Progesterone, which, we propose, binds to an inactive conformation of the receptor,<sup>4</sup> competes with dexamethasone for binding.<sup>10</sup> "Suboptimal inducers" are assumed to interact with both active and inactive forms, thereby partially converting inactive to active receptors. The final ratio of the forms is determined by their relative affinities for a particular steroid.<sup>4</sup>

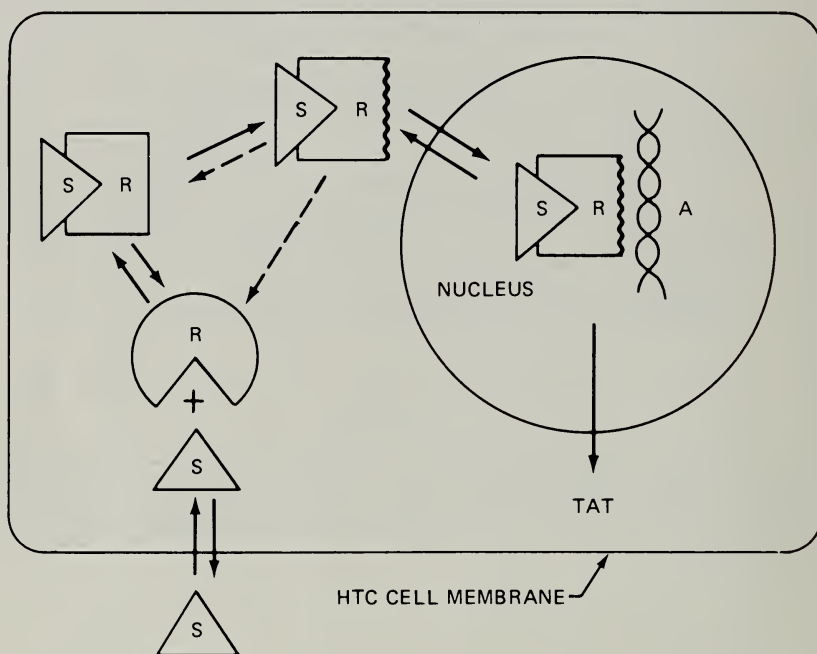


Fig. 3 Early steps in glucocorticoid action. The steroid (S) enters the cell and binds to the cytoplasmic receptor protein (R). In the case of inducer steroids, the receptor-steroid complex has a different conformation from the unbound receptor. Further changes, "activation," occur in the R-S complex exposing a nuclear binding site. The active complex then binds to the nuclear acceptor site (A) and tyrosine aminotransferase (TAT) is eventually induced. [From S. J. Higgins, G. G. Rousseau, J. D. Baxter, and G. M. Tomkins, *Journal of Biological Chemistry*, 248: 5871 (1973).]

When dexamethasone is added to HTC cells, the receptor concentration of the cytosol falls by about 70% and an equivalent amount of receptor-steroid complex appears in the nucleus.<sup>12</sup> When the steroid is removed from the medium, there is a rapid reappearance of the receptor in the cytosol, even in experiments in which macromolecular synthesis is blocked. We think, therefore, that there is a simple equilibrium between the cytoplasmic and nuclear forms of the receptor-steroid complex.

Progesterone, presumably because it binds to the inactive form of the receptor, does not promote its nuclear migration.<sup>12</sup>

The association of receptor-steroid complexes with nuclei is obviously complicated. Essentially three points of view are held by investigators in this field:

1. The nucleus contains specific "acceptor" proteins.<sup>19,20</sup>
2. Nuclear binding, at least as observed in whole cells, is largely nonspecific, and, although there must be specific acceptor sites, they are all but impossible to detect.<sup>21</sup>
3. The sites occupied are related to or identical to the biologically active acceptor sites.

If nuclei are treated with DNase, they lose 30 to 40% of their DNA and their ability to bind receptor-dexamethasone complexes.<sup>13</sup> These experiments obviously suggest that DNA plays an important role in the binding of receptor-steroid complexes. Further experiments<sup>22</sup> show that there is indeed an association of receptor-steroid complexes with purified DNA. This association in some ways resembles nuclear binding since it requires both that the receptor be associated with an inducer steroid and that "activation" of the receptor-steroid complex precede DNA binding. Single-stranded DNA binds activated complex only 30% as well as double-stranded DNA. Ribosomal RNA does not bind. However, DNA from *Escherichia coli* bacteriophages  $\lambda$  and T7 bind receptor-dexamethasone complex as well as rat DNA.

More direct evidence for the role of DNA in the acceptor sites comes from experiments using steroid-sensitive mouse lymphoma cells. Ordinarily these cells are killed after prolonged contact (12 to 24 hr) with physiological concentrations of the glucocorticoids.<sup>23</sup> Steroid-insensitive variants, apparently mutants,<sup>24,25</sup> arise at low frequency, however. Cells bearing one such mutant phenotype that is nuclear transfer deficient (nt-) contain receptor-steroid complexes that fail to migrate to the nucleus. In cell-free experiments the complex has diminished binding to purified DNA.<sup>26,27</sup> In the same vein, a mutant cell containing receptors that localize in the nucleus more avidly than do the normal complexes also binds more tightly to DNA.<sup>27</sup> These results suggest that DNA binding is indeed important for nuclear localization although they do not, as yet, allow us to distinguish between the three alternatives presented previously.

On the basis of observations that only the last two-thirds of  $G_1$  and the whole of S are periods when TAT synthesis can be regulated, we have formulated a model for TAT induction<sup>28</sup> involving a structural gene, which codes for the enzyme, and a regulatory gene, the product of which destabilizes its RNA. This gene product is itself labile. Initially the inactivation of the messenger may be reversible, but ultimately the process leads to permanent degradation (Fig. 2).

During the "controllable" periods of the cycle, the synthesis of TAT messenger takes place and the mRNA is labile. In the nonregulated portion of

the cell cycle, we believe that the expression of both regulatory and structural genes is blocked, so that whatever quantity of RNA is active when the cells arrive at G<sub>2</sub> is now stable. The turnover rate of TAT enzyme molecules appears to be constant throughout the cell cycle, however.

Which of the genes in the model are affected by the steroids? Steinberg et al.,<sup>29</sup> who have been studying this question by comparing the turnover rates of active TAT messenger in the presence and absence of the inducer, have calculated that at a maximum the half-time of mRNA of the messenger inactivation is 1 to 1.5 hr, but whether the receptor-steroid complex favors mRNA production or inhibits its inactivation remains equivocal.

## REFERENCES

1. G. M. Tomkins, in *Advances in Cell Biology*, D. Prescott (Ed.), Vol. 2, p. 299, Appleton-Century-Crofts, Inc., New York, 1971.
2. D. K. Granner, S. Hayashi, E. B. Thompson, and G. M. Tomkins, *J. Mol. Biol.*, **35**: 291 (1968).
3. W. A. Scott, R. Shields, and G. M. Tomkins, *Proc. Nat. Acad. Sci. USA*, **69**: 2937 (1972).
4. H. H. Samuels and G. M. Tomkins, *J. Mol. Biol.*, **52**: 57 (1970).
5. A. Hershko and G. M. Tomkins, *J. Biol. Chem.*, **246**: 710 (1971).
6. D. W. Martin, G. M. Tomkins, and M. Bresler, *Proc. Nat. Acad. Sci. USA*, **63**: 842 (1969).
7. D. W. Martin, Jr. and G. M. Tomkins, *Proc. Nat. Acad. Sci. USA*, **65**: 1064 (1970).
8. L. Sellars and D. Granner, *J. Cell Biol.*, **60**: 337 (1974).
9. B. B. Levinson, J. D. Baxter, G. G. Rousseau, and G. M. Tomkins, *Science*, **175**: 189 (1972).
10. G. G. Rousseau, J. D. Baxter, and G. M. Tomkins, *J. Mol. Biol.*, **67**: 99 (1972).
11. S. J. Higgins, G. G. Rousseau, J. D. Baxter, and G. M. Tomkins, *J. Biol. Chem.*, **248**: 5866 (1973).
12. G. G. Rousseau, J. D. Baxter, S. J. Higgins, and G. M. Tomkins, *J. Mol. Biol.*, **79**: 539 (1973).
13. J. D. Baxter, G. G. Rousseau, M. C. Benson, R. L. Garcea, J. Ito, and G. M. Tomkins, *Proc. Nat. Acad. Sci. USA*, **69**: 1892 (1972).
14. P. L. Ballard, J. D. Baxter, S. J. Higgins, G. G. Rousseau, and G. M. Tomkins, *Endocrinology*, **94**: 998 (1974).
15. W. Rosenau, J. D. Baxter, G. G. Rousseau, and G. M. Tomkins, *Nature (London) New Biol.*, **237**: 20 (1972).
16. C. H. Sibley and G. M. Tomkins, *Cell*, **2**: 213-220 (1974).
17. D. Failla, in preparation.
18. G. Litwack, R. Filler, S. A. Rosenfield, N. Lichtash, C. A. Wishman, and S. Singer, *J. Biol. Chem.*, **248**: 7481 (1973).
19. B. W. O'Malley, T. C. Spelsberg, W. T. Schrader, F. Chytil, and A. W. Steggles, *Nature*, **235**: 141 (1972).
20. G. A. Puca, V. Sica, and E. Nola, *Proc. Nat. Acad. Sci. USA*, **71**: 979 (1974).
21. D. Williams and J. Gorski, *Proc. Nat. Acad. Sci. USA*, **69**: 3464 (1972).
22. G. G. Rousseau, in preparation.
23. K. Horibata and A. W. Harris, *Exp. Cell Res.*, **60**: 61 (1970).

24. C. H. Sibley, U. Gehring, H. Bourne, and G. M. Tomkins, in *Control of Proliferation in Animal Cells* (Vol. 1 of Cold Spring Harbor Conferences on Cell Proliferation), B. Clarkson and R. Baserga (Eds.), May 20-27, 1973, Cold Spring Harbor Laboratory, 1974.
25. C. H. Sibley and G. M. Tomkins, *Cell*, **2**: 221-227 (1974).
26. U. Gehring, in preparation.
27. K. Yamamoto and M. Stampfer, in press.
28. G. M. Tomkins, T. D. Gelehrter, D. K. Granner, D. W. Martin, Jr., H. H. Samuels, and E. B. Thompson, *Science*, **166**: 1474 (1969).
29. R. A. Steinberg, W. A. Scott, B. B. Levinson, R. D. Ivarie, and G. M. Tomkins, Glucocorticoid Induction of Tyrosine Aminotransferase, in *Regulation of Gene Expression in Eukaryotic Cells*, Fogarty International Center Proceedings No. 25, U. S. Government Printing Office, Washington, D. C., in press.



# SEQUENTIAL BIOCHEMICAL EVENTS IN THE MAMMALIAN CELL CYCLE

ROBERT A. TOBEY, LAWRENCE R. GURLEY, C. E. HILDEBRAND,  
PAUL M. KRAEMER, ROBERT L. RATLIFF, and RONALD A. WALTERS  
Cellular and Molecular Radiobiology Group, Los Alamos Scientific Laboratory,  
Los Alamos, New Mexico

---

## ABSTRACT

In examining highly synchronized populations of Chinese hamster (line CHO) cells, we have demonstrated a temporally coordinated series of events that prepare cells for mitosis. Preparations begin prior to initiation of DNA replication and continue through late interphase into mitosis. Two hours before entry into S phase, there is an abrupt increase in the amount of DNA that associates with membrane, and concomitantly phosphorylation of old, preexistent histone f1 begins. The levels of deoxyribonucleoside triphosphates in acid-soluble pools increase at approximately 30 min before the start of DNA replication. As cells traverse through late interphase, cell-surface-associated heparan sulfate is released into the culture medium immediately prior to mitosis. Phosphorylation of histone f3 and a subfraction of f1 occurs specifically as cells traverse from  $G_2$  into M, with dephosphorylation occurring as cells reenter  $G_1$ . Upon exit from mitosis, the deoxyribonucleotides are rapidly degraded. These observations allow us to construct a map of sequentially ordered events in the CHO cell cycle. The results suggest that, even in cultured cells, regulation of proliferation depends upon a complex series of coordinated processes.

The detection of specific sequences of biochemical processes as cells replicate their DNA and divide implies a temporally ordered expression of genetic information during the cell cycle. As part of a long-term program at Los Alamos Scientific Laboratory (LASL), we have examined a number of events involved in cell proliferation using a single cell line, Chinese hamster cells (line CHO), under a uniform set of growth conditions. In this manner direct comparisons may be made between various processes located throughout the cell cycle. In this paper we construct a map showing temporal arrangement of events during the cell cycle and demonstrate the complexity of coordinated processes that exist even in cultured cells. We are not attempting a general review of the extensive

literature concerned with mammalian cell-cycle biochemistry, since numerous excellent reviews are available.<sup>1-4</sup> Instead, we have compiled our cumulative cell-cycle experiences and, in this presentation, attempt to assess the biochemical implications of relationships between various proliferative processes.

## CELL-SYNCHRONIZATION PROCEDURES

Studies of cell-cycle-specific processes are facilitated by use of cell populations synchronized at multiple stages of the cell cycle. A variety of synchronization techniques was employed in our studies. In one procedure cells transferred to medium containing suboptimal quantities of isoleucine become arrested in  $G_1$  but remain capable of synthesizing a variety of macromolecules over a prolonged period without entering a state of gross biochemical imbalance.<sup>5-7</sup> These cells resume cycle traverse following restoration of isoleucine.<sup>5-7</sup> In this manner extremely large quantities of cells (limited only by the size of the culture vessel) can be obtained in  $G_1$ . The kinetics of cell-cycle progression after reversal of the isoleucine-mediated  $G_1$  block are essentially identical to those for cultures allowed to cycle following mitotic selection (Fig. 1a). These techniques are unsuitable for studying late interphase events because of a loss of synchrony due to variations in the rate of cycle progression by individual cells in the population. Additional techniques consequently are required to study events in late interphase. In a second protocol, cells prepared by either the isoleucine-deficiency technique or by mitotic selection are treated with hydroxyurea, with the result that the cells traverse  $G_1$  and accumulate at the  $G_1/S$  boundary.<sup>9</sup> After hydroxyurea removal, the cells enter S phase immediately and commence dividing within 6 hr (Fig. 1b). In another procedure cells released from isoleucine-mediated  $G_1$  arrest are synchronized in mid-S phase by treatment with 20 mM thymidine;<sup>10</sup> thymidine blockade is reversed by washing out excess thymidine. The various procedures for synchrony induction just described were used in the studies that follow.

## HISTONE PHOSPHORYLATION

Recently accumulated data suggest that control of biological activity is partially dependent upon the modulation of the physical state of chromatin arising from reversible chemical modification of histones.<sup>11,12</sup> Furthermore, Balhorn et al.<sup>13</sup> demonstrated a direct correlation between the rate of growth in a variety of tumors and the extent of phosphorylation of histone f1. These observations led us to investigate patterns of histone phosphorylation during the CHO cell cycle.

The histone-phosphorylation patterns in traversing interphase cells from an exponentially growing culture are shown in Fig. 2a and b. In these cells two species of histone are phosphorylated, f1 and f2a2.<sup>14</sup> However, as shown in

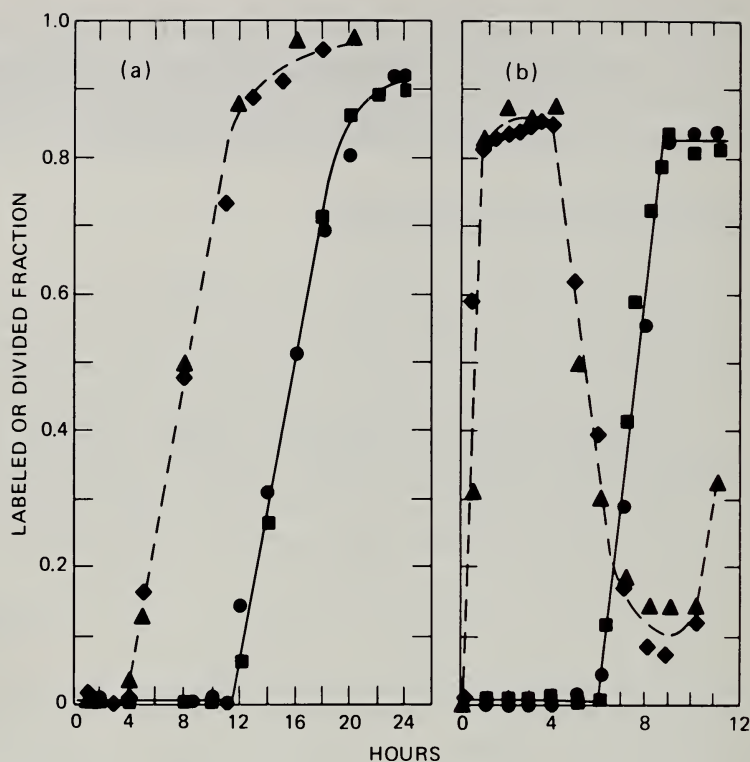


Fig. 1 Techniques used to synchronize CHO cells. (a) Fraction of cells synthesizing DNA (incorporating  $^3\text{H}$ -thymidine during continuous exposure) (▲, ◆); cell number increase in cultures synchronized by the isoleucine-deficiency<sup>5-7</sup> technique (●) and the mitotic-selection<sup>8</sup> technique (■). (b) Fraction of cells synthesizing DNA, (incorporating  $^3\text{H}$ -thymidine during 15-min pulse-labeling periods) (▲, ◆); the fraction of cells dividing in cultures synchronized by the isoleucine-deficiency/hydroxyurea<sup>9</sup> technique (●) and the mitotic-selection/hydroxyurea technique (■). The divided fraction represents  $N/N_0 - 1$ .

Fig. 2c and d, in nonproliferating  $G_1$ -arrested cells, the only phosphorylated species is f2a2.<sup>15</sup> At what stage during transition from a nonproliferating to a proliferating state does phosphorylation of histone f1 commence? For an answer to this question, the rates of synthesis and phosphorylation of histone f1 were determined along with the rate of entry into S phase in arrested cells resuming cycle progression after restoration of isoleucine (Fig. 3). Although bulk synthesis of histone f1 commences at the time that DNA replication begins (Fig. 3a), f1 phosphorylation precedes entry into the DNA synthetic phase by approximately 2 hr (Fig. 3b). Thus, phosphorylation of old, preexistent histone f1 begins significantly before the cells start to replicate DNA. As shown elsewhere,<sup>16</sup> phosphorylation of histones f1 and f2a2 continues at increased rates through S,  $G_2$ , and into M.

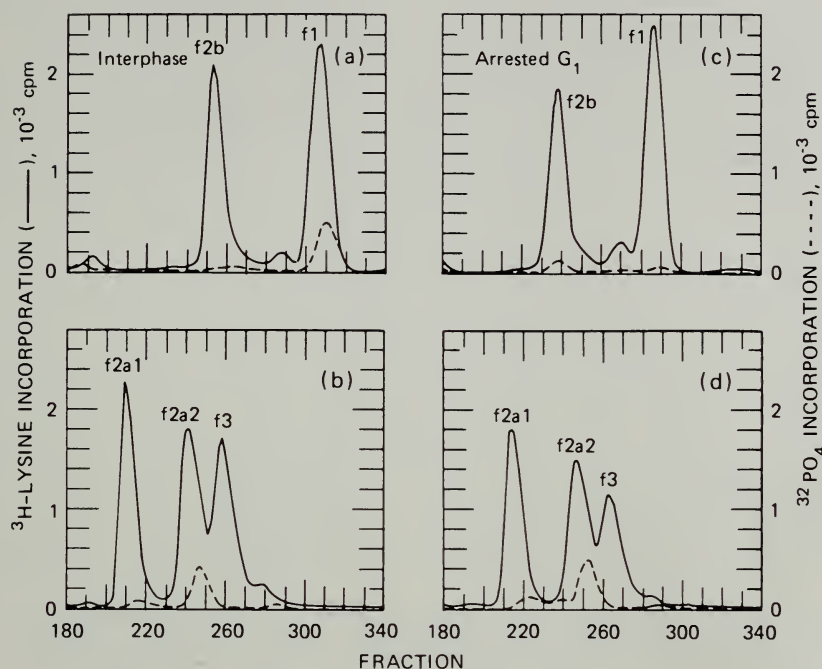


Fig. 2 Preparative gel electrophoretic profiles of histone phosphorylation in traversing interphase CHO cells (parts a and b) and in isoleucine-deficient  $G_1$ -arrested CHO cells (parts c and d). The histones were uniformly prelabeled for 52 hr with  $^3\text{H}$ -lysine (—) and were pulse labeled with  $\text{H}_3\text{}^{32}\text{PO}_4$  (---) for 2 hr before collection to reveal phosphorylated histones. Experimental details for parts a and b and for parts c and d are described in Refs. 14 and 15, respectively.

Interesting changes in the pattern of histone phosphorylation also occur as cells enter and exit from mitosis,<sup>14</sup> as shown in Fig. 4. In these studies monolayer cultures were exposed to Colcemid and  $\text{H}_3\text{}^{32}\text{PO}_4$  for 2 hr, after which the accumulated metaphase-arrested cells (which had been exposed to  $^{32}\text{PO}_4$  during transition from  $G_2$  to M) were dislodged by mitotic selection and the histones were isolated and analyzed. Figure 4a and b shows that, in addition to the phosphorylated f1 and f2a2 species normally seen in late  $G_1$ , S,  $G_2$ , and mitotic cells,<sup>16</sup> there are two additional phosphorylated histones, f3 and a slowly migrating subfraction of f1. These latter two histone species are phosphorylated to a substantially lesser degree in cells already in metaphase arrest when first exposed to  $^{32}\text{PO}_4$  (Fig. 4c and d). In other studies<sup>14</sup> not shown, we demonstrated that the f3 and f1 subfractions are subsequently dephosphorylated when cells reenter  $G_1$ . The preceding results indicate that histone f3 and the f1 subfraction are phosphorylated specifically as cells complete  $G_2$  and are dephosphorylated as cells complete M, suggesting that these phosphorylated species play a role in mitosis.



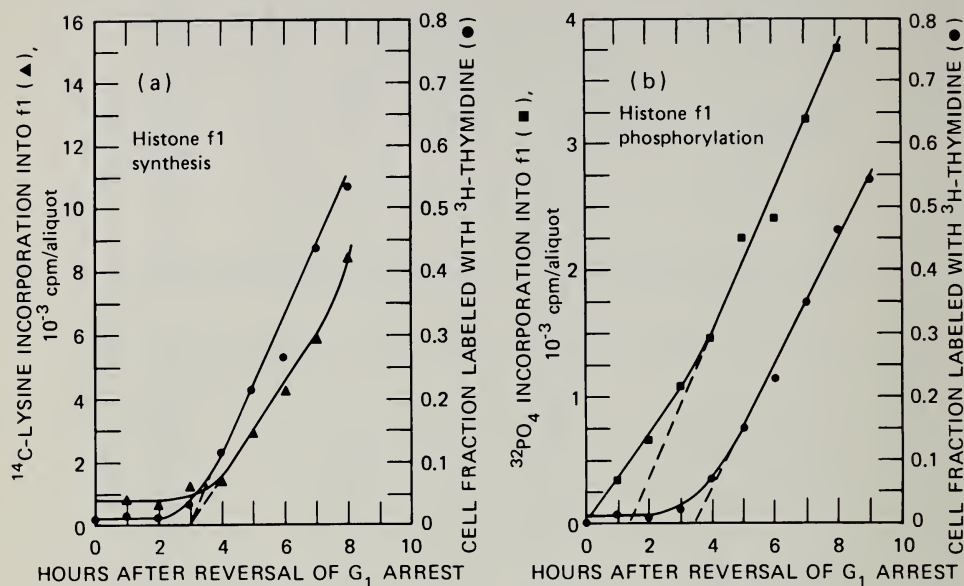


Fig. 3 Rates of synthesis (a) and phosphorylation (b) of histone f1 in CHO cells after reversal of G<sub>1</sub> arrest. ●, fraction of cells synthesizing DNA (incorporating <sup>3</sup>H-thymidine during 1-hr pulse-labeling period). Rates of synthesis (▲) and phosphorylation (■) of f1 were determined by measuring the amounts of <sup>14</sup>C-lysine and H<sub>3</sub><sup>32</sup>PO<sub>4</sub> incorporated during the 1-hr pulse-labeling periods as described previously.<sup>14</sup>

## DNA-LIPOPROTEIN COMPLEXES

Complexes of DNA associated with material containing hydrophobic regions (presumed to represent lipoprotein fragments) can be isolated from cells<sup>17</sup> with the aid of crystals formed by interaction of the detergent sodium lauroyl sarcosinate with MgCl<sub>2</sub>. These complexes contain material that can be labeled with <sup>14</sup>C-thymidine or <sup>14</sup>C-choline. They are resistant to ribonuclease treatment but are sensitive to treatment with deoxyribonuclease, Pronase, or sodium dodecyl sulfate or to heating to temperatures above 37°C.<sup>18,19</sup> Less than 10% of the DNA in the complexes can be attributed to a nonspecific entrapment.<sup>18,19</sup> In view of these properties suggesting that the complexes are comprised of DNA specifically associated with lipoprotein, cell-cycle studies were initiated. Cells whose DNA had been prelabeled with <sup>14</sup>C-thymidine were resuspended in label-free medium following mitotic selection, and the amount of old DNA associated in the complexes was determined at various times thereafter (Fig. 5a). A small amount of DNA is complexed to lipoprotein fragments even during mitosis and early G<sub>1</sub>. However, a sudden increased association commences at approximately 2 hr prior to initiation of DNA replication. To study complexes in late interphase, we synchronized cells with prelabeled DNA by

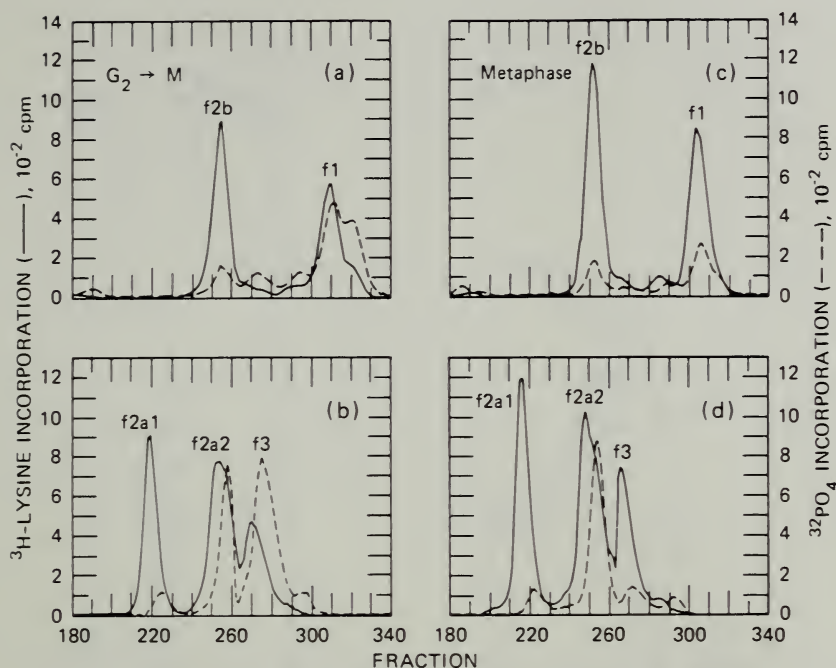


Fig. 4 Preparative gel electrophoretic profiles of histone phosphorylation in CHO cells traversing from  $G_2$  into M (parts a and b) and in CHO cells already in metaphase (parts c and d) during exposure to  $\text{H}_3^{32}\text{PO}_4$ . Cells were uniformly prelabeled with  $^3\text{H}$ -lysine (—) and were pulse labeled for 2 hr with  $\text{H}_3^{32}\text{PO}_4$  (---). For experimental details see Ref. 14.

combined mitotic selection and hydroxyurea treatment. At the time of removal of hydroxyurea (time 0 sample in Fig. 5b, when cells are accumulated near the  $G_1/S$  boundary), the amount of old DNA complexed to lipoprotein is already at a high level, indicating that the amount of DNA in the complexes had increased even though DNA replication was prevented by hydroxyurea. After removal of hydroxyurea there is a further enhancement of DNA associated with lipoprotein which persists through S and into  $G_2$ , then decreases as cells begin to divide. Thus the relationship between DNA and lipoprotein undergoes two major transitions: an increased interaction at 2 hr prior to initiation of DNA synthesis and a decreased association at mitosis.

## DEOXYRIBONUCLEOTIDE POOLS

Before a cell can commence synthesizing DNA, adequate levels of deoxyribonucleoside triphosphates (dNTP) may be present. The cell-cycle-dependent kinetics of deoxyribonucleoside triphosphate levels in acid-soluble pools were determined with cells synchronized by mitotic selection and allowed to traverse

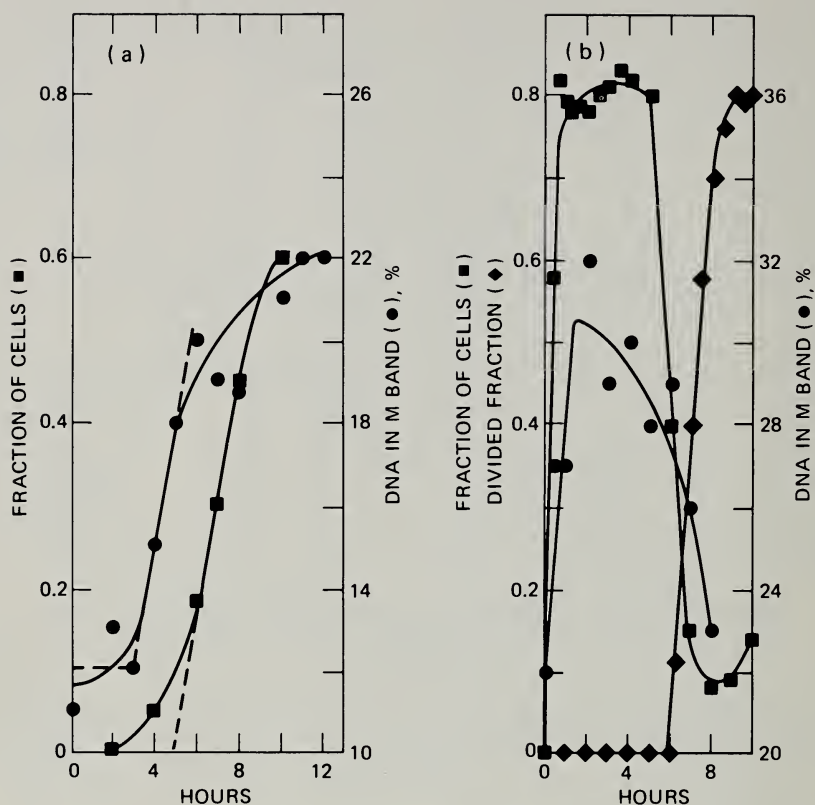


Fig. 5 DNA-lipoprotein complexes in synchronized CHO cells. (a) After mitotic selection, the amount of old prelabeled DNA associated with lipoprotein in sarkosyl crystals<sup>17-19</sup> (●) was determined, and, in addition, the fraction of cells synthesizing DNA (■) (incorporating <sup>3</sup>H-thymidine as in Fig. 1b) was measured in a nonprelabeled culture synchronized in parallel. (b) After mitotic-selection/hydroxyurea treatment, the amount of old prelabeled DNA associated with lipoprotein (●) was determined as in part a, with the fraction of cells synthesizing DNA (■) (labeled with <sup>3</sup>H-thymidine as in Fig. 1b) and divided fraction (◆) determined from a nonprelabeled culture synchronized in parallel. The divided fraction represents  $N/N_0 - 1$ . For experimental details see Refs. 18 and 19.

interphase (Fig. 6). The levels of deoxythymidine-5'-triphosphate (dTTP), deoxyadenosine-5'-triphosphate (dATP), and deoxyguanosine-5'-triphosphate (dGTP) which are at maximal values during mitosis<sup>20</sup> decrease dramatically as cells complete mitosis and enter G<sub>1</sub> (Fig. 6a). Although at a low level during mitosis, the level of deoxycytidine-5'-triphosphate (dCTP) also decreases upon reentry into interphase. During early G<sub>1</sub>, the levels of all four deoxyribonucleoside triphosphates are extremely low, but, within 0.3 to 0.6 hr prior to entry into S phase, the amount of all four species begins to increase in preparation for DNA replication.

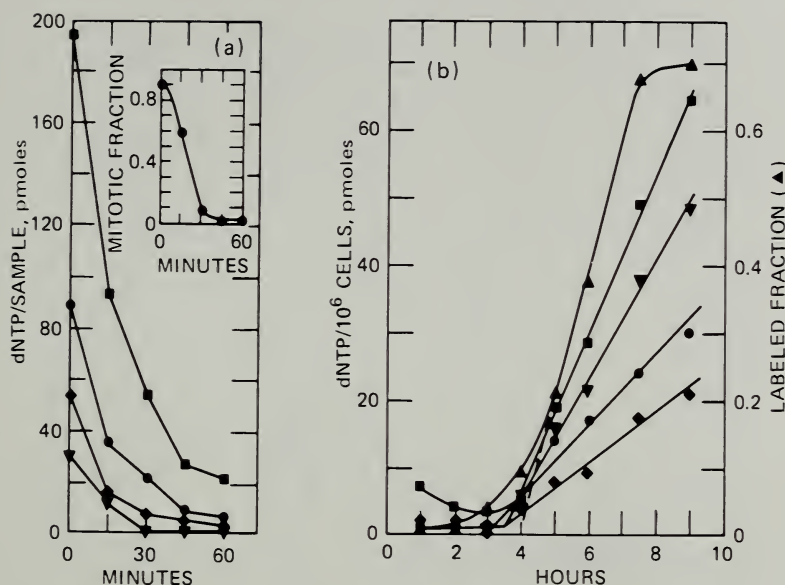


Fig. 6 Levels of deoxyribonucleotides (dNTP) in acid-soluble pools in CHO cells during escape from mitosis (a) and during early interphase (b).

■ dTTP                      ● dATP  
 ▼ dCTP                      ◆ dGTP  
 ▲ Fraction synthesizing DNA  
 (incorporating <sup>3</sup>H-thymidine)

The assays used were similar to those described by Lindberg and Skoog<sup>21</sup> and by Skoog<sup>22</sup> except that *Micrococcus luteus* DNA polymerase and <sup>32</sup>P-labeled deoxyribonucleotides were utilized in our assays.<sup>20</sup> Cells were synchronized by mitotic selection.

In cultures prepared by mitotic selection and allowed to progress through G<sub>1</sub> in the presence of hydroxyurea, the levels of dTTP, dCTP, and dGTP increase at the appropriate time even though DNA synthesis is inhibited (Fig. 7a). In contrast, the level of dATP does not increase in the hydroxyurea-treated medium. Within 3 min after removal of hydroxyurea, the level of dATP increases ninefold, and DNA synthesis commences simultaneously (Fig. 7b). Shortly thereafter, the levels of dTTP, dGTP, and dATP decrease. Then the levels of these three deoxyribonucleotides increase through S, G<sub>2</sub>, and M, whereas the dCTP content increases across S phase and decreases as cells enter G<sub>2</sub>. These results suggest that, in our CHO cell, hydroxyurea specifically prevents accumulation of dATP and thereby inhibits initiation of DNA synthesis. It is further suggested that the pool level of only dCTP is roughly correlated with DNA synthesis.<sup>23</sup>



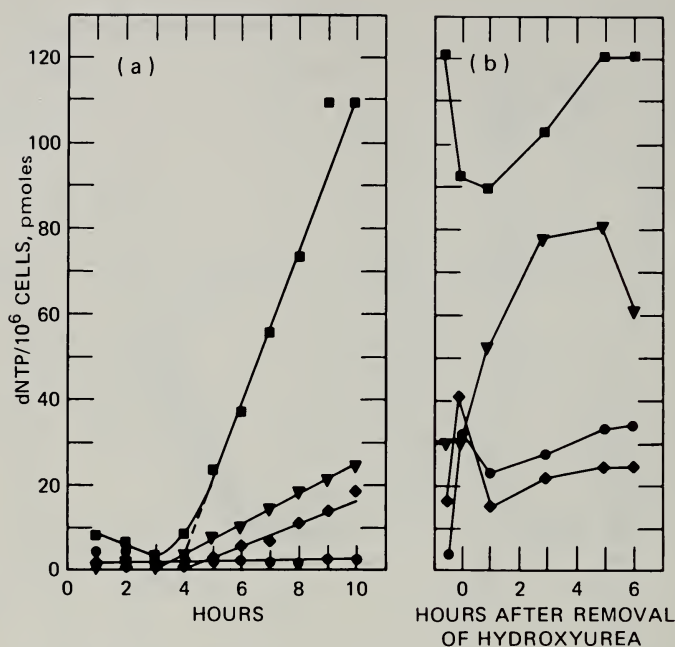


Fig. 7 Levels of deoxyribonucleotides (dNTP) in acid-soluble pools in CHO cells traversing G<sub>1</sub> in the presence of hydroxyurea (a) and following removal of hydroxyurea (b). For experimental details see Ref. 20.

■ dTTP      ● dATP  
▼ dCTP      ◆ dGTP

## CELL-SURFACE HEPARAN SULFATE

Heparan sulfate is an important cell component that becomes integrated into a metabolically active fraction of the cell surface. The presence of this material in a wide variety of mammalian cells<sup>2,4,25</sup> suggests a general role in cellular metabolism. Consequently we determined the content of surface Heparan sulfate at various times in the cell cycle in cultures of CHO cells synchronized by the combined isoleucine-deficiency technique and reversible inhibition of DNA synthesis with excess thymidine.<sup>10</sup> Heparan sulfate was isolated by a combination of molecular sieve and DEAE-cellulose chromatography, and the amount present was then determined by assaying the uronic acid residues.<sup>26</sup> The results shown in Fig. 8 reveal a significant loss of surface heparan sulfate as cells progress through late interphase and divide. Note that the data are plotted as mass per aliquot rather than mass per cell, indicating a net loss of surface heparan sulfate independent of any "per cell" decrease due to cell division. Although not shown in the figure, the following occur: (1) the quantities of cell sap heparan sulfate do not undergo dramatic fluctuations in the premitotic

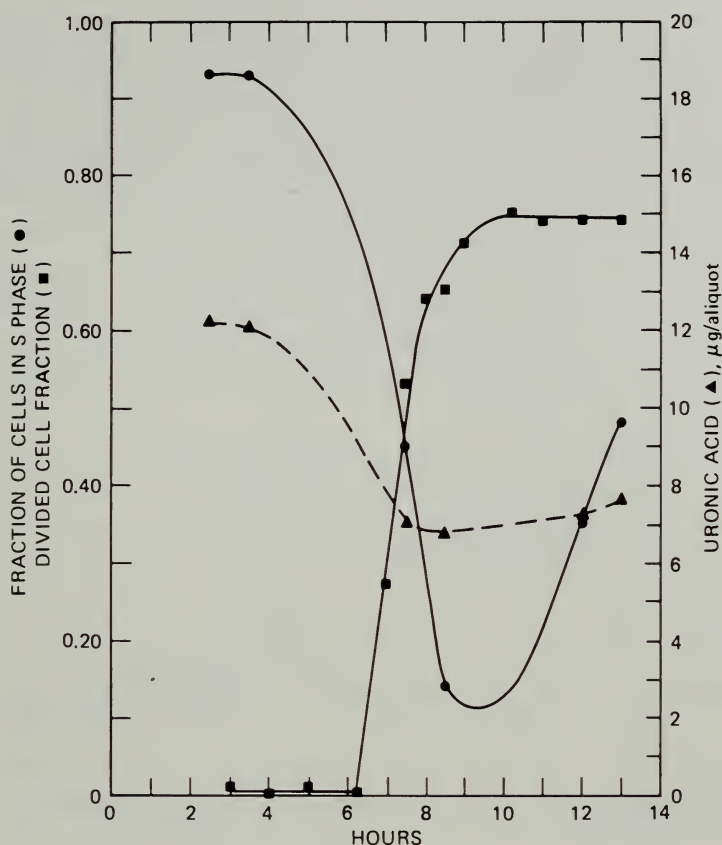


Fig. 8 Mass of surface heparan sulfate in CHO cells synchronized by isoleucine-deficiency/thymidine blockade.<sup>10</sup> Experimental details and uronic acid assays on the isolated heparan sulfate were carried out as described previously.<sup>2,6</sup> ▲, mass surface heparan sulfate; ●, fraction of cells in S phase; ■, divided cell fraction.

period; (2) the rates of synthesis and transport of heparan sulfate to the cell surface remain essentially constant through S and G<sub>2</sub>; and (3) the level of another cell-surface constituent, the surface glycopeptides, does not change significantly during late interphase.<sup>10</sup> Taken together, these results indicate that the loss of cell-surface heparan sulfate is not merely part of a general premitotic loss of cell-surface constituents but, instead, represents a specific cell-surface biochemical change as cells prepare for mitosis.

## TEMPORAL SEQUENCE OF EVENTS

When the results presented in this review were combined with data from previous studies carried out at LASL, it was possible to construct a map

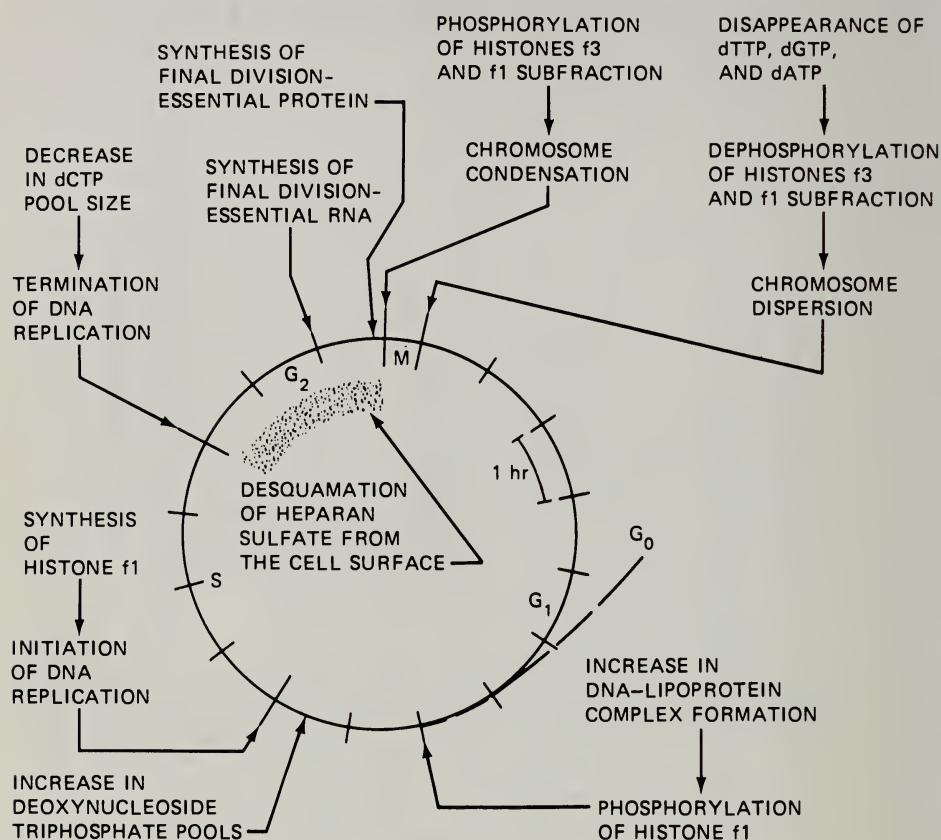


Fig. 9 Temporal sequence of biochemical events in the CHO cell cycle.

illustrating the temporal arrangement of biochemical events during the CHO cell cycle (Fig. 9). Note that the temporal relationships shown in Fig. 9 apply to line CHO cells grown under our cultivation conditions. Our speculative interpretation of the biochemical implications of the relationships between various proliferative processes follows.

For the biochemical markers described, the earliest indication that a cell is preparing for DNA replication occurs in G<sub>1</sub> 2 hr before initiation of DNA synthesis. At this time phosphorylation of histone f1 commences (Fig. 3b), and concomitantly the amount of DNA complexed to lipoprotein greatly increases (Fig. 5a). From nuclear magnetic resonance studies of calf-thymus nucleohistone, Bradbury, Carpenter, and Rattle<sup>27</sup> suggested that phosphorylation of histone f1 may play an integral role in chromatin organization and chromosome condensation. We suggest that, as an early step in preparation for DNA replication, phosphorylation of old, preexistent histone f1 results in an alteration in chromatin structure which allows an enhanced association of chromatin with lipoprotein. That is, phosphorylation of f1 and increased DNA

association with lipoprotein may be coordinated biochemically as well as temporally.

Continued phosphorylation of histone f1 through S, G<sub>2</sub>, and M may indicate that further f1 phosphorylation-mediated changes in chromatin structure are essential for progression through late interphase and mitosis. Regarding this notion, based upon studies of accessibility of DNA to DNase and actinomycin at varying stages of the HeLa cell cycle, Pederson<sup>28</sup> has proposed the existence of a "chromosome cycle" in eukaryotic cells involving continuous alterations in chromatin structure throughout interphase and culminating in chromosome condensation during mitosis. We suggest that phosphorylation of histone f1 may play an integral role in the cell-cycle-specific changes in chromatin accessibility reported by Pederson.

The levels of deoxyribonucleotides begin to increase at approximately 0.5 hr prior to initiation of DNA synthesis (Fig. 6b). As cells enter the S phase, DNA replication begins as does bulk synthesis of histones. Although synthesis of DNA and histone commences at approximately the same time (see Fig. 3a), there is no absolute coordination of these two processes, since histone synthesis and turnover occur under conditions in which DNA synthesis is inhibited.<sup>29,30</sup> Upon completion of DNA synthesis, the level of only the dCTP pool commences decreasing, while the other three deoxyribonucleoside triphosphates increase in content (Fig. 7b).

As cells continue the progression through late interphase, preparations are made for mitosis and cell division. Approximately 70 min prior to cell entry into mitosis, the final species of RNA essential for completion of mitosis is synthesized,<sup>31</sup> while at 12 to 15 min before prophase, the last division-essential protein species is synthesized.<sup>32,33</sup> During the premitotic period there is also a loss of heparan sulfate specifically from the cell surface (Fig. 8). We suggest that the loss of surface heparan sulfate at this time may result in an uncovering or activation of other cell-surface entities which leads to increased reactivity in the immediate premitotic period. In this regard a number of cell-surface changes occur at approximately the time that cells lose surface heparan sulfate. Among the changes are increased reactivity of wheat germ agglutinin sites<sup>34</sup> and blood group antigens,<sup>35</sup> as well as an increase in the neuraminidase-sensitive component of cellular electrophoretic mobility.<sup>36</sup> Thus fluctuations in the quantities of a generally occurring cell-surface constituent such as heparan sulfate may actually represent a mechanism by which expression of other cell-surface entities is regulated.

Phosphorylation of histone f3 and the f1 subfraction at precisely the time that cells complete G<sub>2</sub> (Fig. 4a and b) and subsequent dephosphorylation of these species as cells reenter G<sub>1</sub> strongly suggest that phosphorylation of these histones plays an integral role in chromosome condensation. Our observations are consistent with the speculations of Bradbury, Carpenter, and Rattle<sup>27</sup> that phosphorylation of histone f1 may trigger chromosome condensation. If indeed



phosphorylation of f3 and the f1 subfraction helps to trigger chromosome condensation, phosphorylation of these histone species then represents the final interphase operation, terminating in prophase. Sadgopal and Bonner<sup>3,7</sup> provided evidence for a greater degree of disulfide bond formation within histone f3 from metaphase chromosomes than in the dispersed chromatin of interphase cells. This implies that oxidation of f3 may be involved in maintaining the condensed chromosome structure. We suggest that phosphorylation of histone f3 during the final stages of G<sub>2</sub> may alter f3 conformation and thus result in disulfide bond formation and chromosome condensation.

As the cell enters G<sub>1</sub>, the levels of the deoxyribonucleoside triphosphates drop essentially to zero (Fig. 6a). We believe this represents a specific process rather than simple diffusion of the deoxyribonucleotides into the cytoplasm and subsequent destruction by cytoplasmic phosphatases. Had the latter process occurred, the levels of all four deoxyribonucleoside triphosphates should have decreased at the start of mitosis (when disaggregation of the nuclear membrane occurs) rather than at the end of mitosis.

## CONCLUSIONS

The data reported here represent an initial attempt to identify sequential temporal relationships among a variety of processes during the cell cycle. The results strongly suggest that, even in our relatively simple cultured-cell system, proliferation capacity depends upon a complex series of coordinated events. Once cells are committed to proliferate, a sequence of preprogrammed operations is initiated long before DNA replication commences. Prevention of DNA replication does not necessarily prevent initiation of preparative events, since the phosphorylation of histone f1,<sup>3,8</sup> the increase in lipoprotein-associated DNA (Fig. 5b), and the elevation in level of three of the deoxyribonucleoside triphosphates (Fig. 7a) are all initiated in traversing G<sub>1</sub> cells treated with hydroxyurea. That is, those processes normally prerequisite to initiation of genome replication are sequentially "turned on" in preparation for DNA replication even though DNA synthesis is inhibited. As cells progress through late interphase and prepare to divide, heparan sulfate is lost specifically from the cell surface, and histone f3 and f1 subfraction are phosphorylated as a final G<sub>2</sub> event.

One interesting aspect of our data may relate to control of expression of genetic information during the cell cycle. Various processes that are turned on at varying stages of the cell cycle continue to function throughout the remainder of interphase and are only turned off upon reaching mitosis. For example, f1 histone phosphorylation and enhanced DNA-lipoprotein associations commence initially at 2 hr prior to entry into S phase yet continue on into mitosis. Similarly, the levels of dTTP, dGTP, and dATP all begin to increase, starting at 0.5 hr before S phase, and generally continue to increase across late interphase,

then decrease in late M. Finally, the synthetic rates for various classes of RNA and for bulk protein show a steady increase throughout the entire cell cycle until the mitotic period.<sup>39,40</sup> One possible interpretation of these observations is that, once turned on, the cistrons for these products continue to function throughout the remainder of interphase, turning off during mitosis when chromosome condensation prevents continued accessibility to the DNA. Does such a simplistic mechanism operate in these cells? Is there a precise obligatory sequence of events that prepares cells for DNA replication and division, or will it be possible to invert the order of events or to initiate a late event under conditions in which an early event is inhibited? Answers to these and similar questions concerned with control of proliferation may soon be amenable to biochemical analysis through use of multifaceted experimental approaches similar to those used in this paper.

## ACKNOWLEDGMENTS

We acknowledge the excellent technical assistance of Joseph G. Valdez, John L. Hanners, and Phyllis C. Sanders. This work was performed under the auspices of the U. S. Atomic Energy Commission.

## REFERENCES

1. R. Baserga, Biochemistry of the Cell Cycle: A Review, *Cell Tissue Kinet.*, **1**: 167-191 (1968).
2. O. I. Epifanova and V. V. Terskikh, On the Resting Periods in the Cell Life Cycle, *Cell Tissue Kinet.*, **2**: 75-93 (1969).
3. D. M. Prescott, in *Normal and Malignant Cell Growth*, R. J. M. Fry, M. L. Griem, and W. H. Kirsten (Eds.), pp. 79-92, Springer-Verlag New York Inc., 1969.
4. R. Baserga (Ed.), *The Cell Cycle and Cancer*, pp. 1-447, Marcel Dekker, Inc., New York, 1971.
5. R. A. Tobey and K. D. Ley, Isoleucine-Mediated Regulation of Genome Replication in Various Mammalian Cell Lines, *Cancer Res.*, **31**: 46-51 (1971).
6. M. D. Enger and R. A. Tobey, Effects of Isoleucine Deficiency on Nucleic Acid and Protein Metabolism in Cultured Chinese Hamster Cells: Continued RNA and Protein Synthesis in the Absence of DNA Synthesis, *Biochemistry*, **11**: 269-277 (1972).
7. R. A. Tobey, in *Methods in Cell Biology*, D. M. Prescott (Ed.), Vol. 6, pp. 67-112, Academic Press, Inc., New York, 1973.
8. R. A. Tobey, E. C. Anderson, and D. F. Petersen, Properties of Mitotic Cells Prepared by Mechanically Shaking Monolayer Cultures of Chinese Hamster Cells, *J. Cell. Physiol.*, **70**: 63-68 (1967).
9. R. A. Tobey and H. A. Crissman, Preparation of Large Quantities of Synchronized Mammalian Cells in Late G<sub>1</sub> in the Pre-DNA Replicative Phase of the Cell Cycle, *Exp. Cell Res.*, **75**: 460-464 (1972).
10. P. M. Kraemer and R. A. Tobey, Cell-Cycle Dependent Desquamation of Heparan Sulfate from the Cell Surface, *J. Cell Biol.*, **55**: 713-717 (1972).
11. V. G. Allfrey, in *Histones and Nucleohistones*, D. M. Philips (Ed.), pp. 241-294, Plenum Publishing Corporation, New York, 1971.

12. E. M. Bradbury and C. Crane-Robinson, in *Histones and Nucleohistones*, D. M. Philips (Ed.), pp. 85-134, Plenum Publishing Corporation, New York, 1971.
13. R. Balhorn, M. Balhorn, H. P. Morris, and R. Chalkley, Comparative High Resolution Electrophoresis of Tumor Histones: Variation in Phosphorylation as a Function of Cell Proliferation Rate, *Cancer Res.*, **32**: 1775-1784 (1972).
14. L. R. Gurley, R. A. Walters, and R. A. Tobey, Cell-Cycle-Specific Changes in Histone Phosphorylation Associated with Cell Proliferation and Chromosome Condensation, *J. Cell Biol.*, **60**: 356-364 (1974).
15. L. R. Gurley, R. A. Walters, and R. A. Tobey, The Metabolism of Histone Fractions. VI. Differences in the Phosphorylation of Histone Fractions During the Cell Cycle, *Arch. Biochem. Biophys.*, **154**: 212-218 (1973).
16. L. R. Gurley, R. A. Walters, and R. A. Tobey, Histone Phosphorylation in Late Interphase and Mitosis, *Biochem. Biophys. Res. Commun.*, **50**: 744-750 (1973).
17. F. Hanoaka and M. Yamada, Localization of the Replication Point of Mammalian Cell DNA at the Membrane, *Biochem. Biophys. Res. Commun.*, **42**: 647-653 (1971).
18. C. E. Hildebrand and R. A. Tobey, DNA-Membrane Complexes in Chinese Hamster Cells: Cell-Cycle Studies, *Fed. Proc.*, **32**: 640a (1973).
19. C. E. Hildebrand and R. A. Tobey, Temporal Organization of DNA in Chinese Hamster Cells: Cell Cycle Dependent Association of DNA with Membrane, *Biochim. Biophys. Acta*, **331**: 165-180 (1973).
20. R. A. Walters, R. A. Tobey, and R. L. Ratliff, Cell Cycle Dependent Variations of Deoxyribonucleoside Triphosphate Pools in Chinese Hamster Cells, *Biochim. Biophys. Acta*, **319**: 336-347 (1973).
21. U. Lindberg and L. Skoog, A Method for the Determination of dATP and dTTP in Picomole Amounts, *Anal. Biochem.*, **34**: 152-160 (1970).
22. L. Skoog, An Enzymatic Method for the Determination of dCTP and dGTP in Picomole Amounts, *Eur. J. Biochem.*, **17**: 202-208 (1970).
23. K. L. Skoog, B. A. Nordenskjöld, and K. G. Bjursell, Deoxyribonucleoside Triphosphate Pools and DNA Synthesis in Synchronized Hamster Cells, *Eur. J. Biochem.*, **33**: 428-432 (1973).
24. C. P. Dietrich and H. M. De Oca, Production of Heparin Related Mucopolysaccharides by Mammalian Cells in Culture, *Proc. Soc. Exp. Biol. Med.*, **134**: 955-962 (1970).
25. P. M. Kraemer, Heparan Sulfates of Cultured Cells. II. Acid-Soluble and Precipitable Species of Different Cell Lines, *Biochemistry*, **10**: 1445-1451 (1971).
26. P. M. Kraemer, Heparan Sulfates of Cultured Cells. I. Membrane-Associated and Cell Sap Species in Chinese Hamster Cells, *Biochemistry*, **10**: 1437-1445 (1971).
27. E. M. Bradbury, B. G. Carpenter, and H. W. E. Rattle, Magnetic Resonance Studies on Deoxyribonucleoprotein, *Nature*, **241**: 123-126 (1973).
28. T. Pederson, Chromatin Structure and the Cell Cycle, *Proc. Nat. Acad. Sci. U.S.A.*, **69**: 2224-2228 (1972).
29. L. R. Gurley and J. M. Hardin, The Metabolism of Histone Fractions. II. Conservation and Turnover of Histone Fractions in Mammalian Cells, *Arch. Biochem. Biophys.*, **130**: 1-6 (1969).
30. L. R. Gurley and J. M. Hardin, The Metabolism of Histone Fractions. III. Synthesis and Turnover of Histone f1, *Arch. Biochem. Biophys.*, **136**: 392-401 (1970).
31. R. A. Tobey, D. F. Petersen, E. C. Anderson, and T. T. Puck, Life Cycle Analysis of Mammalian Cells. III. The Inhibition of Division in Chinese Hamster Cells by Puromycin and Actinomycin, *Biophys. J.*, **6**: 567-581 (1966).
32. R. A. Tobey, E. C. Anderson, and D. F. Petersen, RNA Stability and Protein Synthesis in Relation to the Division of Mammalian Cells, *Proc. Nat. Acad. Sci. U.S.A.*, **56**: 1520-1527 (1966).



33. R. A. Walters and D. F. Petersen, Radiosensitivity of Mammalian Cells. II. Radiation Effects on Macromolecular Synthesis, *Biophys. J.*, **8**: 1487-1504 (1968).
34. T. O. Fox, J. R. Sheppard, and M. M. Burger, Cyclic Membrane Changes in Animal Cells: Transformed Cells Permanently Display a Surface Architecture Detected in Normal Cells Only During Mitosis, *Proc. Nat. Acad. Sci. U.S.A.*, **68**: 244-247 (1971).
35. W. J. Kuhns and S. Bramson, Variable Behavior of Blood Group H on HeLa Cell Populations Synchronized with Thymidine, *Nature*, **219**: 938-939 (1968).
36. E. Mayhew, Cellular Electrophoretic Mobility and the Mitotic Cycle, *J. Gen. Physiol.*, **49**: 717-725 (1966).
37. A. Sadgopal and J. Bonner, Proteins of Interphase and Metaphase Chromosomes Compared, *Biochim. Biophys. Acta*, **207**: 227-239 (1970).
38. L. R. Gurley, R. A. Walters, and R. A. Tobey, The Metabolism of Histone Fractions. VII. Phosphorylation and Synthesis of Histones in Late G<sub>1</sub> Arrest, *Arch. Biochem. Biophys.*, **164**: 469-477 (1974).
39. M. D. Enger and R. A. Tobey, RNA Synthesis in Chinese Hamster Cells. II. Increase in Rate of RNA Synthesis during G<sub>1</sub>, *J. Cell Biol.*, **42**: 308-315 (1969).
40. C. H. Blomquist, C. T. Gregg, and R. A. Tobey, Enzyme and Coenzyme Levels, Oxygen Uptake and Lactate Production in Synchronized Cultures of Chinese Hamster Cells, *Exp. Cell Res.*, **66**: 75-80 (1971).



# CYCLE-DEPENDENT THERAPEUTIC AGENTS

VINCENT H. BONO, JR., and ROBERT L. DION

Drug Research and Development, Division of Cancer Treatment,  
National Cancer Institute, Bethesda, Maryland

---

## ABSTRACT

The principal effect of cancer chemotherapeutic drugs is cell death. The susceptibility of cells to the lethal action of drugs depends on certain parameters of their proliferative kinetics: the proliferative fraction, the relative lengths of  $G_1$ , S, and  $G_2$  phases, and the absolute rate of DNA synthesis in S-phase cells. Drugs have been characterized in terms of their concentration-dependent, time-dependent, and phase-dependent cytocidal effects and also in terms of their phase-dependent maturation effects. The use of flow microfluorometry in analyzing drug effects on exponentially proliferating populations of cells is described.

The major biological effect of cancer chemotherapeutic drugs is cell death. Therapeutic advantage is attained when the death of neoplastic cells exceeds the toxicity due to the death of normal host cells, such as hematopoietic and gastrointestinal cells. Since one of the main characteristics of neoplasia is proliferation, attention has been directed to characterizing the kinetics of cell proliferation and to identifying the responses of cells to chemotherapeutic drugs in this context.

The simplest populations to analyze have been certain experimental animal tumors growing in ascites form, e.g., L1210 murine leukemia.<sup>1,2</sup> These are populations in which all cells divide in very short time periods. These populations have high dividing fractions and short cell-cycle times. Their growth kinetics are in these respects like those of growing bacteria. The kinetics<sup>3</sup> of other neoplasms (e.g., late stages of experimental leukemia and solid tumors, such as lymphomas and carcinoma), are much more complex. Populations of these cells take widely varying times to divide; i.e., they have broadly distributed cell-cycle times. A significantly large fraction of the population appears not to divide at all. These cells are considered to be resting, or in a  $G_0$  state. These

characteristics approach the kinetic state of many mature normal tissues. For cells that are actively proliferating, the relative lengths of time spent in  $G_1$ , S, and  $G_2$  and the absolute rate of DNA synthesis in S-phase cells all contribute their characterization.

The susceptibility of cells to the lethal effects of cancer chemotherapeutic drugs depends on these characteristics. Generally, four major experimental systems have been used to characterize drugs effects: concentration-dependent cytotoxic effects; exposure-time-dependent cytotoxic effects; cell-cycle phase-dependent cytotoxic effects; and cell-cycle phase-dependent maturation effects.

## DRUG-CONCENTRATION-DEPENDENT CYTOTOXIC EFFECTS

Exposing a given population of cells to increasing concentrations of a drug has been found to produce several effects. There may be no apparent limit to the fraction of cells that can be killed (a nonspecific drug effect), or there may be a limit, revealing a fraction of cells that is either totally or partially resistant to the lethal effect of increasing drug concentrations. If the resistant fraction of cells are resting cells, or  $G_0$ -state cells, the drug is classified as cycle specific. If, on the other hand, cells in the exposed population are all actively proliferating and cells in the sensitive fraction are identified as being all in one phase of the cell cycle, the drug effect is classified as phase specific.

Using these experimental conditions, Bruce and Valeriote<sup>4</sup> have classified nitrogen mustard ( $HN_2$ ) as phase and cycle nonspecific; vinblastine, methotrexate, azaserine, and cytosine arabinoside as phase specific; and 5-fluorouracil (FU), actinomycin D, Cytosan, and BCNU as cycle specific. Bhuyan and coworkers,<sup>5-7</sup> in a system consisting in cycling cells, have found neocarzinostatin, actinomycin D, FU, BCNU, CCNU, streptozotocin, and chlorambucil to be phase nonspecific and ellipticine, camptothecin, 5-azacytidine, cytosine arabinoside, and FUDR to be phase specific. Barranco, Novak, and Humphrey<sup>8</sup> found BCNU and Bleomycin to be plateau stage specific; i.e., cells in stationary stage are more sensitive to them than cells in exponential growth. This is in contrast to hydroxyurea (HU), which is cycle specific and to which stationary-stage cells are completely resistant. It is as yet uncertain to what extent stationary-stage cells are equivalent to resting, or  $G_0$ , cells.

## TIME-DEPENDENT CYTOTOXIC EFFECTS

At constant drug concentrations the time course of cell survival is an indication of whether all cells are equally sensitive to the drug or some fraction of the population resists the lethal action of the agent. About half the L1210 cells are resistant to  $5 \times 10^{-4}M$  and  $10^{-3}M$  HU (Fig. 1). At the higher concentration there appears to be a significant but slow rate of cell death in the resistant fraction. In contrast, no major fraction of the population resists BCNU,

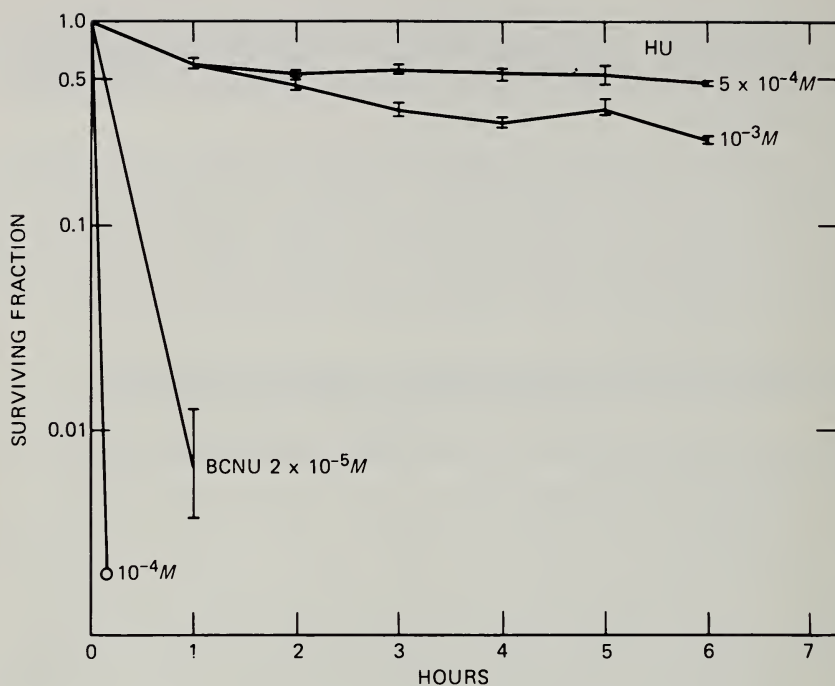


Fig. 1 Survival of L1210 leukemia cells in continuous exposure to hydroxyurea (HU) or BCNU.

and the rate of cell kill is very sensitive to concentration. These properties of BCNU were described by Skipper et al.,<sup>9</sup> who contrasted it to the lack of concentration dependence of the rate of cell kill by cytosine arabinoside, methotrexate, and HU. For drugs with S-phase cytotoxic specificity, the concept of "self-limitation"<sup>9</sup> has been applied. That is, certain drugs, e.g., methotrexate, 6-mercaptopurine, and to some extent FU, appear, in a nonlethal way, to prevent cells from maturing into a susceptible cell type and thus have a self-limiting action. In contrast, cytosine arabinoside and HU appear not to prevent cells from maturing into a cell type that is susceptible to the lethal action of the drug.

## CELL-CYCLE PHASE-DEPENDENT CYTOTOXIC EFFECTS

Cell-synchronizing systems have been used to analyze the survival of drug-exposed populations of a uniform cell-cycle phase. Using synchronized DON cells, Bhuyan et al.<sup>5-7</sup> have found adriamycin, camptothecin, 5-azacytidine, cytosine arabinoside, HU, and FUDR to be most effective on S-phase cells. Most effective on G<sub>1</sub>-phase cells were BCNU, CCNU, and MeCCNU, and most effective on mitotic and G<sub>1</sub>-phase cells were ellipticine and Bleomycin. In considering the meaning of these observations, we must remember that the phase

of maximal sensitivity is being determined at a fixed drug concentration. For example, nitrogen mustard<sup>7</sup> at a low concentration is most effective on mitotic, G<sub>1</sub>-phase, and early S-phase cells, but it is not ordinarily considered to be phase specific since, when it is at high enough concentrations, all cells are susceptible to its lethal action.

## CELL-CYCLE PHASE-DEPENDENT MATURATION EFFECTS

As we have seen, the cell-cycle phase characteristics of the exposed population appear to a significant degree to determine the response of the population to drug exposure. If prior exposure to the same or a different drug alters these characteristics of the population, then the effect of the drug will be different. Thus the effects of a drug on the maturation rates of cells as they progress through the cycle may be of importance in determining either the results of repeated therapeutic doses or the effects of the combined use of two drugs in sequence.

Cell-cycle-phase maturation<sup>10</sup> or progression has been analyzed by radioautographic methods, starting with mitotically selected cells or G<sub>1</sub>-phase arrested cells. The development of flow microfluorometry<sup>11</sup> (FMF) and the technique of fluorescent Fuelgen staining of suspensions of cells has allowed us to measure cell-cycle progression by observing the rate at which cells pass from a G<sub>1</sub>-phase DNA content, through S-phase DNA contents, to a G<sub>2</sub>-phase DNA content. Using both methods of analysis, Tobey<sup>10</sup> and Tobey and Crissman<sup>11</sup> found that the main effect of neocarzinostatin, Bleomycin, Daunomycin, and adriamycin is to slow maturation through G<sub>2</sub> phase. Camptothecin slowed maturation through S phase, whereas cytosine arabinoside and HU both interfered with the G<sub>1</sub>- to S-phase transition and with maturation through S phase.

The techniques of FMF have also been applied to measuring the effects of drugs on the distribution of cell DNA contents in a random or exponentially growing system. The changes in cell DNA-content distributions will reflect the relative effects on progress through the various phases of the cycle.

A highly idealized example of this approach is illustrated in Fig. 2. We can simulate the DNA-content distribution of an exponentially growing population by composing a model based on the assumption that the DNA synthesis rate is constant throughout S phase. Exponential growth defines the relative number of cells of any given age in their progress to mitosis. By arbitrarily selecting the relative lengths of G<sub>1</sub>, S, and G<sub>2</sub> phases, we can calculate the fraction of the total population having any given DNA content between diploid and tetraploid. Thus two curves, the age-frequency curve and the DNA-synthesis-rate curve, can be used to compute the DNA-content frequency curve (Fig. 2, lower right). Assume now that a hypothetical drug slows the proliferation rate of the population of cells but that growth is still exponential at the slower rate. Assume



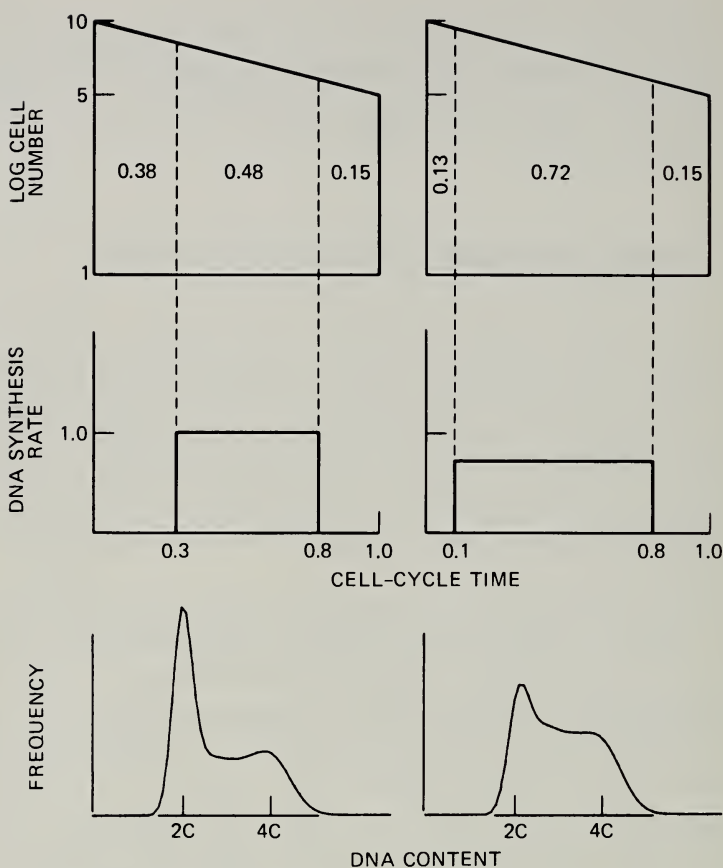


Fig. 2 Computed DNA-content distributions of an exponentially growing cell population.

also that the experimentally determined DNA-content frequency curve was altered (Fig. 2, lower left). Since growth continues to be exponential, the age-frequency curve remains unchanged. Thus the time of onset and completion of DNA synthesis is determined by the observed DNA-content frequency curve. In this case the primary effect is a significant lengthening of the relative duration of S phase. Even though this approach is appealing, it is not practical at this time since most drugs do not alter growth to a single slower exponential rate but instead produce a curve of growth decrease. For this reason, the age-frequency curve is unknown and the altered DNA-content frequency curve cannot be analyzed in this way.

Because of this limitation, we have attempted to exploit this method to characterize rather than to analyze the effects of chemotherapeutic drugs on the DNA-content frequency curve. The methods employed are simple: L1210 leukemia cells are grown in suspension culture, with a doubling time of 12 hr. Culture samples are continuously exposed to test drugs over time periods from 3

to 24 hr and under conditions where the control culture continues in exponential growth for that period. Samples are fixed and analyzed by FMF with a commercially available cytofluorograph. The results are computer processed to present a normalized frequency distribution curve.

The problem to be solved is that of selecting conditions of drug concentration and time of exposure so that the pattern produced is characteristic of the major effects of the drug on cell-cycle maturation. One approach is to use a drug concentration just high enough to prevent any increase in cell numbers over a 24-hr period. The effect of Colcemid is shown in Fig. 3. The progressive maturation and accumulation of cells in mitosis is reflected in the shift of the DNA distribution to a uniform premitotic DNA content. Note that a higher concentration does not slow the rate of progression to the distribution seen at 6 hr.

The effects of macromomycin, a new antitumor drug, are shown in Fig. 4. This protein produced by *Streptomyces macromyceticus* is thought to exert its action at the cell surface. In addition to accumulation of cells with a premitotic

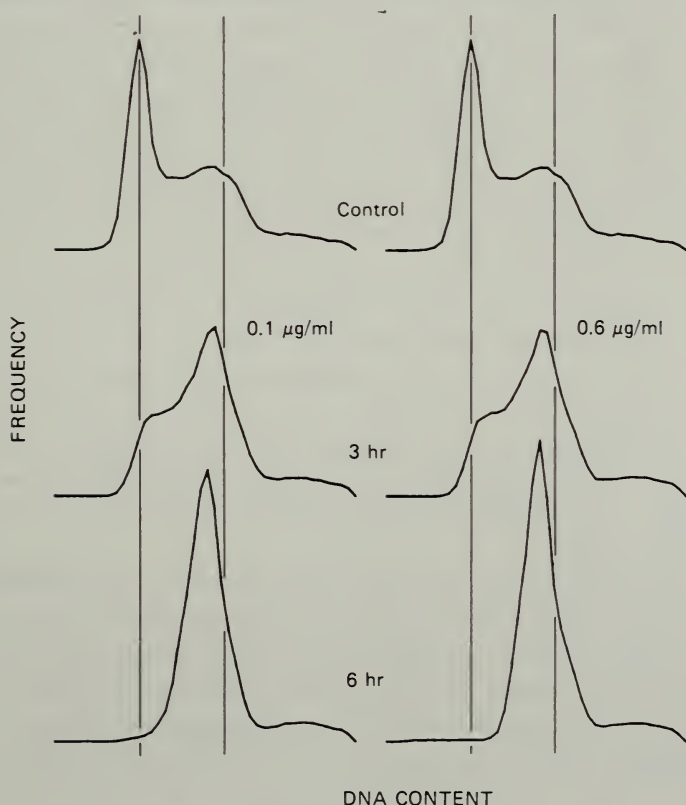


Fig. 3 Time course effect of two concentrations of Colcemid on L1210 cell DNA distributions.

DNA content, there is a slowing of progression of cells through S phase which is concentration dependent. There appears to be no decrease in the rate of maturation of  $G_1$ -phase to S-phase cells.

The distribution patterns after 6 hr of exposure to FU, HU,  $HN_2$ , and BCNU are shown in Fig. 5. The figures in parentheses represent the growth rates relative to control, determined at 24 hr. Both FU and HU produce a deficit of cells with a premitotic DNA content, and there is an accumulation of cells in early S phase for FU and in  $G_1$  phase for HU. In contrast,  $HN_2$  has little effect on the distribution even though the growth rate is 7% of control. This implies that the rate of progression through all phases of the cycle is uniformly reduced. A similar effect is produced by BCNU, but there is also a significant population of cells with DNA content less than  $G_1$ -phase cells. This suggests that considerable degradation of DNA has occurred in association with the cytotoxic effects of this drug.

Since the conditions used are effectively controlling the mitotic division rate to zero, drug effects resulting in either an accumulation or a depletion of  $G_2$ -phase cells will be emphasized. An alternate approach is to select drug concentrations that allow a reduced but significant cell-division rate. In Fig. 6, we see the distribution pattern produced by these four drugs when growth rate was reduced to 70% of control over a 6-hr period. FU gives a pattern very similar to that seen before; results for HU show a smaller decrease in  $G_2$ -phase cells and a higher early S-phase population than results observed under no-growth conditions;  $HN_2$  is characterized by a decrease in  $G_1$ -phase cells; BCNU is distinguished from  $HN_2$  in that it has a less pronounced decrease in  $G_1$ -phase cells and a more pronounced increase in  $G_2$ -phase cells. Note the absence of cells with a DNA content smaller than that of  $G_1$ -phase cells.

Since it is difficult to measure growth rates accurately over a 6-hr period, even with a 12-hr doubling time, a modification of this condition was tried. Using drug concentrations that allow growth rates of about 50% of control as measured at 24 hr, we observed the distributions produced at 6 hr. Figure 7 shows these results. Small variations in growth rates (indicated by the range shown in parentheses) do not alter the distribution pattern. The patterns produced by FU, HU, and BCNU have the same characteristics shown in Fig. 6. Although  $HN_2$  lacks a defined  $G_1$ -phase peak, the accumulation of early S-phase cells is clearly evident.

When DNA distribution curves are measured after 24 hr of drug exposure, small changes in growth rates are associated with significant changes in the DNA distribution (Fig. 8). Here, as BCNU reduces the 24-hr growth rate from 72% to 39% of control, the relative size of  $G_1$  and  $G_2$  peaks reverse. Note, though, that the relative lack of accumulation of S-phase cells remains throughout.

In conclusion, then, an appropriate set of conditions for characterizing drug effects on cell-cycle maturation appears to be satisfied by measuring the early perturbations in the DNA-content distribution at drug concentrations that produce a decrease in cell-division rate of the order of 50% of control.

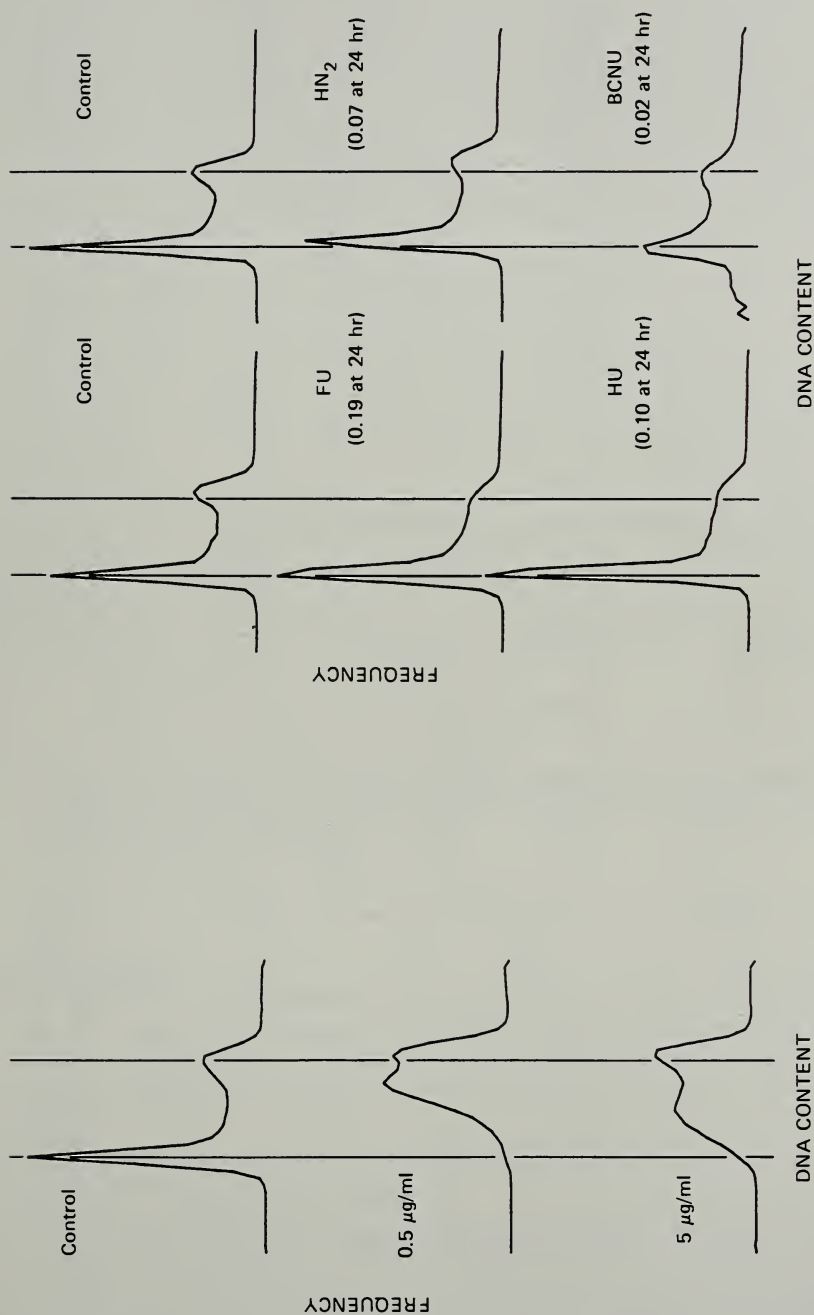


Fig. 4 Effects of two concentrations of macromomycin on L1210 cell DNA distributions at 6 hr.

Fig. 5 Effects of FU, HN<sub>2</sub>, and BCNU on L1210 cell DNA distributions at 6 hr. Growth rates relative to control are given in parentheses.



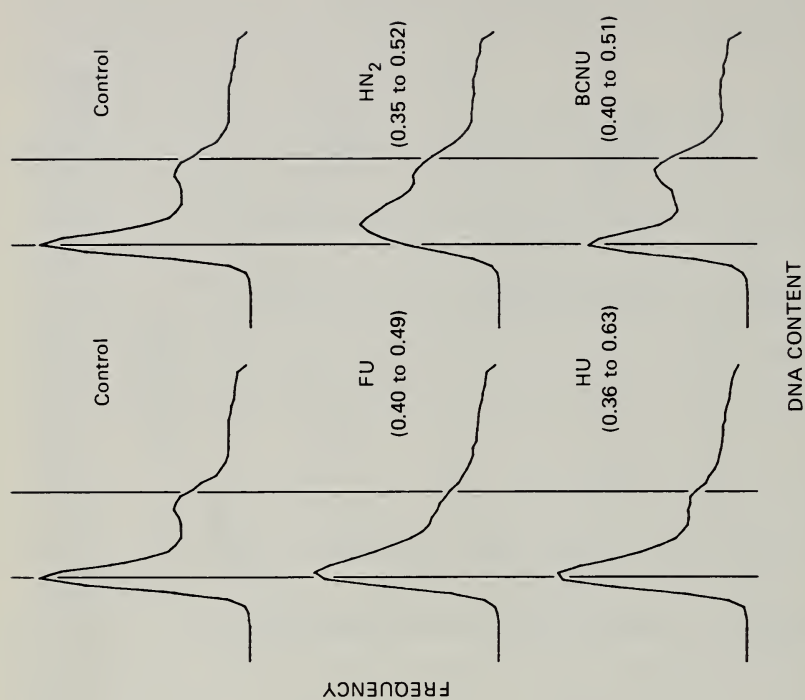


Fig. 6 Effects of FU, HU, HN<sub>2</sub>, and BCNU on L1210 cell DNA distributions at 6 hr when growth rate was reduced to 70% of control as measured at 24 hr.

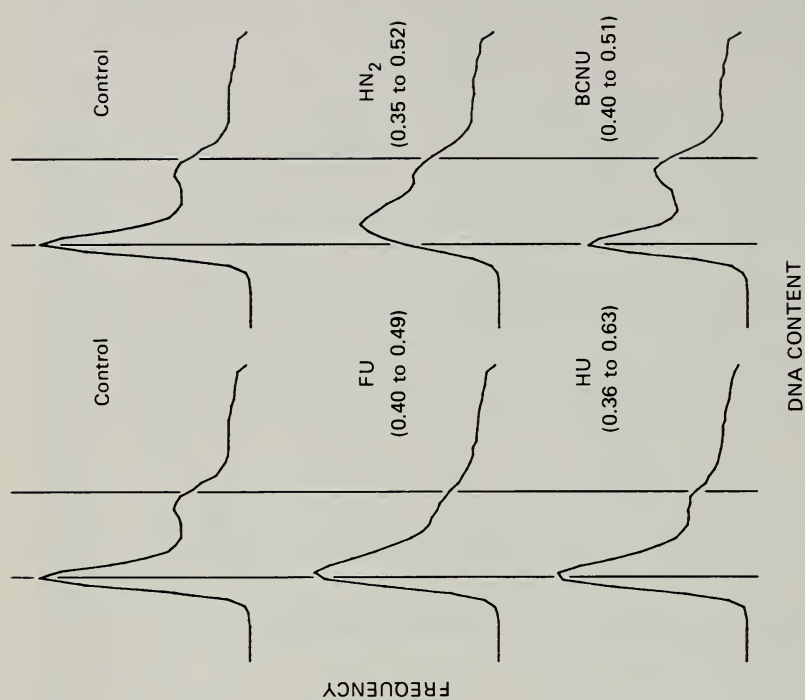


Fig. 7 Effects of FU, HU, HN<sub>2</sub>, and BCNU on L1210 cell DNA distributions at 6 hr when growth rate was reduced to 50% of control as measured at 24 hr. Range of variations in growth rate is shown in parentheses.



Fig. 8 Measurement of L1210 cell DNA distribution curves showing sensitivity to growth rate after 24 hr exposure to BCNU. Growth rate for exposed cells is given in parentheses.

## REFERENCES

1. H. W. Skipper, F. M. Schabel, Jr., and W. S. Wilcox, Experimental Evaluation of Potential Anticancer Agents. XXI. Scheduling of Arabinosyl-cytosine to Take Advantage of Its S-phase Specificity Against Leukemic Cells, *Cancer Chemother. Rep.*, **51**: 125-165 (1967).
2. R. C. Young, V. T. DeVita, and S. Perry, The Thymidine- $^{14}\text{C}$  and  $^3\text{H}$  Double-Labeling Technique in the Study of the Cell Cycle of L1210 Leukemic Ascites Tumor *in Vivo*, *Cancer Res.*, **29**: 1581-1584 (1969).
3. L. F. Lamerton and G. G. Steel, Cell Population Kinetics in Normal and Malignant Tissues, *Progr. Biophys. Mol. Biol.*, **18**: 245-280 (1948).
4. W. R. Bruce and F. A. Valeriote, in *Chemotherapy of Malignant Neoplasms*, F. J. Ansfield (Ed.), pp. 27-28, Charles C Thomas, Publisher, Springfield, Ill., 1973.
5. B. K. Bhuyan, L. G. Scheidt, and T. J. Fraser, Cell Cycle Phase Specificity of Antitumor Agents, *Cancer Res.*, **32**: 398-407 (1972).
6. B. K. Bhuyan, T. J. Fraser, and L. H. Li, Cell Cycle Phase Specificity and Biochemical Effects of Ellipticine on Mammalian Cells, *Cancer Res.*, **32**: 2538-2544 (1972).

7. B. K. Bhuyan and T. J. Fraser, Cytotoxicity of Antitumor Agents in a Synchronous Mammalian Cell System, *Cancer Chemother. Rep.*, **58**: 149-155 (1974).
8. S. C. Barranco, J. K. Novak, and R. M. Humphrey, Response of Mammalian Cells Following Treatment with Bleomycin and 1,3-bis(2-chloroethyl)-1-nitrosourea During Plateau Phase, *Cancer Res.*, **33**: 691-694 (1973).
9. H. E. Skipper, F. M. Schabel, Jr., L. B. Mellett, L. J. Montgomery, H. H. Lloyd, and R. W. Brockman, Implications of Biochemical, Cytokinetic, Pharmacologic and Toxicologic Relationships in the Design of Optimal Therapeutic Schedules, *Cancer Chemother. Rep.*, **54**: 431-450 (1970).
10. R. A. Tobey, A Simple, Rapid Technique for Determination of the Effects of Chemotherapeutic Agents on Mammalian Cell-Cycle Traverse, *Cancer Res.*, **32**: 309-316 (1972).
11. R. A. Tobey and H. A. Crissman, Use of Flow Microfluorometry in Detailed Analysis of Effects of Chemical Agents on Cell Cycle Progression, *Cancer Res.*, **32**: 2726-2732 (1972).

## CELL-CYCLE ANALYSIS: SESSION SUMMARY

DONALD F. PETERSEN, *Session Chairman*

Cellular and Molecular Radiobiology Group, Los Alamos Scientific Laboratory,  
Los Alamos, New Mexico

---

In introducing this session, I commented that Howard and Pelc's cell cycle lacked detail. Clearly, this lack of detail is no longer the case. Superimposing Dr. Mueller's contemporary cell-cycle diagram on the diagrams of Dr. Tomkins and Dr. Tobey provides a truly impressive accumulation of detail relevant to understanding cell-cycle progression. Cell-cycle kinetics in the present stage of development offer a useful tool for studying, as Dr. Holley has done, the fundamental reasons for cycle progression and arrest. We concur and are gratified that he shares our optimism that this new instrumentation "will revolutionize cell biology." The efficiency of data accumulation in culture systems has been amply demonstrated by Dr. Bono's summary of parameters that appear useful in screening antineoplastic agents.

I think the clear message of the presentations in this session is that regulatory phenomena will be a principal preoccupation for some time and that the characterization of the mediator molecules is a major challenge. Dr. Mueller has nominated a lipoprotein factor—perhaps a constituent of membrane held captive under normal circumstances which acts as the mediator for initiating DNA replication if it is somehow allowed to escape and interact with the nucleus. Escape or stimulation of a receptor by a mitogen or hormone is certainly consistent with Dr. Tomkin's elegant model for induction. Documentation of a variety of temporal events by Dr. Tobey and his colleagues begins to point to the complexity of the interrelationships between macromolecular components of chromatin. In the context of this meeting, it is important to emphasize the extent to which their cultures were characterized with respect to cycle position. Because of the inherent and progressive dispersion of synchronized mammalian systems, such documentation is essential for interpretation of any cycle-dependent event.



At a time when chemotherapy and chemotherapy combined with radiotherapy provide the most promising clinical responses in tumor treatment, classification of potential chemotherapeutic agents according to cell-cycle effects appears to be most easily accomplished by the methods under discussion at this meeting. Whether correlation of drug action on the cell cycle and clinical response can be made remains to be seen, but the examples discussed are consistent with the notion that cycle effects reflect mechanism of action. Therefore useful screening protocols appear to be a practical application of the methodology.

Cells that exhibit the peculiar property of contact inhibition or growth control seem to operate under the influence of a large number of regulatory factors. We have seen convincing evidence that a significant number of low-molecular-weight components exert specific influences on growth—amino acids, ions, serum factors, indeed hormones. These observations are at once encouraging in that regulation is experimentally accessible and discouraging because they seem, at least for the moment, to argue against regulation of malignant transformations in situ. However, we can now manipulate cells in culture and assess the consequences of what we have done with immeasurably greater ease than by classical techniques. Progress in the field and our optimism should escalate accordingly.

## SESSION IV

### THE CELL NUCLEUS: OPENING REMARKS

J. HERBERT TAYLOR, *Session Chairman*

Institute of Molecular Biophysics, Florida State University, Tallahassee, Florida

---

In spite of significant advances in many areas of our knowledge of the cell nucleus in the last 25 years, there remain some strange enigmas. From the study of prokaryotes, as well as higher cells, we know the structural features of DNA, its potential coding properties, and the general mode of its replication. However, we lack detailed knowledge of the mechanisms regulating replication and integration of DNA into chromosomes. It has become clear that some, and perhaps all, of the DNA is made in small segments which are then joined together by ligase activity into the long chains typically found in chromosomes, but the meaning of these observations escapes us. The role of RNA in priming replication or in the regulatory system has recently stirred renewed interest in the mechanism and regulation of replication, but we know so little about this aspect that a conceptual rationale for the role of RNA is difficult to formulate.

Beginning with the observations that the DNA in chromosomes consisted of two subunits with properties and behavior in replication similar to the two chains of DNA molecules,<sup>1,2</sup> it became increasingly clear that all the DNA in a chromosome is potentially a single uninterrupted duplex. The latest additions to this evidence are the measurements of viscoelastic properties of DNA carefully released from chromosomes of *Drosophila* which indicate polymers long enough to account for all DNA present in the chromosomes.<sup>3</sup> Although these measurements involve extrapolations that allow errors of a factor of two, it is clear that very long polymers of the order of a whole chromosome can be released and measured. These observations added to the well-demonstrated fact that genomes of prokaryotes consist of a single DNA duplex make the concept of the much longer polymers in higher cells less difficult to accept. Even though the duplex is continuous, the polynucleotide chains may be open at intervals, and certainly this appears to be the situation during replication.<sup>4</sup> Whether the interruptions in the polynucleotide chains occur at specific sites and represent functional subunits is an interesting possibility but is difficult to evaluate at this

time. From the very early autoradiographic studies on DNA replication in chromosomes, it was clear that replication could be initiated simultaneously at many sites in a chromosome.<sup>5</sup> This was strikingly demonstrated by Huberman and Riggs<sup>6</sup> some years ago by what Callan<sup>7</sup> calls fiber autoradiography. Dr. Joel Huberman will give us some recent results relating to the size and rates of chain growth in the presumed units of replication along the long polymers characteristic of chromosomes of Chinese hamster ovary (CHO) cells.

Much excitement has been aroused by the discovery that new methods of staining allow one to identify all chromosomes of the complement of many mammalian species which were formerly indistinguishable. Both fluorescent microscopy and regular light microscopy after certain treatments and staining procedures which denature and allow partial renaturation have been successful. Dr. Frances Arrighi will review some of the developments, show us some interesting examples, and perhaps try to interpret some of the properties of DNA or chromatin on the basis of the staining reactions. Dr. L. L. Deaven will then describe the use of one of these techniques, i.e., the staining of G-bands, to identify and evaluate the quantitative changes in DNA and the correlated changes in chromosome complements which one can observe in aneuploid cell lines.

One of the long-standing puzzles concerning the chromosomes of higher cells is the abundance of DNA compared with the presumed number of genes. The Chinese hamster chromosomes, like those of other mammals, have about 1000 times as much DNA as the genome of a bacterial cell such as *Escherichia coli*. Yet the mammalian cell is not known to require 1000 times as many enzymes and other proteins as a bacterial cell. What then can be the function of the extra DNA? Part of it can be accounted for by repetitious sequences that do not appear to be transcribed at all. These DNAs comprise a large fraction of the genome in some species, but even if half the DNA is consigned to this category, a function for which is unknown, the remaining unique sequences are far more numerous than would appear to be necessary for coding sequences for structural genes. The idea that genes are present in many identical copies has been one explanation, but now the mounting evidence indicates that most of the sequences are represented once or at most a few times in each genome. There are a few well-documented exceptions, such as ribosomal RNA coding sequences,<sup>8</sup> 5S RNA coding sequences,<sup>8</sup> transfer RNA coding sequences, and perhaps a few others. However, when the DNA involved in these special categories is subtracted from the total, the unique sequences are still far more numerous than our present concepts can account for. Another idea which has been proposed by several persons is the concept that most of the extra DNA is involved somehow in regulatory functions, but the models so far are highly speculative. Perhaps the best approach to the problem in the long run is to learn more about the nature of mutable loci that code for specific enzymes or other proteins in higher cells.

For many reasons the study of such mutations is facilitated by the use of cell cultures rather than breeding experiments involving whole animals. Beginning

with the recognition that cells in culture could be induced to fuse under appropriate cultural conditions,<sup>9,10</sup> and later through the interaction with inactive viruses, techniques for studying the genetics of cells in culture have advanced faster than most of us could have envisioned some years ago. The fusion of cells and the union of nuclei in the fused cells give the equivalent of fertilization in vitro along with the resulting hybrid cells. The next step of induced chromosome reduction and segregation is less well developed, but hybrid cells produced by certain combinations have been found in which one set of chromosomes is preferentially lost. By nutritional selective pressure it has been possible to isolate clones of cells in which all except one chromosome of one complement have been eliminated. The locus of the gene being selected for can be associated with the remaining chromosome, the identity of which can be established by the staining procedures previously mentioned.

Mapping of mutant genes is a necessary step in many genetic studies, but the nature of the genetic locus with respect to size, regulatory sequences, and uniqueness in the total complement is needed to answer the more revealing questions referred to above. Comparably, analyses in prokaryotes serve as a guide to solve some of the problems. Others are unique to the eukaryotes. Dr. E. H. Y. Chu, who was one of the first to seize upon these techniques for a study of the nature of mutations in cultured cells, will tell us about genetic markers associated with Chinese hamster chromosomes.

## REFERENCES

1. J. H. Taylor, P. S. Woods, and W. L. Hughes, The Organization and Duplication of Chromosomes as Revealed by Autoradiographic Studies Using Tritium-Labeled Thymidine, *Proc. Nat. Acad. Sci. U.S.A.*, **43**: 122-128 (1957).
2. J. H. Taylor, The Organization and Duplication of Genetic Material, in *Proceedings of the 10th International Congress of Genetics, Montreal, Aug. 20-27, 1958*, Vol. 1, pp. 63-78, University of Toronto Press, Toronto, 1959.
3. R. Kavenoff and B. H. Zimm, Chromosome-Sized DNA Molecules from *Drosophila*, *Chromosoma*, **41**: 1-28 (1973).
4. J. H. Taylor, Replication of DNA in Mammalian Chromosomes: Isolation of Replicating Segments, *Proc. Nat. Acad. Sci., U. S. A.*, **70**: 1083-1087 (1973).
5. J. H. Taylor, Asynchronous Duplication of Chromosomes in Cultured Cells of Chinese Hamster, *J. Biophys. Biochem. Cytol.*, **7**: 445-464 (1960).
6. J. A. Huberman and A. D. Riggs, On the Mechanism of DNA Replication in Mammalian Chromosomes, *J. Mol. Biol.*, **32**: 327-341 (1968).
7. H. G. Callan, Replication of DNA in Chromosomes of Eukaryotes, *Proc. Roy. Soc. (London) Ser. B.*, **181**: 19-41 (1972).
8. D. D. Brown and K. Sugimoto, The Structure and Evolution of Ribosomal and 5S DNAs in *Xenopus laevis* and *Xenopus mulleri*, *Cold Spring Harbor Symp. Quant. Biol.*, **38**: 501-505 (1974).
9. B. Euphrussi, L. J. Scaletta, M. A. Stenchever, and M. C. Yoshida, Hybridization of Somatic Cells *In Vitro*, *Symp. Int. Soc. Cell Biol.*, **3**: 13-28 (1964).
10. G. Barski, Cytogenetic Alterations in Mixed Cultures of Mammalian Somatic Cells *In Vitro*, *Symp. Int. Soc. Cell Biol.*, **3**: 1-12 (1964).



# THE CELL CYCLE AND DNA SYNTHESIS IN MAMMALIAN CELLS

JOEL A. HUBERMAN

Massachusetts Institute of Technology, Cambridge, Massachusetts

---

## ABSTRACT

DNA fiber autoradiography was used to measure the size of replication units and the rate of replication fork movement as a function of time during the S phase of synchronized CHO (Chinese hamster ovary) cells. The rate of fork movement increased by a factor of 3 to 5 from early S phase to late S phase, with the most dramatic change occurring in the first hour of S phase. On the other hand, the size of replication units did not vary significantly throughout S phase.

My understanding of the effect of position in the cell cycle on DNA synthesis has gone through several changes in the 8 years since I became interested in the problem. One way in which my views have evolved—and I suspect many investigators have gone through a similar evolution—is illustrated in Fig. 1. When I first learned about the existence of a discrete period of DNA synthesis during interphase,<sup>1</sup> I assumed that within each cell there was a sharp transition from a nonsynthetic to a synthetic state at the  $G_1/S$  boundary and another sharp transition back to a nonsynthetic state at the  $S/G_2$  boundary, as illustrated in Fig. 1a. Indeed, some early reports<sup>2,3</sup> on rate of DNA synthesis during S phase suggest a nearly constant rate similar to the extreme of Fig. 1a.

Shortly thereafter, my knowledge of cell biology increased, and I learned that, when the total rate of DNA synthesis is measured on a population of synchronized mammalian cells, the rate increases gradually at the beginning of S phase and decreases gradually at the end of S phase, as shown schematically in Fig. 1b. At first I felt this behavior of synchronized populations could be explained by imperfect synchrony in the population; i.e., each cell might have a constant rate of DNA synthesis during S phase (Fig. 1a) and asynchrony might cause the gradual transitions exhibited by the total population (Fig. 1b). But I

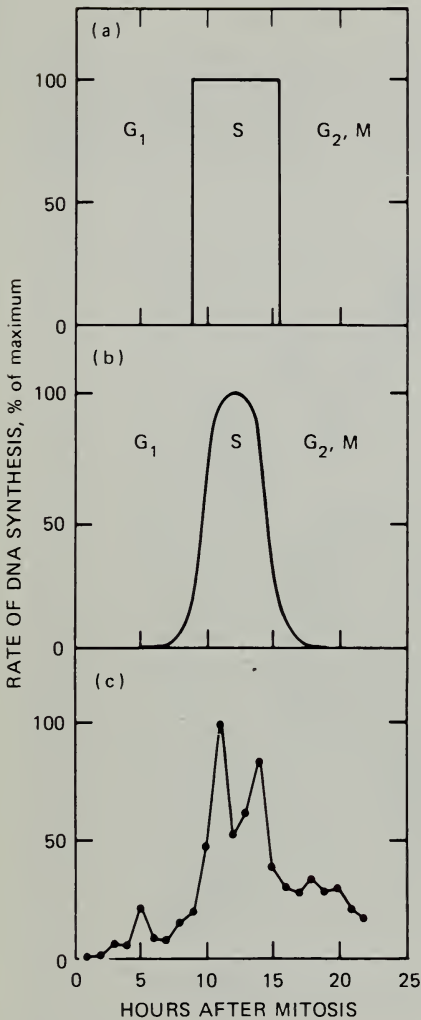


Fig. 1 Possible ways in which the rate of DNA synthesis might vary during the cell cycle. (a) The extreme hypothetical case of constant rate of DNA synthesis throughout S phase. (b) A hypothetical case of gradual increase in rate at the beginning of S phase and gradual decrease in rate at the end of S phase. Experimental data roughly similar to this diagram have been obtained by many investigators, e.g., Klevecz.<sup>14</sup> (c) Data obtained by Klevecz and Kapp<sup>15</sup> for the rate of DNA synthesis during the cell cycle of human WI-38 cells. Cells were synchronized by mitotic selection and then pulse-labeled with <sup>3</sup>H-thymidine for 30 min at hourly intervals after mitosis. Acid-precipitable radioactivity was measured. See Ref. 15 for detailed procedure.

soon learned more about DNA replication, and two more possible explanations occurred to me. The gradual transitions of Fig. 1b might also be explained by gradual changes in the number of replication units operating at one time or by changes in the rate of replication fork movement.

Perhaps I had better explain what I mean by replication units. The concept had its origins in the autoradiographic studies from many laboratories, which have shown that DNA synthesis can occur simultaneously at multiple discrete sites within individual chromosomes. The first such study was performed on Chinese hamster cells by Taylor.<sup>4</sup> He pulse-labeled Chinese hamster cells for 10 min with <sup>3</sup>H-thymidine, allowed the cells to reach mitosis in the absence of radioactive label, and then autoradiographed the mitotic chromosomes. Silver grains, indicative of underlying sites of DNA synthesis, frequently occurred in

several separate positions over individual chromosomes (Fig. 2). The magnitude of the number of separate sites of replication did not become apparent, however, until DNA fiber autoradiography, the technique developed by Cairns,<sup>5</sup> was first applied to mammalian DNA replication by Cairns<sup>6</sup> and by Arthur Riggs and myself.<sup>7</sup> In this technique cells are labeled with  $^3\text{H}$ -thymidine at the highest

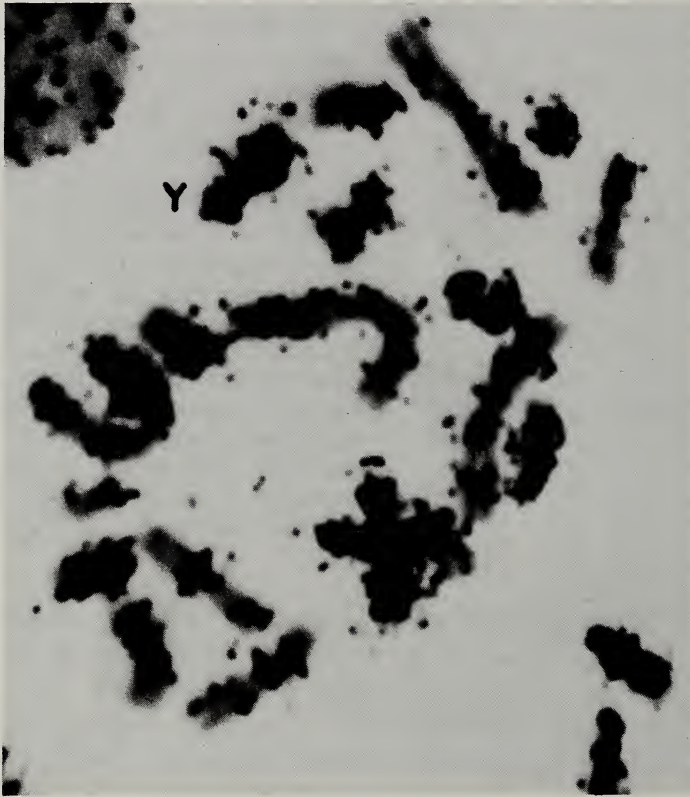


Fig. 2 Separate sites of DNA replication within single chromosomes of a Chinese hamster cell. Cells were pulse-labeled for 10 min with  $^3\text{H}$ -thymidine, then "chased" with cold thymidine until mitosis. The mitotic chromosomes were autoradiographed. Detailed procedure is given by Taylor.<sup>4</sup> Y, position of the Y chromosome. (Photograph courtesy of J. H. Taylor.)

possible specific activity and then gently lysed, and, in one of a number of ways, the cellular DNA is stretched out on a flat surface and autoradiographed. In Fig. 3 are displayed typical autoradiograms obtained after pulse-labeling Chinese hamster cells for 30 min. Individual DNA fibers are stretched out, and each is labeled in several short regions. From the histogram in Fig. 4, one can see that the modal distance between the centers of replicating regions is about  $30\ \mu$ . Since the total Chinese hamster haploid genome contains about 3 pg or  $1 \times 10^6$



Fig. 3 Separate sites of DNA replication within single DNA molecules of Chinese hamster cells. The cells were pretreated with 5-fluorodeoxyuridine for 12 hr, then pulse-labeled with  $^3\text{H}$ -thymidine for 30 min, then lysed. The DNA was spread out on a flat surface and autoradiographed. See Ref. 7 for detailed procedure and original picture.



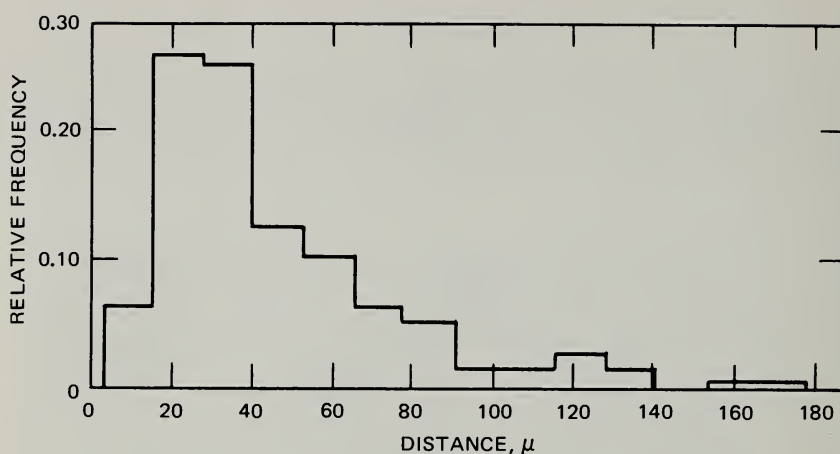


Fig. 4 Distribution of center-to-center distances between labeled regions like those in Fig. 3. Only labeled regions which were in tandem arrays like those of Fig. 3, and thus presumably in single DNA molecules (proof of this is given by Huberman and Riggs<sup>7</sup>), were measured. See Ref. 7 for detailed measuring procedure.

$\mu$  of DNA,<sup>8</sup> there are (very) approximately  $3 \times 10^4$  such regions involved in the replication of the haploid genome.

Additional work by us<sup>7,9</sup> and by others<sup>10-13</sup> also shows that within each such region DNA synthesis takes place at two replication forks which move out from a common origin, as diagrammed in Fig. 5. I will call the DNA replicated by each pair of forks which start at a common origin a "replication unit." Then the conclusion of the previous paragraph can be restated by saying that there are roughly  $3 \times 10^4$  replication units in the haploid Chinese hamster genome. Clearly, variations in the number of replication units operating at one time within single cells could cause the gradual changes in rate of DNA synthesis in whole populations noted in Fig. 1b. It is also clear from Fig. 5 that variations in the rate of replication fork movement could be responsible for those gradual changes.

How, then, can one distinguish among population asynchrony, changes in the number of operating replication units, and changes in the rate of fork movement as explanations of the gradual changes of Fig. 1b? Asynchrony in supposedly synchronized cell populations is a constant problem for cell biologists and one difficult to eliminate. However, recent work by Klevecz<sup>14</sup> and Klevecz and Kapp<sup>15</sup> makes it clear that for some cell lines, at least, variations in rates of DNA synthesis in synchronized populations are so great that they are nearly impossible to explain by asynchrony. Briefly, they find that the unimodal S-phase curve of Fig. 1b is typical of heteroploid cell lines like CHO (Chinese hamster ovary)<sup>14</sup> but that pseudodiploid cells like the Chinese hamster Don C line have a bimodal curve with two periods of maximum rate

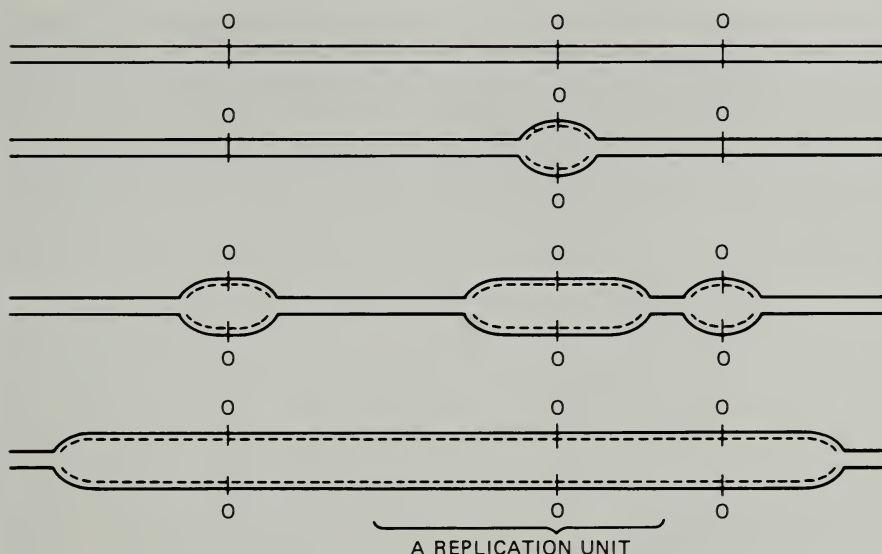


Fig. 5 Diagrammatic representation of bidirectional DNA replication and replication units in mammalian cells. —, parental DNA chains; ---, newly replicated chains. A stretch of DNA containing three replication units, each of which starts replication at an origin (O), is shown. Replication is assumed to terminate when adjacent converging forks collide. (Huberman and Riggs<sup>7</sup> give a slightly different version assuming that replication terminates at specific sites on the DNA molecule. No evidence that distinguishes these two possibilities is presently known.)

during S phase.<sup>14</sup> A true diploid line, human WI-38, has the trimodal S-phase curve<sup>15</sup> shown in Fig. 1c. I can see no way to explain such a curve in terms of asynchrony among cells each having an S phase of 6 hr or more with constant rate of DNA synthesis throughout. Therefore the variations of Fig. 1c must be occurring primarily within single cells.

The overall rate of DNA synthesis is not the only feature that changes during the S phase. The type of DNA replicated varies as well. Most heterochromatin is replicated late in S phase, whereas euchromatin is mostly replicated during early S phase (see review by Lima-de-Faria and Jaworska<sup>16</sup>). Even in the case of such functionally active DNA as ribosomal DNA, there are variations from cell type to cell type in the time during S phase when the DNA is replicated.<sup>17-19</sup>

With this background in mind, I can now formulate the experimental questions that I shall attempt to answer in this paper: (1) Are changes in the rate of DNA synthesis within single cells during S phase due to changes in the number of operating replication units or to changes in the rate of replication fork movement or both? (2) Since the kind of DNA replicated in early S phase is different from that replicated in late S phase, is there also a difference in the size of replication units in early and late S phase?

We first became interested in these questions during recent studies on the direction of DNA synthesis.<sup>9</sup> We were using a modification of the Cairns technique<sup>5</sup> developed by Lark, Consigli, and Toliver<sup>20</sup> in which the cells are lysed with anionic detergent and the DNA fibers are all spread out on the surface of a glass microscope slide. Because the DNA is fixed to the slides almost immediately after the cells are lysed, the DNA from single labeled cells is frequently spread over single small areas of the slide, without interference by DNA from other labeled cells. In the extreme situation of incomplete cell lysis, one can see the DNA of individual cells emerging from the broken nuclei like tails from comets (Fig. 6), but, in the more usual situation of better lysis and spreading, the only sign one has that different regions of the slide contain DNA from different individual cells is that the labeled regions appear more homogeneous in small areas. In Fig. 7, for instance, we see a region where we guess that DNA from one single cell is lying parallel to and to the side of DNA from a second single cell.



Fig. 6 DNA fiber autoradiograph showing DNA presumably from two partially lysed HeLa cells. HeLa cells growing on Petri plates were pulse-labeled with  $^3\text{H}$ -thymidine at 15 Ci/mmol for 15 min and then "chased" with  $^3\text{H}$ -thymidine at 51 Ci/mmol for 15 min (low specific activity  $\rightarrow$  high specific activity shift). The cells were lysed with sodium dodecyl sulfate, and their DNA was spread onto a glass microscope slide and autoradiographed with an exposure time of 15 months. For details of the procedure, see Ref. 9.



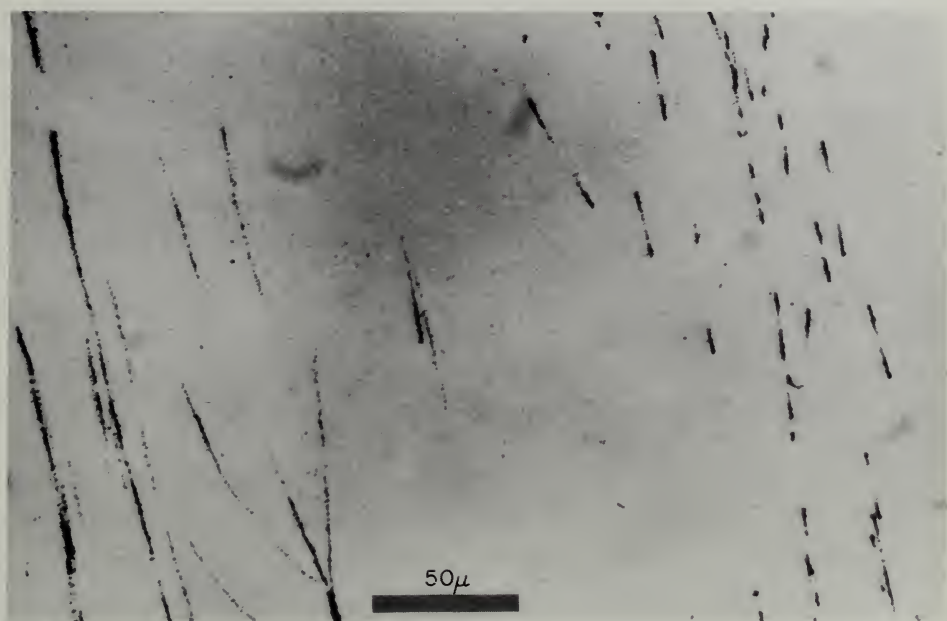


Fig. 7 DNA fiber autoradiograph showing DNA presumably from two different HeLa cells. Radioactive labeling and autoradiographic procedure were identical to those of Fig. 6 except that the autoradiographic exposure time was 7.75 months. Note that the magnification is much higher than for Fig. 6.

When we first saw areas like Figs. 6 and 7, we were struck by the relatively homogeneous appearance of the labeled regions within presumed single cells, and by the extent to which the labeled regions could differ in appearance in different presumed cells, even though all cells had been labeled under identical conditions. We guessed that the differences between cells might be due to the cells' being in different stages of the cell cycle. David Housman, a postdoctoral fellow in our laboratory, undertook to test this possibility by careful DNA fiber autoradiographic study of synchronized cells.

We used CHO cells synchronized by the Colcemid technique of Stubblefield.<sup>21</sup> In our hands the starting cell populations were >99% in mitosis. The entry and departure of our cells into and out of S phase is shown in Fig. 8. A single peak is obtained whose breadth indicates the degree of asynchrony in G<sub>1</sub> for this heteroploid cell line. Note that some cells have entered S phase as early as 2 hr after mitosis.

We obtained a rough estimate for the variation in rate of DNA synthesis within individual CHO cells during S phase by pulse-labeling them for 30 sec with <sup>3</sup>H-TdR, then sectioning them, and autoradiographing the sections.<sup>22</sup> The average grain count over those nuclei which were labeled was much higher in late S phase than in early S phase (Table 1). Known variations in the size of the



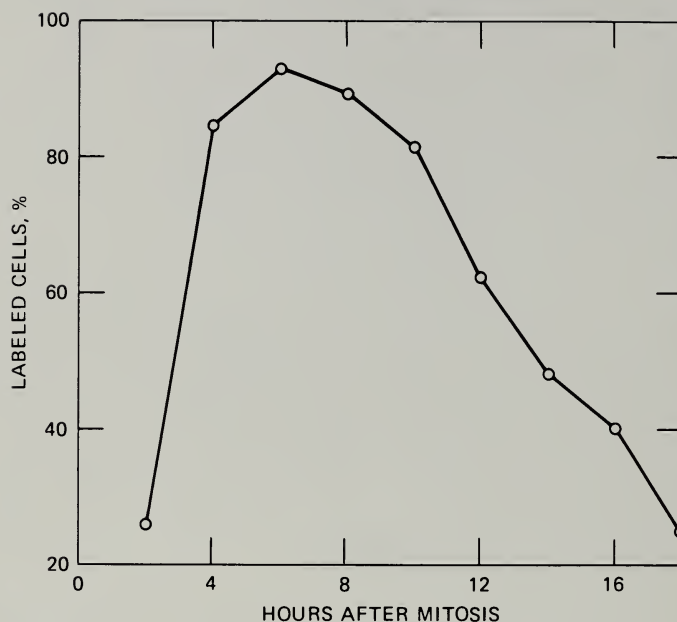


Fig. 8 Passage of synchronized CHO cells through S phase. Cells were synchronized by the Colcemid-reversal method of Stubblefield.<sup>21</sup> At 2-hr intervals after release from mitosis,  $^3\text{H}$ -TdR was added to each plate (20 Ci/mmol; 17  $\mu\text{Ci/ml}$ ). After 10 min the cells were washed twice with cold isotonic saline, collected by trypsinization at room temperature, allowed to swell in hypotonic medium for 10 min, pelleted, fixed with methanol-acetic acid (3:1), spread onto subbed glass slides, and allowed to dry. The slides were coated with Kodak AR-10 autoradiographic stripping film and exposed for 7 days. After development the slides were stained with Giemsa stain, and at least 312 cells were scanned to determine the percent of cells labeled at each time point.

TABLE 1  
RATE OF DNA SYNTHESIS IN SYNCHRONIZED CHO CELLS

Hours after release from mitosis	2	4	6	8	10	12
Average number of grains per cell section after 1 month's exposure*	<1	6	16	16	24	17

\*Cells were synchronized as in Fig. 8, pulse-labeled for 30 sec with  $^3\text{H}$ -thymidine, fixed, sectioned, and autoradiographed with the electron microscope. Data and detailed procedure are given by Huberman, Tsai, and Deich.<sup>22</sup>

thymidine-5'-triphosphate pool during the cell cycle<sup>23</sup> are in the wrong direction to explain these findings by dilution of the added <sup>3</sup>H-thymidine, and variations in the rate of thymidine uptake by the cells are also an unlikely explanation since much longer pulses (10 min) gave similar results (Huberman and Tsai, unpublished data).

As we had anticipated, Housman found that, when *synchronized* cells were pulse-labeled and their DNA was then autoradiographed, the appearance of the DNA autoradiograms was nearly as homogeneous over the whole slide as it had previously been within single presumed cells. In addition, the appearance of the autoradiograms changed during S phase. As illustrated in Fig. 9, when cells were labeled with a 15-min pulse of <sup>3</sup>H-thymidine at low specific activity followed by a 15-min pulse at high specific activity, the lengths of the labeled regions were much shorter if the cells were labeled in very early S phase (2 hr after mitosis) than they were if labeled later in S phase (4 or 10 hr after mitosis). This suggests that the rate of fork movement is less in early S phase than it is in late S phase.

To be certain of these conclusions, Housman made careful measurements of the lengths of DNA segments labeled in a two-specific-activity pulse, like the one in Fig. 9, where the cells were labeled first for 15 min with <sup>3</sup>H-thymidine at low specific activity and then for 15 min with <sup>3</sup>H-thymidine at high specific activity. In order to measure only lengths of DNA which were unbroken and which were replicating throughout the entire labeling period, he measured only low-grain-density regions that were bounded on one side by an unlabeled gap and on the other side by a high-grain-density region (see Fig. 10). Such regions almost certainly began replication at the beginning of the low-specific-activity pulse and continued on until the beginning of the high-specific-activity pulse. Histograms of such labeled lengths at various times during S phase (Fig. 11) reveal a striking two- to three-fold increase in rate of fork movement after early S phase. Housman also made similar measurements on autoradiograms produced by a single 20-min pulse at high specific activity. Although measurements of such single-specific-activity pulses are complicated by the possibilities that replication units may have stopped, started, or fused during the pulse, the measurements are much simpler to make, and Housman could easily make more of them. As shown in Fig. 12, the single-specific-activity measurements made at 2, 3, 6, 7.5, and 10.5 hr are in reasonable agreement with the measurements in Fig. 11 made at similar times. Thus, when a 20-min pulse is used, the single-specific-activity method gives a reasonable estimate of replication rate. From the more extensive measurements in Fig. 12, one can see that there is a gradual increase in rate of fork movement during most of S phase, the maximum rate in late S being four to five times greater than the minimum rate in very early S. A similar conclusion was reached several years ago by Painter and Schaeffer<sup>24</sup> using a buoyant density-shift method for estimating rate of fork movement in HeLa cells. In our earlier DNA autoradiographic experiments,<sup>7</sup> Arthur Riggs and I also attempted to detect variations in the rate of fork

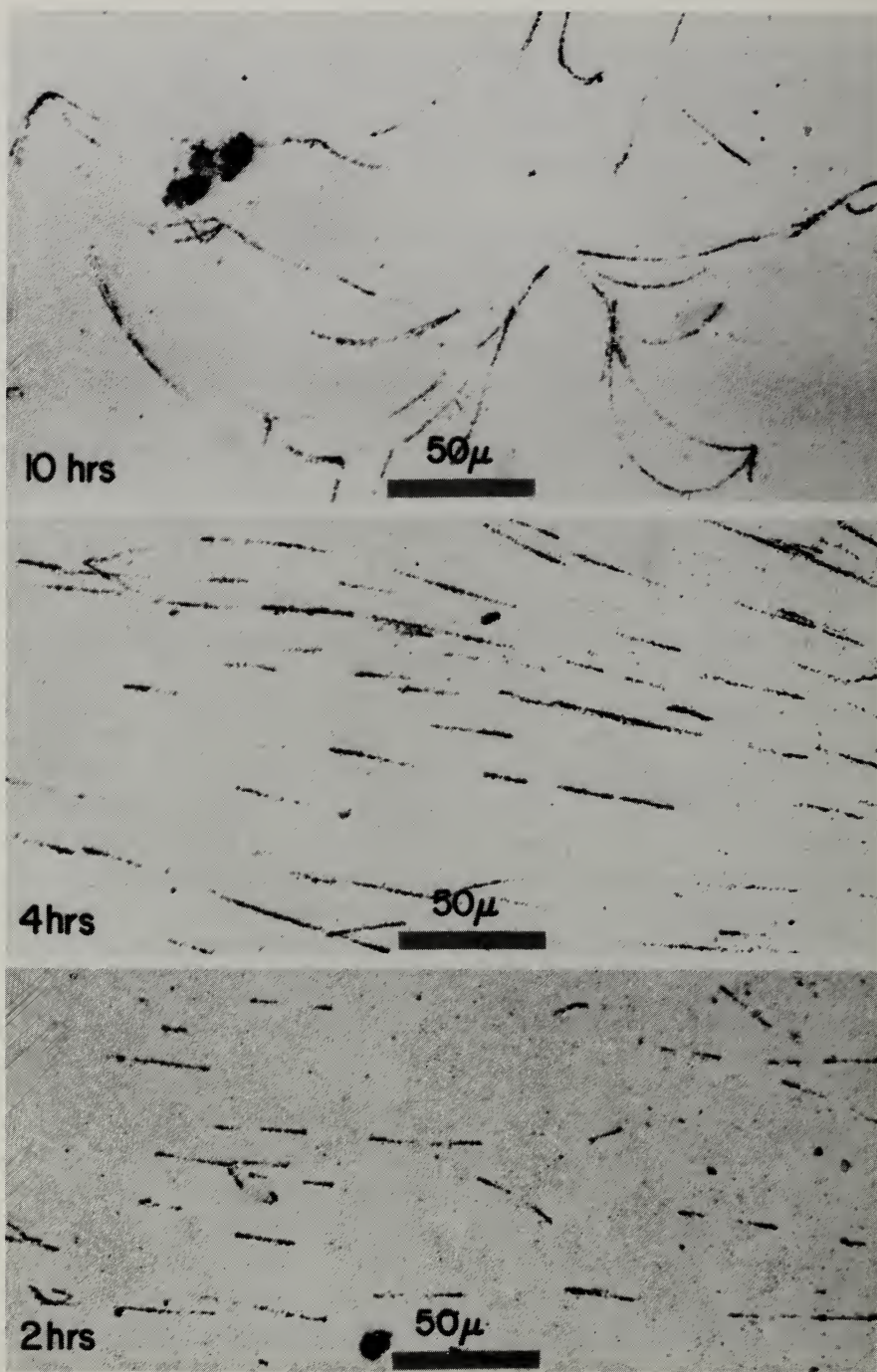


Fig. 9 DNA fiber autoradiograms from CHO cells at different stages of S phase, i.e., very early, early, and late (2, 4, and 10 hr, respectively, after mitosis). Cells were synchronized as in Fig. 8, and, at 2-hr intervals after mitosis, were pulse-labeled first with  $^3\text{H}$ -thymidine at 10 Ci/mmole for 15 min and then with  $^3\text{H}$ -thymidine at 50 Ci/mmole for another 15 min. The cells were then lysed and their DNA autoradiographed as in Fig. 6.



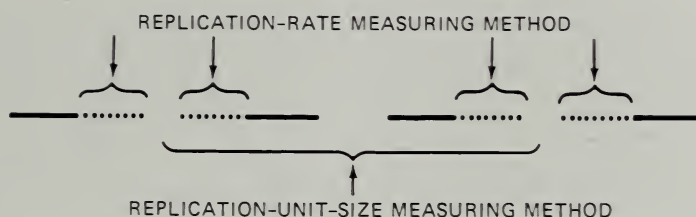


Fig. 10 Methods for measuring replication rate and replication unit size. —, high-grain-density region in DNA fiber autoradiogram; ...., low-grain-density region. The configuration diagrammed is typical for DNA labeled with a low specific activity  $\rightarrow$  high specific activity shift, as in Figs. 6, 7, and 9. Such measurements must be made in uncrowded regions of the slide, unlike the crowded areas in Figs. 6, 7, and 9. See Huberman and Tsai<sup>9</sup> for examples of uncrowded regions.

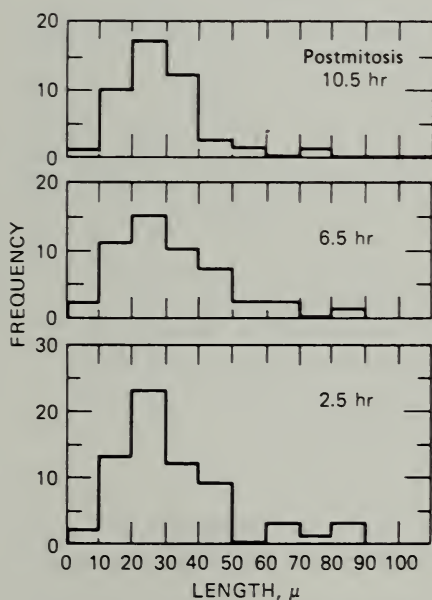


Fig. 11 Length distribution of low-grain-density regions. The DNA autoradiograms were prepared under conditions identical to those of Fig. 9 except that CHO cells were labeled at 2.5, 6.5, and 10.5 hr after mitosis. Low-grain-density regions, selected randomly from uncrowded areas of the slides if they appeared to be parts of single DNA fibers, were measured by the criteria of Fig. 10. Since the low-specific-activity pulse lasted for 15 min, rates of fork movement (in  $\mu/\text{min}$ ) can be obtained by dividing the indicated lengths by 15.

movement during S phase. However, we did not make measurements during the first hour of S phase (which our data now suggest is the period showing the greatest deviation from average), and we used a cruder synchronization procedure (a 12-hr treatment with 5-fluorodeoxyuridine). Therefore our failure at that time to notice any significant variation in rate during S phase is not surprising.

The fact that obvious variations in rate of fork movement can be detected with heteroploid cell lines like CHO (this paper) and HeLa (Painter and Schaeffer<sup>24</sup>) leads one to wonder whether variations might not be even more



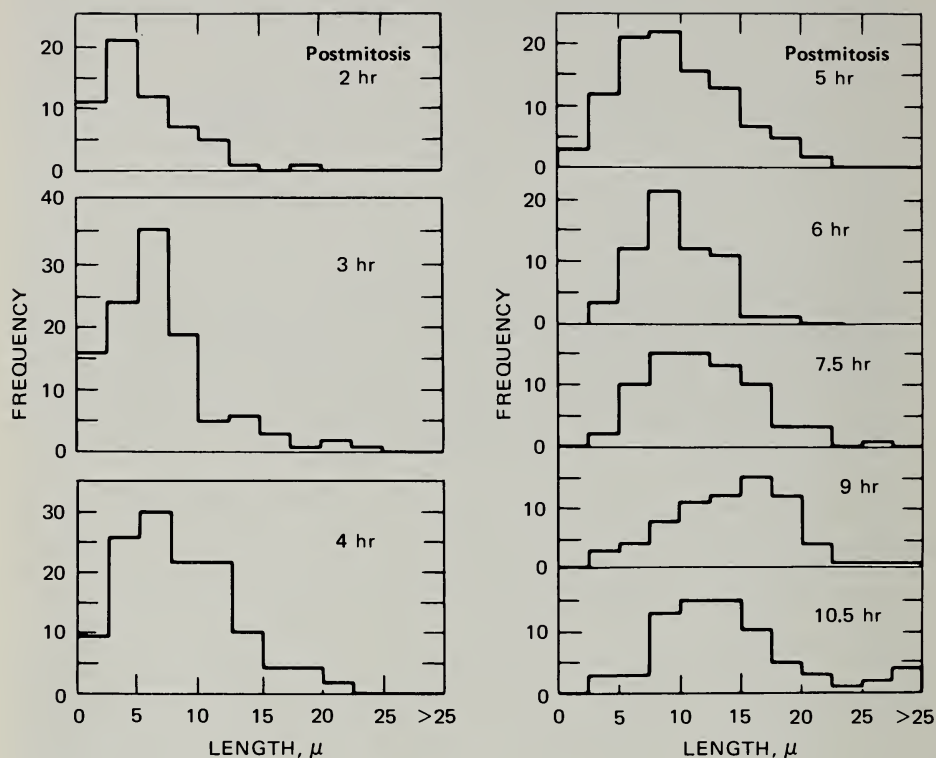


Fig. 12 Distribution of autoradiogram lengths obtained by labeling CHO cells for 20 min with  $^3\text{H}$ -thymidine. Cells were synchronized as in Fig. 8, and, at the indicated time after mitosis, they were pulse-labeled for 20 min with  $^3\text{H}$ -thymidine at 50 Ci/mmole. Cells were lysed and DNA was autoradiographed as in Fig. 6. Autoradiograms for length measurement were selected randomly from uncrowded areas of the slides. Rates of fork movement (in  $\mu/\text{min}$ ) can be obtained by dividing the indicated lengths by 20.

pronounced in diploid lines like the ones with which Klevecz<sup>14,15</sup> has demonstrated bi- or triphasic variations in overall rate of DNA synthesis during S phase.

At this time we have no clues about the molecular factors involved in the observed rate variations. It is possible that some compound which is necessary and rate-limiting for DNA synthesis gradually accumulates during S phase. Perhaps experiments in which DNA synthesis is studied in isolated nuclei will help in finding the cause of the rate variations.

Note that, although the variations in rate of fork movement demonstrated in Figs. 11 and 12 amount to as much as five-fold during the S phase, these variations are insufficient to account for the greater than 20-fold change suggested for total synthesis within single cells by the data in Table 1. Therefore we suggest that changes in the number of operating replication units must be occurring along with the demonstrated variations in fork movement rate.

What about replication unit size? Housman measured the distance between centers of replication units since the position of centers was easier to determine than the sites where replication units terminate or fuse together. His method of measurement is diagrammed in Fig. 10, and his results are presented in Fig. 13. There appears to be no significant difference in replication unit size throughout the S phase, even during the period when the rate of fork movement is changing dramatically. This interesting finding suggests that, if the position of origins is determined by specific sequences,<sup>2,5</sup> then such origin-specific sequences occur as commonly in heterochromatin (which replicates predominantly from 10 to 12 hr after mitosis in these cells<sup>2,2</sup>) as in euchromatin [which replicates

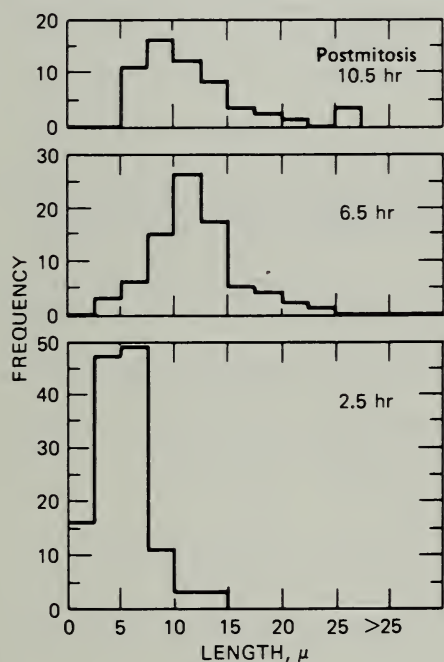


Fig. 13 Lengths of replication units. Measurements were made by the criteria of Fig. 10 on the same autoradiograms used for Fig. 11.

predominantly from 2 to 6 hr after mitosis (Ref. 22 and Huberman and Tsai, unpublished results)]. So far as I know, no one has been able to detect short, simple-sequence heterochromatin (the kind typified by mouse satellite DNA) in CHO cells. It would be interesting to see if the size of replication units is also constant throughout S phase in cell types with a great deal of satellite heterochromatin, such as mouse or kangaroo rat.

I now come to the present time in this description of the evolution of my views on the relation between the cell cycle and DNA synthesis. I have learned that there are variations in the total rate of DNA synthesis per cell during S phase and that these variations may be the result both of changes in the number of replication units operating at any one time and of changes in the rate

of DNA synthesis at each replication fork. How and why such changes occur is a problem that is left for the future. I have also learned that in CHO cells, at least, there is no significant change in replication unit size during S phase. The real significance of this finding will become apparent when we have learned the molecular signals that determine the size and timing of a replication unit.

## ACKNOWLEDGMENTS

Most of the original research reported here was, as noted in the text, carried out by David Housman. In addition, Will Wheatley and Alice Tsai contributed time and effort to some of the experiments. Financial support came from research grants from the National Science Foundation and National Institutes of Health.

## REFERENCES

1. A. Howard and S. R. Pelc, Synthesis of Desoxyribonucleic Acid in Normal and Irradiated Cells and Its Relation to Chromosome Breakage, *Heredity, London. (Suppl.)*, 6: 261-273 (1953).
2. J. L. Edwards, A. L. Koch, P. Youcis, H. Freese, M. B. Laite, and J. T. Donaldson, Some Characteristics of DNA Synthesis and the Mitotic Cycle in Ehrlich Ascites Tumor Cells, *J. Biophys. Biochem. Cytol.*, 7: 273-282 (1960).
3. C. P. Stanners and J. F. Till, DNA Synthesis in Individual L-Strain Mouse Cells, *Biochim. Biophys. Acta*, 37: 406-419 (1960).
4. J. H. Taylor, Asynchronous Duplication of Chromosomes in Cultured Cells of Chinese Hamster, *J. Biophys. Biochem. Cytol.*, 7: 455-464 (1960).
5. J. Cairns, The Bacterial Chromosome and Its Manner of Replication as Seen by Autoradiography, *J. Mol. Biol.*, 6: 208-213 (1963).
6. J. Cairns, Autoradiography of HeLa Cell DNA, *J. Mol. Biol.*, 15: 372-373 (1966).
7. J. A. Huberman and A. D. Riggs, On the Mechanism of DNA Replication in Mammalian Chromosomes, *J. Mol. Biol.*, 32: 327-341 (1968).
8. H. A. Sober (Ed.), *Handbook of Biochemistry*, 2nd ed., pp. H112-H113, The Chemical Rubber Company, Cleveland, 1970.
9. J. A. Huberman and A. Tsai, Direction of DNA Replication in Mammalian Cells, *J. Mol. Biol.*, 75: 5-12 (1973).
10. H. G. Callan, Replication of DNA in the Chromosomes of Eukaryotes, *Proc. Roy. Soc. (London) Ser. B*, 181: 19-41 (1972).
11. R. Hand and I. Tamm, Rate of DNA Chain Growth in Mammalian Cells Infected with Cytocidal RNA Viruses, *Virology*, 47: 331-337 (1972).
12. F. Amaldi, F. Carnevali, L. Leoni, and D. Mariotti, Replicon Origins in Chinese Hamster Cell DNA. I. Labeling Procedure and Preliminary Observations, *Exp. Cell Res.*, 74: 367-374 (1972).
13. H. Weintraub, Bi-directional Initiation of DNA Synthesis in Developing Chick Erythroblasts, *Nature (London) New Biol.*, 236: 195-197 (1972).
14. R. R. Klevecz, Temporal Coordination of DNA Replication with Enzyme Synthesis in Diploid and Heteroploid Cells, *Science*, 166: 1536-1538 (1969).
15. R. R. Klevecz and L. N. Kapp, Intermittent DNA Synthesis and Periodic Expression of Enzyme Activity in the Cell Cycle of WI-38, *J. Cell Biol.*, 58: 564-573 (1973).

16. A. Lima-de-Faria and H. Jaworska, Late DNA Synthesis in Heterochromatin, *Nature*, **217**: 138-142 (1968).
17. F. Amaldi, D. Giacomoni, and R. Zito-Bignami, On the Duplication of Ribosomal RNA Cistrons in Chinese Hamster Cells, *Eur. J. Biochem.*, **11**: 419-423 (1969).
18. D. Giacomoni, and D. Finkel, Time of Duplication of Ribosomal RNA Cistrons in a Cell Line of *Potorous tridactylis* (Rat Kangaroo), *J. Mol. Biol.*, **70**: 725-728 (1972).
19. I. Balazs and C. Schildkraut, DNA Replication in Synchronized Cultured Mammalian Cells. II. Replication of Ribosomal Cistrons in Thymidine-Synchronized HeLa Cells, *J. Mol. Biol.*, **57**: 153-158 (1971).
20. K. G. Lark, R. Consigli, and A. Toliver, DNA Replication in Chinese Hamster Cells: Evidence for a Single Replication Fork per Replicon, *J. Mol. Biol.*, **58**: 873-875 (1971).
21. E. Stubblefield, in *Methods in Cell Physiology*, Vol. 3, D. M. Prescott (Ed.), pp. 25-43, Academic Press, Inc., New York, 1968.
22. J. A. Huberman, A. Tsai, and R. A. Deich, DNA Replication Sites Within Nuclei of Mammalian Cells, *Nature*, **241**: 32-36 (1973).
23. K. L. Skoog, B. A. Nordenskjold, and K. G. Bjursell, Deoxyribonucleoside-Triphosphate Pools and DNA Synthesis in Synchronized Hamster Cells, *Eur. J. Biochem.*, **33**: 428-432 (1973).
24. R. B. Painter and A. W. Schaeffer, Variation in the Rate of DNA Chain Growth Through the S Phase in HeLa Cells, *J. Mol. Biol.*, **58**: 289-295 (1971).
25. F. Amaldi, M. Buongiorno-Nardelli, F. Carnevali, L. Leoni, D. Mariotti, and M. Pomponi, Replicon Origins in Chinese Hamster Cell DNA. II. Reproducibility, *Exp. Cell. Res.*, **80**: 79-87 (1973).



# GENETIC CONSERVATISM IN PHYLOGENY WITH SPECIAL REFERENCES TO CHROMOSOMES

FRANCES E. ARRIGHI

Department of Biology, The University of Texas System Cancer Center,  
M. D. Anderson Hospital and Tumor Institute, Houston, Texas

---

## ABSTRACT

Recent advances in mammalian cytogenetic technique have permitted extension of ideas and conclusions regarding species relationships, evolution pathways, and genetic conservatism. Examples of hybridization homology suggest that specific sequences in the DNA of humans and the great apes were present prior to divergence of Hominidae and Pongidae 30 million years ago. Conventional karyology and banding techniques have shown that differences between the karyotypes of *Peromyscus crinitus* and *P. eremicus* are accountable entirely in heterochromatic regions and that euchromatic regions display striking resemblance. Characteristic G-band patterns of X chromosomes persist in 60 widely divergent mammalian species, again demonstrating that arrangement of genetic material is conservative. Mechanisms for chromosomal changes in phylogeny are reviewed.

Evolutionary trends at the genetic level have been studied mainly by analyses of gene products (phenotypes) and their linkages and/or by chromosome analyses. In *Drosophila* evolution studies, significant achievements were made in genetic cytology even before the dawn of molecular biology.<sup>1</sup> More recently comparison between proteins of certain species, e.g., hemoglobin, histones, and ribosomal cistrons, have indicated that at least certain genes have changed very little in the course of organic evolution.

Observations on chromosome morphology and behavior have yielded a considerable amount of information regarding species relationships, population structure, and meiotic mechanisms. Before the recent period when improvements of cell-culture techniques facilitated the growing of mammalian cells in vitro, chromosome research relied principally on plant and insect materials. Because of a number of newer techniques, mammalian cytogenetics has advanced rapidly and some interesting conclusions have been reached. One of these conclusions, surprisingly, is that the arrangement of genetic material in mammalian

chromosomes and probably in other classes of vertebrates is extremely conservative. This paper summarizes some of the findings in this area of research.

## GENETIC CONSERVATISM

Although genetic studies of man and of the laboratory mouse have had excellent progress, those of other mammals are still in their infancy. Some data, however, are already available in respect to sex-linked genes. The enzyme glucose-6-phosphate dehydrogenase has been shown to be X-linked in man, horse and donkey, two species of European wild hares (*Lepus europaeus* and *L. timidus*), and an American rodent (*Peromyscus maniculatus*).<sup>2</sup> These species belong to the orders Primates, Perissodactyla, Lagomorpha, and Rodentia, respectively. There is also some evidence of sex-linkage of the genes hemophilia A and B in man and in dog and probably in the horse.<sup>2</sup> Some preliminary data, together with cytological findings to be discussed later, suggest that many sex-linked genes are sex-linked in the great majority of species throughout the class Mammalia.

The concept and technique of nucleic acid hybridization gave evolutionists a powerful means for comparing genomes at the molecular level. The more recent procedure of in situ nucleic acid hybridization is especially valuable for linking molecules to chromosomes and nuclei. Pardue et al.<sup>3</sup> used the histone messenger from the sea urchin to locate the histone genes in the polytene chromosomes of *Drosophila*. It is not yet feasible to identify locations of single-copy genes on metaphase chromosomes, but it is reasonably reliable now to locate repetitive DNA sequences. Grain counts of nuclei permit rough estimation of the degree of homology between homologous and heterologous hybrids.<sup>4</sup> Jones and co-workers<sup>5</sup> reported the homology between the human satellite III DNA and the chimpanzee satellite A DNA. These two DNA fractions have the same buoyant density in neutral CsCl gradient; they are localized in specific chromosomes of each species (both homologous and heterologous hybridization); and they both hybridize in specific regions of the chromosomes of the orangutan. These investigators,<sup>5</sup> therefore, speculated that this particular DNA sequence should have been in existence in the ancestral genome of Hominidae and Pongidae prior to divergence, which is estimated to be approximately 30 million years ago.

## CONVENTIONAL KARYOLOGICAL APPROACHES TO PHYLOGENY

Using conventional karyotype analysis, one obtains rather empirical data because within each karyotype many chromosomes possess similar morphology. The chromosomes of the domestic mouse, *Mus musculus*, provide a prime example. The 40 chromosomes of this species have a similar morphology; all are acrocentric and the differences in lengths are so gradual that even pairing is impossible. Only the shortest pair of autosomes and the Y chromosome are

distinctly shorter than the remaining elements and can be identified in good preparations.<sup>6</sup> Therefore cytogenetic data on the mouse were indeed non-existent although a large amount of genetic data was available.

Deciphering phylogenetic relationships by karyological means is understandably difficult by conventional karyotypes. Fortunately, in many cases the karyological changes appear to involve total chromosome or total arm translocations (the Robertsonian mechanism). Thus a karyotype containing two acrocentric pairs of chromosomes can be reduced to one pair of biarmed chromosomes. The number of chromosome arms (the "fundamental number" of Matthey<sup>7</sup>) remains unchanged. In other words, when the karyotypes of many related taxa are compared, one finds this trend: high diploid numbers with a high number of acrocentrics down to low diploid number with a higher number of biarmed chromosomes. The best example is probably found in the tobacco mouse, *Mus poschiavinus*.<sup>8</sup> The chromosomes of this species consist of 14 biarmed chromosomes and 12 acrocentrics ( $2n = 26$ ). If its karyotype is compared with that of the house mouse, the 40 basic elements are preserved. Therefore the fundamental number does not change and the Robertsonian system prevails.

Unfortunately, not all karyotypic changes are as simple and as clear-cut. In many species of the rodent genus *Peromyscus*, the situation is the opposite. The diploid number is always 48, but the number of chromosome arms varies drastically from species to species. In these cases Robertsonian systems cannot explain the changes at all. With the classic cytogenetic explanations, these changes must have been achieved by pericentric inversions and reciprocal translocations. Yet the unexplainable fact is that hybrids from crosses of parents with different fundamental numbers are perfectly normal in their meiotic behavior.<sup>9</sup> In cases where more complex rearrangements have occurred between widely separated taxa, karyological tracing of their relationships was practically impossible. For example, no one even attempted to relate the karyotype of the rhesus macaque ( $2n = 42$ , 84 chromosome arms) to that of the African green monkey ( $2n = 60$ , 120 chromosome arms). Some of these dilemmas now are being resolved because of improved techniques.

## NEWER KARYOLOGICAL APPROACHES TO PHYLOGENY

Recent cytological improvements (i.e., quinacrine fluorescence, or Q-banding; constitutive heterochromatin staining, or C-banding; and Giemsa staining, or G-banding and R-banding)<sup>10</sup> have greatly enhanced the resolution for visualizing metaphase chromosomes. The C-banding is of particular value because it defines the location(s) of the highly repeated DNA sequences. In most, if not all, mammalian species, every pair of chromosomes can now be recognized and delimited. By various banding procedures, therefore, gross chromosomal rearrangement can be identified without difficulty. There is no problem whatsoever in identifying the elements involved in the Robertsonian



process. For example, all fusion products in *Mus poschiavinus* were positively identified by Q-banding.<sup>11</sup> Major inversions in chromosomes of the genus *Rattus* have been found and identified also.<sup>12</sup>

The mystery of the *Peromyscus* karyotypes was almost unequivocally solved.<sup>13-15</sup> Briefly, most short arms of the *Peromyscus* chromosomes are heterochromatic, i.e., C-band positive (Fig. 1). The preliminary data of Clark, Pathak, and Arrighi<sup>16</sup> showed that at least in *P. eremicus*, where every chromosome has a heterochromatic short arm (Fig. 1b), the individual arms indeed contain a high number of satellite (repeated) sequences. Pathak, Hsu, and Arrighi<sup>15</sup> attempted by C-banding and G-banding to compare the two extreme cases of *P. eremicus* (with 48 short arms) and *P. crinitus* (with 8 short arms). All short arms were found to be heterochromatic. In G-band preparations, after the heterochromatic segments are disregarded, the euchromatic elements (long arms) of the two species are matched almost band by band (Figs. 2 and 3). Thus the two species, which conventional karyotypic analysis shows to be drastically different, are in reality extremely similar when only the informational material (euchromatin) is compared.

More amazing, perhaps, is the report of Stock and Hsu,<sup>17</sup> who compared the chromosomes of the rhesus macaque and the African green monkey. These animals have extremely different karyotypes. If the heterochromatic arms in the karyotypes are removed and the fused chromosomes (both Robertsonian fusions and tandem translocations) are located, the G-bands of the two species are again highly homologous. Although the two species of monkeys are widely separated, both belong to the family Cercopithecidae.

Of particular significance is the work of Pathak and Stock,<sup>18</sup> who compared the G-band patterns of the X chromosomes of some 60 species of mammals representing different genera, families, and orders. They found that the X chromosome of mammals, despite the tremendous differences in size and morphology, basically retained some characteristic banding patterns through millions of years of organic evolution. These examples strongly indicate that the arrangement of genetic material in chromosomes appears to be extremely conservative.

## DISCUSSION

Data on molecular biology and cytology suggest that the structure of informational genes and the arrangement patterns of these genes are rather conservative, thus allowing effective tracing of phylogenetic relationship in higher animals. We have presented an example to demonstrate that even highly repeated DNA sequences may also be conservative in nature. The repetitive sequences, however, are comparatively more liable to change. The various amounts of base mismatching found in repetitive DNAs indicate their capability to change. The variable pyrimidine tract lengths of the repeated sequences in the



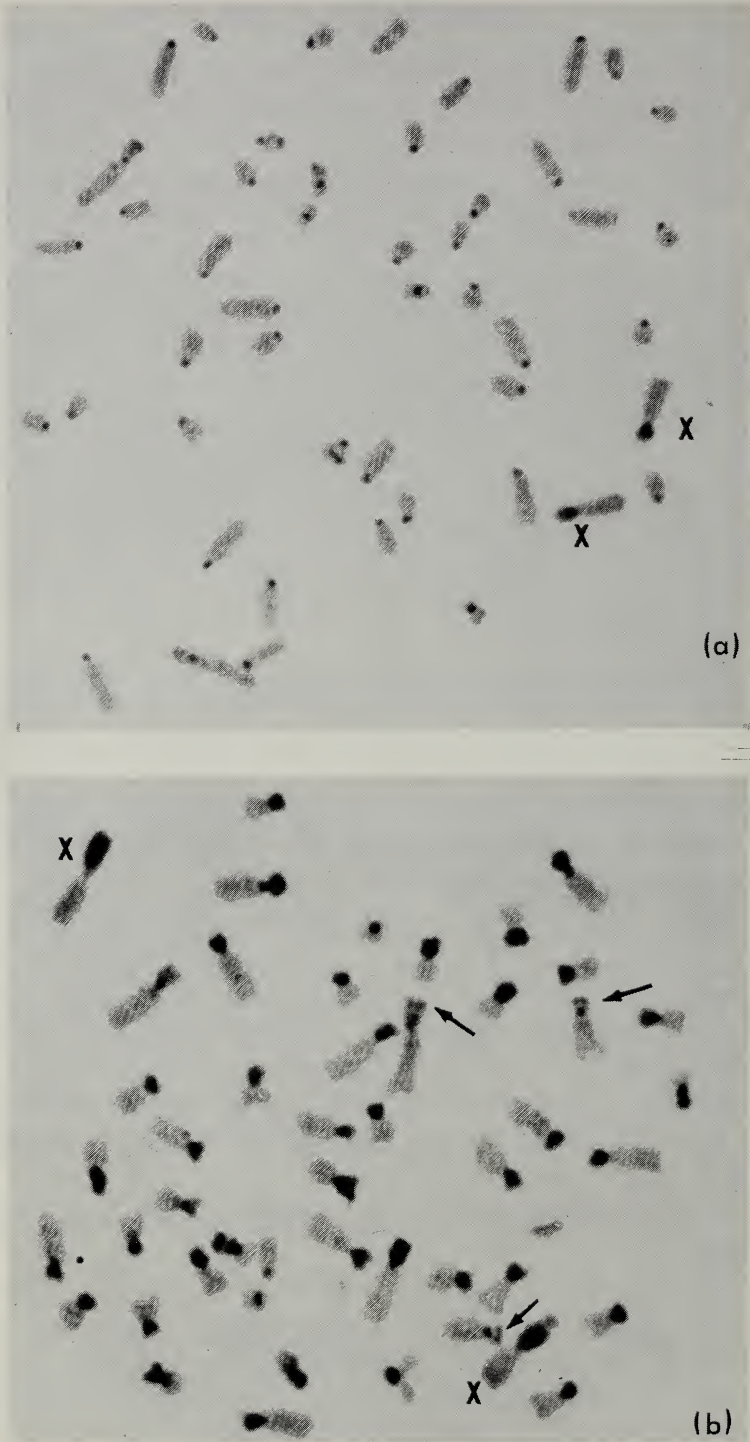


Fig. 1 C-band patterns of *Peromyscus crinitus* and *P. eremicus* depicting sites of constitutive heterochromatin. (a) *P. crinitus*. Note absence of short arms in most chromosomes. (b) *P. eremicus*. The short arms are C-band positive. Arrows indicate secondary constrictions within heterochromatic segments.

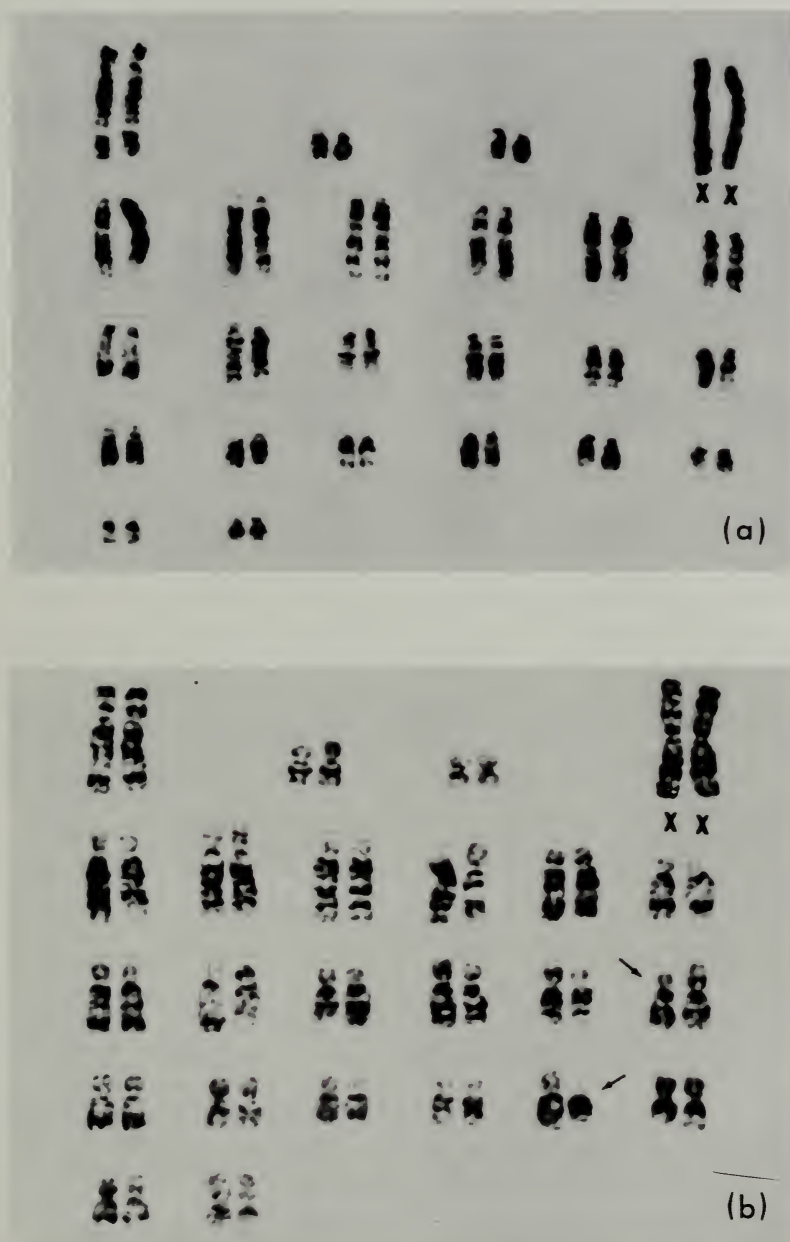


Fig. 2 Karyotypes of *Peromyscus eremicus* and *P. crinitus* showing G-band patterns. (a) *P. crinitus*. (b) *P. eremicus*. Arrows point to chromosome pairs showing matching G-bands in long arms but differing in length of short arms.

[Figures 1 and 2 are from S. Pathak, T. C. Hsu, and F. E. Arrighi, Chromosomes of *Peromyscus* (Rodentia. Cricetidae). IV. The Role of Heterochromatin in Karyotypic Evolution, *Cytogenet. Cell Genet.*, 12: 315-326 (1973).]

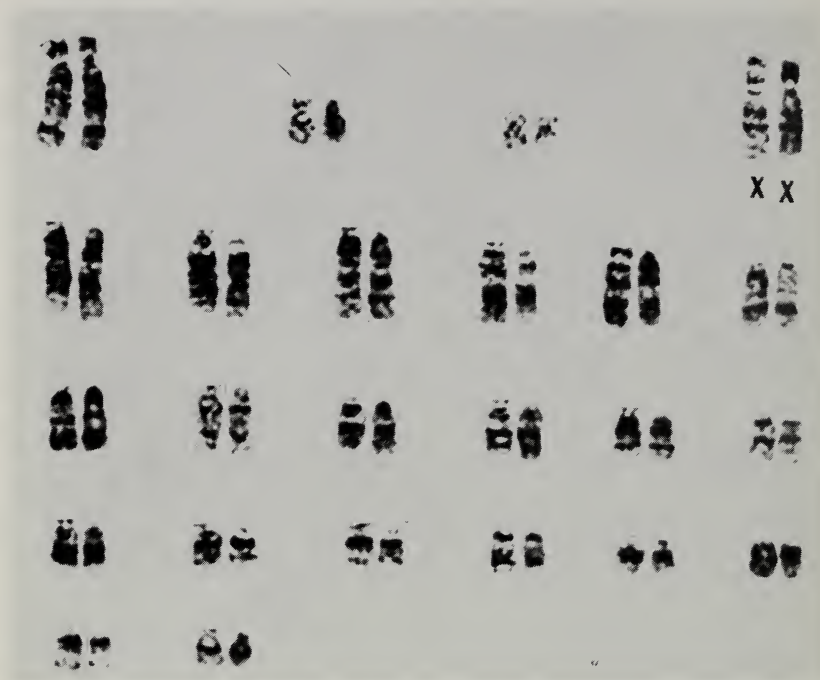


Fig. 3 Artificial G-band karyotype. The chromosomes on the right are from *Peromyscus crinitus* and are unaltered. The chromosomes on the left are from *P. eremicus*. The C-band positive areas have been cut from the *P. eremicus* chromosomes. The G-bands of the long arms then match almost perfectly. [From S. Pathak, T. C. Hsu, and F. E. Arrighi, Chromosomes of *Peromyscus* (Rodentia: Cricetidae). IV. The Role of Heterochromatin in Karyotypic Evolution, *Cytogenet. Cell Genet.*, 12: 315-326 (1973).]

mouse satellite DNA<sup>19</sup> provide another way of looking at its mutagenicity. Indeed, related species may possess highly repeated sequences entirely different from one another.

Similar situations were found in the amount and distribution of constitutive heterochromatin, the chromosomal location of repetitious DNA. The C-bands have been known to be polymorphic within a species<sup>20</sup> between subspecies<sup>13</sup> and species.<sup>15</sup> From the data accumulated thus far, it appears that chromosomal changes in phylogeny are achieved mainly by the following routes:

1. Fusing and possibly splitting of total chromosomal arms.
2. Addition or deletion of heterochromatin, both within a chromosome arm, thereby changing its length, and with the formation of new arms, thereby changing the shape of the chromosome as well as the fundamental number of the karyotype.

The euchromatin material, including its packaging system, appears to change little in the course of phylogenetic divergence.



## REFERENCES

1. J. T. Patterson and W. S. Stone, *Evolution in the Genus Drosophila*, The Macmillan Company, New York, 1952.
2. S. Ohno, *Sex Chromosomes and Sex-Linked Genes*, pp. 58-66, Springer-Verlag New York Inc., New York, 1967.
3. M. L. Pardue, E. Weinberg, L. H. Kedes, and M. L. Birnstiel, Localization of Sequences Coding for Histone Messenger RNA in the Chromosomes of *Drosophila melanogaster*, *J. Cell Biol.*, **55**: 199a (1972).
4. F. E. Arrighi, T. C. Hsu, P. Saunders, and G. F. Saunders, Localization of Repetitive DNA in the Chromosomes of *Microtus agrestis* by Means of *In Situ* Hybridization, *Chromosoma*, **32**: 224-236(1970).
5. K. W. Jones, J. Prosser, G. Corneo, E. Ginelli, and M. Bobrow, Satellite DNA, Constitutive Heterochromatin and Human Evolution, in *Symposia Medica Hoechst 6: Modern Aspects of Cytogenetics: Constitutive Heterochromatin in Man*, pp. 45-74, F. K. Schattauer Verlag GmbH, Stuttgart—New York, 1973.
6. H. F. Stich and T. C. Hsu, Cytological Identification of Male and Female Somatic Cells in the Mouse, *Exp. Cell Res.*, **20**: 248-249(1960).
7. R. Matthey, L'évolution de la formule chromosomiale chez les Vertébrés, *Experientia*, **1**: 50-56; 78-86(1945).
8. A. Gropp, U. Tettenborn, and E. von Lehmann, Chromosomen Variation vom Robertson'schen Typus bei Tabakamaus, *M. poschiavinus*, und ihren Hybriden mit der Laboratoriumsmaus, *Cytogenetics*, **9**: 9-23(1970).
9. A. M. Waterbury, Clonal Variation in the Karyotype of *Peromyscus maniculatus* (Wagner) from California, Ph.D. Dissertation, University of California at Davis, *Dissertation Abstracts International*, **B**, **33**: 1326-1327(1972).
10. Paris Conference, 1971, Standardization in Human Cytogenetics, *Cytogenetics*, **11**: 317-362(1972).
11. L. Zech, E. P. Evans, C. E. Ford, and A. Gropp, Banding Patterns in Mitotic Chromosomes of Tobacco Mouse, *Exp. Cell Res.*, **70**: 263-268(1972).
12. T. H. Yosida and T. Sagai, Banding Pattern Analysis of Polymorphic Karyotypes in the Black Rat by a New Differential Staining Technique, *Chromosoma*, **37**: 387-394(1972).
13. P. A. Duffy, Chromosome Variation in *Peromyscus*. A New Mechanism, *Science*, **176**: 1333-1334(1972).
14. W. N. Bradshaw and T. C. Hsu, Chromosomes of *Peromyscus* (Rodentia, Cricetidae). III. Polymorphism in *Peromyscus maniculatus*, *Cytogenetics*, **11**: 436-451(1972).
15. S. Pathak, T. C. Hsu, and F. E. Arrighi, Chromosomes of *Peromyscus* (Rodentia: Cricetidae). IV. The Role of Heterochromatin in Karyotypic Evolution, *Cytogenetics and Cell Genetics*, **12**: 315-326(1973).
16. R. W. Clark, S. Pathak, and F. E. Arrighi, Similarities and Dissimilarities of Chromosomes and DNA in 2 Species of Deer Mice (*Peromyscus*), *J. Cell Biol.*, **59**: 57a(1973).
17. A. D. Stock and T. C. Hsu, Evolutionary Conservatism in Arrangement of Genetic Material: A Comparative Analysis of Chromosome Banding Between the Rhesus Macaque ( $2n = 42$ , 84 arms) and the African Green Monkey ( $2n = 60$ , 120 arms), *Chromosoma*, **43**: 211-224(1973).
18. S. Pathak and A. D. Stock, The X Chromosomes of Mammals: Karyological Homology as Revealed by Banding Techniques, *Genetics*, in press.
19. E. Southern, Repetitive DNA in Mammals, in *Symposia Medica Hoechst 6: Modern Aspects of Cytogenetics: Constitutive Heterochromatin in Man*, pp. 19-27, F. K. Schattauer Verlag GmbH, Stuttgart—New York, 1973.
20. A. P. Craig-Holmes, F. B. Moore, and M. W. Shaw, Polymorphism of Human C-Band Heterochromatin. I. Frequency of Variants, *Amer. J. Hum. Genet.*, **25**: 181-192(1973).



# ON CHROMOSOME ORGANIZATION

T. C. HSU

Department of Biology, M. D. Anderson Hospital and Tumor Institute,  
The University of Texas, Houston, Texas

---

## ABSTRACT

Research areas related to chromosome organization which require continued active inquiry are chemical structures, macromolecular interrelationships, definition of the basic unit of chromosome organization, strandedness, and distribution of DNA and protein families along the chromosome. New advances in chromosome banding, in situ hybridization, and premature chromosome condensation promise to sustain accumulation of new knowledge at an accelerated rate.

Biologists have been studying various aspects of chromosomes for nearly a century, but, so far as the organization of chromosomes is concerned, our knowledge is still relatively meager. One of the reasons for this poor progress in our understanding of chromosome organization is that biology relies heavily on the progress in biological chemistry. In the area of chromosome studies, elucidation of the chemistry of nucleoproteins is one of the determining factors. However, if we reexamine the history of cytology prior to the proposal of the DNA model, we can easily tell that the past 20 years has been a period of remarkable recrudescence.

Probably the subject of chromosome organization can be divided into a number of interrelated areas, all of which require active exploration:

1. The chemical structures of the macromolecular species that are constituents of the chromosomes. Advances in nucleic acid research and nucleoprotein research have considerably improved our understanding of the kinds and the chemical structures of the macromolecules that are the principal components of the chromosomes. A great deal more research, however, is needed in the chemistry of these, particularly in the chemistry of nonhistone proteins.

2. The interrelationships among the chromosomal macromolecules. Chromosomes are not simply the compact, highly basophilically stained objects observed in mitotic divisions. In interphase and in meiosis, they display entirely different appearances, hence different organizations. Elucidation of chromosome organization in terms of macromolecular (nucleic acids and proteins) relations (their stereochemistry, the role of divalent ions, etc.) must explain all the morphological changes as well as their physiological implications. How the complexes are formed and how they are dissociated remain enigmatic in physical and chemical terms.

3. The basic unit. Electron microscopists have spent a considerable amount of time measuring the width of the various nucleoprotein fibers seen in isolated mitotic chromosomes and in interphase nuclei. Unfortunately, convincing chemical data in conjunction with fine structure observations are still wanting, and how the basic units fold and unfold is still a highly debatable subject.

4. The strandedness. This is an age-old problem: does a mitotic chromatid contain one or more than one basic unit, i.e., strand? Recently the unineme hypothesis appears to receive more experimental support than the multineme hypothesis. Each chromatid, therefore, appears to contain a single DNA double helix.

5. The distribution of DNA and protein families along the chromosome. Advances in modern biology rely both on concepts and on methodology. In fact, methodological and technological inventions and improvements sometimes revolutionize established concepts. On the other hand, new concepts may also stimulate the development of new methodology. In the investigation of the distribution of DNA and protein families along the chromosomes, many significant advances have been made during recent years, probably more than those made during all the past decades added together. If I must single out some most important landmarks, I believe the following three are among the significant discoveries in the history of chromosome cytology:

a. The discovery that metaphase chromosomes are longitudinally differentiated into bright and dark fluorescent zones or bands when cytological preparations stained with a fluorochrome, quinacrine, are viewed with ultraviolet optics. This discovery by the group of investigators under the leadership of T. Caspersson in Stockholm led not only to the practical application that facilitates the recognition of individual chromosomes for cytogenetic analyses of man, mouse, and other species but also to the modification of the concept that the basic chromosomal fibers are randomly folded along a chromatid. In other words, if the basic fiber is indeed folded back and forth along a chromatid, there should be a strict pattern of folding with segments containing similar base composition arranged side by side along the chromatid axis. For example, highly A-T rich segments should line up in parallel with abrupt beginnings and abrupt endings to form a sharp Giemsa or quinacrine-positive band.

Although the fluorescent banding (Q-band) technique lost some of its appeal after the invention of the simpler Giemsa-banding technique, which essentially

tells the same story with practically no more effort than the conventional staining procedure and which requires only an ordinary microscope, the original discovery should still be considered a major contribution.

b. The discovery of the *in situ* nucleic acid hybridization procedure. The group of investigators in the laboratory of J. G. Gall at Yale University invented a procedure for hybridizing labeled nucleic acid molecules with DNA of the chromosomes and nuclei. This discovery led to a flurry of activities testing the locations of various DNA species of various organisms, especially the locations of repeated sequences. A positive correlation was established from these studies, i.e., highly repeated DNA sequences are primarily located in the heterochromatic regions of the chromosomes. As a by-product of this series of investigations, a simple method was developed to reveal constitutive heterochromatin in metaphase chromosomes. It has been found that, although most constitutive heterochromatin pieces are situated in the vicinity of the centromeres, other patterns of distribution are not uncommon. This phenomenon emphatically denies the random-folding concept of chromosomal fibers. This is especially evident with interstitial bands of constitutive heterochromatin because the fibers must be arranged in such a pattern that the highly repeated sequences parallel one another across the width of a chromatid.

The now-famous Giemsa banding (G-band) techniques are derivatives of the original heterochromatin procedure. The deeply stained G-bands correspond, almost band by band, to the brightly fluorescent quinacrine bands. Available data indicate that it is very likely the Giemsa-positive and the quinacrine-positive bands are A-T rich, and the negative areas, G-C rich. It is still debatable, however, whether or not the A-T rich regions, like the constitutive heterochromatin, also lack genetic information. Some investigators think so. I would like to point out that repetitive DNA sequences are not always A-T rich. In many organisms, satellite DNA fractions are G-C rich. They form typical heterochromatin, but they are G and Q negative. It is therefore unsafe to draw conclusions from one staining reaction. At any rate, one thing is clear: the distribution of DNA families along the chromosomes is clustered. Similarly, there is preliminary evidence to show that the distribution of histone families also is not random.

c. The discovery of premature condensed chromosomes. The phenomenon of cell fusion has been used as a tool for studying a variety of research problems in biomedicine. Most of these studies employ chromosome analysis for verifications or as cytogenetic markers. However, the discovery of premature condensed chromosomes (PCC) made by R. T. Johnson and P. N. Rao has great significance directly relating to research on chromosomes. This discovery represents the first time a biologist could see interphase chromosomes in the form of chromosomes. Furthermore, one can differentiate the  $G_1$ , S, and  $G_2$  chromosomes by their morphology. The PCC offers many exciting possibilities for studying chromosome structure and chromosome physiology. The applica-

tion of banding techniques to PCC further enhances the usefulness of this procedure.

Sometimes new techniques can stimulate a surge of research activities for a period of time, but the field will become somewhat stagnant again because of exhaustive applications of these techniques with the lack of newer approaches. Human cytogenetics, for example, followed this pattern between 1959 and 1969 until the fluorescence staining technique on plant chromosomes was discovered. Hopefully this trend does not apply to the area being discussed here. Our technological repertoire of molecular biology and biochemistry should be sufficient to promote further research at an exponential rate, provided research funds are available, for an eventual construction of a plausible chromosome model that may be as important, in the chronicle of biological sciences, as the DNA model proposed 20 years ago.



# CHROMOSOME G-BANDING AND DNA CONSTANCY IN ANEUPLOID\* CELL POPULATIONS

LARRY L. DEAVEN, PHYLLIS C. SANDERS, JULIE L. GRILLY,  
PAUL M. KRAEMER, and DONALD F. PETERSEN  
Cellular and Molecular Radiobiology Group, Los Alamos Scientific Laboratory,  
Los Alamos, New Mexico

---

## ABSTRACT

The evolution of chromosomal aberrations for in vitro cell populations is a poorly understood phenomenon. Recent studies in our laboratory using improved flow microfluorometry techniques seriously challenge the stem-line concept. These observations indicate that, although the DNA content of heteroploid cells is greater than that of diploid parent cells, there is little, if any, increase in variability of cell-to-cell DNA content and that the traditional mechanisms used to explain infrastem-line variability of chromosome number are inadequate. Chromosome banding analysis of several HeLa populations supports these conclusions. Banding studies indicate that the variations in chromosome number per cell are restricted to the small classes of chromosomes and that these variations are compensatory with respect to total cellular content of chromatin. Other trends revealed by the banding patterns are that all these lines maintain at least one haploid set of unaltered chromosomes and that some of the rearranged chromosomes are also altered from the normal sequence of chromosomal DNA synthesis.

Much of our current understanding of the chromosome constitutions of aneuploid cell populations comes from data accumulated a number of years ago. In 1914 Theodor Boveri found that abnormal distributions of chromosomes were associated with errors in embryonic development.<sup>1</sup> This, as well as other studies, led him to suggest that chromosome changes might be the primary cause of cancer. There are other scattered reports in the early literature on

---

\*In this manuscript, the term aneuploid is used to define cells which contain chromosomes that are abnormal in either number or structure. In this context heteroploidy is a type of aneuploidy but emphasizes the variability of chromosome number and structure within a given cell population.

chromosomes of cancer tissues,<sup>2-4</sup> some supporting the Boveri hypothesis,<sup>5</sup> but it was not until the 1950s that any real advances were made in this area. At that time ascites tumor systems were developed,<sup>6</sup> methods for chromosome preparation were improved,<sup>7</sup> and a number of in vitro cell lines were established.<sup>8-10</sup> Analysis of the in vitro cell populations led to some unexpected results. Cancer cytologists had known for some time that tumor cells contained abnormal numbers of chromosomes; however, many investigators were surprised to find extensive aneuploidy in cultured cells previously derived from normal tissues.<sup>11</sup> These changes in karyotype during in vitro cellular evolution have been extensively documented and confirmed and are believed to be similar, if not identical, to the chromosome rearrangements in tumor cells.<sup>12</sup>

Unfortunately, some of the data published during the 1950s have now been shown to be erroneous, whereas other data must be viewed with at least some skepticism. This is not surprising when one considers that much of this literature is concerned with changes in chromosome number and structure and that it was not until the middle of this period (1956) that the correct euploid number for man was established.<sup>13</sup> Nevertheless, a central dogma emerged which attempts to draw together the many observations published at that time. This so-called stem-line theory was originally derived from studies of chromosome patterns in ascites tumors<sup>14</sup> but later was extended by Hsu to include evolved in vitro cell populations.<sup>12</sup> This concept originally defined the stem cells as that portion of the total population having a specific karyotype and being the principal progenitors of tumor growth. Other cells containing different karyotypes were considered to be the products of aberrant mitotic events, to be generally incapable of continued proliferation, and hence to be transient components of the tumor-cell population. Later studies demonstrated that this view was an oversimplification. For example, improved cytogenetic analyses showed that karyotype deviations occurred within what were considered to be stem-line cells,<sup>15</sup> and microspectrophotometric studies suggested that tumors may have multiple stem-lines or no distinct stem-lines. Therefore more-recent discussions have recognized that tumors and in vitro cell lines are in a state of flux with changing forms and modes and that stem-line constancy is not absolute.<sup>12,16</sup>

Microspectrophotometric measurements of cellular DNA content in tumors and of cultured aneuploid lines are also uninterpretable in many cases.<sup>17-19</sup> In some studies cell-cycle progression was not taken into consideration, and in others staining artifacts due to differential chromosome condensation may account for the discrepancies; however, in general, the emerging picture from these data is that chromosomally aneuploid cells contain "aneuploid amounts of DNA." One of the most extensive series of studies of this type is from Atkin's<sup>20</sup> laboratory. Atkin pooled Feulgen-DNA values from several tumors (approximately 1500 cells in the G<sub>1</sub> mode) and compared the resulting coefficient of variation (CV) with analogous distributions for nonmalignant cells (sample sizes, 116, 302, and 839 cells). The CV obtained for aneuploid cells was about 10% but that for normal cells ranged from 6.2 to 8.2%.

## FLOW MICROFLUOROMETRIC MEASUREMENTS

Recent developments in flow microfluorometry (FMF) permit very rapid measurements of large numbers of cells (typical sample size,  $10^5$  cells) with a two- to three-fold improvement in CV as compared with the microspectrophotometric technique. Using this new technology, Kraemer et al.<sup>21,22</sup> were surprised to find that, although the DNA content was increased to approximately 3C, the variability of cellular DNA content in classical heteroploid lines was no greater than in euploid strains from which they were derived. Of particular interest to the study of chromosome changes in evolved cell populations were two experiments involving manipulation of chromosome number and measurements of cellular DNA content in these altered populations. The first of these experiments concerned measurements of the DNA content per cell of Chinese hamster (line CHO) cell populations after treatment with low doses of Colcemid to induce chromosomal nondisjunction.<sup>23</sup> The results (Fig. 1) showed that, when DNA dispersion occurred, FMF distributions clearly indicated it. The alternate experiment involved clonal selection from HeLa cell populations. It had been shown previously that, when wild type HeLa populations were cloned, some of the clones retained tight chromosome number distributions for varying periods of time.<sup>24</sup> When clones from a HeLa stock were examined, one clone was found to contain cells with either 66 or 68 chromosomes, but the parent line had a modal chromosome number of 71 with a perimodal dispersion of about 10 chromosomes. FMF distributions of the parent line and the clone are shown in Fig. 2. Coefficients of variation of the "wild" and cloned cells were 3.52 and 3.75%, respectively, and the DNA contents were identical. This comparison clearly demonstrates that cellular DNA can be constant despite chromosome number variability. Furthermore, taken together, these two experiments strongly suggest that chromosome variability in aneuploid-heteroploid cells cannot always be explained by, or attributed to, mitotic nondisjunction.

Because the FMF data cannot be explained by preexisting concepts, Kraemer et al.<sup>22</sup> have presented an alternative model to explain the loss of karyotype control in heteroploid cell lines. Briefly, this notion suggests that chromosomes normally may not always exist as separate entities, that during some portion of interphase much of the DNA is continuous, and that heteroploidy represents the aberrant packaging of chromosomes which then appears at metaphase as rearrangements. A test of this model in its simplest form could come from analysis of aneuploid lines by Giemsa banding techniques. In this construction it would be predicted that the bulk of the cells should contain one sequence of bands which is broken up in different ways.

## GIEMSA BANDING ANALYSIS

The first G-band analysis of an aneuploid cell line was reported by Deaven and Petersen.<sup>25</sup> They found that, although numerous rearrangements occurred

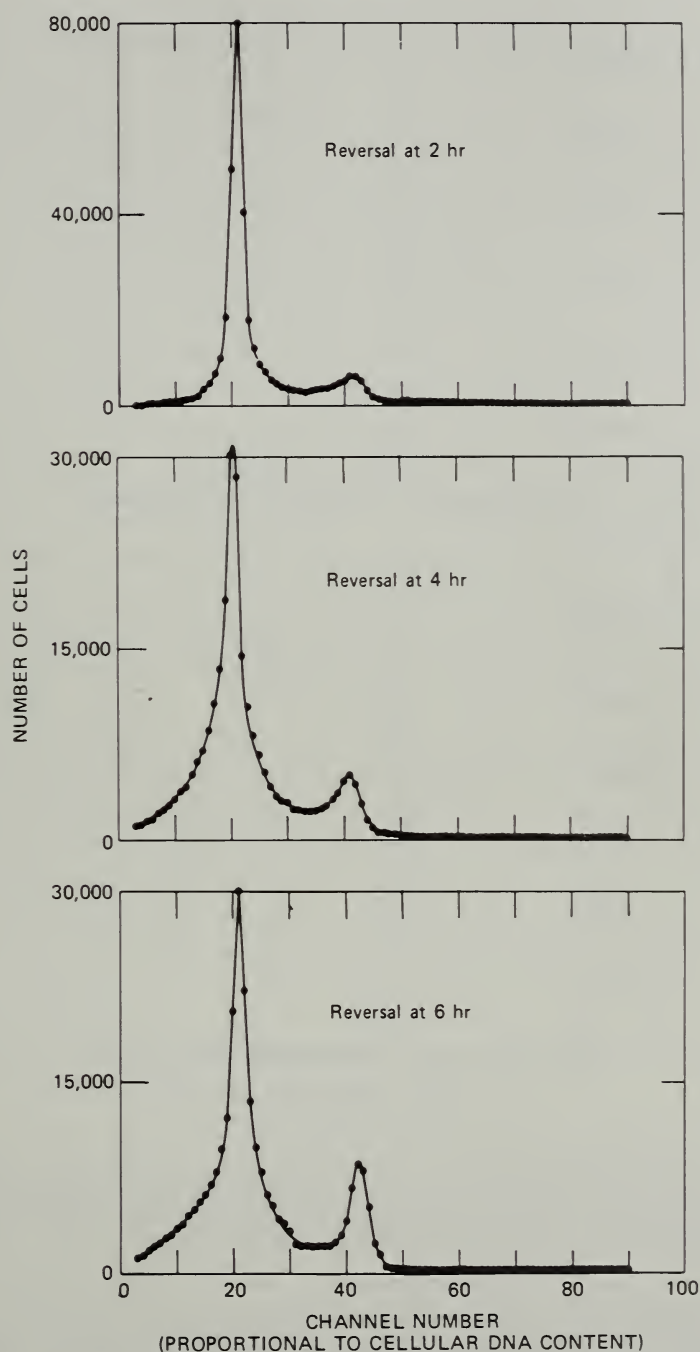
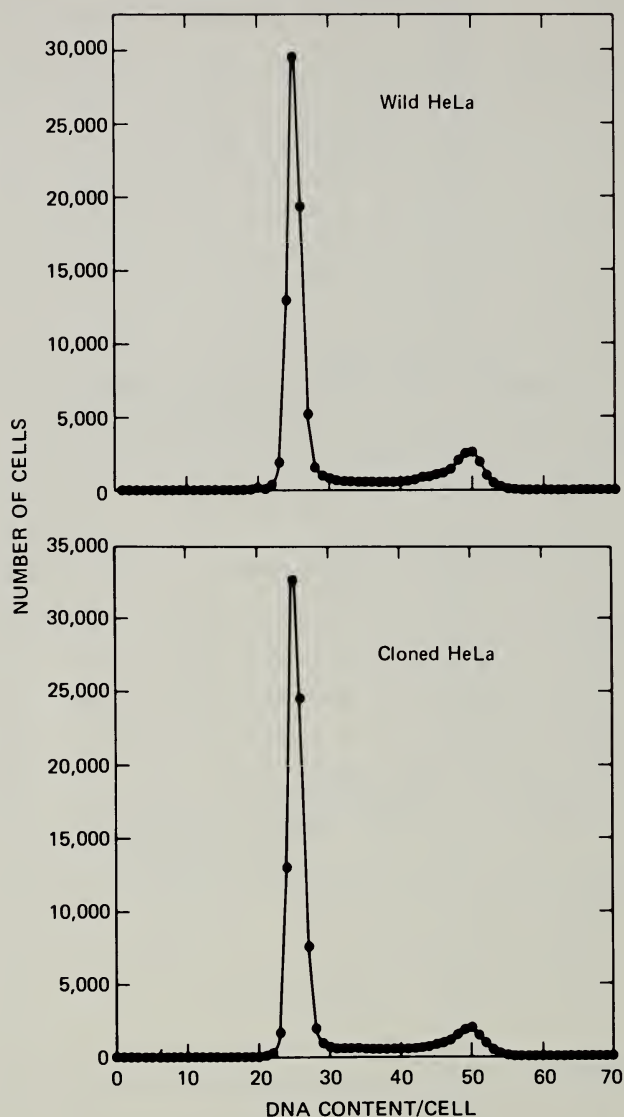


Fig. 1 Progressive Colcemid-induced nondisjunction in Chinese hamster cells (line CHO). Mitotic cells were collected from the same monolayers at 2, 4, and 6 hr after addition of Colcemid, reversed in fresh medium for 4 hr, collected, and stained with the acriflavine-Feulgen technique.





**Fig. 2** Flow microfluorometric DNA distributions of a "wild" type and a cloned population of HeLa cells. The coefficient of variation of the G<sub>1</sub> peak for the wild type is 3.52% and for the clone is 3.75%.

in Chinese hamster (line CHO) cells, essentially all euploid chromatin was present in each cell. This observation is in good agreement with the FMF comparisons of CHO with euploid Chinese hamster cells (4% less DNA in CHO) and with the 3% decrement reported earlier on the basis of chromosome arm-length measurements.<sup>26</sup> In addition, they found that one haploid set of chromosomes remained largely intact. This observation was interesting from a genetic viewpoint because mutagenetic studies also suggested that line CHO was

monosomic for some elements.<sup>26</sup> Although line CHO showed little perimodal dispersion, when it has been observed it has always involved the smallest chromosomes.

FMF measurements of eight HeLa cell lines collected from different laboratories showed that variations in DNA content existed between the independently passaged lines. The distributions shown in Fig. 3 are from two HeLa lines designated HeLa 4 and HeLa 229. They are genetic variants selected for different sensitivities to human enterovirus infection. The DNA distributions in Fig. 3 demonstrate that, although neither of the lines had an elevated dispersion of cellular DNA, line 229 had about 33% more DNA per cell than line 4. Another HeLa line, S-3 (not pictured), contained the same amount of DNA as HeLa 4. Chromosome counts for lines S-3, 4, and 229 were in agreement with the FMF data in that S-3 had a modal number of 66, the mode for 4 was 65, and 229 was higher with a mode of 83 (Fig. 4). All lines showed a dispersion of chromosome numbers around the mode. Mitotic cells were selected from these lines for G-banding with the cold trypsin technique.<sup>27</sup>

As previously reported,<sup>28</sup> the HeLa S-3 chromosomes could be divided conveniently into three groups: (1) normal unaltered chromosomes; (2) altered chromosomes common to many cells in the population; and (3) altered chromosomes unique to one or perhaps a small minority of cells in a population.<sup>5</sup> At least one haploid set of normal human chromosomes remained intact in all cells analyzed. There were suggestions that these HeLa cells were basically triploid; the DNA content was about 1.5 times the human diploid value, and among the larger chromosomes triploid complements could be found. For example, the fifth and sixth abnormal chromosomes in Fig. 5 were subtelocentrics composed of short arms of normal number 1 chromosomes. These two plus the single unaltered number 1 provided a triploid complement for the number 1 short arm DNA. There were other examples of triploidy including chromosomes 7 and 15; however, because there were many small abnormal chromosomes involving what appeared to be complex band rearrangements, a complete analysis was not readily possible.

Figure 6 shows that, although HeLa 4 had the same amount of DNA as S-3 and a similar chromosome number distribution, the actual karyotypes were quite different. Whereas HeLa S-3 cells contained about 40% abnormal chromosomes, there were only about 24% in HeLa 4. The increase in normal chromosomes resulted in many of the individual numbers having triploid groups.

The karyotypes of line 229 (Figs. 7 and 8), which contained 33% more DNA than either S-3 or 4, were similar to the 4 karyotype. Both these lines contained approximately the same ratio of normal-to-abnormal chromosomes; some of the abnormalities were common to both lines, and the major difference was an increase in numbers of copies of preexisting chromosomes in line 229. When a 229 cell containing 76 chromosomes (Fig. 7) was compared to a 229 cell containing 80 chromosomes (Fig. 8), the differences again usually involved variable numbers of

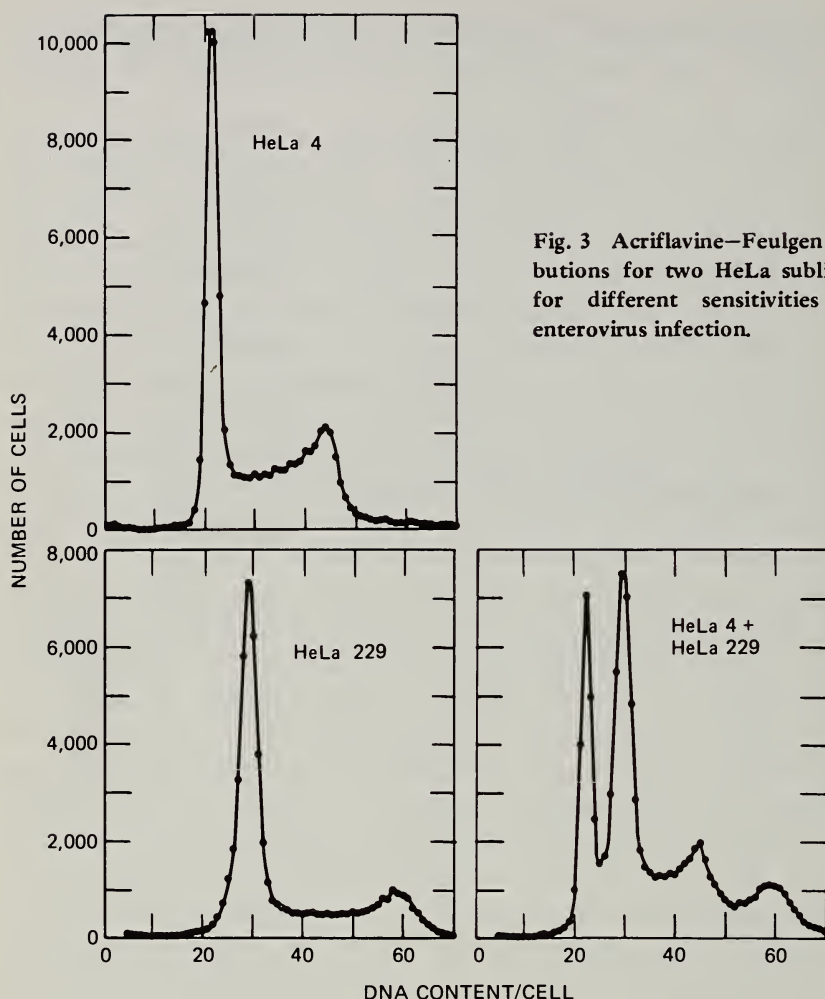


Fig. 3 Acriflavine-Feulgen DNA distributions for two HeLa sublines selected for different sensitivities to human enterovirus infection.

copies within a given group. There was also an indication that these changes were compensatory and that they primarily involved the small chromosomes. For example, the cell in Fig. 7 was a triploid for all C group chromosomes, whereas the cell in Fig. 8 had only two copies of chromosomes 7 and 8. However, the cell in Fig. 8 had four copies of number 9 and one extra copy of numbers 14 and 17. There were additional changes, but they can be summarized by using arm-length measurements rather than discussed individually.

In the human genome total chromosome arm length was found to be approximately proportional to DNA content.<sup>29</sup> Large chromosomes actually contained a little more DNA than expected, and small chromosomes contained a little less than expected on the basis of length;<sup>29</sup> however, the correlation was close enough to provide some independent measure of cell-to-cell variability within and between the HeLa lines. Each normal chromosome and each

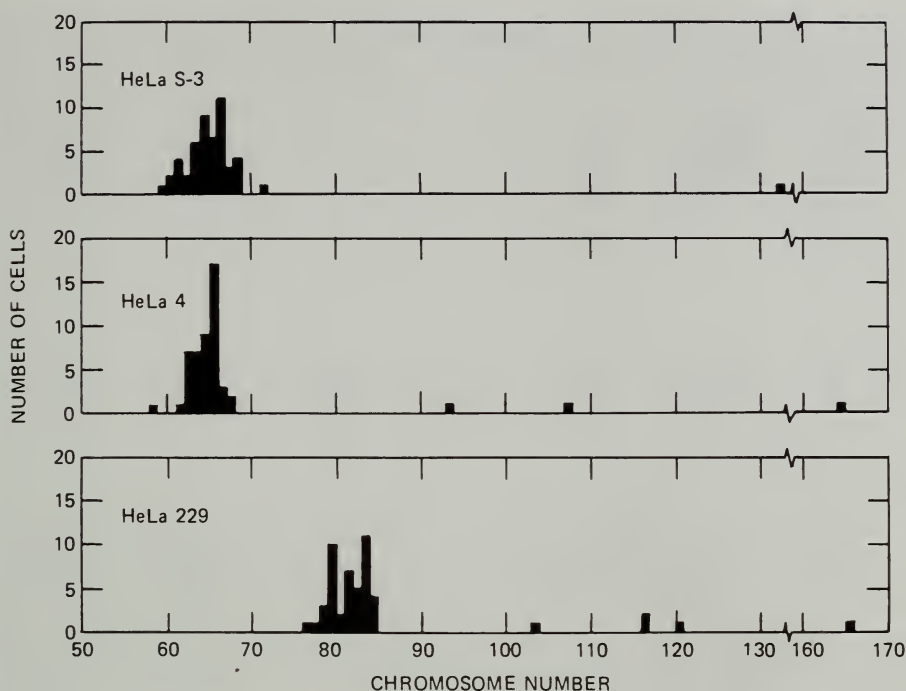


Fig. 4 Chromosome number histograms for two HeLa (S-3 and 4) lines with similar amounts of DNA and for one (229) containing approximately 33% more DNA than the other two.

identifiable portion of the altered chromosomes were assigned a length value from pooled measurements.<sup>30</sup> When an abnormal chromosome could not be positively identified, it was assigned to its appropriate Denver position on the basis of length alone and given that arm length regardless of its banding pattern. When cells from the three HeLa lines were compared on this basis, the difference between lines S-3 and 229 was about 28%, and the difference between 229 and 4 was 32%. This is in good agreement with FMF data that indicated a difference of 33%. When cells within a given line were analyzed (8 from S-3, 7 from 229, and 11 from 4), cell-to-cell dispersion varied from less than 1% to 4.8%. Although these data are limited and preliminary, they do agree with all FMF data collected to date which indicate that both diploid and heteroploid populations vary at most from 3.5 to 6.0%.

One reason why the arm-length measurements showed little variability can be seen by examining the classification data from five S-3 cells in Table 1 and by comparing the chromosomes in Fig. 7 with those in Fig. 8. The cell-to-cell differences in chromosome number primarily involved the small chromosomes (groups D, E, F, and G), occasionally group C, but never the A and B groups. When a group C chromosome was missing, it was replaced by two or more smaller chromosomes that appeared to compensate in size and therefore DNA



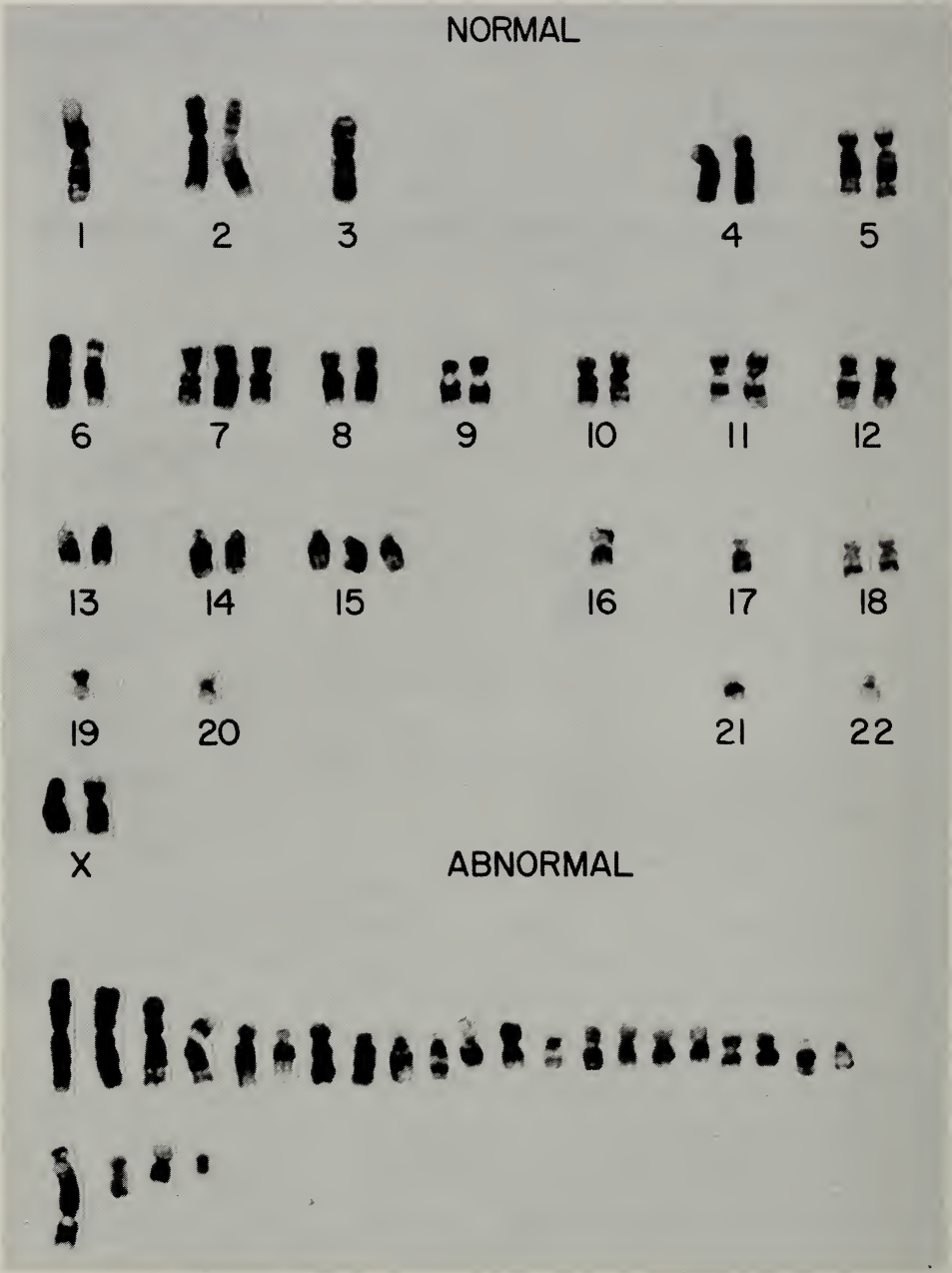


Fig. 5 Giemsa bands induced by the cold trypsin method of a HeLa S-3 cell. Chromosome number, 65.

content for the missing element. A similar observation has been reported previously,<sup>31</sup> but these findings are in marked contrast with those by Minkler, Gofman, and Tandy.<sup>32</sup>

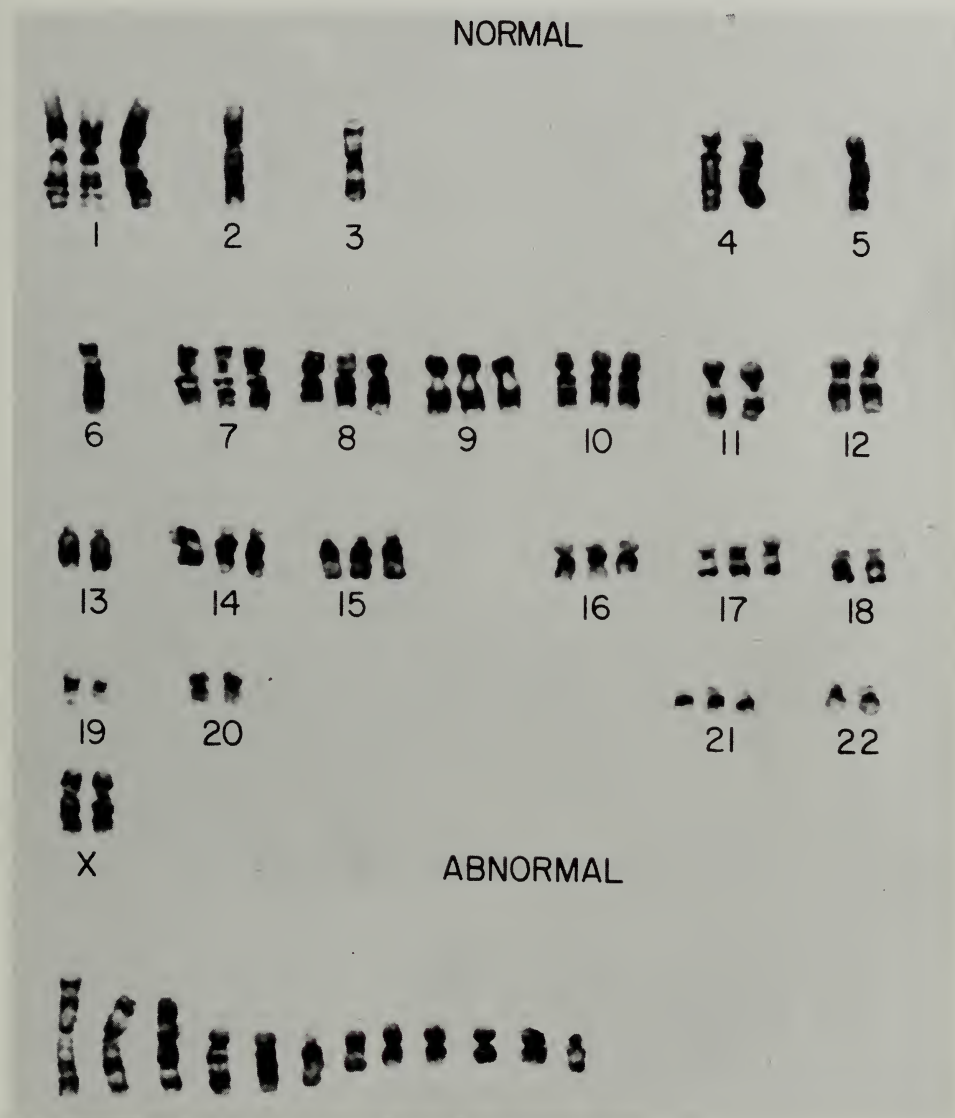


Fig. 6 Cold trypsin-induced Giemsa bands of a HeLa 4 cell. Chromosome number, 64.

Finally, when perimodal cells were compared with those in the mode with respect to specific chromosome content, there were few, if any, systematic differences between them. That is, two modal cells each containing 65 chromosomes can have as many differences between them as are found between a cell with 60 chromosomes and one with 65 chromosomes. These observations all suggest that an infrastem-line is a population of cells interrelated with one another with respect to DNA content but without regard to specific content of chromosomes.

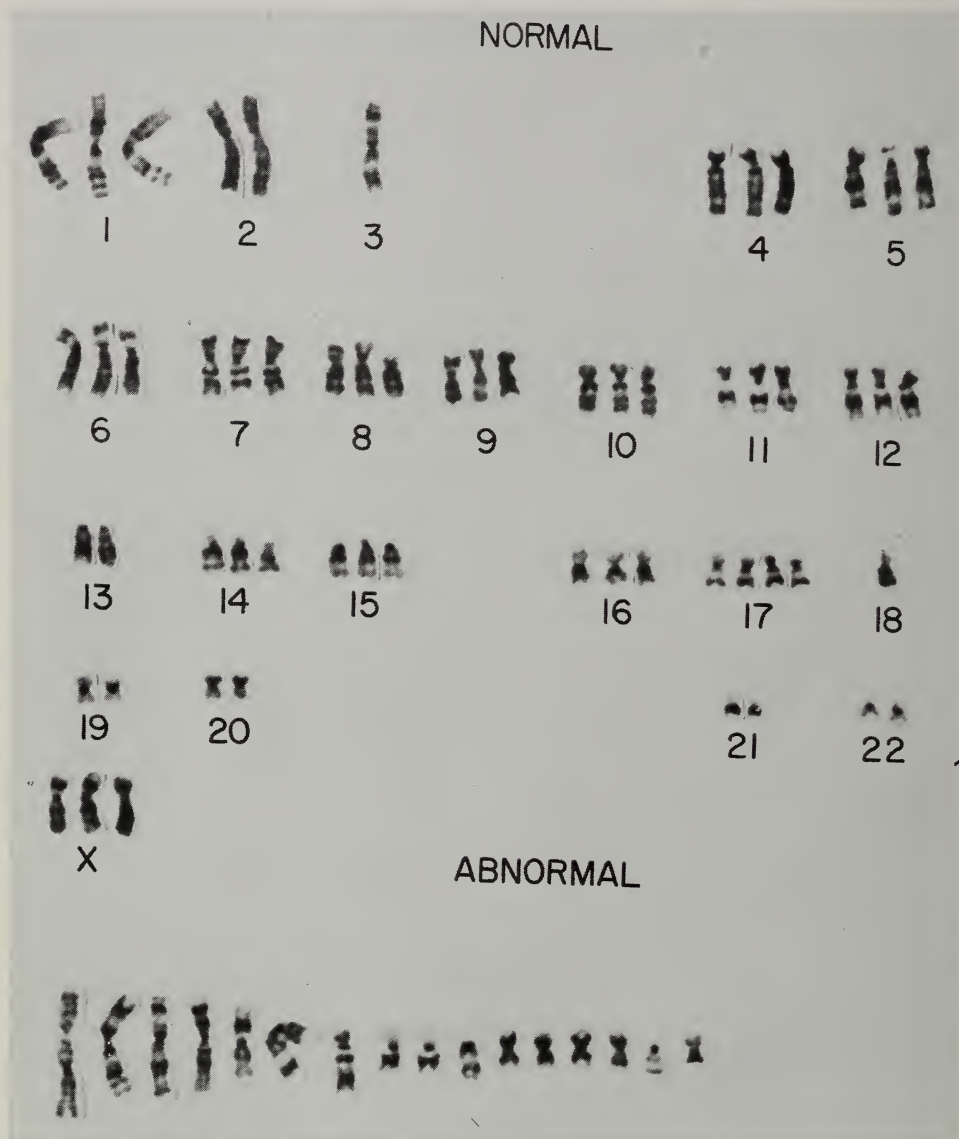


Fig. 7 Cold trypsin-induced Giemsa bands of a HeLa 229 cell. Chromosome number, 76.

Current evidence suggests that chromosome banding analysis will demonstrate even more karyotypic diversity in heteroploid cell populations than was heretofore suspected. What are the relationships between chromosomal variability and genetic variability? The most frequent interpretation given to the existence of diverse karyotypes within an evolving cell population is that of selective adaptation.<sup>12,33</sup> In this context the various karyotypes represent individual genotypes with respect to physiological and/or metabolic optima for a

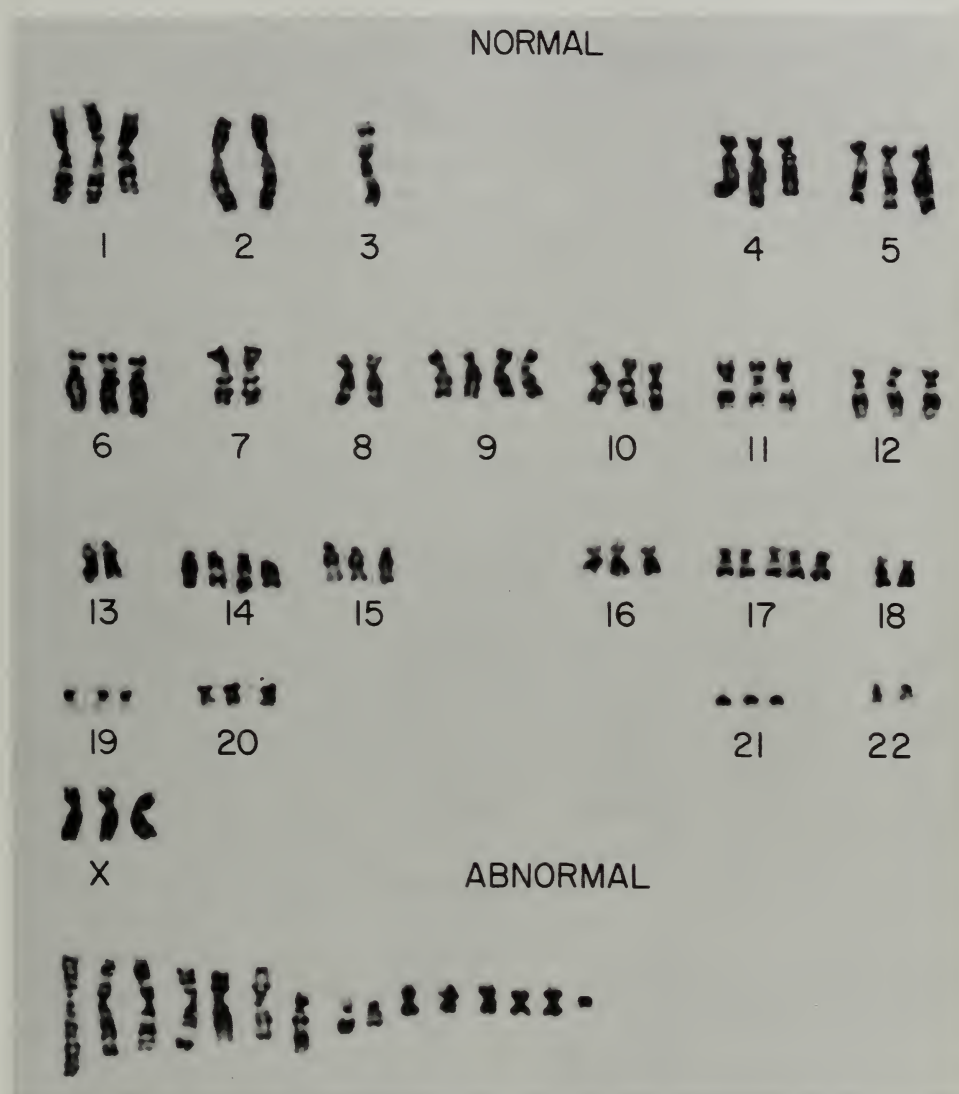


Fig. 8 Cold trypsin-induced Giemsa bands of a HeLa 229 cell. Chromosome number, 80.

given environment. Although some studies suggest that such a correlation exists, at least in a general way,<sup>34,35</sup> the assignment of specific metabolic phenotypes to specific karyotypes has been notoriously difficult.<sup>36,37</sup> In contrast to this view are the observations of Chu and Giles,<sup>24</sup> which indicate that various subclones of HeLa cells vary from one another in karyotype stability under seemingly constant environmental conditions.

Studies of other parameters (e.g., cloning efficiency, dose-survival curves, variability in generation time, and spontaneous mutation rate) suggest that



TABLE 1  
CLASSIFICATION OF THE CHROMOSOMES OF  
FIVE HeLa S-3 CELLS

Normal chromo- some	Cell number					Marker chromo- some	Cell number				
	1	2	3	4	5		1	2	3	4	5
1	1	1	1	1	1	A	1	1	1	1	1
2	11	11	11	11	11	B	1	1	1	1	1
3	1	1	1	1	1	C	1	1	1	1	0
4	11	11	11	11	11	D	1	1	1	1	1
5	11	11	11	11	11	E	1	1	1	1	1
6	11	11	11	11	11	F	1	1	1	1	1
7	111	111	111	111	111	G	1	1	1	1	1
8	11	111	11	111	11	H	1	1	1	1	1
9	111	111	11	111	11	I	11	11	11	1	11
10	1	1	1	1	1	J	1	1	1	1	1
11	11	11	11	11	11	K	1	1	11	1	1
12	11	1	11	11	11	L	1	1	1	1	1
13	11	11	11	11	11	M	1	0	0	0	0
14	11	11	11	11	11	N	11	11	1	11	11
15	111	111	111	111	111	O	0	11	1	1	1
16	11	11	111	111	1	P	1	1	1	1	1
17	1	1	1	1	1	Q	11	0	1	1	11
18	111	11	111	11	111	R	0	1	0	1	1
19	1	1	1	1	1	S	1	1	1	1	1
20	1	1	1	1	1	T	0	1	1	1	1
21	111	111	111	111	1	Unclassi- fied chromo- some	0	111	111	1	111
22	1	1	1	0	1						
X	11	11	11	11	11						
Normal						44	44	40			
Marker						<u>20</u>	<u>24</u>	<u>23</u>	<u>21</u>	<u>24</u>	
Total						64	67	67	65	64	

genetic variability in heteroploid populations is no greater than in the diploid populations from which they were derived (see Kraemer et al. for a more complete discussion<sup>22</sup>). These observations, as well as those of Chu and Giles,<sup>24</sup> suggest that karyotypic variability in itself may be a phenotypic expression controlled in diploid cells but uncontrolled in the heteroploid state.

In CHO cells autoradiographic studies have shown that the normal sequence of chromosomal DNA synthesis is altered. Some of the chromosomal sites that replicate late in euploid cells replicate earlier in CHO, and several late-replicating

chromosomes in CHO cells replicate in early or middle S phase in euploid material. In HeLa cells there are two, and sometimes three, X chromosomes. None of these are late replicating, nor do they replicate simultaneously.<sup>38</sup> Do these changes in time of replication have any relationship with genetic expression? An answer to this question is now possible through the use of known genetic markers on human X chromosomes, and such information may serve to elucidate the paradox of genetic stability in the face of karyotypic diversity.

## DISCUSSION

The literature on chromosomes of evolved cell populations is lengthy and sometimes difficult to understand. We have attempted to summarize the major concepts that have developed as a result of this work, but the reader is referred to reviews of the various subtopics which could be only briefly mentioned in this paper (Refs. 12, 22, 33, 37, 39, and 40). The ambiguity of these data amply demonstrates that, although much has been learned about this subject, the problem is a difficult one and that new approaches will be necessary to achieve a final solution. New developments in FMF and chromosome banding have only begun to be utilized to this end, yet the data obtained have already changed our views of heteroploidy. The FMF determinations amply demonstrate that these cell populations are much more uniform with respect to cellular DNA content than was heretofore suspected. The available chromosome banding data suggest that all populations maintain at least one haploid set of unaltered chromosomes, that cell-to-cell chromosome variability is restricted to the smaller groups of chromosomes, and that chromosome additions or deletions are compensatory with respect to total cellular chromatin. When banding analysis is combined with autoradiography, an altered sequence of chromosomal DNA synthesis is revealed.

Although banding methods allow a much greater resolution of chromosome rearrangements than previous techniques, a word of caution about the interpretation of these data is appropriate. It is fairly easy to band and arrange homologs in euploid cells; however, when each chromosome in a cell may or may not be altered, correct classification is much more difficult. Observations of endoreduplicated chromosomes help to define the limits of banding resolution, but more objective automated scanning systems would be very helpful in solving this problem. Finally, although the exact mechanism for banding is not understood, it seems likely that the bands are somehow related to chromosome supercoiling. Reports of altered supercoiling in abnormal chromosomes have already appeared in the literature,<sup>41</sup> and this might further complicate the correct identification of chromosomes in heteroploid cells.

## ACKNOWLEDGMENT

This work was performed under the auspices of the U. S. Atomic Energy Commission.

## REFERENCES

1. T. Boveri, *Zur Frage der Entwicklung maligner Tumoren*, Gustav Fischer, Jena, 1914.
2. J. Billing, The Number of Chromosomes in the Cells of Cancerous and Other Human Cells, *J. Amer. Med. Ass.*, **88**: 396 (1927).
3. T. Kemp, Über die somatischen Mitosen bei Menschen und wurmblütigen Turen unter normalen und pathologischen Verhältnissen, *Z. Zellforsch. Mikroskop. Anat.*, **11**: 429-444 (1930).
4. M. Levine, Chromosome Number in Cancer Tissue of Man, of Rodent, of Bird, and in Crown Gall Tissue in Plants, *J. Cancer Res.*, **14**: 400-425 (1930).
5. Ö. Winge, Zytologische Untersuchungen über der Natur maligner Tumoren. II. Teerkarzinome bei Mäusen, *Z. Zellforsch. Mikroskop. Anat.*, **10**: 683-735 (1930).
6. G. Klein, Comparative Studies of Mouse Tumors with Respect to Their Capacity for Growth as "Ascites Tumor" and Their Average Nucleic Acid Content per Cell, *Exp. Cell Res.*, **2**: 518-573 (1951).
7. T. C. Hsu, Mammalian Chromosomes In Vitro. I. The Karyotype of Man, *J. Hered.*, **43**: 167-172 (1952).
8. G. O. Gey, W. D. Coffman, and M. T. Bubicek, Tissue Culture Studies of the Proliferative Capacity of Cervical and Normal Epithelium, *Cancer Res.*, **12**: 264-265 (1952).
9. S. Chang, Continuous Subcultivation of Epithelial-Like Cells from Normal Human Tissues, *Proc. Soc. Exp. Biol. Med.*, **87**: 440-443 (1954).
10. H. Eagle, Propagation in a Fluid Medium of a Human Epidermoid Carcinoma, Strain KB, *Proc. Soc. Exp. Biol. Med.*, **89**: 362-364 (1955).
11. A. Levan, Chromosome Studies on Some Human Tumors and Tissues of Normal Origin, Grown In Vivo and In Vitro at the Sloan-Kettering Institute, *Cancer*, **9**: 648-663 (1956).
12. T. C. Hsu, Chromosomal Evolution in Cell Populations, in *International Review of Cytology*, Vol. XII, Academic Press, Inc., New York, 1961.
13. J. H. Tjio and A. Levan, The Chromosome Number of Man, *Hereditas*, **42**: 1-6 (1956).
14. S. Makino, Cytological Studies on Cancer. III. The Characteristics and Individuality of Chromosomes in Tumor Cells of the Yoshida Sarcoma Which Contribute to the Growth of the Tumor, *Gann*, **43**: 17-34 (1952).
15. J. H. Tjio and A. Levan, Comparative Idiogram Analysis of the Rat and the Yoshida Rat Sarcoma, *Hereditas*, **42**: 218-234 (1956).
16. T. S. Hauschka and A. Levan, Cytologic and Functional Characterization of Single Cell Clones Isolated from the Krebs-2 and Ehrlich Ascites Tumors, *J. Nat. Cancer Inst.*, **21**: 77-135 (1958).
17. T. C. Hsu and P. S. Moorhead, Mammalian Chromosomes In Vitro. VII. Heteroploidy in Human Cell Strains, *J. Nat. Cancer Inst.*, **18**: 463-471 (1957).
18. S. Bader, A Cytochemical Study of the Stem Cell Concept in Specimens of Human Ovarian Tumor, *J. Biophys. Biochem. Cytol.*, **5**: 217-229 (1959).
19. H. F. Stich and H. E. Emson, Aneuploid Deoxyribonucleic Acid Content of Human Carcinomas, *Nature*, **184**: 290-291 (1959).
20. N. B. Atkin, Perimodal Variation of DNA Values of Normal and Malignant Cells, *Acta Cytol.*, **13**: 270-273 (1969).



21. P. M. Kraemer, D. F. Petersen, and M. A. Van Dilla, On DNA Constancy in Heteroploidy and the Stem-line Theory of Tumors, *Science*, **174**: 714-717 (1971).
22. P. M. Kraemer, L. L. Deaven, H. A. Crissman, and M. A. Van Dilla, DNA Constancy Despite Variability in Chromosome Number, in *Advances in Cell and Molecular Biology*, Vol. 2, Academic Press, Inc., New York, 1972.
23. H. Kato and T. H. Yosida, Nondisjunction of Chromosomes in a Synchronized Cell Population Initiated by Reversal of Colcemid Inhibition, *Exp. Cell Res.*, **60**: 459-464 (1970).
24. E. H. Y. Chu and N. H. Giles, Comparative Chromosomal Studies on Mammalian Cells in Culture. I. The HeLa Strain and Its Mutant Clonal Derivatives, *J. Nat. Cancer Inst.*, **20**: 383-401 (1958).
25. L. L. Deaven and D. F. Petersen, The Chromosomes of CHO, An Aneuploid Chinese Hamster Cell Line: G-Band, C-Band, and Autoradiographic Analyses, *Chromosoma*, **41**: 129-144 (1973).
26. F. Kao and T. T. Puck, Genetics of Somatic Mammalian Cells. IX. Quantitation of Mutagenesis by Physical and Chemical Agents, *J. Cell. Physiol.*, **74**: 245-257 (1969).
27. L. L. Deaven and D. F. Petersen, Measurements of Mammalian Cellular DNA and Its Localization in Chromosomes, in *Methods in Cell Biology*, Vol. 8, D. M. Prescott (Ed.), pp. 179-204, Academic Press, Inc., New York, 1974.
28. L. L. Deaven and D. F. Petersen, G-Band Analysis of Chromosomal Alterations in Aneuploid Cell Lines, in *Abstracts Presented at the Thirteenth Annual Meeting, The American Society for Cell Biology, Miami Beach, Florida, November 14-17, 1973*, p. 73a, Abstract No. 146, The Rockefeller University Press, New York, 1973.
29. B. Mayall, Lawrence Livermore Laboratory, personal communication, 1973.
30. D. Bergsma (Ed.), Chicago Conference: Standardization in Human Cytogenetics, *Nat. Found. March Dimes Birth Defects Orig. Art. Ser.*, **2**(2): 21 (1966).
31. N. B. Atkin and M. C. Baker, Chromosome Abnormalities as Primary Events in Human Malignant Disease: Evidence from Marker Chromosomes, *J. Nat. Cancer Inst.*, **36**: 539-557 (1966).
32. J. L. Minkler, J. W. Gofman, and R. K. Tandy, A Specific Common Chromosomal Pathway for the Origin of Human Malignancy. II. Evaluation of Long-Term Human Hazards of Potential Environmental Carcinogens, *Adv. Biol. Med. Phys.*, **13**: 107-151 (1970).
33. T. S. Hauschka, The Chromosomes in Ontogeny and Oncogeny, *Cancer Res.*, **21**: 957-974 (1961).
34. T. C. Hsu, Mammalian Chromosomes In Vitro. XIII. Cyclic and Directional Changes of Population Structure, *J. Nat. Cancer Inst.*, **25**: 1339-1354 (1960).
35. T. C. Hsu and D. S. Kellogg, Mammalian Chromosomes In Vitro. XII. Experimental Evolution of Cell Populations, *J. Nat. Cancer Inst.*, **24**: 1067-1093 (1960).
36. M. Vogt, A Genetic Change in a Tissue Culture Line of Neoplastic Cells, *J. Cell. Comp. Physiol.*, **52**(1): 271-286 (1958).
37. T. C. Hsu and D. S. Kellogg, Genetics of In Vitro Cells, in *Genetics and Cancer*, pp. 183-204, University of Texas Press, Austin, 1959.
38. S. Federoff, University of Saskatchewan, personal communication, 1973.
39. N. B. Atkin, Principles and Application of the Deeley Integrating Microdensitometer, in *Introduction to Quantitative Cytochemistry*, Vol. II, G. L. Wied and G. F. Bahr (Eds.), pp. 1-26, Academic Press, Inc., New York, 1970.
40. S. Makino, The Chromosome Cytology of the Ascites Tumors of Rats, with Special Reference to the Concept of the Stemline Cell, *Int. Rev. Cytol.*, **6**: 25-84 (1957).
41. F. Lampert, Chromosome Alterations in Human Carcinogenesis, in *Advances in Cell and Molecular Biology*, Vol. 1, E. J. DuPraw (Ed.), pp. 185-212, Academic Press, Inc., New York, 1971.



# GENETIC MARKERS ASSOCIATED WITH HAMSTER CHROMOSOMES

E. H. Y. CHU, N. C. SUN,\* and C. C. CHANG†

Department of Human Genetics, University of Michigan Medical School,  
Ann Arbor, Michigan

---

## ABSTRACT

Genetic markers are prerequisite to progress in somatic cell genetics. Mutants may be derived either from an individual within a population with a demonstrable change in phenotype or by observation and selection of variants arising either spontaneously or as a result of experimental mutagenesis in cell cultures. The majority of the currently available induced mutants have been derived from established lines of Chinese hamster cells. Although this discussion is restricted to mutations in hamster cells, the problems and methodology are shared by other cultured mammalian cells. This paper explores reasons why Chinese hamster cells are particularly favorable for mutation experiments, the specific markers that have been isolated, mechanisms by which recessive mutations can be detected, and evidence that these phenotypic variants are in fact gene mutations.

One of the important prerequisites for somatic cell genetics is to obtain genetic markers. Essentially there are two ways to obtain mutant cells: either by growing cells derived from a mutant individual with a changed phenotype that is also expressed at the cellular level or by selecting variants that arise in cell cultures. Spontaneous mutations do occur, but the frequency of mutants can be greatly increased with experimental mutagenesis.<sup>1,2</sup> The techniques for induction, isolation, and characterization of mutants in mammalian cells in culture are generally applicable to all cells regardless of species origin. Historically, however, the great majority of induced mutants available to date appear to have been isolated from various established cell lines derived from the Chinese hamster. In

---

\*Present address: National Cancer Institute, Bethesda, Md.

†Postdoctoral fellow supported by National Institutes of Health Genetics Training Grant 5-T01-GM71. Present address: Department of Human Development, Michigan State University, East Lansing, Mich.

this paper discussions will be confined to these apparent mutations observed in the hamster cells. Implicit is the fact that the problems and procedures involved in mutation studies are shared by other cultured mammalian cells as well. It should be noted that diploid human fibroblasts<sup>3,4</sup> and lymphoblastoid cell lines<sup>5</sup> have been employed for mutagenesis studies. Nevertheless, technical difficulties, such as the limited life-span of human diploid fibroblast strains and the low plating efficiencies of both fibroblasts and lymphocytes, have thus far prevented a full utilization of mutant human cells for genetic analysis. As model systems mutants isolated from the hamster and other nonhuman mammalian cells could serve as experimental tools both in the development of techniques and in the elucidation of principles in somatic cell genetics. Specifically we address ourselves here to the following questions: (1) Why are Chinese hamster cells particularly favorable for mutation experiments? (2) What kinds of genetic markers have been isolated in hamster cells? (3) How can recessive mutations be detected in diploid mammalian cells? (4) Are these phenotypic variants the result of gene mutations? A more extensive but somewhat different treatment of these topics has been made in two recent reviews.<sup>6,7</sup> New evidence will be cited which lends stronger support to the genetic origin of somatic variation and indicates the possible existence of regulatory mutations in mammalian cells. Furthermore, the possibility of dominant mutations in these cells is also discussed.

## ADVANTAGES OF USING CHINESE HAMSTER CELLS FOR MUTATION STUDIES

Established cell lines from the Chinese hamster (*Cricetulus griseus*,  $2n = 22$ ) have been used in recent years for induction and analysis of gene mutations, principally in the laboratories of T. T. Puck<sup>8</sup> and L. Siminovitch (cited in Ref. 6) and in our laboratory.<sup>7,9,10</sup> These cells were chosen because of several attributes that suit them particularly well for mutagenesis experiments.

Yerganian<sup>11</sup> was primarily responsible for the introduction into the United States of the Chinese hamster as a laboratory mammal and for the establishment of long-term cell lines from this species which retain either classic diploidy or a new diploid karyotype.<sup>12,13</sup> At the time when most of the "permanent" mammalian cell lines, such as HeLa and L, which were available to investigators were usually polyploid and when homonuclear diploid human cell strains were scarce and difficult to maintain, the low chromosome number and individually identifiable chromosomes of the hamster cells offered an attractive material for cell biology, especially for experimental cytogenetics. More important, it was thought that in aneuploid hamster cells the probability for detecting recessive mutations might be greater than in polyploid cells.

A number of seemingly permanent cell lines have been established in different laboratories from various tissues of the Chinese hamster. Notable among these

are the V79 line from the lung,<sup>12,14</sup> the CHO line from the ovary,<sup>15</sup> and the Don C line also from the lung.<sup>16</sup> Most of these lines possess relatively stable karyotypes and usually have approximately the diploid number of chromosomes. CHO cells have only 4% less DNA per cell than normal Chinese hamster cells.<sup>17</sup> Giemsa-banding studies of the chromosomes in CHO cells indicate that those cells having the modal number of 21 retain practically all the chromatin material of the normal cells.<sup>18</sup>

Different hamster cell lines have been employed for a variety of investigative purposes, and considerable information has been accumulated in the literature concerning the biological properties of the hamster cells. For example, much is known about the hamster cell with respect to its karyotype, cellular structure, growth behavior, mitotic synchronization, biosynthesis of macromolecules, sensitivity to radiation and chemicals, interaction with viruses, frozen storage, etc. The cumulative information has provided an invaluable technical background on the basis of which genetic studies of the hamster cells could proceed. Among these the most important is the successful application to hamster cells of the plating technique developed earlier by Puck and associates.<sup>19</sup> Under standard culture conditions the average generation time of V79 and CHO cells is about 12 hr, and the cloning or plating efficiency of these cells approaches 100%. Compared to many other mammalian cell lines, the time required for formation of macroscopic colonies from single cells is short, e.g., 7 to 10 days. The high plating efficiency of hamster cells is essential for the isolation of rare variants and quantitative analysis of the mutational events. The development of semidefined media leads to the formulation of appropriate media for the selection of nutritional mutants. The possibility of mitotic synchronization by any of the several techniques now available permits the isolation and analysis of mutants which affects specific functions at different stages of the cell cycle. Since both V79 and CHO cells can grow in a temperature range between 32 and 41°C without appreciable change of either growth rate or plating efficiency, temperature-sensitive mutants can be isolated by appropriate selective method at different temperatures within this range. Furthermore, CHO cells grow well either in suspension or in monolayer culture; other hamster cell lines probably can also be adapted to suspension culture. As pointed out by Thompson and Baker,<sup>6</sup> suspension culture allows considerable technical flexibility, such as ease of growth monitoring, convenient cell sampling, and a more precise regulation of culture temperature in water baths. On the other hand, monolayer culture is often more suitable than suspension for certain kinds of experimental operations, such as cloning.

Finally, the hamster cells have specific advantages when used in somatic cell hybridization experiments. Either intraspecific or interspecific fusion involving the hamster cells occurs spontaneously,<sup>20</sup> but the fusion capacity can be greatly enhanced in the presence of such agents as Sendai virus. In the progeny of cell hybrids formed after fusion between hamster and human cells, the human



chromosomes are preferentially eliminated, permitting the assignment of genes to specific human chromosomes.<sup>21,22</sup>

## KINDS OF GENETIC MARKERS ISOLATED IN HAMSTER CELLS

Table 1 summarizes the kinds of mutants that have been isolated, primarily in CHO and V79 hamster cells, in different laboratories. The origin and characteristics of these mutant cell lines have been described in recent reviews<sup>6,7</sup> and will not be detailed here.

Drug-resistant markers are probably the easiest to obtain by direct selection in the presence of a cytotoxic agent. Different classes of chemicals have been used, including the analogs of purines, pyrimidines, and nucleosides, isotopically labeled metabolic precursors, folic acid antagonists, antibiotics, mitotic poisons, and membrane-active drugs. The underlying rationale is that cells resistant to an antimetabolite or to an agent either are defective in certain steps of metabolic pathways or produce abnormal proteins that fail to bind to the extrinsic selective agent. There may be, however, more than one mechanism of resistance for a specific drug. In addition, there are instances in which permeation of the drug into the cell may be impaired.<sup>23-25</sup> In certain cases selective procedures are available for both forward change to drug resistance and reverse change to drug

TABLE 1  
MUTANTS\* ISOLATED FROM VARIOUS CHINESE HAMSTER  
CELL LINES

Drug resistance		Auxotrophy		Conditional lethality	
azg <sup>S</sup> (HGPRT <sup>+</sup> )	azg <sup>r</sup> (HGPRT <sup>-</sup> )	ara-C <sup>r</sup>	gln <sup>-</sup>	gly <sup>-</sup> A,B,C,D	ts
dap <sup>S</sup> (APRT <sup>+</sup> )	dap <sup>r</sup> (APRT <sup>-</sup> )	apt <sup>r</sup>	gly <sup>-</sup>	ade <sup>-</sup> A,B	
		aman <sup>r</sup>	hyp <sup>-</sup>	ino <sup>-</sup>	
		cch <sup>r</sup>	urd <sup>-</sup>	(ade,tdr) <sup>-</sup>	
bu <sup>S</sup> (TK <sup>+</sup> )	bu <sup>r</sup> (TK <sup>-</sup> )	oua <sup>r</sup>	(gly,hyp,tdr) <sup>-</sup>	(gly,ade,tdr) <sup>-</sup>	
		vel <sup>r</sup>	gal <sup>-</sup>	(gly,adr,tdr) <sup>-</sup>	
			pro <sup>-</sup>		
			ser <sup>-</sup>		

\*Abbreviations: azg, 8-azaguanine; dap, 2,6-diaminopurine; bu, 5-bromo-deoxyuridine; ara-C, cytosine arabinoside; apt, amethopterin; aman,  $\alpha$ -amanitin; cch, colchicine; oua, ouabain; vel, vinblastine sulfate; gln, L-glutamine; gly, glycine; hyp, hypoxanthine; urd, uridine; tdr, thymidine; gal, galactose; pro, proline; ser, serine; ade, adenine; ino, inositol; adr, adenosine; ts, temperature sensitive; HGPRT, hypoxanthine-guanine phosphoribosyltransferase; APRT, adenine phosphoribosyltransferase; TK, thymidine kinase.



sensitivity (e.g., azaguanine resistance); in other cases back selection is not possible (e.g., ouabain resistance).

Auxotrophic mutations in mammalian cells are particularly useful in elucidating the nature of metabolic pathways as well as the regulation of cellular metabolism. Selecting for nutritional auxotrophs requires formulating a permissive medium and a nonpermissive medium. Unfortunately, mammalian cells, unlike microorganisms, require amino acids, vitamins, and serum, in addition to inorganic salts and sugar. Almost all auxotrophic mutants isolated to date in hamster cells are those which require one or more of the nonessential nutrients that are not needed by the wild-type parental cells. In the case of the galactose-negative mutants we isolated from V79 cells, the mutants fail to utilize exogenous galactose, fructose, glucose-1-phosphate, glucose-6-phosphate, or galactose-1-phosphate, whereas the parental V79 cells can utilize any one of these compounds instead of glucose (Sun, Chang, and Chu, unpublished data).

For cultured mammalian cells the kinds of nonessential nutrients, which are not many, pose a severe limitation for the kinds of auxotrophs that may potentially be isolated. This approach is further limited by the fact that auxotrophic mutations are usually recessive and the mammalian cells are diploid. However, use can be made of the natural auxotrophic markers present in all mammalian cells. It is perhaps possible to select for dominant "meiotrophic" mutants, i.e., those requiring fewer growth factors than the wild type, as has been done in *Pasteurella pestis*.<sup>2,6</sup>

Perhaps the most useful class of mutants are those which are conditional lethal. This class of mutants offers a convenient experimental handle, such as a shift of the incubation temperature, to discover the nature and timing of gene action. In addition, since amino acid substitution has been shown in a number of instances to cause a changed thermal stability of the mutant protein (e.g., hemoglobin, glucose-6-phosphate dehydrogenase, carbonic anhydrase, or tobacco mosaic virus protein), heritable temperature sensitivity can be taken as an indirect proof for structural gene mutation. Selective or nonselective techniques are available for the isolation of temperature-sensitive mutants in CHO and V79 cells.<sup>2,7,28</sup> Conditional lethality dependent on pH, ionic strength, etc., has not yet been described for mammalian cells, but the principles for selection should be the same as for temperature-sensitive mutants.

Besides the nonspecific temperature-sensitive mutants isolated in the hamster and other mammalian cells in culture, locus-specific temperature-sensitive mutants involving specific gene products will be particularly interesting and significant for elucidating gene expression. A recent example of this type is a temperature-sensitive mutant isolated in CHO cells which exhibited temperature-sensitive leucyl-transfer RNA synthetase activity.<sup>29</sup> Among the galactose-negative mutants we isolated in V79 cells, four appeared to be temperature sensitive. These mutants are capable of utilizing exogenous galactose at 33 but not at 37°C.

## GENE EXPRESSION IN DIPLOID CELLS

Intercistronic complementation was detected in cell hybrids formed between independently isolated mutants of different (e.g.,  $\text{gln}^- \times \text{azg}^r$ ) or similar (e.g.,  $\text{gly}_A^- \times \text{gly}_B^-$ ) function,<sup>20,30,31</sup> leading to the conclusion that nearly all the mutants in hamster cells so far examined behave like recessive characters. There are, however, two infrequent exceptions. In somatic cell hybrids, ouabain resistance appears to be codominant (R. Mankovitz and R. M. Baker, unpublished data cited in Ref. 6), and resistance to vinblastine sulfate is either dominant or codominant.<sup>32</sup>

In theory dominant mutations should be readily recognized in diploid mammalian cells under appropriate selective conditions. As mentioned earlier, meiotrophic mutations are dominant and can be screened for by deprivation of appropriate essential nutrients, one at a time, from the standard growth medium. In addition, the possibility exists that some of the regulatory gene mutations may be dominant. There is already evidence for the existence of regulatory genes in mammalian cells.<sup>33,34</sup> If regulatory mutations comparable to the lactose operon in *Escherichia coli* and numerous other loci in prokaryotes existed in mammalian cells, models for dominant mutations in mammals could be visualized.<sup>35</sup> One example is a mutant of the *i* gene of the lactose operon. In this case the lactose repressor is a tetramer composed of four identical monomers. In the presence of the  $i^-^d$  mutation, defective monomers are made which combine with normal  $i^+$  monomers and affect the entire molecule so that it will not bind to the operator. Of course, mutations at the operator or promotor loci would be dominant. Another possible mechanism for dominant mutations in mammalian cells would be those analogous to the mutations in *E. coli* affecting either adenylate cyclase or cyclic AMP (cAMP) receptor protein.<sup>36,37</sup> In either situation the cAMP-receptor protein complex will not be functioning, thus impairing both its binding to the promotor site and the initiation of normal transcription.

X-linked recessive mutations may be expressed because of the functional haploidy of this chromosome in male mammals. X-linked recessive mutations in somatic cells from female mammals can also be expressed in clones in which the X chromosome bearing the normal allele is genetically inactivated.

The expression of autosomal recessive mutations in diploid cells could be due to homozygosis as a result of mutations of both alleles of the gene. The probability for this event to occur is low, if not impossible. Similarly, the expression of autosomal recessive character could be the result of a mutation or mitotic recombination followed by segregation, changing from a preexisting heterozygous state to the homozygous recessive state. Martin and Sprague<sup>38</sup> presented evidence in human fibroblast cultures of the possible parasexual cycle ( $2n \rightarrow 4n \rightarrow 2n$ ). Autosomal recessive markers thus could be unmasked from a heterozygous parental cell.

Alternatively, Kao and Puck<sup>2</sup> suggested that successful isolation of recessive mutations in diploid cells may depend on the existence of specific monosomies (or partial monosomies). Chasin<sup>39</sup> studied marker segregation in intraspecific hybrids between different hamster cell mutants and found a lack of linkage for the wild-type alleles of at least three recessive mutations (i.e., HGPRT<sup>-</sup>, APRT<sup>-</sup>, and gly<sup>-</sup><sub>A</sub> or gly<sup>-</sup><sub>B</sub>). This result would require the existence of at least three different monosomies or deleted chromosomal regions in the CHO cells. As mentioned earlier, CHO cells possess 96% of the DNA per cell of the normal diploid hamster cells<sup>17</sup> and retain practically all the chromatin of the normal cells, as measured by Giemsa-banding analysis of chromosomes.<sup>18</sup> It is therefore difficult to reconcile these findings with the hemizygoty hypothesis to explain the expression of autosomal recessive characters in diploid cells. The hypothesis is certainly valid and has not been completely ruled out in any single instance.

## GENETIC VS. EPIGENETIC BASIS OF SOMATIC VARIATION

Mutation is generally defined as a permanent hereditary alteration in the genetic material (DNA or RNA). Short of a direct demonstration of a change in the nucleotide sequence and in the absence of sexual phenomenon in somatic cells, phenotypic variation observed in these cells could be interpreted as the result of either genetic alteration or modulation of gene expression. The latter contention has received some experimental support from Harris,<sup>40,41</sup> who observed that mutation rates to thermal tolerance or to drug resistance in Chinese hamster cells are essentially independent of the ploidy level. Furthermore, Mezger-Freed<sup>24,42,43</sup> failed to find any significant increase in spontaneous or induced mutations to 5-bromodeoxyuridine (BUdR) resistance in haploid as compared to diploid lines of frog cells. Unfortunately, there are certain methodological shortcomings in these experiments in that the nature of phenotypic variants observed is unclear. In his experiments Harris determined only the frequency of variants; in Mezger-Freed's earlier studies, only the activity of thymidine kinase in the BUdR-resistant variants and in parental cell lines was compared. It seems that independent and perhaps more rigorous studies are necessary to either verify or refute the possible existence of epigenetic control of gene expression in mammalian cells.

In a recent report Chasin<sup>44</sup> compared the frequency of mutations in CHO cells and in a tetraploid cell line derived from it. The frequency of mutations from glycine auxotrophy to glycine prototrophy was similar in the pseudodiploid and tetraploid cells, as expected for a dominant phenotype. However, forward mutation to 6-thioguanine resistance (presumably HGPRT<sup>-</sup>) was 25-fold lower in the tetraploid as compared to the diploid strain. Freed and Mezger-Freed<sup>25</sup> demonstrated that a thymidine transport (TT) reaction is a required intermediate state in the origin of thymidine kinase (TK) deficient



haploid frog cells. Thus there are two mechanisms of resistance to BUdR:  $TT^-$  and  $TK^-$ . However, whether the individual steps of increasing BUdR resistance are genetic or nongenetic remains unanswered.

Contrariwise, a large body of experimental evidence reviewed elsewhere<sup>6,7</sup> suggests a genetic basis for mammalian somatic cell variations. A number of criteria have been applied to assess the mutational origin of phenotypic variation observed in cultured mammalian cells. These criteria include: (1) random occurrence, (2) retention of stable phenotype in the absence of selection, (3) induction with mutagens, (4) mutagenic specificity, (5) conditional lethality, (6) interallelic complementation, and (7) changes in the activity and physicochemical properties of specific gene products. To be sure, some of the supporting evidence is circumstantial and indirect, and not all criteria have been met in every instance of the observed somatic variation. However, evidence is rapidly accumulating to support the view that at least some of the phenotypic variants isolated from mammalian cells in culture arose from structural gene mutation. The strongest support for this hypothesis is the evidence that these variants contain altered enzymes. Chinese hamster cell variants have been analyzed which contain (1) altered HGPRT (i.e., having immunological cross-reactivity but lacking catalytic activity),<sup>45</sup> (2) altered RNA polymerase (i.e., RNA polymerase that is  $\alpha$ -amanitin resistant),<sup>46</sup> (3) altered dihydrofolate reductase (i.e., altered response toward enzyme inhibitors),<sup>47</sup> and (4) temperature-sensitive leucyl-transfer RNA synthetase (i.e., inability to charge tRNA with leucine at an elevated temperature, 40.5°C).<sup>29</sup> Similar examples of altered proteins in mutant human lymphocytes and mutant mouse L cells have also been reported.<sup>48,49</sup>

In conclusion, mammalian cells are considerably more complex in organization than prokaryotes so that the mechanisms of gene expression probably involve some yet unknown features and far more complicated steps than those revealed in lower organisms. Since stable and heritable epigenetic changes apparently take place during development in intact complex organisms, their occurrence in cultured cells of these organisms is a distinct possibility. It is of paramount importance that such mechanisms at the cellular level are clearly demonstrated. On the other hand, there are increasing lines of evidence to strongly support the view that many, if not all, phenotypic variations observed in cultured mammalian cells are, in fact, due to mutational changes. Further, it might be emphasized that, in addition to alterations in the structural genes, there may be mutations in the regulatory genes or some other forms of novel mechanisms for gene expression in mammalian cells. The Chinese hamster cell in tissue culture has served well as an experimental model for the detection and analysis of mutations. This *in vitro* cell system should continue to be useful as an investigative tool for studies on mutation and gene action in mammals including man.



## ACKNOWLEDGMENT

This research was supported by National Science Foundation Grants GB 34302 and GB 37100.

## REFERENCES

1. E. H. Y. Chu and H. V. Mallng, Mammalian Cell Genetics. II. Chemical Induction of Specific Locus Mutations in Chinese Hamster Cells In Vitro, *Proc. Nat. Acad. Sci. U. S. A.*, **61**: 1306-1312 (1968).
2. F.-T. Kao and T. T. Puck, Genetics of Somatic Mammalian Cells. VII. Induction and Isolation of Nutritional Mutants in Chinese Hamster Cells, *Proc. Nat. Acad. Sci. U. S. A.*, **60**: 1275-1281 (1968).
3. R. DeMars and K. R. Held, The Spontaneous Azaguanine-Resistant Mutants of Diploid Human Fibroblasts, *Humangenetik*, **16**: 87-110 (1972).
4. R. J. Albertini and R. DeMars, Somatic Cell Mutation. Detection and Quantification of X-Ray-Induced Mutation in Cultured, Diploid Human Fibroblasts, *Mutat. Res.*, **18**: 199-224 (1973).
5. K. Sato, R. S. Slesinski, and J. W. Littlefield, Chemical Mutagenesis at the Phosphoribosyltransferase Locus in Cultured Human Lymphoblasts, *Proc. Nat. Acad. Sci. U. S. A.*, **69**: 1244-1248 (1972).
6. L. H. Thompson and R. M. Baker, Isolation of Mutants of Cultured Mammalian Cells, in *Methods in Cell Biology*, Vol. 6, D. M. Prescott (Ed.), pp. 209-281, Academic Press, Inc., New York, 1973.
7. E. H. Y. Chu, Induction and Analysis of Gene Mutations in Cultured Mammalian Somatic Cells, *Genetics, Suppl.*, in press.
8. T. T. Puck, *The Mammalian Cell as a Microorganism. Genetics and Biochemical Studies In Vitro*, Holden-Day, Inc., San Francisco, 1972.
9. E. H. Y. Chu, Induction and Analysis of Gene Mutations in Mammalian Cell Cultures, in *Environmental Chemical Mutagens*, A. Hollaender (Ed.), pp. 411-444, Plenum Publishing Corporation, New York, 1971.
10. E. H. Y. Chu, Mutagenesis in Mammalian Cells, in *Environment and Cancer*, pp. 198-213, The Williams & Wilkins Company, Baltimore, Md., 1972.
11. G. Yerganian, The Striped-Back or Chinese Hamster, *Cricetulus griseus*, *J. Nat. Cancer Inst.*, **20**: 705-727 (1958).
12. D. K. Ford and G. Yerganian, Observations on the Chromosomes of Chinese Hamster Cells in Tissue Culture, *J. Nat. Cancer Inst.*, **21**: 393-425 (1958).
13. D. K. Ford, R. Wakonig, and G. Yerganian, Further Observations on the Chromosomes of Chinese Hamster Cells in Tissue Culture, *J. Nat. Cancer Inst.*, **22**: 765-799 (1959).
14. C. K. Yu, Evaluation and Nature of the Near-Diploid Cells of Chinese Hamster (*Cricetulus griseus*) In Vitro, *Can. J. Genet. Cytol.*, **5**: 307-317 (1963).
15. T. T. Puck, S. J. Cieciura, and A. Robinson, Genetics of Somatic Mammalian Cells. III. Long-Term Cultivation of Euploid Cells from Human and Animal Subjects, *J. Exp. Med.*, **108**: 945-956 (1958).
16. E. Stubblefield, Mammalian Chromosomes In Vitro. XIX. Chromosomes of Don-C, a Chinese Hamster Fibroblast Strain with a Part of Autosome 1b Translocated to the Y Chromosome, *J. Nat. Cancer Inst.*, **37**: 799-817 (1966).
17. P. M. Kraemer, L. L. Deaven, H. A. Crissman, and M. A. Van Dilla, DNA Constancy Despite Variability in Chromosome Number, *Advan. Cell Mol. Biol.*, **2**: 47-108 (1972).

18. L. L. Deaven and D. F. Petersen, The Chromosomes of CHO, an Aneuploid Chinese Hamster Cell Line: G-Band, C-Band, and Autoradiographic Analyses, *Chromosoma*, **41**: 129-144 (1973).
19. T. T. Puck, P. Marcus, and S. J. Cieciura, Clonal Growth of Mammalian Cells *In Vitro*. Growth Characteristics of Colonies from Single HeLa Cells With and Without a "Feeder" Layer, *J. Exp. Med.*, **103**: 273-284 (1956).
20. E. H. Y. Chu, P. Brimer, K. B. Jacobson, and E. V. Merriam, Mammalian Cell Genetics. I. Selection and Characterization of Mutations Auxotrophic for L-Glutamine or Resistant to 8-Azaguanine in Chinese Hamster Cells *In Vitro*, *Genetics*, **62**: 359-377 (1969).
21. F.-T. Kao and T. T. Puck, Genetics of Somatic Mammalian Cells: Linkage Studies with Human-Chinese Hamster Cell Hybrids, *Nature*, **228**: 329-332 (1970).
22. N. C. Sun, C. C. Chang, and E. H. Y. Chu, Chromosome Assignment of the Human Gene for Galactose-1-Phosphate Uridyltransferase, *Proc. Nat. Acad. Sci. U. S. A.*, **71**: 404-407 (1974).
23. R. E. Breslow and R. A. Goldsby, Isolation and Characterization of Thymidine Transport Mutants of Chinese Hamster Cells, *Exp. Cell Res.*, **55**: 339-346 (1969).
24. L. Mezger-Freed, Puromycin Resistance in Haploid and Heteroploid Frog Cells: Gene or Membrane Determined? *J. Cell Biol.*, **51**: 742-751 (1971).
25. J. J. Freed and L. Mezger-Freed, Origin of Thymidine Kinase Deficient (TK<sup>-</sup>) Haploid Frog Cells via an Intermediate Thymidine Transport Deficient (TT<sup>-</sup>) Phenotype, *J. Cell Physiol.*, **82**: 199-212 (1973).
26. E. Englesberg and L. Ingraham, Meiotrophic Mutants of *Pasteurella pestis* and Their Use in Elucidation of Nutritional Requirements, *Proc. Nat. Acad. Sci. U. S. A.*, **43**: 369-373 (1957).
27. L. H. Thompson, R. Mankovitz, R. M. Baker, J. E. Till, L. Siminovitch, and G. F. Whitmore, Isolation of Temperature-Sensitive Mutants of L-Cells, *Proc. Nat. Acad. Sci. U. S. A.*, **66**: 377-384 (1970).
28. D. B. Smith and E. H. Y. Chu, Isolation and Characterization of Temperature-Sensitive Mutants in a Chinese Hamster Cell Line, *Mutat. Res.*, **17**: 113-120 (1973).
29. L. H. Thompson, J. L. Harkins, and C. P. Stanners, A Mammalian Cell Mutant with a Temperature-Sensitive Leucyl-Transfer RNA Synthetase, *Proc. Nat. Acad. Sci. U. S. A.*, **70**: 3094-3098 (1973).
30. F.-T. Kao, R. T. Johnson, and T. T. Puck, Complementation Analysis on Virus-Fused Chinese Hamster Cells with Nutritional Markers, *Science*, **164**: 312-314 (1969).
31. F.-T. Kao, L. Chasin, and T. T. Puck, Genetics of Somatic Mammalian Cells. X. Complementation Analysis of Glycine-Requiring Mutants, *Proc. Nat. Acad. Sci. U. S. A.*, **64**: 1284-1291 (1969).
32. M. Harris, Anomalous Patterns of Mutation in Cultured Mammalian Cells, *Genetics*, *Suppl.*, **73**: 181-185 (1973).
33. R. J. Klebe, T.-R. Chen, and F. H. Ruddle, Mapping of a Human Genetic Regulator Element by Somatic Cell Genetic Analysis, *Proc. Nat. Acad. Sci. U. S. A.*, **66**: 1220-1227 (1970).
34. F.-T. Kao and T. T. Puck, Genetics of Somatic Mammalian Cells: Demonstration of a Human Esterase Activator Gene Linked to the Ade B Gene, *Proc. Nat. Acad. Sci. U. S. A.*, **69**: 3273-3277 (1972).
35. D. E. Comings, The Structure and Function of Chromatin, *Advan. Hum. Genet.*, **3**: 237-431 (1972).
36. I. Pastan and R. Perlman, Cyclic Adenosine Monophosphate in Bacteria, *Science*, **169**: 339-344 (1970).
37. S. Nakanishi, S. Adhya, M. Gottesman, and I. Pastan, Studies on the Mechanism of Action of the *gal* Repressor, *J. Biol. Chem.*, **248**: 5937-5942 (1973).

38. G. M. Martin and C. A. Sprague, Parasexual Cycle in Cultivated Human Somatic Cells, *Science*, **166**: 761-763 (1969).
39. L. A. Chasin, Non-Linkage of Induced Mutations in Chinese Hamster Cells, *Nature (London) New Biol.*, **240**: 50-52 (1972).
40. M. Harris, Mutation Rates in Cells at Different Ploidy Levels, *J. Cell Physiol.*, **78**: 177-184 (1971).
41. M. Harris, Phenotypic Expression of Drug Resistance in Hybrid Cells, *J. Nat. Cancer Inst.*, **50**: 423-429 (1973).
42. L. Mezger-Freed, Effect of Ploidy and Mutagen on Bromodeoxyuridine Resistance in Haploid and Diploid Frog Cells, *Nature (London) New Biol.*, **235**: 245-246 (1972).
43. L. Mezger-Freed, Mutagenesis of Haploid Cultured Frog Cells, *Genetics, Suppl.*, in press.
44. L. A. Chasin, The Effect of Ploidy on Chemical Mutagenesis in Cultured Chinese Hamster Cells, *J. Cell Physiol.*, **82**: 299-308 (1973).
45. A. L. Beaudet, D. J. Roufa, and C. T. Caskey, Mutations Affecting the Structure of Hypoxanthine: Guanine Phosphoribosyltransferase in Cultured Chinese Hamster Cells, *Proc. Nat. Acad. Sci. U. S. A.*, **70**: 320-324 (1973).
46. V. L. Chan, G. F. Whitmore, and L. Siminovitch, Mammalian Cells with Altered Forms of RNA Polymerase II, *Proc. Nat. Acad. Sci. U. S. A.*, **69**: 3119-3123 (1972).
47. A. M. Albrecht, J. L. Biedler, and D. J. Hutchison, Two Different Species of Dihydrofolate Reductase in Mammalian Cells Differentially Resistant to Amethopterin and Methasquin, *Cancer Res.*, **32**: 1539-1546 (1972).
48. S. Povey, S. E. Gardiner, B. Watson, S. Mowbray, H. Harris, E. Arthur, C. M. Steel, C. Blenkinsop, and H. J. Evans, Genetic Studies on Human Lymphoblastoid Lines: Isozyme Analysis on Cell Lines from Forty-one Different Individuals and on Mutants Produced Following Exposure to a Chemical Mutagen, *Ann. Hum. Genet.*, **36**: 247-266 (1973).
49. J. D. Sharp, N. E. Capecchi, and M. R. Capecchi, Altered Enzymes in Drug-Resistant Variants of Mammalian Tissue Culture Cells, *Proc. Nat. Acad. Sci. U. S. A.*, **70**: 3145-3149 (1973).



## THE CELL NUCLEUS: SESSION SUMMARY

J. HERBERT TAYLOR, *Session Chairman*

Institute of Molecular Biophysics, Florida State University, Tallahassee, Florida

---

You have heard from Dr. Huberman's report that the units of replication in CHO cells all fall into the same size class whether replicated early or late in the S phase. However, those initiated early in S phase grow at considerably slower rates than those initiated in middle or late S phase. Callan<sup>1</sup> has demonstrated that the sites of initiation are closer together in S phases of early embryonic cells compared to adult cells, whereas spermatocytes in the premeiotic S phase have considerably fewer initiation sites per chromosome than adult somatic cells and therefore longer spacings between these. The S phases are also proportionately longer, but chain growth is nearly constant except for its response to differences in the temperature at which replication is allowed to proceed.

The question raised in my mind concerns the size of the ultimate unit of replication and how this unit relates to the larger units detected by the various people who have studied the problem. Clearly the short pieces detected in pulse-labeled cells (Okazaki fragments) could be the ultimate unit and conceivably might be the only structurally defined unit along the DNA chains. These units appear to be about 1000 to 1200 nucleotides and can be measured by sedimentation or by electron microscopy.<sup>2</sup> Both methods indicate modal sizes of fragments which would extend along 0.3 to 0.4  $\mu\text{m}$  of native DNA and include 900 to 1200 base pairs. These observations can be correlated with opening of the strands at about the same intervals when DNA is partially melted.<sup>3</sup> However, it is clear from the studies presented by Huberman and previous reports<sup>1,4,5</sup> that initiation begins at a locus and proceeds in both directions at two forks so that loops of a size considerably larger than the Okazaki fragments are produced. Many fragments are presumably polymerized and joined end to end by a ligase activity. The questions raised are whether the Okazaki fragments are unique-sized segments from each locus and whether the



larger units are likewise the same at each S phase at a given stage in development.

From the staining properties of the bands, i.e., Q-bands, G-bands, and C-bands, it appears that the chromosomes are differentiated into regions with respect to the type of DNA contained. Of course, this idea has been held by some since Heitz described the heterochromatic and euchromatic regions in chromosomes of *Drosophila*. The demonstration that repeated sequences DNA (satellite DNA) occupies restricted regions of the chromosome complement<sup>6</sup> was an expansion of that concept. That these regions have characteristic patterns of replication over the S phase has become well-known. However, the meaning of these observations is only dimly revealed to us. Nevertheless, as Dr. Arrighi has demonstrated so well, the cytologist can make good use of the variations without understanding their full significance.

The remarkable indication that cells maintain a characteristic amount of DNA as well as a representative of each chromosomal segment in spite of changes in number and morphology, as presented by Dr. Deaven, is a demonstration of the power of the tools available for chromosome analysis at this time. From a genetic point of view, these observations make good sense, but the concept is not one that we could have held, in view of the apparent changes, except by such careful measurements.

Despite the limited time available to him, Dr. Chu has shown us how much progress we can expect in an analysis of the genome by induction of mutation by mutagenic agents and the genetic analysis of these in cell cultures. The isolation of mutant clones covering a variety of phenotypic changes in the metabolic machinery of the cells indicates that one is dealing with nucleotide sequences similar to those which are being analyzed in prokaryotes. Although we are much further from the kind of analysis that will reveal the regulatory sequences associated with the mutant loci, the type of analysis presented by Dr. Tomkins yesterday leads us to believe that such understanding is rapidly being approached. The pace of new accomplishments allows one to let the mind project the presently unimaginable techniques and technology which might accomplish the fantasy briefly outlined below.

If we in the future could return to the One-Thousandth Symposium on Mammalian Cells, similar to this one at Los Alamos, we might find near this site the huge console of a computer system and building after building stretching away into the mountains beyond. The operator at the console might explain to us, as members of a tour conducted by the director of the laboratory, that a part of these storage facilities contains the computer-stored nucleotide sequences of the chromosome complements of every individual in the country. Upon request he could display the sequences or any relevant part of a genome for us to examine. We might ask then to see the nucleotide sequences for the director, but the operator would explain that since there are approximately 3 billion nucleotide pairs in the chromosome complement this would take a very long time. However, he could produce for us a display of those parts of the complement which differed from the reference genome or wild type that had

recently been established by the International Commission on Genotypes. He would explain that all human reproduction is now controlled, on the basis of this genotypic bank. A large program also would be under way to change some of the more favorably arranged genomes in ways laid out by the International Commission. We would look on with amazement as the colored panels flash sequence after sequence showing mismatches with the reference genome.

## REFERENCES

1. H. G. Callan, Replication of DNA in the Chromosomes of Eukaryotes, *Proc. Roy. Soc. (London) Ser. B.*, **181**: 19-41 (1972).
2. J. H. Taylor, Units of DNA Replication in Chromosomes of Eukaryotes, *Int. Rev. Cytol.*, **37**: 1-20(1974); and unpublished observations made by use of the electron microscope.
3. D. P. Evenson, W. A. Mego, and J. H. Taylor, Subunits of Chromosomal DNA. I. Electron Microscopic Analysis of Partially Denatured DNA, *Chromosoma*, **39**: 225-235 (1972).
4. J. A. Huberman and A. D. Riggs, On the Mechanism of DNA Replication in Mammalian Chromosomes, *J. Mol. Biol.*, **32**: 327-341 (1968).
5. J. A. Huberman and A. Tsai, The Direction of DNA Replication in Mammalian Cells, *J. Mol. Biol.*, **75**: 5-12 (1973).
6. M. L. Pardue and J. G. Gall, Chromosome Localization of Mouse Satellite DNA, *Science*, **168**: 1356-1358 (1970).

## SESSION V

### THE CELL SURFACE: OPENING REMARKS

PAUL M. KRAEMER, *Session Chairman*

Cellular and Molecular Radiobiology Group, Los Alamos Scientific Laboratory,  
Los Alamos, New Mexico

---

This session concerns the cell surface, which is another way of saying that it concerns the external aspects of the plasma membrane. From a biochemical viewpoint, we will be talking within the context of the nature of membranes in general and, in addition, we will be considering those molecular entities which are in, on, or near this particular membrane and which may be relevant to function at the cellular level. A number of speakers in previous sessions have already provided considerable introductory remarks to this session. For instance, Dr. Julius discussed the antigen-binding receptors of immunocompetent cells, which appear to be specific immunoglobulin molecules, and raised the question as to exactly what is the structural difference between the cell-surface variety and the circulating variety that is formed following antigenic stimulation. Two of our speakers will continue the story of the cell surface in immunology. Dr. Mueller discussed his recent work concerning the general changes in exposure of surface proteins as a function of density-dependent control of cell-cycle traverse. Dr. Tomkins referred to several types of hormone receptors, including the nonsteroid type which is presumably resident on the cell surface and which may be directly coupled to cyclic nucleotide metabolism. In addition to these specific areas of interest, there is in the current literature a rapidly expanding body of data and conjecture concerning the general characteristics of cell-surface mechanisms. Dr. Tobey mentioned one of these general ideas in which we have been particularly interested, namely, the data concerning heparan sulfate.

Some of you may have wondered: What is heparan sulfate, why do we not learn to spell heparin correctly, and what has an anticoagulant to do with general notions of cell-surface behavior? Briefly, our story is as follows: The anticoagulant called heparin has been known for 75 or 80 years, and its structural characterization has been essentially completed for some years now. It

has been considered to be a specific differentiated cell product, particularly of mast cells, and to have a molecular weight of, say, 5000 to 20,000. Heparan sulfate was the name given to those fractions in commercial preparation of heparin which lacked anticoagulant potency (in other words, were thrown away). We do not doubt that heparin is and will continue to be a valuable therapeutic agent; however, we suggest that all this classical information may be out of proper physiological context. Our viewpoint is based on a number of straightforward observations that we have published in recent years. For one thing, bona fide heparan sulfate has been isolated from many different types of mammalian cell lines from a variety of animal species, including diploid cells and heteroploid cells. Even lines that have little ability to make other mucopolysaccharides, e.g., the L5178Y lymphoma cell, make heparan sulfate. In each instance, the heparan sulfate could be shown to be present, among other places, as a metabolically active cell-surface component. Consequently we have concluded that heparan sulfate is a general cell-surface constituent and that we should consider the possibility of a general cell-surface function. I should mention that Dr. Muriel Lippman, who is attending this conference, proposed some years ago that certain mucopolysaccharides might have properties for regulating cell growth.

Figure 1 shows the structure of cell-surface heparan sulfate. Like other mucopolysaccharides, this one is now known to be actually a glycoprotein; i.e., it contains a peptide moiety that is rooted into the plasma membrane. The sugar chain is linked to this peptide by a small linkage group shown in Fig. 1. This is of interest because the particular bond between xylose and serine is alkaline labile, and, consequently, we can readily split off the sugar chains. The bulk of the sugar chains consists of repetitive, alternating units of a uronic acid and a glucosamine derivative. A characteristic feature of this particular molecule, which is unique as far as I know, is the N-sulfates on some of the glucosamine units. In addition, there are O sulfates. The  $\alpha 1,4$  linkages are also distinctive. When mammalian cells are treated with trypsin, these fragments break off. In addition, of course, we get a mélange of other surface glycopeptides that vary from cell to cell and presumably include the entities that have cell-specific characteristics. The interesting thing about the heparan sulfate fragments is that they are enormous in size compared to other glycopeptides of the mixture. In a single run, we can readily take all of this mixture and show that only heparan sulfate is excluded from, say, a Bio-Gel A-0.5m column. We found also that a large portion was excluded from Bio-Gel A-5m. This finding was very different from the 5000 to 20,000 molecular weight reported in the literature. Recently Dr. David Smith and I have been trying to characterize this further with equilibrium sedimentation analysis. We have found that the tryptic fragments of the cell-surface heparan sulfate range in size up to a molecular weight of 150,000. When we treat the tryptic fragments with alkaline borohydride, we find that even the individual sugar chains can approach a molecular weight of 50,000. This is so



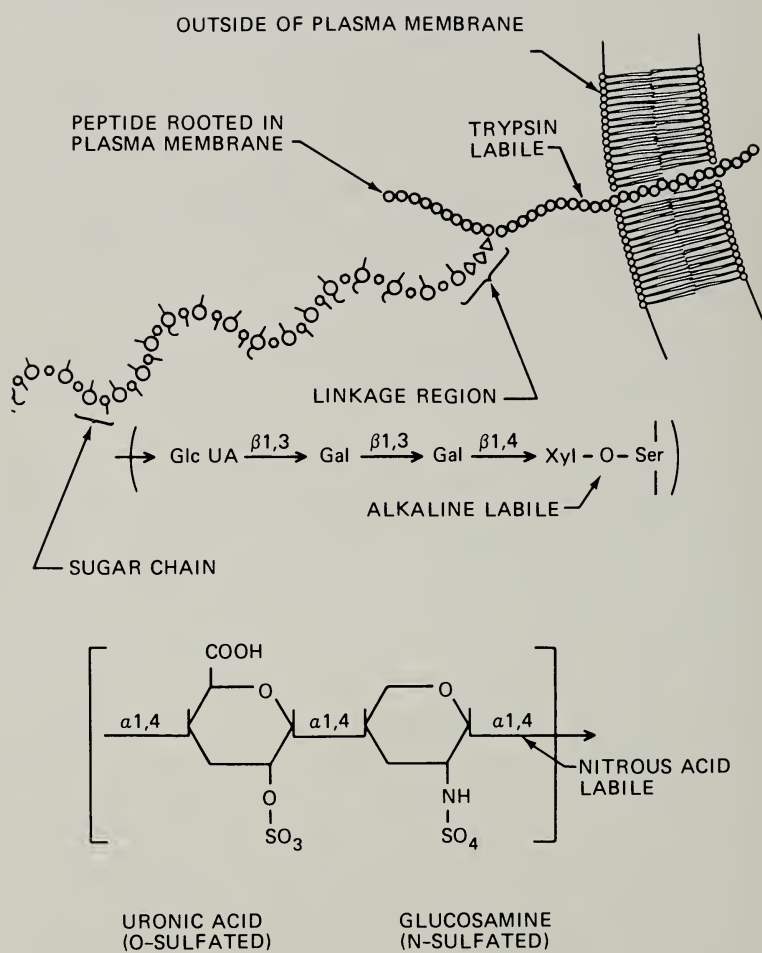
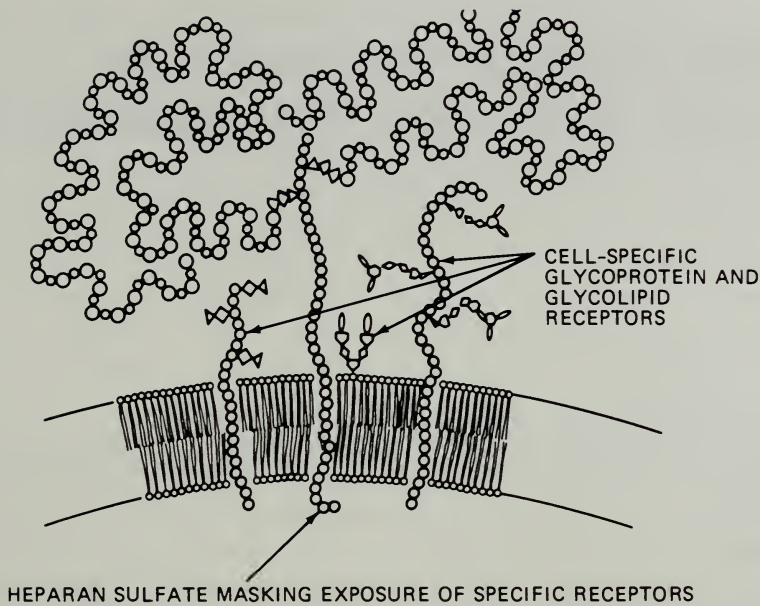


Fig. 1 Diagram showing the major structural features of heparan sulfate of the cell surface.



**Fig. 2** Diagram illustrating the hypothesis that heparan sulfate of the cell surface may regulate exposure of specific receptors.

much bigger than the other cell-surface fragments generated by trypsin treatment that, by combining this feature with the other data, we have come up with a notion that is shown in Fig. 2. Here, we consider heparan sulfate molecules as general cell-surface constituents interspersed on the surface with cell-specific receptors. The particular heparan sulfate molecule illustrated has a peptide moiety rooted in the plasma membrane and has two long sugar chains. The thought here is that these long sugar chains could regulate the exposure of cell-specific receptors.

# CURRENT VIEWS ON THE MOLECULAR ORGANIZATION OF BIOLOGICAL MEMBRANES

GARTH L. NICOLSON

The Salk Institute for Biological Studies, San Diego, California

---

## ABSTRACT

This paper presents an updated version of the Fluid Mosaic Model<sup>1</sup> of membrane structure which incorporates recent data on cytoplasmic control of the cell surface. The intrinsic structure of the plasma membrane is comprised of integral membrane proteins intercalated into a lipid bilayer. Inner-surface peripheral membrane components and membrane-associated contractile components provide two additional levels of membrane organization on the cytoplasmic side of the plasma membrane. These latter classes of membrane components can exert control over the topographic distribution and mobility of cell-surface components, possibly through indirect structural transmembrane linkages across the membrane bilayer. Examples of various types of cytoplasmic control over the cell surface are discussed.

The most important mammalian cell structure involved in the complex interactions of cells with their environments and with other cells is, of course, the plasma membrane. The term "plasma membrane" is used here as a rather broad term describing several actual levels of molecular organization from extracellular mucopolysaccharides, lipid-bilayer intercalated components, and cytoplasmic membrane-associated components. Since the various levels or layers of membrane components are important in describing certain expressions and physiological functions of biological membranes, we have considered more than just the basic permeability barrier of the cell.

The "basic" structure of biological membranes has evolved toward a structural configuration of minimum free energy which incorporates all the various membrane functions and activities essential for the cell. In the Fluid Mosaic Model of membrane structure,<sup>1</sup> the thermodynamic principles that operate to maximize the lowest free-energy environments of membrane lipids, proteins, and saccharides are considered. These principles have been discussed in

detail by Singer.<sup>2</sup> Membrane components that are thermodynamically more stable in aqueous solution, e.g., oligosaccharides, will tend to seek interactions with the aqueous environment (*hydrophilic* interactions). Components that are not thermodynamically stable in aqueous solution, e.g., lipid acyl groups, will tend to interact with each other to the exclusion of the aqueous environment (*hydrophobic* interactions). For example, while most globular membrane-protein components are unstable in aqueous solution and are essential to the structure of the membrane (*integral* membrane proteins), there exists another class of membrane-protein components which is easily removed from the membrane without disruption by mild aqueous treatments (ionic strength, chelating agents, etc.) and are stable in neutral solutions (*peripheral* membrane proteins).<sup>1</sup>

In the basic membrane the structurally important membrane components are the phospholipids and integral membrane proteins. These components are amphipathic (phospholipids) or postulated to be amphipathic (integral membrane proteins); i.e., they are asymmetrical with regard to the hydrophilic and hydrophobic portions of their molecular structures. This has been definitively demonstrated for phospholipid structures and for integral membrane proteins that have been isolated and characterized.<sup>3-5</sup> For the hydrophilic and hydrophobic interactions in the membrane to be maximized, the hydrophilic portions of the components including their oligosaccharides must be presented to the bulk aqueous phase, and their hydrophobic portions must be sequestered away from the aqueous environment inside the membrane. Thus the phospholipids are arranged in an interrupted bilayer consistent with X-ray-diffraction,<sup>6-9</sup> calorimetric,<sup>10</sup> and spin-label<sup>11-15</sup> studies. Integral membrane proteins that have been characterized, such as glycophorin, the major sialoglycoprotein of the human erythrocyte membrane,<sup>4,5,16,17</sup> are also asymmetric molecules. So far, the only protein components positively found to be bearing oligosaccharides and lectin-binding sites are integral membrane proteins with the hydrophobic portions of their structures apparently intercalated into the lipid bilayer and the glycopeptide portions of their structures radiating off the membrane into the aqueous phase.

Figure 1 shows a diagram of the several levels of membrane organization. The basic structural level of the plasma membrane is proposed to be a lipid bilayer with intercalated integral proteins and glycoproteins (integral membrane components). On either side of the basic protein-lipid bilayer structure are protein components that are more loosely bound to the membrane (peripheral membrane components), and on the cytoplasmic side in the cell cytoplasm are additional associated components that may be connected to peripheral or integral membrane components under certain conditions (membrane-associated components).<sup>18</sup> The membrane-associated components may be microfilaments, microtubules, etc., or other cell contractile structures, and their association with the cell membrane is regarded to be transient, depending on cell motility, density, and energy levels.



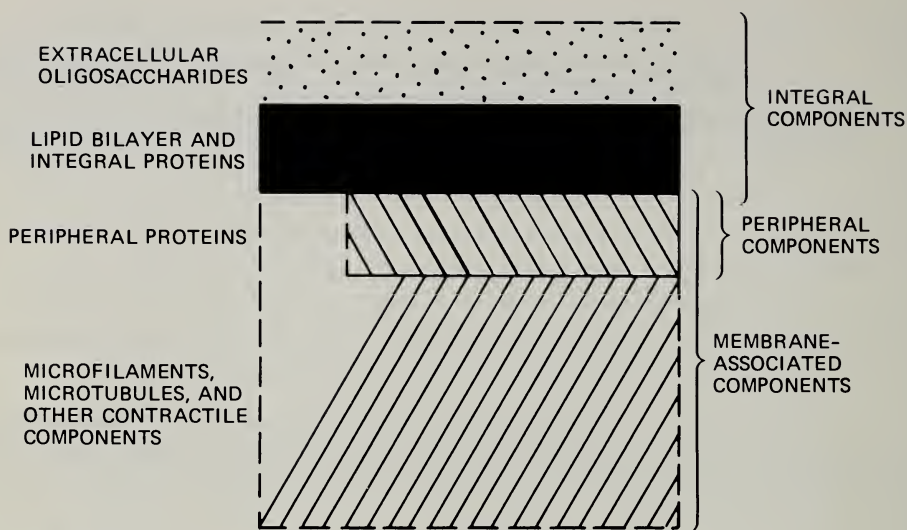
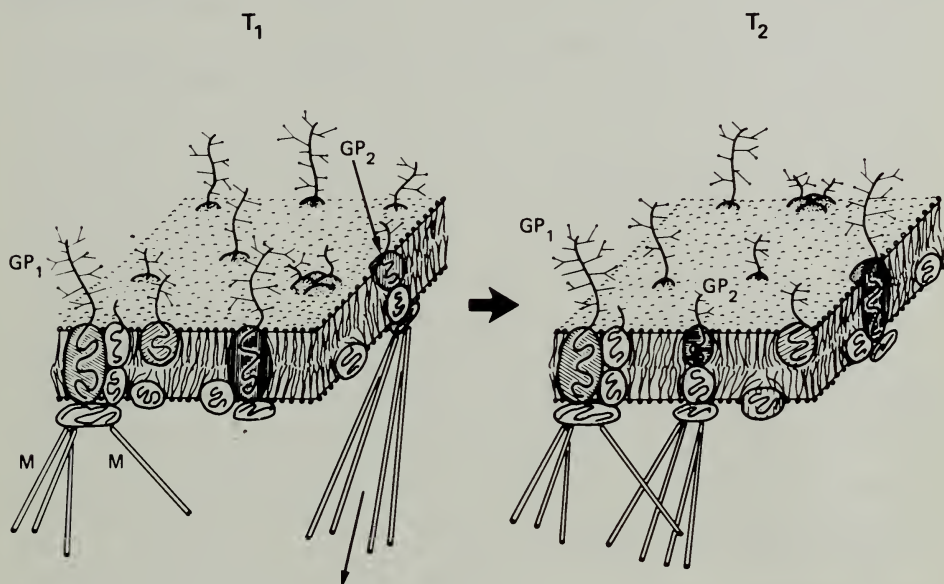


Fig. 1 Levels of cell membrane organization.

## LATERAL MOBILITY OF MEMBRANE COMPONENTS

There is good evidence for mobility of membrane components in the plane of the membrane. Estimates of phospholipid planar diffusion ( $D$ ) from nuclear magnetic resonance and electron paramagnetic resonance spin-label studies indicate rapid motion of these components ( $D \approx 10^{-8}$  cm/sec)<sup>11,14,19-21</sup> but little or no "flip-flop" or rotation from one side of the membrane to the other.<sup>15</sup> Certain protein components also appear to diffuse rapidly, but less rapidly than the lipids in the membrane plane. After Sendai virus-induced fusion of two unlike cells to form a heterokaryon, it takes about 30 to 40 min at 37°C to completely intermix specific surface antigens, such as H-2 histocompatibility antigens,<sup>22</sup> and even less time to aggregate cell-surface immunoglobulin (Ig) and H-2 antigens into "caps" on lymphoid cells.<sup>22-25</sup> Using fluorescent-antibody techniques, Edidin and Fambrough<sup>26</sup> estimated the diffusion constant for certain antigens on muscle fibers to be  $D \approx 10^{-9}$  cm/sec, which is in good agreement with Cone's<sup>27</sup> estimates of the diffusion constant of rhodopsin in the retinal disk membranes using flash photolysis. Saccharides attached to membrane glycoproteins can also be quickly aggregated with lectins on certain cells but not on others.<sup>28-32</sup> The point should be made that different membrane components may be moving laterally at quite different rates<sup>22,25-33</sup> from very fast to very slow or almost nothing, the rate depending on the types of restraints on these moieties that have been applied from outside or inside the cell or both. In Fig. 2, a dynamic version of the Fluid Mosaic Model of membrane structure, the phospholipids are postulated to be diffusing laterally at a high rate in the

membrane and to be rapidly intermixing. Certain integral proteins and glycoproteins are postulated to be moving laterally slower than the phospholipids but considerably faster than some integral glycoproteins and proteins that are relatively "frozen" by external restraints (such as cell-to-cell coupling) or by internal restraints (such as attachment of membrane-associated components)



**Fig. 2** Modified version of the Fluid Mosaic Model of cell membrane structure.  $T_1$  and  $T_2$  represent different points in time. Certain hypothetical integral membrane glycoprotein components are free to laterally diffuse in the membrane plane formed by a lipid bilayer, while others such as the integral glycoprotein-peripheral protein macromolecular complex (GP<sub>1</sub>) are impeded by membrane-associated components (M). Under certain conditions some membrane macromolecular complexes (GP<sub>2</sub>) can be laterally displaced by membrane-associated contractile components in an energy-dependent process. [From G. L. Nicolson, *The Relationship of a Fluid Membrane Structure to Cell Agglutination and Surface Topography*, *Ser. Haematol.*, 6: 277 (1973).]

acting at the inner surface. Such plasma-membrane-associated components as energy-driven contractile structures (microtubule-microfilament systems) may under certain conditions be involved in energy-dependent lateral movements of surface components. Such systems may control antibody- and lectin-induced "capping" of receptors on lymphocytes,<sup>23,34-37</sup> cell motility,<sup>23,34</sup> and endocytosis.<sup>38</sup> But under resting conditions in the absence of contraction of membrane-associated contractile systems, the lateral mobilities of certain linked integral proteins and glycoproteins might be impeded.

## LINKAGE BETWEEN MEMBRANE ORGANIZATIONAL LEVELS

It is immediately obvious that some sort of structural linkage is needed for components from one membrane organizational level to exert control over another level, e.g., for cytoplasmic membrane-associated contractile systems to move an outer-surface-bound immunoglobulin molecule into a cap. Unfortunately, only scant evidence is available on linkages between the various membrane organizational levels. Recently, however, direct interaction has been demonstrated<sup>3,9</sup> between an integral membrane sialoglycoprotein that spans the basic structural level of human erythrocyte membrane (glycophorin<sup>4,5,16</sup>) and an inner-surface peripheral membrane component. In these studies the topographic distribution of glycophorin on the extracellular membrane surface was followed by electron microscopic localization of its sialo residues.<sup>40</sup> Antibodies were made against a membrane component present in the peripheral level of organization, spectrin,<sup>41,42</sup> which is exclusively at the inner membrane surface.<sup>43</sup> The affinity-purified antibodies were sequestered inside human erythrocyte ghosts where they could interact with spectrin molecules. Under conditions of optimal concentration, time, and temperature, antspectrin caused aggregation of spectrin molecules and concomitantly caused aggregation of glycophorin molecules monitored at the outer surface by a transmembrane effect. This process required the sequestration of IgG antibodies (Fab monovalent fragments would not substitute); so the aggregation was dependent on cross-linking spectrin and aggregating it into "clusters." Ji has recently shown that glycophorin and spectrin are close neighbors in the membrane by demonstrating that spectrin can be chemically linked to glycophorin by short bifunctional  $\epsilon$ -amino-reactive imidates.<sup>44</sup>

Interaction or linkage between the membrane-associated level of organization and the cell surface has also been demonstrated recently by indirect means. Berlin and his collaborators<sup>45,46</sup> have shown that microtubule-disrupting drugs such as colchicine, Colcemid, or vinblastine sulfate dramatically affect cell agglutination by concanavalin-A. The agglutination of cells may be related to the mobility and ability of the concanavalin-A receptors to be clustered on the cell surface.<sup>29-32</sup> Other evidence suggesting that membrane-associated components such as microtubules may be structurally linked to the outer plasma membrane surface comes from experiments using dibutyl-*l*-cyclic adenosine monophosphate to modify cell agglutinability by wheat germ agglutinin and its reversal by Colcemid or vinblastine.<sup>47,48</sup>

Although the interrelationships between the various components involved in the structural organization of biological membranes are for the most part unclear (particularly their function), it is now necessary to consider these interrelationships in any scheme of plasma membrane or cell-surface structures. Linkage between the various levels of cell membrane organization may provide the means by which cells can control their surfaces and interactions with other cells and with their environment.



## ACKNOWLEDGMENTS

These studies were supported by grant GB-34178 from the National Science Foundation, contract CB-33879 from the National Cancer Institute, U. S. Public Health Service, and National Cancer Institute Core Grant CA-14195.

## REFERENCES

1. S. J. Singer and G. L. Nicolson, The Fluid Mosaic Model of the Structure of Cell Membranes, *Science*, **175**: 720-731 (1972).
2. S. J. Singer, in *Structure and Function of Biological Membranes*, L. Rothfield (Ed.), pp. 145-222, Academic Press, Inc., New York, 1971.
3. A. Ito and R. Sato, Purification by Means of Detergents and Properties of Cytochrome  $b_5$  from Liver Microsomes, *J. Biol. Chem.*, **243**: 4922-4923 (1968).
4. R. F. Winzler, in *Red Cell Membrane*, G. A. Jamieson and T. J. Greenwalt (Eds.), pp. 157-171, J. B. Lippincott Company, Philadelphia, 1969.
5. J. P. Segrest, I. Kahne, R. L. Jackson, and V. T. Marchesi, Major Glycoprotein of the Human Erythrocyte Membrane: Evidence for an Amphipathic Molecular Structure, *Arch. Biochem. Biophys.*, **155**: 167-183 (1973).
6. J. K. Blasie and C. R. Worthington, Planar Liquid-Like Arrangement of Photopigment Molecules in Frog Retinal Receptor Disk Membrane, *J. Mol. Biol.*, **39**: 417-439 (1969).
7. D. M. Engelman, X-Ray Diffraction Studies of Phase Transitions in the Membrane of *Mycoplasma laidlawii*, *J. Mol. Biol.*, **47**: 115-117 (1970).
8. A. E. Blaurock, Structure of the Nerve Myelin Membrane: Proof of the Low-Resolution Profile, *J. Mol. Biol.*, **56**: 35-52 (1971).
9. M. H. F. Wilkins, A. E. Blaurock, and D. M. Engelman, Bilayer Structure in Membranes, *Nature (London) New Biol.*, **230**: 72-76 (1971).
10. J. M. Stein, M. E. Tourtellotte, J. C. Reinert, R. N. McElhaney, and R. L. Rader, Calorimetric Evidence for the Liquid-Crystalline State of Lipids in a Biomembrane, *Proc. Nat. Acad. Sci. U.S.A.*, **63**: 104-109 (1969).
11. W. L. Hubbell and H. M. McConnell, Spin-Label Studies of the Excitable Membranes of Nerve and Muscle, *Proc. Nat. Acad. Sci. U.S.A.*, **61**: 12-16 (1968).
12. A. D. Keith, A. S. Waggoner, and O. H. Griffith, Spin Labeled Mitochondrial Lipids in *Neurospora crassa*, *Proc. Nat. Acad. Sci. U.S.A.*, **61**: 819-826 (1970).
13. M. E. Tourtellotte, D. Branton, and A. Keith, Membrane Structure: Spin Labeling and Freeze-Etching of *Mycoplasma laidlawii*, *Proc. Nat. Acad. Sci. U.S.A.*, **66**: 909-916 (1970).
14. R. D. Kornberg and H. M. McConnell, Lateral Diffusion of Phospholipids in a Vesicle Membrane, *Proc. Nat. Acad. Sci. U.S.A.*, **68**: 2564-2568 (1971).
15. R. D. Kornberg and H. M. McConnell, Inside-Outside Transitions of Phospholipids in Vesicle Membranes, *Biochemistry*, **10**: 1111-1120 (1971).
16. A. Morawiecki, Dissociation of M- and N-Group Mucoproteins into Subunits in Detergent Solution, *Biochim. Biophys. Acta*, **83**: 339-347 (1964).
17. V. T. Marchesi, T. W. Tillack, R. L. Jackson, J. P. Segrest, and R. E. Scott, Chemical Characterization and Surface Orientation of the Major Glycoprotein of the Human Erythrocyte Membrane, *Proc. Nat. Acad. Sci. U.S.A.*, **69**: 1445-1449 (1972).
18. S. Fleischer, W. L. Zahler, and H. Ozawa, in *Biomembranes*, Vol. 2, L. A. Manson (Ed.), pp. 105-119, Plenum Publishing Corporation, New York, 1971.
19. A. G. Lee, N. J. M. Birdsall, and J. C. Metcalfe, Measurement of Fast Lateral Diffusion of Lipids in Vesicles and in Biological Membranes by  $^1\text{H}$  Nuclear Magnetic Resonance, *Biochemistry*, **12**: 1650-1658 (1973).



20. C. J. Scandella, P. Devaux, and H. M. McConnell, Rapid Lateral Diffusion of Phospholipids in Rabbit Sarcoplasmic Reticulum, *Proc. Nat. Acad. Sci. U.S.A.*, **69**: 2056-2060 (1972).
21. P. C. Jost, O. H. Griffith, R. A. Capaldi, and G. Vanderkooi, Evidence for Boundary Lipid in Membranes, *Proc. Nat. Acad. Sci. U.S.A.*, **70**: 480-484 (1973).
22. L. D. Frye and M. Edidin, The Rapid Intermixing of Cell Surface Antigens After Formation of Mouse-Human Heterokaryons, *J. Cell Sci.*, **7**: 319-333 (1970).
23. R. Taylor, P. Duffus, M. Raff, and S. De Petris, Redistribution and Pinocytosis of Lymphocyte Surface Immunoglobulin Molecules Induced by Anti-Immunoglobulin Antibody, *Nature (London) New Biol.*, **233**: 225-229 (1971).
24. W. C. Davis, H-2 Antigen on Cell Membranes: An Explanation for the Alteration of Distribution by Indirect Labeling Techniques, *Science*, **175**: 1006-1008 (1972).
25. M. Edidin and A. Weiss, Antigen Cap Formation in Cultured Fibroblasts: A Reflection of Membrane Fluidity and of Cell Motility, *Proc. Nat. Acad. Sci. U.S.A.*, **69**: 2456-2459 (1972).
26. M. Edidin and D. Fambrough, Fluidity of the Surface of Cultured Muscle Fibers. Rapid Lateral Diffusion of Marked Surface Antigens, *J. Cell Biol.*, **47**: 27-37 (1973).
27. R. A. Cone, Rotational Diffusion of Rhodopsin in the Visual Receptor Membrane, *Nature (London) New Biol.*, **236**: 39-43 (1972).
28. P. M. Comoglio and R. Guglielmo, Two Dimensional Distribution of Concanavalin A Receptor Molecules on Fibroblast and Lymphocyte Plasma Membranes, *FEBS (Fed. Eur. Biochem. Soc.) Lett.*, **27**: 256-258 (1972).
29. M. Inbar and L. Sachs, Mobility of Carbohydrate Containing Sites on the Surface Membrane in Relation to the Control of Cell Growth, *FEBS (Fed. Eur. Biochem. Soc.) Lett.*, **32**: 124-128 (1973).
30. G. L. Nicolson, Topography of Membrane Concanavalin A Sites Modified by Proteolysis, *Nature (London) New Biol.*, **239**: 193-197 (1972).
31. G. L. Nicolson, in *Control of Proliferation in Animal Cells* (Vol. 1 of Cold Spring Harbor Conferences on Cell Proliferation), B. Clarkson and R. Baserga (Eds.), May 20-27, 1973, pp. 251-270, Cold Spring Harbor Laboratory, 1974.
32. J. Z. Rosenblith, T. E. Ukena, H. H. Yin, R. D. Berlin, and M. J. Karnovsky, A Comparative Evaluation of the Distribution of Concanavalin A-Binding Sites on the Surfaces of Normal, Virally-Transformed, and Protease-Treated Fibroblasts, *Proc. Nat. Acad. Sci. U.S.A.*, **70**: 1625-1629 (1973).
33. P. M. Comoglio and G. Filogamo, Plasma Membrane Fluidity and Surface Motility of Mouse C-1300 Neuroblastoma Cells, *J. Cell Sci.*, **13**: 415-420 (1973).
34. S. de Petris and M. C. Raff, Distribution of Immunoglobulin on the Surface of Mouse Lymphoid Cells as Determined by Immunoferritin Electron Microscopy. Antibody-Induced Temperature-Dependent Redistribution and Its Implications for Membrane Structure, *Eur. J. Immunol.*, **2**: 524-535 (1972).
35. F. Loor, L. Forni, and G. Pernis, The Dynamic State of the Lymphocyte Membrane Factor Affecting the Distribution and Turnover of Surface Immunoglobulins, *Eur. J. Immunol.*, **2**: 203-212 (1972).
36. I. Yahara and G. M. Edelman, Restriction of the Mobility of Lymphocyte Immunoglobulin Receptors by Concanavalin A, *Proc. Nat. Acad. Sci. U.S.A.*, **69**: 608-612 (1972).
37. I. Yahara and G. M. Edelman, The Effects of Concanavalin A on the Mobility of Lymphocyte Surface Receptors, *Exp. Cell Res.*, **81**: 143-155 (1973).
38. R. D. Berlin, Effect of Concanavalin A on Phagocytosis, *Nature (London) New Biol.*, **235**: 44-45 (1972).

39. G. L. Nicolson and R. G. Painter, Anionic Sites of Human Erythrocyte Membranes. II. Trans-Membrane Effects of Anti-Spectrin on the Topography of Positively Charged Colloidal Particles, *J. Cell Biol.*, **59**: 395-406 (1973).
40. G. L. Nicolson, Anionic Sites of Human Erythrocyte Membranes. I. Effects of Trypsin, Phospholipase C, and pH on the Topography of Bound Positively Charged Colloidal Particles, *J. Cell Biol.*, **57**: 373-387 (1973).
41. V. T. Marchesi, E. Steers, T. W. Tillack, and S. L. Marchesi, in *Red Cell Membrane*, G. A. Jamieson and T. J. Greenwalt (Eds.), pp. 117-130, J. B. Lippincott Company, Philadelphia, 1969.
42. M. Clarke, Isolation and Characterization of a Water-Soluble Protein from Bovine Erythrocyte Membranes, *Biochem. Biophys. Res. Comm.*, **45**: 1063-1070 (1971).
43. G. L. Nicolson, V. T. Marchesi, and S. J. Singer, The Localization of Spectrin on the Inner Surface of Human Red Blood Cell Membranes by Ferritin-Conjugated Antibodies, *J. Cell Biol.*, **51**: 265-272 (1971).
44. T. H. Ji, Cross-Linking Sialoglycoproteins of Human Erythrocyte Membranes, *Biochem. Biophys. Res. Comm.*, **53**: 508-514 (1973).
45. R. D. Berlin and T. E. Ukena, Effect of Colchicine and Vinblastine on the Agglutination of Polymorpho-Nuclear Leucocytes by Concanavalin A, *Nature (London) New Biol.*, **238**: 120-122 (1972).
46. H. H. Yin, T. E. Ukena, and R. D. Berlin, Effect of Colchicine, Colcemid and Vinblastine on the Agglutination, by Concanavalin A, of Transformed Cells, *Science*, **178**: 867-868 (1972).
47. A. W. Hsie and T. T. Puck, Morphological Transformation of Chinese Hamster Cells by Dibutyryl Adenosine Cyclic 3':5'-Monophosphate and Testosterone, *Proc. Nat. Acad. Sci. U.S.A.*, **68**: 358-361 (1971).
48. A. W. Hsie, C. Jones, and T. T. Puck, Further Changes in Differentiation State Accompanying the Conversion of Chinese Hamster Cells of Fibroblastic Form by Dibutyryl Adenosine Cyclic 3':5'-Monophosphate and Hormones, *Proc. Nat. Acad. Sci. U.S.A.*, **68**: 1648-1652 (1971).
49. G. L. Nicolson, The Relationship of a Fluid Membrane Structure to Cell Agglutination and Surface Topography, *Ser. Haematol.*, **6**: 275-291 (1973).

# ON SIGNALS GENERATED BY THE BINDING OF MULTIVALENT ANTIGENS TO LYMPHOCYTES

GEORGE I. BELL

Theoretical Division, Los Alamos Scientific Laboratory, Los Alamos, New Mexico

---

## ABSTRACT

The signals that may be transmitted to a lymphocyte by the binding of antigen molecules to antibody-like receptors on the cell surface are classified as microsignals and macrosignals. A microsignal is defined as a signal arising from the binding of one antigen molecule to one receptor molecule; it is an  $m_1$  signal if only a single bond is involved and an  $m_2$  signal for two or more bonds. An  $m_1$  signal might arise from a conformational change in the receptor molecule or from a stabilization of its orientation in the membrane. We concluded that  $m_1$  signals are probably not sufficient to affect cell behavior significantly unless they have a duration of  $\geq$  seconds. A special role may be played by  $m_2$  interactions in the induction or suppression of anti-self-idiotypic antibodies. Macrosignals arise from cross-linking of receptor molecules by multivalent or linked antigen molecules to form an antigen-receptor lattice on the cell surface; they are  $M_1$  signals if passive diffusion of the receptors suffices for lattice formation and signal generation and  $M_2$  signals if active cell movement of the lattice is required. It is argued that times for lattice formation may be of the order of a minute at 37°C. From the action of nonspecific mitogens, we concluded that macrosignals are sufficient to stimulate lymphocytes and that the requirements for T- and B-cell activation differ. In particular, B cells are stimulated by an array of repeating or fixed binding sites. Antigen-specific activation of B cells often requires collaboration of T cells. In these cases, IgT from T cells may aggregate the antigen, sometimes on macrophages, so as to present a stimulating macrosignal to the B cells, but, in addition, the IgT-antigen complexes may bind to and deliver different microsignals to the B cells. In general, antigen-antibody complexes may be the most important signal generators.

According to the clonal selection theory,<sup>1</sup> certain cells of the immune system have on their surfaces antibody-like receptor molecules that are capable of binding antigen. Each of these cells is viewed as producing and having on its surface a set of homogeneous receptor molecules that can specifically bind to certain antigens. Binding of antigen will, under appropriate circumstances,



trigger the cell to proliferate and to produce a clone secreting antibodies similar to the receptor molecules.

In recent years conclusive evidence has been found for the existence of such receptors, particularly on the surfaces of the precursors of antibody-secreting cells, i.e., on B cells, the bone-marrow-derived lymphocytes.<sup>2</sup> In addition, there is less-conclusive evidence<sup>2-4</sup> for antibody-like receptors on T cells, the thymus-derived or -dependent cells which collaborate with B cells to make possible a humoral response to many antigens and which are involved in cell-mediated immunity. On the surface of a typical mouse B cell are approximately  $10^5$  receptor molecules.<sup>5</sup> These have been variously reported to be predominantly IgG molecules<sup>5</sup> or 8S IgM molecules.<sup>3,6</sup> In either case they are probably Y-shaped protein molecules with a combining site for antigen near the end of each arm; each of the arms and the stem are approximately 7 nm in length and 3.5 nm in diameter.<sup>7,8</sup> As will be discussed in more detail later and in accord with the Fluid Mosaic Model of the cell membrane,<sup>9</sup> these receptors are embedded in the cell membrane and are relatively free to move or diffuse in the plane of the membrane. Functionally it is necessary that the antigen-binding sites on receptors be exposed at the outer surface of the membrane. The receptors are then long enough to extend all the way through the membrane and might be viewed as integral proteins.<sup>9,10</sup> However, receptors on B cells are also exposed to binding by anti-immunoglobulin antibodies,<sup>5</sup> including those which specifically attach to the stem (Fc portion) of the receptor molecule;<sup>11</sup> hence at least some of the receptors on B cells must not be very deeply embedded and are perhaps better characterized as peripheral proteins.<sup>9,12</sup> The T-cell receptors may be more deeply embedded.

Since a small lymphocyte has a typical diameter<sup>5</sup> of about  $8\text{ }\mu\text{m}$  and an area (as a sphere) of  $2 \times 10^2\text{ }\mu\text{m}^2 = 2 \times 10^8\text{ nm}^2$ , the area available per receptor is  $2 \times 10^3\text{ nm}^2$  and the distance between receptors is about 45 nm. Thus only of the order of 1% of the membrane is occupied by the receptor molecules. It has been reported<sup>10,13,14</sup> that receptors are gradually shed by resting lymphocytes, with a half-life of the order of hours. These experiments used continuously growing (cycling) diploid lymphocytes<sup>13</sup> or the binding of various agents<sup>10,14</sup> to receptors, which may affect the receptor lifetime and thus may not accurately represent a shedding of unbound receptors from resting cells.

We might postulate<sup>1,15,16</sup> that the binding of sufficient antigen to the receptor sites on a B cell is a necessary and sufficient signal to trigger that cell to proliferate, secrete antibodies, and act out its predestined role in an immune response. We now know that the situation is a good deal more complicated than the prediction by such a simple model—that, for example, the collaboration of several different kinds of cells<sup>17-19</sup> (T cells, B cells, and adherent cells) may be required to initiate a response and that exposure to antigen may sometimes lead to tolerance (diminished capacity to respond) instead of to immunity (enhanced capacity to respond), the specific outcome depending on the physical form of



the antigen.<sup>20,21</sup> This paper examines some of these complications in a systematic way. We begin by classifying the kinds of interactions that multivalent antigens can have with surface receptors and the corresponding signals that might influence cell behavior. Interactions with mitogens which nonspecifically stimulate lymphocytes are also examined. Finally, we briefly discuss interactions that appear to be most important in determining cell behavior in an immune response.

## MICRO SIGNALS AND MACRO SIGNALS

We assume that numerous antibody-like receptor molecules are embedded in the cell membrane and are relatively free to diffuse in the plane of the membrane. We also assume that each receptor molecule has two (or possibly more) exposed sites for specifically binding antigen; receptors with a single binding site per molecule could be included by simple generalization. We wish to consider the interaction of the receptors on a cell surface with an antigen molecule, with antigen molecule referring not only to a well-characterized chemical entity but also to a virus, bacterium, or other cell that can bind specifically to the receptors. The simplest kind of interaction will be the binding of a single antigen molecule to a single receptor binding site. We postulate that such a microscopic interaction delivers to the cell a *microsignal of type one* (or an  $m_1$  signal) to denote that it involves interaction of two molecules at *one* site. For a monovalent antigen, i.e., an antigen molecule with only one antigenic determinant or epitope to bind receptors, this is the only kind of specific interaction that can take place unless the monovalent antigen molecules are somehow linked together or linked to another molecule or cell (see the following discussion). Such  $m_1$  interactions can probably be fairly well characterized as reversible bimolecular reactions<sup>22</sup> such as those which have been studied in the interactions of antibodies with haptens. These reactions have reverse rate constants which are typically<sup>22,23</sup> of the order of 1 to 100 sec<sup>-1</sup> so that a particular  $m_1$  interaction, with monovalent antigen, will be expected to have a duration of a second or less.

The binding of a molecule to a protein frequently produces a change in the conformation of the protein,<sup>24</sup> with very specific consequences on protein binding to other molecules. Therefore an  $m_1$  signal may be a conformational change of the receptor molecule. This conformational change can be imagined to have various effects. It might affect the binding of the receptor to small molecules at the inner surface of the membrane, which could, for example, alter cAMP or cGMP metabolism. It might alter the interaction of the receptor with other molecules in the membrane, or it might alter the other antigen-binding site. We are not aware of any direct evidence of receptor or antibody conformational changes induced by monovalent antigen binding.<sup>25</sup> Indeed, there is evidence, with homogeneous populations of antibodies, that binding of

happen to one binding site does not alter the configuration (affinity) of the other binding site and even that separated arms of the molecule (Fab portions) have the same binding kinetics as do intact molecules.<sup>26</sup> A search for conformational changes induced by hapten binding, using spin-labeled probes,<sup>27</sup> was not successful. A change in circular dichroism, on binding a hapten by homogeneous antibodies, was possibly due to changes in the active site.<sup>28</sup> Of course, these experiments have been performed with free antibodies which may not be identical with receptors. While, in principle, receptors might undergo conformational changes when antibodies do not, we believe such changes, if any, are unimportant for reasons considered in the following discussion.

It appears that an antigen molecule must have some minimum size (molecular weight  $>10^3$  or  $10^4$ ) in order to trigger an immune response.<sup>29</sup> Thus small molecules (haptens) can bind to antibodies and to receptors without much affecting cell behavior. Larger molecules, though monovalent, can induce immune responses, though they are often weak immunogens<sup>29</sup> and sometimes produce tolerance. It is possible to make many haptens immunogenic by simply adding a few amino acids to the hapten.<sup>29</sup> The resulting immunogen induces antibody production but often does not bind the resulting antibodies any better than the hapten. It might appear that such small immunogens can bind only to individual receptor sites and deliver  $m_1$  signals, that therefore  $m_1$  signals exist and are important, but that  $m_1$  signals require binding of antigens that are appreciably larger than the receptor binding site. If this were so, then the function of the material (carrier) that must be added to hapten to make it an immunogen might be to stabilize the orientation of the receptor relative to the plane of the membrane rather than to cause a conformational change. For example, a hydrophilic carrier could tend to orient the receptor to stick its arms out of and its stem into the membrane.

However, it has recently become clear that a function of many carriers is to be recognized by a different cell, a T cell.<sup>17</sup> This recognition may involve binding of the carrier to an antibody-like receptor on the T cell, with a consequent linking of hapten-carrier molecules by such receptors on the T cell or by secreted antibody molecules, perhaps on the surface of a cell for which they are cytophilic. We will discuss these collaborative responses more in the section on intercellular communication, but in the present context their relevance is that monovalent antigens may not end up being presented to the B-cell receptors as isolated monomers. Instead they may be linked together to resemble a multivalent antigen. Therefore an immune response to a small monovalent antigen is not necessarily evidence for the importance of  $m_1$  signals, and the inability of haptens to affect cell behavior is a strong argument against the importance of  $m_1$  signals.

Still another possibility may be mentioned, namely that an  $m_1$  bond must last longer than a second or so for it to be an effective signal. For example, the receptor might take that long to assume a favorable orientation in the

membrane. Then cell behavior would depend on the number and duration of  $m_1$  bonds rather than just an average number of bonds. Cross-linked and multivalent antigens could then deliver effective  $m_1$  signals, whereas haptens and unlinked monomers ordinarily could not. We are not aware of any evidence supporting such a mechanism.

We will now consider interactions that multivalent antigens can have with receptors. A multivalent antigen is defined by the requirement that it have more than one identical epitope per molecule. Evidently such antigens can deliver  $m_1$  signals to a cell by binding to single receptor sites, but they can also bind simultaneously to two or more receptor sites. In particular, a multivalent antigen might bind to two sites on the same receptor molecule. We will call such binding a *microscopic interaction of type two* (or an  $m_2$  interaction) to denote that it is a specific interaction between two molecules at *two* sites. For such an interaction to be possible, the epitopes on the antigen must be appropriately spaced. If we assume a flexible hinge between the arms of a receptor,<sup>7,8</sup> then two epitopes that are simultaneously bound must be separated by a distance between about 4 and 14 nm. Such divalent binding would be tighter than monovalent binding.<sup>22,26</sup> It would serve to stabilize the receptor hinge angle, thus effecting a conformational change and generating an  $m_2$  signal that could be quite different from  $m_1$  signals. In addition, the duration of a double  $m_2$  bond would be expected to be much longer ( $\sim$  hours) than the duration of a single  $m_1$  bond ( $\lesssim$  sec).<sup>22</sup> The duration of  $m_2$  bonds might thus be similar to the half-life for shedding of the receptor.

Since  $m_2$  binding places rather stringent requirements on antigen structure, it might be considered of little general importance in the triggering and regulation of immune responses. If, for example, triggering required  $m_2$  interactions, a bacterium could defeat the immune system by simply spacing its epitopes farther apart than 14 nm. However, two special antigens may be particularly likely to give  $m_2$  signals. The first is an antibody molecule having a shape similar to the receptor and having epitopes near its own combining sites. A cell possessing receptors that could combine with such an antibody would be capable of producing anti-self-idiotypic antibodies. Since idiotypic determinants are probably newly arising self-antigens in adult animals, it is reasonable to expect that the responses to such determinants (self-antigens) might have special features<sup>30</sup> that would possibly involve  $m_2$  signals. For example,  $m_2$  signals might be tolerogenic, to minimize production of anti-self-idiotypic antibodies. Another kind of antigen that would be particularly likely to give  $m_2$  signals would be two small molecules held by one antibody molecule and therefore having an appropriate spacing of epitopes. Such an antigen configuration would, of course, require the presence of external antibody molecules.

We are not aware of direct evidence suggesting that  $m_2$  signals are important in immune responses or, indeed, of investigations designed to determine whether they are important. Possibly experiments in which the degree of hapten coupling



to a carrier was found to have a large effect on cell behavior<sup>20,31</sup> could be interpreted to indicate something about  $m_2$  interactions.

It is likely that a much more important interaction of multivalent antigens involves the simultaneous binding of an antigen molecule to two or more receptor molecules in the membrane. We will call such binding *macroscopic* inasmuch as it involves binding to two or more receptor molecules and possibly interactions with other molecules in the cell membrane, and we define that such binding gives an  $M_1$  signal or signals to the cell. A multivalent antigen will presumably first establish a single bond with a receptor, i.e., involve an  $m_1$  interaction; then, as a second receptor diffuses in the membrane, the antigen can presently establish a second bond, etc. Thus, if many antigen molecules are present, a two-dimensional lattice of antigen-receptor molecules can be built up on the cell membrane. The rate at which such a lattice forms and its general configuration will depend on many factors, in particular on the receptor diffusion rates and affinity for binding antigen and on the antigen size, shape, valence, and concentration.

The rate of diffusion of receptors in membranes is not well known. The mixing of histocompatibility antigens in fused mouse and human cells has been observed,<sup>32</sup> and from this a diffusion constant,  $D = 5 \times 10^{-11}$  cm<sup>2</sup>/sec at 37°C, was estimated.<sup>9</sup> It appears that histocompatibility antigens may be less mobile than antibody-like receptors<sup>33</sup> and hence that receptors may have a larger diffusion constant by perhaps an order of magnitude. For comparison, the diffusion constant of an IgG molecule in water is around  $4 \times 10^{-7}$  cm<sup>2</sup>/sec. If the average distance between receptors is  $d$ , then, in a time of order  $d^2/D$ , the diffusion of receptors will give each point on the cell surface a good chance of having been traversed by a receptor. If we consider a multivalent antigen bound to one or more receptors, a particular unbound epitope is unlikely to be adjacent to a receptor until some time has passed during which, by chance, a receptor diffuses to the appropriate position. Hence the time  $t_D = d^2/D$  represents a diffusion-controlled lower limit for the time to establish secondary bonds to fixed epitopes on a multivalent antigen. (A more mathematical argument is presented in the Appendix of this paper.) For  $D = 5 \times 10^{-11}$  cm<sup>2</sup>/sec and  $d = 45$  nm,  $t_D \approx 0.4$  sec, and as indicated previously  $D$  is likely to be larger, hence  $t_D$  smaller, for receptors at body temperature. Hapten-antibody association rates are typically<sup>22</sup> two or more orders of magnitude slower than the diffusion limits. Receptor and epitope may be oriented more favorably than the random orientations in solution so that a diffusion limit may be more closely approached for the reaction on a membrane. We might expect times for establishing multivalent binding to be about two orders of magnitude longer than  $t_D$  and perhaps of the order of a minute at body temperatures. The receptor diffusion constant will be much smaller at lower temperatures and may also vary with animal species and strain, type of cell, state of differentiation, phase of life cycle, etc. Insofar as antigen-receptor lattice formation may be important in



regulation of immune responses, membrane fluidity may be an important variable.

Rates have been measured<sup>22,34</sup> for establishing multivalent binding of the antigen DNP<sub>16</sub>—guinea pig albumin to guinea pig lymphocytes. The observed times for binding varied with temperature from about 10 min at 4°C to 2 min at 37°C. These are times required for establishing both first and subsequent bonds. However, the first bonds are probably established quite rapidly<sup>22</sup> at the antigen concentrations used, and the times to establish second bonds may well be limiting.

The rate of lattice formation and the lattice configuration will also depend on the character of the multivalent antigen molecule and on antigen concentration. An antigen molecule bound to a receptor will serve as a nucleation site for lattice formation, which may or may not become connected to other nucleation sites. For example, a high concentration of long antigen molecules would appear to favor the rapid formation of a connected lattice over the whole cell surface in a sort of hairnet configuration. A lower concentration of smaller molecules would favor the gradual accumulation of nucleation sites that could diffuse together to form more or less separated lattice islands (patches). Lattice formation is, in many respects, a two-dimensional analogue of precipitation in three dimensions. Therefore lattice formation may not be expected at very low antigen concentrations (receptor excess) or at very high antigen concentrations (antigen excess). In the former case there are not enough antigen molecules to cross-link the receptors; in the latter case each receptor site will tend to be bound to a different antigen molecule. However, additional factors favor lattice formation with multivalent antigens that are big enough to span several receptors. In particular, an antigen molecule that is already bound to one or more receptors has a much greater chance of binding another receptor than does a free antigen molecule. In general, steric considerations would seem much more important for lattice formation than for precipitation, and the analogy between the two phenomena should not be followed too closely.

In recent years experiments have demonstrated and have begun to characterize *in vitro* receptor—ligand lattice formation and its effect on lymphocyte behavior.<sup>5,33,35-40</sup> Many of the experiments have used anti-immunoglobulin antibodies to cross-link the receptors, inasmuch as all B cells can respond to such agents. Multivalent antigen<sup>40</sup> (polymerized flagellin) has been found to have a similar effect on the few cells to which it binds. In addition, immunoglobulins and other agents, usually mitogens, have been used to cross-link other surface moieties on lymphocytes<sup>33,35-39,41,42</sup> and fibroblasts,<sup>43-45</sup> with sometimes similar results, as will be discussed later. These experiments have demonstrated, first of all, that in the absence of multivalent ligands, the receptors are distributed more or less randomly over the cell surface. On binding sufficient multivalent ligand, the receptors become clustered in patches on the cell surface. The formation of patches is a 'passive process that does not require cell metabolism; presumably each patch is a localized

receptor-ligand lattice. The patches are sometimes connected.<sup>37</sup> The rate of patch formation is sensitive to temperature as befits a process depending on receptor diffusion. At 37°C, patches are found within a few minutes, but their rate of formation has not been determined. At 0°C, patches take about 1 hr to form,<sup>39</sup> while at 4°C they are well developed in 20 min.

With metabolically active lymphocytes, connected receptor-ligand patches<sup>38</sup> aggregate to form a single cap at one pole of the cell within about 10 min at 37°C. This capping is not a passive diffusion process but appears rather to be an ordered flow<sup>35,43</sup> of membrane components carrying the patches to one pole. During cap formation, receptors are swept from the cell surface to accumulate in the cap. After cap formation, considerable receptor-ligand material enters the cell,<sup>35,36,38</sup> and after some hours receptors are again present on the cell surface, possibly in larger numbers than before.<sup>36,40</sup> Even in the absence of capping, it appears that a little receptor-antibody material enters the cell<sup>33,46</sup> and that this endocytosis requires a metabolically active cell. Cross-linking of receptors by immunoglobulins has been reported by some investigators to trigger DNA synthesis and mitosis in rabbit lymphocytes,<sup>11</sup> but other researchers have not found this mitogenic action in mice.<sup>47</sup> Cross-linking and capping were not found to alter the immune capability of primed mouse lymphocytes.<sup>47</sup> The extent to which these *in vitro* phenomena occur *in vivo* is not known.

We propose that macroscopic events involving cell metabolism and gross receptor movement be called  $M_2$  events and their signals to the cells be  $M_2$  signals. We presume that such events are a consequence of lattice formation and of the interaction of the lattice with ordered membrane motion. The binding of some antigens might generate  $M_2$  signals without explicit cap formation. In particular, if a lymphocyte encountered a large antigen such as a foreign red cell, the two cells might establish binding contacts, and subsequent lymphocyte membrane motion might be better regarded as orienting the cells rather than as cap formation.

With this definition we have now divided the signals received by a cell on binding multivalent antigen into four categories: two microsignals and two macrosignals. Properties of the interactions giving rise to these signals are summarized in Table 1, and the interactions are sketched in Fig. 1.

We shall now consider agents other than antigens which are capable of triggering lymphocytes. In general, such agents act as nonspecific mitogens; they may deliver macrosignals, but not microsignals, similar to those given by antigens.

## LYMPHOCYTE MITOGENS

Various multivalent ligands bind to the surfaces of lymphocytes and stimulate *in vitro* DNA synthesis, mitosis, and, if B cells are stimulated,

**TABLE 1**  
**PROPERTIES OF SIGNALS**

<b>Microsignals</b>	
$m_1$	Single bond to single receptor. Only signal for unlinked monovalent antigens. First signal for any antigen. Reversible bimolecular reaction (duration $\lesssim$ sec).
$m_2$	Double bond to single receptor. Steric requirements on bivalent or multivalent antigens. Could be due to monomers linked by antibody. Reversible to $m_1$ ? (duration $\sim$ hours) Anti-idiotypic signal?
<b>Macrosignals</b>	
$M_1$	Patching. Requires multivalent antigen or linked monomers. Requires passive diffusion of receptors in membrane. Lattice formed on cell surface—depending on antigen size, shape, valence, affinity, and concentration Irreversible in times of interest.
$M_2$	Capping. Requires $M_1$ (patches). Requires cell metabolism and membrane flow. May be followed by further macrosignals, such as antigen ingestion or receptor re-appearance.

nonspecific antibody synthesis. Among these ligands are certain plant proteins (lectins), including phytohemagglutinin (PHA), concanavalin-A (con-A), and pokeweed mitogen.<sup>48,49</sup> For example, con-A is a tetramer that binds to carbohydrates, specifically to glucose or mannose-like sites on the cell membrane.<sup>49</sup> Con-A and PHA bind equally well to T and B cells.<sup>48</sup> When con-A or PHA are soluble, they are mitogens for T cells (and not for B cells), whereas, when they are cross-linked to a surface and insoluble, they are mitogens for B cells (and not for T cells).<sup>50,51</sup> On the other hand, pokeweed mitogen, either soluble or bound, stimulates either T or B cells.<sup>51</sup> The B-cell mitogens lead to a nonspecific production of antibodies, particularly IgM, by the responding cells.<sup>52</sup>

Con-A and other lectins are believed to cross-link membrane surface carbohydrates. Possibly the antibody-like receptors are sometimes linked by their carbohydrate moieties, but other surface glycoproteins are more often linked. In particular,  $1.4 \times 10^6$  con-A receptors have been reported<sup>53</sup> on lymphocytes, substantially more than the expected  $10^5$  antibody receptors.<sup>5</sup> Similarly, from  $2 \times 10^6$  to  $12 \times 10^6$  receptors have been found and characterized for PHAs of various origins.<sup>54</sup>

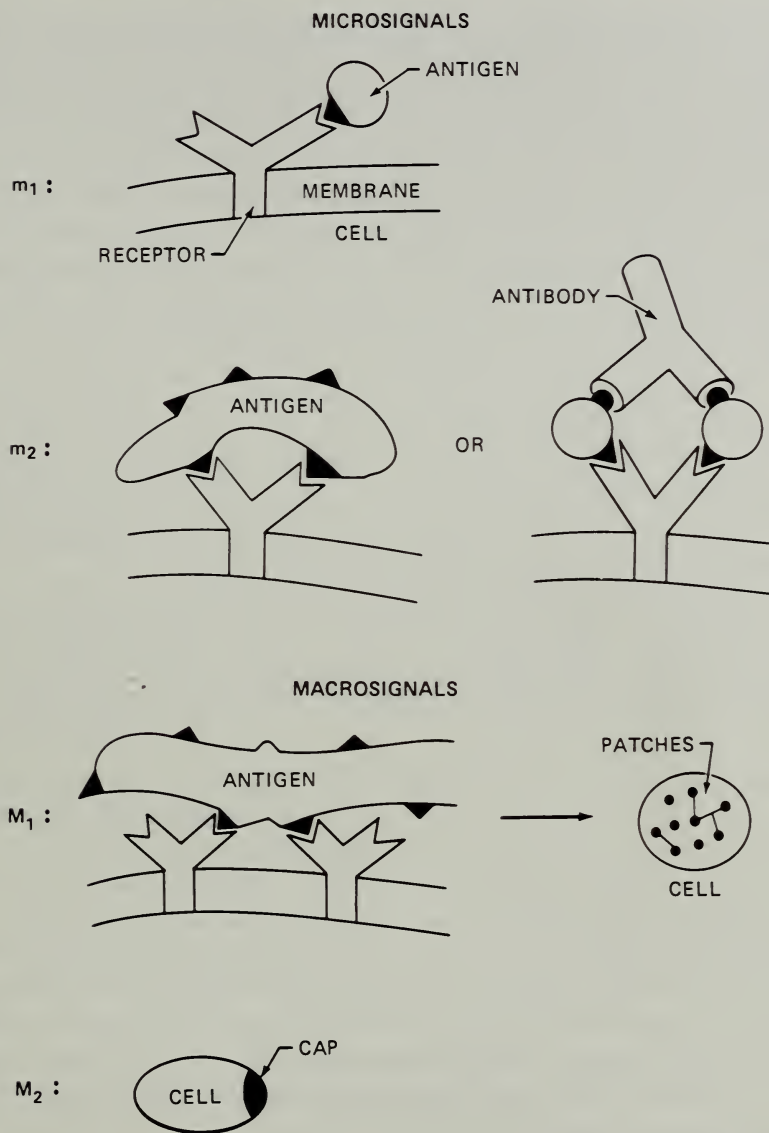


Fig. 1 Antigen configurations for the microsignals and macrosignals.

Soluble con-A concentrations of 10  $\mu\text{g/ml}$  were found to be optimal<sup>49</sup> for stimulating uptake of radioactive thymidine by mouse T cells in vitro; much higher concentrations may have been lethal. At concentrations  $\geq 10 \mu\text{g/ml}$ , con-A was reported to stabilize lymphocyte membranes<sup>53,55</sup> and to inhibit cap formation by anti-immunoglobulin. However, other investigators<sup>33</sup> found that con-A induced cap formation under slightly different conditions.

In attempting to interpret such experiments, we might find it helpful to bear in mind that homologous and heterologous sera, in which lymphocytes are



generally cultivated to maintain cell viability, appear to contain factors that can substantially inhibit or enhance mitogenic effects.<sup>5,6</sup> Some of the factors are straightforward; e.g., serum protein will bind some of the con-A.<sup>5,6</sup> However, there appear to be other factors which are less well understood but which may include mediators of the natural T- and B-cell interactions.<sup>5,6</sup>

Another interesting class of B-cell (but not T-cell) mitogens consists of "thymus-independent" antigens. These are highly multivalent antigens, usually of bacterial origin, which appear capable of triggering *in vivo* immune responses in the absence of T cells. They include lipopolysaccharides (LPS) from gram-negative bacteria,<sup>4,8,57-59</sup> pneumococcal polysaccharide,<sup>59</sup> polymerized flagellin,<sup>59</sup> purified protein derivative of tuberculin,<sup>60</sup> and various other agents.<sup>59</sup> These antigens have all been found (*in vitro*) to stimulate B cells to DNA synthesis and nonspecific antibody synthesis.<sup>59</sup> The mitogenic part of the LPS molecule is known to be lipid A, whereas the antigenic specificity is associated with the polysaccharide region.<sup>58</sup> Also, LPS is a potent adjuvant that can be used to convert a T-cell-dependent antigen into a T-cell-independent antigen and a tolerogenic signal into an immunogenic signal.<sup>58,61</sup>

The nonspecific lymphocyte mitogens presumably do not bind to antigen-combining sites on immunoglobulin receptors and therefore cannot deliver microsignals to the cells similar to the microsignals that arise from specific binding of antigen. The simplest conclusion is that both B and T cells can be induced to synthesize DNA and to divide by macrosignals in the absence of any microsignals. In addition, the stimulated B cells will secrete antibodies. Although both B- and T-cell mitogens probably cross-link membrane components, the requirements for the two kinds of cells differ. In particular, B cells seem to be stimulated by binding to repeated determinants fixed on a surface or on large molecules. From this point of view, we may predict that binding of a small T-cell-dependent antigen to a surface so as to present appropriately spaced and repeating determinants to the B-cell receptors might directly stimulate those B cells which can bind to the antigen. A possible example<sup>20</sup> was found on binding of an appropriate amount of DNP to polymeric flagellin. An antigen is thereby produced which at low doses stimulates strong anti-DNP responses in the apparent absence of T cells.

Mitosis does not appear to be clearly correlated with the induction of capping. Thus we may have capping without mitosis<sup>47</sup> and mitosis without capping.<sup>49</sup> The development of an appropriate ligand-receptor lattice on the cell surface may be sufficient to deliver a stimulating macrosignal ( $M_1$ ) to the cell. At present we can only detect effects of the signals, such as DNA synthesis and antibody secretion, in metabolically active cells. However, we may anticipate that, as the signals become better understood, their effects will be detected prior to gross changes in cell behavior. It has been reported<sup>62</sup> that cyclic GMP levels are greatly elevated in lymphocytes that have been stimulated by soluble PHA and con-A but cyclic AMP levels are little changed. This suggests that cyclic GMP serves as a "second messenger" in lymphocyte stimulation.

Even if the nonspecific mitogens use only macrosignals in stimulating cells, this does not mean that antigens may not deliver important and quite different microsignals. In particular, many of the thymus-independent antigens are effective as immunogens (or tolerogens) at far lower concentrations than as nonspecific mitogens. For example, doses of LPS of  $10^{-17}$  g are effective<sup>63</sup> in priming mice to give an enhanced secondary response, and a dose of  $10^{-9}$  g will give a primary response. In contrast, LPS concentrations around  $10 \mu\text{g/ml}$  are typically used to demonstrate *in vitro* nonspecific action.<sup>58</sup> Thus, when LPS binds to the immunoglobulin surface receptors, it appears far more effective than when it binds to other surface components. One possibility is that binding to the immunoglobulin receptors is much tighter than to other surface components and that *in vivo* a very small dose of LPS will end up mostly attached to the few cells for which it is an immunogen. A second possibility is that specific binding generates microsignals that, at least in conjunction with the appropriate macrosignals, are uncommonly effective. Finally, such antigens may be able to generate their own special microsignals when bound to receptors. For example, when LPS is attached to a cell by polysaccharide-receptor bonds, the lipid A moiety may be particularly effective in interacting with other membrane structures and generating uniquely effective microsignals. Such unique interactions would help to explain the very small amount of LPS which is effective in stimulating animals.

## INTERCELLULAR SIGNALING

For many antigens research<sup>17</sup> has recently established that the antigen must interact with both T and B cells before the B cells become stimulated to proliferate and secrete antibodies. In particular, it appears that the B cells must interact either directly with antigen-activated T cells or with T-cell products before they are stimulated. In a few cases investigators<sup>18,64</sup> have reported that activated T cells release a diffusible antigen-specific, antibody-like molecule (IgT) which, when combined with antigen and located on the surface of cells for which it is cytophilic,<sup>18,65</sup> is capable of stimulating specific B cells. There are many other reports (reviewed in Ref. 17) of cases in which T cells secrete nonspecific factors that activate or suppress B-cell responses. In this paper we cannot examine such experiments in any detail, but we wish to consider the kinds of signals that may be involved in such intercellular communication. In particular, we wish to consider what the T cells may say to the B cells, since that aspect of the communication has been most thoroughly studied.

A possibility suggested<sup>18</sup> by the antigen-specific T-cell products is that IgT molecules serve to aggregate (cross-link) the antigen (perhaps on the surface of the T cell but more probably on the surface of a macrophage<sup>65</sup>) so that presentation of the antigen to the B cell encourages lattice formation and generation of a stimulating macrosignal. Alternatively, the IgT might bind to

other surface receptors on B cells and generate microsignals activating the B cell to antigen-IgT complexes. However, it has been reported that IgT binds preferentially to macrophages.<sup>66</sup> In either case a highly specific interaction between T-cell products and B cells or macrophages is indicated by the finding<sup>66</sup> that antigen-specific collaboration between T and B cells is possible only if the collaborating cells have the same histocompatibility antigens, e.g., H-2 in mice. This suggests that microsignals involving histocompatibility antigens may mediate the collaboration.

A less efficient microsignaling mechanism would involve diffusible T-cell products that are not antigen specific but are labile; binding of these products to any nearby B cell would signal that cell to respond to bound antigen. With this scheme there would be a nonspecific synergism between responses to different antigens, i.e., T cells stimulated by one antigen could signal B cells binding a second and different antigen. Moreover, T cells primed to a particular antigen should be effective in stimulating B cells to respond to another antigen; this conflicts with many observations but is in agreement with others.<sup>17</sup> Therefore we do not believe that diffusible T-cell products which are not antigen-specific can be of primary importance for triggering normal immune responses *in vivo*.

Thus it appears that T cells probably communicate with B cells by releasing, or bearing, antigen-binding factors, which may be the T-cell receptors. These factors serve to aggregate the antigen, perhaps thereby presenting it to the B cell so as to produce a mitogenic macrosignal and perhaps also binding specifically to B cells so as to produce microsignals. More complex intercellular signaling procedures can also be imagined. For example, a macrophage binding the IgT-antigen complex may not only serve to present a stimulating array of antigen and IgT determinants but may also emit other factors that bind to and stimulate B cells.

The requirements for antigen-activation of T cells are even less clear. The T cells can be either activated or paralyzed by antigen,<sup>21</sup> but whether either process requires interaction between T cells or between T-cell products and T cells is not known. These questions could be approached by separating T-cell populations on the basis of their epitope-binding properties, but such experiments have apparently not been done.

## TRANSLATION OF THE SIGNAL

We presume that the precursors of antibody-secreting cells and of the thymus-derived cells participating in immune responses are, prior to contact with antigen, small lymphocytes mainly in a resting ( $G_0$ ) phase. Upon receiving appropriate signals involving bound antigen, the cells are induced to multiply and to differentiate. The cells multiply so that, for example, the number of antibody-secreting cells increases with time; they also appear to differentiate so that, for example, increasing fractions of the cells become plasma cells secreting



IgG. Given a stimulating signal, is the cell response predetermined, or can it be modulated by other factors? In particular, is it possible to get multiplication without differentiation or, alternatively, to get differentiation without multiplication? With regard to the former possibility, we note that clones of antibody-producing cells have been propagated<sup>67</sup> for many ( $\sim 100$ ) cell divisions by using serial transfer of limiting dilutions of spleen cells into irradiated syngenic mice. Thus multiplication does not necessarily imply rapid differentiation of all daughter cells.

There have been numerous suggestions of antigen-induced differentiation without multiplication. For example, it is commonly found (e.g., Ref. 63) that small doses of antigen give rise to no detectable primary response but prime the animal to give an enhanced response to a subsequent injection of antigen. One explanation is that the initial dose stimulated cells to advance part of the way from phase  $G_0$  to  $G_1$  and left them more easily made fully cycling. In this regard lectin stimulation can result in increased antibody secretion prior to DNA synthesis.<sup>56</sup> However, it is usually possible that some cell division may have occurred but escaped detection.<sup>16</sup> These alternatives can be distinguished only by careful quantitative work at the cellular level. A different kind of (terminal) differentiation has been suggested by findings of antibody production during tolerance induction,<sup>68</sup> but again it is difficult to rule out some mitosis during tolerance induction.<sup>69</sup>

We are not aware of any general reasons why contact with antigen may not alter the cell phenotype in a more or less stable manner, without involving mitosis, and indeed other agents such as hormones and cyclic AMP affect cells in this manner, albeit reversibly. We therefore accept the possibility that binding of antigen may, under appropriate conditions, signal a cell to differentiate without multiplying, to multiply and differentiate, or to multiply with little differentiation. Microsignals, arising from bound antigen and possibly also from bound antibodies such as IgT and other factors, and macrosignals presumably form the vocabulary for instructing the cell which path to take. In addition, it appears that signals involving T-cell products are required for switching cells from IgM to IgG production and for selecting cells for high-affinity IgG production.<sup>17</sup>

The cell multiplication caused by a primary exposure to antigen ordinarily will leave an animal with many "memory cells" that enable it to give a more rapid and effective secondary response on subsequent exposure to the same antigen. These memory cells are probably similar to the virgin antigen-sensitive lymphocytes in that they are in  $G_0$  phase and can be stimulated by binding antigen, but, in detail, their binding and responses may be rather different.

## TOLERANCE VS. IMMUNITY

Exposure to antigen may leave an animal with an enhanced capability (immunity) to respond to the same antigen or with a diminished capability



(tolerance) to respond to the same antigen. These capabilities may apply to a humoral response or to a cell-mediated response or to both. In general, it is much easier to tolerize a very young animal.<sup>68</sup> This fact is in agreement with a basic postulate of the original clonal selection theory,<sup>1</sup> whereby tolerance of self-antigens is supposed to be achieved by killing off nascent clones of self-reactive cells when cells encounter antigen at an early phase of maturation.

Many antigens can also induce tolerance in adult animals. Whether a particular antigen induces tolerance or immunity depends on many factors:<sup>68</sup> on the dose of antigen (with very high and sometimes very low doses favoring humoral tolerance); on its state of aggregation (with deaggregation favoring tolerance); and on the degree of hapten conjugation,<sup>20</sup> route of injection, etc. Bretscher and Cohn<sup>70,71</sup> have proposed that these examples of tolerance induction reflect the normal mechanisms by which self-tolerance is established in young animals and maintained in adult animals. The proposed mechanism for humoral responses is that binding of antigen to B- or to T-cell receptors always delivers a paralytic signal, called signal ①, to the cell. Associative antibody, IgT, bound to the antigen can, however, deliver an inductive signal ② to B or T cells. Whether tolerance or immunity results then depends on the absolute number and ratio of signals ① and ②. Bretscher and Cohn further proposed that T cells maturing in the absence of antigen will gradually release IgT. Therefore IgT is present for foreign antigens but not for self-antigens. According to this view, so-called "thymus-independent antigens" are simply antigens that bind IgT uncommonly well.

This theory has a number of very attractive aspects. It relates self-tolerance to the experimental induction of tolerance in adult animals and interprets tolerance induction in a semi-quantitative manner.<sup>71</sup> It explains the termination of tolerance by cross-reacting antigens and predicts cell collaboration and diffusible IgT.

In the context of this paper, it would be natural to regard signal ① as a microsignal arising from binding of antigen to receptor and signal ② as a microsignal arising from binding of IgT to some different kind of receptor that is specific for a common portion of the IgT molecule.\* In this view macrosignals would be unimportant. However, according to Feldmann's experiments,<sup>65</sup> IgT binds to macrophages and not to B cells, and, if this is so, signal ② might more likely be a macrosignal arising from aggregation of antigen on the macrophage surface or possibly an unknown microsignal delivered to the B cell by the macrophage. There are also difficulties in interpreting signal ① as a simple microsignal. If cells were paralyzed by simply binding antigen, then *in vitro* paralysis should be easily obtained by exposure of cells to antigen. However,

---

\*In an early version,<sup>72</sup> signal ① was viewed as an  $m_1$  signal and signal ② as sometimes an  $m_2$  signal.

such procedures do not, in general, induce tolerance.<sup>6,8</sup> Therefore signal ① appears to be more complicated.

Feldmann<sup>31</sup> has argued that cell-bound antigen-antibody complexes are often tolerogenic when in the absence of macrophages. It is reasonable that antigen-antibody complexes should modulate immune responses. For example, a time during an immune response when sufficient antibody has been produced for most antigen to be bound in complexes might be a good time to moderate the clonal expansion or to switch from IgM to IgG synthesis. To relate this to self-tolerance, we could postulate that immature T cells release a different kind of associative antibody, call it Igt, which is not cytophilic and which in combination with antigen stops further maturation of the T cell and paralyzes B cells. The T cells in the absence of antigen would mature to produce IgT. Therefore adult animals would produce Igt for self-antigens and mainly IgT for foreign antigens. Such a model, though distressingly complex, would provide an explanation for the suppression of specific responsiveness by T cells<sup>17</sup> and for serum factors mediating self-tolerance.<sup>73</sup>

Without pursuing these complications further, we conclude that the paralytic and inductive signals ① and ② proposed by Bretscher and Cohn do not seem to be simple microsignals. With regard to such general points as that the induction of tolerance is favored by high antigen doses, many models could be proposed for such effects. For example, the receptor-antigen lattice will clearly depend on antigen concentration. Model calculations might suggest lattice parameters that are tolerogenic as opposed to immunogenic.

## DISCUSSION

We began by classifying the signals that antigen binding can transmit to immunocompetent cells as microsignals and macrosignals. A microsignal is defined as arising from the binding of one antigen molecule to one Ig-receptor molecule either at one binding site ( $m_1$  signal) or at two or more binding sites ( $m_2$  signal). An  $m_1$  signal might be a conformational change in the receptor molecule or a stabilization of receptor orientation relative to the plane of the membrane. We found no direct evidence that  $m_1$  signals are of any importance. In particular, there is no evidence that binding of monovalent antigens to antibodies produces significant conformational changes in those protein molecules. In addition, binding of haptens seems to have no significant effect on cell behavior beyond simply masking the receptors. Therefore we conclude that  $m_1$  signals are probably not sufficient to determine lymphocyte multiplication or differentiation. We presume that formation of antigen-receptor bonds is the essential antigen-recognizing step that must be involved in triggering cell response. However, it appears possible that the individual bonds may not signal anything of importance to the cell (i.e., there may be no  $m_1$  signals) and may serve merely as points of antigen attachment.

We noted, however, the possibility that an antigen-receptor bond might require a certain duration ( $\geq$  sec) in order to deliver an effective  $m_1$  signal. For example, a time for diffusion (translational or rotational) might be necessary before the receptor-antigen complex could find itself in an appropriate location or orientation for delivering a signal. Endocytosis of antigen would also take a fairly long time. In either case long durations of antigen binding could ordinarily be achieved only by multivalent or linked antigens; therefore it would be difficult to distinguish effective  $m_1$  signals of long duration from effects of cross-linking receptors. In principle, we could stabilize  $m_1$  bonds by using techniques of affinity labeling, and it would be of interest to see if such stabilization had any effect on cell behavior.

An  $m_2$  signal will involve an obvious conformational change in a (bivalent) receptor, namely a stabilization of the hinge angle. Such interactions may play a special role in the induction or suppression of anti-idiotypic antibodies. They may also be important when small antigen-antibody complexes bind to a cell. However, in view of the steric requirements on antigen for  $m_2$  binding, we doubt that such signals are of general importance.

Macroscopic signals were defined as those involving the cross-linking of different receptors by multivalent antigens or by antigen-antibody complexes. Signals that arise from passive diffusion and aggregation of receptors in the plane of the membrane were said to be  $M_1$  signals, whereas signals involving active cell metabolism and motion of the membrane were  $M_2$  signals. Multivalent antigens, bound to the cell surface, serve as nucleation centers for the formation of antigen-receptor lattices on the cell surface. The lattice characteristics will depend on the diffusion rate of receptors in the membrane and on antigen size, valence, shape, and concentration. With a high antigen concentration, it may take of the order of a minute at  $37^\circ\text{C}$  for a lattice to be well developed. Lattice formation is responsible for the phenomenon of patching, and the active movement of the lattice to one pole is capping. Capping is frequently followed by endocytosis of the lattice, but antigen ingestion is not required for the stimulation of antibody production.<sup>74</sup>

Various multivalent ligands, including lectins and thymus-independent antigens, are nonspecific lymphocyte mitogens and induce polyclonal antibody synthesis in B cells. These ligands appear to act by cross-linking surface components, and their activity suggests that macrosignals are a sufficient stimulus for lymphocyte multiplication. In particular, B cells (but not T cells) appear to be stimulated by a repeating array of binding sites, including sites fixed to a surface. This suggests that thymus-dependent antigens might become thymus independent by fixing them to a suitable surface. On the other hand, cross-linking of receptors does not always lead to lymphocyte stimulation but can even produce tolerance instead.

For a humoral response to many antigens, the antigen must be recognized by both T and B cells. In some circumstances the activated T cells release a diffusible product (IgT) that is cytophilic for macrophages, and an important



function of the T cells and their products may simply be to aggregate antigen and present it to the B cells so as to favor a stimulating macrosignal. However, it appears likely that other kinds of microsignals, e.g., interactions between IgT and B-cell receptors, are involved. Requirements for T-cell activation are even less clear. Once macrosignals have been invoked as important determinants of cell behavior, it becomes more difficult to anticipate conditions that should be expected to promote tolerance rather than immunity.

The system of humoral immunity presumably evolved, at least in large part, for protection against invading viruses and bacteria and their toxic by-products. The microbes would naturally present themselves to responsive cells as highly multivalent antigens generating strong macrosignals. Initially it might not be desirable for the system to respond much to tiny fragments of the invading microbes since these could not represent viable microbes, and their presence might be negatively correlated with success in defeating the invasion. However, many of these products are toxic so that it also becomes valuable to produce antibodies against the fragments. Perhaps a compromise evolved in which various kinds of fragment (antigen)-antibody complexes were used to regulate the responses to smaller antigens. If, moreover, the humoral-response system evolved as an addition to an existing system of cellular immunity, which involved thymus-derived cells, then it is quite reasonable that IgT-antigen complexes should be highly stimulating to B cells. It is also reasonable that the requirements for antigen activation of T cells may be rather different from the requirements for antigen stimulation of B cells.

When considering the binding of antigen-antibody complexes to lymphocyte surfaces, it becomes more difficult to distinguish effects of microsignals and macrosignals since two or more different kinds of molecules (antigen and antibody) may be interacting with their specific receptors. Nevertheless, we suggest that it is useful to attempt to distinguish between signals that arise from specific binding between individual molecules and signals that arise from a more or less coherent alteration of large areas of cell membrane, such as accompany lattice formation.

## ACKNOWLEDGMENTS

Work was performed under the auspices of the U. S. Atomic Energy Commission.

## REFERENCES

1. F. M. Burnet, *The Clonal Selection Theory of Immunity*, Vanderbilt University Press, Nashville, 1959.
2. N. L. Warner, Surface Immunoglobulins on Lymphoid Cells, in *Contemporary Topics in Immunology*, Vol. 1, M. G. Hanna, Jr. (Ed.), pp. 87-117, Plenum Publishing Corporation, New York, 1972.



3. J. J. Marchalonis, R. E. Cone, and J. L. Atwell, Isolation and Partial Characterization of Lymphocyte Surface Immunoglobulins, *J. Exp. Med.*, **135**: 956-971 (1972).
4. I. Goldschneider and R. B. Cogen, Immunoglobulin Molecules on the Surface of Activated T Lymphocytes in the Rat, *J. Exp. Med.*, **138**: 163-175 (1973).
5. E. Rabellino, S. Colon, H. M. Grey, and E. R. Unanue, Immunoglobulins on the Surface of Lymphocytes, *J. Exp. Med.*, **133**: 156-167 (1971).
6. E. Vitetta, S. Bauer, and J. W. Uhr, Cell Surface Immunoglobulins. II. Isolation and Characterization of Immunoglobulin from Mouse Splenic Lymphocytes, *J. Exp. Med.*, **134**: 242 (1971).
7. N. M. Green, Electron Microscopy of the Immunoglobulins, *Advan. Immunol.*, **11**: 1 (1969).
8. V. R. Sarna, E. W. Silvertown, D. R. Davies, and W. D. Terry, X-Ray Structure of  $\gamma$ G1 Immunoglobulin, *J. Biol. Chem.*, **246**: 3753-3759 (1972).
9. S. J. Singer and G. L. Nicholson, The Fluid Mosaic Model of the Structure of Cell Membranes, *Science*, **175**: 720-731 (1972).
10. E. S. Vitetta and J. W. Uhr, Cell Surface Immunoglobulins. V. Release from Murine Splenic Lymphocytes, *J. Exp. Med.*, **136**: 676-696 (1972).
11. M. W. Fanger, D. A. Hart, J. V. Wells, and A. Nisonoff, Requirement for Cross-Linkage in the Stimulation of Transformation of Rabbit Peripheral Lymphocytes by Antiglobulin Reagents, *J. Immunol.*, **108**: 1484-1492 (1970).
12. D. Wernet, E. S. Vitetta, J. W. Uhr, and E. A. Boyce, Synthesis, Intracellular Distribution, and Secretion of Immunoglobulin and H-2 Antigen in Murine Splenocytes, *J. Exp. Med.*, **138**: 847-857 (1973).
13. R. A. Lerner, P. J. McConahey, I. Jansen, and F. J. Dixon, Synthesis of Plasma Membrane-Associated and Secretory Immunoglobulin in Diploid Lymphocytes, *J. Exp. Med.*, **135**: 136-149 (1972).
14. J. D. Wilson, G. J. V. Nossal, and H. Lewis, Metabolic Characteristics of Lymphocyte Surface Immunoglobulins, *Eur. J. Immunol.*, **2**: 225-232 (1972).
15. G. W. Siskind and B. Benacerraf, Cell Selection by Antigen in the Immune Response, *Advan. Immunol.*, **10**: 1-50 (1969).
16. G. I. Bell, Mathematical Model of Clonal Selection and Antibody Production, *J. Theor. Biol.*, **29**: 191-232 (1970).
17. D. H. Katz and B. Benacerraf, The Regulatory Influence of Activated T Cells on B Cell Responses to Antigen, *Advan. Immunol.*, **15**: 1-94 (1972).
18. M. Feldmann and A. Basten, Cell Interactions in the Immune Response In Vitro. III. Specific Collaboration Across a Cell Impermeable Membrane, *J. Exp. Med.*, **136**: 49-67, 1972.
19. H. C. Claman and D. E. Mosier, Cell-Cell Cooperation in Antibody Formation, *Progr. Allergy*, **16** (1972).
20. M. Feldmann, Induction of Immunity and Tolerance In Vitro by Hapten Protein Conjugates. I. The Relationship Between the Degree of Hapten Conjugation and the Immunogenicity of Dinitrophenylated Polymerized Flagellin, *J. Exp. Med.*, **135**: 735-753 (1972).
21. J. M. Chiller and W. O. Weigle, Cellular Basis of Immunological Unresponsiveness, in *Contemporary Topics in Immunobiology*, Vol. 1, M. G. Hanna, Jr. (Ed.), pp. 119-142, Plenum Publishing Corporation, New York, 1972.
22. G. I. Bell and C. P. DeLisi, Antigen Binding to Receptors on Immunocompetent Cells, *Cell. Immunol.*, **10**: 415-431 (1974).
23. I. Pecht, D. Givol, and M. Sela, Dynamics of Hapten-Antibody Interaction. Studies on a Myeloma Protein with Anti-2,4-Dinitrophenyl Specificity, *J. Mol. Biol.*, **67**: 421 (1972).
24. D. E. Koshland, Jr., Protein Shape and Biological Control, *Sci. Amer.*, **229**: 52-64 (October 1973).

25. H. Metzger, The Antigen Receptor Problem, *Annu. Rev. Biochem.*, **39**: 889-928 (1970).
26. C. L. Hornick and F. Karush, Antibody Affinity. III. The Role of Multivalency, *Immunochemistry*, **9**: 325-340 (1972).
27. L. A. Steiner and G. Feher, A Search for Changes in Antibody Conformation Utilizing Spin-Labeled Probes, *Biophys. Soc. Abstr.*, **11**: 185a (1971).
28. D. A. Holowka, A. D. Strosberg, J. W. Kimball, E. Haber, and R. E. Cathou, Changes in Intrinsic Circular Dichroism of Several Homogeneous Anti-Type III Pneumococcal Antibodies on Binding of a Small Hapten, *Proc. Nat. Acad. Sci. U. S. A.*, **69**: 3399-3403 (1972).
29. F. Borek, Molecular Size and Shape of Antigen, in *Immunogenicity*, Vol. 25 of *Frontiers of Biology*, F. Borek (Ed.), pp. 45-86, North-Holland Publishing Company, Amsterdam, 1972.
30. N. J. Jerne, The Immune System, *Sci. Amer.*, **229**: 52-60 (July 1973).
31. M. Feldmann, Induction of Immunity and Tolerance In Vitro by Hapten Protein Conjugates. III. Hapten Inhibition Studies of Antigen Binding to B Cells in Immunity and Tolerance, *J. Exp. Med.*, **136**: 532-545 (1973).
32. C. D. Frye and M. Edidin, Rapid Intermixing of Cell Surface Antigens After Formation of Mouse-Human Heterokaryons, *J. Cell Sci.*, **7**: 319-335 (1970).
33. E. Unanue, W. P. Perkins, and M. J. Karnovsky, Ligand-Induced Movement of Membrane Macromolecules. I. Analysis by Immunofluorescence and Ultrastructural Radioautography, *J. Exp. Med.*, **136**: 885-906 (1972).
34. J. M. Davie and W. E. Paul, Receptors on Immunocompetent Cells. IV. Direct Measurement of Avidity of Cell Receptors and Cooperative Binding on Multivalent Ligands, *J. Exp. Med.*, **135**: 643-659 (1972).
35. R. B. Taylor, W. P. H. Duffus, M. C. Raff, and S. de Petris, Redistribution and Pinocytosis of Lymphocyte Surface Immunoglobulin Molecules Induced by Anti-Immunoglobulin Antibody, *Nature (London) New Biol.*, **233**: 225-229 (1971).
36. F. Loor, L. Forni, and B. Pernis, Dynamic State of the Lymphocyte Membrane. Factors Affecting the Distribution and Turnover of Surface Immunoglobulins, *Eur. J. Immunol.*, **2**: 203-212 (1972).
37. M. J. Karnovsky, E. R. Unanue, and M. Leventhal, Ligand Induced Movement of Lymphocyte Membrane Macromolecules. II. Mapping of Surface Moieties, *J. Exp. Med.*, **136**: 907-930 (1972).
38. E. R. Unanue, M. J. Karnovsky, and H. D. Engers, Ligand-Induced Movement of Lymphocyte Membrane Macromolecules. III. Relationship Between the Formation and Fate of Anti-Ig—Surface-Ig Complexes and Cell Metabolism, *J. Exp. Med.*, **137**: 675-689 (1973).
39. S. de Petris and M. C. Raff, Normal Distribution, Patching, and Capping of Lymphocyte Surface Immunoglobulin Studied by Electron Microscopy, *Nature (London) New Biol.*, **241**: 257-259 (1973).
40. E. Diener and V. H. Paetkau, Antigen Recognition: Early Surface Receptor Phenomena Induced by Binding of a Tritium-Label Antigen, *Proc. Nat. Acad. Sci. U. S. A.*, **69**: 2364-2368 (1972).
41. K. C. Lee, R. E. Langman, V. H. Paetkau, and E. Diener, Antigen Recognition. III. Effect of Phytomitogens on Antigen-Receptor Capping and the Immune Response In Vitro, *Eur. J. Immunol.*, **3**: 306-309 (1973).
42. G. M. Edelman, I. Yahara, and J. L. Wang, Receptor Mobility and Receptor-Cytoplasmic Interactions in Lymphocytes, *Proc. Nat. Acad. Sci. U. S. A.*, **70**: 1442-1446 (1973).
43. M. Edidin and A. Weiss, Antigen Cap Formation in Cultured Fibroblasts: A Reflection of Membrane Fluidity and of Cell Motility, *Proc. Nat. Acad. Sci. U. S. A.*, **69**: 2456-2459 (1972).

44. S. de Petris, M. C. Raff, and L. Mallucci, Ligand-Induced Redistribution of Concanavalin A on Normal, Trypsinized, and Transformed Fibroblasts, *Nature (London) New Biol.*, **244**: 275-278 (1973).
45. G. Nicolson, Temperature-Dependent Mobility of Concanavalin A Sites on Tumor Cell Surfaces, *Nature (London) New Biol.*, **243**: 218-220 (1973).
46. V. Santer, A. D. Bankhurst, and G. J. V. Nossal, Ultrastructural Distribution of Surface Immunoglobulin Determinants on Mouse Lymphoid Cells, *Exp. Cell. Res.*, **72**: 377-386 (1972).
47. D. H. Katz and E. R. Unanue, Immune Capacity of Lymphocytes After Cross-Linking of Surface Immunoglobulin Receptors by Antibody, *J. Immunol.*, **109**: 1022-1030 (1972).
48. G. Janossy, J. H. Humphrey, M. B. Pepys, and M. F. Greaves, Complement Independence of Stimulation of Mouse Splenic B Lymphocytes by Mitogens, *Nature (London) New Biol.*, **245**: 108-112 (1973), and the references in the article.
49. G. M. Edelman, Antibody Structure and Molecular Immunology, *Science*, **180**: 830-840 (1973).
50. J. Andersson, G. M. Edelman, G. Möller, and O. Sjöberg, Activation of B Lymphocytes by Locally Concentrated Concanavalin A, *Eur. J. Immunol.*, **2**: 233-235 (1972).
51. M. F. Greaves and S. Bauminger, Activation of T and B Lymphocytes by Insoluble Phytomitogens, *Nature (London) New Biol.*, **235**: 67-70 (1972).
52. J. Andersson and F. Melchers, Induction of Immunoglobulin M Synthesis and Secretion in Bone-Marrow-Derived Lymphocytes by Locally Concentrated Concanavalin A, *Proc. Nat. Acad. Sci. U. S. A.*, **70**: 416-420 (1973).
53. I. Yahara and G. M. Edelman, Restriction of the Mobility of Lymphocyte Immunoglobulin Receptors by Concanavalin A, *Proc. Nat. Acad. Sci. U. S. A.*, **69**: 608-616 (1972).
54. C. A. Presant and S. Kornfeld, Characterization of the Cell Surface Receptors for *Agaricus bisporus* Hemagglutinin, *J. Biol. Chem.*, **247**: 6937-6945 (1972).
55. G. M. Edelman, I. Yahara, and J. L. Wang, Receptor Mobility and Receptor-Cytoplasmic Interactions in Lymphocytes, *Proc. Nat. Acad. Sci. U. S. A.*, **70**: 1442-1446 (1973).
56. A. Coutinho, G. Möller, J. Andersson, and W. W. Bullock, In Vitro Activation of Mouse Lymphocytes in Serum-Free Medium: Effect of T and B Cell Mitogens on Proliferation and Antibody Synthesis, *Eur. J. Immunol.*, **3**: 299-306 (1973).
57. J. Andersson, O. Sjöberg, and G. Möller, Induction of Immunoglobulin and Antibody Synthesis In Vitro by Lipopolysaccharides, *Eur. J. Immunol.*, **2**: 349-353 (1972).
58. J. M. Chiller, B. J. Skidmore, D. C. Morrison, and W. O. Weigle, Relationship of the Structure of Bacterial Lipopolysaccharide to Its Function in Mitogenesis and Adjuvanticity, *Proc. Nat. Acad. Sci. U. S. A.*, **70**: 2129-2133 (1973).
59. A. Coutinho and G. Möller, B Cell Mitogenic Properties of Thymus-Independent Antigens, *Nature (London) New Biol.*, **245**: 12-14 (1973).
60. B. M. Sultzter and B. S. Nilsson, PPD-Tuberculin—a B-Cell Mitogen, *Nature (London) New Biol.*, **240**: 198-200 (1972).
61. J. M. Chiller and W. O. Weigle, Termination of Tolerance to Human Gamma Globulin in Mice by Antigen and Bacterial Lipopolysaccharide, *J. Exp. Med.*, **137**: 740-750 (1973).
62. J. W. Hadden, E. M. Hadden, M. K. Haddox, and N. D. Goldberg, Guanosine 3' : 5'-Cyclic Monophosphate: A Possible Intracellular Mediator of Mitogenic Influences in Lymphocytes, *Proc. Nat. Acad. Sci. U. S. A.*, **69**: 3024-3027 (1972).
63. J. A. Rudbach, Molecular Immunogenicity of Bacterial Lipopolysaccharide Antigens: Establishing a Quantitative System, *J. Immunol.*, **106**: 993-1001 (1971).
64. H. Yu and J. Gordon, Helper Specific Function in Antibody Synthesis Mediated by Soluble Factor(s), *Nature (London) New Biol.*, **244**: 20-21 (1973).



65. M. Feldmann, Cell Interactions in the Immune Response In Vitro. V. Specific Collaboration via Complexes of Antigen and Thymus-Derived Cell Immunoglobulins, *J. Exp. Med.*, **136**: 737-760 (1972).
66. D. H. Katz, T. Hamaoka, M. E. Dart, and B. Benacerraf, Cell Interactions Between Histoincompatible T and B Lymphocytes. The H-2 Gene Complex Determines Successful Physiologic Lymphocyte Interactions, *Proc. Nat. Acad. Sci. U. S. A.*, **2624-2628** (1973).
67. A. R. Williamson and B. A. Askonas, Senescence of an Antibody-Forming Cell Clone, *Nature (London) New Biol.*, **238**: 337-339 (1972).
68. W. O. Weigle, Immunological Unresponsiveness, *Advan. Immunol.*, **16**: 61-122 (1973).
69. G. I. Bell, Mathematical Model of Clonal Selection and Antibody Production. III. The Cellular Basis of Immunological Paralysis. *J. Theor. Biol.*, **33**: 379-398 (1971).
70. P. Bretscher and M. Cohn, A Theory of Self-Nonself Discrimination, *Science*, **169**: 1042-1048 (1970).
71. P. Bretscher, The Control of Humoral and Associative Antibody Synthesis, *Transplant. Rev.*, **11**: 217-267 (1972).
72. P. Bretscher and M. Cohn, Minimal Model for the Mechanism of Antibody Induction and Paralysis by Antigen, *Nature (London)*, **220**: 444-448 (1968).
73. P. W. Wright, R. E. Hargreaves, S. C. Bansal, I. D. Bernstein, and K. E. Hellström, Allograft Tolerance: Presumptive Evidence That Serum Factors from Tolerant Animals That Block Lymphocyte-Mediated Immunity In Vitro Are Soluble Antigen-Antibody Complexes, *Proc. Nat. Acad. Sci. U. S. A.*, **70**: 2539-2543 (1973).
74. G. J. V. Nossal and G. L. Ada, *Antigens, Lymphoid Cells, and the Immune Response*, Academic Press, Inc., New York, 1971.

## APPENDIX: THE DIFFUSION LIMIT TO LATTICE-FORMATION RATES

We approximate diffusion in the plane of the membrane by diffusion on a plane surface. The diffusion coefficient,  $D$ , is defined by the requirement that if the receptor density,  $N(r)$ , per unit area, has a gradient  $\nabla N$ , then there is a current  $-D\nabla N$ , which represents the number of receptors crossing a unit length per unit time. The steady-state diffusion equation in polar coordinates, with  $r$  the distance from the epitope center and circular symmetry, is

$$\frac{D}{r} \frac{d}{dr} \left( r \frac{dN(r)}{dr} \right) = 0 \quad (1)$$

To get a diffusion limit to the receptor-epitope reaction rate, we assume that any receptor that gets to  $r = r_0$  is absorbed. Thus we solve Eq. 1 subject to the boundary conditions  $N(r_0) = 0$  and  $N(R) = N_0$ , where  $R$  is some radius large compared to  $r_0$ . The result is

$$N(r) = N_0 \frac{\ln(r/r_0)}{\ln(R/r_0)} \quad (2)$$

The inward flow of receptors across  $r = r_0$ ,  $J(r_0)$ , is  $2\pi r_0 D (dN/dr)_{r=r_0}$  or



$$J(r_0) = \frac{2\pi DN_0}{\ln(R/r_0)} \quad (3)$$

Since  $N_0$  is the receptor density far away from the combining site,  $N_0$  equals  $1/d^2$ , with  $d$  a distance between receptors. Moreover, we wish  $N(r)$  to be about  $N_0$  when  $r = d$ , i.e.,  $R \approx d$ . Hence

$$J(r_0) \approx \frac{2\pi D/d^2}{\ln(d/r_0)} \quad (4)$$

The reciprocal of this quantity represents a mean diffusion time for establishing a secondary bond, i.e.,

$$t_d \approx \frac{d^2}{D} \frac{\ln(d/r_0)}{2\pi} \quad (5)$$

If  $d \approx 45$  nm and  $r_0 \approx 1$  nm, the numerical factor multiplying  $d^2/D$  is 0.6, and it was set to 1 in the qualitative discussion of the main part of this paper. Of course, the epitope may move as well as the receptors; so these arguments cannot be precise.

In three dimensions, these arguments give precisely the Smoluchowski equation,  $k_a = 4\pi rD$ , for diffusion-limited forward rate constants.

# HETEROGENEITY OF ANTIBODY-BINDING AFFINITY

GREGORY W. SISKIND\*

Division of Allergy and Immunology, Department of Medicine,  
Cornell University Medical College, New York, New York

---

## ABSTRACT

The antibody response of an individual animal to a haptenic determinant is highly heterogeneous with regard to affinity. Average affinity increases progressively with time after immunization. The rate of increase is greater after lower doses of antigen. Tolerance induction tends to depress mainly high-affinity antibody synthesis, whereas passive antibody mainly effects low-affinity antibody production.

It appears probable that some form of clonal selection<sup>1</sup> mechanism operates in the process of induction of antibody synthesis by B lymphocytes. It is assumed in such a theory that cells are restricted with regard to the specificity of the antibody that they can synthesize and that this restriction occurs prior to antigen injection and without the necessity for the presence of antigen. B lymphocytes are presumed to have on their surface antibody molecules with binding properties identical to the binding property of the antibody produced by the particular cell and its progeny after stimulation by antigen.<sup>2</sup> In essence, antigen interacts with cells having cell-surface associated antibody molecules capable of binding the particular antigen. Interaction of antigen (perhaps after some preliminary processing or localization) with cell-associated antibody triggers the particular cell to proliferate and secrete antibody. This selective stimulation, on the basis of interaction of antigen with cell-associated antibody, would be responsible for the specificity observed in the immune response.

According to this theory a simple relationship should exist between the binding properties of the serum antibodies and those of the cell-associated

---

\*Career Scientist of the Health Research Council of the City of New York under Investigatorship I-593.

TABLE 1

EFFECT OF TIME AFTER IMMUNIZATION ON ANTIBODY AFFINITY\*

Time after immunization, days	Affinity ( $-\Delta F_I^0$ 35%), kcal/mole
14	9.06 $\pm$ 0.46
28	10.25 $\pm$ 0.44
90	11.31 $\pm$ 0.24
360	11.46 $\pm$ 0.34

\*A population of 64 adult rabbits (half male and half female) was immunized with 0.5 mg DNP-BGG in complete Freund's adjuvant and bled at the times indicated. Antibody affinity was determined, with DNP-glycine as ligand, by the Farr technique. "Average" affinities were calculated from the region of the binding curves falling between 1 and 35% of antibody-binding sites occupied by hapten. Data are summarized from Werblin et al.<sup>1,4</sup> and are presented as mean  $\pm$  standard deviation.

antibodies present on the population of B lymphocytes stimulated to synthesize antibody.<sup>2</sup> Since antibody-forming cells differentiate with respect to the specificity (affinity) of the antibody they produce prior to antigen exposure, one would expect that the populations of antibody molecules would be heterogeneous with respect to affinity for the antigenic determinant. Furthermore, one would expect that high-affinity antibody-producing cells would preferentially bind antigen and thus be preferentially stimulated to proliferate and to secrete antibody. This would be especially significant in the presence of low concentrations of antigen when only high-affinity antibody-forming cells would bind significant amount of antigen.

Previous experimental results have generally agreed with these and other predictions based on such a theoretical framework. Antihapten antibody produced by individual animals is generally highly heterogeneous.<sup>3-6</sup> Average affinity has been shown<sup>3,7,8</sup> to increase progressively with time after immunization (Table 1). The rate of increase in affinity is faster<sup>3,7,8</sup> with lower doses of antigen (Table 2). Tolerance induction by the neonatal injection of a large dose of antigen depresses mainly high-affinity antibody synthesis with a consequent decrease in average affinity.<sup>9</sup> Those cells bearing higher affinity cell-associated antibody molecules preferentially capture antigen during the process of tolerance induction and are thus preferentially rendered tolerant. This results in the observed low affinity of the residual antibody formed.<sup>9</sup> On the other hand, passively injected antibody which competes with cells for available antigen mainly depresses low-affinity antibody synthesis.<sup>7,10</sup>

Most past studies of antibody affinity calculated an average association constant based on the assumption that antibodies are normally (symmetrically) distributed with respect to affinity about some mean value. On the basis of this

TABLE 2  
EFFECT OF ANTIGEN DOSE ON ANTIBODY BINDING AFFINITY\*

Antigen dose, mg	Early response		Peak response		Late response	
	Time, days	$-\Delta F_{av}^0$ , kcal/mole	Time, days	$-\Delta F_{av}^0$ , kcal/mole	Time, days	$-\Delta F_{av}^0$ , kcal/mole
0.05	21	7.56	42	9.68	360	9.03
0.05	21	7.97	42	10.06	360	9.62
0.5	11	8.21	42	9.38	180	8.42
0.5	11	7.03	90	9.71	360	8.55
5.0	11	7.39	180	10.27	360	9.24
5.0	11	7.66	180	10.86	360	10.64
50.0	7	7.15	360	10.34	720	10.39

\*Seven rabbits were immunized with the indicated dose of DNP-BGG in complete Freund's adjuvant and were bled periodically for up to 2 years after immunization. Affinities were measured on each sample, by equilibrium dialysis, with DNP-glycine as ligand. The distribution of affinities was computed from the binding data, and average affinities ( $-\Delta F_{av}^0$ ) were calculated from the distributions.<sup>5</sup> For each animal the affinity, at the earliest bleeding in which sufficient antibody was present to do adequate measurements, is presented under Early response. Listed under Peak response are the time and affinity of the bleeding from each animal that had the highest average affinity. Listed under Late response are the time and average affinity of the last bleeding obtained on each animal. Derived from the data of Werblin et al.<sup>6</sup>

assumption, binding data are plotted as described by Sips<sup>11</sup> or in some comparable manner.<sup>12</sup> A straight line is fit to the data, and the "average" association constant is taken as being equal to the reciprocal of the free-hapten concentration at which 50% of the antibody-binding sites are occupied by hapten as indicated by this regression line.

Recently we reported<sup>5,6</sup> that, in most cases, binding data actually are not linear when plotted in the Sips<sup>11</sup> manner, which implies that antibodies are not distributed symmetrically with respect to affinity. These observations introduce uncertainty into the traditional methods for expressing average affinity. If the binding data are not linear, the regression line will vary, depending on the region of the binding curve in which the data points fall. Furthermore, the "average" affinity calculated in this way would no longer represent the peak of a symmetrical distribution of antibody affinities.

To cope with this situation, we have suggested two approaches.<sup>5</sup> The first approach is very simple and involves merely calculating an average affinity using binding data falling over a defined range of antibody sites bound. That is, one can consider using binding data that fall between 1 and 25% of the antibody sites occupied by hapten. The data are plotted in the usual Sips<sup>11</sup> manner, and a straight line is fit to the data by linear regression analysis. This line is extrapolated to indicate the concentration of free hapten which would be



required to bind 50% of the antibody-binding sites. This type of average affinity in essence reflects mainly the binding properties of the highest affinity subpopulations present in the sample. This procedure ignores the low-affinity antibodies also generally present. However, the procedure has a number of advantages over the routine methods for computing average affinity: (1) Since the data used are restricted to a defined region of the binding curve, determinations made on different antibody samples are more critically comparable. (2) Since the data are considered only from a restricted region of the curve, the data points used are more truly linear. (3) In many experimental situations one is more interested in detecting changes in high-affinity antibodies than in considering the entire antibody population. (4) Since the complete curves are nonlinear, different values for average affinity will be computed by conventional methods depending on where in the binding curve the experimental points fall. If the experimental points are restricted to a defined region of the binding curve, this type of error is minimized and what is being measured is more precisely defined. (5) Such estimates of affinity can be obtained from relatively few experimental points.

When a more complete description of the binding properties of an antibody sample is required, the procedure previously described is clearly inadequate. For a more precise description of the actual population of antibodies present, we developed an iterative approximation procedure, employing a computer, to calculate that distribution of affinities which would best approximate the distribution of affinities actually present. This procedure was previously described and justified in detail.<sup>5</sup> The procedure can provide a very detailed and accurate picture of the distribution of antibody affinities present in a sample. However, for the computation procedure to be employed effectively, it requires large numbers of data points (25 to 50) ranging from 1 to 90% of the antibody sites occupied by hapten.

When binding data obtained by equilibrium dialysis are analyzed by this approximation procedure, the following pattern of change in affinity with time after immunization is observed.<sup>5,6</sup> Initially, a heterogeneous population of relatively low affinity antibodies is present. With time after immunization high-affinity antibodies appear and gradually come to constitute a major portion (up to 85%) of the total antibody. Low-affinity antibodies persist in significant amounts throughout the course of the response. Very late in the immune response (6 months to 1 year in the rabbit), as the total antibody concentration falls, the relative proportion of high-affinity antibodies is reduced, and average affinity decreases (Table 2). That is, there appears to be a preferential loss of high-affinity antibodies, relative to low-affinity antibodies, very late after immunization (Table 3). It is of particular note that, while the relative concentration of high-affinity antibodies fall, high-affinity "memory" cells are still present. Boosting animals very late after immunization when the average affinity has dropped still results in the prompt synthesis of large amounts of very high affinity antibodies.<sup>13</sup>

TABLE 3  
PERSISTENCE OF LOW-AFFINITY ANTIBODY\*

Antigen dose, mg	Time after immunization, days	Antibody concentration		Low-affinity antibody, %
		Total, mg/ml	Low affinity, mg/ml	
5.0	7	0.17	0.16	97
	11	0.40	0.36	89
	21	1.08	0.71	66
	42	1.88	0.58	31
	90	1.29	0.12	9
	180	0.94	0.15	16
	360	0.53	0.23	44
0.5	11	0.16	0.14	90
	21	0.50	0.27	54
	42	3.16	0.98	31
	90	4.75	0.90	19
	360	0.46	0.26	57

\*Two rabbits were immunized with the dose of DNP-BGG indicated, in complete Freund's adjuvant, and were bled repeatedly at the times indicated. The total antibody concentration was determined by saturation of binding sites with DNP-glycine. Antibody affinities were determined from the binding of DNP-glycine using equilibrium dialysis and the distribution of affinities computed from the binding data. Antibodies with association constants falling between  $1.0 \times 10^4$  and  $1.8 \times 10^6$  liters/mole were designated "low affinity," and the amount and percentage of low-affinity antibodies in each sample was calculated. Data are derived from Werblin et al.<sup>6</sup>

Selection for high-affinity antibody synthesis proceeds more rapidly after immunization with lower doses of antigen. As a consequence the time required to reach the maximum average affinity antibody that rabbits will produce is slower<sup>6</sup> after larger doses of antigen (Table 2). All rabbits show this progressive increase in affinity with time after immunization. Some animals tend to produce a high-affinity subpopulation of antibodies, containing up to 80% of an animal's total specific antibody, which is of relatively restricted heterogeneity.<sup>6</sup> Why certain animals exhibit this tendency is not known. However, it is clear<sup>6</sup> that the phenomenon occurs more often in animals immunized with high doses of antigen [over 5 mg dinitrophenylated bovine gamma globulin (DNP-BGG) in complete Freund's adjuvant].

In examining a population of rabbits, one finds a considerable (approximately 1.5 kcal/mole) variation<sup>14</sup> in the maximum affinity anti-DNP antibody produced by individual rabbits (Table 1). It is of note that rabbits synthesizing relatively low affinity antibodies at one time during the course of the immune response have a statistically significant tendency to retain their position at the low end of the population distribution with respect to antibody affinity. Thus

individual rabbits appear to differ with respect to the affinity of the highest affinity anti-DNP antibody that they can synthesize. The basis for this individual variation is not known.

Thus, immunizing rabbits with a relatively simple hapten results in the production of a highly heterogeneous population of antibody molecules with respect to their affinity for the antigenic determinant. This presumably reflects the heterogeneous population of B lymphocytes which is stimulated to proliferate and to produce antibody. From this heterogeneous population of B lymphocytes, that subpopulation which produces high-affinity antibodies captures antigen preferentially and is preferentially stimulated to proliferate. This "high-affinity" subpopulation comes to predominate in the total population of antibody-forming cells, and the average affinity of the serum antibody increases. Procedures that specifically depress antibody synthesis have a profound effect on antibody affinity. B-cell tolerance mainly depresses high-affinity antibody synthesis. Passive antibody, in contrast, preferentially depresses low-affinity antibody synthesis. Nonspecific depression of the immune response, when of moderate degree, has little effect on antibody affinity. These observations are all consistent with a simple clonal selection hypothesis in which antigen acts to select high-affinity B lymphocytes in what amounts to a microevolutionary process.

Very late after immunization there is a preferential loss of high-affinity antibody synthesis. High-affinity memory cells remain since boosting results in the prompt appearance of large amounts of very high affinity antibody. The preferential loss of high-affinity antibody synthesis late in the immune response cannot be readily explained. The observation does suggest the presence of additional antigen-mediated processes that control whether cells proliferate and become memory cells or become active antibody-producing cells.

## ACKNOWLEDGMENT

This study was supported in part by Grant AM-13701 from the National Institutes of Health, U. S. Public Health Service.

## REFERENCES

1. F. M. Burnet, *The Clonal Selection Theory of Acquired Immunity*, Vanderbilt University Press, Nashville, Tenn., 1959.
2. G. W. Siskind and B. Benacerraf, Cell Selection by Antigen in the Immune Response, *Advan. Immunol.*, **10**: 1-50 (1969).
3. G. W. Siskind and H. N. Eisen, Effect of Variations in Antibody Hapten Association Constant upon the Biologic Activity of the Antibody, *J. Immunol.* **95**: 436-441 (1965).
4. T. P. Werblin and G. W. Siskind, Effect of Tolerance and Immunity on Antibody Affinity, *Transplant. Rev.*, **8**: 104-136 (1972).
5. T. P. Werblin and G. W. Siskind, Distribution of Antibody Affinities: Technique of Measurement, *Immunochemistry*, **9**: 987-1011 (1972).

6. T. P. Werblin, Y. T. Kim, F. Quagliata, and G. W. Siskind, Studies on the Control of Antibody Synthesis. III. Changes in Heterogeneity of Antibody Affinity During the Course of the Immune Response, *Immunology*, **24**: 477-492 (1973).
7. G. W. Siskind, P. Dunn, and J. G. Walker, Studies on the Control of Antibody Synthesis. II. Effect of Antigen Dose and of Suppression by Passive Antibody on the Affinity of Antibody Synthesized, *J. Exp. Med.*, **127**: 55-66 (1968).
8. E. A. Goidl, W. E. Paul, G. W. Siskind, and B. Benacerraf, The Effect of Antigen Dose and Time After Immunization on the Amount and Affinity of Anti-Hapten Antibody, *J. Immunol.*, **100**: 371-375 (1968).
9. G. A. Theis and G. W. Siskind, Selection of Cell Populations in Induction of Tolerance: Affinity of Antibody Formed in Partially Tolerant Rabbits, *J. Immunol.*, **100**: 138-141 (1968).
10. K. S. Heller and G. W. Siskind, Effect of Tolerance and of Antibody Mediated Immune Suppression on the Avidity of the Cellular and Humoral Immune Response, *Cell. Immunol.*, **6**: 59-65 (1973).
11. R. Sips, On the Structure of a Catalyst Surface, *J. Chem. Phys.*, **16**: 490 (1948).
12. F. Karush, Immunologic Specificity and Molecular Structure, *Advan. Immunol.*, **2**: 1-40 (1962).
13. Y. T. Kim and G. W. Siskind, Cornell University Medical College, unpublished observations.
14. T. P. Werblin, Y. T. Kim, R. Mage, B. Benacerraf, and G. W. Siskind, The Generation of Antibody Diversity. I. Studies on the Population Distribution of Anti-DNP Antibody Affinities and on the Influence of Allotype on Antibody Affinity and Concentration, *Immunology*, **25**: 17-32 (1973).



# CELL ADHESION

CARL G. HILLERQVIST,\* WARREN L. ROTTMANN, BERNT T. WALTHER,  
and SAUL ROSEMAN

Department of Biology and McCollum-Pratt Institute, The Johns  
Hopkins University, Baltimore, Maryland

---

## ABSTRACT

The adhesion of cells to other cells and to such substrata as collagen is thought to be an important physiological process very possibly involved in morphogenesis, metastasis of tumor cells, etc. We have chosen to define cell adhesion as the first detectable event, the *rate* at which cells attach to substrata or to other cells. With a rapid, quantitative assay devised for measuring adhesion, labeled cells are permitted to attach to the substratum, to a homologous cell layer, or to a heterologous cell layer, and the attachment of the single cells is followed with time of incubation. Kinetic and inhibitor studies show that different processes or cell-surface components are involved in cell-cell and in cell-substratum attachment. The assay method was devised to facilitate the isolation of the intercellular adhesive components. Experiments were conducted with a model adhesive compound, concanavalin-A, to determine if the assay would detect such components.

Direct attempts to isolate adhesive compounds from tissue-culture fibroblasts (3T3 cells and SV40-transformed 3T3 cells) indicate that lipids may be involved in the process. Two active fractions have thus far been obtained, of which one is a potent inhibitor of intercellular adhesion and the other stimulates adhesion in the assay described above.

Other approaches to the intercellular adhesion phenomenon taken in this laboratory suggest that cell-surface carbohydrates may be involved. One set of experiments showed that L-glutamine was required for the intercellular adhesion of mouse teratoma cells to each other and that the only compounds found to replace L-glutamine were D-glucosamine and D-mannosamine. Glucosamine also stimulates the adhesion of SV40/3T3 and 3T3 cells to homologous cell layers. These results are in accord with established biosynthetic pathways leading to the formation of complex carbohydrates. A different approach has recently been undertaken. Analogues of cell-surface complex carbohydrates are covalently linked to small

---

\*Present address: Department of Biochemistry, Vanderbilt School of Medicine, Vanderbilt University, Nashville, Tenn.

Sephadex beads. Galactose beads were found to specifically stimulate the adhesion of SV40/3T3 cells to the beads and to each other.

The net result of these studies suggests that complex cell-surface carbohydrates (and possibly lipids) are involved in the process of intercellular adhesion.

Intercellular adhesion is assumed to play an important role in diverse biological phenomena, including morphogenesis, intercellular communications, and metastasis of tumor cells.<sup>1,2</sup> Despite great interest in cell adhesion, there is no generally accepted definition. Rather, the phenomenon is defined operationally by the method used to observe it. It is questionable that these methods measure the same molecular events.<sup>3</sup> We have chosen to define cell adhesion as the first measurable event, the *rate* at which single cells adhere to other cells or substrata. Adhesion between similar cells is designated specific or homologous adhesion. Adhesion between cells of different origins is designated nonspecific or heterologous intercellular adhesion. Three assays for intercellular adhesion were developed in our laboratory.

The first assay measured the rate of aggregate formation by determining the decrease in the number of single cells with a Coulter electronic particle counter.<sup>4</sup> This method, although rapid and reproducible, cannot readily discriminate between homologous and heterologous adhesion.

The second assay is a modification of a method described by Roth and Weston<sup>5</sup> and measures the adhesion of single cells to cell aggregates.<sup>6</sup> This method is capable of measuring both specific and nonspecific adhesion. However, only a small percentage of the single-cell population adheres to the aggregates over the course of a 1- or 2-hr incubation. It is therefore possible that the adhered single cells do not reflect the adhesive properties of the entire single-cell population. In a third assay, using cell monolayers in place of the aggregates overcame<sup>7</sup> this last objection.

## QUANTITATIVE ASSAY FOR INTERCELLULAR ADHESION

The third assay thus offers a number of advantages in measuring the rate of cell adhesion. Cell adhesion is functionally defined as the rate at which single cells attach to a confluent layer of cells. Radioactively labeled cells are dissociated, suspended in serum-free medium, and incubated with cultured cell layers. After incubation on a reciprocal shaker at 37°C, the unattached cells are aspirated off and the monolayers are washed twice. The radioactivity remaining on the cell layers reflects the number of adhering cells. The rate is determined by incubation of replicate cell layers and suspensions for various times. The cells attach at a rate dependent on the number of single cells in the suspension. Single cells attach individually to the cell layers. Furthermore, the rate of adhesion of single cells to the cell layers parallels the disappearance of single cells from the suspension (measured with the Coulter counter technique). That the assay is

applicable for measuring both homologous and heterologous adhesion was demonstrated with chick embryonic secondary cultures. Neural retina and liver cells attached to homologous cell layers at rates significantly higher than to reciprocal heterologous cell layers.

The monolayer assay was developed to facilitate the isolation of components involved in intercellular adhesion. Therefore it was necessary to demonstrate that the assay can detect substances that might be either stimulatory or inhibitory as schematically depicted in Fig. 1. Cells are assumed to interact in some type of acceptor-donor mechanism. The adhesive rate observed for a particular cell type would then depend on the availability, the total number, and the binding efficiency of those sites on the outer surfaces of the cells.

Accordingly, adhesion could be stimulated either by increasing the number of active sites or by inducing clusters of sites via membrane fluidity changes. Removing or suppressing the synthesis of interfering cell-surface components would also result in a higher adhesive rate. In contrast, inhibition would result from inhibiting the synthesis of interacting sites or by blocking them through haptenlike competition. Similar inhibitory effects would result from the interaction of acceptors and donors of individual cells or from sequestering of sites. Increased synthesis or secretion of interfering cell-surface components

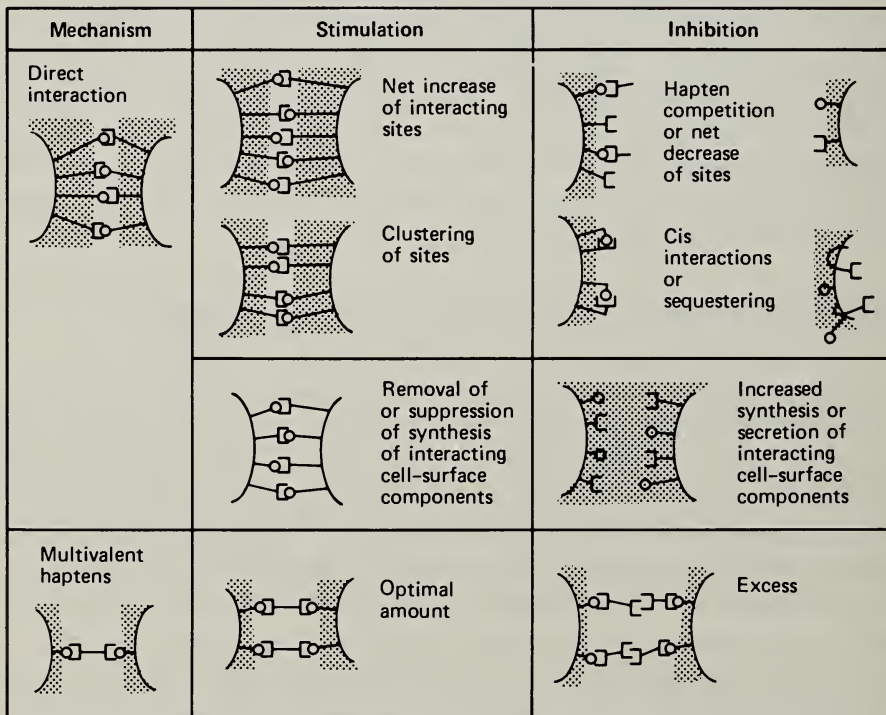


Fig. 1 Factors affecting intercellular adhesion.



would also cause inhibition of the adhesion rate. If the interacting molecules were multivalent either in native form or as a result of aggregation or micelle formation, then such components would stimulate adhesion when added in optimal amounts but would inhibit when added in excess.

As a result of these considerations, concanavalin-A, known to agglutinate SV40-transformed 3T3 mouse fibroblasts as well as freshly trypsinized 3T3 cells,<sup>8</sup> was tested in this assay as a model multivalent adhesive substance. Trypsinized 3T3 single cells were added to trypsin-treated cell layers in both the presence and absence of concanavalin-A. The result was a multifold stimulation of the observed rate of cell attachment. This observation was investigated in detail, and a quantitative assay for lectin agglutination was developed.<sup>9</sup> Inhibition of intercellular adhesion was demonstrated by using drugs that have been reported to interact mainly with the plasma membranes.<sup>10-12</sup> Cytochalasin B ( $5 \times 10^{-6}M$ ) completely inhibited the intercellular adhesion of SV3T3—flat revertant cells but had no effect on the adhesion of those cells to a plastic substrate. Chlorpromazine ( $10^{-5}M$ ) inhibited SV40/3T3 and 3T3 homologous and heterologous adhesion and also adhesion to plastic but had little effect on the agglutination mediated by concanavalin-A. These experiments suggest that intercellular adhesion phenomena of the cells studied are distinct from cell-surface phenomena involved in concanavalin-A-mediated agglutination and adhesion of cells to a plastic substratum.

## ISOLATION OF CELL COMPONENTS THAT AFFECT ADHESION

Since this assay can quantitatively measure the modification of adhesion caused by various compounds, experiments were initiated to isolate components from SV40/3T3 cells that may be directly involved in the phenomenon. Presumably these substances may constitute the molecular basis of intercellular adhesion and/or cell—cell recognition. Initial efforts have focused on the isolation of glycopeptide and lipid fractions that influence the adhesive rate. Lyophilized cells were subjected to standard extraction and enzymatic degradation techniques to obtain crude preparations of lipids, gangliosides, and glycopeptides. Lipids were fractionated by silicic acid chromatography. An aliquot of the ganglioside fraction was subjected to mild acid hydrolysis, and the "asialogangliosides" were recovered by gel chromatography. The effect of the different fractions on the rate of adhesion of SV40/3T3 cells was tested in the monolayer assay. The concentration, expressed as cell equivalents, was calculated by comparing the number of cells from which the fractions were isolated with the number of cells contained in a cell layer. If one assumes 100% yields, the amounts used were equal to 10 cell equivalents. A lipid fraction thought to contain glycolipids completely inhibited intercellular adhesion (Fig. 2), whereas the ganglioside, glycopeptide, and asialoganglioside fractions had no significant effect on the rate of adhesion.



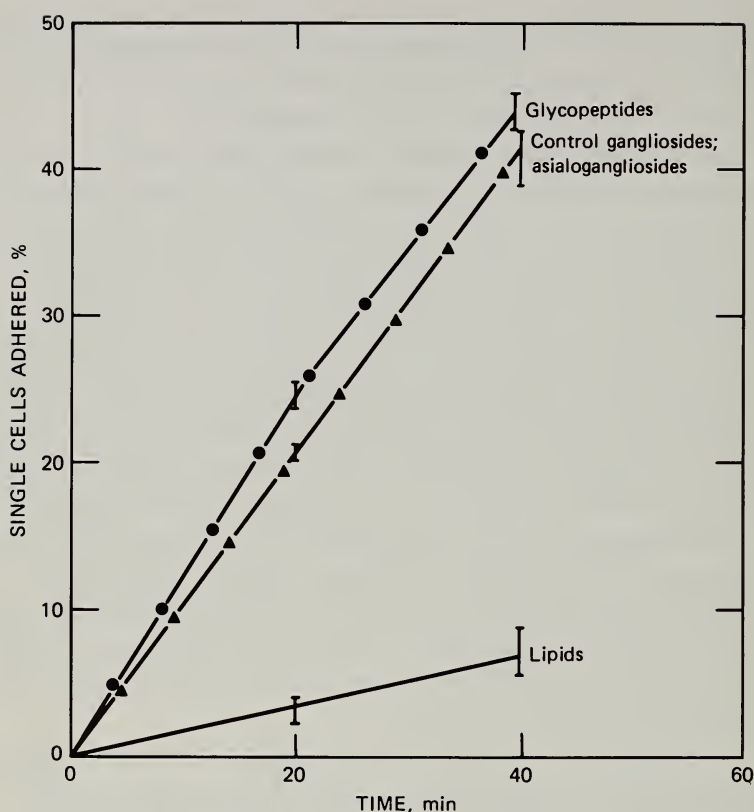


Fig. 2 Effect on the adhesion rate by fractions isolated from SV40/3T3 cells. Each fraction is at a concentration of 10 cell equivalents.

This observation led to efforts focused on extensive fractionation of cell lipids. Total cell lipids, from which gangliosides had been removed, were subjected to fractionation on silicic acid columns. Concentrations of 0.1, 1.0, and 10 cell equivalents of various fractions were assayed. The second chloroform fraction contained total inhibitory activity at 10 cell equivalents; 1 cell equivalent caused a 40% inhibition. Analytical thin-layer chromatography (TLC) of this fraction revealed two spots. By preparative TLC the inhibitory activity was recovered in the fastest migrating fraction (Fig. 3). This fraction contained a  $C_{16}$  fatty acid (~10%), a  $C_{18}$  fatty acid (~5%), and a polyunsaturated hydroxy fatty acid (~80%), as demonstrated by combined gas chromatography and mass spectrometry analysis. Neither of the free fatty acids (stearic, palmitic) had any inhibitory effect at comparable concentrations. Whether the inhibitory effect is due to steric hindrance through micelle formation or to a more specific interaction with cell-surface components involved in adhesion is under investigation. Two fractions, eluted off the silicic acid column with methanol and presumably containing higher glycolipids and phospholipids, showed a concen-

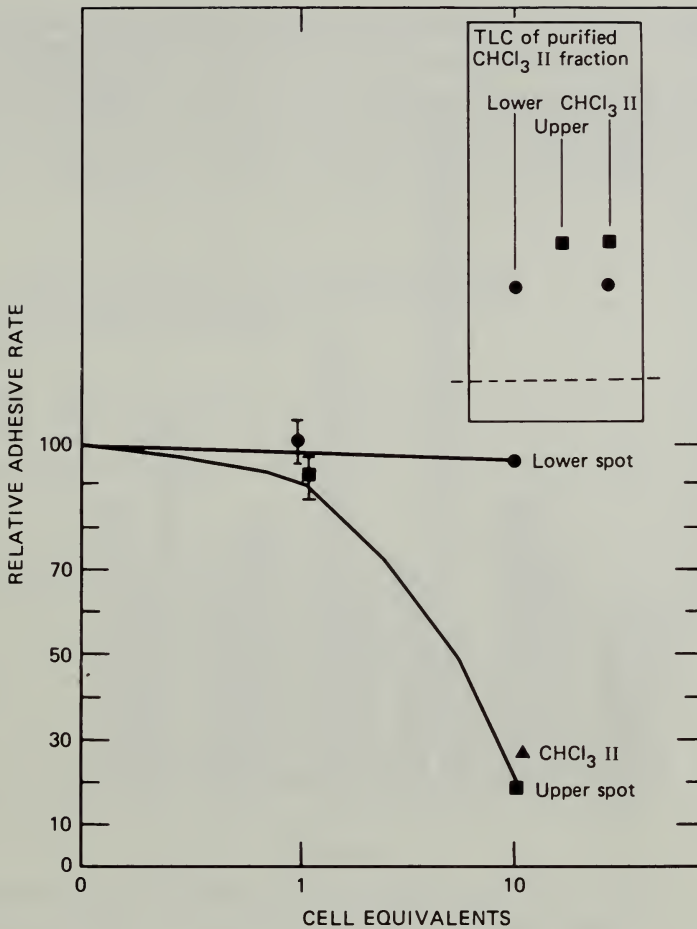


Fig. 3 Effect on the adhesion rate of lipid fractions isolated by preparative thin-layer chromatography from the second chloroform cut from a silicic acid column.

tration-dependent stimulatory effect on adhesion. The effect was larger at 1 cell equivalent than at 10 cell equivalents. The second methanol cut exhibited a slightly higher stimulatory activity than the first (1.9- and 1.6-fold, respectively). None of the other fractions, including all the blanks obtained by running parallel blind experiments, nor the crude lipid fraction caused any significant deviation from the control adhesion rate. Furthermore, a variety of authentic phospholipids were inactive.

Three spots were detected in both methanol fractions by TLC analysis (Fig. 4). These spots were isolated from both methanol cuts by preparative TLC. The fractions were tested (1 cell equivalent) for effect on the homologous intercellular adhesion (20 min incubation, 37°C) of SV40/3T3 cells, 3T3 cells, and baby hamster kidney fibroblasts (BHK). None of the fractions ( $I_x$ ,  $I_a$ , and

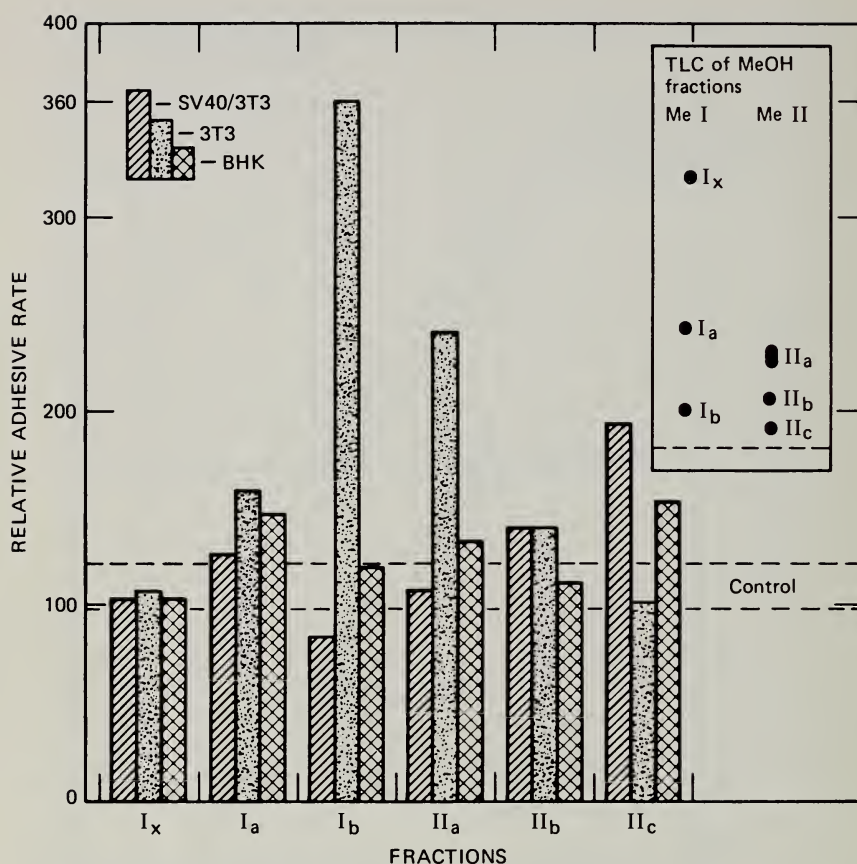


Fig. 4 Effect of polar lipids obtained by preparative thin-layer chromatography on the homologous adhesion rate of SV40/3T3 cells, 3T3 cells, and BHK cells. Fractions  $I_x$ ,  $I_a$ , and  $I_b$  were obtained from the first methanol cut, and  $II_a$ ,  $II_b$ , and  $II_c$  were obtained from the second methanol cut from a silicic acid column.

$I_b$ ) obtained from the first methanol cut (Me I) demonstrated the stimulatory activity with SV40/3T3 cells that the total Me I fraction contained. This might be significant but could also imply that a minor component exhibiting the stimulatory effect was overlooked in the isolation procedure. Fraction  $II_c$  had a stimulatory effect on the adhesion of SV40/3T3 cells, similar to that exhibited by the crude Me II cut, and did not stimulate the adhesion of 3T3 cells. The stimulatory effect of  $II_c$  detected with BHK cells indicates a non-cell-specific interaction. The most dramatic effect was observed with fractions  $I_b$  and  $II_a$  since they specifically stimulated the adhesion of 3T3 cells by a factor of 3.6 and 2.5, respectively. It was further demonstrated that the activity of fraction  $I_b$  significantly decreased at higher concentration, whereas the rate of adhesion increased as a function of the concentration of fraction  $II_a$ . The mechanism of

action of fractions I<sub>b</sub> and II<sub>a</sub> on intercellular adhesion is under investigation. It is conceivable that these lipids may alter membrane fluidity or may form multivalent complexes in the form of micelles (Fig. 1). In all experiments the cells appear normal on microscopic observation after 20 min incubation with those various lipids, but possible artifacts of this type have not yet been eliminated.

## POSSIBLE ROLE OF COMPLEX CARBOHYDRATES IN INTERCELLULAR ADHESION

Although many hypotheses have been offered, there are no current experimental data clearly demonstrating the molecular events involved in intercellular adhesion. Tyler<sup>13</sup> and Weiss<sup>14</sup> independently suggested that the adhesion of cells was due to cell-surface-located antigen-antibody-like interactions. The model is attractive but fails to explain satisfactorily how cells during certain stages of development and growth can detach and readhere to other or similar cells. Roseman<sup>15</sup> has proposed a model for cell adhesion where the interacting sites consist of cell-surface glycosyltransferases and their complex carbohydrate substrates. Aspects of this model could be used to explain the specificity of intercellular adhesion and to explain how cell surfaces might be modified during certain types of cell-cell interactions observed in embryogenesis and mitosis. The involvement of complex carbohydrates in cell adhesion was first proposed by Oppenheimer et al.,<sup>16</sup> who demonstrated that L-glutamine was required for the aggregation of teratoma cells. Trypsin-dissociated teratoma cells aggregated in a complex medium (Medium 199) but not in a glucose-balanced salt solution. The active component in the complex medium was demonstrated to be L-glutamine. D-Glucosamine and D-mannosamine also enhanced the aggregation rate of the teratoma cells when added to the balanced salt solution to that observed in the complex medium. L-Glutamine is required as an amino-group donor for the biosynthesis of amino-containing sugars. Consequently it is necessary for the biosynthesis of a majority of animal complex carbohydrates. These observations are therefore consistent with the hypothesis that complex carbohydrates are involved in intercellular adhesion.

Recent observations made with 3T3 cells and a low adhesive line of SV40/3T3 cells are in agreement with the observations discussed above. Prior to an adhesion assay, both the cell layers and the cells to be used as a single-cell suspension are grown on plates in Dulbecco's modified Eagle medium containing 10% calf serum. When the SV40/3T3 cell layers only were cultured in medium supplemented with D-glucosamine (1mM), a 2.5 stimulation over the control adhesive rate was obtained. If, however, the single cells were grown in medium containing D-glucosamine, the adhesive rate was 60% of the control, regardless of the type of monolayers used ( $\pm$  GlcNH<sub>2</sub>). Neither D-galactosamine, D-galactose, nor N-acetyl-D-galactosamine had any detectable effect on the adhesive



rate when added to the medium at 1mM final concentration. Furthermore, the stimulatory effect of D-glucosamine on the adhesive rate was a function of the concentration of the sugar; at a 50 $\mu$ M concentration there was no deviation from the control rate.

The stimulation of the adhesive rate, observed in culturing SV40/3T3 cell layers in D-glucosamine supplemented medium was also observed with Swiss 3T3 cells (Fig. 5). However, a further enhancement of the adhesive rate was obtained when the cells for the nontrypsinized cell suspension also were grown in the presence of D-glucosamine. This added stimulatory effect was abolished if the

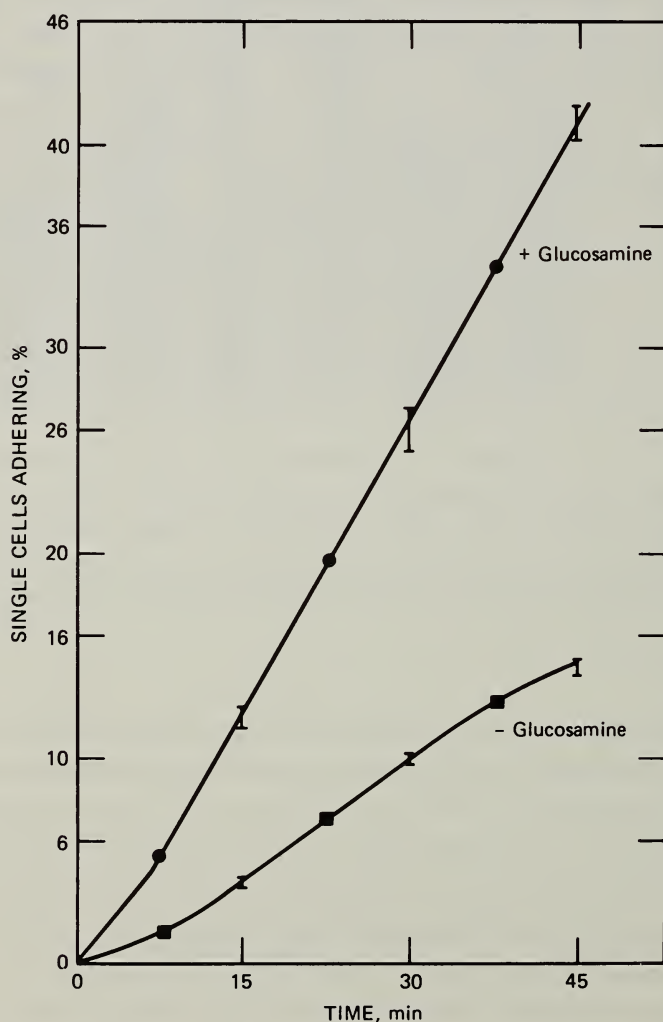


Fig. 5 Effect of 1mM glucosamine on the adhesive rate of Swiss 3T3 cells. Glucosamine was supplemented to the growth medium for 24 hr prior to the adhesion assay.

single cells were subjected to trypsinization. There was no D-glucosamine effect on the adhesive rate of the highly adhesive SV40 Swiss 3T3 cells with either the monolayers or the single cells. D-Glucosamine had no visible effect on cell morphology when used at a concentration of 1mM. It also has no effect on either growth rate or the degree of growth control of these cells. One interpretation of these results is that during standard growth conditions 3T3 cells and low adhesive SV40/3T3 cells fail to synthesize optimal amounts of cell-surface complex carbohydrates containing amino sugars, which are involved in intercellular adhesion. This would result in a "characteristic" low adhesive rate for these cell types. Supplementation with D-glucosamine overcomes this biosynthetic deficiency. The D-glucosamine inhibitory effect observed with SV40/3T3 single cells could be due to increased synthesis of one of the interacting sites, thus promoting "*cis*-interactions." Studying cell adhesion in the presence of serum with the assumption that carbohydrates are involved raises questions concerning the effect of the glycosyltransferases and glycosidases which are present in sera and which vary in both amount and type in different kinds of sera. These facts have to be taken into consideration also in studying glycopeptide and glycolipid composition of cell lines and of a given line as a function of growth. Differences obtained might very well be caused by variations in orientation of those components in the membrane, making them more or less available as substrates for those serum enzymes.

Another approach to investigate the possible involvement of complex carbohydrates in intercellular adhesion is to synthesize "artificial cell surfaces" and to study the interaction of cells with those surfaces. Chipowsky, Lee, and Roseman<sup>17</sup> recently reported results of such an approach. Sephadex beads were activated and coupled with various thio-glycosides via a 6-carbon spacer arm. Thio-glycosides were used to avoid possible enzymatic cleavage of the sugar residues in subsequent experiments with cells. The  $\beta$ -thio-glycosides of D-glucose, D-galactose, and N-acetyl-D-glucosamine were coupled to the beads. Cyanogen bromide-activated beads, as well as beads reacted only with the spacer arm 6-amino-hexanol, were tested as controls. The derivatized beads were incubated with trypsin-dissociated SV40/3T3 cells in serum-free medium and observed microscopically. The cells bound extensively to the galactose-containing beads. This interaction caused a subsequent nucleation phenomenon in which the adhering cells became more adhesive toward other cells. This produced large aggregates of cells and beads. Cells showed little or no affinity for the other types of derivatized beads.

This result demonstrates that SV40/3T3 cells have surface components that specifically recognize and bind to carbohydrates. This directly supports the concept that cell-surface carbohydrates are involved in intercellular adhesion and/or recognition.

According to the Roseman hypothesis,<sup>15</sup> intercellular adhesion is the result of binding between complex carbohydrates and glycosyltransferases, or between

carbohydrates per se via hydrogen bonds. Experiments indicating the presence of cell-surface glycosyltransferases are accumulating. Further, there are indications that these enzymes indeed are involved in cell adhesion.<sup>18-23</sup> Originally it was demonstrated<sup>24</sup> that when neural retina cells were incubated in the presence of uridine 5'-diphosphate-galactose, galactose was incorporated into endogenous acceptors or into exogenous acceptors when the latter were added. Two of the exogenous acceptors were high-molecular-weight glycoproteins. Subsequently, cell-surface glycosyltransferases were detected in blood platelets,<sup>18,19</sup> rat intestinal epithelial cells,<sup>20</sup> and fibroblasts.<sup>21,22</sup> However, the direct involvement of cell-surface glycosyltransferases in cell adhesion remains to be demonstrated.

## SUMMARY

The data discussed in this paper support the hypothesis that complex carbohydrates are involved in intercellular adhesion. The biological role of the lipids shown to exert both stimulatory and inhibitory effects is as yet uncertain. At present the data do not distinguish between a direct (biological) and an indirect (artifactual) effect of these exogenously added cell lipids. Hopefully an extension of these studies will define the molecular mechanisms underlying this important biological phenomenon.

## REFERENCES

1. M. Abercrombie and E. J. Ambrose, The Surface Properties of Cancer Cells: A Review, *Cancer Res.*, **22**: 525 (1962).
2. L. Weiss and E. Mayhew, The Cell Periphery, *New Engl. J. Med.*, **276**: 1354 (1967).
3. P. B. Armstrong, Wilhelm Roux, *Arch. Entwicklungsmech. Organ.*, **168**: 125 (1971).
4. C. W. Orr and S. Roseman, Intercellular Adhesion, *J. Membrane Biol.*, **1**: 109 (1969).
5. S. Roth and J. A. Weston, The Measurement of Intercellular Adhesion, *Proc. Nat. Acad. Sci. U. S. A.*, **58**: 974 (1967).
6. S. Roth, E. J. McGuire, and S. Roseman, An Assay for Intercellular Adhesive Specificity, *J. Cell Biol.*, **51**: 525 (1971).
7. B. T. Walther, R. Ohman, and S. Roseman, A Quantitative Assay for Intercellular Adhesion, *Proc. Nat. Acad. Sci. U. S. A.*, **70**: 1569 (1973).
8. H. Lis and N. Sharon, The Biochemistry of Plant Lectins (Phytohemagglutinins), *Ann. Rev. Biochem.*, **42**: 541 (1973).
9. W. L. Rottmann, B. T. Walther, C. G. Hellerqvist, J. Umbreit, and S. Roseman, A Quantitative Assay for Concanavalin A-Mediated Cell Agglutination, *J. Biol. Chem.*, **249**: 373 (1974).
10. R. D. Estensen and P. G. W. Plagemann, Cytochalasin B: Inhibition of Glucose and Glucosamine Transport, *Proc. Nat. Acad. Sci. U. S. A.*, **69**: 1430 (1972).
11. A. S. Horn, J. T. Coyle, and S. H. Snyder, Catecholamine Uptake by Synaptosomes from Rat Brain, *Mol. Pharmacol.*, **7**: 66 (1971).

12. I. Clausen, H. Harving, and A. B. Dahl-Hansen, The Relationship Between the Transport of Glucose and Cation Across Cell Membranes in Isolated Tissues, *Biochim. Biophys. Acta*, **298**: 393 (1973).
13. A. Tyler, An Auto-Antibody Concept of Cell Structure, Growth and Differentiation, *Growth*, **10**(Symp. 6): 7 (1947).
14. P. Weiss, The Problem of Specificity in Growth and Development, *Yale J. Biol. Med.*, **19**: 235 (1947).
15. S. Roseman, The Synthesis of Complex Carbohydrates by Multiglycosyltransferase Systems and Their Potential Function in Intercellular Adhesion, *Chem. Phys. Lipids*, **5**: 270 (1971).
16. S. B. Oppenheimer, M. Edidin, C. W. Orr, and S. Roseman, An L-glutamine Requirement for Intercellular Adhesion, *Proc. Nat. Acad. Sci. U. S. A.*, **63**: 1395 (1969).
17. S. Chipowsky, Y. C. Lee, and S. Roseman, Adhesion of Cultured Fibroblasts to Insoluble Analogues of Cell-Surface Carbohydrates, *Proc. Nat. Acad. Sci. U. S. A.*, **70**: 2309 (1973).
18. G. A. Jamiesson, C. L. Urban, and A. J. Barker, Enzymatic Basis to Platelet : Collagen Adhesion as the Primary Step in Haemostasis, *Nature (London) New Biol.*, **234**: 5 (1971).
19. H. B. Bosmann, Platelet Adhesiveness and Aggregation: The Collagen : Glycosyl, Polypeptide : N-acetylgalactosaminyl and Glycoprotein : Galactosyl Transferase of Human Platelets, *Biochem. Biophys. Res. Comm.*, **43**: 1118 (1971).
20. M. M. Weiser, Glycosyltransferases and Endogenous Acceptors of the Undifferentiated Cell Surface Membrane, *J. Biol. Chem.*, **248**: 2542 (1973).
21. H. B. Bosmann, Cell Surface Glycosyltransferases and Acceptors in Normal and RNA- and DNA-Virus Transformed Fibroblasts, *Biochim. Biophys. Res. Comm.*, **48**: 523 (1972).
22. S. Roth, A Molecular Model for Cell Interactions, *Quart. Rev. Biol.*, **48**(4): 541-563 (1973).
23. S. Roth and Diane White, Intercellular Contact and Cell Surface Transferase Activity, *Proc. Nat. Acad. Sci. U. S. A.*, **69**: 485 (1972).
24. S. Roth, E. J. McGuire, and S. Roseman, Evidence for Cell-Surface Glycosyltransferases, *J. Cell Biol.*, **51**: 536 (1971).



## THE CELL SURFACE: SESSION SUMMARY

PAUL M. KRAEMER, *Session Chairman*

Cellular and Molecular Radiobiology Group, Los Alamos Scientific Laboratory,  
Los Alamos, New Mexico

---

I would like to relate some of the material you have been hearing in these last sessions with that of the first sessions where the emphasis was on instrumentation. It has been part of the theme of this symposium to see if the time is now ripe for some of these problems in cell biology to be approached with modern instrumentation, and I would like to give, in a somewhat personal, subjective, and anecdotal fashion, some experiences that I think are instructive to this interaction between cell biologists and biophysicists. The first project where we had this interaction working vigorously concerned studies of DNA content in heteroploid cells and other types of cells, done mostly with single-parameter analysis. We found during this period that, to get reliable, reproducible data, we had to produce, as biologists, the "high-quality sample." We had to observe scrupulously the staining reaction and the dispersal procedure. The cell population sampled had to be a first-class population in growth terms, or many artifacts could result and the interpretations actually become confused as, in fact, did happen in some instances. At that time, in our interaction, we began putting little placards on the wall, so to speak, and our motto was "Garbage in and garbage out" in referring to the problems of getting reliable data. We have recently had a more advanced view toward this interaction which came about through our studies of a cell-surface problem.

I would like to go back to some aspects that Dr. John Steinkamp talked about. Figure 1 shows something about the lectin-binding project and about this type of analysis where we have the advantages of more sophisticated multiparameter methods. The diagram shows boxes that represent signals taken on-line at various points in the analysis. In single-parameter lectin studies, we obtained the type of data shown in the top left box. In lectin-binding studies this had some disadvantages. First, since lectins are agglutinins, monodispers-

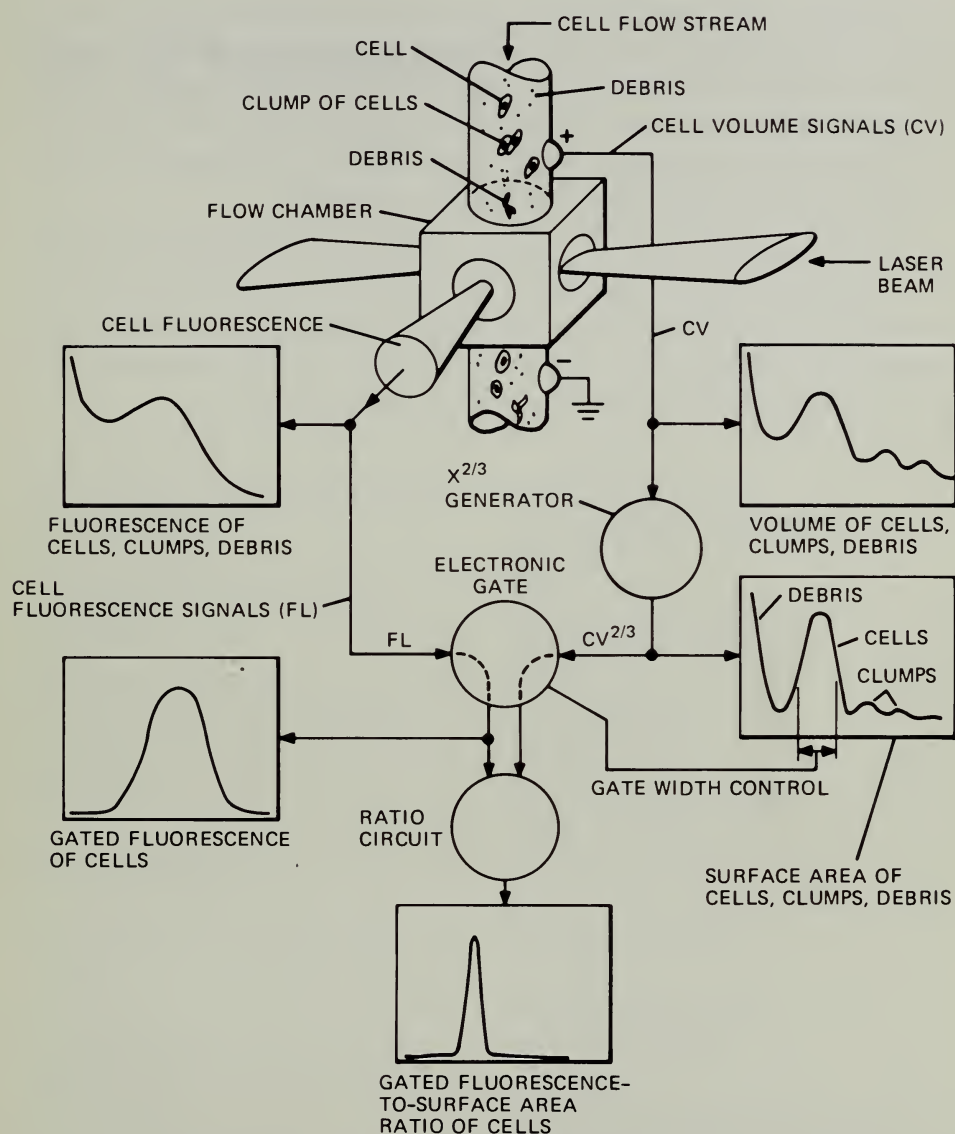


Fig. 1 Diagram illustrating the multiparameter analysis of lectin binding to the cell surface. The boxes represent on-line portrayals of the signals at various points in the analysis. The lowest box represents the final distribution that can be used in comparative studies.

ity—almost by definition—could be troublesome; also, the signal was weaker. Since we did not want to perturb the cell surface and for the same reason could not disperse the population with trypsin, we obviously could not clean up the populations with trypsin. In any case, the primary source of dispersion of the parameter we were measuring was something in which we were not primarily interested, namely, the simple fact that cells in the population were of different

sizes. However, with multiparameter analysis we found that we can start with a mixture of cells, debris, and clumps and that, by signal processing of the two parameters (volume and fluorescence), we can then form a new parameter which we believe has more relevance to what we are studying (that is, the density of binding sites). We can compare this new kind of data for different cell lines or the same cell line under different physiological conditions.

Thus, as cell biologists, we are now challenging the biophysicists to learn to analyze such difficult samples as those from an exfoliative cytology study where loss of information might result from extensive efforts to produce pure, clean, monodispersed cells. We are now challenging the biophysicists to no longer say, "Garbage in and garbage out," but more or less to say, "We can handle your sample, garbage and all, and still find out what we need to know."

## LIST OF PARTICIPANTS

---

C. W. ABELL  
The University of Texas Medical Branch  
Galveston, Tex.

R. E. ANDERSON  
University of New Mexico School of  
Medicine  
Albuquerque, N. Mex.

FRANCES E. ARRIGHI  
M. D. Anderson Hospital and Tumor  
Institute  
The University of Texas  
Houston, Tex.

R. AUER  
Particle Technology, Inc.  
Los Alamos, N. Mex.

J. W. BACUS  
Rush Presbyterian St. Luke's Medical  
Center  
Chicago, Ill.

S. C. BARRANCO  
The University of Texas Medical Branch  
Galveston, Tex.

P. H. BARTELS  
University of Arizona  
Tucson, Ariz.

J. S. BEDFORD  
Vanderbilt University Hospital  
Nashville, Tenn.

B. K. BHUYAN  
The Upjohn Company  
Kalamazoo, Mich.

D. BILLEN  
University of Florida  
Gainesville, Fla.

V. H. BONO, Jr.  
National Cancer Institute  
National Institutes of Health  
Bethesda, Md.

JOAN M. BULL  
National Cancer Institute  
National Institutes of Health  
Bethesda, Md.

G. L. CAMPBELL  
The Wistar Institute  
Philadelphia, Pa.

MARILYN J. CAMPBELL  
Particle Technology, Inc.  
Los Alamos, N. Mex.

E. H. Y. CHU  
University of Michigan  
Ann Arbor, Mich.

J. A. CROLL  
Particle Technology, Inc.  
Los Alamos, N. Mex.

W. R. CRAIN  
M. D. Anderson Hospital and Tumor  
Institute  
The University of Texas  
Houston, Tex.

G. DUDA  
Division of Biomedical and Environmental  
Research  
U. S. Atomic Energy Commission  
Washington, D. C.

URSULA EHMANN  
University of California  
San Francisco, Calif.



M. M. ELKIND  
Argonne National Laboratory  
Argonne, Ill.

M. B. EPSTEIN  
University of California  
Los Angeles, Calif.

S. FEDEROFF  
University of Saskatchewan  
Saskatoon, Saskatchewan, Canada

D. FINDLEY  
University of California  
Los Angeles, Calif.

M. J. FULWYLER  
Particle Technology, Inc.  
Los Alamos, N. Mex.

B. L. GLEDHILL  
Lawrence Livermore Laboratory  
Livermore, Calif.

R. HAGEMANN  
Allegheny General Hospital  
Pittsburgh, Pa.

G. M. HAHN  
Stanford University School of Medicine  
Stanford, Calif.

C. G. HELLERQVIST  
The Johns Hopkins University  
Baltimore, Md.

D. R. HENDERSON  
University of New Mexico School of  
Medicine  
Albuquerque, N. Mex.

R. W. HOLLEY  
The Salk Institute  
San Diego, Calif.

H. A. HOPKINS  
University of Virginia Hospital  
Charlottesville, Va.

L. E. HOPWOOD  
Colorado State University  
Fort Collins, Colo.

J. A. HUBERMAN  
Massachusetts Institute of Technology  
Cambridge, Mass.

R. M. HUMPHREY  
M. D. Anderson Hospital and Tumor  
Institute  
The University of Texas  
Houston, Tex.

MARYLOU INGRAM  
Jet Propulsion Laboratory  
California Institute of Technology  
Pasadena, Calif.

S. W. JORDAN  
University of New Mexico School of  
Medicine  
Albuquerque, N. Mex.

M. H. JULIUS  
Stanford University School of Medicine  
Stanford, Calif.

H. E. KAHN, Jr.  
National Cancer Institute  
National Institutes of Health  
Bethesda, Md.

R. O. KELLEY  
University of New Mexico School of  
Medicine  
Albuquerque, N. Mex.

C. R. KEY  
University of New Mexico School of  
Medicine  
Albuquerque, N. Mex.

K. KOHN  
National Cancer Institute  
National Institutes of Health  
Bethesda, Md.

S. KORNFIELD  
Washington University School of Medicine  
St. Louis, Mo.

G. LEARY  
Department of Biology  
University of New Mexico  
Albuquerque, N. Mex.

J. M. LEHMAN  
University of Colorado School of Medicine  
Denver, Colo.

K. D. LEY  
University of Florida  
Gainesville, Fla.

MURIEL LIPPMAN  
National Cancer Institute  
National Institutes of Health  
Bethesda, Md.

M. LOKEN  
Stanford University School of Medicine  
Stanford, Calif.

W. B. LOONEY  
University of Virginia Medical Center  
Charlottesville, Va.

BONNIE McWILLIAMS  
University of New Mexico School of  
Medicine  
Albuquerque, N. Mex.

G. MAUL  
The Wistar Institute  
Philadelphia, Pa.

B. H. MAYALL  
Lawrence Livermore Laboratory  
Livermore, Calif.

M. R. MELAMED  
Memorial Hospital for Cancer and Allied  
Diseases  
New York City, N. Y.

M. L. MENDELSON  
Lawrence Livermore Laboratory  
Livermore, Calif.

G. C. MUELLER  
McArdle Laboratory  
University of Wisconsin  
Madison, Wis.

G. L. NICOLSON  
The Salk Institute  
San Diego, Calif.

J. H. NILSON  
Department of Biology  
University of New Mexico  
Albuquerque, N. Mex.

A. NORMAN  
University of California  
Los Angeles, Calif.

T. O'CONNOR  
National Cancer Institute  
National Institutes of Health  
Bethesda, Md.

T. T. O'DELL, JR.  
Oak Ridge National Laboratory  
Oak Ridge, Tenn.

L. PACKER  
University of California  
Berkeley, Calif.

J. PAPACONSTANTINOU  
Oak Ridge National Laboratory  
Oak Ridge, Tenn.

ANN PARTRIDGE  
Los Alamos Medical Center  
Los Alamos, N. Mex.

M. K. PATTERSON, JR.  
The Noble Foundation, Inc.  
Ardmore, Okla.

W. Z. PENLAND, JR.  
National Cancer Institute  
National Institutes of Health  
Bethesda, Md.

L. PEUSNER  
Arthur D. Little, Inc.  
Cambridge, Mass.

G. E. POWERS  
Colorado State University  
Fort Collins, Colo.

JOAN ROBERTS  
Technical Information Center  
U. S. Atomic Energy Commission  
Oak Ridge, Tenn.

E. A. SCHENK  
University of Rochester Medical Center  
Rochester, N. Y.

S. SHACKNEY  
National Cancer Institute  
National Institutes of Health  
Bethesda, Md.

G. W. SISKIND  
Cornell University Medical Center  
New York, N. Y.

R. G. SWEET  
Stanford University School of Medicine  
Stanford, Calif.

M. TALLEY  
Department of Biology  
University of New Mexico  
Albuquerque, N. Mex.

J. H. TAYLOR  
Florida State University  
Tallahassee, Fla.

L. H. THOMPSON  
Lawrence Livermore Laboratory  
Livermore, Calif.

W. TOLLES  
State University of New York  
Brooklyn, N. Y.

L. J. TOLMACH  
Washington University School of Medicine  
St. Louis, Mo.

G. M. TOMKINS  
University of California  
San Francisco, Calif.

M. A. TRUMP  
Particle Technology, Inc.  
Los Alamos, N. Mex.

M. A. VAN DILLA  
Lawrence Livermore Laboratory  
Livermore, Calif.

A. VOGEL  
Cold Spring Harbor Laboratory  
Cold Spring Harbor, N. Y.

A. E. WECHSLER  
Arthur D. Little, Inc.  
Cambridge, Mass.

S. S. WEST  
University of Alabama in Birmingham  
Birmingham, Ala.

L. L. WHEELLESS  
University of Rochester Medical Center  
Rochester, N. Y.

G. L. WIED  
University of Chicago  
Chicago, Ill.

T. YAMAMOTO  
Atomic Bomb Casualty Commission  
Tokyo, Japan

ROSALIND YANISHEVSKY  
Lawrence Livermore Laboratory  
Livermore, Calif.

P. ZAMORA  
Department of Biology  
University of New Mexico  
Albuquerque, N. Mex.

R. ZUCKER  
Papanicolaou Cancer Research Institute  
Miami, Fla.

#### LOS ALAMOS SCIENTIFIC LABORATORY

H. M. AGNEW  
E. C. ANDERSON  
B. J. BARNHART  
MARY L. BARTLETT  
G. I. BELL  
L. L. BRANDT  
M. T. BUTLER  
EVELYN W. CAMPBELL  
L. J. CARR  
ELVA H. CLINARD  
L. S. CRAM  
H. A. CRISSMAN  
P. N. DEAN  
L. L. DEAVEN  
C. P. DeLISI  
M. D. ENGER  
JEAN C. FORSLUND

GEORGIA T. FRITZ  
W. B. GOAD  
E. R. GRILLY  
JULIE GRILLY  
L. R. GURLEY  
C. E. HILDEBRAND  
C. E. HOLLEY  
D. M. HOLM  
P. K. HORAN  
JUDITH Y. HUTSON  
J. H. JETT  
P. M. KRAEMER  
P. F. MULLANEY  
BILLIE J. NOLAND  
J. D. PERRINGS  
D. F. PETERSEN

R. L. RATLIFF  
C. R. RICHMOND  
ANGELA ROMERO  
G. C. SALZMAN  
PHYLLIS C. SANDERS  
A. G. SAPONARA  
G. C. SAUNDERS  
L. M. SCHERR  
J. D. SEAGRAVE  
D. A. SMITH  
J. A. STEINKAMP  
R. F. TASCHEK  
R. A. TOBEY  
T. T. TRUJILLO  
G. L. VOELZ  
R. A. WALTERS

# INDEX

- 
- Acidic nuclear protein  
  BUdR effect on synthesis, 133  
  synthesis during cell cycle, 133
- Acridine orange  
  fluorescence distributions  
    dog leukocytes, 66  
    HeLa cells, 100  
  staining procedure, 66, 100
- Acriflavine—Feulgen staining procedure, 96
- Aggregates, Feulgen positive, 46
- Algorithm, learning, 19, 21
- Analysis of cells (*see* Cell analysis)
- Antibody-forming cells, 112-113
- Antigen-binding cells, 112-113
- Argon laser, 62, 108
- Autoradiography  
  chromosome, 224  
  DNA fiber, 182, 186
- B cells  
  activation of, 257  
  clonal-selection theory, 254, 268, 282  
  immunoglobulin-like receptors of, 242, 255, 261  
  mitogen effects on, 261-262  
  mitogen receptors of, 262  
  and T cells, 111  
  and thymus-independent antigens, 264, 268  
  tolerance induction in, 267, 278
- Cannulation technique, 45
- Carcinoma in situ, 31
- Cell analysis  
  absorption, 59  
  acridine orange, 66, 100  
  antibody-forming cells, 112-113  
  antigen-binding cells, 112-113  
  automation, 59, 61, 89, 94, 107, 122  
    clinical, 89  
  cell surface area, 64  
  cell surface fluorescence, 64  
  cell volume, 59, 61  
    DNA content and, 68, 100  
  in cellular-immunology applications, 107  
  characterization of antibody-forming  
    cell precursors, 112  
  Chinese hamster cells, 64, 97  
  chromosome numbers, 76  
  "Coulter counting," 59, 61  
  DNA content, 66, 68, 76, 80, 97, 100  
    and cell volume, 68, 100  
    and protein content, 66, 100  
  dog leukocytes, 66  
  FACS (fluorescence-activated cell  
    sorting), 107  
  flow systems, 59, 61, 91, 107, 122  
  fluorescein-conjugated antibodies, 110  
  fluorescein-conjugated lectins  
    (con A-F), 64  
  fluorescence, 59, 61, 76, 94, 107  
    and light scattering, 107, 110  
  fluorescence-gated scatter, 110  
  future developments, 122  
  gated single parameter, 64, 107  
  HeLa cells, 64, 66, 68, 100  
  light scattering, 59, 61-62, 107, 110  
    fluorescence and, 107, 110



- mouse spleen, 66
- mouse tumor (MCA-1) cells, 66
- multiparameter, 61, 107
- murine thymocytes, 110
- normal, transformed, and revertant
  - mouse cells, 76
- protein content, 66, 100
- ratios of cell parameters, 64, 100
- slit-scan technique, 29
- splenic lymphocytes, 111
- surface area, 62
- T and B cells, 111
- transformed and revertant cell lines, 76
- two-color fluorescence, 61, 66, 100
- two parameter, 66, 107
- viable-cell count methodology, 110
- Cell chromosome studies
  - mouse cells, 76
  - 3T3 cells, 77
- Cell cycle
  - drug phase-dependent maturation effects, 171
  - effect of chemotherapeutic drugs, 170
  - flow microfluorometry, 126, 171
  - maps, 130, 147, 162
- Cell fusion, 38
- Cell-growth properties of 3T3 and SV40-transformed 3T3 revertants, 78
- Cell mutants
  - (*See also* Mutants)
  - auxotrophs, 232
  - meiotrophic, 232
  - temperature sensitive, 230
- Cell revertants
  - chromosome number, 80
  - DNA content per cell, 80
  - SV40-transformed 3T3, 76
- Cell-sample-preparation methods
  - (*See also* Cell-staining methods)
  - dispersal techniques, 95
  - fixation techniques, 95
  - flow systems, 94
- Cell separation
  - antibody-forming cell precursors in mice, 112
  - in cellular-immunology application, 107
  - dog leukocytes, 68
  - HeLa cells, 68
  - isolation of antibody-forming cell precursors, 112
  - mouse leukocytes, 66
  - mouse tumor (MCA-1) cells, 66
- Cell sorting
  - applications, 61, 110
  - in cellular-immunology application, 107
  - electronic, 59
  - fluorescence activated (FACS), 107
  - future developments, 122
  - instrumentation, 61, 107
  - multiparameter, 61
- Cell-staining methods
  - acridine orange, 66, 100
  - acriflavine-Feulgen, 96
  - DNA and protein specific, 66, 100
  - DNA specific, 66, 68, 96
  - ethidium bromide, 97
  - for flow systems, 64, 94, 111
  - fluorescein-conjugated lectins, 101
  - fluorescein isothiocyanate, 66
  - fluorescein-labeled antibodies, 101, 111
  - immunofluorescent, 101, 111
  - mithramycin, 97
  - propidium iodide, 97
  - protein specific, 97
  - suspension, 33
- Cell surface
  - area analysis, 64
  - area distribution, 64
  - fluorescence, 64
  - heparan sulfate, 160
  - macromomycin effect, 173
- Cell synchronization (*see* Synchronized cells)
- Cell transformation
  - normal to malignant, 76
  - SV40-transformed 3T3 cells, 76
- Cell-volume analysis, 59, 61, 100
- Cell-volume distributions
  - CHO, HeLa, and 929 cells, 100
  - DNA-content and, 68, 100
  - HeLa cells, 64, 68
- Cellular adhesion
  - assays for, 285
  - complex carbohydrates and, 291
  - to galactose coupled to Sephadex, 293
  - glycosyltransferases and, 291, 294
  - to homologous and heterologous cells, 285
  - inhibition of, 286
  - models of, 291
  - stimulation of, 286
  - to substrata, 284-285
  - trypsin effect on, 291

- Cellular immunology
  - antigen-binding cells as precursors to antibody-forming cells, 113
  - cell analysis and sorting applications, 107
  - characterization of antibody-forming cell precursors, 112
  - flow-systems applications, 107
  - functional specificity of KLH-binding cells, 113
  - isolation and adoptive response of DNP-binding cells, 115
  - precursor and plaque-forming cells, 117
- Centromeric indices, 10-11
- Chemotherapeutic drugs
  - cell-cycle effects, 170
  - cytotoxic effects, 169
- Chinese hamster cell strain, 39
- Chromatin
  - distribution patterns, 23
  - interaction with hormone-receptor complexes, 146
- Chromophore
  - concentration of, 6
  - mass of, 6
- Chromosomes
  - (See also Cell chromosome studies)
  - alterations in the number per cell, 76
  - autoradiography, 224
  - autosomal, 11
  - banding, 202, 210, 214
  - condensation and histone phosphorylation, 153, 163
  - and DNA content per cell, 79
  - DNA-synthesis sites, 185
  - euchromatic region, 201
  - fundamental number, 202, 206
  - heterochromatic region, 201
  - heteroploidy, 212
  - image analysis, 9
  - karyotype analysis, 57
  - metaphase, 9, 40
  - molecular organization, 208
  - premature condensation, 210
  - strandedness, 209
  - tumor cells, 213
- Classification rule, 19, 21
- Coulter counting, 59, 61
- Counting
  - Coulter, 59, 61
  - electrical resistance, 59, 62
- CYDAC (cytophotometric data conversion), 9, 39
- Cytocidal effects
  - cell cycle dependent, 170
  - concentration dependent, 169
  - time dependent, 169
- Cytodiagnosis, 19
- Cytology, 1-2
- Cytology automation
  - blood typing and cross matching, 92
  - cancer-cell detection, 91
  - cell-measurement instrumentation, 89
  - cellular-specimen concentration, 92
  - clinical laboratory, 89
  - clinical tests requirements, 90
  - differential white blood cell counts, 91
  - record keeping, 89
  - requirements for proper selection of cellular characteristics, 93
  - routine tests, 91
  - specimen handling, 89
  - urinalysis, 91
- Cytophotometer scanning, 6
- Cytophotometric data conversion (CYDAC), 9, 39
- Cytophotometry, 3
  - absorption, 4
  - flow systems, 4
  - imaging systems, 4
- Cytotoxicity test, anti- $\theta$ , 45
- Deoxyribonucleotide pools, 157
- DNA (deoxyribonucleic acid)
  - complex binding, 149
  - lipoprotein complexes, 156-157
  - receptor steroid, 149
  - replication fork, 188, 193, 197-198
  - replication units, 182, 188, 197, 239
  - synthesis sites within chromosomes, 185
- DNA content and chromosomes per cell, 79
- DNA-content distributions
  - and cell-volume distributions, 68, 100
  - CHO, HeLa, and 929 cells, 100
  - HeLa cells, 66, 68
  - mouse spleen, 66
  - mouse tumor (MCA-1) cells, 66
  - normal, transformed, and revertant mouse cells, 76, 80
  - and protein-content distributions, 66, 100
  - WI-38 and HeLa cells, 97
- DNA-fiber autoradiography, 182, 186
- DNA-lipoprotein complexes, 156

- DNA replicase  
  actinomycin D inhibition of, 138  
  MPB inhibition of, 138  
  requirement for DNA synthesis, 138  
  requirement for protein synthesis, 138  
  soluble cytoplasmic fraction factors for activity, 139  
  in synchronized HeLa cells, 136
- DNA replication  
  deoxyribonucleotide pools, 157  
  drug effects, 171  
  histone phosphorylation, 153  
  limiting event, 139  
  lipoprotein complexes, 157  
  need for salt-extractable protein, 142  
  nuclear, 135  
  prerequisite events, 164  
  sites, 140
- DNA-specific cell-staining methods, 66, 68, 96, 100  
  and protein-specific methods, 66, 100
- Dysplastic cell, nonkeratinizing, 31
- Eigenvalues, 18
- Eigenvectors, 18
- Electrical-resistance counting, 59, 62
- Enzyme induction  
  cell-cycle dependence, 146  
  control, 146  
  gene expression, 145  
  glucocorticosteroids and, 146  
  intracellular mediators, 146  
  membranes, 146  
  messenger RNA, 146  
  nuclear acceptor proteins, 149  
  progesterone as anti-inducer, 146  
  regulatory gene and, 149  
  steroid-insensitive cell variants, 149  
  steroid receptors, 146  
  tyrosine aminotransferase (TAT), 146
- Errors  
  distributional, 6  
  systematic, 6
- Ethidium bromide staining procedure, 97
- Euchromatin replication time, 189
- FACS (Fluorescence-activated cell sorting), 107
- Feature set, 21, 23
- Feature vector, 23
- Fibroblasts  
  human diploid, 41  
  mouse embryo, 41
- Flow microfluorometry (FMF), 39, 41, 59, 61, 78, 94, 107  
  analysis of drug effects on cell cycle, 171  
  life-cycle analysis, 126, 171
- Flow systems  
  automation concepts, 89  
  cell-analysis methods, 59, 61, 91, 107  
  cell-preparation methods, 94  
  cell-sorting techniques, 59, 61, 107  
  cell-staining methods, 64, 94, 111  
  in cellular-immunology applications, 107  
  instrumentation techniques, 59, 61, 107
- Fluid Mosaic Model, 246, 255, 259
- Fluorescein-conjugated lectins (con A-F), staining procedure, 64, 101
- Fluorescein isothiocyanate staining procedure, 66
- Fluorescence  
  cytoplasmic, 31  
  nuclear, 31
- Fluorescence-activated cell sorting (FACS), instrumentation and applications, 107
- Fluorescence analysis of cells, 59, 61, 76, 94, 107, 110
- Fluorescence cell-staining techniques, 64, 94, 111
- Flying-spot scanning cytophotometer (CYDAC), 9, 39
- FMF (*see* Flow microfluorometry)
- G<sub>1</sub> phase  
  cytotoxic drugs, 170-171  
  enzyme induction, 146  
  isoleucine deficiency, 153
- Gated-single-parameter analysis  
  cell surface area fluorescence, 64  
  cell volume and DNA content, 69  
  concepts, 62  
  fluorescence and light scattering, 107, 110
- Gene expression, enzyme induction, 145
- Gene regulation in cell cycle, 164-165
- Genetic markers, 228
- Glucocorticosteroids and enzyme induction, 146
- Helium-neon laser, 108
- Heparan sulfate  
  in cell cycle, 163  
  and cell surface, 160  
  isolation of, 160  
  structure and function of, 243

- Heterochromatin replication time, 189
- Histone phosphorylation  
in cell cycle, 154  
chromatin-lipoprotein complexes, 156  
chromosome condensation and, 153, 163  
in  $G_1$  arrest and mitosis, 154
- Histone synthesis  
control, 129  
cytoplasmic polysomes, 130  
DNA synthesis coupled, 131  
messenger RNA, 131  
repressors, 132  
synchronized cells, 129
- Homolog difference, 11
- Hormone-receptor complexes  
and enzyme induction, 146  
interaction with chromatin, 146
- Hybridization in situ, 201, 210
- Hydroxyurea  
cell synchronization, 153  
cycle-specific drug, 169  
dATP synthesis, 159
- Image partitioning, 9
- IMANCO quantimet system, 8
- Immune response, cell analysis and sorting applications, 107
- Immunofluorescence assay, 45
- Immunofluorescent staining procedures, 101, 111
- Immunogens  
effect of size, 257  
function of carrier, 257  
interactions with B-cell receptors, 257  
monovalent antigens as, 256-257  
multivalent antigens as, 258, 260  
lattice formation by, 260  
tolerance induction by, 257, 265, 267, 278
- Immunoglobulins  
affinity distribution of, 278  
diffusion coefficient of, 259  
IgG to IgM transition, 255  
kinetics of affinity change, 278  
macrophage role in synthesis of, 265  
structure of, 255, 258  
T-cell role in synthesis of, 257, 264-266
- Immunology, cellular (*see* Cellular immunology)
- Instrumentation  
cell analysis, 59, 61, 107  
cell sorting, 61, 107
- Karyokinesis, 41
- Learning, unsupervised, 23
- Learning algorithm, 19, 21
- Lectin (con A-F) binding distributions, 64
- Leukemia, chronic myelogenous, 11
- Life-cycle analysis  
conventional, 126  
microfluorometric, 126
- Life-cycle parameters  
density effect, 126  
monolayer culture, 126  
suspension culture, 126
- Light scattering  
analysis of cells, 59, 61-62, 107, 110  
distributions, 110
- Line-scan segments, 17
- Linear discriminant, 21
- Linearity  
photometric, 7  
spatial, 7
- Lymphocytes  
B (bone marrow derived), 44  
radiosensitivity, 44  
T (thymus derived), 44  
thoracic duct, 46  
mouse, 25
- Markov process, 16
- Membranes and steroid receptors, 146
- Metaphase spreads, 9
- Microfluorometry, flow systems, 39, 41, 59, 61, 78, 94, 107
- Microphotometer, rapid-scanning, 15
- Mithramycin staining procedure, 97
- Mitogens  
cap induction by, 250, 264  
cell agglutination by, 250  
cross linking of cell surface components by, 260  
effects on B cells, 261-262  
serum factors and, 264  
specificity of, 262
- Mitosis  
cytotoxic drugs, 171  
and deoxyribonucleotide pools, 157  
DNA-lipoprotein complexes, 156  
and histone phosphorylation, 153
- Morphometric analysis, 44, 46
- Multiparameter cell-analysis and -sorting instrumentation, applications, 61
- Multivariate distribution, 17



- Mutants  
(*See also* Cell mutants)  
destabilization by regulatory gene product, 149  
histone messenger, 131  
steroid insensitive, 149
- Myoblasts, 38
- Myotubes, striated, 38
- Neoplasia, chemotherapeutic drugs, 168
- Neuron tracking, 56
- Nuclear area, 47
- Nuclear DNA  
incorporation of nucleoside triphosphates by HeLa cells in hypotonic solution, 135  
replication in synchronized HeLa cells, 135-138
- Nuclear DNA content, 38
- Nucleus-to-cell diameter ratio, 16, 31
- Nucleus-to-cytoplasm ratio, 29
- Optical density, 5, 15, 46  
baseline, 8
- Picture element, 6
- Plasma membrane  
amphipathic components of, 247  
contractile components associated with, 249  
Fluid Mosaic Model of, 246, 255, 259  
forces influencing the stability of, 247  
linkage of components of, 250  
mobility of components of, 248-249, 259  
proteins of  
capping of, 249, 261  
factors affecting the exposure of, 243  
integral, 247, 255  
lattice formation in, 260  
patching of, 260-261  
peripheral, 247, 255  
structurally important components of, 247
- Polyloid cells, 38
- Propidium iodide staining procedure, 97
- Protein-content distributions  
CHO, HeLa, and 929 cells, 100  
DNA-content distributions and, 66, 100  
HeLa cells, 66
- Protein-specific cell-staining methods, 97  
and DNA-specific methods, 66, 100
- Proteins (*see* Plasma membrane, proteins of)
- Ratio analysis of cell parameters, 64, 66, 68, 100
- Reconstruction, three dimensional, 56
- Regression coefficients, 18
- Regulatory gene and enzyme induction, 150
- Resolution  
photometric, 7  
spatial, 7
- Revertants (*see* Cell revertants)
- Scanning-cytophotometry applications, 8
- Simian virus 40 (SV40), 38
- Slit-scan cell-analysis technique, 29
- Slit-scan cytofluorometer  
low-resolution scanning with, 30  
prescreening with, 31  
resolution of, 29
- Slit-scan flow system, 37
- Sorting of cells (*see* Cell sorting)
- S phase, cytotoxic drugs, 171
- S-phase reactions  
acidic nuclear protein synthesis, 135  
histone synthesis, 129-131  
nuclear DNA replication, 135  
synchronized HeLa cells, 129
- Squamous cells  
fluorescence of, 31  
stripped nuclei, 31
- Staining methods (*see* Cell-staining methods)
- Statistical analysis, multilevel, 11
- Steroid receptors  
allosteric forms, 146  
and DNA binding, 149  
and membranes, 146  
as nonhistone chromosomal proteins, 146  
nuclear and cytoplasmic forms, 149  
in nuclear-transfer-deficient mutants, 149
- Surface, cell (*see* Cell surface)
- SV40, 38
- Synchronization procedures, 153  
amethopterin, 135  
hydroxyurea, 153  
isoleucine, 153  
thymidine, 153
- Synchronized cells  
cell-cycle maps, 130, 147, 162

- chemotherapeutic drugs, 168
- Chinese hamster cells, 152
- and DNA replication, 135
- Don cells, 170
- effects of cancer, ascites cells, 168
- and enzyme induction, 145
- G<sub>0</sub> state, 169
- heparan sulfate, 160
- and histone synthesis, 129, 153
- and nuclear acidic proteins, 133
- synchronization procedures, 135, 153
- temporal sequence of events, 128, 146, 161
- T cells
  - B cells and, 111
  - role in synthesis of immunoglobulins, 257, 264-266
- Training set, 18, 21
- Transformation, neoplastic, 40
- Tumors
  - carcinoma in situ, 31
  - polyoma, 40
  - primary Syrian hamster, 40
- Two-color fluorescence analysis of DNA and protein, 66, 100
- Two-parameter cell analysis
  - DNA-content and cell-volume distributions, 68, 100
  - DNA- and protein-content distributions, 66, 100
  - fluorescence and light scattering, 107, 110
- Two-parameter cell sorting, 69, 107
- Tyrosine aminotransferase, glucocorticosteroid induction, 146
- Unsupervised learning, 23
- Vacuolization of nuclei, 50
- Virus, polyoma, 38

# NOTICE

This book was prepared as an account of work sponsored by the United States Government. Neither the United States nor the United States Energy Research and Development Administration, nor any of their employees, nor any of their contractors, subcontractors, or their employees, makes any warranty, express or implied, or assumes any legal liability or responsibility for the accuracy, completeness or usefulness of any information, apparatus, product or process disclosed, or represents that its use would not infringe privately owned rights.

# THE CELL CYCLE IN MALIGNANCY AND IMMUNITY

James C. Hampton, Chairman

*Proceedings of a symposium  
held at Richland, Washington,  
October 1-3, 1973*

January 1975  
614 pages, 6 by 9 inches  
Library of Congress Catalog Card No. 74-600181

The papers in this volume are concerned with the detection and treatment of cancer and investigate the use of surgery, radiation, chemotherapeutic agents, and immunotherapy. Tumor growth and treatment relate directly to the life cycles of tumor-cell populations and to points in the cell cycle where therapeutic agents, individually and in combination, can be most effective. This volume illustrates the kind of innovative approaches necessary to solve the problem of detection and points the way to more effective treatment of a dreaded and deadly disease.

*Major areas of investigation:*

- Biochemistry of the cell cycle
- Regulation of the cell cycle
- Perturbations of cellular kinetics by  
physical and chemical agents
- The cell cycle in malignancies and  
normal tissues
- Cell-cycle analysis in tumor therapy
- The cell cycle in lymphoid tissues

Available as CONF-731005  
for \$13.60 (\$16.10 foreign) from  
National Technical Information Service  
U. S. Department of Commerce  
Springfield, Va. 22161

## PHYSICAL MECHANISMS IN RADIATION BIOLOGY

Raymond D. Cooper and Robert W. Wood, Editors

*Proceedings of a conference sponsored by the  
Division of Biomedical and Environmental Research  
U. S. Atomic Energy Commission  
Held at Airlie, Virginia, Oct. 11-14, 1972*

This conference brought together radiation biologists, radiation chemists, and biophysicists to discuss the chain of events leading to the production by radiation of primary lesions in biological cells. The objectives of the meeting were to review understanding of physical mechanisms, to pinpoint deficiencies in present knowledge, and to recommend directions and areas of study for future emphasis. The representatives of the different sciences attempted to pool their knowledge of initial interactions in cells and to determine how theories and results in one discipline relate to those developed in another discipline. The first such compilation in 20 years, the book contains reports on the kinds of research being done, extensive discussions among the specialists, and summaries of what is known and of the problems that remain to be dealt with.

---

Available as CONF-721001  
for \$10.60 from  
National Technical Information  
Service  
U. S. Department of Commerce  
Springfield, Virginia 22161

Paperbound  
6 by 9 in.  
330 pages  
Library of Congress  
catalog card number:  
74-600124



# NUCLEAR SCIENCE ABSTRACTS

*Nuclear Science Abstracts* provides the only comprehensive abstracting and indexing coverage of the international nuclear science literature. It is a semimonthly publication of the U.S. Energy Research and Development Administration and is published by the ERDA Technical Information Center. *Nuclear Science Abstracts* covers the nuclear-energy-related scientific and technical reports of ERDA and its contractors, other U.S. Government agencies, other governments, universities, and industrial and research organizations. In addition, books, conference proceedings, individual conference papers, patents, and journal literature on a worldwide basis are abstracted and indexed.

## SUBSCRIPTIONS AND PRICES

*Nuclear Science Abstracts* is available to the public on a subscription basis from the Superintendent of Documents, U.S. Government Printing Office, Washington, D.C. 20402. It is published in two volumes each calendar year, each volume containing 12 regular issues. The annual subscription rate for the two volumes is \$121.05 for domestic subscribers and \$151.35 for foreign subscribers. A single issue costs \$5.05 domestic rates or \$6.35 foreign rates. Domestic rates apply to the United States, Canada, Mexico, and Central and South American countries except Argentina, Brazil, Guyana, French Guiana, Surinam, and British Honduras.

## INDEXES

Indexes covering subject, author, corporate author, and report number are in-

cluded in each issue. These indexes are cumulated for each volume, i.e., for 12 issues on a 6-month volume basis. They are sold on an annual subscription basis (24 issues in 2 volumes) at \$44.40 for domestic subscribers and \$55.50 for foreign subscribers. They are also sold separately by volume on the basis of pagination at the time of publication. The indexes provide a detailed and convenient key to the world's nuclear literature.

## EXCHANGES

*Nuclear Science Abstracts* is available on an exchange basis to universities, research institutions, industrial firms, and publishers of scientific information; inquiries regarding the exchange provision should be directed to the ERDA Technical Information Center, P.O. Box 62, Oak Ridge, Tennessee 37830.

---

## Volumes of Interest in the U. S. ENERGY RESEARCH AND DEVELOPMENT ADMINISTRATION TECHNICAL INFORMATION CENTER BIBLIOGRAPHY SERIES

*Both volumes are available by report number from the National Technical Information Service, Department of Commerce, Springfield, Virginia 22161*

### Human Radiation Dose Studies: A Selected Bibliography

This bibliography covers technical reports and journal articles abstracted in *Nuclear Science Abstracts* from January 1962 to June 1973. It contains 1010 abstracts, arranged by NSA volume and abstract number, and a subject index. (TID-3348; \$7.60)

### Bibliography on Nuclear Medicine

This volume provides references to 1589 publications related to nuclear medicine which were abstracted in *Nuclear Science Abstracts* from January 1972 to June 1973. Each bibliographic citation is followed by NSA subject indexing to provide additional information on the contents of the document. Entries are indexed by personal author, corporate author, subject, and report number. (TID-3319-S5; \$10.60)

DATE DUE

SEP 19 1978

SEP 7 1981

ERDA SYMPOSIUM  
U. S. Department of Comm

in Service,

Reactor Kinetics and Cont  
Dynamic Clinical Studies v  
Noise Analysis in Nuclear S  
Radioactive Fallout from M  
Radioactive Pharmaceutica  
Neutron Dynamics and Co  
Luminescence Dosimetry (I  
Neutron Noise, Waves, and  
Use of Computers in Analy  
(CONF-660527), 1967, S

Compartments, Pools, and  
Thorium Fuel Cycle (CONF  
Radioisotopes in Medicine:  
Abundant Nuclear Energy  
Fast Burst Reactors (CONF  
Biological Implications of t  
Radiation Biology of the F  
Inhalation Carcinogenesis (I  
Myeloproliferative Disorder  
Medical Radionuclides: Rac  
Morphology of Experiment  
Precipitation Scavenging (1  
Neutron Standards and Flu  
Survival of Food Crops and  
Biomedical Implications of  
Radiation-Induced Voids in  
Clinical Uses of Radionuclid

GAYLORD

PRINTED IN U.S.A

I, \$9.00

01), 1972,

Interactive Bibliographic Systems (CONF-711010), 1973, \$7.60  
Radionuclide Carcinogenesis (CONF-720505), 1973, \$13.60  
Carbon and the Biosphere (CONF-720510), 1973, \$10.60  
Technology of Controlled Thermonuclear Fusion Experiments and the Engineering Aspects of Fusion  
Reactors (CONF-721111), 1974, \$16.60  
Thermal Ecology (CONF-730505), 1974, \$13.60  
The Cell Cycle in Malignancy and Immunity (CONF-731005), 1975, \$13.60  
Mammalian Cells: Probes and Problems (CONF-731007), 1975, \$7.60  
Cooling Tower Environment—1974 (CONF-740302), 1975, \$13.60

LIBRARY  
**NIH**

Amazing Research.  
Amazing Help.

<http://nihlibrary.nih.gov>

10 Center Drive  
Bethesda, MD 20892-1150  
301-496-1080

NIH LIBRARY



4 0119 2493



NIH LIBRARY



3 1496 00172 0864

Technical Information Center, Office of Public Affairs  
U. S. ENERGY RESEARCH AND DEVELOPMENT ADMINISTRATION